Tesi di dottorato preparata presso

UNIVERSITÀ DEGLI STUDI FIRENZE

Università di Firenze, Università di Perugia, INdAM consorziate nel CIAFM

nel quadro di una convenzione di cotutela con

Aix–Marseille Université

DOTTORATO DI RICERCA
IN MATEMATICA, INFORMATICA, STATISTICA

Curriculum in Matematica
CICLO XXXVI

Sede amministrativa Università degli Studi di Firenze
Coordinatore Prof. Matteo Focardi

Studi di metastabilità a bassa temperatura

Settore Scientifico Disciplinare MAT/06

Dottorando:
Simone Baldassarri

Tutori
Dr. Gianmarco Bet
Prof. Alexandre Gaudillière
Prof.ssa Francesca R. Nardi

Coordinatore
Prof. Matteo Focardi

Anni 2020-2023

NNT/NL : 2023AIXM0001/000ED000

THÈSE DE DOCTORAT

Soutenue à Florence
en cotutelle avec l'Université de Florence
le 14 décembre 2023 par

Simone Baldassarri

Études de métastabilité à basse température

Discipline
Mathématiques

École doctorale
ED184

Laboratoire
I2M, UMR 7373

Composition du jury

Nils BERGLUND Université d'Orleans	Rapporteur
Gioia CARINCI Università degli Studi di Modena e Reggio Emilia	Rapporteuse
Alessandra BIANCHI Università degli Studi di Padova	Examinatrice
Fabienne CASTELL Aix-Marseille Université	Examinatrice
Ellen SAADA Université de Paris Cité, CNRS	Examinatrice
Paolo DAI PRA Università degli Studi di Verona	Président du jury
Gianmarco BET Università degli Studi di Firenze	Co-directeur de thèse
Alexandre GAUDILLIÈRE Aix-Marseille Université, CNRS	Directeur de thèse

DICHIARAZIONE GIURATA

Io sottoscritto, Simone Baldassarri, con la presente dichiaro che il lavoro presentato in questo manoscritto è il mio lavoro, svolto sotto la direzione scientifica di Gianmarco Bet, Alexandre Gaudillière e Francesca R. Nardi, nel rispetto dei principi di onestà, integrità e responsabilità inerenti alla missione di ricerca. Il lavoro di ricerca e la stesura di questo manoscritto sono stati realizzati nel rispetto sia della carta etica nazionale delle professioni di ricerca sia della carta dell'Università di Aix-Marseille relativa alla lotta contro il plagio.

Quest'opera non è stata precedentemente presentata in Italia o all'estero in una versione identica o simile ad un organismo esaminatore.

Fatta a Firenze il 07 Settembre 2023

AFFIDAVIT

Je soussigné, Simone Baldassarri, déclare par la présente que le travail présenté dans ce manuscrit est mon propre travail, réalisé sous la direction scientifique de Gianmarco Bet, Alexandre Gaudillière et Francesca R. Nardi, dans le respect des principes d'honnêteté, d'intégrité et de responsabilité inhérents à la mission de recherche. Les travaux de recherche et la rédaction de ce manuscrit ont été réalisés dans le respect à la fois de la charte nationale de déontologie des métiers de la recherche et de la charte d'Aix-Marseille Université relative à la lutte contre le plagiat.

Ce travail n'a pas été précédemment soumis en France ou à l'étranger dans une version identique ou similaire à un organisme examinateur.

Fait à Florence le 07 Septembre 2023

LIST OF PUBLICATIONS

1. S. Baldassarri, V. Jacquier, A. Zocca, “Critical configurations of the hard-core model on square grid graphs", arXiv preprint, arXiv:2308.05041 (2023).
2. S. Baldassarri, A. Gaudillière, F. den Hollander, F.R. Nardi, E. Olivieri, E. Scoppola, “Droplet dynamics in a two-dimensional rarefied gas under Kawasaki dynamics", arXiv preprint, arXiv:2304.14099 (2023).
3. S. Baldassarri, A. Gallo, V. Jacquier, A. Zocca, “Ising model on clustered networks: A model for opinion dynamics", *Physica A: Statistical Mechanics and its Applications*, **623** (2023).
4. S. Baldassarri, V. Jacquier, “Metastability for Kawasaki dynamics on the hexagonal lattice", *Journal of Statistical Physics*, **190(46)**, 1–44 (2023).
5. S. Baldassarri, G. Bet, “Asymptotic normality of degree counts in a general preferential attachment model", *Markov Processes and Related Fields*, **28(4)**, 577–603 (2022).
6. S. Baldassarri, F.R. Nardi, “Critical Droplets and sharp asymptotics for Kawasaki dynamics with weakly anisotropic interactions", *Stochastic Processes and their Applications*, **147**, 107–144 (2022).
7. S. Baldassarri, F.R. Nardi, “Critical Droplets and sharp asymptotics for Kawasaki dynamics with strongly anisotropic interactions", *Journal of Statistical Physics*, **186(34)**, 1–46 (2022).
8. S. Baldassarri, F.R. Nardi, “Metastability in a lattice gas with strong anisotropic interactions under Kawasaki dynamics", *Electronic Journal of Probability*, **26(137)**, 1–66 (2021).
9. S. Baldassarri, A. Gaudillière, F. den Hollander, F.R. Nardi, E. Olivieri, E. Scoppola, “Homogeneous nucleation for two-dimensional Kawasaki dynamics", in preparation.

LIST OF PARTICIPATION IN INTERNATIONAL CONFERENCES

1. Invited talk “Droplet dynamics in a two-dimensional rarefied gas under Kawasaki dynamics", *Stochastic Process, metastability and applications*, Nancy (France), 31/05-02/06/2023 (held online due to healthy issues)
2. Invited talk “Droplet dynamics in a two-dimensional rarefied gas under Kawasaki dynamics", Università di Roma Tre (Italy), 09/05/2023
3. Invited talk “Droplet dynamics in a two-dimensional rarefied gas under Kawasaki dynamics", *Analysis and simulations of metastable systems*, CIRM Marseille (France), 03-07/04/2023
4. Invited talk “Droplet growth for anisotropic models with Kawasaki dynamics on a finite box with open boundary conditions", *iPOD Seminar Leiden*, Leiden (The Netherlands), 03/11/2022
5. Invited talk “Nucleation for the metastable Kawasaki dynamics with strongly anisotropic interactions", *Francesca Romana Nardi: A life in probability, building communities across Europe*, Firenze (Italy), 18-22/07/2022
6. Poster Session “Critical Droplets and sharp asymptotics for Kawasaki dynamics with strongly anisotropic interactions", *Probability and Mathematical Physics 2022*, University of Helsinki (Finland), 28/06-07/07/2022
7. Contributed talk “Critical Droplets and sharp asymptotics for Kawasaki dynamics with strongly anisotropic interactions", *Third Italian Meeting on Probability and Mathematical Statistics*, University of Bologna (Italy), 13-16/06/2022
8. Contributed talk “Critical Droplets and sharp asymptotics for Kawasaki dynamics with strongly anisotropic interactions", *Mathematical Physics and Probability Seminar*, 13/04/2022 (online)
9. Invited talk “Critical Droplets and sharp asymptotics for Kawasaki dynamics with strongly anisotropic interactions", *Seminar Interacting Random Systems*, WIAS Berlin (Germany), 06/04/2022
10. Working group *“QuAMProcs–Quantitative Analysis of Metastable Processes”*, Inria Paris, 08-09/03/2022.
11. Invited talk “Metastability in a lattice gas with strong anisotropic interactions under Kawasaki dynamics", *Insalate di Matematica*, Università degli Studi Milano-Bicocca (Italy), 10/02/2022
12. Contributed talk “Metastability in a lattice gas with strong anisotropic interactions under Kawasaki dynamics", *GIM Seminars*, 14/01/2022 (online)
13. Contributed talk “Critical Droplets and sharp asymptotics for Kawasaki dynamics with strongly anisotropic interactions, *Probability Seminar Essen*, 21/12/2021 (online)
14. Contributed 2-hours mini course “Metastability in a lattice gas evolving under Kawasaki dynamics", *First Conference Of Young Applied Mathematicians in Leuca*, Santa Maria di Leuca (Italy), 13/09-17/09/2021
15. Workshop *“Rencontres de Probabilités 2021”*, mini courses taught by Valentin Féray, Patricia Gonçalves and Claudio Landim, 21-22/10/2021 (online).
16. Workshop *“Junior female researchers in probability”*, 04-06/10/2021 (online)
17. *Young European Probabilists* Workshop (YEP XVII: "Interacting particle systems"), mini courses taught by Patricia Gonçalves, Jan Swart and Cristina Toninelli, 30/08-03/09/2021 (online).
18. Workshop *“Random excursions with Jean Bertoin”*, organized by Sorbonne Université, Paris (France), 05-09/07/2021 (online).
19. Workshop *“Recent Progress on Random Walks”*, organized by CIRM, Marseille (France), 12-16/04/2021 (online).

ABSTRACT

We investigate the metastable behaviour of discrete systems at low temperature evolving under the stochastic Kawasaki and Glauber dynamics to analyze the transition to the liquid phase of a supersatured vapour and the spread of an opinion inside a network, respectively. Concerning the second issue, to capture a realistic description of networks we finally consider the problem of metastability for a growing random graph. The first step in this direction is the analysis of the asymptotic properties of such a model, which we address in this work. The thesis is divided into four parts as follows.

The first two parts are devoted to the analysis of the exit from metastability for a lattice gas at very low temperature and low density that evolves according to the conservative *Kawasaki dynamics* in a discrete domain Λ_β whose volume is exponentially large in the inverse temperature β. Particles perform simple exclusion on Λ_β and each of them has a positive activation energy Δ, but when they occupy neighbouring sites they feel a binding energy.

In the first part of the thesis, we consider variations of the *local* version of this model, namely, the gas evolves inside a finite domain $\Lambda \subset \Lambda_\beta$ and we investigate how the transition from metastability to stability takes place. We start by considering $\Lambda \subset \mathbb{Z}^2$, so that neighbouring particles feel a binding energy $-U_1 < 0$ in the horizontal direction and $-U_2 < 0$ in the vertical direction. It turns out that the dynamical behaviour drastically changes whether $U_1 = U_2$ (isotropy), $U_1 < 2U_2$ (weak anisotropy) or $U_1 > 2U_2$ (strong anisotropy). For all these regimes, our focus is the identification of the *critical configurations* that have to be crossed with high probability. The derivation of some geometrical properties of the saddles allows us to identify the full geometry of the minimal gates for the nucleation. We observe very different behaviour in the three regimes.

Next, we consider the domain Λ as a subset of the two-dimensional hexagonal lattice and we assume isotropic interactions between neighbouring particles. We derive the asymptotic behaviour of the transition time from metastability to stability in the limit as β goes to infinity. We also provide a characterization of the shape of the critical droplets and we emphasize that their description differs from that appearing in the standard square lattice since this feature strongly depends on the underlying geometry. Indeed, the particular shape of the hexagonal lattice induces an increment of the regularizing motions of particles in such a way new mechanisms of entering the critical configurations set appear.

In the second part of the thesis, we deal with the original Kawasaki dynamics on the square lattice in the isotropic regime. This analysis is much harder than in small volumes, indeed now particles are conserved in all the domain and a detailed control of the interaction between droplets and the gas of "isolated particles" is needed: the role of the *entropy* turns out to be crucial. We analyze how subcritical droplets form and dissolve when the volume is "moderately large": the evolution of the gas consists of *droplets wandering around on multiple space-time scales*. Based on these results, we are able to predict that the exit from metastability in "very large" volumes occurs via *homogeneous nucleation*, i.e., a critical droplet appears in a box of moderate volume.

In the third part of the thesis, we consider the exit from metastability for systems that evolve under the *non-conservative Glauber dynamics*, which, contrary to Kawasaki dynamics, has its own peculiar features. In particular, we investigate opinion dynamics on networks with a community structure, assuming that individuals can update their binary opinion as the result of the interactions with an external influence and with other individuals in the network. In the very low temperature regime homogeneous opinion patterns prevail and, as such, it takes evereyone a long time to change opinion. We provide estimates for such a transition time and we fully identify the critical configurations for the dynamics.

In the final part, we consider a growing random graph, known as *preferential attachment model*, such that at each step a new vertex is added and forms m connections. It is well known that the proportion of nodes with a given degree at step n converges to a constant as $n \to \infty$. Our goal is to find the asymptotic distribution of the fluctuations around this limiting value. In particular, we prove a central limit theorem for the joint distribution of all degree counts.

Studiamo il comportamento metastabile di sistemi discreti a bassa temperatura che evolvono sotto le dinamiche stocastiche di Kawasaki e Glauber per analizzare rispettivamente il passaggio alla fase liquida di un vapore sovrasaturo e la diffusione di un'opinione all'interno di una rete. Per quanto riguarda la seconda questione, per ottenere una descrizione realistica delle reti consideriamo alla fine il problema della metastabilità per un grafo aleatorio dinamico. Il primo passo in questa direzione è l'analisi delle proprietà asintotiche di tale modello, che affrontiamo in questo lavoro. La tesi è divisa in quattro parti come segue.

Le prime due parti sono dedicate all'analisi della fuga dalla metastabilità per un gas reticolare a temperatura e densità molto basse che evolve secondo la *dinamica conservativa di Kawasaki* in un dominio discreto Λ_β di volume esponenzialmente grande nella temperatura inversa β. Le particelle eseguono un'esclusione semplice in Λ_β ed ciascuna di esse ha un'energia positiva di attivazione Δ, ma quando occupano siti vicini risentono di un'energia di legame.

Nella prima parte della tesi consideriamo variazioni della versione *locale* di questo modello, cioè il gas evolve all'interno di dominio finito $\Lambda \subset \Lambda_\beta$ ed indaghiamo come avviene la transizione dalla metastabilità alla stabilità. Iniziamo considerando $\Lambda \subset \mathbb{Z}^2$, cosicché particelle vicine risentono di un'energia di legame $-U_1 < 0$ nella direzione orizzontale e $-U_2 < 0$ in quella verticale. Il comportamento dinamico del sistema cambia radicalmente se $U_1 = U_2$ (isotropia), $U_1 < 2U_2$ (debole anisotropia) o $U_1 > 2U_2$ (forte anisotropia). Per tutti i regimi identificheremo le *configurazioni critiche* che vengono attraversate con alta probabilità. Grazie ad alcune loro properietà geometriche, riusciamo ad identificare la geometria completa dei varchi minimali per la nucleazione. Osserviamo comportamenti molto diversi nei tre regimi.

Consideriamo in seguito il dominio Λ come sottoinsieme del reticolo esagonale ed assumiamo interazioni isotrope tra particelle vicine. Deriviamo il comportamento asintotico del tempo di transizione dalla metastabilità alla stabilità e forniamo una caratterizzazione delle gocce critiche, sottolineando che la loro descrizione differisce da quella che appare nel reticolo quadrato. Essa dipende, infatti, dalla geometria sottostante e la particolare forma del reticolo esagonale induce un incremento dei moti regolarizzanti delle particelle in modo tale che appaiano nuovi meccanismi di ingresso nell'insieme delle configurazioni critiche.

Nella seconda parte della tesi ci occupiamo della dinamica originale di Kawasaki sul reticolo quadrato con interazioni isotrope. Questa analisi è molto più difficile di quella in volume finito, infatti adesso le particelle sono conservate in tutto il dominio ed è quindi necessario un controllo dettagliato delle interazioni tra le gocce ed il gas di "particelle isolate": il ruolo dell'*entropia* diventa cruciale. Analizziamo come le gocce sottocritiche si formano e si dissolvono quando il volume è "moderatamente grande": l'evoluzione del gas consiste di *gocce erranti su più scale spazio-temporali*. Sulla base di questi risultati possiamo prevedere che l'uscita dalla metastabilità in volumi "molto grandi" avvenga tramite *nucleazione omogenea*, cioè una goccia critica appare in una scatola di volume moderato.

Nella terza parte della tesi consideriamo la fuga dalla metastabilità per sistemi che evolvono secondo la *dinamica non conservativa di Glauber*, che, contrariamente alla dinamica di Kawasaki, ha delle caratteristiche peculiari. Indaghiamo in particolare le dinamiche di opinione su reti con una struttura di comunità, assumendo che gli individui possano aggiornare la loro opinione binaria come risultato delle interazioni con un'influenza esterna e con altri individui nella rete. Nel limite di temperatura molto bassa prevalgono motivi di opinioni omogenee e, pertanto, ci vuole molto tempo affinché tutti cambino idea. Forniamo stime per tale tempo di transizione e identifichiamo completamente le configurazioni critiche per la dinamica.

Nell'ultima parte della tesi consideriamo un grafo aleatorio dinamico nel tempo, noto come *modello ad attaccamento preferenziale*, tale che ad ogni passo viene aggiunto un nuovo vertice di grado m. È noto che la proporzione di nodi con un dato grado al passo n converge ad una costante per $n \to \infty$. Il nostro obiettivo è, quindi, trovare la distribuzione asintotica delle fluttuazioni attorno a questo valore limite. In particolare dimostriamo un teorema del limite centrale per la distribuzione congiunta di tutti i conteggi dei gradi.

RÉSUMÉ

Nous étudions le comportement métastable de systèmes discrets à basse température qui évoluent sous la dynamique stochastique de Kawasaki et Glauber pour analyser respectivement le passage à la phase liquide d'une vapeur sursaturée et la diffusion d'un avis dans un réseau. Quant à la deuxième question, pour obtenir une description réaliste des réseaux nous considèrons enfin le problème de la métastabilité pour un graphe aléatoire dynamique. La première étape dans cette direction est l'analyse des propriétés asymptotiques de ce modèle, que nous affrontons dans ce travail. La thèse est divisée en quatre parties comme suit.

Les deux premières parties sont dédiées à l'analyse de la fuite de la métastabilité pour un gaz de réseau à température et densité très basses évoluant sous la *dynamique conservative de Kawasaki* dans un domaine discret Λ_β, de volume exponentiellement grand en la température inverse β. Les particules effectuent une exclusion simple dans Λ_β et ont une énergie d'activation positive Δ, mais des particules voisines sont affectées par une énergie de liaison.

Dans la première partie de la thèse nous considérons des variantes de la version *locale* de ce modèle, c'est-à-dire que le gaz évolue à l'intérieur d'un domaine fini $\Lambda \subset \Lambda_\beta$ et nous étudions comment s'effectue la transition de la métastabilité à la stabilité. Nous démarrons en considérant $\Lambda \subset \mathbb{Z}^2$, de sorte que les particules voisines sont affectées par une énergie de liaison $-U_1 < 0$ dans la direction horizontale et $-U_2 < 0$ dans la direction verticale. Le comportement dynamique du système change radicalement si $U_1 = U_2$ (isotropie), $U_1 < 2U_2$ (faible anisotropie) ou $U_1 > 2U_2$ (forte anisotropie). Pour ces régimes nous identifierons les *configurations critiques* qui sont traversées avec grande probabilité. Grâce à certaines de leurs propriétés géométriques, nous pouvons identifier la géométrie des entrées minimales pour la nucléation. Nous observons des comportements très différents en les trois régimes.

Nous considérons ensuite le domain Λ comme un sous–ensemble du réseau hexagonal et supposons des interactions isotropes entre particules voisines. Nous dérivons le comportement asymptotique du temps de transition de la métastabilité à la stabilité et nous caractérisons les gouttes critiques, soulignant que leur description diffère de celle dans le réseau carré. De fait, celles-ci dépendent de la géométrie sous-jacente et la forme particulière du réseau hexagonal induit une augmentation des mouvements de régularisation des particules de sorte que nouveaux mécanismes d'entrée apparaissent dans l'ensemble des configurations critiques.

Dans la deuxième partie de la thèse nous traitons la dynamique originale de Kawasaki sur le réseau carré avec des interactions isotropes. Cette analyse est beaucoup plus difficile que l'analyse en volumes finis, car les particules sont désormais conservées dans tout le domaine et un contrôle détaillé des interactions entre les gouttes et le gaz de "particules isolées" est donc nécessaire : le rôle de l'*entropie* devient crucial. Nous analysons comment les gouttes sous-critiques se forment et se dissolvent quand le volume est "modérément grand" : l'évolution du gaz consiste en *gouttes errant sur plusieurs échelles d'espace-temps*. Nous pouvons donc prédire que la fuite de la métastabilité dans des volumes "très grands" se produit par *nucléation homogène*: une goutte critique apparaît dans une boîte de volume modéré.

Dans la troisième partie nous considérons la fuite de la métastabilité pour des systèmes évoluant selon la *dynamique non–conservative de Glauber*, qui présente des caractéristiques particulières. Nous étudions une dynamique d'opinion dans les réseaux avec communautés, en supposant que les individus peuvent mettre à jour leur opinion binaire à la suite d'interactions avec une influence externe et avec d'autres individus du réseau. Dans la limite de température très basse les opinions homogènes prévalent et, par conséquent, l'opinion de chacun change après beaucoup de temps. Nous fournissons des estimations de ce temps de transition et identifions pleinement les configurations critiques pour la dynamique.

Dans la dernière partie de la thèse nous considérons un graphe aléatoire dynamique, le *modèle d'attachement préférentiel*, qui est tel qu'à chaque étape un nouveau sommet de degré m est ajouté. Il est bien connu que la proportion des sommets avec un degré donné à l'étape n converge vers une constante pour $n \to \infty$. Nous établissons donc la distribution asymptotique des fluctuations autour de cette valeur limite. En particulier, nous prouvons un théorème central limite pour la distribution conjointe de tous les nombres de degrés.

RINGRAZIAMENTI

Guardandomi indietro posso dire che questo viaggio è stato intenso, indimenticabile, e davvero carico di emozioni. Dividersi tra Firenze e Marsiglia non è stato affatto facile, e, se sono stato in grado di arrivare dove sono adesso, è grazie all'aiuto ed al supporto di persone meravigliose con le quali ho avuto il piacere di condividere questo percorso. Desidero ringraziare qui tutti coloro che mi hanno accompagnato nell'avventura ed hanno contribuito alla realizzazione di questo lavoro.

Prima di tutto vorrei esprimere la mia più profonda gratitudine ai miei supervisori: Francesca, Gianmarco ed Alex. La vostra positività e profonda passione per la ricerca sono state per me un continuo stimolo a non pormi mai limiti. Mi avete aiutato ad acquisire fiducia, a credere in me stesso e nella mia ricerca, e a diventare un probabilista migliore. Spero con tutto il cuore di aver fatto mia questa mentalità.

Francesca, grazie per avermi fatto scoprire e condotto per mano alla scoperta dello straordinario mondo della metastabilità. Mi sembra ieri che eravamo seduti attorno ad un tavolo, in pausa pranzo, a discutere la direzione più giusta da percorrere insieme. Sempre con il sorriso stampato sulle labbra, avevi per me parole di conforto quando le cose non andavano come volevamo. La tua incredibile tenacia ha fatto sì che, anche adesso che non ci sei più, io riesca comunque a proseguire questo bellissimo viaggio, tenendomi stretti i tuoi consigli – tua eredità più grande e bella. Sono stato circondato dai tuoi amici e collaboratori più stretti, attraverso i quali io continuo a sentirti, perché tanto di te ce l'ho con me. Ti sentirò sempre. Ogni volta in cui, se fossi stata davanti a me, a parlare con me, mi avresti incoraggiato, mi avresti detto "Simone, stai andando bene, continua così!". E io ci crederò un po' di più, come sempre.

Gianmarco, grazie per aver condiviso con me il tuo profondo intuito e i tuoi consigli costruttivi. Sempre con una prospettiva positiva, mi hai costantemente spinto a fare un passo avanti nella mia ricerca. Il tuo continuo supporto mi ha fatto esprimere al meglio. Non mi hai mai fatto sentire solo. Trovare un amico, oltre che un collega, è un dono prezioso e molto raro.

Alex, à partir du moment où la vie nous a réuni tu ne m'as jamais laissé seul. Tu m'as accueilli dans ta vie de la manière la plus naturelle possible. Nos discussions, strictement en italien, ont toujours été une source d'inspiration, tant dans la recherche que dans la vie. Tu as définitivement fait de moi une personne meilleure. Désormais les *calissons* auront toujours un goût spécial. Un immense merci va à Clothilde pour son hospitalité généreuse et sa profonde gentillesse.

Desidero ringraziare Nils Berglund, Gioia Carinci, Alessandra Bianchi, Fabienne Castell, Paolo Dai Pra e Ellen Saada per aver accettato di far parte della mia commissione di dottorato, e per il fatto che leggeranno e commenteranno questa tesi.

Je tiens à remercier Nils Berglund, Gioia Carinci, Alessandra Bianchi, Fabienne Castell, Paolo Dai Pra et Ellen Saada d'avoir acceptés de faire partie de mon comité doctoral, et de lire et commenter cette thèse.

Sono immensamente grato anche a Betta e Frank. Grazie per l'entusiasmo con cui mi avete permesso di prendere parte alla grande avventura che vi coinvolge e che dura ormai da molto tempo: è davvero molto bello far parte del *Kawasaki team*. Non potrò mai dimenticare la vostra immensa professionalità e conoscenza. Lavorare con voi è stato ed è tuttora motivo di profondo orgoglio per me: cercherò di fare tesoro e portare sempre con me i vostri preziosissimi consigli. Ricorderò con molto affetto la vostra accoglienza ad ogni mia singola visita a Leiden e Roma, che rimarranno per me sempre dei luoghi speciali.

Un grazie particolare va anche ai miei collaboratori Alessandro, Anna e Vanessa: poter fare matematica con degli amici è un lusso a cui non vorrei mai rinunciare.

Una menzione speciale spetta senza alcun dubbio alla parte restante del gruppo di Firenze, Luisa ed Eugenio: poter sempre contare su di voi è la cosa più bella che ci sia.

Merci à mon ami *marseillais* Brice, qui m'a accompagné dans ma première expérience loin de chez moi. Je me souviendrai avec grand plaisir des moments passés ensemble !

Un profondo grazie va ai miei genitori, Riccardo e Maria Grazia, ed al mio fratellone Matteo. Grazie per avermi fatto credere nelle mie potenzialità e ad avermi insegnato a non pormi mai limiti. Non potete nemmeno immaginare quanto mi riempia il cuore vedervi orgogliosi di me. Adesso non sarei qui senza di voi. Un ringraziamento speciale va senza dubbio alle mie cugine Chiara e Francesca, alle quali voglio un bene infinito e che ringrazio per esserci sempre.

Un grazie infinito va a tutti i miei amici pistoiesi, Bala, Edo, Jack, Mala e Met, che in un modo o nell'altro sono riusciti sempre a starmi vicini nonostante la lontananza. Vi voglio bene!

Il mio ultimo pensiero va a te, Gaia. Grazie per essere stata con me fino alla fine. Più di chiunque altro hai condiviso con me le gioie e le difficoltà di questo percorso, non abbandonandomi mai. Senza di te al mio fianco non avrei ottenuto questo traguardo. Non hai mai smesso di credere in me e mi hai aiutato a dare sempre il massimo e a non tirarmi indietro mai. Sei il mio punto fermo. Grazie per tutti i momenti vissuti e per quelli che ci saranno. Per il passato, il presente e il futuro insieme.

"Which contain the greatest amount of Science, do you think, the books, or the minds?"... And I considered a minute before replying: "If you mean living minds, I don't think it's possible to decide. There is so much written Science that no living person has ever read: and there is so much thought-out Science that hasn't yet been written".

Lewis Carrol, Sylvie and Bruno

CONTENTS

1 INTRODUCTION

1.1 OVERVIEW

In this thesis we focus on the metastable behaviour of discrete systems at low temperature that evolve under stochastic dynamics.

Metastability is ubiquitous in nature and the need to capture the behavior of systems subject to such a phenomenon is the main motivation of this research. Indeed, metastability naturally arises in a large variety of systems — physics, chemistry, biology, economics and sociology. In this work we mainly focus on discrete systems aiming at capturing features coming from both statistical physics and sociology fields.

Behind the phenomenon of metastability there are some common features, such as a large variability in the moment of the onset of some dramatic change in the properties of the system, a much shorter time for the actual transition (i.e., between the onset of a noticeable change and the moment a new state is reached), and unpredictability of the time of the onset of the transition. It is formally described as a dynamical phenomenon that occurs when a system is close to a first order phase transition. After changing some thermodynamic parameters, the system remains for a considerable (random) time in the old phase, the metastable state, before suddenly making a transition to the new phase, the stable state. In other words, on a short time scale, the system behaves as if it was in equilibrium, while, on a long time scale, it moves between different regions of the state space (see Figure 1.1). The transition occurs when the system manages to create a sufficiently large droplet, the so–called *critical droplet*, of the new phase inside the old phase (see Figure 1.2). In the study of metastablity there are three main issues that are tipically investigated. The first one is the study of the *typical transition time* from the metastable to the stable states, i.e., the time necessary to arrive at the equilibrium phase. The second and third issues concern the geometrical description of the *gate configurations* (also called *critical configurations*) and the *tube of typical trajectories*. These issues are physically more interesting, because they provide information about the configurations that will be crossed by the dynamics. Roughly speaking, the system fluctuates in a neighborhood of the metastable state until it visits the set of critical configurations and then finally reaches the equilibrium: the typical paths that the system follows with high probability form the tube of typical trajectories.

The first main challenge of the mathematical approach to metastability is of a qualitative nature, namely, to explain why in a large variety of systems the same type of metastable behaviour is observed. Many such systems are described from first principles as many-body systems subject to classical or quantum dynamics. While the corresponding equations of motion are known, they are typically very hard to analyze, in particular, over the extremely long time intervals in which metastable behaviour occurs. Also, metastability manifestly

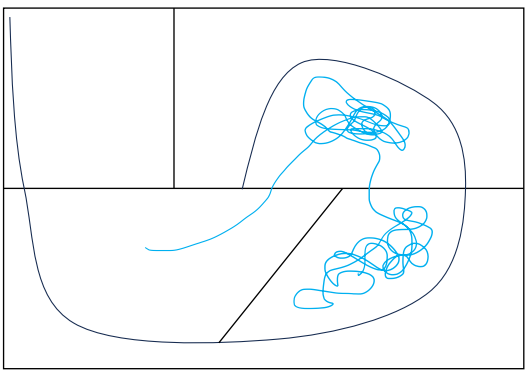

Figure 1.1 – The paradigm picture of metastability.

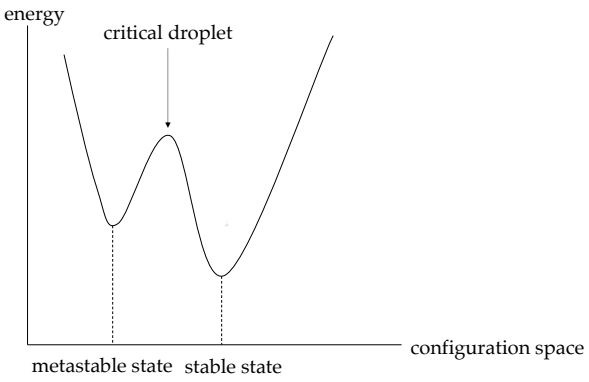

Figure 1.2 – The paradigm picture of the energy landscape.

exhibits randomness (the unpredictable time of the occurrence of the transition), the source of which may be difficult to extract from the underlying deterministic dynamics. It may be due to quantum effects, or external perturbations of a (non-closed) system. A first simplification is to pass to a description of the system as a stochastic dynamics. There is a wide variety of different models where metastability emerges and where the explanation of the underlying universality is possible.

The second main challenge is of a quantitative nature. Given the parameters of some underlying model, we would like to be able to compute as precisely as possible the quantities controlling the metastable phenomena, in particular, the distribution of the times of the transitions between metastable and stable states. Again, this is hard because most metastable systems of practical relevance are many-body systems whose dynamics is not easy to capture, neither analytically nor numerically, and because extremely long time scales may be involved. Understanding metastability on the quantitative level is of considerable practical interest, as it affects the behaviour and functioning of many systems in nature.

In this thesis, we investigate the metastable behaviour of interacting particle systems, described by the standard Ising model, evolving under the stochastic Kawasaki (Section 1.3) and Glauber dynamics (Section 1.4), with particular attention to the geometrical shape of the critical configurations, namely, those crossed by the dynamics with high probability. In particular, we focus on mathematical models describing both phase transitions in statistical physics and spreads of an opinion inside a community. While the first issue has been investigated starting from the early mathematical papers on metastability, the second one has thrived in recent decades, when the advent of the computer age has incited an increasing interest in the fundamental properties of complex networks. To this end, when interpreting the Ising model as a model for cooperative behaviour, studying it in a setting where the underlying domain is a lattice is not appropriate. Hence, in recent years there has been a large interest in studying metastability for the Ising model on random graphs, which are itself models for complex networks. See for instance [33, 34, 38, 55, 56], where this problem was addressed for static random graphs, such as the configuration model, the random regular graph and Erdös–Rényi graphs.

In this work, we start our analysis of metastability for interacting particle systems describing the evolution of individuals' opinions by considering as underlying structure a static (not random) network with a non trivial community structure. The main object of interest is how the social system governs the interactions among individuals when it is influenced by external factors, for example advertisements and political policies. However, the need to capture a *realistic description* of certain type of networks leads to consider *dynamic random graphs*, which model the *growth* of the graph in time. To this end, the last part of this thesis is devoted to the analysis of a particular type of dynamic model, known as *preferential attachment model*. Our ultimate goal is to characterize the metastable behaviour of such a model. In this work we analyze the asymptotic properties of this graph, which represents a first step in this direction.

The idea behind preferential attachment models is simple. In a graph that evolves in time, the newly added vertices are connected to the already existing ones. Think of such vertex as a

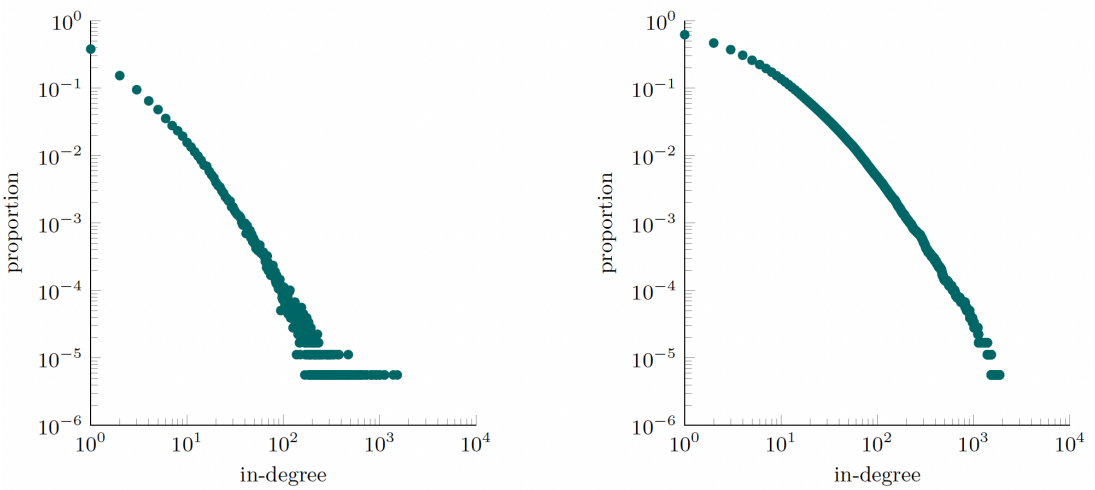

Figure 1.3 – The in–degree distribution for the citation network of papers in probability and statistics in Web of Science. On the left (resp. right) we report the log–log plot of probability mass function (resp. complementary cumulative distribution function). Figure taken from [69].

new individual in a social population, which we model as a graph by letting the individuals be the vertices and the edges be the relations between pairs of individuals. Is it then realistic that the edges connect to each already–present individual with equal probability, or is the newcomer more likely to get to know socially active individuals, who already know many people? If the latter is true, it should be more likely that the edges are connected to vertices that already have a high degree. A possible model for such a growing graph was proposed in [19], and has incited an enormous research effort since.

Such a model has been shown to lead to power–law degree sequences, i.e., the degrees of the vertices show an enormous amount of variability and the number of vertices with degree at least k decays slowly for large k, the so–called *scale–free phenomenon*. This implies that degrees are highly variable and there exist vertices with extremely high degree. Often, the tail of the empirical degree distribution seems to fall off as an inverse power of k. The existence of power–law degree sequences in various real–world networks is quite striking, and models offering a convincing explanation can teach us about the mechanisms that give rise to their scale–free nature. Let us illustrate this with the example of citation networks. In these networks, the vertices are scientific papers, and a directed edge between two papers represents a reference of the first paper to the second. Thus, the in–degree of a paper is its number of citations, while the out–degree is its number of references. In Figure 1.3 we depict the in–degree distribution, in log–log scale, of the citation network of probability and statistics papers in the period 1980 to May 2015 from Web of Science. We can see that the in–degree distribution resembles a power law. Indeed, let N_k be the number of vertices with degree k. When it approximately is proportional to an inverse power of k, i.e., $N_k \approx c_n k^{-\tau}$ for some normalizing constant c_n and some exponent τ, then

$$\log N_k \approx \log c_n - \tau \log k,$$

so that the plot of $\log k \to \log N_k$ is close to a straight line.

A possible explanation for the occurrence of power–law degree sequences is offered by the preferential attachment paradigm. In preferential attachment models, vertices are added sequentially with a number of edges connected to them. These edges are attached to a receiving vertex with a probability proportional to the degree of the receiving vertex at that time, thus favoring vertices with large degrees. For this model, it is shown in [30] that the number of vertices with degree k decays proportionally to k^{-3}, and this result is a special case of the more general result on the asymptotic degree sequence of preferential attachment models (see Section 1.5).

In the preferential attachment models, it is well known that the proportion of nodes with a given degree at step n converges to a constant as $n \to \infty$ (see Section 1.5 for more details). In this thesis we find the asymptotic distribution of the fluctuations around this limiting value.

In particular, we will prove a central limit theorem for the joint distribution of all degree counts.

1.2 MATHEMATICAL APPROACHES TO METASTABILITY

The study of metastability has a long and rich history. In this section we give a brief summary of the most important developments that shaped the work presented in this thesis focused on very low temperature systems. A mathematical description to study metastability was first attempted in [77, 100] inspired on Gibbsian equilibrium Statistical Mechanics within the context of the van der Waals–Maxwell theory. The *pathwise approach* to metastability was initiated in the late 1960's and early 1970's by Freidlin and Wentzell. They introduced the theory of *large deviations on path space* in order to analyze the long–term behaviour of dynamical systems under the influence of weak random perturbations. Their realisation that the metastable behaviour is controlled by large deviations of the random processes driving the dynamics has permeated most of the mathematical literature on the subject since. We refer to the monograph [57] for an extensive discussion. The application of these ideas in a statistical physics context was initiated in 1984 [39] and was developed in [95–97]. This series of works realised that the theory put forward by Freidlin and Wentzell can be applied to study the metastable behaviour of interacting particle systems.

The pathwise approach focuses on the *dynamics* of the transition from metastable to stable state. The advantage of this approach is that it gives a detailed description of metastable behavior of the system and it made possible to answer the three questions of metastability. By identifying the most likely path between metastable states, the time of the transition and the tube of typical trajectories can be determined. A modern version of the pathwise approach containing the information about time and critical droplets disentangled with respect to the tube of typical trajectories can be found in [44, 45, 85, 92]. This approach developed over the years has been extensively applied to study metastability in Statistical Mechanics lattice models. In this context, this approach and the one that follows [31, 85, 97] have been developed with the aim of finding answers valid with maximal generality and to reduce as much as possible the number of model dependent inputs necessary to describe the metastable behavior of any given system. The pathwise approach was applied in finite volume at low temperature for single-spin-flip Glauber dynamics, see e.g. [4, 10, 14, 24, 39, 40, 42, 49, 79, 80, 89, 93], for Kawasaki dynamics, see e.g. [13, 16–18, 67, 71, 72, 74, 75, 90], and for parallel dynamics, see e.g. [43, 46–48]. The drawback of the pathwise approach is that it is generally hard to identify and control the rate function, especially for systems with a spatial interaction, for which the dynamics is non–local. Consequently, this approach typically leads to relatively crude results on the crossover time.

This limitation can be overcome via the use of another approach, the so–called *potential-theoretic approach*, initiated in [31] and summerized in the monograph [32]. In this approach, the metastability phenomenon is interpreted as a sequence of visits of the path to different metastable sets. This method focuses on a precise analysis of hitting times of these sets with the help of *potential theory*. In the potential-theoretic approach the mean transition time is given in terms of the so-called *capacities* between two sets. Crucially capacities can be estimated by exploiting powerful variational principles. This means that the estimates of the average crossover time that can be derived are much sharper than those obtained via the pathwise approach. The potential theoretic approach was applied to models at finite volume and at low temperature, see e.g. [35, 37, 70, 73, 91].

These mathematical approaches, however, are not completely equivalent as they rely on different definitions of metastable states (see [44, Section 3] for a comparison) and thus involve different properties of hitting and transition times. The situation is particularly delicate for evolutions of infinite-volume systems, irreversible systems and degenerate systems, as discussed in [27, 44, 45, 48]. New difficulties appear when entropy has a larger role to play in the model. The more involved infinite volume limit at low temperature, higher temperature or vanishing magnetic field was studied for instance in [11, 36, 41, 52, 53, 62, 63, 66, 75, 86, 87, 105, 106] for Ising-like models under single-spin-flip Glauber and Kawasaki dynamics. More recent approaches are developed in [6, 20, 21, 28, 29, 82].

1.3 METASTABILITY FOR CONSERVATIVE SYSTEMS

Let us take the example of a supersaturated vapor. Consider a vapor below its critical temperature, near its condensation point. Compress, isothermically, a certain amount of vapor, free of impurities, up to the saturated vapor pressure (at the corresponding temperature). Then continue to slowly increase the pressure, trying to avoid significant density gradients inside the sample. With such careful experimentation we can prepare what is called a supersaturated vapor: indeed, we observe that the system is still in a pure gaseous phase. It persists in this situation of apparent equilibrium for a very long time; this is called a "metastable state", as opposed to a stable state, which, for the given values of the thermodynamic parameters, would correspond to coexistence of liquid and vapor. The stationary situation with a pure phase that we have described above persists until an external perturbation or a spontaneous fluctuation induces the nucleation of the liquid phase, starting an irreversible process that leads to a final stable state where liquid and vapor are segregated, and coexist at the saturated vapor pressure. The lifetime of the metastable state decreases as the degree of supersaturation increases, up to a threshold value for the pressure (the spinodal point) where the gas becomes unstable. The above-described behavior is typical of an evolution that is conservative in the sense that it preserves the number of molecules. To model mathematically phenomena such as the one described above and superheated or supercooled water, it is often proposed to use lattice gas models evolving according to Kawasaki dynamics since the dynamics conserves the number of particles. We emphasize that conservative dynamics are challenging to analyze because the particles conservation implies that droplets must exchange particles with the gas surrounding them many times over long time intervals. Thus, the dynamics is *non-local* in its very essence.

1.3.1 *Kawasaki dynamics*

We consider a two–dimensional lattice gas at very low temperature and density that evolves according to Kawasaki dynamics, i.e., particles are subject to exclusion and interaction in a domain inside $\mathbb{Z}^2$. More precisely, let β be the inverse temperature of the gas. We fix the density of the gas equal to $\rho = e^{-\Delta\beta}$, with $\Delta > 0$ an *activity parameter*. In order to have particles at all, we see that the domain we consider cannot be finite, but its size has to be at least exponentially large in β. Thus, we consider that our system evolves in a square box $\Lambda_\beta \subset \mathbb{Z}^2$, centered at the origin and with periodic boundary conditions, such that $|\Lambda_\beta| = e^{\Theta\beta}$, with $\Theta > \Delta$. We will see in Section 1.3.4 that the parameter Θ plays a crucial role in the analysis.

With each site $x \in \Lambda_\beta$ we associate an occupation variable $\eta(x)$, assuming the values 0 or 1, where $\eta(x) = 0$ (resp. $\eta(x) = 1$) means that the site x is empty (resp. occupied). A lattice gas configuration is denoted by $\eta \in \mathcal{X}_\beta := \{0,1\}^{\Lambda_\beta}$. With each configuration η we associate an energy, the so–called *Hamiltonian* of the system, given by

$$H(\eta) = -U \sum_{\{x,y\}\in\Lambda_\beta^*} \eta(x)\eta(y), \tag{1.3.1}$$

where Λ_β^* denotes the set of bonds between nearest-neighbour sites in Λ_β, i.e., there is a *binding energy* $-U < 0$ between neighbouring particles. Let

$$|\eta| = \sum_{x\in\Lambda_\beta} \eta(x) \tag{1.3.2}$$

be the number of particles in Λ_β in the configuration η, and let

$$\mathcal{V}_N = \{\eta \in \mathcal{X}_\beta : \ |\eta| = N\} \tag{1.3.3}$$

be the set of configurations with N particles. We define Kawasaki dynamics as the continuous-time Markov chain $X = (X(t))_{t\geqslant 0}$ with state space $\mathcal{V}_N$ given by the generator

$$(\mathcal{L}f)(\eta) = \sum_{\{x,y\}\in\Lambda_\beta^*} c(x,y,\eta)[f(\eta^{x,y}) - f(\eta)], \qquad \eta \in \mathcal{X}_\beta, \tag{1.3.4}$$

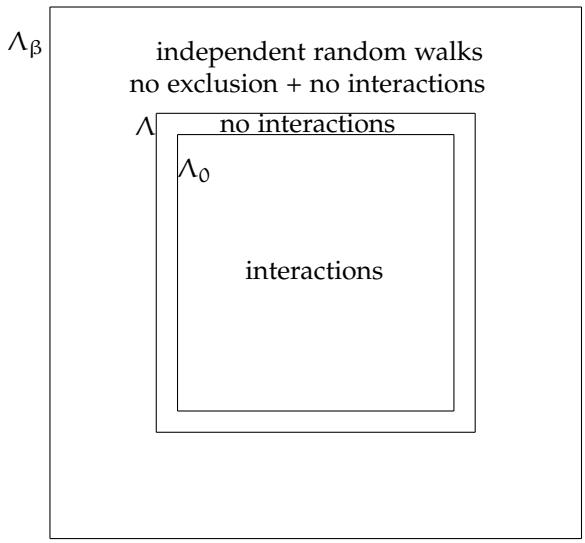

Figure 1.4 – Schematic representation of the domain Λ_β in the simplified model.

where

$$\eta^{x,y}(z) = \begin{cases} \eta(z) & \text{if} \quad z \neq x, y, \\ \eta(x) & \text{if} \quad z = y, \\ \eta(y) & \text{if} \quad z = x, \end{cases} \tag{1.3.5}$$

and

$$c(x, y, \eta) = e^{-\beta[H(\eta^{x,y}) - H(\eta)]_+}. \tag{1.3.6}$$

Equations (1.3.4)–(1.3.6) represent the standard *Metropolis dynamics* associated with H, and is *conservative* because it preserves the number of particles, i.e., $|X(t)| = |X(0)| = N$ for all $t > 0$. The *canonical Gibbs measure* ν_N defined as

$$\nu_N(\eta) = \frac{e^{-\beta H(\eta)} \mathbb{1}_{\mathcal{V}_N}(\eta)}{Z_N}, \qquad Z_N = \sum_{\eta \in \mathcal{V}_N} e^{-\beta H(\eta)}, \qquad \eta \in \mathcal{X}_\beta, \tag{1.3.7}$$

is the reversible equilibrium of this stochastic dynamics for any N:

$$\nu_N(\eta) c(x, y, \eta) = \nu_N(\eta^{x,y}) c(x, y, \eta^{x,y}). \tag{1.3.8}$$

Varying the parameters U and Δ leads to a dramatic change in the behaviour of the gas. Indeed, the choice $\Delta \in (0, U)$ represents the unstable gas, $\Delta = U$ represents the spinoidal point, $\Delta \in (U, 2U)$ corresponds to the *metastable regime*, $\Delta = 2U$ is the condensation point and $\Delta > 2U$ corresponds to a stable gas. We refer to [67, 75] for an extensive discussion on these points, while in Section 1.3.2 we justify the aforementioned metastable regime.

To rigorously analyze this fully conservative model, the idea is to focus the attention on what happens in the *simplified model* introduced in [75]. This model can be obtained from the Kawasaki dynamics defined above after considering exclusion only inside a finite β-independent square box $\Lambda \subset \Lambda_\beta$ and interactions only in

$$\Lambda_0 := \Lambda \setminus \partial^- \Lambda, \tag{1.3.9}$$

where

$$\partial^- \Lambda := \{x \in \Lambda : \exists y \notin \Lambda \text{ such that } |y - x| = 1\} \tag{1.3.10}$$

is the internal boundary of Λ, so that the dynamics of the gas outside Λ is that of independent random walks (see Figure 1.4). The introduction of this model is justified by the fact that, for the original Kawasaki dynamics, the interaction between clusters and the "isolated" particles

of the gas can be approximated by the interaction between clusters and a gas of independent random walks. As widely explained in [75], the nucleation for the simplified model can be tackled via the analysis of the local version of the model, the so–called *local model*. Roughly speaking, in this model particles live and evolve only inside the finite window Λ, where the effect on Λ of the gas in $\Lambda_\beta \setminus \Lambda$ may be described in terms of the creation of new particles at rate ρ at sites on the internal boundary of Λ and the annihilation of particles with rate 1 at sites on the external boundary of Λ. We refer to Section 1.3.2 for the precise definition of the local model. To summarize, the steps to address the issue of the exit from metastability for the fully conservative Kawasaki dynamics are the following:

STEP 1: Analyze the nucleation time and the tube of typical trajectories for the local model. These issues have been addressed in [67, 75].

STEP 2: Extend these results to the simplified model. This issue has been addressed in [75].

STEP 3: Prove that the simplified model is a good approximation for the interactions between clusters and gas in a finite window for the original Kawasaki dynamics. This issue has been addressed in [65].

STEP 4: Get the estimate for the nucleation time and the tube of typical trajectories for the original Kawasaki dynamics. This issue is investigated in this thesis (see Section 1.3.4).

As it will be clear throughout the thesis, step 4 is highly non trivial and requires a careful investigation. We refer to Section 1.3.4 for the main ideas to tackle this problem. Note that step 3 gives us the correct way to control the behaviour of the gas in $\Lambda_\beta \setminus \Lambda$. It is clear that the starting point is the analysis of the local model, which is introduced and studied in Section 1.3.2.

1.3.2 *The local model on the square lattice*

In this section, we introduce the local model and we present the main results already present in the literature together with those that are derived in this thesis. Consider a finite box $\Lambda = \{0, ..., L\}^2 \subset \mathbb{Z}^2$ centered at the origin. The side length L is fixed, but arbitrary, and later we will require L to be sufficiently large. Our configuration space is $\mathcal{X} := \{0,1\}^\Lambda$. To be as general as possible, with each configuration $\eta \in \mathcal{X}$ we define the *local Hamiltonian energy* $\widehat{H}(\eta)$ as

$$\widehat{H}(\eta) := -U_1 \sum_{(x,y)\in\Lambda^*_{0,h}} \eta(x)\eta(y) - U_2 \sum_{(x,y)\in\Lambda^*_{0,v}} \eta(x)\eta(y) + \Delta \sum_{x\in\Lambda} \eta(x), \tag{1.3.11}$$

where $\Lambda^*_{0,h}$ (resp. $\Lambda^*_{0,v}$) is the set of the horizontal (resp. vertical) unoriented bonds joining nearest-neighbors points in Λ_0 (recall (1.3.9)). Thus, the interaction is acting only inside $\Lambda \setminus \partial^-\Lambda$; the binding energy associated to a horizontal (resp. vertical) bond is $-U_1 < 0$ (resp. $-U_2 < 0$). Note that $\widehat{H}(\eta)$ is obtained after augmenting the energy in (1.3.1) by adding a term $\Delta|\eta|$ and by distinguishing between horizontal and vertical bonds. This models the presence of an external reservoir that keeps the density of particles in Λ_β fixed at $\rho = e^{-\beta\Delta}$. We may assume without loss of generality that $U_1 \geqslant U_2$. The dynamical behaviour of the local model changes drastically based on the relation between the parameters U_1 and U_2. In particular, we identify three interesting regimes: *isotropic* ($U_1 = U_2 = U$), *weakly anisotropic* ($U_1 < 2U_2$) and *strongly anisotropic* ($U_1 > 2U_2$). Although our analysis for the original model is concerned only with the isotropic case (as it is clear by the Hamiltonian defined in (1.3.1)), we define the local model in this general setup because we are interested in its analysis for all these three regimes. The *locally conservative Kawasaki dynamics* can be defined as the standard dynamics with different behaviours at the boundary of Λ. To be precise, let $b = (x \to y)$ be an oriented bond, i.e., an *ordered* pair of nearest neighbour sites, and define

$$\begin{aligned} \partial^*\Lambda^{out} &:= \{b = (x \to y) : x \in \partial^-\Lambda, y \notin \Lambda\}, \\ \partial^*\Lambda^{in} &:= \{b = (x \to y) : x \notin \Lambda, y \in \partial^-\Lambda\}, \\ \Lambda^{*,orie} &:= \{b = (x \to y) : x, y \in \Lambda\}, \end{aligned} \tag{1.3.12}$$

and put $\bar{\Lambda}^{*,\mathrm{orie}} := \partial^*\Lambda^{\mathrm{out}} \cup \partial^*\Lambda^{\mathrm{in}} \cup \Lambda^{*,\,\mathrm{orie}}$. Two configurations $\eta, \eta' \in \mathcal{X}$ with $\eta \neq \eta'$ are said to be *communicating states* if there exists a bond $b \in \bar{\Lambda}^{*,\mathrm{orie}}$ such that $\eta' = T_b\eta$, where $T_b\eta$ is the configuration obtained from η in any of these ways:

— for $b = (x \to y) \in \Lambda^{*,\,\mathrm{orie}}$, $T_b\eta$ denotes the configuration obtained from η by interchanging particles along b:

$$T_b\eta(z) := \begin{cases} \eta(z) & \text{if } z \neq x, y, \\ \eta(x) & \text{if } z = y, \\ \eta(y) & \text{if } z = x. \end{cases} \tag{1.3.13}$$

— For $b = (x \to y) \in \partial^*\Lambda^{\mathrm{out}}$ we set:

$$T_b\eta(z) := \begin{cases} \eta(z) & \text{if } z \neq x, \\ 0 & \text{if } z = x. \end{cases} \tag{1.3.14}$$

This describes the annihilation of a particle along the border.

— for $b = (x \to y) \in \partial^*\Lambda^{\mathrm{in}}$ we set:

$$T_b\eta(z) := \begin{cases} \eta(z) & \text{if } z \neq y, \\ 1 & \text{if } z = y. \end{cases} \tag{1.3.15}$$

This describes the creation of a particle along the border.

Since in finite volume is equivalent and more convenient dealing with a discrete time stochastic process, we define Kawasaki dynamics as the discrete time Markov chain $(\eta_t)_{t\in\mathbb{N}}$ on the state space $\mathcal{X}$ given by the following transition probabilities: for $\eta \neq \eta'$:

$$P(\eta, \eta') := \begin{cases} |\bar{\Lambda}^{*,\,\mathrm{orie}}|^{-1} e^{-\beta[H(\eta')-H(\eta)]_+} & \text{if } \exists b \in \bar{\Lambda}^{*,\mathrm{orie}} : \eta' = T_b\eta, \\ 0 & \text{otherwise,} \end{cases} \tag{1.3.16}$$

where $[a]_+ = \max\{a, 0\}$ and $P(\eta, \eta) := 1 - \sum_{\eta' \neq \eta} P(\eta, \eta')$. This describes a standard Metropolis dynamics with open boundary conditions: along each bond touching $\partial^-\Lambda$ from the outside, particles are created with rate $\rho = e^{-\Delta\beta}$ and are annihilated with rate 1, while inside Λ_0 particles are conserved. Note that an exchange of occupation numbers $\eta(x)$ for any x inside the ring $\Lambda \setminus \Lambda_0$ does not involve any change in energy.

Remark 1.3.1. *The stochastic dynamics defined by (1.3.16) is reversible with respect to the Grand–canonical Gibbs measure*

$$\mu(\eta) := \frac{e^{-\beta\widehat{H}(\eta)}}{Z}, \qquad Z := \sum_{\eta\in\mathcal{X}} e^{-\beta\widehat{H}(\eta)}, \qquad \eta \in \mathcal{X}. \tag{1.3.17}$$

In the remainder of this section we will present the main results concerning metastability and nucleation for the local model in all the three regimes. First, note that the metastable regime corresponds to taking

$$\Delta \in (U_1, U_1 + U_2). \tag{1.3.18}$$

Indeed, a special feature of Kawasaki dynamics is that in the metastable regime (1.3.18) particles move along the border of a droplet more rapidly than they arrive from the boundary of the box. More precisely, the condition $\Delta > U_1$ implies that the arrival of new particles is slower than the dissociation of protruding particles (see Figure 1.5 on the left), whereas the condition $\Delta < U_1 + U_2$ implies that the arrival of new particles is faster than the dissociation of non–protruding particles (see Figure 1.5 on the right). Note that in the case of isotropic interactions the condition in (1.3.18) reads as $U < \Delta < 2U$. For all these three regimes we have that the empty box

$$\square := \{\eta \in \mathcal{X} : \eta(x) = 0 \ \forall\, x \in \Lambda\} \tag{1.3.19}$$

is the unique metastable state and the full box

$$\blacksquare := \{\eta \in \mathcal{X} : \eta(x) = 1 \ \forall\, x \in \Lambda_0, \eta(x) = 0 \ \forall\, x \in \Lambda \setminus \Lambda_0\} \tag{1.3.20}$$

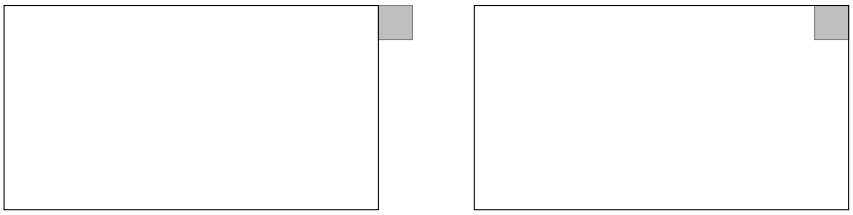

Figure 1.5 – In both clusters we represent in grey the particle we want to detach: the one on the left (resp. right) is protruding (resp. non–protruding) and detaching it has a probability of order $e^{-U_1\beta}$ (resp. $e^{-(U_1+U_2)\beta}$).

is the unique stable state, provided that L is sufficiently large. This assumption is needed to have $\widehat{H}(\blacksquare) < \widehat{H}(\square) = 0$ and later we will provide an explicit lower bound for L. Thus, the exit from metastability consists in analyzing the transition from $\square$ to $\blacksquare$. The main objects of the analysis are the estimate of this transition time and the geometrical description of the *critical droplets* the system has to cross to perform the nucleation, the so–called *gate* for the transition. In addition, a crucial role both from a probabilistic and physical point of view is the description of the union of all the *minimal gates*, where a minimal gate is a gate that is minimal by inclusion. These have the physical meaning of "minimal sets of critical configurations" and are a crucial step in the description of the typical trajectories.

To make the previous assumption on L precise, we introduce the so–called *critical lengths*. In particular, in the isotropic regime $U_1 = U_2 = U$ we define the critical length as

$$\ell_c := \left\lceil \frac{U}{2U-\Delta} \right\rceil, \tag{1.3.21}$$

while in the anisotropic regimes ($U_1 \neq U_2$) we define the horizontal and vertical critical lengths as

$$\ell_1^* := \left\lceil \frac{U_1}{U_1+U_2-\Delta} \right\rceil, \qquad \ell_2^* := \left\lceil \frac{U_2}{U_1+U_2-\Delta} \right\rceil, \tag{1.3.22}$$

respectively. Thus, we require that

$$L > \begin{cases} 2\ell_c & \text{for the isotropic regime,} \\ 2\ell_1^* & \text{for the anisotropic regimes.} \end{cases} \tag{1.3.23}$$

In addition, we need some non–degeneracy assumptions. In particular, for the isotropic model we assume that

$$\frac{U}{2U-\Delta} \notin \mathbb{N}, \tag{1.3.24}$$

while for the anisotropic models we assume that

$$\frac{U_1}{U_1+U_2-\Delta} \notin \mathbb{N}, \qquad \frac{U_2}{U_1+U_2-\Delta} \notin \mathbb{N}. \tag{1.3.25}$$

To avoid pathological trivial cases, we further assume that

$$\Delta \in \begin{cases} \left(\frac{3}{2}U, 2U\right) & \text{for the isotropic regime,} \\ \left(U_1 + \frac{U_2}{2}, U_1+U_2\right) & \text{for the anisotropic regimes.} \end{cases} \tag{1.3.26}$$

Note that condition (1.3.26) ensures that all the critical lengths are larger than two. In the remainder of this section assume that conditions (1.3.23)-(1.3.26) are in force. By [16, 75, 90] it is well known which is the shape of the canonical critical droplets for the three regimes. In particular, they consist in a rectangular shape, with the addition of a protuberance (i.e., one particle attached to a side of the rectangular cluster) and a free particle anywhere in Λ (i.e., a particle that does not interact with the others). See Figure 1.6 on the left and Figure 1.7. More

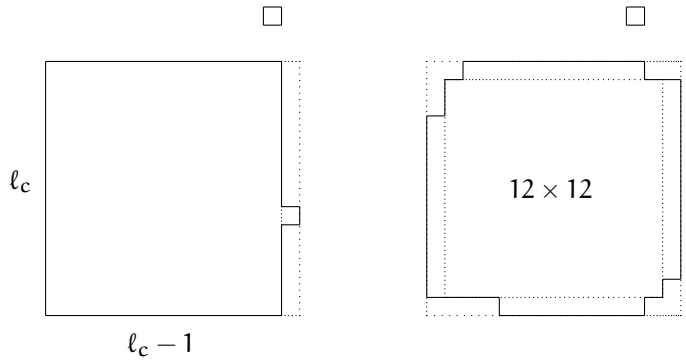

Figure 1.6 – Critical configurations in the isotropic regime for $\ell_c = 14$.

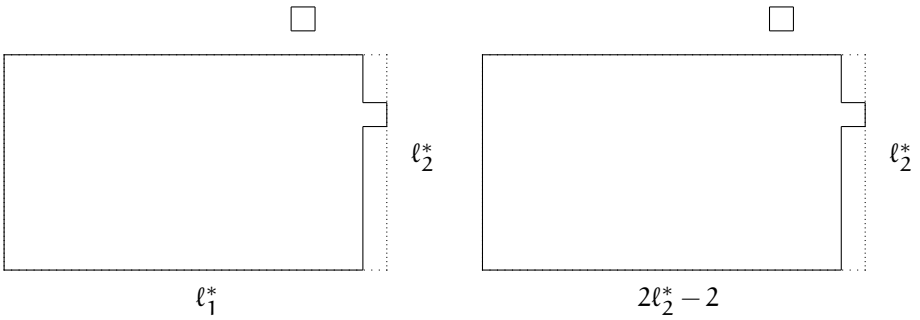

Figure 1.7 – Canonical critical configurations in the weakly anisotropic regime (on the left) and in the strongly anisotropic regime (on the right).

precisely, they constitute a *gate* for the transition, namely, a set of configurations that will be crossed with probability tending to 1 in the limit as β goes to infinity. To define it rigorously, a central role is played by the set of *optimal paths*, which are those paths (i.e., sequence of communicating configurations) realizing the minimum value among all the paths going from $\square$ to $\blacksquare$ of the maximal energy reached in a single path. Formally, we set

$$(\square \to \blacksquare)_{opt} := \{\omega : \square \to \blacksquare : \max_{\xi \in \omega} \widehat{H}(\xi) = \Phi(\square, \blacksquare)\}, \tag{1.3.27}$$

where $\omega : \square \to \blacksquare$ is a general path connecting $\square$ to $\blacksquare$ and

$$\Phi(\square, \blacksquare) := \min_{\omega : \square \to \blacksquare} \max_{\xi \in \omega} \widehat{H}(\xi) \tag{1.3.28}$$

is the *communication height* between $\square$ and $\blacksquare$. Thus, we define a gate $\mathcal{C}^*(\square, \blacksquare)$ for the transition from $\square$ to $\blacksquare$ as a subset of the set of *minimal saddles* $\mathcal{S}(\square, \blacksquare)$, such that any path $\omega \in (\square \to \blacksquare)_{opt}$ crosses the set $\mathcal{C}^*(\square, \blacksquare)$, where

$$\mathcal{S}(\square, \blacksquare) := \{\zeta \in \mathcal{X} : \exists \omega \in (\square \to \blacksquare)_{opt}, \omega \ni \zeta \text{ such that } \widehat{H}(\zeta) = \Phi(\square, \blacksquare)\}. \tag{1.3.29}$$

A first important difference that comes out in the different regimes is that in the strongly anisotropic one the shape of the critical droplets is not *Wulff*, where the Wulff shape is that minimizing the energy of a droplet at fixed volume. Indeed, the Wulff shape corresponds to rectangular droplets of horizontal and vertical dimensions ℓ_1 and ℓ_2, respectively, such that $\ell_1 - \ell_2$ is of order

$$\bar{\ell} := \left\lceil \frac{U_1 - U_2}{U_1 + U_2 - \Delta} \right\rceil, \tag{1.3.30}$$

which are called *standard rectangles*. Note that in the isotropic regime this means that the square clusters are Wulff–shaped. By the shape of the canonical critical droplets it easy to check that in the isotropic models the Wulff shape concides with the critical shape, so that it is not possible to distinguish among them. A rigorous analysis of the non equivalence between critical configurations and Wulff shape motivates the study of anisotropic models

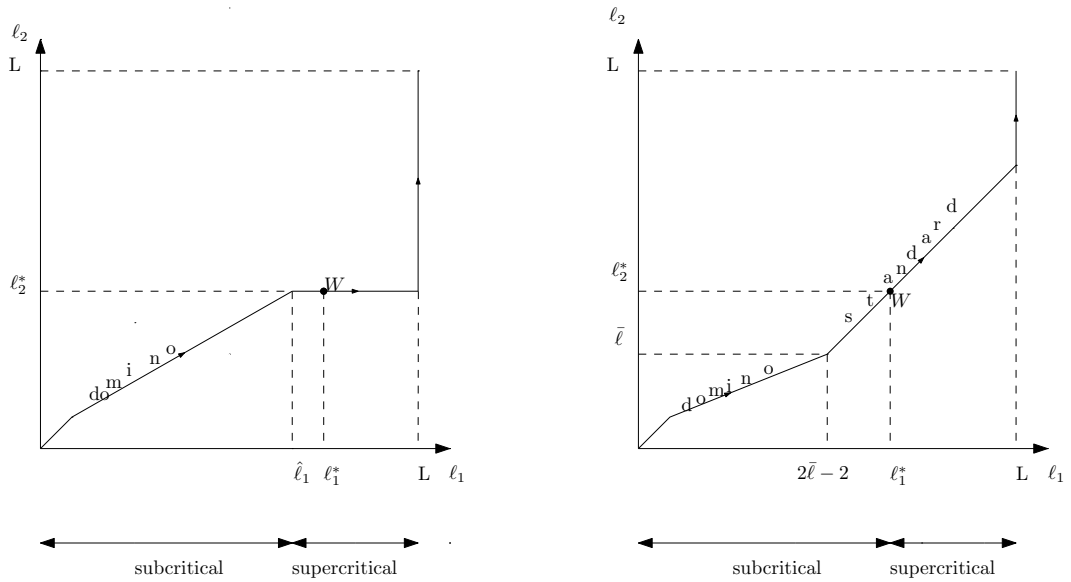

Figure 1.8 – Typical path for strong anisotropy (on the left) and weak anisotropy (on the right), in which we highlight with W the critical Wulff–shaped configuration.

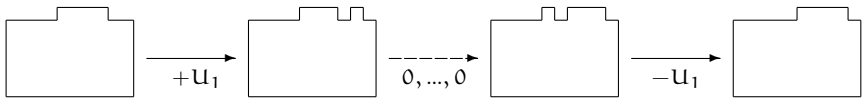

Figure 1.9 – 1-translation of the horizontal north bar at cost U_1.

and is a first step in showing the robustness of the argument rooted in the dynamical nature of metastable systems. On the one hand, also in the weakly anisotropic model the critical droplet has a Wulff shape, but the evolution of the system does not follow Wulff-shaped configurations. Indeed, it follows the so–called *domino rectangles*, which are rectangles for which the horizontal dimension is "almost" twice as long as the vertical one (see Figure 1.8 on the left). On the other hand, in the strongly anisotropic regime the Wulff shape is not a critical configuration. Indeed, the rectangular custer is not standard, but is a *domino rectangle*, and the dynamics crosses the critical Wulff-shape only in its supercritical part (see Figure 1.8 on the right). In conclusion, in both anisotropic regimes the Wulff shape is not relevant in the nucleation pattern as for the anisotropic Glauber dynamics, see [79]. The locally conservative dynamics and the movement of particles along the border of the droplet give a regularization effect. Surprisingly, as mentioned above, this effect does not drive the nucleation process along Wulff-shaped configurations, especially in the assumption of strong anisotropy. We refer to [16, 90] for an extensive discussion.

We denote by $\mathcal{C}^* = \mathcal{C}^*(\square, \blacksquare)$ the set of critical configurations and define $\Gamma^* := \Phi(\square, \blacksquare)$. In [16, 75, 90] the authors proved that Γ^* coincide with the energy of the configurations belonging to $\mathcal{C}^*$ and that $\mathcal{C}^*$ is a gate for the transition. In addition, they proved that with probability tending to 1 in the limit as β goes to infinity, the system creates the critical droplet and reaches the stable state $\blacksquare$ in a time of order $e^{\Gamma^*\beta}$ when it starts from the metastable state $\square$. In particular, there exists an explicit formula for the energy barrier Γ^* which depends on the parameters U_1, U_2 and Δ of the Hamiltonian energy and we refer to those papers for further details.

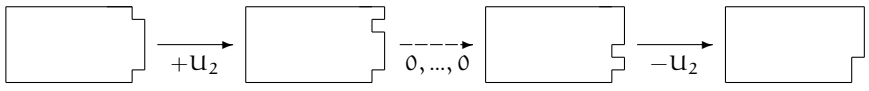

Figure 1.10 – 1-translation of the vertical east bar at cost U_2.

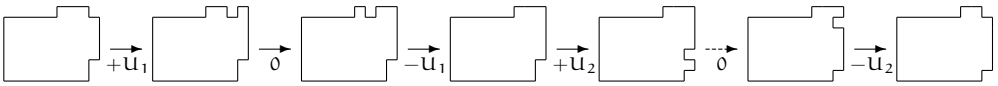

Figure 1.11 – Sliding of a unit square around the "north-east corner" at cost U_1.

GEOMETRICAL DESCRIPTION OF THE GATE

A relevant issue for the dynamical characterization of the system is the description of *all* the "relevant" critical configurations. This description turns out to be very rich when we deal with the conservative Kawasaki dynamics. Indeed, a crucial feature of this dynamics is that particles can move along the border of the droplet as a part of regularizing motions. There are two types of relevant motions: the *translation of a bar* and the *sliding of a bar*. Intuitively, a bar can be thought as a set of connected particles that are attached to a cluster and the translation of a bar consists in the iteration of the 1–translation depicted in Figures 1.9-1.10. The sliding of a bar consists instead in moving a bar attached to a cluster around a corner of the cluster and can be defined as the iteration of the motion depicted in Figure 1.11. We will introduce later in Section 3.2.1 point 5 the precise definition of bars and of these motions. The aforementioned motions are crucial for the full geometrical description of the gate. To this end, we need some geometrical definitions. First, we define the set $\bar{\mathcal{Q}}$ (resp. $\widetilde{\mathcal{Q}}$) as the set of configurations having only one cluster anywhere in Λ_0 consisting of a $\ell_1 \times \ell_2$ rectangle with a single protuberance attached to one of the shortest (resp. longest) sides, where

$$(\ell_1, \ell_2) = \begin{cases} (\ell_c - 1, \ell_c) & \text{for the isotropic regime,} \\ (\ell_1^* - 1, \ell_2^*) & \text{for the weakly anisotropic regime,} \\ (2\ell_2^* - 3, \ell_2^*) & \text{for the strongly anisotropic regime.} \end{cases}$$

By denoting with n_c the number of particles of the clusters in $\mathcal{Q} = \bar{\mathcal{Q}} \cup \widetilde{\mathcal{Q}}$, we define

$$\begin{aligned} \bar{\mathcal{D}} &:= \{\eta' \in \mathcal{V}_{n_c} | \, \exists\, \eta \in \bar{\mathcal{Q}} : \widehat{H}(\eta) = \widehat{H}(\eta') \text{ and } \Phi_{|\mathcal{V}_{n_c}}(\eta, \eta') \leqslant \widehat{H}(\eta) + U_1\}, \\ \widetilde{\mathcal{D}} &:= \{\eta' \in \mathcal{V}_{n_c} | \, \exists\, \eta \in \widetilde{\mathcal{Q}} : \widehat{H}(\eta) = \widehat{H}(\eta') \text{ and } \Phi_{|\mathcal{V}_{n_c}}(\eta, \eta') \leqslant \widehat{H}(\eta) + U_1\}, \end{aligned} \tag{1.3.31}$$

where we recall that $\mathcal{V}_{n_c}$ is the set of configurations with n_c particles and $\Phi_{|\mathcal{V}_{n_c}}(\eta, \eta')$ means that we are computing the communication height between η and η' by looking only at paths crossing configurations inside the set $\mathcal{V}_{n_c}$. Note that $\bar{\mathcal{Q}} \subset \bar{\mathcal{D}}$ (resp. $\widetilde{\mathcal{Q}} \subset \widetilde{\mathcal{D}}$). To keep the notation concise we have adopted the same notation for all the three scenarios, but one may replace U_1 with U in the isotropic case. Note that the last condition in (1.3.31) is the same as requiring that

$$\Phi_{|\mathcal{V}_{n_c}}(\eta, \eta') < \Gamma^* + \widehat{H}(\square) = \Gamma^*,$$

which comes from the fact that to describe gates we are interested only in the optimal paths, so that the energy along them cannot exceed the value Γ^*. Roughly speaking, in the isotropic and weakly anisotropic cases one can think of $\bar{\mathcal{D}}$ and $\widetilde{\mathcal{D}}$ as the sets of configurations consisting of a rectangular cluster with four bars attached to its four sides such that the sum of the lengths of the bars is fixed. Concerning the strongly anisotropic model, this characterization comes out only for the set $\bar{\mathcal{D}}$, while the configurations in $\widetilde{\mathcal{D}}$ have a cluster with a different shape. The reason why this difference arises is that in the strongly anisotropic regime there is a larger rigidity of the dynamics, so that the motion of particles along the border of a cluster is more unlikely. We will elaborate more on this later and we will see the strong impact that this effect has on some other dynamical features. Concerning the isotropic regime, the full geometrical characterization has been achieved in [35, Theorem 1.4.1], while it constitutes a novelty of this thesis for what concerns the anisotropic regimes.

First, let us focus on the isotropic regime. In [35] the authors proved that the gate for the transition $\mathcal{C}^*$ can be expressed as $\mathcal{C}^* = \mathcal{D}^{fp}$, where

$$\mathcal{D} := \bar{\mathcal{D}} \cup \widetilde{\mathcal{D}} \tag{1.3.32}$$

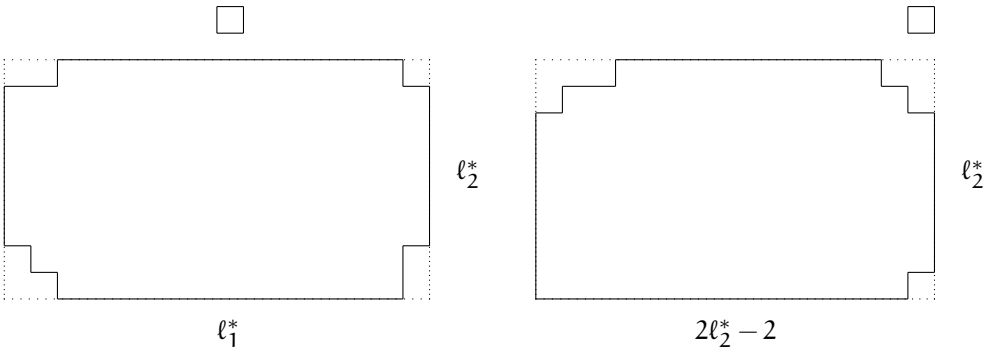

Figure 1.12 – Critical configurations in $\mathcal{C}^*$ in the weakly (resp. strongly) anisotropic regime on the left (resp. right). Moreover, if we remove the free particle we obtain a configuration in $\bar{\mathcal{D}} \setminus \bar{\mathcal{Q}}$.

and the upper index "fp" indicates the addition of a free particle anywhere inside the box Λ (see Figure 1.6 on the right). Let us see the key ingredients to prove the aforementioned geometrical characterization of the gate. Clearly, we have that

$$\widehat{H}(\mathcal{C}^*) = \widehat{H}(\mathcal{D}^{fp}) = \widehat{H}(\mathcal{D}) + \Delta = \widehat{H}(\mathcal{Q}) + \Delta = \Gamma^*$$

and therefore

$$\widehat{H}(\mathcal{D}) = \widehat{H}(\mathcal{Q}) = \Gamma^* - \Delta.$$

The key ingredients to get the claim are the following (recall (1.3.28)):

(i) Prove that $\Phi(\square, \blacksquare) \leqslant \Gamma^*$.

(ii) Prove that $\Phi(\square, \blacksquare) \geqslant \Gamma^*$.

(iii) Get the geometrical characterization of the set $\mathcal{D}$.

For point (i), it suffices to construct a path connecting $\square$ to $\blacksquare$ which does not exceed the energy value Γ^*. For this we refer to [35, Section 2.3.1].

Concerning point (ii), the proof comes into three steps. The first one is that any optimal path $\omega \in (\square \to \blacksquare)_{opt}$ (recall (1.3.27)) must pass through a configuration consisting of a single $(\ell_c - 1) \times \ell_c$ rectangular cluster somewhere in Λ_0. This step is achieved by using a standard isoperimetric inequality–type argument [1], which ensures that the configurations consisting of $\ell_c(\ell_c - 1)$ particles with minimal energy are those in which the particles form a single $(\ell_c - 1) \times \ell_c$ rectangular cluster. Let us denote by η such a unique configuration modulo translations and rotations. Note that

$$\widehat{H}(\eta) = \Gamma^* - 2\Delta + U.$$

The second step consists in proving that all the optimal paths must cross the set $\mathcal{Q}$. Starting from η, to reach $\blacksquare$ a new particle has to enter inside Λ_0: this brings us to the energy $\Gamma^* - \Delta + U$. Before any new particle is created, the energy must lower by at least U: the unique way to do this is to move the free particle until it attaches to the cluster, giving rise to a configuration in $\mathcal{Q}$. The final steps is to show that to reach $\blacksquare$ from $\mathcal{Q}$ the energy has to reach the value Γ^*. By [1] we deduce that the unique allowed move is to add a free particle, giving rise to a configuration with energy Γ^*.

Point (iii) provides the full description of the gate. Indeed, once the system is in $\mathcal{Q}$, before the arrival of the next particle, it can reach *all* configurations that have the same energy, the same number of particles and can be reached at cost less or equal to U, which are precisely those belonging to $\mathcal{D}$. To get this, one has to study all the possible motions of particles that can take place on the boundary of the droplet as represented in Figures 1.9-1.11.

Along the way we have also characterized the entrance in the set of critical configurations. Indeed, from the steps above, it follows that any $\omega \in (\square \to \blacksquare)_{opt}$ passes first through $\mathcal{Q}$, then possibly through $\mathcal{D} \setminus \mathcal{Q}$, and finally through $\mathcal{C}^*$. This refined analysis of the dynamics is crucial when one tries to find sharper estimates regarding the mean transition time. We will see in the next paragraph how to achieve this issue.

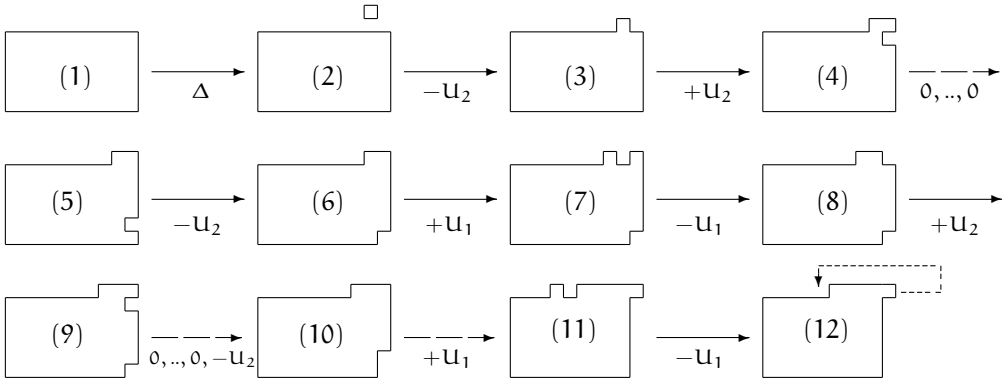

Figure 1.13 – Second mechanism to enter the gate in the strongly anisotropic regime: configuration (1) consists in a $(2\ell_2^* - 1) \times (\ell_1^* - 1)$ rectangular cluster and has energy equal to $\Gamma^* - \Delta + U_2 - U_1$, thus configurations (7) and (11) have energy equal to Γ^*. In (12) we indicate with a dashed arrow the detachment of the protuberance at cost U_1 and afterwards the movement of the free particle until it connects to the cluster that decreases the energy by $U_1 + U_2$. When the free particle is detached the dynamics reaches the set $\mathcal{C}^*$.

Let us now consider the weakly anisotropic regime. First, note that in this case

$$\widehat{H}(\bar{\mathcal{D}}) = \Gamma^* - \Delta < \Gamma^* - \Delta + U_1 - U_2 = \widehat{H}(\widetilde{\mathcal{D}}). \tag{1.3.33}$$

The main difference that arises with respect to the isotropic regime is that in the weakly anisotropic regime the gate $\mathcal{C}^*$ can be expressed as $\mathcal{C}^* = \bar{\mathcal{D}}^{fp}$, see Figure 1.12 on the left (compare with (1.3.32)). The reason why only the set $\bar{\mathcal{D}}$ is relevant for the set $\mathcal{C}^*$ is the following. Starting from the set $\widetilde{\mathcal{D}}$, the dynamics either passes through the set $\bar{\mathcal{D}}$ or it is not possible that a free particle is created without exceeding the energy level Γ^*. Indeed, by (1.3.33) we know that any $\eta \in \widetilde{\mathcal{D}}$ has energy $\widehat{H}(\eta) = \Gamma^* - \Delta + U_1 - U_2$. By the optimality of the path, starting from such η it is possible to create a free particle only after lowering the energy. This is possible only if $\eta \in \widetilde{\mathcal{Q}}$, where it is possible to detach the protuberance and reattach it to a vertical side, thus we obtain a configuration in $\bar{\mathcal{Q}}$.

Concerning the strongly anisotropic regime, it is reasonable to expect that also in this case only $\bar{\mathcal{D}}$ is the relevant set for the gate. This is indeed the case. However, configurations in $\widetilde{\mathcal{D}}$ have a very different shape in the strongly anisotropic regime compared to those for the isotropic and weakly anistropic regimes. More precisely, configurations in this set now do not consist in a unique rectangular droplet with four bars attached to its four sides. Indeed, starting from a configuration $\eta \in \widetilde{\mathcal{Q}}$, only a move at cost U_2 is allowed. Otherwise, if a move at cost U_1 takes place, then the resulting configuration has energy $\Gamma^* - \Delta + 2U_1 - U_2 > \Gamma^*$, thus the described path would be not optimal. We deduce therefore that the gate $\mathcal{C}^*$ can be expressed as $\mathcal{C}^* = \bar{\mathcal{D}}^{fp}$ (see Figure 1.12 on the right).

Despite the fact that the structure of the gate is similar for the three scenarios, we emphasize that the entrance in them is very different. In particular, for the strongly anisotropic case there are two different mechanisms to enter the gate, while for the other two scenarios there is a unique one, see [18, Lemma 7.13]. In particular, we proved that any $\omega \in (\square \to \blacksquare)_{opt}$ enters the set $\mathcal{C}^*$ in one of the following ways:

(i) ω passes through $\bar{\mathcal{Q}}$, then possibly through $\bar{\mathcal{D}} \setminus \bar{\mathcal{Q}}$, and finally reaches $\mathcal{C}^*$;

(ii) ω follows the path described in Figure 1.13.

This is a consequence of a larger rigidity of the dynamics in the strongly anisotropic case. An important part of the regularizing motions of particles along the border of the clusters is lost, and because of this a new mechanism for entering in the critical configurations set appears.

GEOMETRICAL DESCRIPTION OF THE UNION OF ALL THE MINIMAL GATES

On the one hand, it is clear that the properties that are strictly related to the horizontal and vertical dimensions are the same for both weakly and strongly anisotropic cases. On the other hand, some properties that involve the motion of particles along the border of the droplet are

very different. Intuitively, one may think of the weakly anisotropic case as an "interpolation" between the isotropic and strongly anisotropic ones. Indeed, it has some properties similar to the first, others to the latter. We now highlight this difference in the description of the set

$$\mathcal{G}(\square,\blacksquare) := \bigcup_{\mathcal{W}(\square,\blacksquare)\text{ minimal gate}} \mathcal{W}(\square,\blacksquare),$$

where a *minimal gate* $\mathcal{W}(\square,\blacksquare)$ is a gate minimal by inclusion, i.e., $\mathcal{W}(\square,\blacksquare)$ is a gate and for any $\mathcal{W} \subsetneq \mathcal{W}(\square,\blacksquare)$ there exists $\omega' \in (\square \to \blacksquare)_{opt}$ such that $\omega' \cap \mathcal{W}' = \emptyset$. Note that the set $\mathcal{G}(\square,\blacksquare)$ represents the union of all the minimal gates for the transition from $\square$ to $\blacksquare$. For the isotropic case more motions along the border are allowed and thus an explicit geometric description of the set is more difficult, but for the anisotropic cases we fully obtain it, since the condition $U_1 \neq U_2$ makes the sliding of particles along the border of the droplet more unlikely. Among the anisotropic cases, the structure of the set $\mathcal{G}(\square,\blacksquare)$ strongly depends on how large is U_1 with respect to U_2, indeed in the case $U_1 > 2U_2$ less slidings along the border are allowed and thus the structure of the union of minimal gates is less rich than the weakly anisotropic case. This characterization for all the three scenarios represents a novel contribution of this thesis.

The starting point for this analysis is the introduction of the concept of *unessential saddle*. Roughly speaking, a saddle $\zeta \in \mathcal{S}(\square,\blacksquare)$ (recall (1.3.29)) is called unessential if it can be "bypassed" by an optimal path in one of its neighborhoods, namely, if for any optimal path crossing ζ there exists another optimal path not crossing ζ such that the two paths do not differ too much. Formally, this happens if for any $\omega \in (\square \to \blacksquare)_{opt}$ such that $\omega \cap \zeta \neq \emptyset$ we have $\{\arg\max_\omega \widehat{H}\} \setminus \{\zeta\} \neq \emptyset$ and there exists $\omega' \in (\square \to \blacksquare)_{opt}$ such that $\{\arg\max_{\omega'} \widehat{H}\} \subseteq \{\arg\max_\omega \widehat{H}\} \setminus \{\zeta\}$. Then we refer to *essential saddles* as those that are not unessential. The notion of essential saddles is crucial in the attempt to characterize the union of minimal gates thanks to [85, Theorem 5.1]. Indeed, the authors proved that a saddle is essential if and only if it belongs to the union of all the minimal gates. Thanks to this equivalence, we reduce our study to the identification of the set of all the essential saddles that has to be crossed during the transition in the three different regimes.

First, we provide a *model–independent strategy* that is useful to eliminate some unessential saddles. More precisely, we require some model–dependent inputs in order to prove that two types of saddles are unessential and therefore they are not in the union of the minimal gates. In order to apply this strategy to Kawasaki dynamics, we need to verify that the required model–dependent inputs are valid for our model in the three scenarios. This study, together with the characterization of the essential saddles, relies on a detailed analysis of the motion of particles along the border of the droplet, which is a typical feature of Kawasaki dynamics. In order not to burden the explanation of the basic ideas too much, we present here this model–independent strategy directly applied to Kawasaki dynamics for the transition from $\square$ to $\blacksquare$, while we refer to Section 3.1.2 for the general strategy.

Recall [45, eq. (3.40)] for the definition of cycle: in the case of Metropolis dynamics this definition coincides with [85, eq. (2.7)]. We need the following definition. Given $\sigma \in \mathcal{X}$, $\Gamma > 0$ and $\mathcal{A}$ a set of target configurations, we say that the *initial cycle* for the transition from σ to $\mathcal{A}$ with depth Γ is

$$\mathcal{C}^\sigma_{\mathcal{A}}(\Gamma) := \{\sigma\} \cup \{\eta \in \mathcal{X} : \Phi(\sigma,\eta) - \widehat{H}(\sigma) < \Gamma = \Phi(\sigma,\mathcal{A}) - \widehat{H}(\sigma)\}. \tag{1.3.34}$$

In words, this initial cycle contains all the configurations that can be reached by σ by spending less energy than the communication height between σ and the target set $\mathcal{A}$. Note that in definition (1.3.34) we emphasize the dependence on σ and $\mathcal{A}$, and that Γ is identified by them. Note that the definition of $\mathcal{C}^\sigma_{\mathcal{A}}(\Gamma)$ coincides with $\mathcal{C}_{\mathcal{A}}(\sigma)$ defined in [85, eq. (2.25)]. We will focus on the two specific intial cycles $\mathcal{C}^{\square}_{\blacksquare}(\Gamma^*)$ and $\mathcal{C}^{\blacksquare}_{\square}(\Gamma^* - \widehat{H}(\blacksquare))$. Roughly speaking, in order to apply the general strategy to our model, we need the following model–dependent inputs (we encourage the reader to inspect Figure 1.14):

(i) Identify the set of metastable and stable states and the energy barrier between them, which are $\square$, $\blacksquare$ and Γ^* in our model, respectively.

(ii) Find a gate for the transition, which is $\mathcal{C}^*$ in our model.

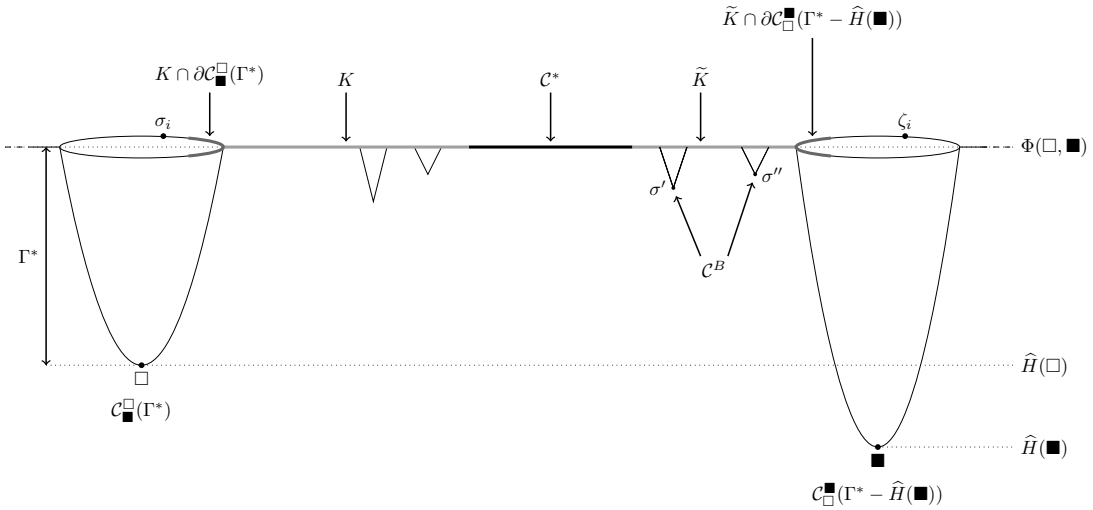

Figure 1.14 – Example of the energy landscape for the transition between $\square$ and $\blacksquare$. We depict on the left (resp. right) the cycle of the metastable (resp. stable) state $\mathcal{C}^{\square}_{\blacksquare}(\Gamma^*)$ (resp. $\mathcal{C}^{\blacksquare}_{\square}(\Gamma^* - \widehat{H}(\blacksquare))$). We indicate in black $\mathcal{C}^*$, in light gray K and $\widetilde{K}$, emphasizing in dark gray the part of K and $\widetilde{K}$ that intersect the boundaries of the two previous cycles. We give an example of two configurations σ and σ' that are in $\mathcal{C}^B$.

(iii) Find two sets of configurations $\mathcal{C}^G$ and $\mathcal{C}^B$ such that when the dynamics reaches $\mathcal{C}^G$, it has made it "over the hill", while when it reaches $\mathcal{C}^B$ it has not.
(iv) Identify the subsets K (resp. $\widetilde{K}$) of the saddles that are visited by the optimal paths "just before entering" (resp. "just after visiting") the gate.

Definition 1.3.2. *A saddle σ is of the first type if it is not in $\mathcal{C}^* \cup K$ and belongs to the boundary of the cycle $\mathcal{C}^{\square}_{\blacksquare}(\Gamma^*)$, i.e., $\sigma \in \partial\mathcal{C}^{\square}_{\blacksquare}(\Gamma^*) \cap (\mathcal{S}(\square, \blacksquare) \setminus (\mathcal{C}^* \cup K))$.*

Definition 1.3.3. *A saddle ζ is of the second type if it is not in $\mathcal{C}^* \cup \widetilde{K}$ and belongs to the boundary of the cycle $\mathcal{C}^{\blacksquare}_{\square}(\Gamma^* - \widehat{H}(\blacksquare))$, i.e., $\zeta \in \partial\mathcal{C}^{\blacksquare}_{\square}(\Gamma^* - \widehat{H}(\blacksquare)) \cap (\mathcal{S}(\square, \blacksquare) \setminus (\mathcal{C}^* \cup \widetilde{K}))$.*

Thus, provided that we addressed conditions (i)-(iv) for our model, the following results hold:

1. Any saddle σ of the first type is unessential.
2. Any saddle ζ of the second type is unessential.

On the one hand, we emphasize that point 1 is guaranteed only by the model–dependent inputs (i), (ii) and (iv). Indeed, the idea of the proof is the following. Given an optimal path ω passing through a saddle σ of the first type and crossing the cycle $\mathcal{C}^{\square}_{\blacksquare}(\Gamma^*)$ for the last time in the configuration η, thanks to [85, Lemma 2.28] we know that there exists a path contained in that cycle $\mathcal{C}^{\square}_{\blacksquare}(\Gamma^*)$, so that it does not cross the saddle σ, such that it can proceed as ω starting from η. Thus, the path ω' obtained by the concatenation of these two paths has the desired property, namely,

$$\{\arg\max_{\omega'} \widehat{H}\} \subseteq \{\arg\max_{\omega} \widehat{H}\} \setminus \{\sigma\}.$$

On the other hand, we emphasize that for point 2 all the model–dependent inputs are necessary. In particular, point (iii) turns out to be crucial. Indeed, the idea of the proof is the following. For point (iii) we deduce that every optimal path ω passing through a saddle of the second type ζ has to cross a saddle $\eta \in \mathcal{C}^* \cup \widetilde{K}$ that communicates with $\mathcal{C}^G$ via one step of the dynamics. Thus, we can define the optimal path ω' as the path ω up to the saddle η, then it reaches the set $\mathcal{C}^G$ and afterwards proceed into $\mathcal{C}^{\blacksquare}_{\square}(\Gamma^* - \widehat{H}(\blacksquare))$. It is easy to check that the path ω' has the desired property.

To characterize all the essential saddles, the idea is therefore to partition the saddles that are not in $\mathcal{C}^*$ in three types: the saddles σ of the first type, the saddles ζ of the second type, and the saddle ξ of the third type, which are all the saddles that are not of the first and second

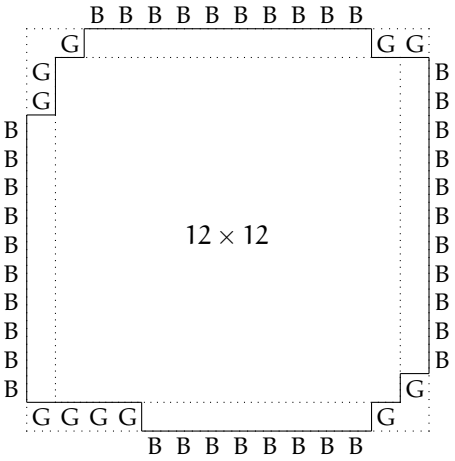

Figure 1.15 – Good sites (G) and bad sites (B) for $\ell_c = 14$.

type. The reason why we exclude the saddles belonging to $\mathcal{C}^*$ is that they are all essential, as we will see later in detail. After the identification of points (iii) and (iv) above, namely, the sets $\mathcal{C}^B$, $\mathcal{C}^G$, K and $\widetilde{K}$, the strategy explained above tells us that the saddles of the first and second type are unessential. Thus, in order to characterize the set $\mathcal{G}(\square, \blacksquare)$ we need to characterize the essential saddles of the third type, which is a task that needs to be addressed by hand for any model and turns out to be intricate for the conservative Kawasaki dynamics.

First, we introduce the sets $\mathcal{C}^G$ and $\mathcal{C}^B$ with the properties claimed in point (iii) above. To this end, we set

$$L^* := \begin{cases} L - \ell_c & \text{for the isotropic regime,} \\ L - \ell_2^* & \text{for the anisotropic regimes.} \end{cases} \tag{1.3.35}$$

For $\eta \in \mathcal{C}^*$, we associate $(\hat{\eta}, x)$ with $\hat{\eta} \in \mathcal{D}$ protocritical droplet and $x \in \Lambda$ the position of the free particle. We denote by $\mathcal{C}^G(\hat{\eta})$ (resp. $\mathcal{C}^B(\hat{\eta})$) the configurations that can be reached from $(\hat{\eta}, x)$ by a path that moves the free particle towards the cluster and attaches the free particle in $\partial^- CR(\hat{\eta})$ (resp. $\partial^+ CR(\hat{\eta})$), where $CR(\hat{\eta})$ is the *circumscribed rectangle* of $\hat{\eta}$, namely, the smallest rectangle containing $\hat{\eta}$. In Figure 1.15 and Figure 1.16 on the left we explicitly depict the good and bad sites for a specific $\hat{\eta}$ for isotropic and strongly anisitropic interactions, respectively. Let

$$\mathcal{C}^G = \bigcup_{\hat{\eta} \in \mathcal{D}} \mathcal{C}^G(\hat{\eta}), \qquad \mathcal{C}^B = \bigcup_{\hat{\eta} \in \mathcal{D}} \mathcal{C}^B(\hat{\eta}). \tag{1.3.36}$$

To prove that these specific sets satisfy the conditions required in (iii), we argue as follows. We claim that for all the three regimes the following properties hold:

1. If $\eta \in \mathcal{C}^G$, then there exists a path $\omega : \eta \to \blacksquare$ such that $\max_{\zeta \in \omega} \widehat{H}(\zeta) < \Gamma^*$.
2. If $\eta \in \mathcal{C}^B$, then there are no $\omega : \eta \to \square$ or $\omega : \eta \to \blacksquare$ such that $\max_{\zeta \in \omega} \widehat{H}(\zeta) < \Gamma^*$.

These two properties are precisely the ones required in point (iii). The proof for the isotropic case is presented in [35], while for the anisotropic cases are presented in [17, 18] and use similar arguments.

We identify now the sets K and $\widetilde{K}$ in (iv). These consist of the saddles that are visited by the optimal paths just before entering and just after visiting the set $\mathcal{C}^*$, respectively. For the three regimes we have that $K = \emptyset$. To identify the saddles of the second type, note that we need only to identify the set $\widetilde{K} \cap \partial \mathcal{C}^{\blacksquare}_{\square}(\Gamma^* - \widehat{H}(\blacksquare))$. We proved that this set has a quite intricate structure in the isotropic and weakly anisotropic cases, while it is empty for the strongly anisotropic case. Again, this difference relies on a larger rigidity of motions of particles in the strongly anisotropic regime. This analysis is very technical and therefore we do not report here the ingredients of the proof, but we refer to Sections 3.4, 4.3 and 5.3 for the precise and detailed argument we used in the three regimes.

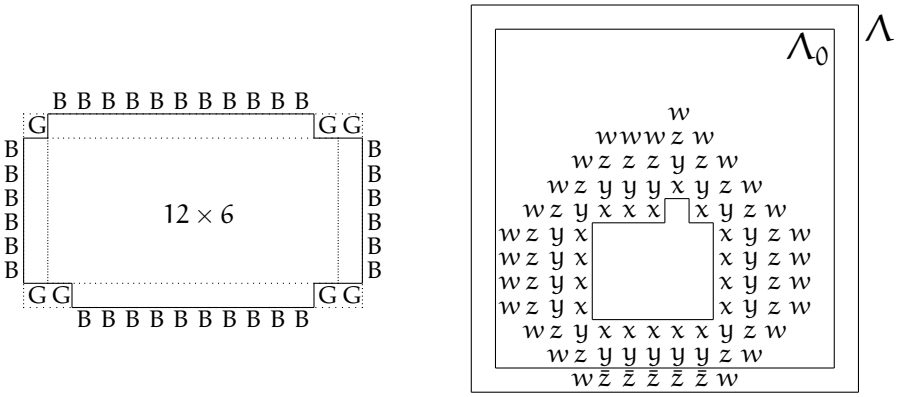

Figure 1.16 – On the left-hand side we represent good sites (G) and bad sites (B) for $\ell_2^* = 8$. On the right-hand side we depict with x the sites in $B_1(\hat{\eta})$, with y the sites in $\bar{B}_2(\hat{\eta})$, with z and $\bar{z}$ the sites in $\bar{B}_3(\hat{\eta})$ and with $\bar{z}$ and w the sites in $\bar{B}_4(\hat{\eta})$.

To prove that $\mathcal{C}^*$ is only composed by essential saddles, we need first to introduce two sets that will be crucial in our argument. For $\eta \in \mathcal{C}^*$, let $\hat{\eta} \in \mathcal{D}$ be the configuration obtained from η by removing the free particle. For $A \subseteq \Lambda$ and $x \in \Lambda$, we denote by $d(x, A)$ the lattice distance between x and A. We need the following definitions.

Definition 1.3.4. *Let Λ_4 be Λ without its four frame-angles. We define, recursively,*

$$B_1(\hat{\eta}) := \{x \in \Lambda_4 |\, x \notin \hat{\eta},\ d(x, \hat{\eta}) = 1\}$$

and

$$B_2(\hat{\eta}) := \{x \in \Lambda_4 |\, x \notin \hat{\eta},\ d(x, B_1(\hat{\eta})) = 1\},$$
$$\bar{B}_2(\hat{\eta}) := B_2(\hat{\eta}),$$

and

$$B_3(\hat{\eta}) := \{x \in \Lambda_4 |\, x \notin B_1(\hat{\eta}),\ d(x, B_2(\hat{\eta})) = 1\},$$
$$\bar{B}_3(\hat{\eta}) := B_3(\hat{\eta}) \cup \{\bar{B}_2(\hat{\eta}) \cap \partial^- \Lambda_4\},$$

and for $i = 4, 5, ..., L^*$

$$B_i(\hat{\eta}) := \{x \in \Lambda_4 |\, x \notin B_{i-2}(\hat{\eta}),\ d(x, B_{i-1}(\hat{\eta})) = 1\},$$
$$\bar{B}_i(\hat{\eta}) := B_i(\hat{\eta}) \cup \{\bar{B}_{i-1}(\hat{\eta}) \cap \partial^- \Lambda_4\}.$$

In words, $B_1(\bar{\eta})$ is the ring of sites in Λ_4 at distance 1 from $\hat{\eta}$, while $\bar{B}_i(\hat{\eta})$ is the ring of sites in Λ_4 at distance i from $\hat{\eta}$ union all the sites in $\partial^- \Lambda_4$ at distance $1 < j < i$ from $\hat{\eta}$ ($i = 2, 3, ..., L^*$) (see Figure 1.16 on the right-hand side). Note that, depending on the location of $\hat{\eta}$ in Λ, the sets $\bar{B}_i(\hat{\eta})$ coincide for large enough i. The maximal number of rings is L^*. We define

$$\mathcal{C}^*(i) := \{(\hat{\eta}, x) : \hat{\eta} \in \mathcal{D}, x \in \bar{B}_i(\hat{\eta})\}, \qquad i = 2, 3, ..., L^*. \tag{1.3.37}$$

First, note that the sets $\mathcal{C}^*(i)$ are not disjoint. From the definitions of the sets $\mathcal{C}^*$ and (1.3.37), we deduce that

$$\mathcal{C}^* = \bigcup_{i=2}^{L^*} \mathcal{C}^*(i). \tag{1.3.38}$$

The proof of $\mathcal{C}^* \subseteq \mathcal{G}(\square, \blacksquare)$ is achieved via two steps:

STEP 1: The saddles in $\mathcal{C}^*(2)$ are essential.

STEP 2: The set $\mathcal{C}^*(i)$ belongs to a minimal gate for any $i = 3, ..., L^*$.

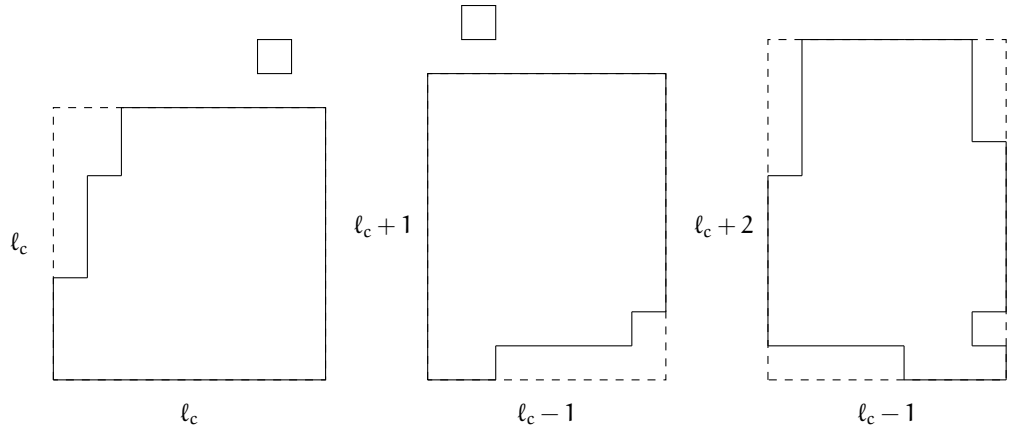

Figure 1.17 – Critical configurations in the isotropic case.

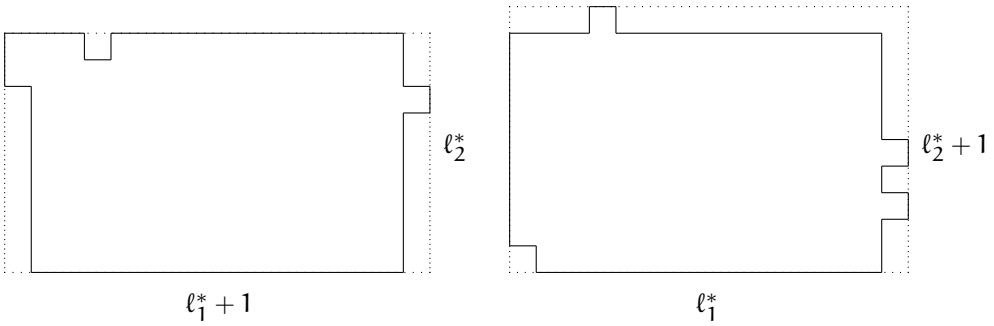

Figure 1.18 – Critical configurations in the weakly anisotropic case.

On the one hand, the proof of step 1 is the same for the three regimes and is based on the fact that it is always possible to find an optimal path that crosses the set $\mathcal{C}^*(2)$ only in a given configuration η. On the other hand, the proof of step 2 differs whether we are dealing with isotropic or weakly anisotropic regimes, and with the strongly anisotropic regime.

We start by considering the isotropic and weakly anisotropic cases. Step 2 is achieved by proving that the set $\mathcal{C}^*(i)$ is a minimal gate for any $i = 3, ..., L^*$, for isotropic and weakly anisotropic interactions. Indeed, by the fact that $\mathcal{C}^*$ is a gate it follows that also each $\mathcal{C}^*(i)$ is. In addition, it is always possible to find an optimal path that crosses the set $\mathcal{C}^*(i)$ only in a given configuration η, so that the set $\mathcal{C}^*(i) \setminus \{\eta\}$ is not a gate anymore, showing therefore the minimality of such a gate.

The analysis is different when we are dealing with the strongly anisotropic case. Indeed, since there are two possible ways to reach the set $\mathcal{C}^*(2)$, to find the minimal gates for any $i = 3, ..., L^*$ we need to consider $\mathcal{C}^*(i)$ union some particular saddles belonging to the path described in Figure 1.13. This implies anyway step 2.

Finally, in order to obtain the full geometrical description of the union of all the minimal gates we need to describe the essential saddles of the third type for all the three scenarios. This part is very technical and requires detailed geometrical definitions, so we skip the details here and refer instead to Sections 3.5, 4.4 and 5.4. Here we report only some examples of configurations belonging to $\mathcal{G}(\square, \blacksquare)$ to give an idea about the shape of all the essential saddles. In Figure 1.17 we show three configurations belonging to the set $\mathcal{G}(\square, \blacksquare)$ in the isotropic case. Note that the configuration on the right has no free particle, indeed it is obtained during the sliding of a bar around a corner of the droplet. We emphasize that in this case many motions along the border are allowed and thus a totally explicit geometric description of the set $\mathcal{G}(\square, \blacksquare)$ is harder to obtain. In Figure 1.18 we show two configurations belonging to the set $\mathcal{G}(\square, \blacksquare)$ in the weakly anisotropic case. Finally, in Figure 1.19 we show two configurations belonging to the set $\mathcal{G}(\square, \blacksquare)$ in the strongly anisotropic case.

We conclude this part concerning the geometrical analysis of all the minimal gates by providing the basic ideas to derive this geometrical description. The first step consists in

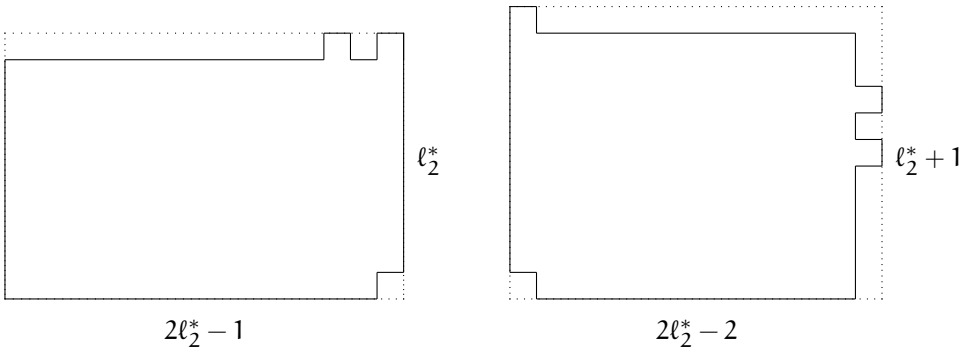

Figure 1.19 – Critical configurations in the strongly anisotropic case.

dividing the saddles that remain to be analyzed in those reached before reaching $\mathcal{G}^B$ and those reached after crossing that set. The former saddles are clearly unessential. Indeed, we can argue as follows. Let ξ be such a saddle.

If ξ is reached before crossing the set $\mathcal{C}^G$, then it is obtained from a configuration $\eta \in \mathcal{C}^*$ without attaching the free particle. Thus, we deduce that the only possibility is that η is composed by a protocritical droplet $\hat{\eta} \in \mathcal{D}$ and a free particle at distance two from the cluster. We deduce therefore that, starting from ξ, the only transition that does not raise the energy is the reverse move giving rise to η, so that ξ is an unessential saddle.

If ξ is reached after crossing the set $\mathcal{C}^G$, due to the properties of the set $\mathcal{C}^G$ it directly follows the unessentiality of the saddle ξ.

This means that it remains only to analyze the saddles obtained after crossing the set $\mathcal{C}^B$. This is the hardest part. Indeed, it depends on all the different types of motions of particles that can take place on the border of the clusters. We emphasize that all the saddles reached after a sliding of a bar around a corner are essential and the analysis concern their full geometrical characterization.

SHARP ESTIMATES

Concerning the asymptotic expectation of the tunneling time, using the pathwise approach, it is not possible to characterize a certain function $f(\beta)$ such that $\log f(\beta)/\beta \to 0$ in the limit as $\beta \to +\infty$ and $\mathbb{E}_\square \tau_\blacksquare = f(\beta) e^{\Gamma^* \beta}(1 + o(1))$, or the presence of a constant factor. To this end, a more detailed study of the so-called *pre-factor* $f(\beta)$ is given in [35] for the two and three dimensional isotropic model using the *potential theoretic approach*. The novel contribution of this thesis regarding the sharp estimate of the mean transition time concerns the estimate of the prefactor for the anisotropic models.

A key role in this analysis is played by the *Dirichlet form*

$$\mathcal{E}(h) = \frac{1}{2} \sum_{\eta,\eta' \in \mathcal{X}} \mu(\eta) P(\eta,\eta')[h(\eta) - h(\eta')]^2, \qquad h : \mathcal{X} \to [0,1], \tag{1.3.39}$$

where μ is the Gibbs measure defined in (1.3.17) and $P(\eta,\eta')$ is the transition probability defined in (1.3.16). Given two non-empty disjoint sets $\mathcal{A}, \mathcal{B} \subseteq \mathcal{X}$, the *capacity* of the pair $\mathcal{A}, \mathcal{B}$ is defined by

$$\mathrm{CAP}(\mathcal{A},\mathcal{B}) = \min_{\substack{h:\mathcal{X}\to[0,1] \\ h_{|\mathcal{A}} \equiv 1, h_{|\mathcal{B}} \equiv 0}} \mathcal{E}(h), \tag{1.3.40}$$

where $h_{|\mathcal{A}} \equiv 1$ means that $h(\eta) = 1$ for all $\eta \in \mathcal{A}$ and $h_{|\mathcal{B}} \equiv 1$ means that $h(\eta) = 0$ for all $\eta \in \mathcal{B}$. The right-hand side of (1.3.40) has a unique minimizer $h^*_{\mathcal{A},\mathcal{B}}$, called the *equilibrium potential* of the pair $\mathcal{A}, \mathcal{B}$, given by

$$h^*_{\mathcal{A},\mathcal{B}} = \mathbb{P}_\eta(\tau_\mathcal{A} < \tau_\mathcal{B}), \qquad \eta \in \mathcal{X} \setminus (\mathcal{A} \cup \mathcal{B}). \tag{1.3.41}$$

By applying the general strategy carried out in [31] and summarized in the monograph [32] for our model, the sharp estimate of the mean transition time is

$$\mathbb{E}_\square(\tau_\blacksquare) = \frac{1}{Z\,\mathrm{CAP}(\square,\blacksquare)}(1 + o(1)), \qquad \beta \to \infty. \tag{1.3.42}$$

To get an explicit variatonal formula for the prefactor starting from (1.3.42), we need first to introduce a graph representation of the configuration space. View $\mathcal{X}$ as a graph whose vertices are configurations and whose edges connect communicating configurations. Let

- $\mathcal{X}^*$ be the subgraph of $\mathcal{X}$ obtained by removing all vertices η with $\widehat{H}(\eta) > \Gamma^*$ and all edges incident to these vertices;
- $\mathcal{X}^{**}$ be the subgraph of $\mathcal{X}^*$ obtained by removing all vertices η with $\widehat{H}(\eta) = \Gamma^*$ and all edges incident to these vertices.

Note that the sets $\mathcal{C}^{\square}_{\blacksquare}(\Gamma^*)$ and $\mathcal{C}^{\blacksquare}_{\square}(\Gamma^* - \widehat{H}(\blacksquare))$ are the connected components of $\mathcal{X}^{**}$ containing $\square$ and $\blacksquare$, respectively. Consider the set

$$\mathcal{X}^{**} \setminus (\mathcal{C}^{\square}_{\blacksquare}(\Gamma^*) \cup \mathcal{C}^{\blacksquare}_{\square}(\Gamma^* - \widehat{H}(\blacksquare))) = \bigcup_{i=1}^{I} \mathcal{X}(i), \tag{1.3.43}$$

where each $\mathcal{X}(i)$ is a *well* in $\mathcal{S}(\square, \blacksquare)$, i.e., a set of communicating configurations with energy strictly less than Γ^* but with communication height Γ^* towards both $\square$ and $\blacksquare$. Among all the wells $\mathcal{X}(i)$, we can highlight the wells $\mathcal{Z}_j^{\square}$ (resp. $\mathcal{Z}_j^{\blacksquare}$) of the unessential saddles of the first (resp. second) type σ_j (resp. ζ_j) (recall Definitions (1.3.2) and (1.3.3)). To obtain the sharp estimate of $Z^{\text{CAP}}(\square, \blacksquare)$ we follow the general strategy outlined in [31, 37]:

- All the terms in the Dirichlet form involving configurations η with $H(\eta) > \Gamma^*$, i.e., $\eta \in \mathcal{X} \setminus \mathcal{X}^*$, contribute at most $Ce^{-(\Gamma^*+\delta)\beta}$ for some $\delta > 0$ and can be neglected. Thus, effectively we can replace $\mathcal{X}$ by $\mathcal{X}^*$.
- Show that $h^*_{\square,\blacksquare} = O(e^{-\delta\beta})$ on $\mathcal{C}^{\blacksquare}_{\square}(\Gamma^* - \widehat{H}(\blacksquare))$ and $h^*_{\square,\blacksquare} = 1 - O(e^{-\delta\beta})$ on $\mathcal{C}^{\square}_{\blacksquare}(\Gamma^*)$ for some $\delta > 0$.
- Prove sharp upper and lower bounds for $h^*_{\square,\blacksquare}$ on $\mathcal{X}^* \setminus (\mathcal{C}^{\square}_{\blacksquare}(\Gamma^*) \cup \mathcal{C}^{\blacksquare}_{\square}(\Gamma^* - \widehat{H}(\blacksquare)))$.

In addition, a novel contribution of this thesis is to prove that it also holds

$$h^*_{\square,\blacksquare} = O(e^{-\delta\beta}) \text{ on } \bigcup_{j=1}^{J_{\blacksquare}} (\{\zeta_j\} \cup \mathcal{Z}_j^{\blacksquare}) \tag{1.3.44}$$

and

$$h^*_{\square,\blacksquare} = 1 - O(e^{-\delta\beta}) \text{ on } \bigcup_{j=1}^{J_{\square}} (\{\sigma_j\} \cup \mathcal{Z}_j^{\square}) \tag{1.3.45}$$

for some $\delta > 0$. This allows a full understanding of the role of the unessential and essential saddles in the prefactor of the mean excursion time. Indeed, also the unessential saddles σ_j and ζ_j have to be considered in this estimate. However, since the equilibrium potential is constantly equal to 1 (resp. 0) on σ_j (resp. ζ_j), the transitions that involve these unessential saddles do not contribute to the prefactor.

In [35] the authors estimated the constant pre-factor for the continuous time version of the isotropic model and found that it does not depend on the parameter β, but on the size of the box and the cardinality of the set of critical droplets with size ℓ_c, namely, the cardinality of the set $\mathcal{D}$. Note that in the discrete time model we defined in Section 1.3.2, the occupation variables for at most one bond between nearest-neighbour sites per time step is changed, so that in continuous time dynamics the mean transition time is rescaled by a factor $1/|\bar{\Lambda}^{*,\text{orie}}|$. These estimates of the pre-factor are possible once the geometrical description of the critical configurations and of its neighborhood are found. In particular, the authors proved that there exists a constant $K = K(\Lambda, \ell_c)$ such that

$$\mathbb{E}_{\square}(\tau_{\blacksquare}) = Ke^{\Gamma^*\beta}(1 + o(1)), \quad \beta \to \infty. \tag{1.3.46}$$

The authors derived a representation for the constant K in terms of certain capacities associated with two–dimensional simple random walk. This representation depends on the geometry of $\mathcal{C}^*$ and its *immediate vicinity*, i.e., the configurations $\eta \in \mathcal{X} \setminus \mathcal{C}^*$ for which there exists $\eta' \in \mathcal{C}^*$ such that $\eta' = \tau_b\eta$ for a bond $b \in \bar{\Lambda}^{*,\text{orie}}$ (recall (1.3.12)). This immediate vicinity is actually *rather complex*, due to the fact that when the free particle attaches itself *improperly* to the protocritical droplet (i.e., in a bad site), it triggers a motion of particles along the border of the

droplet. Consequently, no easily computable formula for K is available. It turns out, however, that the behavior of K for large Λ can be computed explicitly. Indeed, in [35] the authors proved that

$$\lim_{\Lambda\to\mathbb{Z}^2} \frac{|\Lambda|}{\log|\Lambda|} K(\Lambda,\ell_c) = \frac{1}{4\pi N(\ell_c)}, \tag{1.3.47}$$

where

$$N(\ell_c) = \sum_{k=1}^{4} \binom{4}{k} \left[\binom{\ell_c+k-2}{2k-1} + 2\binom{\ell_c+k-3}{2k-1} \right]$$

is the cardinality of $\mathcal{D}$ modulo shifts. The intuition behind this result is the following. The average time it takes for the dynamics to enter $\mathcal{C}^*$ when starting from $\square$ is

$$\frac{1}{|\mathcal{D}|}\frac{1}{|\partial\Lambda^{*,in}|} e^{\Gamma^*}(1+o(1)), \quad \beta\to\infty, \tag{1.3.48}$$

where $|\mathcal{D}|$ counts the number of protocritical droplets and $|\partial\Lambda^{*,in}|$ counts the number of directed bonds from $\partial^+\Lambda$ to $\partial^-\Lambda$ along which the free particle can be created (recall (1.3.12)). Let $\pi(\Lambda,\ell_c)$ be the probability, averaged with respect to the uniform distribution for the protocritical droplet on $\mathcal{D}$ and the uniform distribution for the free particle entering on $\partial^*\Lambda^{in}$, that the free particle moves from $\partial^-\Lambda$ to the protocritical droplet and attaches itself *properly* (i.e., in a good site). This is the probability that the dynamics, after it enters the set $\mathcal{C}^*$, moves onwards to $\blacksquare$ rather than returns to $\square$. Then

$$\frac{1}{\pi(\Lambda,\ell_c)}(1+o(1)), \quad \beta\to\infty \tag{1.3.49}$$

is the average number of times a free particle just created in $\partial^-\Lambda$ attempts to move to the protocritical droplet and attaches itself properly before it finally manages to do so. The average nucleation time is the product of (1.3.48) and (1.3.49), and so we conclude that

$$K(\Lambda,\ell_c) = \frac{1}{|\mathcal{D}||\partial^*\Lambda^{in}|\pi(\Lambda,\ell_c)}. \tag{1.3.50}$$

Now, we have

$$\lim_{\Lambda\to\mathbb{Z}^2} \frac{|\mathcal{D}|}{|\Lambda|} = N(\ell_c). \tag{1.3.51}$$

Furthermore, we have

$$\lim_{\Lambda\to\mathbb{Z}^2} |\partial^*\Lambda^{in}|\pi(\Lambda,\ell_c)\log|\Lambda| = 4\pi. \tag{1.3.52}$$

Indeed, the term $4\pi/\log|\Lambda|$ is the probability for large Λ that a particle, after detaching itself from the protocritical droplet, reaches $\partial^-\Lambda$ before reattaching itself. Due to the recurrence of simple random walk in two dimensions, for large Λ this probability is independent of the shape and the location of the protocritical droplet, as long as it is far from $\partial^-\Lambda$. By reversibility, the reverse motion has the same probability, which explains (1.3.52). Then (1.3.47) follows by combining (1.3.50)-(1.3.52).

If the free particle attaches in a bad site to the protocritical droplet, then either it may again detach itself or it may cause some motion of particles along the border of the droplet, after which another particle may detach itself, possibly leaving behind a different protocritical droplet. However, since for large Λ a free particle has a small probability to escape from the protocritical droplet and return to $\partial\Lambda$, it must eventually attach itself in a good site.

The asymptotics in (1.3.47) does not depend on the shape of Λ, i.e., it would be the same if Λ were a circle rather than a large square. Furthermore, in the three-dimensional case similar results are obtained in [35] but with less control over the geometry and the constant.

Concerning the anisotropic models, the proof relies again on the tools developed in the potential theoretic approach and the estimates which are obtained are similar. However, for

the strongly anisotropic regime something different happens. Indeed, since the entrance in the set of critical configurations is crucial for the estimate of the prefactor, the fact that in this regime there are two different mechanisms to do so means that a better estimate can be found. We refer to Section 5.1.2 for more details.

As we said above, how the dynamics enters the gate is a relevant property to derive. In [35] the authors prove that this entrance in the isotropic regime is uniform in the following sense:

$$\lim_{\beta\to\infty} \mathbb{P}_{\square}\left(\eta_{\tau_{\mathcal{C}^*-}} = \eta \mid \tau_{\mathcal{C}^*} < \tau_{\square}\right) = \frac{1}{|\mathcal{D}|} \text{ for any } \eta \in \mathcal{D}, \tag{1.3.53}$$

where $\tau_{\mathcal{C}^*-}$ is the time just prior to $\tau_{\mathcal{C}^*}$. This is reasonable, indeed the protocritical droplets in $\mathcal{D}$, seen just prior to the creation of the free particle in $\partial^- \Lambda$, occur with equal probability. This is what we expect also in the weakly anisotropic regime, while this is not the case in the strongly anisotropic regime. We refer to [17, 18] for all the technical details, while here we elaborate on the general strategy behind.

The monograph [32] provides a general framework to prove that the entrance in the gate is uniform. In particular, the authors prove the *uniform entrance distribution* subject to two hypotheses. More precisely, we introduce the sets $\mathcal{P}^*_{PTA}$ and $\mathcal{C}^*_{PTA}$ as follows. Think of $\mathcal{P}^*_{PTA}$ as the set of configurations where the dynamics, starting from the metastable state, is "almost on top of the hill", and of $\mathcal{C}^*_{PTA}$ as the set of configurations where the dynamics "has reached the top of the hill" and is "capable of crossing over" to the stable state without returning to "the valley around the metastable state". See [32, Definition 16.3] for the precise definition. Thus, the hypotheses are

(H1) There is a unique metastable and a unique stable state.

(H2) All the configurations in $\mathcal{C}^*_{PTA}$ have the same number of configurations in $\mathcal{P}^*_{PTA}$ from which they can be reached via an allowed move.

Since there is a unique way to enter the gate in the weakly anisotropic regime, nothing different with respect to the isotropic case happens. However, the situation is completely different in the case of strong anisotropy. Indeed, we have proved that in this model the set $\mathcal{P}^*_{PTA}$ coincides with $\bar{\mathcal{D}}$ union some protocritical doplets involved in the second mechanism to enter the gate (such as configurations (6) and (10) in Figure 1.13), and $\mathcal{C}^*_{PTA}$ coincides with $\mathcal{C}^*(L^*)$ union some saddles involved in the second mechanism to enter the gate. First, note that $\mathcal{C}^* \neq \mathcal{C}^*_{PTA}$. Also note that condition (H2) follows from the result concerning the two mechanisms to enter the gate. Thus, since both (H1) and (H2) hold, [32, Theorem 16.4(b)] should hold, i.e., the entrance has a uniform distribution, but this is not true. More precisely, this model represents a counterexample of [32, Theorem 16.4(b)]. This depends on the hypotheses (H2), that takes into account only the map from $\mathcal{C}^*_{PTA}$ to $\mathcal{P}^*_{PTA}$ and not the reverse one. Therefore we propose to replace the hypotheses (H2) with

(H2′) All the configurations in $\mathcal{C}^*_{PTA}$ have the same number of configurations in $\mathcal{P}^*_{PTA}$ from which they can be reached via an allowed move and viceversa.

We are convinced that this could be the correct hypotheses, indeed the analysis of the uniform entrance distribution in $\mathcal{C}^*_{PTA}$ has to take into account the number of configurations in $\mathcal{P}^*_{PTA}$ that communicate with $\mathcal{C}^*_{PTA}$ via one step of the dynamics. Now it is clear that this model does not satisfy (H2′), indeed each configuration in $\bar{\mathcal{D}}$ has exactly $4L-4$ configurations in $\mathcal{C}^*$ from which it can be reached via an allowed move, while each of the other configurations composing $\mathcal{P}^*_{PTA}$ has only one configuration in $\mathcal{C}^*_{PTA}$ with this property. Therefore [32, Theorem 16.4(b)] does not hold for this model.

Finally, for all the three regimes we also examined the rate of convergence to the stationary distribution of the Metropolis Markov chain $\{\eta_t\}_{t\in\mathbb{N}}$. We measured the rate of convergence in terms of the total variational distance and the mixing time, which describes the time required for the distance to stationarity to become small. More precisely, for any $0 < \varepsilon < 1$, we define the *mixing time* as

$$t_{mix}(\varepsilon) := \min\left\{ n \geqslant 0 : \max_{x\in\mathcal{X}} \|P^n(x,\cdot) - \mu(\cdot)\|_{TV} \leqslant \varepsilon \right\}, \tag{1.3.54}$$

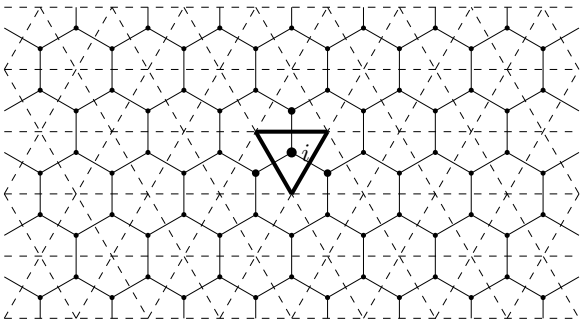

Figure 1.20 – We highlight in black the sites j such that $d(i,j) \neq 0$ on the hexagonal lattice.

where $\|\nu - \nu'\|_{TV} := \frac{1}{2}\sum_{x\in\mathcal{X}} |\nu(x) - \nu'(x)|$ for any two probability measures ν, ν' on $\mathcal{X}$. Another classical notion to investigate the speed of convergence of Markov chains is the *spectral gap*, which is defined as

$$\rho := a^{(2)}, \tag{1.3.55}$$

where $1 = a^{(1)} > a^{(2)} \geqslant \ldots \geqslant a^{(|\mathcal{X}|)} \geqslant -1$ are the eigenvalues of the matrix $(P(x,y))_{x,y\in\mathcal{X}}$ defined in (1.3.16).

Thus, we proved that for all the three regimes and for any $\varepsilon \in (0,1)$ it holds

$$\lim_{\beta\to\infty} \frac{1}{\beta} \log t_{mix}(\varepsilon) = \Gamma^* = \lim_{\beta\to\infty} -\frac{1}{\beta} \log \rho.$$

In addition, there exist two constants $0 < c_1 \leqslant c_2 < \infty$ independent of β such that for every $\beta > 0$

$$c_1 e^{-\beta\Gamma^*} \leqslant \rho \leqslant c_2 e^{-\beta\Gamma^*}.$$

1.3.3 *The local model on the hexagonal lattice*

In this section, we introduce the local model on the hexagonal lattice and we present the main results derived in this thesis. Consider the discrete hexagonal lattice $\mathbb{H}^2$ embedded in $\mathbb{R}^2$ and let $\mathbb{T}^2$ be its dual, so that $\mathbb{T}^2$ is the triangular lattice. Two sites of the discrete hexagonal lattice are said to be *nearest neighbors* when they share an edge of the lattice, see Figure 1.20. We consider an hexagon in $\mathbb{H}^2$ with radius L and we define $\Lambda \subset \mathbb{T}^2$ as the union between this hexagon and all the sites, that are not in the hexagon, with lattice distance one from the hexagon. Recall equation (1.3.9) for the definition of the set Λ_0, which is defined as Λ without its internal boundary. With this choice of the finite β-independent domain Λ, we deduce that Λ_0 is an hexagon with radius L, see Figure 1.21. Note that Λ_0 contains $6L^2$ sites. The side length L is fixed, but arbitrary, and later we will require L to be sufficiently large. Recall the definition of the configuration space as $\mathcal{X} = \{0,1\}^\Lambda$. With each configuration $\eta \in \mathcal{X}$, we associate the local Hamiltonian energy $\widehat{H}(\eta)$ defined in (1.3.11), where we take $U_1 = U_2 = U$ and we replace the vertical and horizontal bonds on the square lattice with the bonds connecting nearest-neighbor sites on the hexagonal lattice. Thus, we can write the energy as

$$\widehat{H}(\eta) := -U \sum_{(x,y)\in\Lambda_0^*} \eta(x)\eta(y) + \Delta \sum_{x\in\Lambda} \eta(x), \tag{1.3.56}$$

where

$$\Lambda_0^* = \{(x,y) \in \Lambda_0 \times \Lambda_0 : |x-y| = 1\}$$

is the set of non-oriented bonds in Λ_0. Thus, the interaction consists of a binding energy $-U < 0$ for each nearest-neighbor pair of particles in Λ_0. In addition, there is an activation

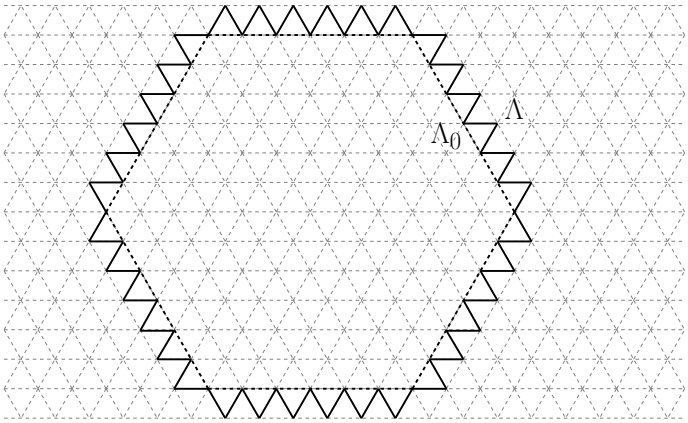

Figure 1.21 – We depict the set Λ with a straight line, while we depict the hexagon Λ_0 with a dashed line.

energy $\Delta > 0$ for each particle in Λ. Here we consider only the isotropic regime, namely, the binding energy associated to each bond is the same, because in this thesis we derived results only in this scenario. However, as we have done for the model evolving on the square lattice, it is possible to consider *anisotropic interactions*. This is left as a future research direction. The locally conservative Kawasaki dynamics on the hexagonal lattice can be therefore defined as in Section 1.3.2 with a different choice of the domain Λ. For this model, the metastable regime corresponds to taking

$$\Delta \in \left(U, \frac{3}{2}U\right). \tag{1.3.57}$$

We can justify this condition as follows. The condition $\Delta > U$ has the same interpretation given above, but now the condition $\Delta < 2U$ is not enough as in the square lattice. Indeed, for more than one particle attached to an hexagonal shape it is possible to detach a single particle alternatively at cost U and $2U$, see Figure 1.22. Thus, the required upper bound on Δ can be viewed as an average of these two costs. We have that the empty hexagon

$$\hexagon := \{\eta \in \mathcal{X} : \eta(x) = 0 \ \forall\, x \in \Lambda\} \tag{1.3.58}$$

is the unique metastable state and the full hexagon

$$\hexagon := \{\eta \in \mathcal{X} : \eta(x) = 1 \ \forall\, x \in \Lambda_0, \eta(x) = 0 \ \forall\, x \in \Lambda \setminus \Lambda_0\} \tag{1.3.59}$$

is the unique stable state, provided that L is sufficiently large. This assumption is needed to have $\widehat{H}(\hexagon) < \widehat{H}(\hexagon) = 0$ and later we will provide an explicit lower bound for L. Note that equations (1.3.58)–(1.3.59) coincide with equations (1.3.19)–(1.3.20), but here we use a different definition of Λ and therefore we change notation only to make clear which lattice we are referring to. Thus, the exit from metastability consists in analyzing the transition from $\hexagon$ to $\hexagon$. We will focus on the estimate of this transition time and on the geometrical description of the *critical droplets* the system has to cross to perform the nucleation.

The main motivation of this analysis is the following. We investigate how the underlying lattice affects the dynamical properties of the system. The choice of the hexagonal lattice comes from a recent study done for this model evolving under the non–conservative Glauber dynamics (see Section 1.4.1) in [4, 78], because it has been shown how a certain class of parallel dynamics (shaken dynamics in [2, 3]) on the square lattice induces a collection of parallel dynamics on a family of Ising models on the hexagonal lattice with non-isotropic interactions, where the spins in each of the two partitions are alternatively updated. Our result concerning the gate indicates that the underlying lattice is crucial for the dynamics of the system. One could be tempted to simply conjecture that the critical configurations are the counterparts on the hexagonal lattice of those arising for the same model on the square lattice, for example by replacing the rectangular shape with an hexagonal one, but this conjecture is false. Indeed, we will prove that for this model there exist two different sizes for the critical droplets depending

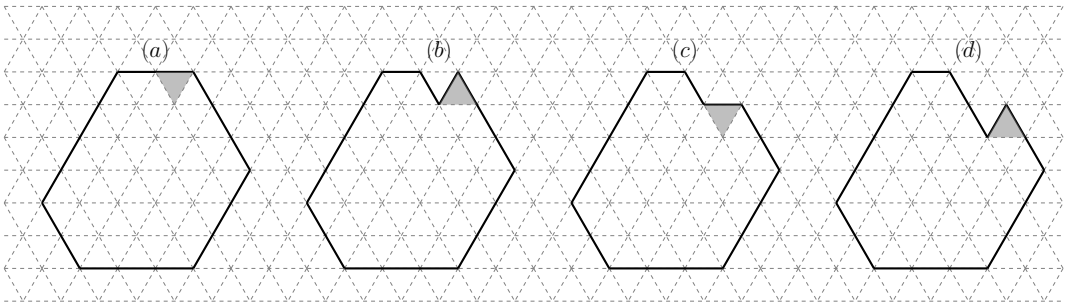

Figure 1.22 – In all the clusters we represent in grey the particle that is detaching: this has a probability of occurring of order $e^{-2U\beta}$ (resp. $e^{-U\beta}$) for clusters (a) and (c) (resp. (b) and (d)).

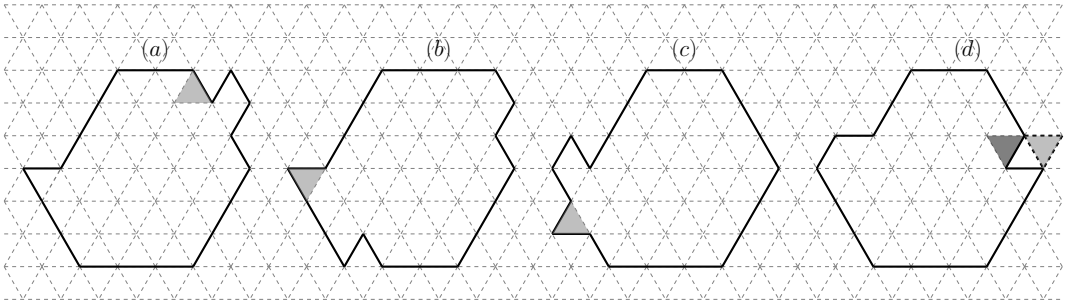

Figure 1.23 – In (b) we depict a configuration obtained starting from the configuration represented in (a). In particular, in (a) we highlight in grey the triangular face that moves towards the elementary rhombus on the right at cost U, while in (b) we highlight in grey the single protuberance. In (d) we depict a configuration obtained starting from the configuration represented in (c). In particular, in (c) we highlight in grey the single protuberance, while in (d) we highlight in light grey the free particle and in dark grey the last triangular face that has been moved towards left.

on the value of the fractional part of the ratio $(\Delta - U)/(3U - 2\Delta)$. This situation occurs also for the model evolving under Glauber dynamics considered in [4], but we want to stress that its characterization is very different. Indeed, the main difference between Kawasaki and Glauber dynamics is that the former conserves the number of particles and therefore the structure of the gates is much richer. In particular, for Glauber dynamics there is a *unique* minimal gate, but for Kawasaki dynamics their characterization is not trivial and therefore much more interesting to derive. The geometrical description of the minimal gates is out of the scope of this thesis and is left as a future research direction, but we encourage the reader to inspect the differences between Theorem 6.1.4 and [4, Theorem 2.13] to keep in mind the different nature of the gate for the transition for these two different dynamics.

COMPARISON WITH KAWASAKI DYNAMICS ON THE SQUARE LATTICE

Here, we make a comparison between the isotropic model on the hexagonal lattice and other models evolving under Kawasaki dynamics on the square lattice in order to emphasize the different behavior of the system depending on the geometry of the lattice. The locally conservative dynamics and the movement of particles give a regularization effect, but we stress that the particular shape of the hexagonal lattice induces an increment of these regularizing motions in such a way that new mechanisms of entering the critical configurations set appear, see Remarks 1.3.5 and 1.3.6 for more details. This is a first crucial difference between the two isotropic models. Indeed, on the square lattice a new mechanism to enter the gate appears only in the strongly anisotropic setting, see [16, 17]. For the weakly anisotropic and isotropic models there is a unique way to enter the gate: a rectangular shape with a single protuberance is reached and then a free particle enters from the boundary of the box, see [18, 90] for more details. On the square lattice, before the entrance of the free particle it is possible that particles move only along the border of the cluster, while on the hexagonal lattice this phenomenon can

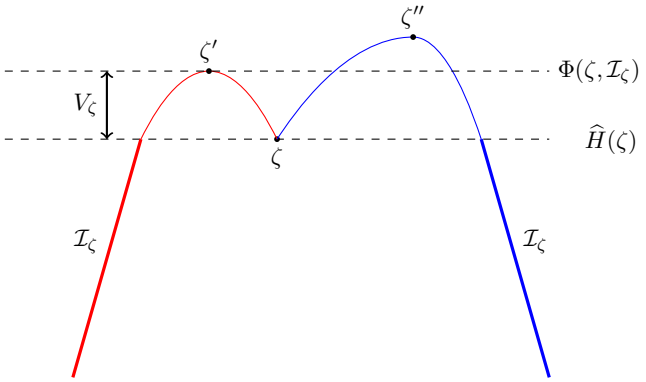

Figure 1.24 – Stability level V_ζ for a configuration ζ.

also appear for particles in an internal region of the cluster, see Figure 1.23(a)-(b) and (c)-(d) for two examples of the first and last configuration obtained in such a way. As a consequence, in this case the complete geometrical characterization is hard to obtain, and is left as a future research direction. The reason we observe this very different behavior rests on the specific structure of the underlying lattice. Indeed, on the hexagonal lattice, when a particle that does not belong to the border of a cluster moves, if it attaches to a protuberance then the energy increases by U (2 bonds are broken and one is created when the moving particle attaches to the protuberance), while this is false on the square lattice. Indeed, in that case the energy increases by $2U$ (3 bonds are broken and one is created when the moving particle attaches to the protuberance). This difference turns out to be crucial when the dynamics is close to critical configurations. This phenomenon can be also found in the different metastable regime for this model with respect to the one on the square lattice. This is peculiar of Kawasaki dynamics, indeed for Glauber dynamics this does not happen, see [4, Condition 2.6]. This behavior is also responsible for the particular shape of the critical droplets, which present two different protuberances and not only one as in the square lattice case. As it will be clear throughout the work, we come to the conclusion that the geometry of the lattice significantly influences the behavior of the system subject to Kawasaki dynamics and this makes it very interesting to study.

IDENTIFICATION OF STABLE AND METASTABLE STATES

Here we give the main ideas to deduce that ⎔ (resp. ⬢) is the unique metastable (resp. stable) state. The key notion is that of *stability level* of a configuration σ, which is defined as the energy barrier (see Figure 1.24)

$$V_\zeta := \Phi(\zeta, \mathcal{I}_\zeta) - \widehat{H}(\zeta), \tag{1.3.60}$$

where $\mathcal{I}_\zeta$ is the set of states with energy below $\widehat{H}(\zeta)$:

$$\mathcal{I}_\zeta := \{\eta \in \mathcal{X} \,|\, \widehat{H}(\eta) < \widehat{H}(\sigma)\}. \tag{1.3.61}$$

We set $V_\sigma := \infty$ if $\mathcal{I}_\sigma$ is empty. Since the set of metastable states is formally defined as

$$\mathcal{X}^m := \left\{\sigma \in \mathcal{X} \,|\, V_\sigma = \max_{\eta \in \mathcal{X}\setminus\mathcal{X}^s} V_\eta\right\}, \tag{1.3.62}$$

the idea is to prove that there exists $V^* > 0$ such that the only configurations with a stability level greater than V^* are ⎔ and ⬢. In particular, $V^* = \Delta + U$. This proof is divided in two steps. First of all, we prove that the configurations satisfying certain geometrical properties have a stability level smaller than or equal to $\Delta + U$, and then we show that all configurations, different from ⎔ and ⬢, has a stability level smaller than or equal to $\Delta + U$. This implies that the system reaches with high probability either the state ⎔, which is local minimizer of the Hamiltonian, or the ground state ⬢, thanks to $\widehat{H}(⬢) < \widehat{H}(⎔)$, in a time shorther than $e^{(V^*+\varepsilon)\beta}$, uniformly in the starting configuration for any $\varepsilon > 0$. For all the technical details we refer to Section 6.3.

TRANSITION TIME AND DESCRIPTION OF A GATE

Before stating the results we have derived, we provide a heuristic discussion from a static point of view. Consider the metastable regime (1.3.57) and the limit β tending to infinity. Let us make a rough computation of the probability to see a regular hexagon of radius r of occupied sites centered at the origin. We denote by μ^* the restricted ensemble, namely, the Grand–canonical Gibbs measure defined in (1.3.17) restricted to a suitable subset of configurations, where all sufficiently large clusters are suppressed. Under restricted ensemble we have

$$\mu^*(\text{regular hexagon of radius } r) \approx \rho^{6r^2} e^{3U(3r^2-r)\beta},$$

since the density of the gas ρ is close to the probability to find a particle at a given site and $-U$ is the binding energy between two particles at the neighboring sites, with $3(3r^2-r)$ the number of bonds for an hexagon with radius r. Writing $\rho = e^{-\Delta\beta}$ we obtain

$$\mu^*(\text{regular hexagon of radius } r) \approx e^{-\beta[6r^2\Delta+3(r-3r^2)U]},$$

where the exponent has a saddle point at

$$\bar{r} = \frac{U}{2(3U-2\Delta)}.$$

This means that droplets with radius $r < \bar{r}$ appear with a probability that decreases in r and droplets with radius $r \geqslant \bar{r}$ a probability that increases in r. This would leave to the conclusion that $\bar{r}$ is the radius of the critical droplet. We will see in the sequel that the situation is more delicate (see (1.3.63) for the precise definition of the critical radius r^*), indeed the dynamical mechanism for the transition between hexagonal droplets, which is not considered here, have an influence on the growth or shrinkage of the droplets. The choice $\Delta \in (U, \frac{3}{2}U)$ corresponds to $r^* \in (1, \infty)$, i.e., to a non-trivial critical droplet.

To make the previous assumption on L precise, we introduce the so–called *critical radius* as

$$r^* := \left\lfloor \frac{U}{2(3U-2\Delta)} - \frac{1}{2} \right\rfloor = \left\lfloor \frac{\Delta-U}{3U-2\Delta} \right\rfloor. \tag{1.3.63}$$

We require that

$$L > 2r^* + 3. \tag{1.3.64}$$

In addition, we require some non–degeneracy assumptions. In particular, we assume that

$$\frac{\Delta-U}{3U-2\Delta} \notin \mathbb{N}. \tag{1.3.65}$$

To avoid pathological trivial cases, we further assume that

$$\Delta \in \left(\frac{7}{5}U, \frac{3}{2}U\right). \tag{1.3.66}$$

Note that condition (1.3.66) ensures that all the critical lengths are larger than two. In the remainder of this section assume that conditions (1.3.64)–(1.3.66) are in force. Thanks to (1.3.65), we can write

$$r^* = \frac{\Delta-U}{3U-2\Delta} - \delta,$$

with $\delta \in (0,1)$ the fractional part of $(\Delta-U)/(3U-2\Delta)$ fixed. We will see that δ plays a crucial role in this analysis. Indeed, depending whether $\delta \in (0, \frac{1}{2})$ or $\delta \in (\frac{1}{2}, 1)$ the system has a different behaviour. Our goal is to provide estimates for the transition time from $\hexagon$ and $\hexagon$, and to characterize the critical droplets.

Next, we prove that the gate for the transition $\mathcal{C}^* = \mathcal{C}^*(\hexagon, \hexagon)$ contains those configurations consisting of one free particle and a unique cluster having a shape close to an hexagon with

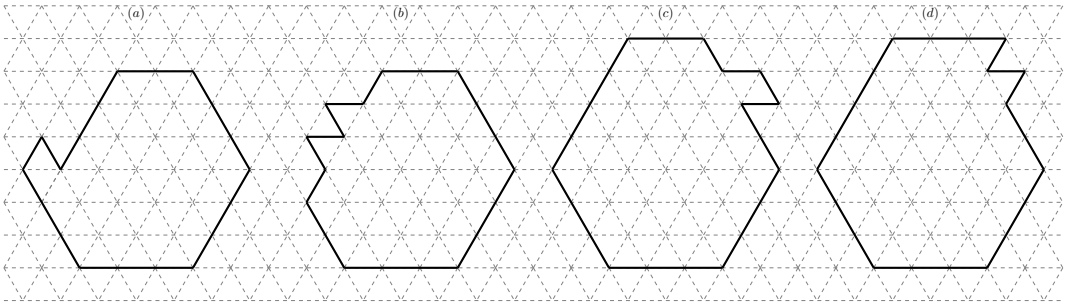

Figure 1.25 – On the left there are two examples of configurations in $\widetilde{\mathcal{S}}(A_1^*-1)$, $\widetilde{\mathcal{D}}(A_1^*-1)$. On the right there are two examples of configurations in $\widetilde{\mathcal{S}}(A_2^*-1)$, $\widetilde{\mathcal{D}}(A_2^*-1)$.

radius r^*. To this end, we argue as follows. First, we define the *critical area* A^* as the number of particles in the configurations in $\mathcal{C}^*$. Formally, it is defined as

$$A^* := \begin{cases} A_1^* & \text{if } \delta \in (0, \frac{1}{2}), \\ A_2^* & \text{if } \delta \in (\frac{1}{2}, 1), \end{cases} \tag{1.3.67}$$

where A_1^* and A_2^* are two explicit constants depending on r^*. To characterize the critical droplets, we give an intuitive definition of the configurations denoted by $\widetilde{\mathcal{S}}(A^*-1)$ and $\widetilde{\mathcal{D}}(A^*-1)$ that play the role of protocritical configurations. In particular, configurations in $\widetilde{\mathcal{S}}(A^*-1)$ (resp. $\widetilde{\mathcal{D}}(A^*-1)$) have a unique cluster with area A^*-1 and shape as in Figure 1.25(a)-(c) (resp. Figure 1.25(b)-(d)). By denoting by $n(\eta)$ the number of free particles of the configuration η, let

$$\begin{aligned} \mathcal{K}(A^*-1) := \{\eta' \in \mathcal{V}_{A^*-1} \,|\, \exists\, \omega = (\eta, \omega_1, ..., \omega_n, \eta') : \eta \in \widetilde{\mathcal{S}}(A^*-1) \cup \widetilde{\mathcal{D}}(A^*-1), \\ \widehat{H}(\eta) = \widehat{H}(\eta'), n(\omega_j) = 0 \,\forall\, j = 1, ..., n \text{ and } \Phi_{\mathcal{V}_{A^*-1}}(\eta, \eta') \leqslant \widehat{H}(\eta) + U\} \end{aligned} \tag{1.3.68}$$

be the set of configurations obtained starting from $\widetilde{\mathcal{S}}(A^*-1) \cup \widetilde{\mathcal{D}}(A^*-1)$ by a path that does not create free particles, the energy along it increases by U at most and the starting and final configurations have the same energy. Note that the last condition in (1.3.68) is the same as requiring that $\Phi_{\mathcal{V}_{A^*-1}} < \Gamma_H^*$, where

$$\Gamma_H^* := \widehat{H}(\mathcal{K}(A^*-1)) + \Delta = \widehat{H}(\widetilde{\mathcal{S}}(A^*-1)) + \Delta = \widehat{H}(\widetilde{\mathcal{D}}(A^*-1)) + \Delta.$$

The set $\mathcal{K}(A^*-1)$ plays the same role as the sets $\widetilde{\mathcal{D}}$ and $\bar{\mathcal{D}}$ introduced for the model evolving on the square lattice. Indeed, the conditions required in (1.3.68) are analogous to those required in (1.3.31), with the additional request that the path connecting $\eta \in \widetilde{\mathcal{S}}(A^*-1) \cup \widetilde{\mathcal{D}}(A^*-1)$ to $\eta' \in \mathcal{V}_{A^*-1}$ do not create any free particle. This condition ensures that η' is not obtained from η by moving a protuberance, because on the hexagonal lattice this does happen by first detaching the protuberance itself. We do not need this condition on the square lattice because a protuberance can be moved along a side of a cluster without ever detaching.

In this thesis we will prove that the set $\mathcal{C}^* = \mathcal{K}(A^*-1)^{fp}$ is a gate for the transition from ⬡ to ⬢, so that the energy value Γ_H^* coincides with the energy of the critical configurations. We emphasize that we have not obtained a full geometrical characterization of this set. Indeed, to get this we need to geometrically identify the set $\mathcal{K}(A^*-1)$. This is left as a future research direction.

Remark 1.3.5. *Unlike what happens on the square lattice, on the hexagonal lattice many more ways to move particles at cost U can occur. We stress this crucial property of the hexagonal lattice since it has a strong impact on the geometrical description of the gate. Indeed, for instance, concerning a configuration as in Figure 1.26(a), note that it is possible to move a protuberance belonging to the elementary rhombus on the left at cost U. The key fact is that these are not the unique possibilities, as occurs on the square lattice, indeed in this case it is possible to move also particles that belong to the internal part of a cluster. For example, it is possible to move towards the elementary rhombus an entire*

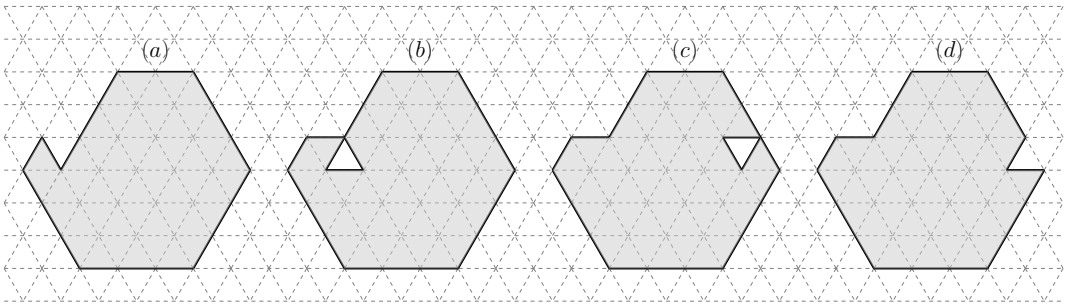

Figure 1.26 – In this figure we depict an example of motions of particles that belong to the internal part of a cluster at cost U. We represent the cluster in grey. Starting from the configuration represented in (a), by moving a particle towards the empty site, the energy increases by U and the configuration that is obtained is the one represented in (b). From now on, the empty site moves at cost 0 until the path reaches the configuration depicted in (c). Finally, the path reaches the configuration in (d) by lowering the energy by U, thus the starting and final configuration have the same energy.

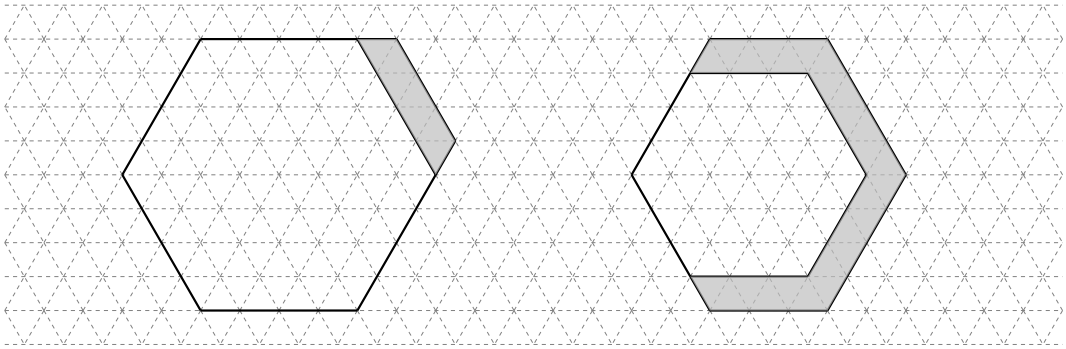

Figure 1.27 – Two examples of quasi–regular hexagons.

row of particles giving rise to a configuration with the same energy (see Figure 1.26 for the entire path). For this reason the geometrical characterization of the gate is much richer and more interesting than the one derived for the square lattice. Moreover, these additional regularizing motions of particles lead to several mechanisms to enter the gate. We point the reader to Remark 1.3.6 for more details.

To prove that the set $\mathcal{C}^*$ is a gate for the transition and that the system, with probability tending to 1 in the limit as β goes to infinity, creates the critical droplet and reaches $\hexagon$ in a time of order $e^{\Gamma^*_H \beta}$ when it starts from $\hexagon$, the key ingredients are the following:

(i) Prove that $\Phi(\hexagon, \hexagon) \leqslant \Gamma^*_H$.
(ii) Prove that $\Phi(\hexagon, \hexagon) \geqslant \Gamma^*_H$.
(iii) Prove that any $\omega \in (\hexagon \to \hexagon)_{opt}$ crosses the set $\mathcal{C}^*$.

For (i), it suffices to construct a *reference path* ω^* connecting $\hexagon$ to $\hexagon$ which does not exceed the energy value Γ^*_H. In particular, this path is composed by increasing clusters as close as possible to quasi–regular hexagonal shape, see Figure 1.27. The idea of the construction of ω^* is the following: we first construct a skeleton path $\{\bar{\omega}_r\}_{r=0}^L$ given by a sequence of configurations that contain a regular hexagon with radius r. Obviously $\bar{\omega}_r$ is not a path since the transition from $\bar{\omega}_r$ to $\bar{\omega}_{r+1}$ cannot occur in a single step of the dynamics. Thus, in order to obtain a path we interpolate each element of the skeleton path. This is done in two steps. First, between $\bar{\omega}_r$ and $\bar{\omega}_{r+1}$, we introduce a sequence of configurations $\tilde{\omega}_r^1, ..., \tilde{\omega}_r^{i_r}$ given by $\bar{\omega}_r$ plus a bar, i.e., a quasi-regular hexagon. Again, these configurations are given by a single increasing droplet. Finally, we introduce a second interpolation to obtain a path ω^* from the sequence of configurations $\tilde{\omega}_r^i$. Its construction goes as follows. Between every couple of consecutive configurations in $\tilde{\omega}$, for which the cluster is increased by one particle, a sequence of configurations with a new particle is inserted. In particular, the new particle is initially created at the boundary of Λ and then brought to the correct site via consecutive moves of this free particle.

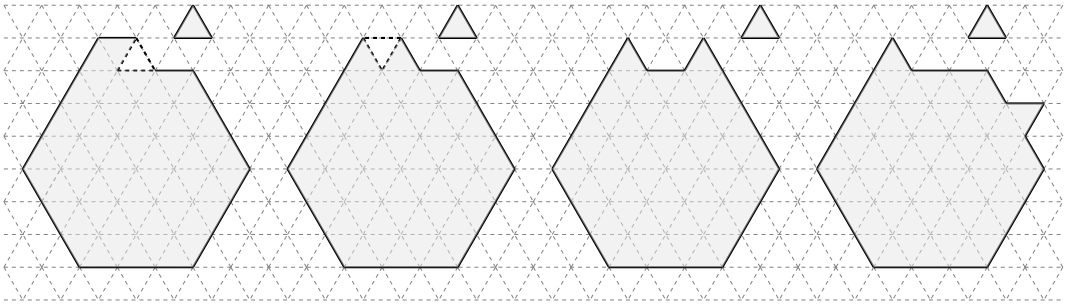

Figure 1.28 – From the left to the right we depict in light grey the possible configurations belonging to $\mathcal{X}_{A_1^*-1}$ and crossed by an optimal path. In dashed dark grey, we depict the future position of the free particle to cover the angle of $\frac{5}{3}\pi$ in the first two examples.

For point (ii), we need to introduce the set $\mathcal{E}_{B_i}(r)$, which contains the configurations having a unique cluster with a shape of quasi–regular hexagon, that is a regular hexagon with i bars attached clockwise. See Figure 1.27, where on the left (resp. right) we depict a configuration in $\mathcal{E}_{B_1}(4)$ (resp. $\mathcal{E}_{B_4}(3)$). Then the proof proceeds in three steps:

1. If $\delta \in (0, \frac{1}{2})$ (resp. $\delta \in (\frac{1}{2}, 1)$), prove that any $\omega \in (\hexagon \to \hexagonblack)_{opt}$ must pass through a configuration $\mathcal{E}_{B_5}(r^*)$ (resp. $\mathcal{E}_{B_1}(r^*+1)$).
2. If $\delta \in (0, \frac{1}{2})$ (resp. $\delta \in (\frac{1}{2}, 1)$), prove that any $\omega \in (\hexagon \to \hexagonblack)_{opt}$ must pass through a configuration having cluster belonging to the set $\mathcal{E}_{B_5}(r^*)$ (resp. $\mathcal{E}_{B_1}(r^*+1)$). with the addition of two particles
3. Any $\omega \in (\hexagon \to \hexagonblack)_{opt}$ must reach the energy level Γ_H^*.

To prove these three points, we consider separately the cases $\delta \in (0, \frac{1}{2})$ and $\delta \in (\frac{1}{2}, 1)$. To give an idea of the proofs, here we focus only on the case $\delta \in (0, \frac{1}{2})$. To prove point 1, the idea is the following. By denoting by $\widetilde{A}$ the number of particles of the configurations in $\mathcal{E}_{B_5}(r^*)$ and by using an isoperimetric–type argument carried out in [4], we deduce that in $\mathcal{V}_{\widetilde{A}}$ the unique (modulo translations and rotations) configuration of minimal perimeter, and hence minimal energy, is the one in $\mathcal{E}_{B_5}(r^*)$. Since

$$\widehat{H}(\mathcal{E}_{B_5}(r^*)) = \Gamma_H^* - 3\Delta + 2U,$$

any other configuration in $\mathcal{V}_{\widetilde{A}}$ has energy at least $\Gamma_H^* - 3\Delta + 3U$. To increase the particle number starting from any such configuration, a particle must be created at cost Δ. But the resulting configuration would have energy $\Gamma_H^* - 2\Delta + 3U$, which exceeds Γ_H^* due to the condition $2\Delta < 3U$. Thus, this would let to a path exceeding the energy value Γ_H^* and therefore the path would not be optimal. Note that $\widetilde{A} = A_1^* - 3$. Thanks to point 1, to prove point 2 we argue as follows. Since the path has to cross $\mathcal{V}_{A_1^*-1}$, starting from a quasi–regular hexagon with area $A_1^* - 3$, a free particle is created giving rise to a configuration with energy $\Gamma_H^* - 2\Delta + 2U < \Gamma_H^*$. Before any new free particle is created, the energy has to decrease by at least U. The unique way to do so this is to move the particle towards the cluster and attach it to the quasi–regular hexagon, which lowers the energy to $\Gamma_H^* - 2\Delta + U$. Now it is possible to create another particle at cost Δ giving rise to a configuration with energy $\Gamma_H^* - \Delta + U < \Gamma_H^*$. Again, before creating a new free particle, the energy has to decrease by at least U. The unique way to do so this is to move the particle until it is attached to the cluster, which lowers the energy to $\Gamma_H^* - \Delta$. This gives us a configuration η composed by a cluster belonging to $\mathcal{E}_{B_5}(r^*)$ with the addition of two particles, as claimed. To conclude the argument with point 3, we use again an isoperimetric–type argument carried out in [4], which ensures that the minimal energy in $\mathcal{V}_{A_1^*-1}$ is realized, altough not uniquely, in a configuration as η above. Since it is not possible to reduce the energy without lowering the particles number and any further move to increase the particles number involves the creation of a new particle, the energy must reach the value Γ_H^*.

Finally, thanks to points 2 and 3 above, to get (iii) we need to prove that any optimal path connecting $\hexagon$ to $\hexagonblack$ crosses the set $\mathcal{V}_{A^*-1}$ in a configuration belonging to $\mathcal{K}(A^*-1)$ (recall

(1.3.68)) before a new particle is created, giving rise to a configuration in $\mathcal{C}^*$. This part of the proof is technical and requires a detailed analysis. Indeed, point 2 above does not tell us how the two additional particles are attached to the quasi–regular hexagonal cluster, see for instance Figure 1.28 for four admissible examples when $\delta \in (0, \frac{1}{2})$. Note that in the first two examples it is possible to attach the free particle lowering the energy by $2U$, while in the other two cases the energy decreases by U only. This is responsible for a different behavior of the dynamics in these two cases. Indeed, the first two configurations belong to the set $\mathcal{K}(A_1^* - 1)^{fp}$, while the others do not. The idea of the proof is that, when the dynamics reaches a configuration different from the first two represented in Figure 1.28, then it cannot directly reach the cycle of the stable state, but it has to rearrange the clusterized particles to get a configuration in $\mathcal{K}(A_1^* - 1)^{fp}$. This will prove the desired statement.

Remark 1.3.6. *We emphasize that the result concerning the gate that we obtain is different from [35, Proposition 2.3.7]. Indeed, on the square lattice the authors were able to prove that any optimal path from the metastable to the stable state reaches a square or quasi-square shape, then a protuberance is attached and finally a free particle enters the box. However, points 2 and 3 do not suffice to characterize the entrance in the gate. Indeed, several mechanisms to enter the gate appear on the hexagonal lattice. Clearly, one of these possibilities is to add a free particle starting from a configuration in $\mathcal{K}(A_i^* - 1)$. But there are many other ways to enter $\mathcal{K}(A_i^* - 1)^{fp}$. For example, suppose that $0 < \delta < \frac{1}{2}$ and an optimal path $\omega : \hexagon \to \hexagonfull$ crosses a configuration η of the type of the third cluster depicted in Figure 1.28. Starting from such η, it is possible that the free particle is attached to the cluster in such a way that it forms an elementary rhombus together with a triangular face already attached. Thus, the energy reaches the value $\Gamma_H^* - U$. Thus, it is possible to move the other triangular face at cost U and, when it is detached, the path ω crosses a configuration in $\mathcal{K}(A_1^* - 1)^{fp}$, but the path does not cross the set $\mathcal{K}(A_1^* - 1)$. With this example we want to put the attention on the fact that several mechanisms to enter the gate appear due to the particular shape of the lattice. Indeed, on the square lattice it does not matter which side the protuberance is attached to because it is possible to move it along the side at zero cost.*

The last result that we have proven is a first step towards the characterization of the tube of typical trajectories, which is out of the scope of this thesis. In particular, we characterize subcritical and supercritical quasi-regular hexagons, i.e., subcritical quasi-regular hexagons shrink to $\hexagon$, while supercritical quasi-regular hexagons grow to $\hexagonfull$ in the following sense. Let $\mathcal{E}^-_{B_i}(r)$ (resp. $\mathcal{E}^+_{B_i}(r)$) be the set of configurations composed by a single quasi-regular hexagon contained in (resp. containing) $\mathcal{E}_{B_i}(r)$. The following statements hold:

(i) When $\delta \in (0, \frac{1}{2})$, we have

$$\begin{aligned} &\text{if } \eta \in \mathcal{E}^-_{B_5}(r^*) \quad \Longrightarrow \lim_{\beta\to\infty} \mathbb{P}_\eta(\tau_{\hexagon} < \tau_{\hexagonfull}) = 1, \\ &\text{if } \eta \in \mathcal{E}^+_{B_0}(r^* + 1) \quad \Longrightarrow \lim_{\beta\to\infty} \mathbb{P}_\eta(\tau_{\hexagonfull} < \tau_{\hexagon}) = 1. \end{aligned} \tag{1.3.69}$$

(ii) When $\delta \in (\frac{1}{2}, 1)$, we have

$$\begin{aligned} &\text{if } \eta \in \mathcal{E}^-_{B_1}(r^* + 1) \quad \Longrightarrow \lim_{\beta\to\infty} \mathbb{P}_\eta(\tau_{\hexagon} < \tau_{\hexagonfull}) = 1, \\ &\text{if } \eta \in \mathcal{E}^+_{B_2}(r^* + 1) \quad \Longrightarrow \lim_{\beta\to\infty} \mathbb{P}_\eta(\tau_{\hexagonfull} < \tau_{\hexagon}) = 1. \end{aligned} \tag{1.3.70}$$

The proof relies on the notion of cycle, recall (1.3.34). To prove (i) and (ii) we need [92, Theorem 3.2], which states that every state in a cycle is visited by the process before the exit with high probability. Using this result, we need to prove the following:

1. When $0 < \delta < \frac{1}{2}$, then
   (i) if η is a quasi-regular hexagon contained in $\mathcal{E}_{B_4}(r^*)$, then there exists a cycle $\mathcal{C}^{\hexagon}_{\hexagonfull}(\Gamma_H^*)$ containing η and $\hexagon$ and not containing $\hexagonfull$;
   (ii) if η is a quasi-regular hexagon containing $\mathcal{E}_{B_0}(r^* + 1)$, then there exists a cycle $\mathcal{C}^{\hexagonfull}_{\hexagon}(\Gamma_H^* - \widehat{H}(\hexagonfull))$ containing η and $\hexagonfull$ and not containing $\hexagon$;
2. When $\frac{1}{2} < \delta < 1$, then
   (i) if η is a quasi-regular hexagon contained in $\mathcal{E}_{B_0}(r^* + 1)$, then there exists a cycle $\mathcal{C}^{\hexagon}_{\hexagonfull}(\Gamma_H^*)$ containing η and $\hexagon$ and not containing $\hexagonfull$;

(ii) if η is a quasi-regular hexagon containing $\mathcal{E}_{B_2}(r^* + 1)$, then there exists a cycle $\mathcal{C}^{\hexagon}_{\hexagon}(\Gamma^*_H - \widehat{H}(\hexagon))$ containing η and $\hexagon$ and not containing $\hexagon$.

This can be achieved by means of the reference path ω^* introduce above. For all the technical details we refer to Section 6.3.6.

1.3.4 *Towards the original model: the role of the entropy*

In this section we come back to the original model introduced in Section 1.3.1, namely, particles now live and evolve on a square box whose size grows exponentially in the inverse temperature β. We are interested in how the gas *nucleates* in large volumes, i.e., how the particles form and dissolve subcritical droplets until they manage to build a critical droplet that is large enough to trigger the nucleation. The analysis of this model is much harder than that of the local model, because now particles are conserved in all the domain and a detailed control of the interaction between droplets and the gas of "isolated particles" is needed.

In this setting the role of the *entropy* turns out to be crucial. The notion of entropy enters into every attempt to explain metastability. Indeed, one can argue that metastable states are determined by the *maximum entropy* (or minimum free energy) principle under suitable constraints. The decay from the metastable to the stable state is a typical thermodynamic irreversible process towards the absolute maximum of entropy (or absolute minimum of free energy). The transition towards stability is a large–deviation phenomenon that can be described in terms of suitable rate functions. The exit from metastability to stability is, in general, intrinsically random. For physically relevant systems the transition mechanism involves what can be called time entropy: the transition takes place after long random waiting times inside suitable *permanence sets*, which are regions inside the state space built as the connected unions of cycles. Spatial entropy comes into play: in large volumes, even at low temperatures, entropy is competing with energy because the metastable state and the states that evolve from it under the dynamics have a non-trivial spatial structure. If we want to understand the behaviour of such systems, then a coarse–grained description becomes imperative, since on the microscopic level the competition between energy and entropy does not allow for a proper understanding of metastable states and their transition paths.

The problem of nucleation for Kawasaki dynamics in large volumes is tackled in a series of three works. We adopt the point of view that the identification of "tube of typical trajectories" is the key towards getting full control on the metastable crossover. Already in the early mathematical papers on metastability [39, 95, 96, 107], and later in papers on Kawasaki dynamics in finite volume [67, 75], the main strategy was to identify sets of configurations of *increasing regularity* that are *resistant* to the dynamics on corresponding increasing time scales. These sets of configurations form the backbone in the construction of the "tube of typical trajectories". In particular, the idea was to define temporal configurational environments within which the trajectories of the process remain confined with high probability on appropriate time scales. This approach involves an analysis of all the possible evolutions of the process, and requires the exclusion of rare events via large deviation a priori estimates.

In the first paper [65] the authors proved an *ideal gas approximation*, i.e., they showed that the dynamics is well approximated by a process of *Independent Random Walks* (IRWs). Indeed, if the lattice gas is sufficiently rarefied, then each particle spends most of its time moving like a random walk. When two particles occupy nearest–neighbour sites, the binding energy inhibits their random walk motion, and these pauses are long when the temperature is low. However, if the time intervals in which a particle is interacting with the other particles are short compared to the time intervals in which it is free, then the interaction can be represented as a small perturbation of a free random walk motion. The most challenging situation is when the temperature and the density of the gas tends to zero simultaneously, which is precisely our case. The reason is that low temperature corresponds to strong interaction, so that the ideal gas approximation is far from trivial. This is also the more interesting situation from a physical point of view. Indeed, $e^{-2U\beta}$ is the density of the saturated gas at the condensation point, see [76]. For densities smaller than this, namely, $\Delta > 2U$, we have a stable gas so rarefied that it behaves like an ideal gas *up to very large times*. If we pick $\Delta < U$, we get an unstable gas, which behaves like an ideal gas only *up to short times*. If we pick $U < \Delta < 2U$, avoiding the appearance of droplets of the liquid phase, we get a metastable gas. In this

regime we still have a rarefied gas, and the authors proved that it behaves like an ideal gas *up to relatively large times*. The ideal gas is represented by a process of IRWs and the ideal gas approximation is described by a process of *Quasi–Random Walks* (QRWs), which is defined as follows. It consists of a process of N labelled particles that can be coupled to a process of N IRWs in such a way that the two processes follow the same paths outside rare time intervals, called *pause intervals*, in which the paths of the QRW–process remain confined to small regions. In the metastable regime, typically some pauses are much shorter than $e^{\Delta\beta}$, while others are much longer. The authors showed that the low–density Kawasaki dynamics with labelled particles is a QRW–process. We encourage the reader to inspect the main properties of QRWs, which will be a key tool for the analysis of this model. In particular, we refer to [62, Theorems 3.2.3, 3.2.4, 3.2.5, 3.3.1] for the *non-superdiffusivity* property and for upper and lower bounds on the *spread-out property*, respectively.

Let us now discuss the main difficulties arising in analyzing a fully conservative dynamics by showing the differences appearing with respect to the local and the simplified model. On the one hand, in the local model (see Section 1.3.2) particles move according to Kawasaki dynamics only insite a finite box Λ_0 and at the boundary particles are created and annihilated. Thus, there is no effect of the droplets in Λ_0 on the gas outside Λ_0. Concerning the simplified model (see Section 1.3.1), the gas reservoir now consists of IRWs. The total number of particles is fixed and this model is well approximated by the local model for $\beta \to \infty$ as far as its metastable behaviour is concerned, see [75]. Note that the gas outside Λ_0 influences the Kawasaki gas inside Λ_0 and vice versa. This mutual influence was described by means of QRWs: the gas particles perform random walks, interspersed with pause intervals during which they interact with the other particles, and interspersed with jumps corresponding to the difference between the positions of the particle at the end and at the beginning of a pause interval. Due to the fact that Λ_0 is finite, the jumps are small with respect to the displacement of the random walks on time scales that are exponentially large in β. Moreover, the number of pause intervals is controlled by the rare returns of the random walk to Λ_0. These two ingredients —few pause intervals and small jumps— were sufficient to control the dynamics. For what concerns the fully conservative model, as long as the clusters are small, we may expect the jumps in the QRWs to be small: at most of the order of the size of the clusters. The crucial obstacle in approximating the gas particles by QRWs is that the interaction acts everywhere. Particles must arrive from or return to the gas, which acts as a reservoir, and therefore the dynamics is not really local. Thus, it is not possible to decouple the dynamics of the particles inside Λ_0 from the dynamics of the gas outside Λ_0. Therefore we need to replace the control on the rare returns of a random walk to a fixed finite box by a control on the number of particle–particle and particle–cluster collisions. This is achieved with the help of non–collision estimates developed in [61].

In this thesis, which corresponds to the second work of the series, we use the results in [65] to analyse how subcritical droplets form and dissolve on multiple space-time scales when the volume is *moderately large*, namely, $\Theta < 2\Delta - U$. In large volumes the possible evolutions of the Kawasaki lattice gas are much more involved than in small volumes, and multiple events must be considered and controlled compared to the case of finite volume treated earlier. In particular, it is important to control the *history* of the particles. For this reason we introduce several new tools, such as assigning colours to the particles that summarises information about how they interacted with the surrounding gas in the past. The focus remains on the "tube of typical trajectories", even though the control of all the possible evolutions of the Kawasaki lattice gas requires the use of multiple graphs describing multiple temporal configurational environments. These graphs will be identified in Section 7.5, which is the core of this analysis and contains the proofs of all the principal lemmas.

Finally, in the follow–up paper [12], which is the last in a series of three papers dealing with Kawasaki dynamics in large volumes, we consider the setting where the volume is *very large*, namely, $\Theta < \Gamma^* - (2\Delta - U)$ (recall that Γ^* is the energy of the critical droplet in the local model), and use the results in the first two papers [11, 62] to identify the *nucleation time*. The outcome of the three papers together shows the following:

(1) Subcritical droplets behave as Quasi-Random Walks, see [65].

(2) Most of the time the configuration consists of *quasi-squares* and *free particles*. That is why we use the terminology *droplet dynamics*. The crossover time between configurations of this type is identified on a time scale that is exponential in β (see Theorem 7.1.2).
(3) Starting from configurations consisting of quasi-squares and free particles, the dynamics typically *resist*, i.e., the dimensions of the quasi-squares do not change, for an exponential time scale in β depending only on the dimensions of the smallest quasi-square (see Theorem 7.1.3).
(4) Starting from configurations consisting of quasi-squares and free particles, the dynamics typically either creates a larger quasi-square or a smaller quasi-square, depending on the dimensions of the starting quasi-square (see Theorem 7.1.5). There is a non-negligible probability that a *subcritical* quasi-square follows an *atypical* transition, in that it grows a larger quasi-square, and this lets the dynamics *escape from metastability* (see Theorem 7.1.6).
(5) The crossover from the gas to the liquid (= nucleation) occurs because a *supercritical quasi-square* is created somewhere in a moderately large box and *subsequently grows into a large droplet*. This issue will be addressed in [12].
(6) The configurations in moderately large boxes behave as if they are *essentially independent* and as if the surrounding gas is *ideal*. No information travels between these boxes on the relevant time scale that grows exponentially fast with β. The supercritical quasi-square appears more or less independently in different boxes, a phenomenon referred to as *homogeneous nucleation*. This issue will be addressed in [12].
(7) The *tube of typical trajectories leading to nucleation* is described via a series of events on which the evolution of the gas consists of *droplets wandering around on multiple space-time scales*. This control is achieved via what we call the *deductive approach* in Section 7.5.
(8) The asymptotics of the nucleation time is identified on a time scale that is exponential in β and depends on the *entropic factor* related to the size of the box. This issue will be addressed in [12].

We will see that in the metastable regime $\Delta \in (U, 2U)$ small droplets with "side length" smaller than a critical length will have a tendency to shrink, while large droplets will have a tendency to grow. We will refer to the former as *subcritical droplets* and to the latter as *supercritical droplets*. The initial configuration η_0 is chosen according to the *restricted* measure $\mu_{\mathcal{R}}$, which is the grand-canonical Gibbs measure associated with H and conditioned to $\mathcal{R}$, i.e., *conditioned on all the droplets in Λ_β being subcritical*. More precisely, recalling the definition of the critical length for the local model ℓ_c given in (1.3.21), we define

$$\mathcal{R} := \{\eta \in \mathcal{X}_\beta : \text{all clusters of } \eta \text{ have volume less than } \ell_c(\ell_c - 1) + 2\} \tag{1.3.71}$$

and the restricted measure $\mu_{\mathcal{R}}$ is defined as

$$\mu_{\mathcal{R}}(\eta) = \frac{e^{-\beta[H(\eta)+\Delta|\eta|]}}{Z_{\mathcal{R}}} \mathbb{1}_{\mathcal{R}}(\eta), \qquad \eta \in \mathcal{X}_\beta, \tag{1.3.72}$$

where

$$Z_{\mathcal{R}} = \sum_{\eta \in \mathcal{R}} e^{-\beta[H(\eta)+\Delta|\eta|]}. \tag{1.3.73}$$

To describe the evolution of our system in terms of a droplet dynamics, we will show that on an appropriate time scale the dynamics typically returns to the set of configurations consisting of quasi-square droplets, provided the volume is not too large. The main results of this thesis allow such a description of the dynamics in terms of growing and shrinking wandering droplets. As part of the nucleation process, droplets grow and shrink by exchanging particles with the gas surrounding them, as is typical for a conservative dynamics. In particular, we will identify the main growing and shrinking rates for these droplets up to a time horizon going beyond the exit of $\mathcal{R}$: up to the formation of a first large droplet with volume of order $\lambda(\beta)$, with λ a slowly increasing but unbounded function. In the follow-up paper [12], these theorems will be used to identify the nucleation time, i.e., the time of exit of $\mathcal{R}$. Our theorems only concern the *initial phase* of the nucleation, until the critical droplet grows into a droplet that is roughly $\sqrt{\lambda(\beta)}$ times the size of the critical droplet. They provide no information on

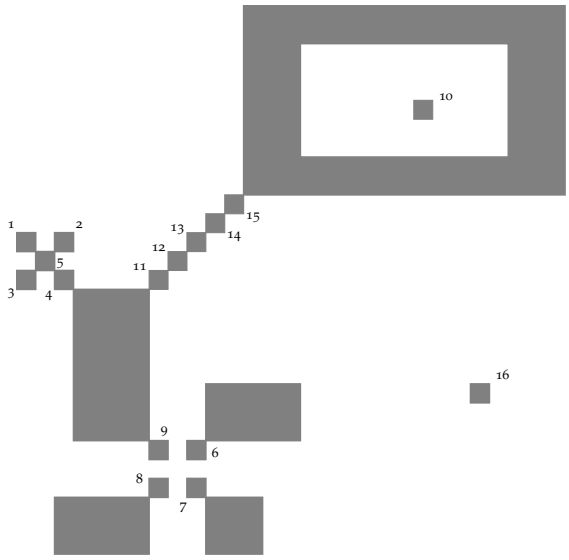

Figure 1.29 – Each particle is represented by a unit square. A particle is clusterised when it is part of a cluster. A particle is free when it is not touching any other particles and can be moved to infinity by moving non–clusterised particles only. Particles 1–5 and 16 are free, particles 6–9, 10, 11–15 are not free. All other particles are clusterised.

what happens *afterwards*, when the droplet grows even further and becomes macroscopically large. In that regime the gas around the droplet becomes depleted, smaller droplets move around and coalesce into larger droplets, etc. It remains a major challenge to describe what precisely happens in this regime, which lies *beyond* metastability.

To make precise the time horizon we are interested in, we need the following definitions. We set

$$\mathcal{R}' := \left\{ \eta \in \mathcal{X}_\beta : \begin{array}{l} \text{all clusters of } \eta \text{ have volume at most } \ell_c(\ell_c - 1) + 2 \\ \text{except for at most one cluster with volume less than } \frac{1}{8}\lambda(\beta) \end{array} \right\}, \tag{1.3.74}$$

where $\lambda(\beta)$ is an unbounded but slowly increasing function of β satisfying

$$\lambda(\beta) \log \lambda(\beta) = o(\log \beta), \qquad \beta \to \infty, \tag{1.3.75}$$

e.g. $\lambda(\beta) = \sqrt{\log \beta}$. For $C^\star > 0$ large enough, our theorems will hold up to time $T^\star$ defined as

$$T^\star = e^{C^\star \beta} \wedge \min\{t \geqslant 0 : X(t) \notin \mathcal{R}'\}. \tag{1.3.76}$$

We will see in [12] that our dynamics starting from $\mu_{\mathcal{R}}$ typically exits $\mathcal{R}'$ within a time that is exponentially large in β, and with a probability tending to 1 does so through the formation of a single large cluster $\mathcal{C}$ of volume $\frac{1}{8}\lambda(\beta)$, rather than through two supercritical droplets. Hence, $T^\star$ indeed coincides with the appearance time of $\mathcal{C}$, provided $C^\star$ is large enough.

As in [62], the notion of active and sleeping particle will be crucial throughout this analysis. Since the precise definition requires additional notations, we give here an intuitive description only. For precise definitions we refer to Section 7.4.3.1.

The division of particles into active and sleeping is related to the notion of free particles, which is slightly different for the original model with respect to that in the local model. Intuitively, a particle is *free* if it does not belong to a cluster (= a connected component of nearest-neighbour particles) and can be moved to infinity without clusterisation, i.e., by moving non-clusterised particles only (see Figure 1.29). Let

$$D = U + d,$$

with $d > 0$ sufficiently small. For $t > e^{D\beta}$, a particle is said to be *sleeping* at time t if it was not free during the time interval $[t - e^{D\beta}, t]$. Non-sleeping particles are called *active*. (Note that being active or sleeping depends on the history of the particle.) By convention, we say

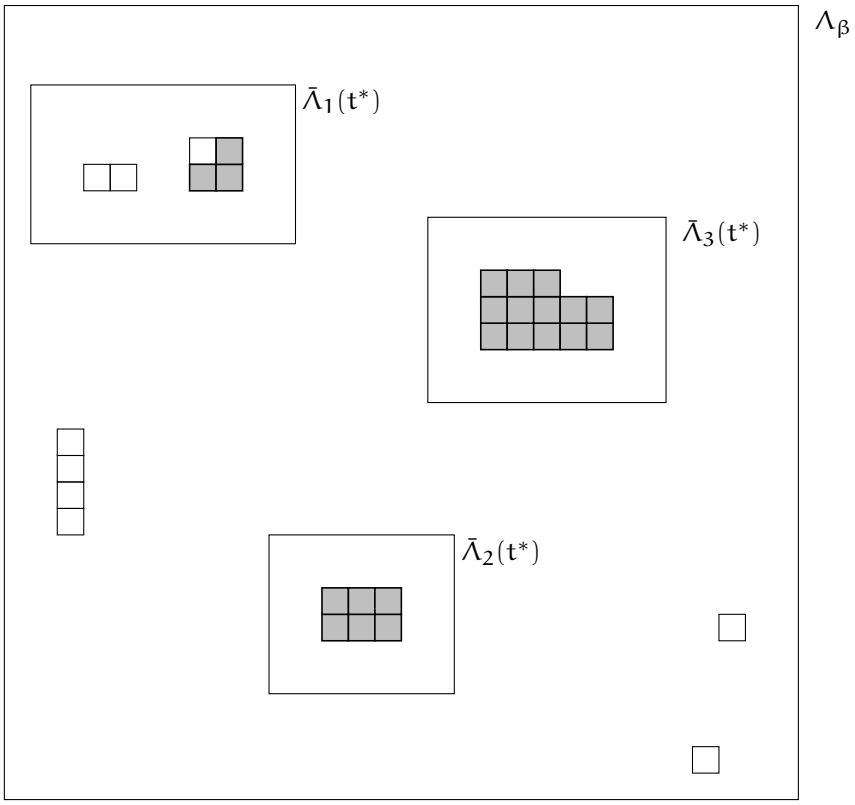

Figure 1.30 – An example of local boxes $\bar\Lambda(t^*) = (\bar\Lambda_i(t^*))_{1\leqslant i\leqslant 3}$ for $t^* > 0$, where the gray and the white particles are sleeping, respectively, active.

that prior to time $e^{D\beta}$ sleeping particles are those that belong to a large enough *quasi-square*, where quasi-squares are clusters with sizes $\ell_1 \times \ell_2$ in the set

$$QS = \{(\ell_1, \ell_2) \in \mathbb{N}^2 \colon\ \ell_1 \leqslant \ell_2 \leqslant \ell_1 + 1\}. \tag{1.3.77}$$

In order to declare all the particles in the quasi-square as sleeping before time $e^{D\beta}$ we require that $\ell_1 \geqslant 2$.

To define a finite box Λ as the union of a finite number k of disjoint local boxes $\bar\Lambda_i$, $1 \leqslant i \leqslant k$, in analogy with the local model introduced in [75], we associate with each configuration a local configuration

$$\bar\eta \in \{0,1\}^{\bar\Lambda} = \prod_{1\leqslant i\leqslant k} \{0,1\}^{\bar\Lambda_i},$$

which we identify with $\{0,1\}^\Lambda$. These local boxes allow us to control the global properties of the gas in terms of its local properties, namely, via the duality between gas and droplets, which is represented by the duality between active and sleeping particles, respectively. First, the local boxes have to contain all the sleeping particles. Second, the local boxes are dynamic, namely, $\bar\Lambda_i = \bar\Lambda_i(t)$. Indeed, droplets can move and we want to avoid seeing sleeping particles outside of the local boxes. In particular, the boxes follow the droplets, i.e., must be redefined only when the following events occur: two droplets are too close to each other, or a cluster is too close to the boundary of a box, or a particle outside the boxes falls asleep, or particles in a box all turn active. At any time $t \geqslant 0$, we require that the collection of the $k(t)$ local boxes $\bar\Lambda(t) = (\bar\Lambda_i(t))_{1\leqslant i\leqslant k(t)}$ satisfy the afore mentioned conditions. We refer to Définition 7.1.1 for the technical details. See Figure 1.30 for an example of local boxes.

Since at each time t all the sleeping particles belong to $\bar\Lambda(t)$, the boxes induce a partition of the sleeping particles. We say that a *coalescence occurs at time* t if there exist two sleeping particles that are in different local boxes at time t^-, but are in the same local box at time t, i.e., if there exist $1 \leqslant i_1, i_2 \leqslant k(t^-)$, $i_1 \neq i_2$, $1 \leqslant i^* \leqslant k(t)$ and two sleeping particles s_1, s_2 such that $s_j \in \bar\Lambda_{i_j}(t^-)$ and $s_j \in \bar\Lambda_{i^*}(t)$, $j = 1, 2$. This phenomenon is related to the

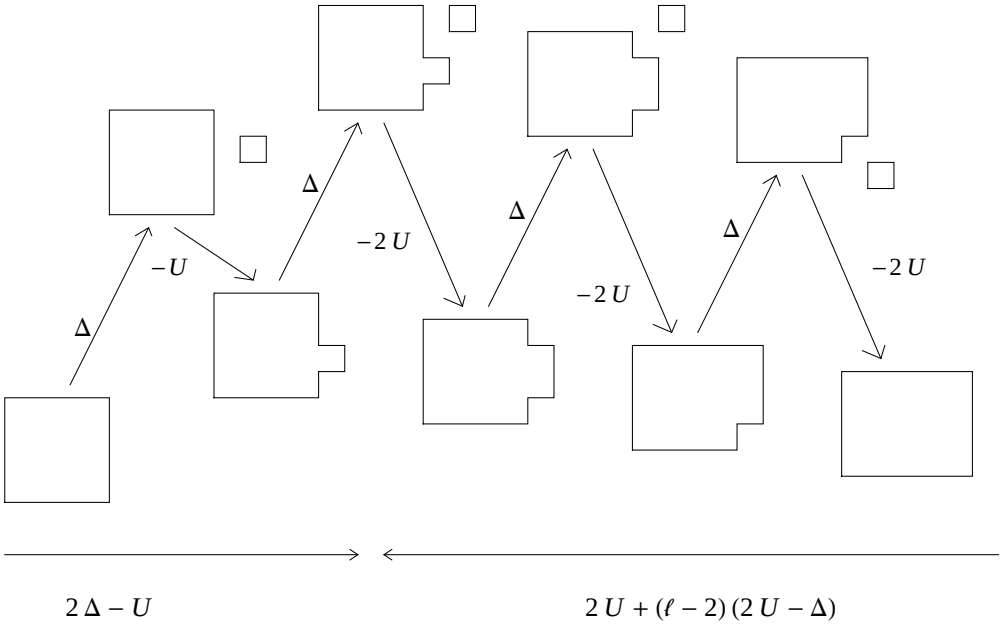

Figure 1.31 – Cost of adding or removing a row of length ℓ in a finite volume.

possibility that two droplets join to form a single larger droplet. Coalescence is difficult to control quantitatively, which is why in the present work we limit ourselves to what happens *in the absence of coalescence*. In the follow-up paper [12] we show that metastable nucleation is unlikely to occur via coalescence.

Let $\mathcal{X}_{\Delta^+}$ be the set of configurations without droplets or with droplets that are quasi-squares with $\ell_1 \geqslant 2$ (and with additional regularity conditions on the gas surrounding droplets to be specified in Définition 7.2.9). Let $\mathcal{X}_E$ be the set of configurations in $\mathcal{X}_{\Delta^+}$ without droplets (see (7.3.1) and Définition 7.2.9). Define $(\bar{\tau}_k)_{k\in\mathbb{N}_0}$ as the sequence of return times in $\mathcal{X}_{\Delta^+}$ after an active particle is seen in Λ, where $\bar{\tau}_0$ is the first hitting time of $\mathcal{X}_{\Delta^+}$. See (7.1.5) for the precise definition. Recall that $|\Lambda_\beta| = e^{\Theta\beta}$. We assume that $\Delta < \Theta \leqslant \theta$, with θ defined as follows. Let $\varepsilon = 2U - \Delta$, and let $r(\ell_1, \ell_2)$ be the *resistance* of the $\ell_1 \times \ell_2$ quasi-square with $1 \leqslant \ell_1 \leqslant \ell_2$ given by (see Figure 1.31)

$$\begin{aligned} r(\ell_1, \ell_2) &= \min\{(\ell_1 - 2)\varepsilon + 2U, 2\Delta - U\} \\ &= \min\{(2U - \Delta)\ell_1 - U + 2\Delta - U, 2\Delta - U\}. \end{aligned} \tag{1.3.78}$$

Let $\theta = 2\Delta - U - \gamma$ be the resistance of the largest subcritical quasi-square. Since this quasi-square has sizes $(\ell_c - 1) \times \ell_c$, we have $2\Delta - U - \gamma = 2U + ((\ell_c - 1) - 2)\varepsilon$, so that

$$\gamma = \Delta - U - (\ell_c - 2)\varepsilon. \tag{1.3.79}$$

We will see that $\gamma > 0$ is an important parameter. The previously mentioned regularity conditions on the gas use an extra parameter $\alpha > 0$ (see below Définition 7.2.9), which can be chosen as small as desired. Since we defined $D = U + d$, Δ^+ is defined by $\Delta^+ = \Delta + \alpha$. Call a function $f(\beta)$ superexponentially small, written $\mathrm{SES}(\beta)$, if

$$\lim_{\beta\to\infty} \frac{1}{\beta} \log f(\beta) = -\infty. \tag{1.3.80}$$

MAIN THEOREMS: GROWING AND SHRINKING RATES OF DROPLETS

The main theorems we have derived control the transitions between configurations consisting of quasi-squares and free particles, the times scales on which these transitions occur, and the most likely trajectories they follow.

Theorem (I) Our first result describes the typical return times to the set $\mathcal{X}_{\Delta^+}$. In particular, we prove that, starting from $\mu_{\mathcal{R}}$, with probability $1 - \mathrm{SES}(\beta)$ it holds that the return times on the set $\mathcal{X}_{\Delta^+}$ are of order $e^{(\Delta+\alpha)\beta}$.

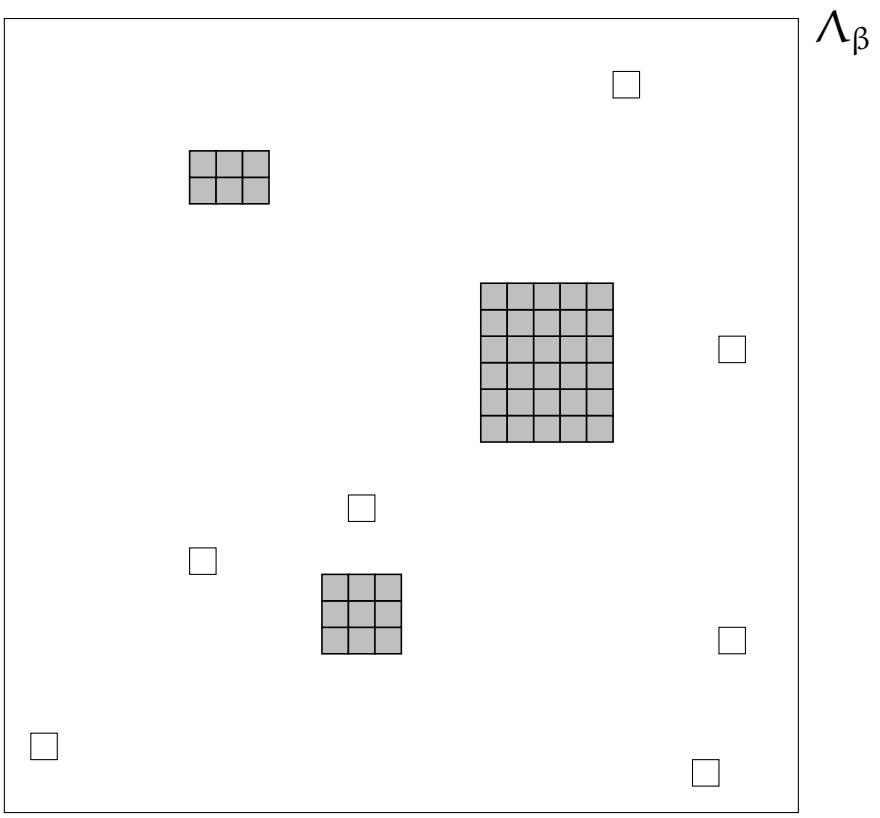

Figure 1.32 – An example of a configuration $\eta \in \mathcal{X}_{\Delta^+}$, where the gray and the white particles are sleeping, respectively, are active, such that $\pi(\eta) = \{(2,3),(3,3),(5,6)\}$.

Theorem (II) Our second theorem describes the typical update times for a configuration in $\mathcal{X}_{\Delta^+}$. Denoting by π a projection from $\mathcal{X}_{\Delta^+}$ to a finite space

$$\bar{\mathcal{X}}_\Delta = \bigcup_{k \geqslant 0} QS^1 \times \cdots \times QS^k, \tag{1.3.81}$$

where QS^i are the sizes of the quasi-square clusters contained in the local boxes $\bar{\Lambda}_i$ and are defined in (1.3.77). See Figure 1.32. We can define a dynamics on the space $\bar{\mathcal{X}}_\Delta$ of sizes of quasi-squares, arranged for example in increasing lexicographic order. For $i \in \mathbb{N}_0$, we denote by $(\ell_{1,i}, \ell_{2,i})$ in QS, with $\ell_{1,i} \geqslant 2$, the sizes of the smallest quasi-square at time $\bar{\tau}_i$, if any, and otherwise we set $\ell_{1,i} = \ell_{2,i} = 0$. Recall (1.3.78), and define the resistance of a configuration in $\mathcal{X}_E$ by

$$r(0,0) = 4\Delta - 2U - \theta. \tag{1.3.82}$$

We prove that, starting from $\mu_{\mathcal{R}}$ and unless a coalescence occurs, for any $i \in \mathbb{N}_0$ the projected dynamics typically remains in $\pi(X(\bar{\tau}_i))$ through successive visits in $\mathcal{X}_{\Delta^+}$ for a time of order $e^{r(\ell_{1,i},\ell_{2,i})\beta}$. Note that for $\ell_{1,i} \geqslant \ell_c$ all the quasi-squares have the same resistance $2\Delta - U$. For the case in which $X(\bar{\tau}_i)$ has no quasi-square, its resistance $r(0,0)$ involves the resistance of the empty configuration in the local model and a spatial entropy that comes from the position in Λ_β where the new droplet can appear.

Theorem (III) Our third result describes the typical transition of the system between two successive visits to $\mathcal{X}_{\Delta^+}$ conditional on the dynamics not returning to the same configuration at time $\bar{\tau}_{i+1}$. Given a configuration $X(\bar{\tau}_i) \in \mathcal{X}_{\Delta^+}$, define the typical transition π'_i as follows. For $\ell_{1,i} \geqslant \ell_c$, set

$$\begin{aligned}\pi'_i = \big\{\pi(\eta') \colon\ & \eta' \text{ is a configuration obtained from } X(\bar{\tau}_i) \\ & \text{by adding a row to an arbitrary quasi-square}\big\}.\end{aligned} \tag{1.3.83}$$

See Figure 1.33. For $\ell_{1,i} < \ell_c$, we need to distinguish between the cases $\ell_{2,i} \geqslant 3$, $\ell_{2,i} = 2$ and $\ell_{2,i} = 0$. If $\ell_{1,i} < \ell_c$ and $\ell_{2,i} \geqslant 3$ (respectively, $\ell_{2,i} = 2$), then we define π'_i as the singleton

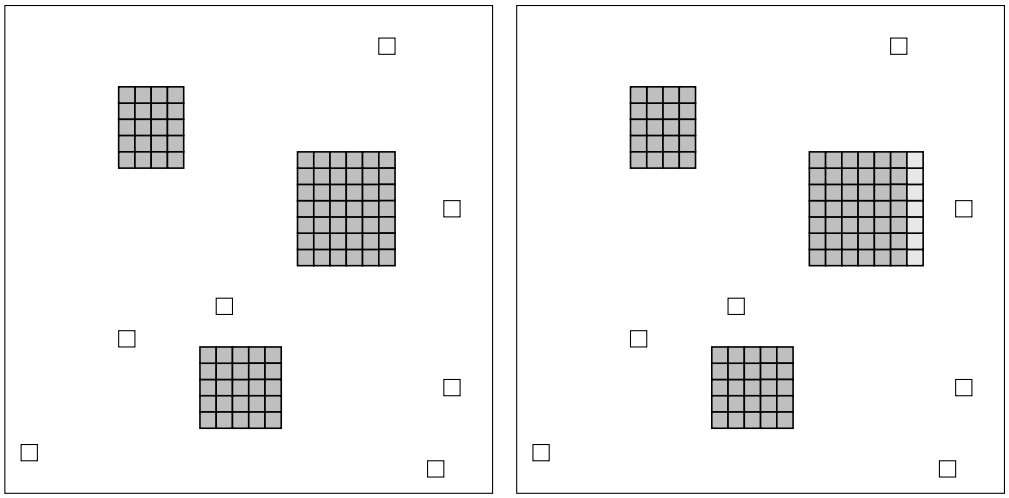

Figure 1.33 – For $\ell_c = 4$, on the left an example of a configuration $\eta \in \mathcal{X}_{\Delta^+}$ such that $\pi(\eta) = \{(4,5),(5,5),(6,7)\}$ and on the right one possible typical transition $\pi' = \{(4,5),(5,5),(7,7)\}$, where the gray and the white particles are sleeping, respectively, are active.

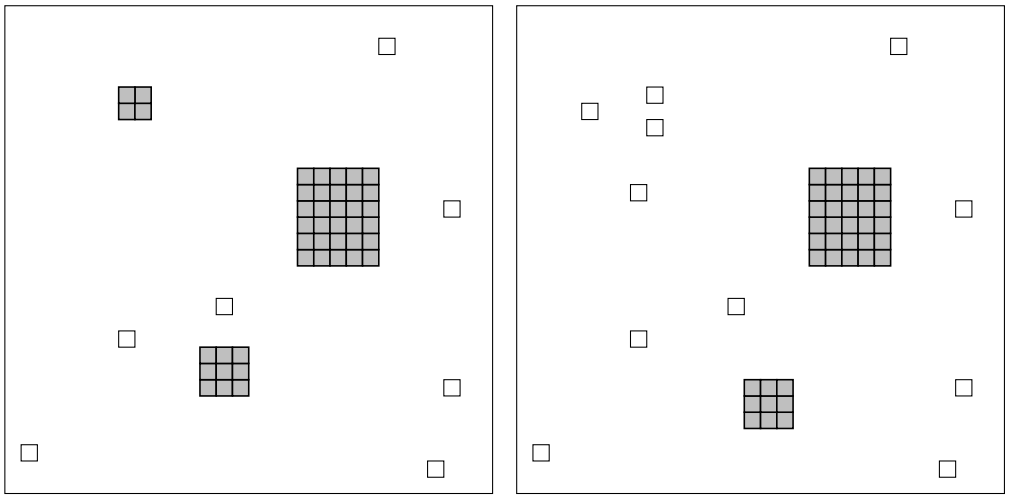

Figure 1.34 – On the left an example of a configuration $\eta \in \mathcal{X}_{\Delta^+}$ such that $\pi(\eta) = \{(2,2),(3,3),(5,6)\}$ and on the right the typical transition $\pi' = \{(3,3),(5,6)\}$, where the gray and the white particles are sleeping, respectively, are active.

made up of the collection of sizes of quasi-squares obtained from $\pi(X(\bar{\tau}_i))$ by modifying one of the smallest quasi-squares, which becomes $(\ell_{2,i} - 1) \times \ell_{1,i}$ (respectively, 0×0). If $\ell_{1,i} = \ell_{2,i} = 0$, then we define $\pi'_i = \{\pi(\eta')\}$, where η' is the configuration obtained from $X(\bar{\tau}_i)$ by creating a 2×2 square droplet, namely, $\pi'_i = \{(2,2)\}$. See Figure 1.34. Thus, we prove that

$$\lim_{\beta\to\infty} P_{\mu_{\mathcal{R}}}\left(\begin{array}{l}\text{if } \bar{\tau}_{i+1} \leqslant T^\star, \text{ then } \pi(X(\bar{\tau}_{i+1})) \in \pi'_i \text{ or} \\ \text{a coalescence occurs between } \bar{\tau}_i \text{ and } \bar{\tau}_{i+1}\end{array}\,\middle|\, \pi(X(\bar{\tau}_{i+1})) \neq \pi(X(\bar{\tau}_i))\right) = 1. \tag{1.3.84}$$

Theorem (IV) Our fourth and last theorem characterises the atypical transitions of the system, starting from a subcritical configuration consisting of a single quasi-square, between two successive visits to $\mathcal{X}_{\Delta^+}$, with no creation of new boxes and conditional on the dynamics not returning to the same configuration at time $\bar{\tau}_i$. To this end, given $X(\bar{\tau}_i) \in \mathcal{X}_{\Delta^+}$ with $2 \leqslant \ell_{1,i} < \ell_c$, we define $\pi''_i = (\ell_{2,i}, \ell_{1,i} + 1)$. This result provides a lower bound for the atypical transition of "going against the drift" in the case of a subcritical quasi-square. As we will show in the follow-up paper [12], the *escape from metastability* occurs via nucleation of a supercritical droplet somewhere in the box Λ_β. Indeed, we will characterize the time the dynamics needs to exit $\mathcal{R}$, as well as the typical paths of configurations visited by the

wandering cluster until the formation of a large droplet. The results of this thesis, which are limited to the case $\Theta < 2\Delta - U - \gamma$, will allow us to accomplish this task for larger values of Θ, namely, $\Theta < \Gamma^* - (2\Delta - U)$, where we recall that Γ^* is the energy of the critical droplet in the local model.

Remark 1.3.7. *The techniques developed in this thesis make it possible to prove that, for any quasi-square configuration of size $\ell_1 \times \ell_2$ in $\mathcal{X}_{\Delta^+}$, the cluster exits any finite box centered around the cluster with a volume that does not depend on β, within a time of order $e^{\Gamma(\ell_1,\ell_2)\beta}$. This is the reason why we speak of a* wandering cluster. *We will not state nor use this result as a formal theorem.*

The remainder of this section is devoted to provide the idea of the proofs of these four main theorems. The starting point is to formulate certain regularity properties for the initial configuration that we can impose because their failure is extremely unlikely. In particular, we introduce a subset of configurations $\mathcal{X}^* \subset \mathcal{X}_\beta$, which we refer to as the *typical environment*, with the property that if our system is started from the restricted ensemble, then it escapes from $\mathcal{X}^*$ within any time scale that is exponential in β only with a negligible probability, i.e.,

$$P_{\mu_{\mathcal{R}}}(\tau_{\mathcal{X}_\beta \setminus \mathcal{X}^*} \leqslant \mathsf{T}^\star) = \mathrm{SES}(\beta).$$

This result allows us to work with configurations in $\mathcal{X}^*$. Replacing the original dynamics by the dynamics restricted to $\mathcal{X}^*$, we can couple the two dynamics in such a way that they have the same trajectories up to any time that is exponential in β with probability $1 - \mathrm{SES}(\beta)$.

The basic idea to prove theorem (I) is to group configurations into a sequence of subsets of configurations of increasing regularity and prove a recurrence property to these sets on an increasing sequence of time scales, i.e, the dynamics reaches these sets within the reference time with probability $1 - \mathrm{SES}(\beta)$. This is a standard argument for metastable systems at low temperature, which has been carried out in full detail for a simplified version of our model [75]. Here we indicate the differences with respect to the earlier work. First, we emphasize that, alongside the local model, we need to introduce two additional sets to control the regularity of the gas surrounding the droplets. In addition, the local boxes now are not fixed, but they move with the droplets. Thus, a delicate control of them is needed: in particular, we have to control the probability that a new box is created within the reference time.

To prove Theorems (II)–(IV), we need to provide bounds on the probability of transitions between configurations consisting of quasi–square and free particles. In particular, providing upper bounds on the probability that typical and atypical transitions occur represents the main hurdles. Indeed, we need to control all the possible mechanisms to grow and shrink. These hurdles are organised into what we call the *deductive approach*: the tube of typical trajectories leading to nucleation is described via a series of events, whose complements have negligible probability, on which the evolution of the gas consists of *droplets wandering around on multiple space-time scales* in a way that can be captured by a coarse-grained Markov chain on a space of droplets.

1.4 METASTABILITY FOR NON–CONSERVATIVE SYSTEMS

Let us consider the example of a ferromagnetic system below the critical temperature. We let the system start from an equilibrium state when a positive external magnetic field has slowly switched off, and then we let it evolve, after having introduced a small negative magnetic field. We observe that the initial situation, which is characterized by a positive magnetization, persists for a long macroscopic time. In other words, the system instead of undergoing the right phase transition, remains for a long time in an apparently stationary situation until some external perturbation or some spontaneous large fluctuation will nucleate the new phase, starting an irreversible process leading the system to the true equilibrium phase, with negative magnetization. The above-described behavior is typical of an evolution that is non–conservative in the sense that the magnetization is not preserved. To model mathematically phenomena such as the one described above it is often proposed to use lattice models evolving according to Glauber dynamics since the dynamics does not conserve the total magnetization of the system. We emphasize that non–conservative dynamics have their peculiar features with respect to the conservative ones, and in the remainder of this section we aim at highlighting them.

1.4.1 *Glauber dynamics*

We consider a finite set of sites V. With each site we associate a spin value (-1 or $+1$) and we define the configuration space $\mathcal{X} = \{-1, +1\}^V$. We can associate with each configuration σ the Hamiltonian energy $\widetilde{H}(\sigma)$. Here we do not report the particular choice of the set V and the energy $\widetilde{H}(\sigma)$, because it changes depending on the phenomenon we want to model. This choice will be shown in Section 1.4.2 where we deal with the spread of an opinion inside a community. With β being the inverse temperature, we consider the usual single-flip Metropolis dynamics $(X_t)_{t\in\mathbb{N}}$ on $\mathcal{X}$ induced by $\widetilde{H}$. The transition probabilities of Glauber dynamics are therefore given by

$$P(\sigma,\eta) = q(\sigma,\eta)e^{-\beta[\widetilde{H}(\eta)-\widetilde{H}(\sigma]_+}, \quad \text{for all } \sigma \neq \eta, \tag{1.4.1}$$

where $[\cdot]_+$ denotes the positive part and $q(\sigma,\eta)$ is a connectivity matrix independent of β, defined, for all $\sigma \neq \eta$, as

$$q(\sigma,\eta) = \begin{cases} \frac{1}{|V|} & \text{if } \exists\, x \in V \text{ such that } \sigma^{(x)} = \eta, \\ 0 & \text{otherwise,} \end{cases} \tag{1.4.2}$$

where

$$\sigma^{(x)}(z) = \begin{cases} \sigma(z) & \text{if } z \neq x, \\ -\sigma(x) & \text{if } z = x. \end{cases} \tag{1.4.3}$$

This dynamics is *reversible* with respect to the Gibbs measure

$$\mu(\sigma) = Z^{-1}\exp(-\beta\widetilde{H}(\sigma)),$$

where $Z = \sum_{\sigma\in\mathcal{X}} \widetilde{H}(\sigma)$ is the normalizing constant, in the sense that our Markov chain $(X_t)_{t\in\mathbb{N}}$ satisfies the detailed balance condition.

1.4.2 *A model for opinion dynamics*

In this section, we focus on the Ising model as a first simple canonical model for public opinion dynamics, c.f. [109, 110], in presence of a binary choice. In this context, the state of a spin describes the current opinion of an individual, the external magnetic field captures the exposure to biased information and/or one-sided marketing/campaigning, and the couplings between neighboring spins model the effect of peer interactions on personal opinions. In Ising-like binary opinion models, the temperature of the system approximates all the more or less random events which may influence individuals' opinions but are not explicitly accounted for in the model, cf. [110]. In this thesis, we study the metastable behavior of the Ising model on a network with communities in the very low-temperature limit, which is instrumental to describe a situation where peer interactions and external factors have a strong influence on everyone's opinion. The low temperature favors homogeneous opinion patterns in which there are fewer individuals that disagree with the peers they interact with, which at a macroscopic level means that opinions become very rigid and hard to change, e.g., on a very polarizing issue.

The basic Ising model can be augmented to have more than two opinions and possibly asymmetric interactions between them, like in [111] where the authors consider an Ising–like model with three opinions but where the two most extreme opinions do not interact with each other. Since we are mostly interested in the interplay between opinion dynamics and network topology, in this thesis we focus on the simpler case of a binary opinion. The voter model is another Ising–like model to study the evolution of binary opinions which features a different (and possibly irreversible) majority update rule, see e.g. [8, 51, 94]. For a more broad review of mathematical and physical opinion dynamics models, we refer the interested reader to [114].

It is clear that assuming the underlying structure is a lattice or the complete graph is not ideal when modeling public opinion dynamics, since individuals have very heterogeneous social networks and interaction patterns. In particular, it is reasonable to assume that each individual has only a finite number of interactions and that he/she would tend to align more with the opinion of individuals in the community we belong to rather than that of complete strangers. Aiming to understand the role of the community structure in opinion dynamics, here we consider a very heterogeneous family of networks with very dense communities and very weak interactions between these communities. Various opinion dynamics models have been studied on networks with a community structure, e.g., [83, 108], but mostly by means of numerical simulations, while in this thesis we focus on rigorous mathematical results.

We are primarily interested in understanding the interplay between opinion dynamics and the community structure of the underlying network. Aiming to derive closed–form results, we choose a specific family of simple but prototypical clustered networks. More specifically, we consider the Ising model on a graph G consisting of k clusters of equal size, which are locally complete graphs, and such that each node is connected to a single node in each of the other clusters. With this choice, we obtain a network with very dense communities which are only sparsely connected to each other.

The structure of the network heavily influences both static (i.e., the configurations' energy) and dynamic properties (the likelihood of the system's trajectories) of the Ising model. In this setting, it is of interest to study the metastability or tunneling phenomena that the opinion dynamic model may exhibit. For instance, in presence of a positive external magnetic field, the metastable state of the system describes the diffusion of a second very rigid opinion which is not aligned with the mainstream one.

Informally, the metastable configurations are those in which the system persists for a long time before reaching one of the stable configurations, i.e., those minimizing the system's energy. In the context of the clustered network that we consider in this thesis, the set of metastable states heavily depends on the relative strength of the interactions between the network communities and that of the external magnetic field. In absence of an external magnetic field, the two opinions are equally likely and the two homogeneous opinion patterns are both stable states. In this case, it is still interesting to study how, starting with all individuals agreeing on one opinion, the whole network can transition to the opposite opinion, how long this will take and what are the most likely trajectories of this process.

Formally, for every $k \geqslant 2$ and every $n \geqslant 2$ we consider an undirected graph $G = \mathcal{G}(k, n)$ consisting of k clusters, each of which is a complete subgraph of size n, in which we further connect each node, $i = 1, \dots, n$ also to its $k-1$ "twins" in the other $k-1$ clusters (those with the same reminder modulo n), hence obtaining a regular graph where each node has degree $n+k-2$. The vertex set of $\mathcal{G}(k, n)$ is $V = \bigcup_{i=1}^{k} V^{(i)}$ where $V^{(i)} := \{n \cdot (i-1) + 1, \dots, n \cdot i\}$ are the nodes in the i-th cluster. The edge set of $\mathcal{G}(k, n)$ is $E = E_{\text{int}} \cup E_{\text{cross}}$, where $E_{\text{int}} = \bigcup_{i=1}^{k} E_{\text{int}}^{(i)}$ is the collection of *internal edges*, e.g., edges inside a cluster, and E_{cross} that of the edges across clusters, to which we refer as *cross-edges*. The graph $\mathcal{G}(k, n)$ then has $\frac{1}{2}kn(n+k-2)$ edges, $n\binom{k}{2}$ of which are cross-edges and $\binom{n}{2}$ inside each cluster. Figure 1.35 depicts an instance of $\mathcal{G}(3, 5)$.

With each site $i \in V$ we associate a spin variable $\sigma(i) \in \{-1, +1\}$. On the configuration space $\mathcal{X} = \{-1, +1\}^V$, we define the energy function $\widetilde{H}$ as

$$\widetilde{H}(\sigma) := -\sum_{(i,j)\in E_{\text{int}}} \sigma_i \sigma_j - \varepsilon \sum_{(i,j)\in E_{\text{cross}}} \sigma_i \sigma_j - h \sum_{i\in V} \sigma_i, \quad \sigma \in \mathcal{X}, \tag{1.4.4}$$

where we assume the strength of interaction across clusters is parametrized by a scalar $\varepsilon \in [-1, 1]$, while is equal to 1 along all the other internal edges and $h \geqslant 0$ is the external magnetic field. We will consider the case $h \in [0, 1]$ where, as it will be shown, the system exhibits a metastable behavior. It is reasonable to assume that the opinions of individuals that belong to a different community have less influence over each community. For this reason, the interactions across different network clusters are assumed to be weaker than those inside each cluster, since their strength is equal to $|\varepsilon| \leqslant 1$. Moreover, by taking negative values for ε, we can model situations in which individuals tend to disagree with individuals from other communities. The presence of a nonzero external magnetic field of intensity h

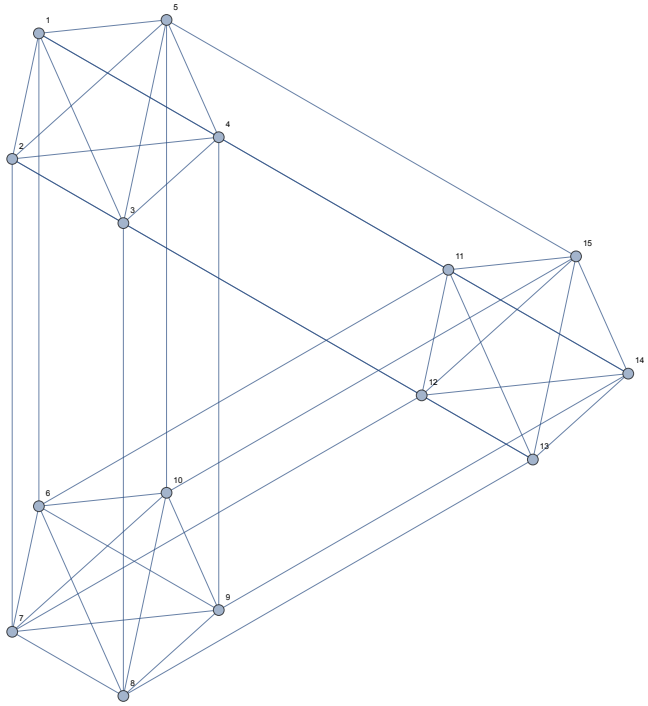

Figure 1.35 – Representation of the graph $\mathcal{G}(3,5)$.

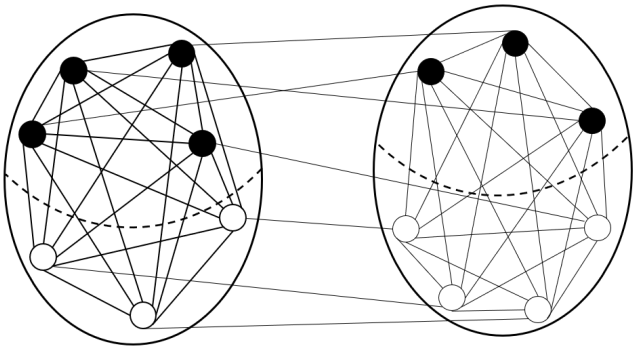

Figure 1.36 – Example of a configuration in $C(4,3,3)$ on the network $\mathcal{G}(2,7)$ with the color-coded spins (black for $+1$ and white for -1). The first cluster has $p_1 = 4$ spins $+1$, has $p_2 = 3$ spins -1 and there are $a = 3$ agreeing edges between plus spins.

favors configurations in which the spins are aligned in the direction of the field. Since every individual spin feels the external field, its energetical contribution has to be proportional to the number of spins with a certain sign.

Glauber dynamics is then defined as the discrete time Markov chain with transition probabilities defined in (1.4.1) with the Hamiltonian defined in (1.4.4). For this model, depending on the values of the parameter ε and of the external magnetic field h we will characterize the asymptotic properties of the transition time from the set of metastable (or stable) states to the set of stable states, as well as providing a characterizion of the critical configurations crossed by the dynamics with probability tending to one in the limit of very–low temperature.

In this thesis we will be interested to the case $k = 2$. Figure 1.36 depicts an instance of $\mathcal{G}(2,7)$. The reason behind this choice is twofold: firstly, the case $k = 2$ already exhibits a very diverse and rich behaviour, and, secondly, the more general case with $k > 2$ clusters is not conceptually harder to tackle, but simply heavier in terms of notation and terminology. Having a network with only $k = 2$ clusters $V^{(1)}$ and $V^{(2)}$ allows for a very compact notation for spin configurations that are equivalent modulo relabelling of the nodes. For a configuration $\sigma \in \mathcal{X}$ and $i = 1, 2$, let $V_+^{(i)}(\sigma)$ the subset of nodes in cluster i whose spin is equal $+1$ in σ and

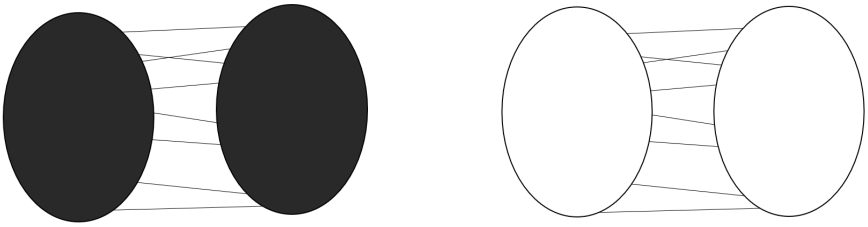

Figure 1.37 – The two uniform configurations $+\mathbf{1}$ and $-\mathbf{1}$, where we represent in white (resp. black) the minus (resp. plus) spins.

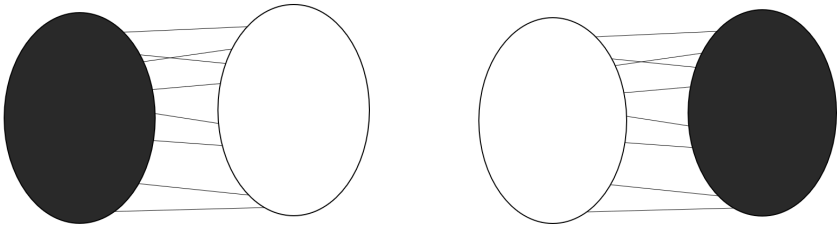

Figure 1.38 – The two mixed configurations $\pm\mathbf{1}$ and $\mp\mathbf{1}$, where we represent in white (resp. black) the minus (resp. plus) spins.

$E_+(\sigma)$ the subset of edges connecting $V_+^{(1)}(\sigma)$ and $V_+^{(2)}(\sigma)$. For $0 \leqslant p_1, p_2 \leqslant n$ and $0 \leqslant a \leqslant n$, we define the subset $C(p_1, p_2, a) \subset \mathcal{X}$ as

$$C(p_1, p_2, a) := \left\{ \sigma \in \mathcal{X} \,:\, |V_+^{(1)}(\sigma)| = p_1,\ |V_+^{(2)}(\sigma)| = p_2,\ \text{and } |E_+(\sigma)| = a \right\}.$$

In words, $C(p_1, p_2, a)$ is the collection of configurations σ on $\mathcal{G}(2, n)$ such that

— σ has $0 \leqslant p_1 \leqslant n$ spins $+1$ on the first cluster and $0 \leqslant p_2 \leqslant n$ spins $+1$ on the second cluster;

— σ has a of agreeing cross-edges between spins $+1$ in the first cluster and spins $+1$ on the second cluster.

Note that the number a of agreeing edges given n, p_1, p_2 must satisfy the following inequality

$$\max\{0, p_1 + p_2 - n\} \leqslant a \leqslant \min\{p_1, p_2\}, \tag{1.4.5}$$

since there cannot be a negative amount of edges between any pair of sub-clusters. We remark that the parameters p_1, p_2 and a uniquely identify the set of configurations in $C(p_1, p_2, a)$, modulo relabelling of the nodes. Indeed, it implicitly gives information also about spins -1 in the following sense:

— σ has $0 \leqslant n - p_1 \leqslant n$ spins -1 on the first cluster and $0 \leqslant n - p_2 \leqslant n$ spins -1 on the second cluster;

— σ has $p_1 - a$ disagreeing cross-edges between spins $+1$ on the first cluster and spins -1 on the second cluster;

— σ has $p_2 - a$ disagreeing cross-edges between spins -1 on the first cluster and spins $+1$ on the second cluster;

— σ has $n + a - p_1 - p_2$ agreeing cross-edges between spins -1 on the first cluster and spins -1 on the second cluster.

Figure 1.36 shows an example of a configuration in $C(4, 3, 3)$ on the network $\mathcal{G}(2, 7)$.

We further denote by $+\mathbf{1}, -\mathbf{1}$ the two homogeneous configurations on $\mathcal{G}(2, n)$ consisting of all $+1$ spins and all -1 spins, see Figure 1.37. We refer to the configurations which are not globally homogeneous but are locally uniform inside each cluster as *mixed configurations* and denote them as $\pm\mathbf{1}, \mp\mathbf{1}$. Clearly, there are only 2 of them on $\mathcal{G}(2, n)$, see Figure 1.38.

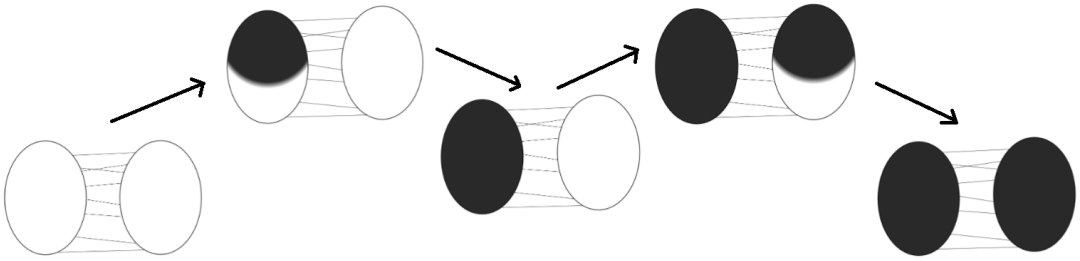

Figure 1.39 – Here we depict the reference path $\bar{\omega}$ by representing the saddles, the metastable and stable states that it crosses, where we represent in white (resp. black) the spins -1 (resp. $+1$).

MAIN THEOREMS: CASE $h = 0$

Here we focus on the case $h = 0$, namely, there is no external magnetic field. The first result we provide is the identification of metastable and stable states. In particular, we have that the set of stable states is

$$\mathcal{X}^s = \begin{cases} \{+\mathbf{1}, -\mathbf{1}\} & \text{if } \varepsilon > 0, \\ \{+\mathbf{1}, -\mathbf{1}, \pm\mathbf{1}, \mp\mathbf{1}\} & \text{if } \varepsilon = 0, \\ \{\pm\mathbf{1}, \mp\mathbf{1}\} & \text{if } \varepsilon < 0, \end{cases} \tag{1.4.6}$$

and the set of metastable states is

$$\mathcal{X}^m = \begin{cases} \{\pm\mathbf{1}, \mp\mathbf{1}\} & \text{if } \varepsilon > 0, \\ \{+\mathbf{1}, -\mathbf{1}\} & \text{if } \varepsilon < 0. \end{cases} \tag{1.4.7}$$

In view of this, it is clear that the interesting phenomenon to consider is now the *tunneling transition*, namely, the transition between two stable states. Due to the symmetry of the system, one can conjecture that the gate $\mathcal{C}^*$ for this transition is composed by two types of configurations. The first one corresponds to having $\frac{n}{2}$ spins $+1$ in one of the two clusters, 0 spins $+1$ in the other cluster and 0 agreeing cross–edges between spins $+1$ in the two clusters. The second one corresponds to having $\frac{n}{2}$ spins $+1$ in one of the two clusters, n spins $+1$ in the other cluster and $\frac{n}{2}$ agreeing cross–edges between spins $+1$ in the two clusters. Note that if n is odd, then $\frac{n}{2}$ should be replaced by $\frac{n+1}{2}$ or $\frac{n-1}{2}$ depending whether $\varepsilon \geqslant 0$ or $\varepsilon < 0$. Then, we deduce that the system performs the transition between the two stable states in a time of order $e^{\Gamma^* \beta}$ in the limit as $\beta \to \infty$, where Γ^* is the energy of the critical configurations and can be explicitly expressed in terms of n and ε. Let us denote by s_1 the starting stable state and by s_2 the target stable state. As we have seen in Section 1.3.3, the key ingredients are the following:

(i) Prove that $\Phi(s_1, s_2) \leqslant \Gamma^*$.
(ii) Prove that $\Phi(s_1, s_2) \geqslant \Gamma^*$.
(iii) Prove that any $\omega \in (s_1 \to s_2)_{opt}$ crosses the set $\mathcal{C}^*$.

For point (i), it suffices to construct a reference path connecting s_1 to s_2 which does not exceed the energy value Γ^*. If $\varepsilon \geqslant 0$, we define a reference path $\bar{\omega}$ from $-\mathbf{1}$ to $+\mathbf{1}$, while if $\varepsilon < 0$ we define a path $\hat{\omega}$ from $\pm\mathbf{1}$ to $\mp\mathbf{1}$. In words, these paths are constructed in the following way. The path $\bar{\omega}$, which starts from $-\mathbf{1}$, consists in flipping one by one the minus spins in one community until the path reaches either $\pm\mathbf{1}$ or $\mp\mathbf{1}$ and afterward the remaining minuses are flipped one by one until the path reaches $+\mathbf{1}$ (see Figure 1.39). The construction of the path $\hat{\omega}$ is made in a similar way (see Figure 1.40).

Again, points (ii) and (iii) can be proven via an isoperimetric inequality–type argument. In particular, the idea is to partition the state space in subsets $\mathcal{C}(p)$ of configurations having precisely p plus spins, see Figure 1.41 for an example, and finally characterize those configurations that minimize the energy when p is fixed. We refer to Chapter 8 for all the details.

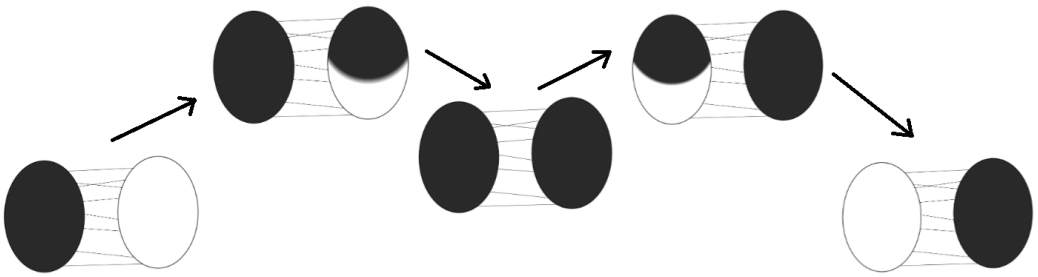

Figure 1.40 – Here we depict the reference path $\hat{\omega}$ by representing the saddles, the metastable and stable states that it crosses, where we represent in white (resp. black) the spins -1 (resp. $+1$).

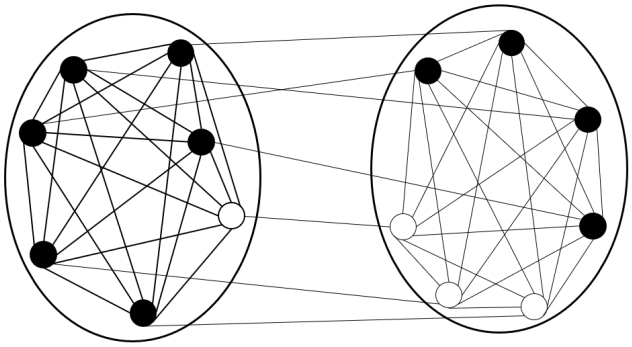

Figure 1.41 – An example of a configuration σ on the network $\mathcal{G}(2,7)$ that belongs to the manifold $\mathcal{C}(10)$, since it has $p = 10$ $+1$ spins, specifically $p_1 = 6$ in the first cluster and $p_2 = 4$ in the second cluster ($+1/-1$ spins are colored in black/white, respectively).

MAIN THEOREMS: CASE $h > 0$

We focus here on the case $h > 0$, which describes the situation in which there is a positive external magnetic field that favors plus spins. Moreover, we assume that $0 < h \leqslant 1$ in order to avoid the energetical contribution of the external magnetic field prevails over the binding energies associated with internal edges. As it will be clear later, the dynamical behavior of the system is different in the two cases $0 < h \leqslant |\varepsilon| \leqslant 1$ and $0 \leqslant |\varepsilon| < h \leqslant 1$, especially when $\varepsilon < 0$. Indeed, this corresponds to a different "importance" given to the cross-edges and the external magnetic field. In particular, we have that the set of stable states is

$$\mathcal{X}^s = \begin{cases} \{+\mathbf{1}\} & \text{if } 0 \leqslant \varepsilon \leqslant 1 \text{ or } 0 < -\varepsilon < h \leqslant 1, \\ \{+\mathbf{1}, \pm\mathbf{1}, \mp\mathbf{1}\} & \text{if } h = -\varepsilon, \\ \{\pm\mathbf{1}, \mp\mathbf{1}\} & \text{if } 0 < h < -\varepsilon \leqslant 1, \end{cases} \tag{1.4.8}$$

and the set of metastable states is

$$\mathcal{X}^m = \begin{cases} \{-\mathbf{1}\} & \text{if } 0 \leqslant \varepsilon \leqslant 1 \text{ or } h = -\varepsilon, \\ \{\pm\mathbf{1}, \mp\mathbf{1}\} & \text{if } 0 < -\varepsilon < h \leqslant 1, \\ \{+\mathbf{1}\} & \text{if } 0 < h < -\varepsilon \leqslant 1. \end{cases} \tag{1.4.9}$$

Thus, our interest is to investigate the asymptotic behavior as $\beta \to \infty$ of the tunneling time (resp. transition time to the stable state) for the system started at the stable state s_1 (resp. metastable state m) to reach for the first time the other stable state s_2 (resp. the stable state s) if $0 < h < -\varepsilon \leqslant 1$ (resp. if $0 \leqslant \varepsilon \leqslant 1$ or $0 < -\varepsilon < h \leqslant 1$). As before, the strategy to characterize the gate and estimate the transition time is to prove the corresponding version of points (i)–(iii) above. Here we argue only about point (i) by exhibiting the reference paths, while we refer to Chapter 8 for all the details concerning points (ii) and (iii).

If $\varepsilon \geqslant 0$, consider the path $\bar{\omega}$ represented in Figure 1.39. If $0 < h < -\varepsilon \leqslant 1$, we define $\check{\omega} : \pm\mathbf{1} \to \mp\mathbf{1}$ as the path represented in Figure 1.42. If $0 < -\varepsilon < h \leqslant 1$, we define $\tilde{\omega} : \pm\mathbf{1} \to +\mathbf{1}$ as the path represented in Figure 1.43.

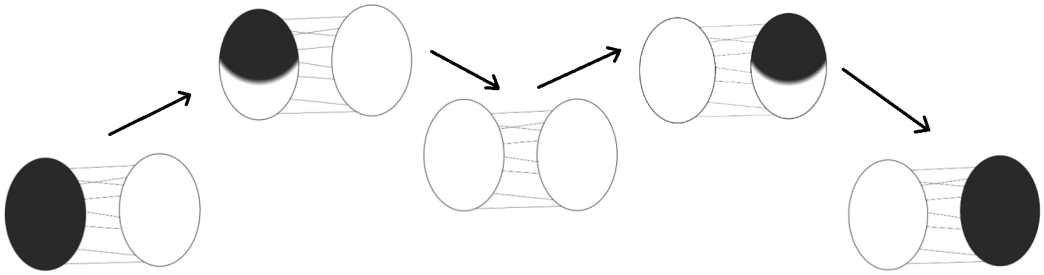

Figure 1.42 – Here we depict the reference path $\check{\omega}$ by representing the saddles, the metastable and stable states that it crosses, where we represent in white (resp. black) the minus (resp. plus) spins.

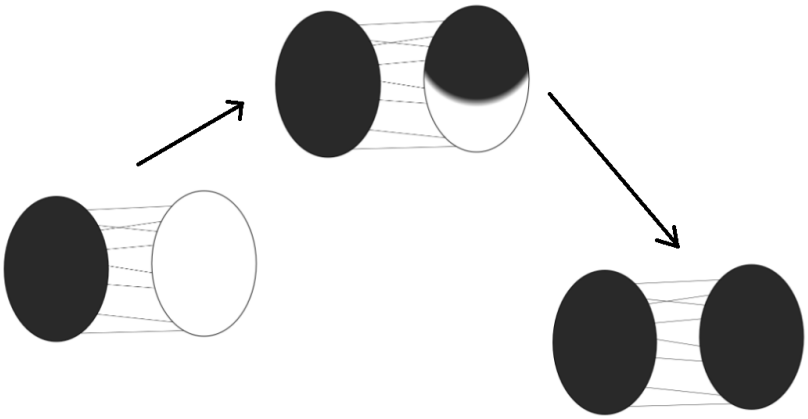

Figure 1.43 – Here we depict the reference path $\tilde{\omega}$ by representing the saddles, the metastable and stable states that it crosses, where we represent in white (resp. black) the minus (resp. plus) spins.

In this thesis, we investigated opinion dynamics inside a community of individuals via the analysis of metastability for the Ising model on the graph $\mathcal{G}(2, n)$. Depending on the different parameters ε and h, we showed that the stable and metastable states of the system are different. Thus, according to the different scenarios, we used the framework of the pathwise approach [85, 92] to analyze the transition or tunneling time, respectively, and to describe the critical configurations. Moreover, we showed that the presence of a positive external magnetic field, which can be interpreted as external information or influence, makes the situation much richer, especially in the case $\varepsilon < 0$ in which communities tend to have diverging opinions. More specifically, the set of stable states is completely different according to the role given to the external information with respect to influence between communities, namely, depending on whether $h < -\varepsilon$ or not. This model is our first attempt to analyze the spread of an opinion inside two communities. First, the extension to a general number k of communities naturally arises in this context and will be the focus of future work, together with the computation of the prefactor for the mean transition time. This represents a challenging task in the case $k > 2$, as one needs to take into account all the mechanisms of spreading the new opinion among different communities. Further, one may consider models with more than two opinions (Potts model) or with different interaction strengths among communities. We believe that the opinion dynamics inside a population of individuals with a nontrivial network topology is a topic of great interest with many several interesting directions to explore further in future research work.

1.5 PREFERENTIAL ATTACHMENT RANDOM GRAPHS

In this section, we focus on the analysis of the limiting behaviour of the preferential attachment random graphs. The unprecedented growth in size and complexity of social and economic networks in the last two decades has sparked considerable interest in the

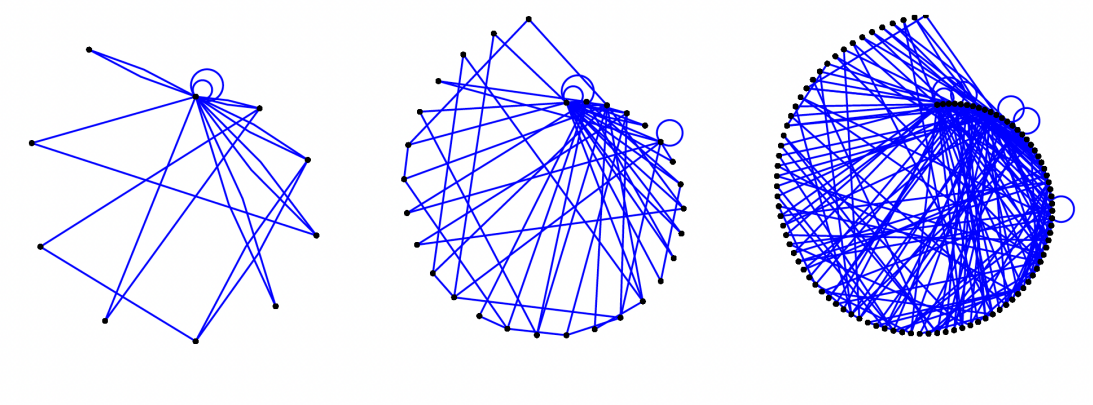

Figure 1.44 – Preferential attachment random graph with $m = 2$ and $\delta = 0$ of sizes 10, 30 and 100. Figure taken from [69].

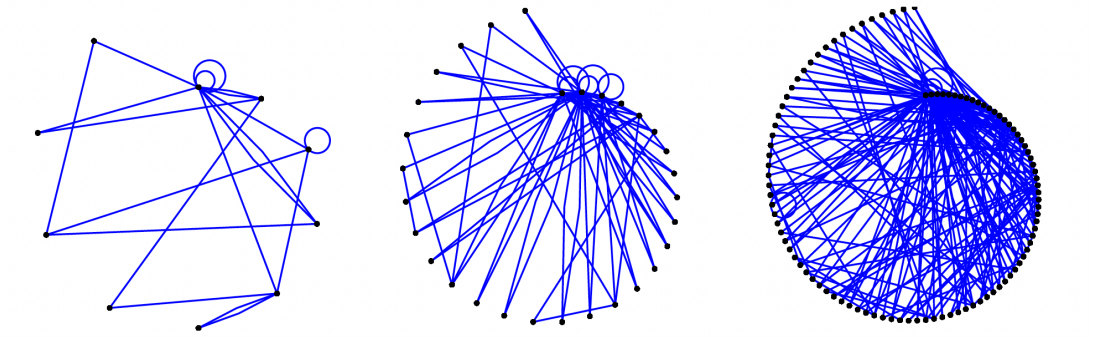

Figure 1.45 – Preferential attachment random graph with $m = 2$ and $\delta = -1$ of sizes 10, 30 and 100. Figure taken from [69].

understanding of the fundamental properties of such networks. In this context, the preferential attachment (PA) model, introduced in [19], is a well-known model for a network that grows in time. More precisely, the PA model consists of a sequence of graphs of increasing size such that each graph is obtained from the previous according to a certain probabilistic rule. Namely, at each step a new vertex is added and it forms connections with the vertices in the graph in such a way that connections with vertices having larger degrees are more likely. Here, we consider the PA model without self-loops described for example in [59]. In particular, each graph in the sequence is connected.

Several different PA models appear in the literature, depending on the concrete details of the attachment mechanism. For instance, in [30, 58, 104, 113, 115] the authors investigate a *directed* PA model, while in [23, 50, 58, 59, 88, 103] an *undirected* version is considered. However, classical PA networks do not always fit real-world network data well, or in many applications it is natural to assign some kind of features to the vertices or to the edges. This led to consider some extensions of the classical PA model. For example, in [7] the authors consider a general family of preferential attachment models with multi-type edges, while [5, 84, 98] investigate a PA model which mixes PA rules with uniform attachment rules. In this work we consider the PA model without self-loops described in [59]. We make this choice in order to simplify the calculations, but we believe that our result also holds, for example, for the PA model with self-loops considered in the standard reference [69, Chapter 8]. We argue this in more detail later on. See Figures 1.44 and 1.45 for examples of such random graphs with self-loops, where each new node has a fixed number $m \in \mathbb{N}$ of edges attached to it and δ is a parameter of the model (see (1.5.1) for the precise definition). This is a particular case of the model considered in [59], where m is a random variable and is sampled for each new node.

Our main result is a central limit theorem for the proportion of nodes with a given degree. In fact, we prove this *jointly* for all degree counts. In particular, we give an explicit expression

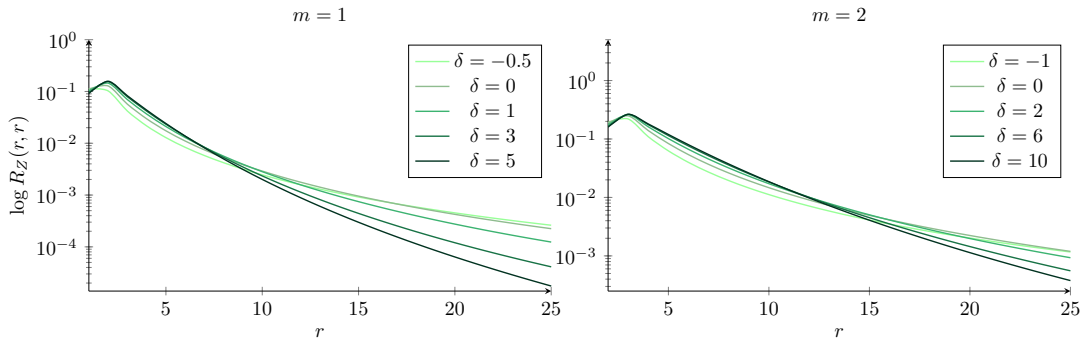

Figure 1.46 – $R_Z(r,r)$ for $m = 1$ and $\delta = -0.5, 0, 1, 3, 5$ on the left-hand side and $R_Z(r,r)$ for $m = 2$ and $\delta = -1, 0, 2, 6, 10$ on the right-hand side. To highlight the different behaviour of the various variance functions, we use the logarithmic axis on the y-axis.

for the asymptotic covariance. The first results concerning the study of the asymptotic normality of degree counts in the preferential attachment models without self-loops is given in [88] by using martingale central limit theorems. Our results generalize those obtained in [103] for the preferential attachment tree. More precisely, in [103] the authors consider a PA model with self-loops and such that $m = 1$. Note that here we consider the PA model with $m \geqslant 1$ and without self-loops. However, this does not influence the asymptotic behavior of the degree counts, since as the graph size goes to infinity, the probability that a new vertex forms a self-loop tends to zero. Because of this one would expect to recover the results in [103] when plugging $m = 1$ in our result. Indeed this is the case if one takes into account a few minor mistakes in [103] which we will discuss later. Note that a major difference between the two models is the resulting connectivity structure. Our model produces a connected graph with probability 1 (w.p. 1), while the model in [103] is disconnected w.p. 1. However, this does not play a role in the distribution of the degree counts. In [99] the authors studied the joint degree counts in linear preferential attachment random graphs. The results are stated in terms of weight of vertices, but they can be tought of as degree, since each time a vertex receives a new edge, its weight increases by one. The main difference between our and their model is that we consider the attachment probabilities proportional to a linear function of the degree of an old vertex (see (1.5.1)), while in [99] they are proportional to the degree of an old vertex.

In practice, in real-world networks not all nodes that enter the network have the same degree, and thus it would be interesting to extend our result to the case of a random initial degree distribution. Promising results on this model have been obtained in [54, 59]. Moreover, in this thesis we assume that the parameters of the model are known, but in many practical situations one is given a realization of the graph and the task is estimating the unknown parameters, see [60, 101, 112]. If we consider a more general class of preferential attachment graphs, for which a model-free approach is used and therefore the exact distribution of the graph is not known (see for instance [81]), we expect that the techniques presented in this work could be used to derive central limit theorem for all the degree counts. This is an interesting open problem.

Let us now describe in detail the random graph model that we consider. Fix once and for all an integer $m \geqslant 1$. Formally, the preferential attachment model is a sequence of random graphs $(PA_s)_{s=1}^t$. The index s is interpreted as a time parameter. At time s, the graph PA_s has a set $V = \{0, 1, ..., s\}$ of $s+1$ vertices. For $s = 1$ the graph PA_1 consists of the vertices 0 and 1, connected by m edges. For $s \geqslant 2$, the graph PA_s is obtained from PA_{s-1} by adding a new vertex s with degree m as follows. Define $PA_{s,0}$ =PA_{s-1} and $PA_{s,1}$,...,$PA_{s,m}$ as the intermediate graphs obtained by adding a new edge sequentially to $PA_{s,0}$. For $i = 1, ..., m$, $PA_{s,i}$ is obtained from $PA_{s,i-1}$ by drawing an edge from s to a randomly selected vertex among $\{0, 1, ..., s-1\}$. The probability that a vertex s is connected to some vertex i is proportional to the degree of i. In other words, vertices with large degrees are more likely to attract new edges. We denote by $N_k(s,i)$ for $i = 1, ..., m$ the number of vertices of degree k after the i-th edge has been attached at time s, excluding the vertex s. We

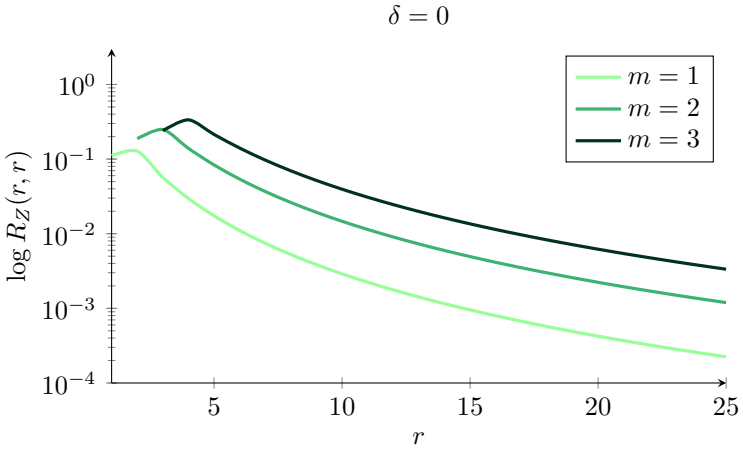

Figure 1.47 – $R_Z(r,r)$ for $\delta = 0$ and $m = 1, 2, 3$. To highlight the different behaviour of the various variance functions, we use the logarithmic axis on the y-axis.

set $N_k(s+1,0) := N_k(s,m)$. Furthermore, we denote by $D_{s,i}$ the degree of the vertex which has been attached to the i—th edge added when constructing PA_s from PA_{s-1}. Consider now the σ-algebra $\mathcal{F}_{s,i}$ generated by the preferential attachment construction up until the attachment of the i-th edge of the new vertex at time s. The conditional probability that the i-th edge connects to a vertex of degree $D_{s,i}$ is

$$\mathbb{P}(D_{s,i} = k|\mathcal{F}_{s,i-1}) = \frac{(k+\delta)N_k(s,i-1)}{\sum_j (j+\delta)N_j(s,i-1)}, \tag{1.5.1}$$

where $\delta > -m$ is an affine parameter. The normalizing constant in (1.5.1) takes the simple form [59]

$$\sum_{j=1}^{\infty} (j+\delta)N_j(s,i-1) = s(2m+\delta) - 2m + i - 1. \tag{1.5.2}$$

For the standard PA model considered in [69, Chapter 8] it is shown that there exists a probability mass function $\{p_k,\ k \geqslant m\}$ such that, uniformly on $i \in \{0,...,m\}$,

$$\lim_{s\to\infty} \frac{N_k(s,i)}{s} = p_k \in (0,1), \tag{1.5.3}$$

almost surely, where p_k is given by

$$p_k = (2+\delta/m)\frac{\Gamma(k+\delta)\Gamma(m+2+\delta+\delta/m)}{\Gamma(m+\delta)\Gamma(k+3+\delta+\delta/m)}. \tag{1.5.4}$$

Here $\Gamma(\cdot)$ is the Gamma function. When the graph size goes to infinity, the probability that a new vertex forms a self-loop tends to zero and thus it easy to check that (1.5.3) and (1.5.4) hold still for our model without self-loops following the proof proposed in [69, Section 8.6].

In order to state our main result, we require some further notation. We say that the events $(A_n)_n$ hold with high probability when $P(A_n) \to 1$ as $n \to \infty$. Given a random vector $(X_1^{(n)}, X_2^{(n)}, ...)$, we write $(X_1^{(n)}, X_2^{(n)}, ...) \Rightarrow (X_1, X_2, ...)$ to indicate that for any $k \in \mathbb{N}$, as $n \to \infty$ $(X_1^{(n)}, X_2^{(n)}, ..., X_k^{(n)})$ converges to $(X_1, X_2, ..., X_k)$ in distribution as vectors in $\mathbb{R}^n$. Our main result is the following. As $s \to \infty$, we prove that

$$\left(\sqrt{s}\Big(\frac{N_k(s,i)}{s} - p_k\Big),\ k = m, m+1, ...\right) \Rightarrow (Z_k,\ k = m, m+1, ...), \tag{1.5.5}$$

where $(Z_k,\ k = m, m+1, ...)$ is a mean zero Gaussian process with covariance function R_Z given by (9.1.2). The proof relies on the careful construction of an appropriate martingale.

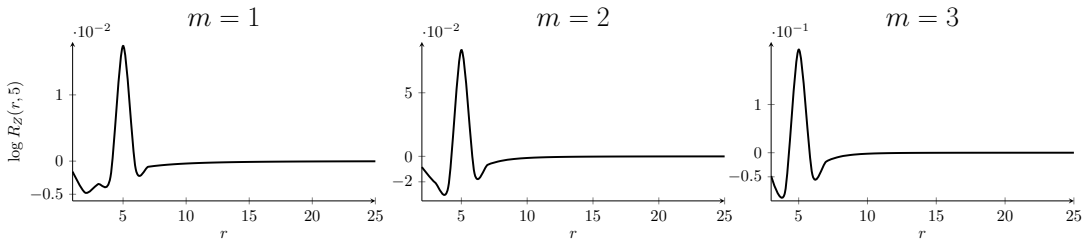

Figure 1.48 – $R_Z(r,5)$ for $\delta = 0$ and $m = 1, 2, 3$.

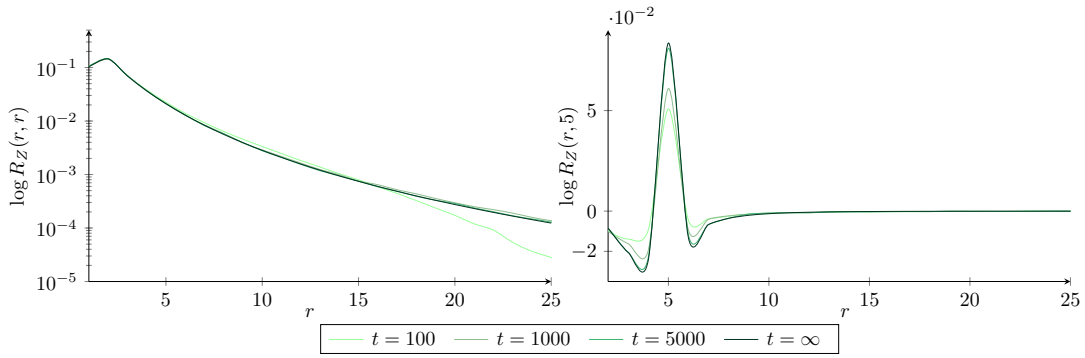

Figure 1.49 – Left-hand side: $R_Z(r,r)$ for $\delta = 1$ and $m = 1$ ($t = \infty$) compared with the numerical simulations stopped at time $t = 100, 1000, 5000$. Each empirical curve was obtained by taking the average of $N = 10000$ simulations. Right-hand side: $R_Z(r,5)$ for $\delta = 0$ and $m = 2$ ($t = \infty$) compared with the numerical simulations stopped at time $t = 100, 1000, 5000$. Each empirical curve was obtained by taking the average of $N = 10000$ simulations. To highlight the different behaviour of the various variance functions, we use the logarithmic axis on the y-axis.

Since the expression in (9.1.2) is remarkably complicated, here we do not report it and we refer to Chapter 9 for the explicit formula. In addition, we plot it for various parameter choices to help the understanding. In Figure 1.46 we plot the function $r \mapsto R_Z(r,r)$ for fixed $m = 1$ (resp. $m = 2$) and various values of δ. On the other hand, in Figure 1.47 we plot the function $R_Z(r,r)$ for fixed $\delta = 0$ and various values of m. In Figure 1.48 we plot the function $R_Z(r,5)$ for $\delta = 0$ and $m = 1, 2, 3, 4$. Finally, in Figure 1.49 on the left-hand- side we compare the asymptotic covariance function $R_Z(r,r)$ for fixed $m = 1, \delta = 1$ with the empirical variance obtained by numerically simulating the PA model up until time $t = 100, 1000, 5000$. Furthermore, in Figure 1.49 on the right-hand side, we compare the asymptotic covariance function $R_Z(r,5)$ for fixed $m = 2, \delta = 0$ with the empirical covariance obtained by numerical simulation of the PA model up until time $t = 100, 1000, 5000$. While we do not have rigorous results on the convergence speed of the rescaled vertex counts, Figure 1.49 suggests that the convergence is indeed quite fast.

Remark 1.5.1. *As explained in [69, Chapter 8], it is possible to define the preferential attachment model with $m > 1$ in terms of the model with $m = 1$ by collapsing vertices, thus one could be tempted to directly apply this construction to the results derived in [103] for the model with $m = 1$. This is a possible approach which presents its own difficulties and now we try to highlight them. The central limit theorem that we want to prove involves the number of vertices with a fixed degree, thus we need to find a relation between that quantity for the model $m > 1$ and $m = 1$ in order to use the result obtained in [103]. This is not straightforward, indeed a rich control over the graph construction is required at each step.*

Remark 1.5.2. *Here we choose to update the degrees during the attachment of a new vertex, but it is possible to consider also the case in which we update the degrees of the vertices only when the m-th edge is added. In this case, after constructing a suitable martingale with respect to the filtration $(\mathcal{F}_s)_{s \geqslant 1}$ generated by the construction of the preferential attachment graph until time s, it is possible*

to reproduce the same computations. Thus, we are able to prove a similar result for this model by using the techniques presented here.

Following the argument carried out in [88], we are able to prove a central limit theorem for the vector composed by the rescaled number of vertices with degree greater than k. In this case, the covariance matrix of the limiting normal law becomes simple and now we compute it. Define the number of vertices with degree greater than k as

$$\psi_k(s,i) := \sum_{j \geqslant k} N_j(s,i) \tag{1.5.6}$$

and

$$\psi(s,i) := (\psi_m(s,i), \psi_{m+1}(s,i), ...). \tag{1.5.7}$$

Note that we can write

$$\begin{aligned} &\psi(1,i) = (0,...,0), \\ &\psi(s,i+1) = \psi(s,i) + \delta_{D_{s,i}}, \end{aligned} \tag{1.5.8}$$

where $\delta_{D_{s,i}}$ is the vector with all the coordinates equal to 0 except the $D_{s,i}$-th one, that is equal to 1. From (1.5.3) it follows that the differences of the vector valued process $\{\psi(s,i),\ s \geqslant 1,\ i = 1,...,m\}$ become more and more indipendent and identically distributed in the limit as $s \to \infty$. Let $\pi_k(s,i) := \mathbb{P}(D_{s,i} = k | \mathcal{F}_{s,i-1})$ and

$$\pi_k := \lim_{s\to\infty} \pi_k(s,i) = \frac{k+\delta}{2m+\delta} p_k. \tag{1.5.9}$$

Thus, as $s \to \infty$, it holds true that

$$\left(\sqrt{s}\Big(\frac{\psi_k(s,i)}{s} - \pi_k \Big),\ k = m, m+1, ... \right) \Rightarrow (Z_k,\ k = m, m+1, ...), \tag{1.5.10}$$

where $(Z_k,\ k = m, m+1, ...)$ is a mean zero Gaussian process with covariance matrix $V = (v_{r\ell})_{k\times k}$ given by the limit of the upper left minor size $i \times i$ of the infinite conditional covariance matrix $\mathrm{Var}(\delta_{D_{s,i}} | \mathcal{F}_{s,i-1})$, namely

$$\begin{aligned} v_{rr} &= \pi_r(1-\pi_r) = \frac{(r+\delta)p_r(2m+\delta-(r+\delta)p_r)}{(2m+\delta)^2}, \\ v_{r\ell} &= -\pi_r\pi_\ell = -\frac{(r+\delta)(\ell+\delta)}{(2m+\delta)^2} p_r p_\ell,\ r \neq \ell. \end{aligned} \tag{1.5.11}$$

1.6 OUTLINE OF THE THESIS

This thesis is organized as follows. Chapter 2 represents the Italian translation of Chapter 1. Chapters 3-7 are devoted to the study of the metastable conservative Kawasaki dynamics, while Chapter 8 to the study of the metastable non–conservative Glauber dynamics. Finally, in Chapter 9 we investigate the asymptotic properties of the preferential attachment model. More precisely, the content of each chapter is the following.

In Chapter 3, our first goal is to provide the geometrical description of the union of all the minimal gates $\mathcal{G}(\square, \blacksquare)$ in the isotropic case. We will prove that there are many distinct minimal gates, which we will geometrically characterize together with their union. To this end, we first give a *model-independent strategy* that is useful to eliminate some unessential saddles, i.e., those that are not essential, for the characterization of the set $\mathcal{G}(m, \mathcal{X}^s)$, where m is the unique metastable state and $\mathcal{X}^s$ is the set of stable states. We then apply this strategy to the two–dimensional isotropic model that evolves under Kawasaki dynamics, where $m = \square$ and $\mathcal{X}^s = \{\blacksquare\}$. In order to do this, we need to verify that the required model-dependent inputs are valid for our model. This study, together with the characterization of the essential saddles, relies on a detailed analysis of the motion of particles along the border of the droplet, which is a typical feature of the Kawasaki dynamics. Additionally, we give some model–independent

results concerning the sharp asymptotics of the mean transition time, which clarify the role of the unessential saddles in the computation of the prefactor. We conclude this chapter by investigating the spectral gap and mixing time of the process. The content of this chapter is based on the published paper [18] and its extended version [15].

In Chapter 4, we geometrically characterize the set $\mathcal{G}(\square, \blacksquare)$ in the weakly anisotropic case. We do this thanks to the model–independent strategy carried out in Chapter 3 and the specific analysis of the dynamics of the system. Additionally, we prove sharp asymptotics for the transition time and for the uniform entrance distribution. We conclude this chapter by investigating the spectral gap and mixing time of the process. The content of this chapter is based on the published paper [18] and its extended version [15].

Chapter 5 is devoted to the geometrical description of the set $\mathcal{G}(\square, \blacksquare)$ in the strongly anisotropic regime. We will prove that there are many distinct minimal gates that we will geometrically characterize together with their union. We apply the model-independent strategy carried out in Chapter 3 to this model in order to eliminate some unessential saddles. Thus, we need to verify that the required model-dependent inputs are valid in our case. This study together with the characterization of the essential saddles rely on a detailed analysis of the motion of particles along the border of the droplet. On the one hand this is a typical feature of the Kawasaki dynamics, on the other hand this is peculiar in the strongly anisotropic case. Additionally, we prove sharp asymptotics for the transition time and we investigate the spectral gap and mixing time. This chapter is based on [17].

In Chapter 6, we study the local Kawasaki dynamics on the hexagonal lattice with isotropic interactions. In particular, we investigate the critical configurations and the tunneling time between ⎔ (empty hexagon) and ⬢ (full hexagon) for this model. Our main results are the following. First, we identify the metastable and stable states and we prove a convergence in probability, expectation and law for the transition time, answering the first question of metastability. Then, we prove that the system reaches with high probability either the state ⎔ or ⬢ in a time shorter than $e^{\beta(V^*+\varepsilon)}$, uniformly in the starting configuration for any $\varepsilon > 0$, where $V^* = \Delta + U$. In other words, the dynamics speeded up by a factor of order $e^{\beta V^*}$ reaches with high probability $\{⎔, ⬢\}$. Finally, we provide a characterization of a gate for the transition, answering the second issue of metastability. We emphasize that this result reflects how the underlying lattice is crucial for the dynamics of the system. This chapter is based on [13].

In Chapter 7, we consider the fully conservative model on the two-dimensional square lattice. We will use the results of [62] to analyze how subcritical droplets form and dissolve on multiple space-time scales when the volume is moderately large, namely, the box has volume $e^{\Theta\beta}$, with $\Delta < \Theta < 2\Delta - U$. Since the dynamics is conservative, we need to control non-local effects in the way droplets are formed and dissolved. This is done via an *axiomatic approach*: the tube of typical trajectories leading to nucleation is described via a series of events, whose complements have negligible probability, on which the evolution of the gas consists of droplets wandering around on multiple space-time scales in a way that can be captured by a coarse-grained Markov chain on a space of droplets. This chapter is based on the preprint [11].

In Chapter 8, we analyze the Ising model on a specific family of clustered networks, by identifying the set of metastable and stable states and by estimating the asymptotic behavior of the transition time between them in the low-temperature limit. In the context of the clustered network that we consider in this chapter, the set of metastable states depends heavily on the relative strength of the interactions between the network communities and that of the external magnetic field. In absence of an external magnetic field, the two opinions are equally likely and the two homogeneous opinion patterns are both stable states. In this case, it is still interesting to study how, starting with all individuals agreeing on one opinion, the whole network can transition to the opposite opinion, how long this will take and what are the most likely trajectories of this process. This chapter is based on [10].

In Chapter 9, our main result is a central limit theorem for the proportion of nodes with a given degree for a general preferential attachment model. To this end, we use martingale central limit theorems. In fact, we prove this *jointly* for all degree counts. In particular, we give an explicit expression for the asymptotic covariance and we also use numerical simulations to

argue that the convergence is quite fast. The proof relies on the careful construction of an appropriate martingale. The content of this chapter is based on [9].

2 INTRODUZIONE

2.1 PANORAMICA

In questa tesi ci concentriamo sul comportamento metastabile di sistemi discreti a bassa temperatura che evolvono sotto dinamiche stocastiche.

La metastabilità è onnipresente in natura e la necessità di catturare il comportamento di sistemi soggetti a tale fenomeno è la motivazione principale di questa ricerca. Infatti, la metastabilità nasce naturalmente in una grande varietà di sistemi – fisica, chimica, biologia, economia e sociologia. In questo lavoro ci concentriamo principalmente sui sistemi discreti mirando a catturare le caratteristiche provenienti da entrambi i campi della fisica statistica e della sociologia.

Dietro il fenomeno della metastabilità ci sono alcune caratteristiche comuni, come una grande variabilità nel momento dell'insorgenza di qualche cambiamento drammatico nelle proprietà del sistema, un tempo molto più breve per la transizione effettiva (cioè, tra l'inizio di un cambiamento notevole e il momento in cui si raggiunge un nuovo stato), e imprevedibilità del momento dell'inizio della transizione. È formalmente descritto come un fenomeno dinamico che si verifica quando un sistema è vicino a una transizione di fase del primo ordine. Dopo aver modificato alcuni parametri termodinamici, il sistema rimane per un tempo considerevole (casuale) nella vecchia fase, lo stato metastabile, prima di fare improvvisamente una transizione verso la nuova fase, lo stato stabile. In altre parole, in breve tempo, il sistema si comporta come se fosse in equilibrio, mentre, su una scala a lungo termine, si muove tra diverse regioni dello spazio degli stati (si veda la Figura 2.1). La transizione avviene quando il sistema riesce a creare una goccia sufficientemente grande, la cosiddetta *goccia critica*, della nuova fase all'interno della vecchia fase (si veda la Figura 2.2). Nello studio della metastabilità ci sono tre questioni principali che sono tipicamente indagate. La prima è lo studio del *tempo di transizione tipico* dagli stati metastabili a quelli stabili, cioè il tempo necessario per arrivare alla fase di equilibrio. La seconda e la terza questione riguardano la descrizione geometrica delle configurazioni che formano il *varco della transizione* (chiamate anche *configurazioni critiche*) ed il *tubo delle traiettorie tipiche*. Questi problemi sono fisicamente più interessanti, perché forniscono informazioni sulle configurazioni che saranno attraversate dalla dinamica. Grossomodo, il sistema fluttua in vicinanza dello stato metastabile fino a quando non visita l'insieme delle configurazioni critiche e infine raggiunge l'equilibrio: i cammini tipici che il sistema segue con alta probabilità formano il tubo delle traiettorie tipiche.

La prima sfida principale dell'approccio matematico alla metastabilità è di natura qualitativa, vale a dire, a spiegare perché in una grande varietà di sistemi si osserva lo stesso tipo di comportamento metastabile. Molti di questi sistemi sono descritti dai primi principi come sistemi multicorpo soggetti a dinamica classica o quantistica. Mentre sono note le

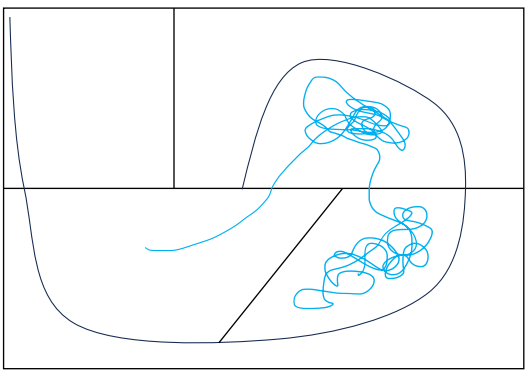

Figura 2.1 – Immagine paradigmatica della metastabilità.

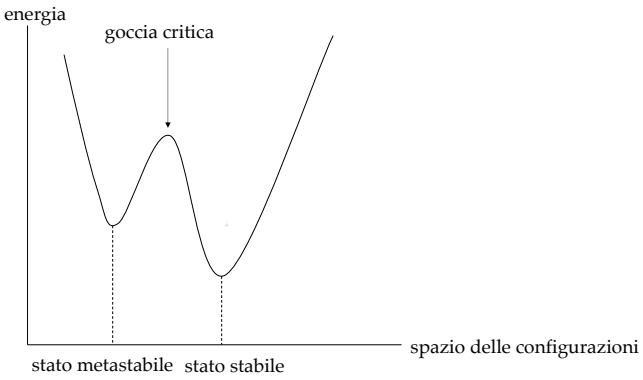

Figura 2.2 – Immagine paradigmatica del panorama energetico.

corrispondenti equazioni del moto, sono in genere molto difficili da analizzare su intervalli di tempo estremamente lunghi in cui si verifica un comportamento metastabile. Inoltre, la metastabilità mostra manifestamente casualità (il momento imprevedibile del verificarsi della transizione), la cui origine può essere difficile da estrarre dalle dinamiche deterministiche sottostanti. Questo può essere dovuto agli effetti quantistici, o alle perturbazioni esterne di un sistema (non chiuso). Una prima semplificazione è passare ad una descrizione del sistema attraverso una dinamica stocastica. C'è una grande varietà di modelli diversi dove emerge la metastabilità e dove è possibile la spiegazione dell'universalità sottostante.

La seconda sfida principale è di natura quantitativa. Dati i parametri di qualche modello sottostante, vorremmo poter calcolare nel modo più preciso possibile le quantità che controllano i fenomeni metastabili, in particolare, la distribuzione dei tempi delle transizioni tra stati metastabili e stabili. Ancora una volta, questo è difficile perché la maggior parte dei sistemi metastabili di rilevanza pratica sono sistemi multicorpo la cui dinamica non è facile da catturare, né analiticamente né numericamente, e perché possono essere coinvolte scale di tempo estremamente lunghe. La comprensione della metastabilità a livello quantitativo è di notevole interesse pratico, in quanto influisce sul comportamento e il funzionamento di molti sistemi in natura.

In questa tesi indaghiamo il comportamento metastabile di sistemi di particelle interagenti, descritti dal modello standard di Ising, che evolve sotto la dinamica stocastica di Kawasaki (Sezione 2.3) e di Glauber (Sezione 2.4), con particolare attenzione alla forma geometrica delle configurazioni critiche, cioè quelle attraversate dal sistema con alta probabilità. In particolare, ci concentriamo su modelli matematici che descrivono sia le transizioni di fase in fisica statistica sia come si diffonde un'opinione all'interno di una comunità. Mentre il primo problema è stato indagato a partire dai primi lavori matematici sulla metastabilità, il secondo ha prosperato negli ultimi decenni, quando l'avvento dell'era dei computer ha suscitato un interesse sempre più crescente nelle proprietà fondamentali delle reti complesse. A tal fine, quando si interpreta il modello di Ising come modello di comportamento cooperativo, non è appropriato studiarlo in un ambiente dove il dominio sottostante è un reticolo. Quindi, negli ultimi anni c'è stato un grande interesse nello studio della metastabilità per il modello di Ising su grafi aleatori, che sono modelli per reti complesse. Ci riferiamo per esempio a [33, 34, 38, 55, 56], dove questo problema è stato affrontato per grafi aleatori statici, come il modello di configurazione, il grafo aleatorio regolare ed i grafi di Erdös-Rényi.

In questo lavoro iniziamo la nostra analisi della metastabilità per sistemi di particelle interagenti che descrivono l'evoluzione delle opinioni di invidui considerando come struttura sottostante una rete statica (non casuale) con una struttura comunitaria non banale. L'oggetto principale di interesse è come il sistema sociale governa le interazioni tra individui quando è influenzato da fattori esterni, per esempio pubblicità e politiche sociali. Tuttavia, la necessità di ottenere una *descrizione realistica* di alcuni tipi di reti porta a considerare *grafi aleatori dinamici*, che modellizzano la *crescita* del grafo nel tempo. A tal fine, l'ultima parte di questa tesi è dedicato all'analisi di un particolare tipo di modello dinamico, noto come *modello ad attaccamento preferenziale*. Il nostro obiettivo finale è quello di caratterizzare il comportamento

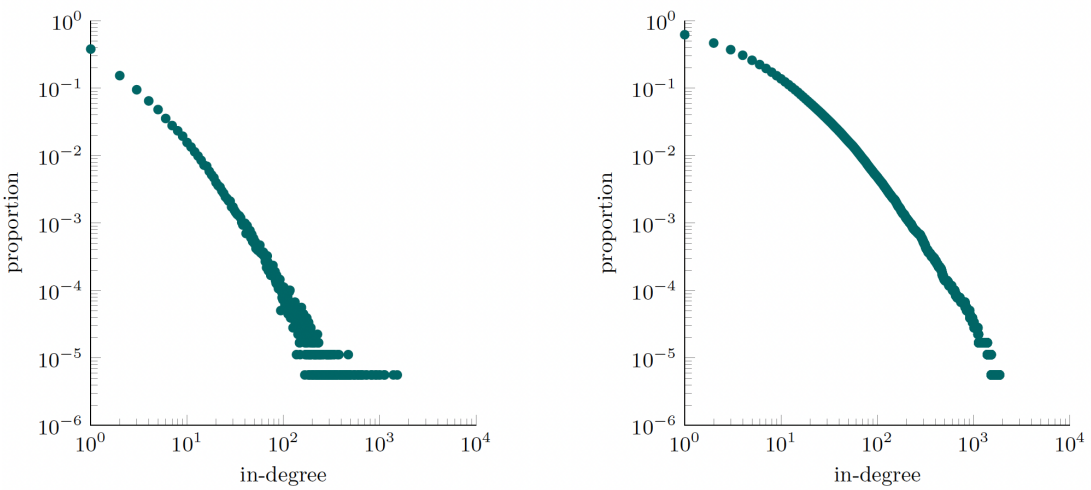

Figura 2.3 – La distribuzione dei gradi interni per la rete delle citazioni di articoli di probabilità e statistica in Web of Science. Sulla sinistra (risp. destra) riportiamo il grafico in scala log–log plot della funzione di probabilità di massa (risp. funzione di distribuzione cumulativa complementare). Figura presa da [69].

metastabile di tale modello. In questo lavoro analizziamo le proprietà asintotiche di questo grafo, che rappresenta un primo passo in questa direzione.

L'idea alla base dei modelli ad attacco preferenziali è semplice. In un grafo che si evolve nel tempo, i vertici appena aggiunti sono collegati a quelli già esistenti. Pensiamo a questo vertice come ad un nuovo individuo in una popolazione sociale, che rappresentiamo come un grafo in cui gli individui sono i vertici ed i lati sono le relazioni tra coppie di individui. È realistico assumere che i lati si connettano ad ogni individuo già presente con pari probabilità, o il nuovo arrivato ha più probabilità di conoscere persone socialmente attive, le quali conoscono già molte persone? Se quest'ultimo è vero, dovrebbe essere più probabile che i lati siano collegati ai vertici che hanno già un alto grado. Un possibile modello per tale grafo dinamico è stato proposto in [19], e da allora ha incitato un enorme sforzo di ricerca.

È stato dimostrato che tale modello porta a delle sequenze di gradi che seguono una legge di potenza, cioè, i gradi dei vertici mostrano un'enorme quantità di variabilità ed il numero di vertici con grado almeno k decade lentamente per k grande, il cosiddetto *fenomeno senza scala*. Questo implica che i gradi sono altamente variabili ed esistono vertici con grado estremamente elevato. Spesso, la coda della distribuzione del grado empirico sembra decadere come una potenza inversa di k. L'esistenza di sequenze di gradi che seguono una legge di potenza in varie reti del mondo reale è abbastanza sorprendente, e i modelli che offrono una spiegazione convincente possono darci informazioni circa i meccanismi che danno origine alla loro natura senza scala. Cerchiamo di illustrare questo fenomeno con l'esempio delle reti di citazione. In queste reti, i vertici sono articoli scientifici, e un lato diretto tra due articoli rappresenta un riferimento del primo articolo al secondo. Così, il grado interno di un articolo è il suo numero di citazioni, mentre il grado esterno è il suo numero di riferimenti. Nella Figura 2.3 rappresentiamo la distribuzione in gradi, in scala log-log, della rete di citazioni di articoli di probabilità e statistica dal 1980 al Maggio 2015 in Web of science. Possiamo vedere che la distribuzione dei gradi interni assomiglia a una legge di potenza. Infatti, sia N_k il numero di vertici con grado k. Quando è approssimativamente proporzionale a una potenza inversa di k, cioè, $N_k \approx c_n k^{-\tau}$ per qualche costante di normalizzazione c_n ed esponente τ, si ottiene che

$$\log N_k \approx \log c_n - \tau \log k,$$

in modo che il grafico di $\log k \to \log N_k$ è vicino ad una linea retta.

Una possibile spiegazione del manifestarsi delle sequenze di gradi che seguono una legge di potenza è offerto dal paradigma dell'attaccamento preferenziale. Nei modelli ad attacco preferenziale, i vertici sono aggiunti in sequenza con un certo numero di lati collegati a loro. Questi lati sono attaccati ad un vertice ricevente con una probabilità proporzionale al grado del vertice ricevente in quel momento, favorendo così i vertici con un alto grado. Per questo

modello, in [30] è mostrato che il numero di vertici con grado k decade proporzionalmente a k^{-3}, e questo risultato è un caso speciale di un risultato più generale sulla sequenza dei gradi asintotica di modelli ad attaccamento preferenziale (si veda la Sezione 2.5).

Nei modelli ad attaccamento preferenziale, è noto che la proporzione dei nodi con un dato grado al passo n converge a una costante quando $n \to \infty$ (si veda la Sezione 2.5 per maggiori dettagli). In questa tesi troviamo la distribuzione asintotica delle fluttuazioni intorno a questo valore limite. In particolare, dimostreremo un teorema di limite centrale per la distribuzione congiunta di tutti i conteggi dei gradi.

2.2 APPROCCI MATEMATICI ALLA METASTABILITÀ

Lo studio della metastabilità ha una storia lunga e ricca. In questa sezione diamo un breve riassunto degli sviluppi più importanti che hanno dato forma al lavoro presentato in questa tesi, che è focalizzato su sistemi a temperatura molto bassa. In [77, 100] è stata tentata per la prima volta una descrizione matematica per lo studio della metastabilità, che è ispirata alla Meccanica Statistica dell'equilibrio di Gibbs nel contesto della teoria di van der Waals-Maxwell. L'*approccio traiettoriale* alla metastabilità nasce tra la fine degli anni '60 e l'inizio degli anni '70 da Freidlin e Wentzell. Hanno introdotto la teoria di *grandi deviazioni sullo spazio dei cammini* per analizzare il comportamento a lungo termine di sistemi dinamici sotto l'influenza di perturbazioni casuali deboli. La loro realizzazione che il comportamento metastabile è controllato da grandi deviazioni del processo aleatorio che guida la dinamica ha influenzato da allora la maggior parte della letteratura matematica sull'argomento. Ci riferiamo alla monografia [57] per un'ampia discussione. L'applicazione di queste idee in un contesto di fisica statistica è stato avviato nel 1984 [39] ed è stato sviluppato in [95–97]. Questa serie di lavori ha realizzato che la teoria proposta da Freidlin e Wentzell può essere applicata per studiare il comportamento metastabile di sistemi di particelle interagenti.

L'approccio traiettoriale si concentra sulla *dinamica* della transizione dallo stato metastabile allo stato stabile. Il vantaggio di questo approccio è che fornisce una descrizione dettagliata del comportamento metastabile del sistema ed ha permesso di rispondere alle tre domande della metastabilità. Individuando il cammino più probabile tra stati metastabili è possibile determinare sia il tempo della transizione sia il tubo delle traiettorie tipiche. Una versione moderna dell'approccio traiettoriale contenente le informazioni sul tempo e sulle gocce critiche divise rispetto a quelle sul tubo delle traiettorie tipiche si trova in [44, 45, 85, 92]. Questo approccio si è sviluppato nel corso degli anni ed è stato ampiamente applicato per studiare la metastabilità nei modelli reticolari di Meccanica Statistica. In questo contesto, questo approccio e quello che segue [31, 85, 97] sono stati sviluppati con l'obiettivo di trovare risposte valide con la massima generalità e ridurre il più possibile il numero di ipotesi dipendenti dal modello necessarie per descrivere il comportamento metastabile di un dato sistema. L'approccio traiettoriale è stato applicato in volume finito a bassa temperatura per la dinamica di Glauber a singola inversione di spin, vedere ad esempio [4, 10, 14, 24, 39, 40, 42, 49, 79, 80, 89, 93], per la dinamica di Kawasaki, vedi ad es. [13, 16–18, 67, 71, 72, 74, 75, 90], e per dinamiche parallele, vedere ad esempio [43, 46–48]. Lo svantaggio dell'approccio traiettoriale è che la funzione di tasso è generalmente difficile da identificare e controllare, specialmente per i sistemi con un'interazione spaziale, per cui la dinamica non è locale. Di conseguenza, questo approccio in genere conduce a risultati relativamente grezzi sul tempo di transizione.

Questa limitazione può essere superata attraverso l'uso di un altro approccio, il cosiddetto *approccio potenziale–teorico*, avviato in [31] e riassunto nella monografia [32]. In questo approccio, il fenomeno della metastabilità viene interpretato come una sequenza di visite del cammino a diversi insiemi metastabili. Questo metodo si concentra su un'analisi precisa dei tempi di arrivo in questi insiemi con l'aiuto della *teoria del potenziale*. Nell'approccio potenziale–teorico il tempo medio di transizione è dato in termini delle cosiddette *capacità* tra due insiemi. Le capacità possono essere stimate sfruttando potenti principi variazionali. Questo significa che le stime del tempo medio di transizione che si possono ricavare sono molto più forti rispetto a quelle ottenute tramite l'approccio traiettoriale. L'approccio potenziale–teorico è stato applicato ai modelli a volume finito e a bassa temperatura, vedi ad es. [35, 37, 70, 73, 91].

Questi approcci matematici, tuttavia, non sono del tutto equivalenti poiché si basano su definizioni diverse degli stati metastabili (vedi [44, Sezione 3] per un confronto) e quindi coinvolgono proprietà diverse dei tempi di arrivo e di transizione. La situazione è particolarmente delicata per evoluzioni di sistemi a volume infinito, sistemi irreversibili e sistemi degeneri, come discusso in [27, 44, 45, 48]. Nuove difficoltà compaiono quando l'entropia ha un ruolo più importante da giocare nel modello. Le situazioni più interessanti sono il limite di volume infinito, temperatura più alta o campo magnetico evanescente, che sono state studiate ad esempio in [11, 36, 41, 52, 53, 62, 63, 66, 75, 86, 87, 105, 106] per modelli di tipo Ising che evolvono secondo dinamica di Glauber e Kawasaki. Approcci più recenti sono stati sviluppati in [6, 20, 21, 28, 29, 82].

2.3 METASTABILITÀ PER SISTEMI CONSERVATIVI

Prendiamo l'esempio di un vapore sovrasaturo. Consideriamo un vapore al di sotto della sua temperatura critica, vicino al suo punto di condensazione. Comprimiamo isotermicamente una certa quantità di vapore, privo di impurità, fino alla pressione del vapore saturo (alla temperatura corrispondente). In seguito continuiamo ad aumentare lentamente la pressione, cercando di evitare significativi gradienti di densità all'interno del campione. Con una sperimentazione così attenta possiamo preparare quello che viene chiamato un vapore sovrasaturo. Osserviamo, infatti, che il sistema è ancora in una fase gassosa pura. Persiste in questa situazione di apparente equilibrio per molto tempo: questo è chiamato "stato metastabile", in contrasto con uno stato stabile, che, per dati valori dei parametri termodinamici, corrisponderebbe alla coesistenza di liquido e vapore. La situazione stazionaria con una fase pura che abbiamo descritto sopra persiste fino a quando una perturbazione esterna o una fluttuazione spontanea induce la nucleazione della fase liquida, avviando un processo irreversibile che porta ad uno stato stabile finale, dove liquido e vapore sono separati, ma coesistono alla pressione di vapore saturo. La durata dello stato metastabile diminuisce all'aumentare del grado di sovrasaturazione, fino ad un valore di soglia per la pressione (il punto spinodale) dove il gas diventa instabile. Il comportamento sopra descritto è tipico di un'evoluzione conservativa, cioè il numero di molecole viene preservato. Per modellizzare matematicamente fenomeni come questo e come l'acqua surriscaldata o sopraffusa viene spesso proposto l'utilizzo modelli di gas reticolari che evolvono secondo la dinamica Kawasaki, poiché tale dinamica conserva il numero di particelle. Sottolineiamo che le dinamiche conservatrici sono difficili da analizzare a causa della conservazione delle particelle: ciò implica che le gocce molte volte devono scambiarsi particelle con il gas che le circonda in lunghi intervalli di tempo. Pertanto la dinamica è *non locale* nella sua essenza.

2.3.1 *Dinamica di Kawasaki*

Consideriamo un gas reticolare bidimensionale a temperatura e densità molto basse che si evolve secondo la dinamica di Kawasaki, cioè le particelle sono soggette ad esclusione ed interazione in un dominio all'interno di $\mathbb{Z}^2$. Più precisamente, sia β la temperatura inversa del gas. Fissiamo la densità del gas uguale a $\rho = e^{-\Delta\beta}$, con $\Delta > 0$ un *parametro di attività*. Per avere particelle vediamo che il dominio che consideriamo non può essere finito, ma la sua dimensione deve essere almeno esponenzialmente grande in β. Pertanto consideriamo che il nostro sistema evolva in una scatola quadrata $\Lambda_\beta \subset \mathbb{Z}^2$ centrata nell'origine, con condizioni al bordo periodiche e tale che $|\Lambda_\beta| = e^{\Theta\beta}$, con $\Theta > \Delta$. Vedremo nella Sezione 2.3.4 che il parametro Θ gioca un ruolo cruciale nell'analisi.

Ad ogni sito $x \in \Lambda_\beta$ associamo una variabile di occupazione $\eta(x)$, che può assumere i valori 0 o 1, dove $\eta(x) = 0$ (risp. $\eta(x) = 1$) significa che il sito x è vuoto (risp. occupato). Una configurazione di gas reticolare è indicata da $\eta \in \mathcal{X}_\beta := \{0,1\}^{\Lambda_\beta}$. Ad ogni configurazione η associamo un'energia, la cosiddetta *Hamiltoniana* del sistema, data da

$$H(\eta) = -U \sum_{\{x,y\}\in\Lambda_\beta^*} \eta(x)\eta(y), \tag{2.3.1}$$

dove Λ_β^* denota l'insieme dei legami tra i siti primi–vicini in Λ_β, cioè, c'è una *energia di legame* $-U < 0$ tra particelle vicine. Sia

$$|\eta| = \sum_{x \in \Lambda_\beta} \eta(x) \tag{2.3.2}$$

il numero di particelle in Λ_β nella configurazione η, e sia

$$\mathcal{V}_N = \{\eta \in \mathcal{X}_\beta : \ |\eta| = N\} \tag{2.3.3}$$

l'insieme delle configurazioni con N particelle. Definiamo la dinamica di Kawasaki come la catena di Markov a tempo continuo $X = (X(t))_{t \geqslant 0}$ con spazio degli stati $\mathcal{V}_N$ data dal generatore

$$(\mathcal{L}f)(\eta) = \sum_{\{x,y\} \in \Lambda_\beta^*} c(x, y, \eta)[f(\eta^{x,y}) - f(\eta)], \qquad \eta \in \mathcal{X}_\beta, \tag{2.3.4}$$

dove

$$\eta^{x,y}(z) = \begin{cases} \eta(z) & \text{if} \quad z \neq x, y, \\ \eta(x) & \text{if} \quad z = y, \\ \eta(y) & \text{if} \quad z = x, \end{cases} \tag{2.3.5}$$

e

$$c(x, y, \eta) = e^{-\beta[H(\eta^{x,y}) - H(\eta)]_+}. \tag{2.3.6}$$

Le equazioni (2.3.4)–(2.3.6) rappresentano la *dinamica di Metropolis* standard associata ad H, che è *conservativa* perché conserva il numero di particelle, cioè, $|X(t)| = |X(0)| = N$ per ogni $t > 0$. La *misura canonica di Gibbs* ν_N, definita come

$$\nu_N(\eta) = \frac{e^{-\beta H(\eta)} \mathbb{1}_{\mathcal{V}_N}(\eta)}{Z_N}, \qquad Z_N = \sum_{\eta \in \mathcal{V}_N} e^{-\beta H(\eta)}, \qquad \eta \in \mathcal{X}_\beta, \tag{2.3.7}$$

è l'equilibrio reversibile di questa dinamica stocastica per ogni N:

$$\nu_N(\eta) c(x, y, \eta) = \nu_N(\eta^{x,y}) c(x, y, \eta^{x,y}). \tag{2.3.8}$$

Variare i parametri U e Δ porta a un drastico cambiamento del comportamento del gas. Infatti, la scelta $\Delta \in (0, U)$ rappresenta il gas instabile, $\Delta = U$ rappresenta il punto spinoidale, $\Delta \in (U, 2U)$ corrisponde al *regime metastabile*, $\Delta = 2U$ è il punto di condensazione e $\Delta > 2U$ corrisponde a un gas stabile. Ci riferiamo a [67, 75] per un'ampia discussione su questi punti, mentre nella Sezione 2.3.2 giustifichiamo il suddetto regime metastabile.

Per analizzare rigorosamente questo modello completamente conservativo, l'idea è quella di focalizzare l'attenzione su cosa accade nel *modello semplificato* introdotto in [75]. Questo modello può essere ottenuto dalla dinamica di Kawasaki sopra definita dopo aver considerato esclusione solo all'interno di una scatola quadrata $\Lambda \subset \Lambda_\beta$ finita e indipendente da β ed interazioni solo in

$$\Lambda_0 := \Lambda \setminus \partial^- \Lambda, \tag{2.3.9}$$

dove

$$\partial^- \Lambda := \{x \in \Lambda : \exists y \notin \Lambda \text{ tale che } |y - x| = 1\} \tag{2.3.10}$$

è il bordo interno di Λ, in modo che la dinamica del gas fuori da Λ sia quella di passeggiate aleatorie indipendenti (si veda la Figura 2.4). L'introduzione di questo modello è giustificato dal fatto che, per la dinamica originale di Kawasaki, l'interazione tra un cluster e le particelle "isolate" del gas può essere approssimato dall'interazione tra cluster ed un gas di passeggiate aleatorie indipendenti. Come ampiamente spiegato in [75], la nucleazione per il modello semplificato può essere affrontato attraverso l'analisi della versione locale del modello, il

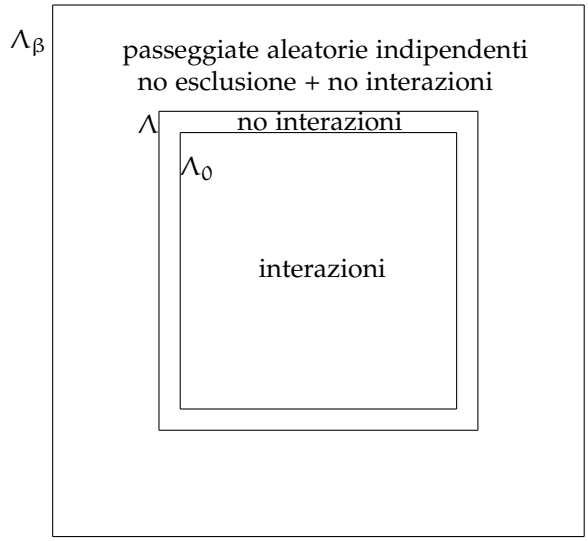

Figura 2.4 – Rappresentazione schematica del dominio Λ_β nel modello semplificato.

cosiddetto *modello locale*. In parole povere, in questo modello le particelle vivono ed evolvono solo all'interno della scatola finita Λ, dove l'effetto su Λ del gas in $\Lambda_\beta \setminus \Lambda$ può essere descritto in termini di creazione di nuove particelle a tasso ρ nei siti sul bordo interno di Λ e l'annichilazione di particelle a tasso 1 nei siti sul bordo esterno di Λ. Ci riferiamo alla Sezione 2.3.2 per la precisa definizione del modello locale. Riassumendo, i passi per affrontare il problema dell'uscita dalla metastabilità per la dinamica di Kawasaki completamente conservativa sono i seguenti:

PASSO 1: Analizzare il tempo di nucleazione ed il tubo delle traiettorie tipiche per il modello locale. Questi problemi sono stati affrontati in [67, 75].

PASSO 2: Estendere questi risultati al modello semplificato. Questo problema è stato risolto in [75].

PASSO 3: Dimostrare che il modello semplificato è una buona approssimazione per le interazioni tra un cluser ed il gas che lo circonda in una finestra finita per la dinamica originale di Kawasaki. Questo problema è stato affrontato in [65].

PASSO 4: Ottenere la stima del tempo di nucleazione ed il tubo delle traiettorie tipiche per la dinamica originale di Kawasaki. Questo problema è indagato in questa tesi (vedi Sezione 2.3.4).

Come risulterà chiaro nel corso della tesi, il passo 4 è altamente non banale e richiede un'attenta indagine. Ci riferiamo alla Sezione 2.3.4 per le idee principali per affrontare questo problema. Notiamo che il passaggio 3 ci fornisce il modo corretto per controllare il comportamento del gas in $\Lambda_\beta \setminus \Lambda$. È chiaro che il punto di partenza è l'analisi del modello locale, che viene introdotto e studiato nella Sezione 2.3.2.

2.3.2 *Il modello locale sul reticolo quadrato*

In questa sezione introduciamo il modello locale e presentiamo i principali risultati già presenti in letteratura insieme a quelli che sono derivati in questa tesi. Consideriamo una scatola finita $\Lambda = \{0, ..., L\}^2 \subset \mathbb{Z}^2$ centrata nell'origine. La lunghezza del lato L è fissa, ma arbitraria, e più tardi richiederemo che L sia sufficientemente grande. Il nostro spazio degli stati è $\mathcal{X} := \{0,1\}^\Lambda$. Per essere più generici possibile, ad ogni configurazione $\eta \in \mathcal{X}$ associamo l'*energia hamiltoniana locale* $\widehat{H}(\eta)$ come

$$\widehat{H}(\eta) := -U_1 \sum_{(x,y)\in\Lambda^*_{0,h}} \eta(x)\eta(y) - U_2 \sum_{(x,y)\in\Lambda^*_{0,v}} \eta(x)\eta(y) + \Delta \sum_{x\in\Lambda} \eta(x), \tag{2.3.11}$$

dove $\Lambda^*_{0,h}$ (risp. $\Lambda^*_{0,v}$) è l'insieme dei legami non orientati orizzontali (risp. verticali) che uniscono i punti primi–vicini in Λ_0 (si ricordi (2.3.9)). Pertanto, l'interazione agisce solo

all'interno $\Lambda \setminus \partial^- \Lambda$; l'energia di legame associata ad un legame orizzontale (risp. verticale) è $-U_1 < 0$ (risp. $-U_2 < 0$). Si noti che $\widehat{H}(\eta)$ si ottiene aumentando l'energia in (2.3.1) di un termine $\Delta|\eta|$ e distinguendo tra legami orizzontali e verticali. Questo modella la presenza di un serbatoio esterno che conserva la densità delle particelle in Λ_β fissata a $\rho = e^{-\beta\Delta}$. Possiamo assumere senza perdita di generalità che $U_1 \geqslant U_2$. Il comportamento dinamico del modello locale cambia drasticamente in base alla relazione tra i parametri U_1 e U_2. In particolare individuiamo tre regimi interessanti: *isotropo* ($U_1 = U_2 = U$), *debolmente anisotropo* ($U_1 < 2U_2$) e *fortemente anisotropo* ($U_1 > 2U_2$). Sebbene la nostra analisi per il modello originale riguarda solo il caso isotropo (come è chiaro dall'Hamiltoniana definita in (2.3.1)), definiamo il modello locale in modo generale perché ci interessa la sua analisi per tutti e tre i regimi. La *dinamica di Kawasaki localmente conservativa* può essere definita come la dinamica originale con comportamenti diversi al bordo di Λ. Per essere precisi, sia $b = (x \to y)$ un legame orientato, cioè una coppia *ordinata* di siti vicini, e definiamo

$$\begin{aligned} \partial^*\Lambda^{out} &:= \{b = (x \to y) : x \in \partial^-\Lambda, y \notin \Lambda\}, \\ \partial^*\Lambda^{in} &:= \{b = (x \to y) : x \notin \Lambda, y \in \partial^-\Lambda\}, \\ \Lambda^{*,orie} &:= \{b = (x \to y) : x, y \in \Lambda\}, \end{aligned} \tag{2.3.12}$$

e poniamo $\bar{\Lambda}^{*,orie} := \partial^*\Lambda^{out} \cup \partial^*\Lambda^{in} \cup \Lambda^{*,orie}$. Due configurazioni $\eta, \eta' \in \mathcal{X}$, con $\eta \neq \eta'$, si dicono *stati comunicanti* se esiste un legame $b \in \bar{\Lambda}^{*,orie}$ tale che $\eta' = T_b\eta$, dove $T_b\eta$ è la configurazione ottenuta da η in uno dei modi segunti:

— per $b = (x \to y) \in \Lambda^{*,orie}$, $T_b\eta$ denota la configurazione ottenuta da η scambiando particelle lungo b:

$$T_b\eta(z) := \begin{cases} \eta(z) & \text{if } z \neq x, y, \\ \eta(x) & \text{if } z = y, \\ \eta(y) & \text{if } z = x. \end{cases} \tag{2.3.13}$$

— Per $b = (x \to y) \in \partial^*\Lambda^{out}$ poniamo:

$$T_b\eta(z) := \begin{cases} \eta(z) & \text{if } z \neq x, \\ 0 & \text{if } z = x. \end{cases} \tag{2.3.14}$$

Questo descrive l'annichilazione di una particella lungo il bordo.

— per $b = (x \to y) \in \partial^*\Lambda^{in}$ poniamo:

$$T_b\eta(z) := \begin{cases} \eta(z) & \text{if } z \neq y, \\ 1 & \text{if } z = y. \end{cases} \tag{2.3.15}$$

Questo descrive la creazione di una particella lungo il bordo.

Poiché in volume finito trattare un processo stocastico a tempo discreto è equivalente e più conveniente rispetto ad un processo a tempo continuo, definiamo la dinamica di Kawasaki come la catena di Markov a tempo discreto $(\eta_t)_{t\in\mathbb{N}}$ sullo spazio degli stati $\mathcal{X}$ data dalle seguenti probabilità di transizione: per $\eta \neq \eta'$:

$$P(\eta, \eta') := \begin{cases} |\bar{\Lambda}^{*,orie}|^{-1} e^{-\beta[H(\eta')-H(\eta)]_+} & \text{se } \exists b \in \bar{\Lambda}^{*,orie} : \eta' = T_b\eta, \\ 0 & \text{altrimenti,} \end{cases} \tag{2.3.16}$$

dove $[a]_+ = \max\{a, 0\}$ e $P(\eta, \eta) := 1 - \sum_{\eta' \neq \eta} P(\eta, \eta')$. Questo descrive una dinamica di Metropolis standard con condizioni al contorno aperte: lungo ciascun legame che tocca $\partial^-\Lambda$ dall'esterno le particelle vengono create con tasso $\rho = e^{-\Delta\beta}$ e sono annientate con tasso 1, mentre all'interno di Λ_0 le particelle sono conservate. Si noti che uno scambio di numeri occupazionali $\eta(x)$ per ogni x all'interno dell'anello $\Lambda \setminus \Lambda_0$ non comporta alcuna variazione di energia.

Osservazione 2.3.1. *La dinamica stocastica definita da* (2.3.16) *è reversibile rispetto alla misura di Gibbs gran canonica*

$$\mu(\eta) := \frac{e^{-\beta\widehat{H}(\eta)}}{Z}, \qquad Z := \sum_{\eta\in\mathcal{X}} e^{-\beta\widehat{H}(\eta)}, \qquad \eta \in \mathcal{X}. \tag{2.3.17}$$

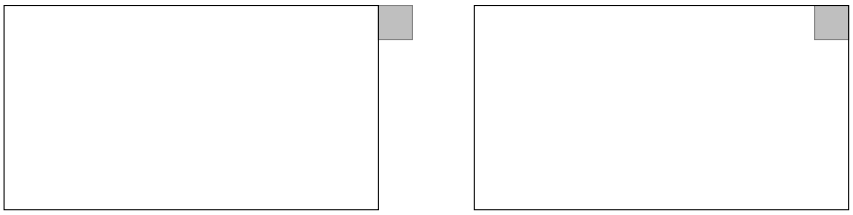

Figura 2.5 – In entrambi i cluster rappresentiamo in grigio la particella che sta per staccarsi: quella a sinistra (risp. destra) è sporgente (risp. non sporgente) e staccarla ha una probabilità dell'ordine di $e^{-U_1\beta}$ (risp. $e^{-(U_1+U_2)\beta}$).

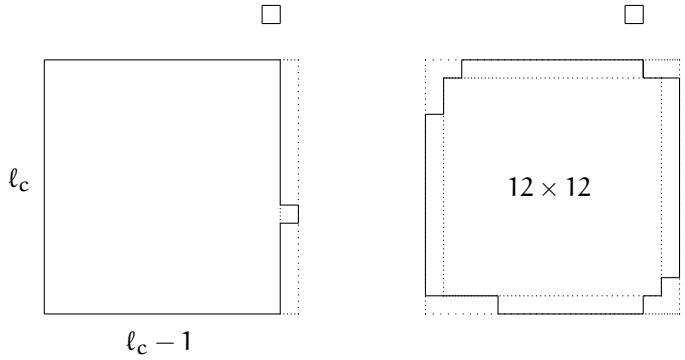

Figura 2.6 – Configurazioni critiche nel regime isotropo per $\ell_c = 14$.

Nel resto di questa sezione presenteremo i principali risultati riguardanti la metastabilità e la nucleazione per il modello locale in tutti e tre i regimi. Innanzitutto, si noti che il regime metastabile corrisponde a prendere

$$\Delta \in (U_1, U_1 + U_2). \tag{2.3.18}$$

Una caratteristica particolare della dinamica di Kawasaki è che nel regime metastabile (2.3.18) le particelle si muovono lungo il bordo di una goccia più rapidamente di quanto arrivino dal bordo della scatola. Più precisamente, la condizione $\Delta > U_1$ implica che l'arrivo di nuove particelle è più lento della dissociazione delle particelle sporgenti (si veda la Figura 2.5 a sinistra), mentre la condizione $\Delta < U_1 + U_2$ implica che l'arrivo di nuove particelle è più veloce della dissociazione delle particelle non sporgenti (si veda la Figura 2.5 a destra). Si noti che nel caso di interazioni isotrope la condizione in (2.3.18) si legge come $U < \Delta < 2U$. Per tutti questi tre regimi abbiamo che la scatola vuota

$$\square := \{\eta \in \mathcal{X} : \eta(x) = 0 \ \forall\, x \in \Lambda\} \tag{2.3.19}$$

è l'unico stato metastabile e la scatola piena

$$\blacksquare := \{\eta \in \mathcal{X} : \eta(x) = 1 \ \forall\, x \in \Lambda_0, \eta(x) = 0 \ \forall\, x \in \Lambda \setminus \Lambda_0\} \tag{2.3.20}$$

è l'unico stato stabile, purché L sia sufficientemente grande. Questa ipotesi è necessaria per avere $\widehat{H}(\blacksquare) < \widehat{H}(\square) = 0$ e più avanti forniremo un limite inferiore esplicito per L. L'uscita dalla metastabilità consiste quindi nell'analizzare la transizione da $\square$ a $\blacksquare$. I principali oggetti dell'analisi sono la stima di questo tempo di transizione e la descrizione geometrica delle *gocce critiche* che il sistema deve attraversare per eseguire la nucleazione, il cosiddetto *varco* per la transizione. Inoltre, un aspetto cruciale sia da un punto di vista probabilistico che fisico è la descrizione dell'unione di tutti i *varchi minimali*, dove un varco minimale è un varco che è minimo per inclusione. Questi hanno il significato fisico di "insiemi minimi di configurazioni critiche" e sono un passo cruciale nella descrizione delle traiettorie tipiche.

Per rendere precisa l'ipotesi precedente su L, introduciamo le cosiddette *lunghezze critiche*. In particolare, nel regime isotropo $U_1 = U_2 = U$ definiamo la lunghezza critica come

$$\ell_c := \left\lceil \frac{U}{2U - \Delta} \right\rceil, \tag{2.3.21}$$

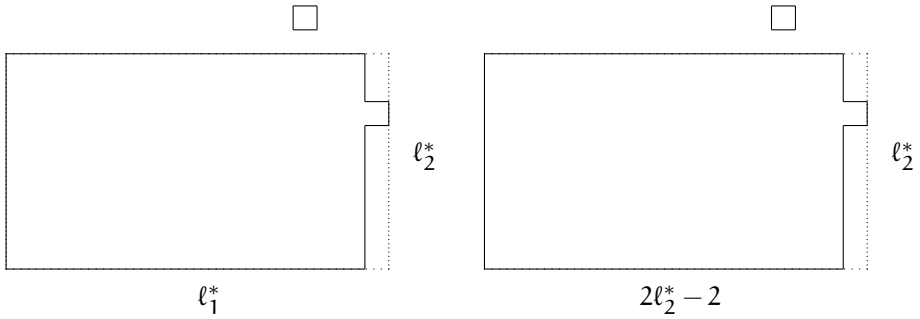

Figura 2.7 – Configurazioni critiche canoniche nel regime debolmente anisotropo (sulla sinistra) e nel regime fortemente anisotropo (sulla destra).

mentre nei regimi anisotropi ($U_1 \neq U_2$) definiamo rispettivamente la lunghezza critica orizzontale e verticale come

$$\ell_1^* := \left\lceil \frac{U_1}{U_1 + U_2 - \Delta} \right\rceil, \qquad \ell_2^* := \left\lceil \frac{U_2}{U_1 + U_2 - \Delta} \right\rceil. \tag{2.3.22}$$

Richiediamo quindi

$$L > \begin{cases} 2\ell_c & \text{per il regime isotropo,} \\ 2\ell_1^* & \text{per i regimi anisotropi.} \end{cases} \tag{2.3.23}$$

Abbiamo bisogno inoltre di alcune ipotesi di non degenerazione. In particolare, per il modello isotropo assumiamo

$$\frac{U}{2U - \Delta} \notin \mathbb{N}, \tag{2.3.24}$$

mentre per i modelli anisotropi assumiamo

$$\frac{U_1}{U_1 + U_2 - \Delta} \notin \mathbb{N}, \qquad \frac{U_2}{U_1 + U_2 - \Delta} \notin \mathbb{N}. \tag{2.3.25}$$

Per evitare casi banali patologici, assumiamo inoltre

$$\Delta \in \begin{cases} \left(\frac{3}{2}U, 2U\right) & \text{per il regime isotropo,} \\ \left(U_1 + \frac{U_2}{2}, U_1 + U_2\right) & \text{per i regimi anisotropi.} \end{cases} \tag{2.3.26}$$

Notiamo che la condizione (2.3.26) garantisce che tutte le lunghezze critiche siano maggiori di due. Nel resto di questa sezione assumeremo che tali condizioni (2.3.23)-(2.3.26) siano valide. Da [16, 75, 90] è ben nota la forma delle gocce critiche canoniche per i tre regimi: sono costituite da una forma rettangolare con l'aggiunta di una protuberanza (cioè una particella attaccata a un lato del cluster rettangolare) e di una particella libera ovunque in Λ (cioè una particella che non interagisce con le altre). Si veda la Figura 2.6 a sinistra e la Figura 2.7. Più precisamente, queste costituiscono un *varco* per la transizione, cioè un insieme di configurazioni che sarà attraversato con probabilità tendente a 1 nel limite di β che va all'infinito. Per definire rigorosamente il concetto di varco, un ruolo centrale è giocato dall'insieme dei *cammini ottimali*, che sono quei cammini (ovvero sequenze di configurazioni comunicanti) che tra tutti quelli che vanno da $\square$ a $\blacksquare$ realizzano il valore minimo dell'energia massima raggiunta in un singolo cammino. Poniamo formalmente

$$(\square \to \blacksquare)_{opt} := \{\omega : \square \to \blacksquare : \max_{\xi \in \omega} \widehat{H}(\xi) = \Phi(\square, \blacksquare)\}, \tag{2.3.27}$$

dove $\omega : \square \to \blacksquare$ è un cammino generico che collega $\square$ a $\blacksquare$ e

$$\Phi(\square, \blacksquare) := \min_{\omega : \square \to \blacksquare} \max_{\xi \in \omega} \widehat{H}(\xi) \tag{2.3.28}$$

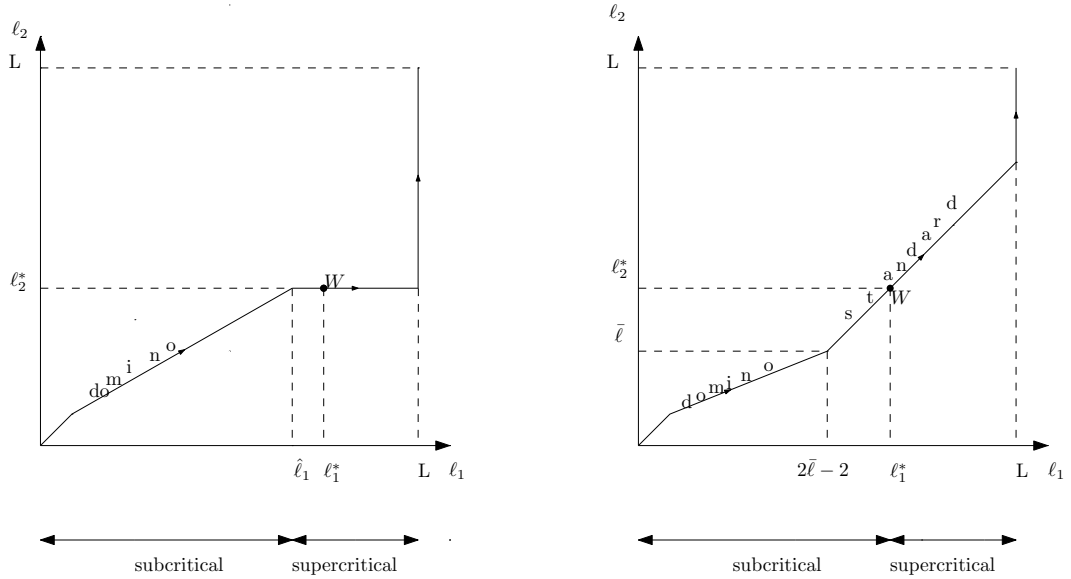

Figura 2.8 – Cammino tipico per forte anisotropia (a sinistra) e debole anisotropia (a destra), in cui si evidenzia con W la forma della configurazione critica di Wulff.

è l'*altezza di comunicazione* tra $\square$ e $\blacksquare$. Definiamo quindi un varco $\mathcal{C}^*(\square,\blacksquare)$ per il passaggio da $\square$ a $\blacksquare$ come sottoinsieme dell'insieme delle *selle minime* $\mathcal{S}(\square,\blacksquare)$ tale che ogni cammino $\omega \in (\square \to \blacksquare)_{opt}$ attraversa l'insieme $\mathcal{C}^*(\square,\blacksquare)$, dove

$$\mathcal{S}(\square,\blacksquare) := \{\zeta \in \mathcal{X} : \exists \omega \in (\square \to \blacksquare)_{opt}, \omega \ni \zeta \text{ tale che } \widehat{H}(\zeta) = \Phi(\square,\blacksquare)\}. \tag{2.3.29}$$

Una prima importante differenza che viene fuori nei diversi regimi è quella che nel regime fortemente anisotropo la forma delle gocce critiche non è *Wulff*, dove la forma di Wulff è quella che minimizza l'energia di una goccia a volume fissato. In effetti la forma di Wulff corrisponde a gocce rettangolari di dimensioni orizzontali e verticali rispettivamente pari a ℓ_1 e ℓ_2 tale che $\ell_1 - \ell_2$ sia di ordine

$$\bar{\ell} := \left\lceil \frac{u_1 - u_2}{u_1 + u_2 - \Delta} \right\rceil, \tag{2.3.30}$$

che si chiamano *rettangoli standard*. Si noti che nel regime isotropo ciò significa che i cluster quadrati hanno la forma di Wulff. Dalla forma delle gocce critiche canoniche è facile verificare che nel modello isotropo la forma di Wulff coincide con la forma critica, cosicché non è possibile distinguerle. Un'analisi rigorosa della non equivalenza tra configurazioni critiche e forma di Wulff motiva lo studio dei modelli anisotropi ed è un primo passo per mostrare la robustezza dell'argomentazione radicata nella natura dinamica dei sistemi metastabili. Da un lato osserviamo che anche nel modello debolmente anisotropo la goccia critica ha una forma Wulff, ma in questo caso l'evoluzione del sistema non segue configurazioni con forma di Wulff. In effetti il sistema segue i cosiddetti *rettangoli domino*, che sono rettangoli per i quali la dimensione orizzontale è "quasi" il doppio di quella verticale (si veda la Figura 2.8 a sinistra). Dall'altro lato osserviamo che nel regime fortemente anisotropo le configurazioni critiche non hanno forma di Wulff. Il custer rettangolare, infatti, non è standard, ma è un *rettangolo domino*, e la dinamica incrocia la forma critica di Wulff solo nella sua parte supercritica (si veda la Figura 2.8 a destra). In conclusione, in entrambi i regimi anisotropi la forma di Wulff non è rilevante nello schema di nucleazione come accade per la dinamica anisotropa di Glauber, si veda [79]. La dinamica localmente conservativa e il movimento delle particelle lungo il bordo delle gocce dà un effetto di regolarizzazione. Sorprendentemente, come accennato in precedenza, questo effetto non guida il processo di nucleazione lungo configurazioni con forma di Wulff, soprattutto nell'ipotesi di forte anisotropia. Ci riferiamo a [16, 90] per un'ampia discussione.

Indichiamo con $\mathcal{C}^* = \mathcal{C}^*(\square,\blacksquare)$ l'insieme delle configurazioni critiche e definiamo $\Gamma^* := \Phi(\square,\blacksquare)$. In [16, 75, 90] gli autori hanno dimostrato che Γ^* coincide con l'energia delle

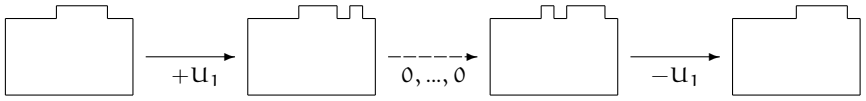

Figura 2.9 – 1-traslazione della barra orizzontale nord a costo U_1.

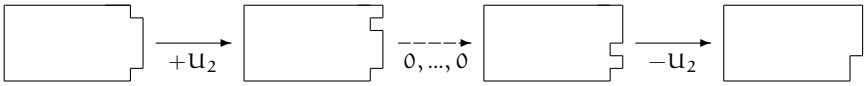

Figura 2.10 – 1-traslazione della barra verticale est a costo U_2.

configurazioni appartenenti a $\mathcal{C}^*$ e che $\mathcal{C}^*$ è un varco per la transizione. Hanno dimostrato inoltre che, con probabilità tendente a 1 nel limite di β che tende all'infinito, il sistema crea la goccia critica e raggiunge lo stato stabile ■ in un tempo di ordine $e^{\Gamma^* \beta}$ quando parte dallo stato metastabile □. Esiste in particolare una formula esplicita per l'energia di barriera Γ^* che dipende dai parametri U_1, U_2 e Δ dell'energia Hamiltoniana e rimandiamo a quei lavori per ulteriori dettagli.

DESCRIZIONE GEOMETRICA DEL VARCO

Una questione significativa per la caratterizzazione dinamica del sistema è la descrizione di *tutte* le configurazioni critiche "rilevanti". Questa descrizione risulta essere molto ricca quando affrontiamo la dinamica conservativa di Kawasaki. Una caratteristica cruciale di questa dinamica, infatti, è che le particelle possono muoversi lungo il bordo delle gocce come parte di movimenti di regolarizzazione. Ci sono due tipi di movimenti rilevanti: la *traslazione di una barra* e lo *scorrimento di una barra*. Intuitivamente, una barra può essere pensata come un insieme di particelle connesse che sono collegate ad un cluster e la traslazione di una barra consiste nell'iterazione dell'1–traslazione rappresentata nelle Figure 2.9-2.10. Lo scorrimento di una barra consiste invece nello spostamento di una barra attaccata ad un cluster attorno ad un angolo del cluster e può essere definito come l'iterazione del moto raffigurato in Figura 2.11. Presenteremo più avanti nella Sezione 3.2.1 punto 5 la precisa definizione delle barre e di questi movimenti. Le citate mosse sono cruciali per la descrizione geometrica completa del varco. A tal fine abbiamo bisogno di alcune definizioni geometriche. Per prima cosa definiamo l'insieme $\bar{\Omega}$ (risp. $\widetilde{\Omega}$) come l'insieme delle configurazioni che hanno soltanto un cluster in Λ_0 costituito da un rettangolo di dimensioni $\ell_1 \times \ell_2$ con una sola protuberanza attaccata ad uno dei lati più corti (risp. lunghi), dove

$$(\ell_1, \ell_2) = \begin{cases} (\ell_c - 1, \ell_c) & \text{per il regime isotropo,} \\ (\ell_1^* - 1, \ell_2^*) & \text{per il regime debolmente anisotropo,} \\ (2\ell_2^* - 3, \ell_2^*) & \text{per il regime fortemente anisotropo.} \end{cases}$$

Indicando con n_c il numero di particelle dei cluster in $\Omega = \bar{\Omega} \cup \widetilde{\Omega}$, definiamo

$$\begin{aligned} \bar{\mathcal{D}} &:= \{\eta' \in \mathcal{V}_{n_c} | \; \exists\, \eta \in \bar{\Omega} : \widehat{H}(\eta) = \widehat{H}(\eta') \text{ e } \Phi_{|\mathcal{V}_{n_c}}(\eta, \eta') \leqslant \widehat{H}(\eta) + U_1\}, \\ \widetilde{\mathcal{D}} &:= \{\eta' \in \mathcal{V}_{n_c} | \; \exists\, \eta \in \widetilde{\Omega} : \widehat{H}(\eta) = \widehat{H}(\eta') \text{ e } \Phi_{|\mathcal{V}_{n_c}}(\eta, \eta') \leqslant \widehat{H}(\eta) + U_1\}, \end{aligned} \tag{2.3.31}$$

dove ricordiamo che $\mathcal{V}_{n_c}$ è l'insieme delle configurazioni con n_c particelle e $\Phi_{|\mathcal{V}_{n_c}}(\eta, \eta')$ significa che stiamo calcolando l'altezza di comunicazione tra η e η' guardando soltanto i cammini che attraversano le configurazioni all'interno dell'insieme $\mathcal{V}_{n_c}$. Si noti che $\bar{\Omega} \subset \bar{\mathcal{D}}$ (risp. $\widetilde{\Omega} \subset \widetilde{\mathcal{D}}$). Per mantenere la notazione concisa abbiamo adottato la stessa per tutti e tre gli

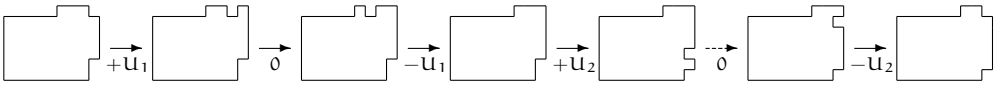

Figura 2.11 – Scorrimento di un quadrato unitario attorno all' "angolo nord-est" a costo U_1.

scenari, ma uno può sostituire U_1 con U nel caso isotropo. Si noti che l'ultima condizione in (2.3.31) equivale a richiedere

$$\Phi_{|\mathcal{V}_{n_c}}(\eta,\eta') < \Gamma^* + \widehat{H}(\square) = \Gamma^*,$$

che deriva dal fatto che per descrivere i varchi ci interessano soltanto i cammini ottimali, in modo che l'energia lungo di loro non può superare il valore Γ^*. In parole povere, nei casi isotropo e debolmente anisotropo si può pensare a $\bar{\mathcal{D}}$ e $\widetilde{\mathcal{D}}$ come gli insiemi delle configurazioni costituite da un cluster rettangolare con quattro barre attaccate ai suoi quattro lati tale che la somma delle lunghezze delle barre è fissato. Per quanto riguarda il modello fortemente anisotropo, questa caratterizzazione viene fuori solo per l'insieme $\bar{\mathcal{D}}$, mentre le configurazioni in $\widetilde{\mathcal{D}}$ hanno un cluster con una forma diversa. Il motivo per cui sorge questa differenza risiede nel fatto che nel regime fortemente anisotropo c'è una maggiore rigidità della dinamica, in modo che il moto delle particelle lungo il bordo di un cluster sia più improbabile. Ne parleremo meglio in seguito e vedremo il forte impatto che questo effetto ha su altre caratteristiche della dinamica. Per quanto riguarda il regime isotropo, la caratterizzazione geometrica completa è stata ottenuta in [35, Teorema 1.4.1], mentre per i regimi anisotropi costituisce una novità di questa tesi.

Concentriamoci innanzitutto sul regime isotropo. In [35] gli autori hanno dimostrato che il varco per la transizione $\mathcal{C}^*$ può essere espresso come $\mathcal{C}^* = \mathcal{D}^{fp}$, dove

$$\mathcal{D} := \bar{\mathcal{D}} \cup \widetilde{\mathcal{D}} \tag{2.3.32}$$

e l'indice superiore "fp" indica l'aggiunta di una particella libera ovunque all'interno della scatola Λ (si veda Figura 2.6 a destra). Vediamo gli ingredienti chiave per dimostrare la suddetta caratterizzazione geometrica del varco. Abbiamo chiaramente che

$$\widehat{H}(\mathcal{C}^*) = \widehat{H}(\mathcal{D}^{fp}) = \widehat{H}(\mathcal{D}) + \Delta = \widehat{H}(\mathcal{Q}) + \Delta = \Gamma^*$$

e quindi

$$\widehat{H}(\mathcal{D}) = \widehat{H}(\mathcal{Q}) = \Gamma^* - \Delta.$$

Gli ingredienti chiave per ottenere l'asserto sono i seguenti (si ricordi (2.3.28)):

(i) Dimostrare che $\Phi(\square, \blacksquare) \leqslant \Gamma^*$.
(ii) Dimostrare che $\Phi(\square, \blacksquare) \geqslant \Gamma^*$.
(iii) Ottenere la descrizione geometrica dell'insieme $\mathcal{D}$.

Per il punto (i) è sufficiente costruire un cammino che collega $\square$ a $\blacksquare$ per cui l'energia lungo di esso non superi il valore critico Γ^*. Per questo facciamo riferimento a [35, Sezione 2.3.1].

Per quanto riguarda il punto (ii), la dimostrazione si articola in tre passi. Il primo è che qualsiasi cammino ottimale $\omega \in (\square \to \blacksquare)_{opt}$ (si ricordi (2.3.27)) deve passare attraverso una configurazione costituita da un singolo cluster rettangolare di dimensioni $(\ell_c - 1) \times \ell_c$ da qualche parte in Λ_0. Questo passo si ottiene utilizzando un argomento standard di tipo disuguaglianza isoperimetrica [1], che garantisce che le configurazioni costituite da $\ell_c(\ell_c - 1)$ particelle con energia minima sono quelle in cui le particelle formano un unico cluster rettangolare di dimensioni $(\ell_c - 1) \times \ell_c$. Indichiamo con η tale configurazione, che è unica modulo traslazioni e rotazioni. Notiamo che

$$\widehat{H}(\eta) = \Gamma^* - 2\Delta + U.$$

Il secondo passo consiste nel dimostrare che tutti i cammini ottimali devono attraversare l'insieme $\mathcal{Q}$. Partendo da η, per raggiungere $\blacksquare$ è necessario che una nuova particella entri all'interno di Λ_0: questo porta l'energia del sistema a raggiungere il valore $\Gamma^* - \Delta + U$. Prima che venga creata una nuova particella, l'energia deve dunque diminuire di almeno U: l'unico modo per farlo è spostare la particella libera finché non si attacca al cluster, dando luogo ad una configurazione in $\mathcal{Q}$. Il passo finale consiste nel dimostrare che per raggiungere $\blacksquare$ da $\mathcal{Q}$ l'energia deve raggiungere il valore Γ^*. Da [1] deduciamo che l'unica mossa consentita è aggiungere una particella libera, dando luogo ad una configurazione con energia Γ^*.

Il punto (iii) fornisce la descrizione completa del varco. Infatti, una volta che il sistema è in $\mathcal{Q}$, prima dell'arrivo della particella seguente, il sistema può raggiungere *tutte* le configurazioni

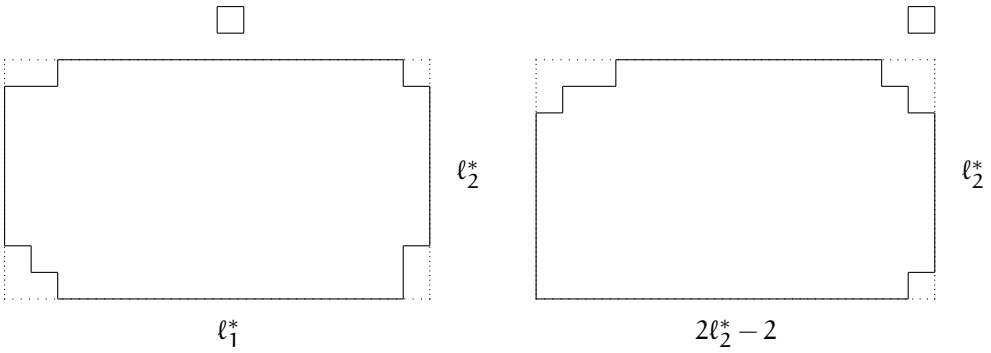

Figura 2.12 – Configurazioni critiche in $\mathcal{C}^*$ nel regime debolmente (risp. fortemente) anisotropo sulla sinistra (resp. destra). Inoltre, se la particella libera viene rimossa, otteniamo una configurazione in $\bar{\mathcal{D}} \setminus \bar{\mathcal{Q}}$.

che hanno la stessa energia, lo stesso numero di particelle e che possono essere raggiunte ad un costo inferiore o uguale ad U, che sono appunto quelle appartenenti a $\mathcal{D}$. Per ottenere questo bisogna studiare tutti i possibili moti delle particelle che possono avvenire sul bordo della goccia, come rappresentato nelle Figure 2.9-2.11.

Attraverso questo ragionamento abbiamo anche caratterizzato l'ingresso nell'insieme delle configurazioni critiche. Dai passaggi precedenti, infatti, segue che ogni $\omega \in (\square \to \blacksquare)_{opt}$ attraversa prima l'insieme $\mathcal{Q}$, poi eventualmente l'insieme $\mathcal{D} \setminus \mathcal{Q}$, ed infine l'insieme $\mathcal{C}^*$. Questa analisi raffinata della dinamica è cruciale quando si cerca di trovare stime più forti relative al tempo medio di transizione. Vedremo nel prossimo paragrafo come risolvere questa problematica.

Consideriamo ora il regime debolmente anisotropo. Notiamo innanzitutto che in questo caso

$$\widehat{H}(\bar{\mathcal{D}}) = \Gamma^* - \Delta < \Gamma^* - \Delta + U_1 - U_2 = \widehat{H}(\widetilde{\mathcal{D}}). \tag{2.3.33}$$

La principale differenza che viene fuori rispetto al regime isotropo è che in presenza di debole anisotropia il varco $\mathcal{C}^*$ può essere espresso come $\mathcal{C}^* = \bar{\mathcal{D}}^{fp}$, si veda la Figura 2.12 a sinistra (si confronti con (2.3.32)). Il motivo per cui soltanto l'insieme $\bar{\mathcal{D}}$ è rilevante per l'insieme $\mathcal{C}^*$ è il seguente. Partendo dall'insieme $\widetilde{\mathcal{D}}$, la dinamica passa attraverso l'insieme $\bar{\mathcal{D}}$ oppure non è possibile che si crei una particella libera senza superare il livello di energia Γ^*. Infatti, da (2.3.33) sappiamo che qualsiasi configurazione $\eta \in \widetilde{\mathcal{D}}$ ha energia $\widehat{H}(\eta) = \Gamma^* - \Delta + U_1 - U_2$. Per l'ottimalità del cammino, partendo da tale η è possibile creare una particella libera solo dopo aver abbassato l'energia. Questo è possibile solo se $\eta \in \widetilde{\mathcal{Q}}$, infatti in tal caso possiamo staccare la protuberanza e riattaccarla su un lato verticale, ottenendo così una configurazione in $\bar{\mathcal{Q}}$.

Per quanto riguarda il regime fortemente anisotropo, è lecito aspettarsi che anche in questo caso soltanto $\bar{\mathcal{D}}$ è l'insieme rilevante per il varco. Questo è infatti ciò che succede. Tuttavia, le configurazioni in $\widetilde{\mathcal{D}}$ hanno una forma molto diversa nel regime fortemente anisotropo rispetto a quelli isotropi e debolmente anistropi. Più precisamente, le configurazioni in questo insieme ora non consistono più in un'unica goccia rettangolare con quattro barre attaccate ai suoi quattro lati. Partendo da una configurazione $\eta \in \widetilde{\mathcal{Q}}$, infatti, soltanto una mossa a costo U_2 è ammessa. Altrimenti, se avvenisse una mossa a costo U_1, la configurazione risultante avrebbe energia $\Gamma^* - \Delta + 2U_1 - U_2 > \Gamma^*$, quindi il cammino descritto non sarebbe ottimale. Deduciamo quindi che il varco $\mathcal{C}^*$ può essere espresso come $\mathcal{C}^* = \bar{\mathcal{D}}^{fp}$ (si veda la Figura 2.12 a destra).

Nonostante il fatto che la struttura del varco sia simile per i tre scenari, sottolineiamo che l'ingresso in essi è molto diverso. In particolare, per il caso fortemente anisotropo ci sono due diversi meccanismi per entrare nel varco, mentre per gli altri due scenari ce n'è uno unico, si veda [18, Lemma 7.13]. In particolare abbiamo dimostrato che ogni $\omega \in (\square \to \blacksquare)_{opt}$ raggiunge l'insieme $\mathcal{C}^*$ in uno dei seguenti modi:

(i) ω passa per $\bar{\mathcal{Q}}$, quindi eventualmente attraverso $\bar{\mathcal{D}} \setminus \bar{\mathcal{Q}}$, e infine raggiunge $\mathcal{C}^*$;

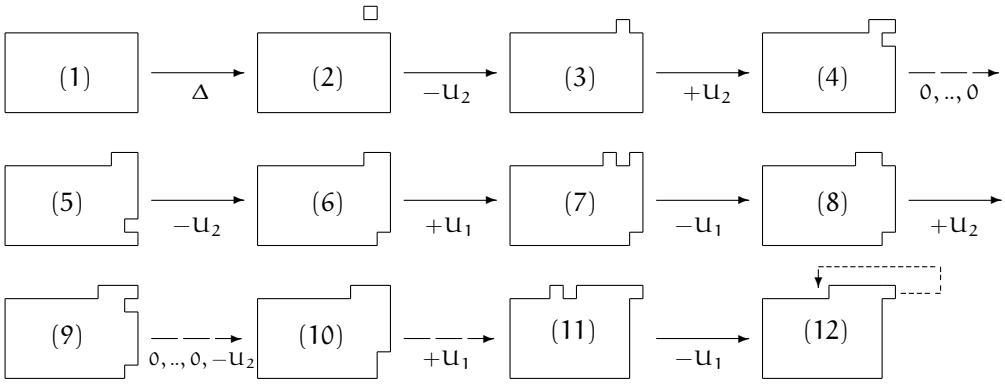

Figura 2.13 – Secondo meccanismo per l'ingresso nel varco nel regime fortemente anisotropo: la configurazione (1) consiste in un cluster rettangolare di dimensioni $(2\ell_2^* - 1) \times (\ell_1^* - 1)$ ed ha energia pari a $\Gamma^* - \Delta + U_2 - U_1$, quindi le configurazioni (7) e (11) hanno energia pari a Γ^*. In (12) indichiamo con una freccia tratteggiata il distacco della protuberanza a costo U_1 ed in seguito il movimento della particella libera fino a che non si attacca al cluster, facendo sì che l'energia decresca di $U_1 + U_2$. Quando la particella libera si stacca la dinamica raggiunge l'insieme $\mathcal{C}^*$.

(ii) ω segue il cammino descritto in Figura 2.13.

Questa è la conseguenza di una maggiore rigidità della dinamica nel caso fortemente anisotropo. Una parte importante dei moti di regolarizzazione delle particelle lungo il bordo dei cluster si viene a perdere e per questo motivo appare un nuovo meccanismo per entrare nell'insieme delle configurazioni critiche.

DESCRIZIONE GEOMETRICA DELL'UNIONE DI TUTTI I VARCHI MINIMALI

Da un lato è chiaro che le proprietà strettamente correlate alle dimensioni orizzontali e verticali sono le stesse per i casi anisotropi. D'altra parte, alcune proprietà che coinvolgono il moto delle particelle lungo il bordo delle gocce sono molto diverse. Si potrebbe pensare intuitivamente del caso debolmente anisotropo come una "interpolazione" tra quello isotropo e fortemente anisotropo. In effetti, ha alcune proprietà simili al primo, altre al secondo. Evidenziamo ora questa differenza nella descrizione dell'insieme

$$\mathcal{G}(\square, \blacksquare) := \bigcup_{\mathcal{W}(\square,\blacksquare) \text{ varco minimale}} \mathcal{W}(\square, \blacksquare),$$

dove un *varco minimale* $\mathcal{W}(\square, \blacksquare)$ è un varco minimo per inclusione, cioè $\mathcal{W}(\square, \blacksquare)$ è un varco e per qualsiasi $\mathcal{W} \subsetneq \mathcal{W}(\square, \blacksquare)$ esiste $\omega' \in (\square \to \blacksquare)_{opt}$ tale che $\omega' \cap \mathcal{W}' = \emptyset$. Si noti che l'insieme $\mathcal{G}(\square, \blacksquare)$ rappresenta l'unione di tutti i varchi minimali per il passaggio da $\square$ a $\blacksquare$. Per il caso isotropo sono consentiti più spostamenti lungo il bordo dei cluster e quindi è più difficile fornire una descrizione geometrica esplicita di tale insieme, mentre per i casi anisotropi la otteniamo pienamente, poiché la condizione $U_1 \neq U_2$ rende più improbabile lo spostamento delle particelle lungo il bordo delle gocce. Tra i casi anisotropi, la struttura dell'insieme $\mathcal{G}(\square, \blacksquare)$ dipende fortemente da quanto è grande U_1 rispetto a U_2, infatti nel caso $U_1 > 2U_2$ sono consentiti meno scivolamenti lungo il bordo e quindi la struttura dell'unione dei varchi minimali è meno ricca rispetto a quella nel caso debolmente anisotropo. Questa caratterizzazione per tutti e tre gli scenari rappresenta un contributo innovativo di questa tesi.

Il punto di partenza di questa analisi è l'introduzione del concetto di *sella non essenziale*. In parole povere, una sella $\zeta \in \mathcal{S}(\square, \blacksquare)$ (si ricordi (2.3.29)) è detta non essenziale se può essere "aggirata" da un cammino ottimale in uno dei suoi dintorni, vale a dire, se per qualsiasi cammino ottimale che attraversa ζ esiste un altro cammino ottimale che non attraversa ζ in modo tale che i due cammini non differiscano troppo. Formalmente, questo accade se per qualsiasi $\omega \in (\square \to \blacksquare)_{opt}$ tale che $\omega \cap \zeta \neq \emptyset$ abbiamo $\{\arg\max_\omega \widehat{H}\} \setminus \{\zeta\} \neq \emptyset$ ed esiste $\omega' \in (\square \to \blacksquare)_{opt}$ tale che $\{\arg\max_{\omega'} \widehat{H}\} \subseteq \{\arg\max_\omega \widehat{H}\} \setminus \{\zeta\}$. Definiamo quindi le *selle essenziali* come quelle che non sono non essenziali. La nozione di selle essenziali è cruciale nel tentativo di caratterizzare l'unione dei varchi minimali grazie a [85, Teorema

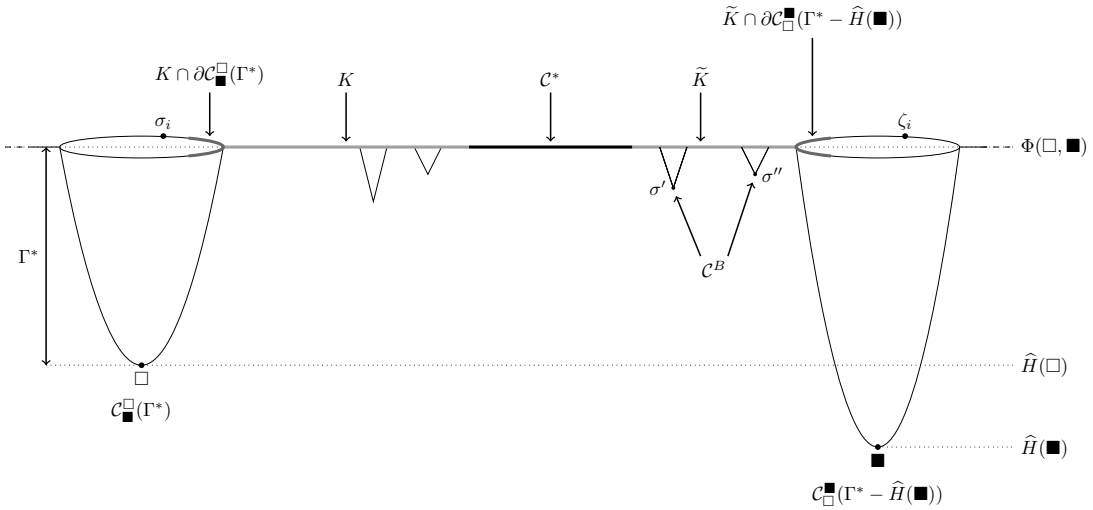

Figura 2.14 – Esempio del panorama energetico per la transizione tra $\square$ e $\blacksquare$. Rappresentiamo sulla sinistra (risp. destra) il ciclo dello stato metastabile (risp. stabile) $\mathcal{C}^{\square}_{\blacksquare}(\Gamma^*)$ (risp. $\mathcal{C}^{\blacksquare}_{\square}(\Gamma^* - \widehat{H}(\blacksquare))$). Indichiamo $\mathcal{C}^*$ in nero, K e $\widetilde{K}$ in grigio chiaro, evidenziando in grigio scuro la parte di K e $\widetilde{K}$ che interseca i bordi dei due cicli precedenti. Forniamo un esempio di due configurazioni σ e σ' che sono in $\mathcal{C}^B$.

5.1]. Infatti gli autori hanno dimostrato che una sella è essenziale se e solo se appartiene all'unione di tutti i varchi minimali. Grazie a questa equivalenza possiamo ridurre il nostro studio all'identificazione dell'insieme di tutte le selle essenziali che devono essere attraversate durante la transizione nei tre diversi regimi.

Per prima cosa forniamo una *strategia indipendente dal modello* utile ad eliminare alcune selle non essenziali. Più precisamente abbiamo bisogno di alcuni input dipendenti dal modello per dimostrare che due tipologie di selle non sono essenziali e quindi non appartengono all'unione dei varchi minimali. Per applicare questa strategia alla dinamica di Kawasaki dobbiamo quindi verificare che gli input richiesti sono validi per il nostro modello nei tre scenari. Questo studio, insieme alla caratterizzazione delle selle essenziali, si basa su un'analisi dettagliata del movimento delle particelle lungo il bordo delle gocce, che è una caratteristica tipica della dinamica di Kawasaki. Per non appesantire troppo la spiegazione delle idee di base, presentiamo qui questa strategia indipendente dal modello applicata direttamente alla dinamica di Kawasaki per la transizione da $\square$ a $\blacksquare$, mentre ci riferiamo alla Sezione 3.1.2 per la strategia generale.

Si ricordi [45, eq. (3.40)] per la definizione di ciclo: nel caso di una dinamica di Metropolis questa definizione coincide con [85, eq. (2.7)]. Abbiamo bisogno della seguente definizione. Dati $\sigma \in \mathcal{X}$, $\Gamma > 0$ ed un insieme di configurazioni di arrivo $\mathcal{A}$, diciamo che il *ciclo iniziale* per la transizione da σ ad $\mathcal{A}$ con profondità Γ è

$$\mathcal{C}^{\sigma}_{\mathcal{A}}(\Gamma) := \{\sigma\} \cup \{\eta \in \mathcal{X} : \Phi(\sigma, \eta) - \widehat{H}(\sigma) < \Gamma = \Phi(\sigma, \mathcal{A}) - \widehat{H}(\sigma)\}. \tag{2.3.34}$$

In parole, questo ciclo iniziale contiene tutte le configurazioni raggiungibili da σ spendendo meno energia rispetto all'altezza di comunicazione tra σ e l'insieme di arrivo $\mathcal{A}$. Si noti che nella definizione (2.3.34) sottolineiamo la dipendenza da σ e $\mathcal{A}$, e che Γ è identificato da essi. Si noti che la definizione di $\mathcal{C}^{\sigma}_{\mathcal{A}}(\Gamma)$ coincide con $\mathcal{C}_{\mathcal{A}}(\sigma)$ definito in [85, eq. (2.25)]. Ci concentreremo sui due specifici cicli iniziali $\mathcal{C}^{\square}_{\blacksquare}(\Gamma^*)$ e $\mathcal{C}^{\blacksquare}_{\square}(\Gamma^* - \widehat{H}(\blacksquare))$. In parole povere, per applicare la strategia generale al nostro modello, abbiamo bisogno dei seguenti input dipendenti dal modello (incoraggiamo il lettore ad ispezionare la Figura 2.14):

(i) Identificare l'insieme degli stati metastabili e stabili e la barriera energetica tra loro, che nel nostro modello sono rispettivamente $\square$, $\blacksquare$ e Γ^*.
(ii) Trovare un varco per la transizione, che nel nostro modello è $\mathcal{C}^*$.
(iii) Trovare due insiemi di configurazioni $\mathcal{C}^G$ e $\mathcal{C}^B$ tali che quando la dinamica raggiunge $\mathcal{C}^G$, l'ha fatto "oltre la collina", mentre quando raggiunge $\mathcal{C}^B$ no.
(iv) Identificare i sottoinsiemi K (risp. $\widetilde{K}$) delle selle che sono visitate dai cammini ottimali "appena prima di entrare" (risp. "appena dopo aver visitato") il varco.

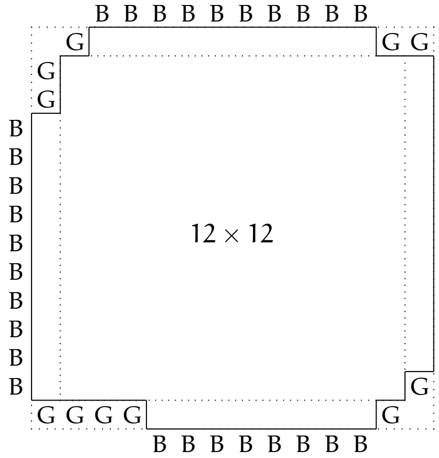

Figura 2.15 – Siti buoni (G) e siti cattivi (B) per $\ell_c = 14$.

Definizione 2.3.1. *Una sella σ è del primo tipo se non è in $\mathcal{C}^* \cup K$ e appartiene al bordo del ciclo $\mathcal{C}^{\square}_{\blacksquare}(\Gamma^*)$, cioè $\sigma \in \partial\mathcal{C}^{\square}_{\blacksquare}(\Gamma^*) \cap (\mathcal{S}(\square, \blacksquare) \setminus (\mathcal{C}^* \cup K))$.*

Definizione 2.3.2. *Una sella ζ è del secondo tipo se non è in $\mathcal{C}^* \cup \widetilde{K}$ e appartiene al bordo del ciclo $\mathcal{C}^{\blacksquare}_{\square}(\Gamma^* - \widehat{H}(\blacksquare))$, cioè $\zeta \in \partial\mathcal{C}^{\blacksquare}_{\square}(\Gamma^* - \widehat{H}(\blacksquare)) \cap (\mathcal{S}(\square, \blacksquare) \setminus (\mathcal{C}^* \cup \widetilde{K}))$.*

Quindi, a condizione che le condizioni (i)-(iv) siano verificate per il nostro modello, valgono i seguenti risultati:

1. Ogni sella σ del primo tipo è non essenziale.
2. Ogni sella ζ del secondo tipo è non essenziale.

Da un lato sottolineiamo che il punto 1 è garantito solo dagli input dipendenti dal modello (i), (ii) e (iv). Infatti, l'idea della dimostrazione è la seguente. Dato un cammino ottimale ω che passa da una sella σ del primo tipo e attraversa il ciclo $\mathcal{C}^{\square}_{\blacksquare}(\Gamma^*)$ per l'ultima volta nella configurazione η, grazie a [85, Lemma 2.28] sappiamo che esiste un cammino contenuto in quel ciclo $\mathcal{C}^{\square}_{\blacksquare}(\Gamma^*)$, cosicché non attraversa la sella σ, tale che può procedere come ω a partire da η. Pertanto il cammino ω' ottenuto dalla concatenazione di questi due cammini ha la proprietà desiderata, cioè

$$\{\arg\max_{\omega'} \widehat{H}\} \subseteq \{\arg\max_{\omega} \widehat{H}\} \setminus \{\sigma\}.$$

Sottolineiamo invece che per il punto 2 tutti gli input dipendenti dal modello sono necessari. In particolare il punto (iii) risulta cruciale. Infatti, l'idea della dimostrazione è la seguente. Per il punto (iii) deduciamo che ogni cammino ottimale ω che attraversa una sella del secondo tipo ζ deve attraversare una sella $\eta \in \mathcal{C}^* \cup \widetilde{K}$ che comunica con $\mathcal{C}^G$ attraverso un passo della dinamica. Possiamo quindi definire il cammino ottimale ω' come il cammino uguale ad ω fino alla sella η che poi raggiunge l'insieme $\mathcal{C}^G$, procedendo successivamente in $\mathcal{C}^{\blacksquare}_{\square}(\Gamma^* - \widehat{H}(\blacksquare))$. È facile verificare che il cammino ω' ha la proprietà desiderata.

Per caratterizzare tutte le selle essenziali, l'idea è quindi quella di partizionare le selle che non sono in $\mathcal{C}^*$ in tre tipi: le selle σ del primo tipo, le selle ζ del secondo tipo, e le selle ξ del terzo tipo, che sono tutte le selle che non sono né del primo né del secondo tipo. Il motivo per cui escludiamo le selle appartenenti a $\mathcal{C}^*$ è che sono tutte essenziali, come vedremo più avanti nel dettaglio. Dopo l'individuazione dei punti (iii) e (iv) precedenti, vale a dire gli insiemi $\mathcal{C}^B$, $\mathcal{C}^G$, K e $\widetilde{K}$, la strategia spiegata sopra ci dice che le selle del primo e del secondo tipo sono non essenziali. Per caratterizzare l'insieme $\mathcal{G}(\square, \blacksquare)$ dobbiamo quindi caratterizzare le selle essenziali del terzo tipo, che è un compito che deve essere affrontato a mano per qualsiasi modello e risulta essere intricato per la dinamica conservativa di Kawasaki.

Introduciamo in primo luogo gli insiemi $\mathcal{C}^G$ e $\mathcal{C}^B$ con le proprietà rivendicate al punto (iii) precedente. A tal fine poniamo

$$L^* := \begin{cases} L - \ell_c & \text{per il regime isotropo,} \\ L - \ell_2^* & \text{per i regimi anisotropi.} \end{cases} \tag{2.3.35}$$

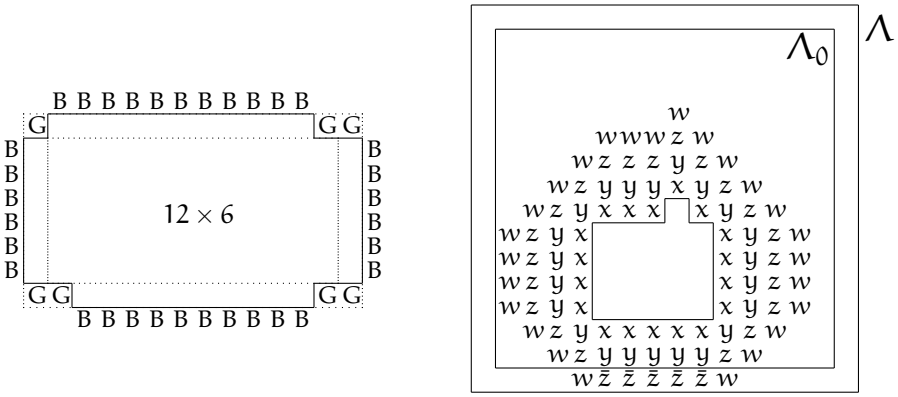

Figura 2.16 – Sulla sinistra rappresentiamo i siti buoni (G) e i siti cattivi (B) per $\ell_2^* = 8$. Sulla sinistra rappresentiamo con x i siti in $B_1(\hat{\eta})$, con y i siti in $\bar{B}_2(\hat{\eta})$, con z e $\bar{z}$ i siti in $\bar{B}_3(\hat{\eta})$ e con $\bar{z}$ e w i siti in $\bar{B}_4(\hat{\eta})$.

Ad ogni $\eta \in \mathcal{C}^*$ associamo la coppia $(\hat{\eta}, x)$, dove $\hat{\eta} \in \mathcal{D}$ rappresenta la goccia protocritica e $x \in \Lambda$ la posizione della particella libera. Indichiamo con $\mathcal{C}^G(\hat{\eta})$ (risp. $\mathcal{C}^B(\hat{\eta})$) le configurazioni raggiungibili da $(\hat{\eta}, x)$ da un cammino che sposta la particella libera verso il cluster e la attacca in $\partial^- CR(\hat{\eta})$ (risp. $\partial^+ CR(\hat{\eta})$), dove $CR(\hat{\eta})$ è il *rettangolo circoscritto* di $\hat{\eta}$, cioè il rettangolo più piccolo contenente $\hat{\eta}$. Nelle Figure 2.15 e 2.16 a sinistra per un $\hat{\eta}$ specifico rappresentiamo esplicitamente i siti buoni e cattivi rispettivamente per interazioni isotrope e fortemente anisotrope. Siano

$$\mathcal{C}^G = \bigcup_{\hat{\eta} \in \mathcal{D}} \mathcal{C}^G(\hat{\eta}), \qquad \mathcal{C}^B = \bigcup_{\hat{\eta} \in \mathcal{D}} \mathcal{C}^B(\hat{\eta}). \tag{2.3.36}$$

Per dimostrare che questi insiemi specifici soddisfano le condizioni richieste in (iii), ragioniamo come segue. Affermiamo che per tutti e tre i regimi valgono le seguenti proprietà:

1. Se $\eta \in \mathcal{C}^G$, allora esiste un cammino $\omega : \eta \to \blacksquare$ tale che $\max_{\zeta \in \omega} \widehat{H}(\zeta) < \Gamma^*$.
2. Se $\eta \in \mathcal{C}^B$, allora non ci sono $\omega : \eta \to \square$ oppure $\omega : \eta \to \blacksquare$ tale che $\max_{\zeta \in \omega} \widehat{H}(\zeta) < \Gamma^*$.

Queste due proprietà sono precisamente quelle richieste al punto (iii). La dimostrazione per il caso isotropo è presentata in [35], mentre per i casi anisotropi sono presentate in [17, 18] e usa argomentazioni simili.

Identifichiamo ora gli insiemi K e $\widetilde{K}$ in (iv). Questi insiemi sono costituiti rispettivamente dalle selle che sono visitate dai cammini ottimali appena prima di entrare e subito dopo la visita all'insieme $\mathcal{C}^*$. Per i tre regimi abbiamo che $K = \emptyset$. Per identificare le selle del secondo tipo osserviamo che abbiamo bisogno soltanto di identificare l'insieme $\widetilde{K} \cap \partial \mathcal{C}^{\blacksquare}_{\square}(\Gamma^* - \widehat{H}(\blacksquare))$. Abbiamo dimostrato che questo insieme ha una struttura piuttosto complessa nei casi isotropi e debolmente anisotropi, mentre è vuoto per il caso fortemente anisotropo. Questa differenza si basa ancora una volta su una maggiore rigidità dei moti delle particelle nel regime fortemente anisotropo. Questa analisi è molto tecnica e quindi non riportiamo qui gli ingredienti della prova, ma ci riferiamo alle Sezioni 3.4, 4.3 e 5.3 per l'argomentazione precisa e dettagliata che abbiamo usato nei tre regimi.

Per dimostrare che $\mathcal{C}^*$ è composto soltanto da selle essenziali, dobbiamo prima introdurre due insiemi che saranno cruciali nella nostra argomentazione. Per ogni $\eta \in \mathcal{C}^*$ sia $\hat{\eta} \in \mathcal{D}$ la configurazione ottenuta da η rimuovendo la particella libera. Per $A \subseteq \Lambda$ e $x \in \Lambda$, indichiamo con $d(x, A)$ la distanza sul reticolo tra x e A. Abbiamo bisogno delle seguenti definizioni.

Definizione 2.3.3. *Sia Λ_4 ottenuto da Λ rimuovendo i suoi quattro angoli. Definiamo ricorsivamente*

$$B_1(\hat{\eta}) := \{x \in \Lambda_4 |\, x \notin \hat{\eta},\ d(x, \hat{\eta}) = 1\}$$

e

$$B_2(\hat{\eta}) := \{x \in \Lambda_4 |\, x \notin \hat{\eta},\ d(x, B_1(\hat{\eta})) = 1\},$$
$$\bar{B}_2(\hat{\eta}) := B_2(\hat{\eta}),$$

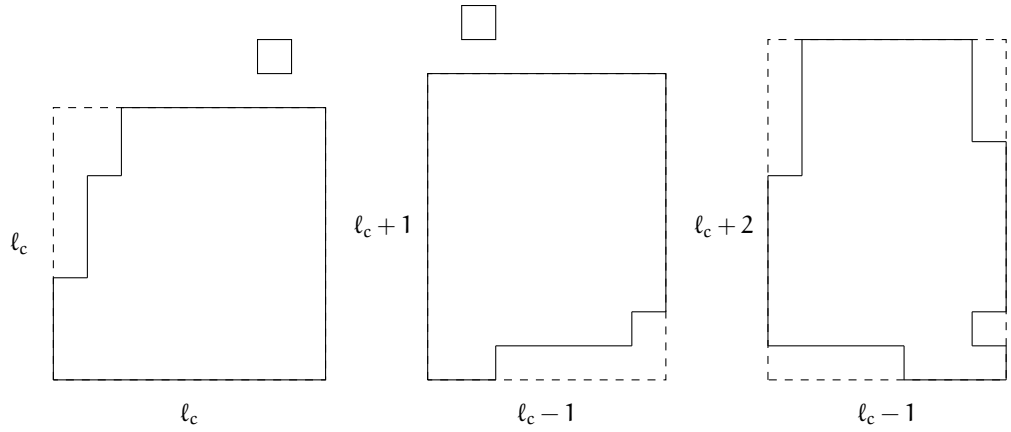

Figura 2.17 – Configurazioni critiche nel caso isotropo.

e

$$B_3(\hat{\eta}) := \{x \in \Lambda_4 |\ x \notin B_1(\hat{\eta}),\ d(x, B_2(\hat{\eta})) = 1\},$$
$$\bar{B}_3(\hat{\eta}) := B_3(\hat{\eta}) \cup \{\bar{B}_2(\hat{\eta}) \cap \partial^- \Lambda_4\},$$

e per $i = 4, 5, ..., L^*$

$$B_i(\hat{\eta}) := \{x \in \Lambda_4 |\ x \notin B_{i-2}(\hat{\eta}),\ d(x, B_{i-1}(\hat{\eta})) = 1\},$$
$$\bar{B}_i(\hat{\eta}) := B_i(\hat{\eta}) \cup \{\bar{B}_{i-1}(\hat{\eta}) \cap \partial^- \Lambda_4\}.$$

In parole, $B_1(\bar{\eta})$ è l'anello dei siti in Λ_4 a distanza 1 da $\hat{\eta}$, mentre $\bar{B}_i(\hat{\eta})$ è l'anello dei siti in Λ_4 a distanza i da $\hat{\eta}$ e da tutti i siti in $\partial^- \Lambda_4$ a distanza $1 < j < i$ da $\hat{\eta}$ ($i = 2, 3, ..., L^*$) (si veda Figura 2.16 sulla destra). Si noti che, a seconda della posizione di $\hat{\eta}$ in Λ, gli insiemi $\bar{B}_i(\hat{\eta})$ coincidono per i sufficientemente grande. Il numero massimo di anelli è L^*. Definiamo

$$\mathcal{C}^*(i) := \{(\hat{\eta}, x) : \hat{\eta} \in \mathcal{D}, x \in \bar{B}_i(\hat{\eta})\}, \qquad i = 2, 3, ..., L^*. \tag{2.3.37}$$

Notiamo per prima cosa che gli insiemi $\mathcal{C}^*(i)$ non sono disgiunti. Dalla definizione dell'insieme $\mathcal{C}^*$ e da (2.3.37) deduciamo che

$$\mathcal{C}^* = \bigcup_{i=2}^{L^*} \mathcal{C}^*(i). \tag{2.3.38}$$

La dimostrazione del fatto che $\mathcal{C}^* \subseteq \mathcal{G}(\square, \blacksquare)$ si ottiene attraverso due passi:

PASSO 1: Le selle in $\mathcal{C}^*(2)$ sono essenziali.

PASSO 2: L'insieme $\mathcal{C}^*(i)$ appartiene ad un varco minimale per ogni $i = 3, ..., L^*$.

Da un lato si ha che la dimostrazione del passo 1 è la stessa per i tre regimi e si basa sul fatto che è sempre possibile trovare un cammino ottimale che attraversi l'insieme $\mathcal{C}^*(2)$ solo in un data configurazione η. La dimostrazione del passo 2 è invece diversa se abbiamo a che fare regimi isotropi o debolmente anisotropi, e con il regime fortemente anisotropo.

Iniziamo considerando i casi isotropo e debolmente anisotropo. Il passo 2 si ottiene dimostrando che l'insieme $\mathcal{C}^*(i)$ è un varco minimale per ogni $i = 3, ..., L^*$. Dal fatto che $\mathcal{C}^*$ è un varco segue infatti che anche ogni $\mathcal{C}^*(i)$ lo è. Inoltre è sempre possibile trovare un cammino ottimale che attraversi l'insieme $\mathcal{C}^*(i)$ solo in una data configurazione η, in modo che l'insieme $\mathcal{C}^*(i) \setminus \{\eta\}$ non è più un varco, mostrando quindi la minimalità di un tale varco.

L'analisi è invece diversa quando si ha a che fare con il caso fortemente anisotropo. Infatti, poiché ci sono due modi possibili per raggiungere l'insieme $\mathcal{C}^*(2)$, per trovare i varchi minimali dobbiamo considerare per ogni $i = 3, ..., L^*$ l'unione dell'insieme $\mathcal{C}^*(i)$ con alcune particolari selle appartenenti al cammino descritto in Figura 2.13. Questo implica comunque il passo 2.

Infine, per ottenere la descrizione geometrica completa dell'unione di tutti i varchi minimali, dobbiamo descrivere le selle essenziali del terzo tipo per tutti e tre gli scenari. Questa parte

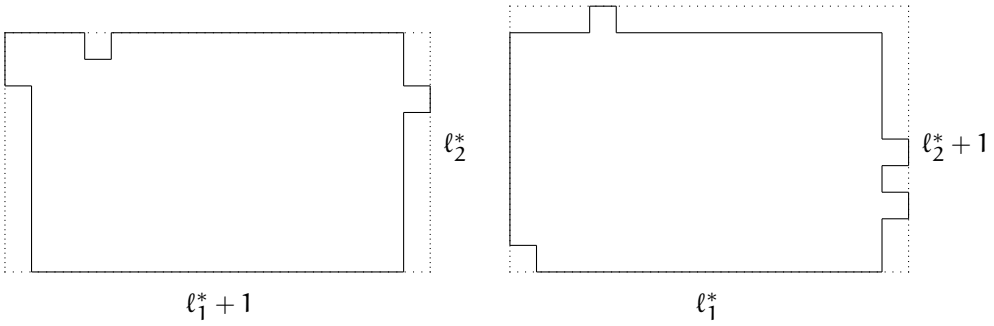

Figura 2.18 – Configurazioni critiche nel caso debolmente anisotropo.

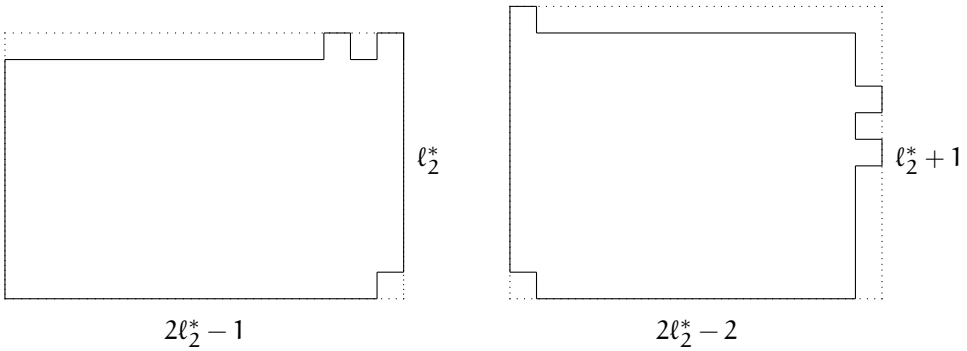

Figura 2.19 – Configurazioni critiche nel caso fortemente anisotropo.

è molto tecnica e richiede definizioni geometriche dettagliate, quindi qui saltiamo i dettagli e facciamo invece riferimento alle Sezioni 3.5, 4.4 e 5.4. Di seguito riportiamo solo alcuni esempi di configurazioni appartenenti a $\mathcal{G}(\square, \blacksquare)$ per dare un'idea della forma di tutte le selle essenziali. In Figura 2.17 mostriamo tre configurazioni appartenenti all'insieme $\mathcal{G}(\square, \blacksquare)$ nel caso isotropo. Si noti che la configurazione a destra non ha particelle libere e si ottiene durante lo scorrimento di una barra attorno ad un angolo della goccia. Sottolineiamo che in questo caso molti movimenti lungo il bordo sono ammessi e quindi una descrizione geometrica del tutto esplicita dell'insieme $\mathcal{G}(\square, \blacksquare)$ è più difficile da ottenere. In Figura 2.18 mostriamo due configurazioni appartenenti all'insieme $\mathcal{G}(\square, \blacksquare)$ nel caso debolmente anisotropo. Infine, in Figura 2.19 mostriamo due configurazioni appartenenti all'insieme $\mathcal{G}(\square, \blacksquare)$ nel caso fortemente anisotropo. Concludiamo questa parte riguardante l'analisi geometrica di tutti i varchi minimali fornendo le idee di base per derivare questa descrizione geometrica. Il primo passo consiste nel dividere le selle che restano da analizzare in quelle raggiunte prima di raggiungere $\mathcal{G}^B$ e dopo aver attraversato quell'insieme. Le prime tipologie di selle sono chiaramente non essenziali. Possiamo infatti argomentare come segue. Sia ξ una tale sella.

Se ξ viene raggiunta prima di attraversare l'insieme $\mathcal{C}^G$, allora è ottenuta da una configurazione $\eta \in \mathcal{C}^*$ senza attaccare la particella libera. Deduciamo quindi che l'unica possibilità è che η sia composta da un goccia protocritica $\hat{\eta} \in \mathcal{D}$ e da una particella libera a distanza due dal cluster. Deduciamo quindi che, partendo da ξ, l'unica transizione che non aumenta l'energia è la mossa inversa che dà origine a η, quindi ξ è una sella non essenziale.

Se ξ viene raggiunta dopo aver attraversato l'insieme $\mathcal{C}^G$, per le proprietà dell'insieme $\mathcal{C}^G$ segue direttamente la non essenzialità della sella ξ.

Ciò significa che resta solo da analizzare le selle ottenute dopo aver attraversato l'insieme $\mathcal{C}^B$. Questa è la parte più difficile, infatti dipende da tutti i diversi tipi di moti di particelle che possono aver luogo al bordo dei cluster. Sottolineiamo che tutte le selle raggiunte dopo uno scivolamento di una barra attorno ad un angolo sono essenziali e l'analisi riguarda quindi la loro completa caratterizzazione geometrica.

STIME PIÙ FORTI

Per quanto riguarda il valore atteso asintotico del tempo di transizione, utilizzando l'approccio

traiettoriale non è possibile stabilire se la funzione $f(\beta)$ tale che $\mathbb{E}_{\square}\tau_{\blacksquare} = f(\beta)e^{\Gamma^*\beta}(1+o(1))$ nel limite di $\beta \to +\infty$ è tale che $\log f(\beta)/\beta \to 0$ oppure è un fattore costante e indipendente da β. A tal fine, uno studio più dettagliato del cosiddetto *prefattore* $f(\beta)$ è dato in [35] per il modello isotropo in due e tre dimensioni utilizzando l'*approccio potenziale–teorico*. Il contributo innovativo di questa tesi relativo alle stime più forti del tempo medio di transizione riguarda la stima del prefattore per i modelli anisotropi.

Un ruolo chiave in questa analisi è giocato dalla *forma di Dirichlet*

$$\mathcal{E}(h) = \frac{1}{2}\sum_{\eta,\eta'\in\mathcal{X}} \mu(\eta)P(\eta,\eta')[h(\eta)-h(\eta')]^2, \qquad h : \mathcal{X} \to [0,1], \tag{2.3.39}$$

dove μ è la misura di Gibbs definita in (2.3.17) e $P(\eta,\eta')$ è la probabilità di transizione definita in (2.3.16). Dati due insiemi disgiunti e non vuoti $\mathcal{A},\mathcal{B} \subseteq \mathcal{X}$, la *capacità* della coppia $\mathcal{A},\mathcal{B}$ è definita da

$$\mathrm{CAP}(\mathcal{A},\mathcal{B}) = \min_{\substack{h:\mathcal{X}\to[0,1]\\ h_{|\mathcal{A}}\equiv 1, h_{|\mathcal{B}}\equiv 0}} \mathcal{E}(h), \tag{2.3.40}$$

dove $h_{|\mathcal{A}} \equiv 1$ significa che $h(\eta) = 1$ per ogni $\eta \in \mathcal{A}$ e $h_{|\mathcal{B}} \equiv 1$ significa che $h(\eta) = 0$ per ogni $\eta \in \mathcal{B}$. Il lato destro di (2.3.40) ha un unico minimizzatore $h^*_{\mathcal{A},\mathcal{B}}$, detto *potenziale di equilibrio* della coppia $\mathcal{A},\mathcal{B}$, dato da

$$h^*_{\mathcal{A},\mathcal{B}} = \mathbb{P}_\eta(\tau_{\mathcal{A}} < \tau_{\mathcal{B}}), \qquad \eta \in \mathcal{X}\setminus(\mathcal{A}\cup\mathcal{B}). \tag{2.3.41}$$

Applicando al nostro modello la strategia generale sviluppata in [31] e riassunta nella monografia [32], la stima precisa del tempo medio di transizione è

$$\mathbb{E}_{\square}(\tau_{\blacksquare}) = \frac{1}{Z\mathrm{CAP}(\square,\blacksquare)}(1+o(1)), \qquad \beta\to\infty. \tag{2.3.42}$$

Per ottenere una formula variazionale esplicita per il prefattore partendo da (2.3.42), dobbiamo prima introdurre una rappresentazione attraverso un grafo dello spazio delle configurazioni. Visualizzamo quindi $\mathcal{X}$ come un grafo i cui vertici sono configurazioni e i cui lati connettono configurazioni comunicanti. Poniamo

- $\mathcal{X}^*$ come il sottografo di $\mathcal{X}$ ottenuto rimuovendo tutti i vertici η con $\widehat{H}(\eta) > \Gamma^*$ e tutti i lati incidenti a questi vertici;
- $\mathcal{X}^{**}$ come il sottografo di $\mathcal{X}^*$ ottenuto rimuovendo tutti i vertici η con $\widehat{H}(\eta) = \Gamma^*$ e tutti i lati incidenti a questi vertici.

Si noti che gli insiemi $\mathcal{C}^{\square}_{\blacksquare}(\Gamma^*)$ e $\mathcal{C}^{\blacksquare}_{\square}(\Gamma^* - \widehat{H}(\blacksquare))$ sono le componenti connesse di $\mathcal{X}^{**}$ contenenti rispettivamente $\square$ e $\blacksquare$. Consideriamo l'insieme

$$\mathcal{X}^{**}\setminus(\mathcal{C}^{\square}_{\blacksquare}(\Gamma^*)\cup\mathcal{C}^{\blacksquare}_{\square}(\Gamma^*-\widehat{H}(\blacksquare))) = \bigcup_{i=1}^{I}\mathcal{X}(i), \tag{2.3.43}$$

dove ogni $\mathcal{X}(i)$ è una *valle* in $\mathcal{S}(\square,\blacksquare)$, cioè un insieme di configurazioni comunicanti con energia strettamente inferiore a Γ^* ma con altezza di comunicazione Γ^* verso sia $\square$ che $\blacksquare$. Tra tutte le valli $\mathcal{X}(i)$ possiamo evidenziare le valli $\mathcal{Z}^{\square}_j$ (risp. $\mathcal{Z}^{\blacksquare}_j$) delle selle non essenziali del primo (risp. secondo) tipo σ_j (risp. ζ_j) (ricordiamo le Definizioni (2.3.1) e (2.3.2)). Per ottenere la stima precisa di $Z\mathrm{CAP}(\square,\blacksquare)$ seguiamo la strategia generale delineata in [31, 37]:

- Tutti i termini nella forma di Dirichlet che coinvolgono configurazioni η con $H(\eta) > \Gamma^*$, cioè $\eta \in \mathcal{X}\setminus\mathcal{X}^*$, contribuiscono al massimo di $Ce^{-(\Gamma^*+\delta)\beta}$ per qualche $\delta > 0$ e quindi possono essere trascurati. Quindi, effettivamente, possiamo sostituire $\mathcal{X}$ con $\mathcal{X}^*$.
- Mostrare che $h^*_{\square,\blacksquare} = O(e^{-\delta\beta})$ su $\mathcal{C}^{\blacksquare}_{\square}(\Gamma^* - \widehat{H}(\blacksquare))$ e $h^*_{\square,\blacksquare} = 1 - O(e^{-\delta\beta})$ su $\mathcal{C}^{\square}_{\blacksquare}(\Gamma^*)$ per qualche $\delta > 0$.
- Dimostrare stime superiori ed inferiori più precise per $h^*_{\square,\blacksquare}$ su $\mathcal{X}^*\setminus(\mathcal{C}^{\square}_{\blacksquare}(\Gamma^*)\cup\mathcal{C}^{\blacksquare}_{\square}(\Gamma^* - \widehat{H}(\blacksquare)))$.

Inoltre, un contributo innovativo di questa tesi è dimostrare che vale anche

$$h^*_{\square,\blacksquare} = O(e^{-\delta\beta}) \text{ su } \bigcup_{j=1}^{J_{\blacksquare}}(\{\zeta_j\}\cup\mathcal{Z}^{\blacksquare}_j) \tag{2.3.44}$$

e

$$h^*_{\square,\blacksquare} = 1 - O(e^{-\delta\beta}) \text{ su } \bigcup_{j=1}^{J_\square} (\{\sigma_j\} \cup \mathcal{Z}_j^\square) \tag{2.3.45}$$

per qualche $\delta > 0$. Ciò consente una piena comprensione del ruolo delle selle non essenziali ed essenziali nel calcolo del prefattore del tempo medio di escursione. Infatti anche le selle non essenziali σ_j e ζ_j devono essere considerate in questa stima. Tuttavia, poiché il potenziale di equilibrio è costantemente uguale ad 1 (risp. 0) su σ_j (risp. ζ_j), le transizioni che coinvolgono queste selle non essenziali non contribuiscono al calcolo del prefattore.

In [35] gli autori hanno fornito una stima del prefattore per la versione a tempo continuo del modello isotropo ed hanno dimostrato che è una costante che non dipende dal parametro β, ma soltanto dalla dimensione della scatola e dalla cardinalità dell'insieme delle gocce critiche di dimensione ℓ_c, cioè dalla cardinalità dell'insieme $\mathcal{D}$. Notiamo che nel modello a tempo discreto che abbiamo definito in Sezione 2.3.2, ad ogni passo temporale vengono scambiate le variabili di occupazione per al massimo un legame tra i siti primi vicini, cosicché per le dinamiche a tempo continuo il tempo medio di transizione viene riscalato di un fattore $1/|\bar{\Lambda}^{*,\mathrm{orie}}|$. Queste stime del prefattore sono possibili una volta che viene fornita la descrizione geometrica delle configurazioni critiche e di quelle che si trovano nei loro dintorni. Gli autori hanno dimostrato in particolare che esiste una costante $K = K(\Lambda, \ell_c)$ tale che

$$\mathbb{E}_\square(\tau_\blacksquare) = K e^{\Gamma^*\beta}(1 + o(1)), \quad \beta \to \infty. \tag{2.3.46}$$

Gli autori hanno derivato una rappresentazione per la costante K in termini di determinate capacità associate ad una passeggiata aleatoria semplice bidimensionale. Questa rappresentazione dipende dalla geometria di $\mathcal{C}^*$ e delle sue *immediate vicinanze*, cioè quelle configurazioni $\eta \in \mathcal{X} \setminus \mathcal{C}^*$ per cui esiste $\eta' \in \mathcal{C}^*$ tale che $\eta' = T_b\eta$ per un legame $b \in \bar{\Lambda}^{*,\mathrm{orie}}$ (ricorda (2.3.12)). Questa immediata vicinanza è in realtà *piuttosto complessa*: questo è dovuto al fatto che quando la particella libera si attacca *impropriamente* alla goccia protocritica (cioè in un sito cattivo), questa innesca un movimento di particelle lungo il bordo della goccia. Di conseguenza nessuna formula facilmente calcolabile per K è disponibile. Si scopre, tuttavia, che il comportamento di K per un grande volume Λ può essere calcolato in modo esplicito. Infatti, in [35] gli autori hanno dimostrato che

$$\lim_{\Lambda\to\mathbb{Z}^2} \frac{|\Lambda|}{\log|\Lambda|} K(\Lambda, \ell_c) = \frac{1}{4\pi N(\ell_c)}, \tag{2.3.47}$$

dove

$$N(\ell_c) = \sum_{k=1}^{4} \binom{4}{k} \left[\binom{\ell_c + k - 2}{2k-1} + 2\binom{\ell_c + k - 3}{2k-1} \right]$$

è la cardinalità di $\mathcal{D}$ modulo spostamenti. L'intuizione alla base di questo risultato è la seguente. Il tempo medio necessario alla dinamica per raggiungere $\mathcal{C}^*$ quando parte da $\square$ è

$$\frac{1}{|\mathcal{D}|} \frac{1}{|\partial\Lambda^{*,\mathrm{in}}|} e^{\Gamma^*}(1 + o(1)), \quad \beta \to \infty, \tag{2.3.48}$$

dove $|\mathcal{D}|$ conta il numero di gocce protocritiche e $|\partial\Lambda^{*,\mathrm{in}}|$ conta il numero di legami diretti da $\partial^+\Lambda$ a $\partial^-\Lambda$ lungo i quali può essere creata la particella libera (si ricordi (2.3.12)). Sia $\pi(\Lambda, \ell_c)$ la probabilità, mediata rispetto alla distribuzione uniforme per la goccia protocritica su $\mathcal{D}$ e la distribuzione uniforme per la particella libera che entra in $\partial^*\Lambda^{\mathrm{in}}$, che la particella libera si muova da $\partial^-\Lambda$ alla goccia protocritica e si attacchi *propriamente* (cioè in un sito buono). Questa è la probabilità che la dinamica, dopo essere entrata nell'insieme $\mathcal{C}^*$, vada avanti verso $\blacksquare$ anziché tornare a $\square$. Allora

$$\frac{1}{\pi(\Lambda, \ell_c)}(1 + o(1)), \quad \beta \to \infty \tag{2.3.49}$$

è il numero medio di volte in cui una particella libera appena creata in $\partial^- \Lambda$ tenta di arrivare alla goccia protocritica e di attaccarsi correttamente prima di riuscire a farlo. Il tempo medio di nucleazione è il prodotto di (2.3.48) e (2.3.49), e quindi concludiamo che

$$K(\Lambda, \ell_c) = \frac{1}{|\mathcal{D}||\partial^* \Lambda^{in}|\pi(\Lambda, \ell_c)}. \tag{2.3.50}$$

Ora abbiamo che

$$\lim_{\Lambda \to \mathbb{Z}^2} \frac{|\mathcal{D}|}{|\Lambda|} = N(\ell_c). \tag{2.3.51}$$

Inoltre abbiamo che

$$\lim_{\Lambda \to \mathbb{Z}^2} |\partial^* \Lambda^{in}|\pi(\Lambda, \ell_c) \log |\Lambda| = 4\pi. \tag{2.3.52}$$

Infatti, il termine $4\pi/\log|\Lambda|$ è la probabilità per un grande volume Λ che una particella, dopo essersi staccata dalla goccia protocritica, raggiunga $\partial^- \Lambda$ prima di riattaccarsi. A causa della ricorrenza di una passeggiata aleatoria semplice in due dimensioni, per grandi volumi Λ questa probabilità è indipendente dalla forma e dalla posizione della goccia protocritica, fintanto che è lontana da $\partial^- \Lambda$. Per la reversibilità, la mossa inversa ha la stessa probabilità, che spiega (2.3.52). Allora (2.3.47) segue combinando (2.3.50)-(2.3.52).

Se la particella libera si attacca alla goccia protocritica in un sito cattivo, allora può di nuovo staccarsi oppure può causare un movimento di particelle lungo il bordo della goccia, dopo di che un'altra particella può staccarsi, possibilmente formando una diversa goccia protocritica. Tuttavia, poiché per dei grandi volume Λ una particella libera ha una piccola probabilità di sfuggire alla goccia protocritica e tornare a $\partial\Lambda$, alla fine deve attaccarsi in un sito buono.

La stima asintotica in (2.3.47) non dipende dalla forma di Λ, cioè sarebbe la stessa se Λ fosse un cerchio piuttosto che una grande scatola. Inoltre, nel caso tridimensionale in [35] sono stati ottenuti risultati simili, ma con meno controllo sulla geometria e sulla costante.

Per quanto riguarda i modelli anisotropi, la dimostrazione si basa ancora sugli strumenti sviluppati nell'approccio potenziale–teorico e le stime che si ottengono sono simili. Tuttavia, per il regime fortemente anisotropo accade qualcosa di diverso. Infatti, poichè l'ingresso nell'insieme delle configurazioni critiche è cruciale per la stima del prefattore, il fatto che in questo regime ci sono due diversi meccanismi per farlo significa che è possibile trovare una stima migliore. Ci riferiamo alla Sezione 5.1.2 per ulteriori dettagli.

Come abbiamo detto sopra, come la dinamica entra nel varco è una proprietà rilevante da derivare. In [35] gli autori dimostrano che questa entrata nel regime isotropo è uniforme nel seguente senso:

$$\lim_{\beta \to \infty} \mathbb{P}_\square \left(\eta_{\tau_{\mathcal{C}^*-}} = \eta \mid \tau_{\mathcal{C}^*} < \tau_\square \right) = \frac{1}{|\mathcal{D}|} \text{ per ogni } \eta \in \mathcal{D}, \tag{2.3.53}$$

dove $\tau_{\mathcal{C}^*-}$ è l'istante appena prima di $\tau_{\mathcal{C}^*}$. Questo è ragionevole, infatti le gocce protocritiche in $\mathcal{D}$, viste appena prima della creazione della particella libera in $\partial^- \Lambda$, appaiono con uguale probabilità. Questo è quello che ci aspettiamo anche nel regime debolmente anisotropo, mentre questo non è il caso in presenza di forte anisotropia. Ci riferiamo a [17, 18] per tutti i dettagli tecnici, mentre qui approfondiamo la strategia generale dietro.

La monografia [32] fornisce un quadro generale per dimostrare che l'ingresso nel varco è uniforme. In particolare, gli autori dimostrano la *distribuzione uniforme dell'ingresso* nel caso in cui due ipotesi siano soddisfatte. Più precisamente, introduciamo gli insiemi $\mathcal{P}^*_{PTA}$ e $\mathcal{C}^*_{PTA}$ come segue. Pensiamo a $\mathcal{P}^*_{PTA}$ come all'insieme delle configurazioni dove la dinamica, partendo dallo stato metastabile, è "quasi in cima alla collina", e a $\mathcal{C}^*_{PTA}$ come l'insieme delle configurazioni dove la dinamica "ha raggiunto la cima della collina" ed è "capace di passare" allo stato stabile senza tornare alla "valle intorno allo stato metastabile". Si rimanda a [32, Definizione 16.3] per la definizione precisa. Quindi le ipotesi richieste sono

(H1) Esiste un unico stato metastabile ed un unico stato stabile.

(H2) Tutte le configurazioni in $\mathcal{C}^*_{PTA}$ hanno lo stesso numero di configurazioni in $\mathcal{P}^*_{PTA}$ da cui possono essere raggiunti tramite un mossa consentita.

Dal momento che c'è un modo unico per entrare nel varco nel regime debolmente anisotropo, non accade niente di diverso rispetto al caso isotropo. Tuttavia, la situazione è completamente diversa in caso di forte anisotropia. Infatti, abbiamo dimostrato che in questo modello l'insieme $\mathcal{P}^*_{PTA}$ coincide con l'unione di $\bar{\mathcal{D}}$ e di gocce protocritiche coinvolte nel secondo meccanismo per entrare nel varco (come le configurazioni (6) e (10) in Fig. 2.13), e $\mathcal{C}^*_{PTA}$ coincide con l'unione di $\mathcal{C}^*(L^*)$ e di alcune selle coinvolte nel secondo meccanismo per entrare nel varco. Innanzitutto notiamo che $\mathcal{C}^* \neq \mathcal{C}^*_{PTA}$. Si noti inoltre che la condizione (H2) segue dal risultato relativo ai due meccanismi per entrare nel varco. Quindi, poiché valgono sia (H1) che (H2), [32, Teorema 16.4(b)] dovrebbe valere, cioè l'ingresso ha una distribuzione uniforme, ma questo non è vero. Più precisamente, questo modello rappresenta un controesempio di [32, Teorema 16.4(b)]. Questo dipende dall' ipotesi (H2), che tiene conto solo della mappa da $\mathcal{C}^*_{PTA}$ a $\mathcal{P}^*_{PTA}$ e non di quella inversa. Pertanto proponiamo di sostituire l'ipotesi (H2) con

(H2′) Tutte le configurazioni in $\mathcal{C}^*_{PTA}$ hanno lo stesso numero di configurazioni in $\mathcal{P}^*_{PTA}$ da cui possono essere raggiunte tramite una mossa consentita e viceversa.

Siamo convinti che questa possa essere l'ipotesi corretta, infatti l'analisi della distribuzione dell'ingresso uniforme in $\mathcal{C}^*_{PTA}$ deve tener conto del numero di configurazioni in $\mathcal{P}^*_{PTA}$ che comunicano con $\mathcal{C}^*_{PTA}$ attraverso un passo della dinamica. Ora è chiaro che questo modello non soddisfa (H2′), infatti ogni configurazione in $\bar{\mathcal{D}}$ ha esattamente $4L-4$ configurazioni in $\mathcal{C}^*$ da cui è possibile raggiungerla tramite una mossa consentita, mentre ciascuna delle altre configurazioni che appartiene a $\mathcal{P}^*_{PTA}$ ha una sola configurazione in $\mathcal{C}^*_{PTA}$ con questa proprietà. Pertanto [32, Teorema 16.4(b)] non vale per questo modello.

Abbiamo infine analizzato per tutti e tre i regimi il tasso di convergenza alla distribuzione stazionaria della catena di Markov di Metropolis $\{\eta_t\}_{t\in\mathbb{N}}$. Abbiamo misurato il tasso di convergenza in termini della distanza in variazionale totale e del tempo di mescolamento, che descrive il tempo necessario affinché la distanza dalla stazionarietà diventi piccola. Più precisamente, per ogni $0 < \varepsilon < 1$, definiamo il *tempo di mescolamento* come

$$t_{mix}(\varepsilon) := \min\left\{ n \geqslant 0 : \max_{x\in\mathcal{X}} \|P^n(x,\cdot) - \mu(\cdot)\|_{TV} \leqslant \varepsilon \right\}, \tag{2.3.54}$$

dove $\|\nu - \nu'\|_{TV} := \frac{1}{2}\sum_{x\in\mathcal{X}} |\nu(x) - \nu'(x)|$ per ogni due misure di probabilità ν, ν' su $\mathcal{X}$. Un'altra nozione classica per indagare la velocità di convergenza delle catene di Markov è il *gap spettrale*, che è definito come

$$\rho := a^{(2)}, \tag{2.3.55}$$

dove $1 = a^{(1)} > a^{(2)} \geqslant \ldots \geqslant a^{(|\mathcal{X}|)} \geqslant -1$ sono gli autovalori della matrice $(P(x,y))_{x,y\in\mathcal{X}}$ definita in (2.3.16).

Abbiamo quindi dimostrato che per tutti e tre i regimi e per ogni $\varepsilon \in (0,1)$ vale

$$\lim_{\beta\to\infty} \frac{1}{\beta} \log t_{mix}(\varepsilon) = \Gamma^* = \lim_{\beta\to\infty} -\frac{1}{\beta} \log \rho.$$

Esistono inoltre due costanti $0 < c_1 \leqslant c_2 < \infty$ indipendenti da β tale che per ogni $\beta > 0$ vale

$$c_1 e^{-\beta\Gamma^*} \leqslant \rho \leqslant c_2 e^{-\beta\Gamma^*}.$$

2.3.3 *Il modello locale sul reticolo esagonale*

In questa sezione introduciamo il modello locale sul reticolo esagonale e presentiamo i principali risultati ricavati in questa tesi. Consideriamo il reticolo esagonale discreto $\mathbb{H}^2$ immerso in $\mathbb{R}^2$ e sia $\mathbb{T}^2$ il suo duale, cosicché $\mathbb{T}^2$ è il reticolo triangolare. Diremo che due siti del reticolo esagonale discreto sono *primi vicini* quando condividono un lato del reticolo, si veda la Figura 2.20. Consideriamo un esagono in $\mathbb{H}^2$ con raggio L e definiamo $\Lambda \subset \mathbb{T}^2$ come l'unione tra questo esagono e tutti i siti, che non appartengono all'esagono, a distanza reticolare uno dall'esagono. Richiamiamo l'equazione (2.3.9) per la definizione dell'insieme Λ_0, che è definito come Λ senza il suo bordo interno. Con questa scelta del dominio finito Λ indipendente da β, deduciamo che Λ_0 è un esagono di raggio L, si veda la Figura 2.21. Notiamo che Λ_0 contiene $6L^2$ siti. La lunghezza del lato L è fissa, ma arbitraria, e più

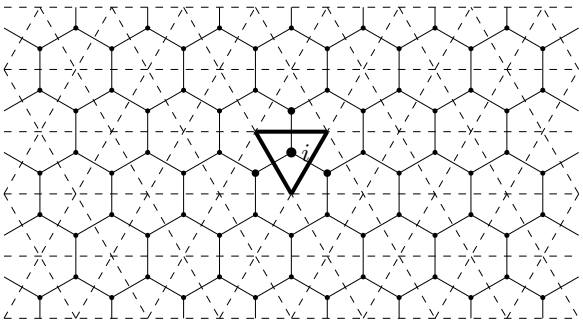

Figura 2.20 – Evidenziamo in nero i siti j tali che $d(i,j) \neq 0$ sul reticolo esagonale.

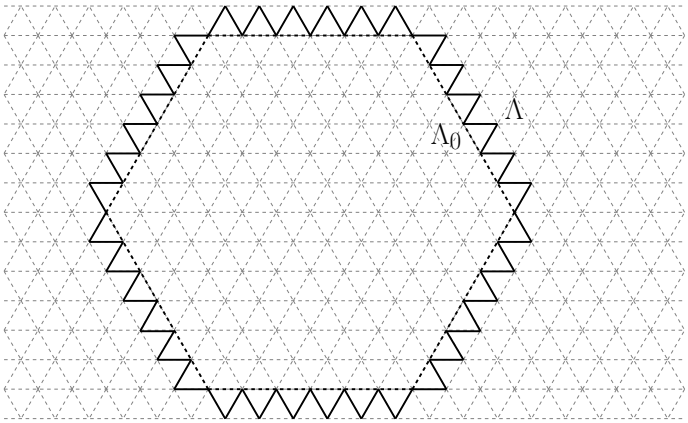

Figura 2.21 – Rappresentiamo l'insieme Λ con una linea dritta, mentre rappresentiamo l'esagono Λ_0 con una linea tratteggiata.

avanti richiederemo che L sia sufficientemente grande. Ricordiamo la definizione dello spazio delle configurazioni come $\mathcal{X} = \{0,1\}^{\Lambda}$. Ad ogni configurazione $\eta \in \mathcal{X}$ associamo l'energia hamiltoniana locale $\widehat{H}(\eta)$ definita in (2.3.11), dove prendiamo $U_1 = U_2 = U$ e sostituiamo i legami verticali e orizzontali sul reticolo quadrato con i legami che collegano i siti primi vicini sul reticolo esagonale. Possiamo quindi scrivere l'energia come

$$\widehat{H}(\eta) := -U \sum_{(x,y)\in\Lambda_0^*} \eta(x)\eta(y) + \Delta \sum_{x\in\Lambda} \eta(x), \tag{2.3.56}$$

dove

$$\Lambda_0^* = \{(x,y) \in \Lambda_0 \times \Lambda_0 : |x-y| = 1\}$$

è l'insieme dei legami non orientati in Λ_0. L'interazione consiste pertanto in un'energia di legame $-U < 0$ per ciascuna coppia di particelle prime vicine in Λ_0. C'è inoltre un'energia di attivazione $\Delta > 0$ per ogni particella in Λ. Qui consideriamo solo il regime isotropo, cioè l'energia di legame associata ad ogni legame è la stessa, perché in questa tesi abbiamo derivato dei risultati solo in questo scenario. Tuttavia, come abbiamo fatto per il modello che evolve sul reticolo quadrato, è possibile considerare *interazioni anisotrope*. Questo è lasciato come futura direzione di ricerca. La dinamica localmente conservativa di Kawasaki sul reticolo esagonale può essere quindi definita come nella Sezione 2.3.2 con una diversa scelta del dominio Λ. Per questo modello il regime metastabile corrisponde a prendere

$$\Delta \in \Big(U, \frac{3}{2}U\Big). \tag{2.3.57}$$

Possiamo giustificare questa condizione come segue. La condizione $\Delta > U$ ha la stessa interpretazione data sopra, ma ora la condizione $\Delta < 2U$ non è sufficiente come nel reticolo

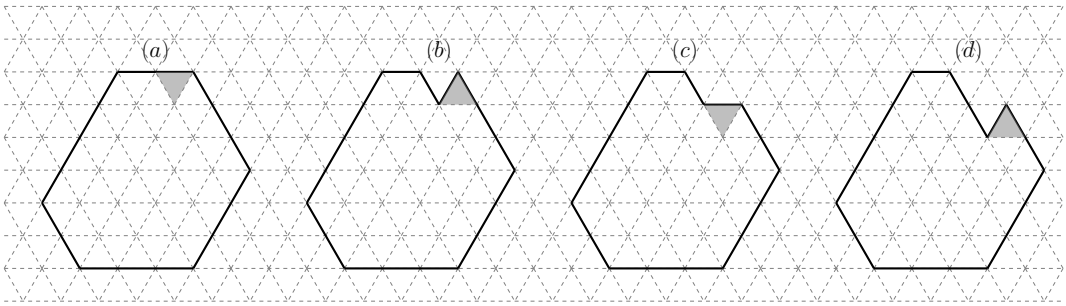

Figura 2.22 – In tutti i cluster rappresentiamo in grigio la particella che si sta staccando: questa mossa ha una probabilità di verificarsi di ordine $e^{-2U\beta}$ (risp. $e^{-U\beta}$) per i cluster (a) e (c) (risp. (b) e (d)).

quadrato. Anzi, per più di una particella attaccata ad un cluster esagonale è possibile staccare una singola particella alternativamente a costo U e $2U$, si veda la Figura 2.22. Pertanto, il limite superiore richiesto su Δ può essere visto come una media di questi due costi. Abbiamo che l'esagono vuoto

$$\hexagon := \{\eta \in \mathcal{X} : \eta(x) = 0 \ \forall\, x \in \Lambda\} \tag{2.3.58}$$

è l'unico stato metastabile e l'esagono pieno

$$\hexagon := \{\eta \in \mathcal{X} : \eta(x) = 1 \ \forall\, x \in \Lambda_0, \eta(x) = 0 \ \forall\, x \in \Lambda \setminus \Lambda_0\} \tag{2.3.59}$$

è l'unico stato stabile, purché L sia sufficientemente grande. Questa ipotesi è necessaria per avere $\widehat{H}(\hexagon) < \widehat{H}(\hexagon) = 0$ e più avanti forniremo un limite inferiore esplicito per L. Notiamo che le equazioni (2.3.58)–(2.3.59) coincidono con le equazioni (2.3.19)–(2.3.20), ma qui usiamo una diversa definizione di Λ e pertanto cambiamo notazione solo per rendere esplicito a quale reticolo ci riferiamo. L'uscita dalla metastabilità consiste quindi nell'analizzare la transizione da $\hexagon$ a $\hexagon$. Ci concentreremo sulla stima di questo tempo di transizione e sulla descrizione geometrica delle *gocce critiche* che il sistema deve attraversare per eseguire la nucleazione.

La motivazione principale di questa analisi è la seguente. Indaghiamo come il reticolo sottostante influisce sulle proprietà dinamiche del sistema. La scelta del reticolo esagonale deriva da un recente studio fatto per questo modello che evolve sotto la dinamica non conservativa di Glauber (si veda la Sezione 2.4.1) in [4, 78], perché è stato mostrato come una certa classe di dinamiche parallele (dinamiche scosse in [2, 3]) sul reticolo quadrato induce una collezione di dinamiche parallele su una famiglia di modelli di Ising sul reticolo esagonale con interazioni non isotrope, dove gli spin in ciascuna delle due partizioni sono alternativamente aggiornati. Il nostro risultato riguardante il varco indica che il reticolo sottostante è fondamentale per la dinamica del sistema. Si potrebbe semplicemente congetturare che le configurazioni critiche sono le controparti sul reticolo esagonale di quelle derivanti dallo stesso modello sul reticolo quadrato, ad esempio sostituendo la forma rettangolare con una esagonale, ma questa congettura è falsa. In effetti, dimostreremo che per questo modello esistono due diverse dimensioni per le gocce critiche a seconda del valore della parte frazionaria del rapporto $(\Delta - U)/(3U - 2\Delta)$. Questa situazione si verifica anche per il modello che evolve sotto la dinamica di Glauber considerato in [4], ma ci teniamo a sottolineare che la sua caratterizzazione è molto diversa. In effetti, la differenza principale tra la dinamica di Kawasaki e quella di Glauber è che la prima conserva il numero di particelle e quindi la struttura dei varchi è molto più ricca. In particolare, per la dinamica di Glauber c'è un *unico* varco minimale, mentre per la dinamica di Kawasaki la loro caratterizzazione non è banale e quindi molto più interessante da derivare. La descrizione geometrica dei varchi minimali esula dagli scopi di questa tesi ed è lasciata come futura direzione di ricerca, ma incoraggiamo il lettore a ispezionare le differenze tra Teorema 6.1.4 e [4, Teorema 2.13] per tenere presente la diversa natura del varco della transizione per queste due diverse dinamiche.

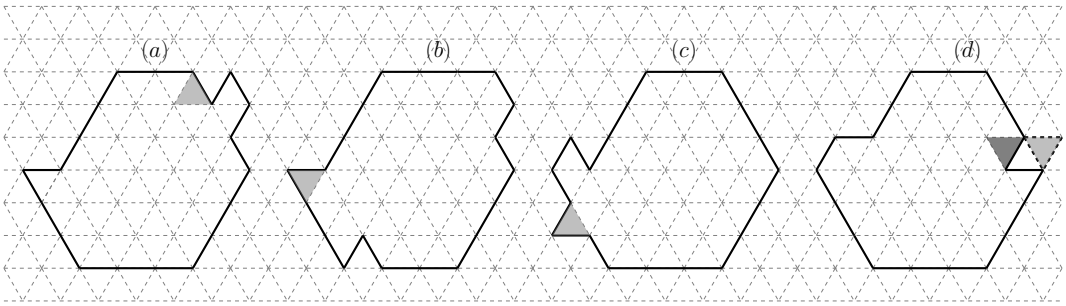

Figura 2.23 – In (b) rappresentiamo una configurazione ottenuta da quella rappresentata in (a). In particolare in (a) evidenziamo in grigio la faccia triangolare che si muove verso il rombo elementare sulla destra a costo U, mentre in (b) evidenziamo in grigio la protuberanza singola. In (d) rappresentiamo una configurazione ottenuta da quella rappresentata in (c). In particolare in (c) evidenziamo in grigio la protuberanza singola, mentre in (d) evidenziamo in grigio chiaro la particella libera ed in grigio scuro l'ultima faccia triangolare che è stata mossa verso sinistra.

CONFRONTO CON LA DINAMICA DI KAWASAKI SUL RETICOLO QUADRATO

Qui facciamo un confronto tra il modello isotropo sul reticolo esagonale e altri modelli che evolvono sotto la dinamica di Kawasaki sul reticolo quadrato per enfatizzare il diverso comportamento del sistema in base alla geometria del reticolo sottostante. La dinamica localmente conservativa e il movimento delle particelle danno un effetto di regolarizzazione, ma sottolineiamo che la forma particolare del reticolo esagonale induce un incremento di questi movimenti regolarizzanti in modo tale che appaiono nuovi meccanismi di ingresso nell'insieme delle configurazioni critiche, si vedano le Osservazioni 2.3.2 e 2.3.3 per maggiori dettagli. Questa è una prima differenza cruciale tra i due modelli isotropi. Sul reticolo quadrato, infatti, un nuovo meccanismo per entrare nel varco appare solo in presenza di forte anisotropia, si veda [16, 17]. Per i modelli debolmente anisotropi e isotropi c'è un modo unico per entrare nel varco: una forma rettangolare con una sola protuberanza viene raggiunta e quindi entra una particella libera dal bordo della scatola, vedere [18, 90] per maggiori dettagli. Sul reticolo quadrato, prima dell'ingresso della particella libera, soltanto le particelle lungo il bordo del cluster possono muoversi, mentre sul reticolo esagonale questo fenomeno può verificarsi anche per le particelle in una regione interna del cluster, vedere Figura 2.23(a)-(b) e (c)-(d) per due esempi della prima e dell'ultima configurazione ottenute in tal modo. Di conseguenza, in questo caso la caratterizzazione geometrica completa è difficile da ottenere, ed è lasciata come futura direzione di ricerca. Il motivo per cui osserviamo questo comportamento molto diverso poggia sulla struttura specifica del reticolo sottostante. Infatti, sul reticolo esagonale, quando una particella che non appartiene al bordo di un cluster si muove, se si attacca ad una protuberanza l'energia aumenta di U (2 legami vengono spezzati ed uno viene creato quando la particella in movimento si attacca alla protuberanza), mentre questo è falso sul reticolo quadrato. Infatti, in quel caso l'energia aumenta di 2U (3 legami vengono spezzati e uno viene creato quando la particella in movimento si attacca alla protuberanza). Questa differenza risulta essere cruciale quando la dinamica è vicina alle configurazioni critiche. Questo fenomeno può anche essere trovato nel diverso regime metastabile per questo modello rispetto a quello sul reticolo quadrato. Questo è peculiare delle dinamica di Kawasaki, infatti per la dinamica di Glauber ciò non accade, si veda [4, Condizione 2.6]. Anche questo comportamento è responsabile della particolare forma delle gocce critiche, che presentano due diverse protuberanze e non solo una come nel caso del reticolo quadrato. Come risulterà chiaro nel corso del lavoro, arriviamo alla conclusione che la geometria del reticolo influenza significativamente il comportamento del sistema soggetto alla dinamica di Kawasaki e questo aspetto lo rende molto interessante da studiare.

IDENTIFICAZIONE DEGLI STATI STABILI E METASTABILI

Qui daremo le idee principali per dedurre che ⬡ (risp. ⬢) è l'unico stato metastabile (risp.

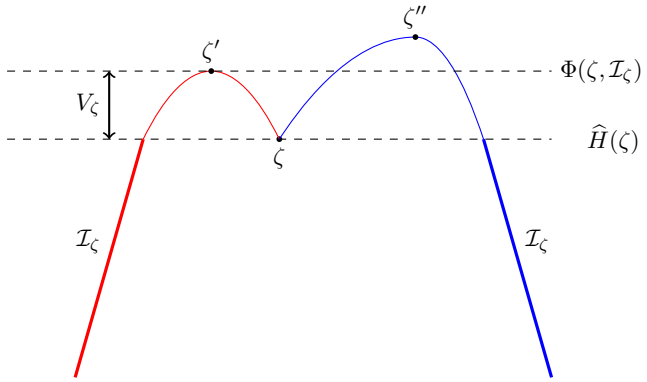

Figura 2.24 – Livello di stabilità V_ζ per una configurazione ζ.

stabile). La nozione chiave è quella di *livello di stabilità* di una configurazione σ, che è definita come la barriera energetica (si veda la Figura 2.24)

$$V_\zeta := \Phi(\zeta, \mathcal{I}_\zeta) - \widehat{H}(\zeta), \tag{2.3.60}$$

dove $\mathcal{I}_\zeta$ è l'insieme degli stati con energia inferiore a $\widehat{H}(\zeta)$:

$$\mathcal{I}_\zeta := \{\eta \in \mathcal{X} \,|\, \widehat{H}(\eta) < \widehat{H}(\sigma)\}. \tag{2.3.61}$$

Poniamo $V_\sigma := \infty$ se $\mathcal{I}_\sigma$ è vuoto. Poiché l'insieme degli stati metastabili è formalmente definito come

$$\mathcal{X}^m := \left\{\sigma \in \mathcal{X} \,|\, V_\sigma = \max_{\eta \in \mathcal{X}\setminus\mathcal{X}^s} V_\eta\right\}, \tag{2.3.62}$$

l'idea è dimostrare che esiste $V^* > 0$ tale che le uniche configurazioni con un livello di stabilità maggiore di V^* sono ⬡ e ⬢. In particolare $V^* = \Delta + U$. Questa dimostrazione si divide in due passi. Prima di tutto dimostriamo che le configurazioni che soddisfano determinate proprietà geometriche hanno un livello di stabilità minore o uguale a $\Delta + U$, e poi mostriamo che tutte le configurazioni, diverse da ⬡ e ⬢, hanno un livello di stabilità minore o uguale a $\Delta + U$. Questo implica che il sistema raggiunge con alta probabilità lo stato ⬡, che è il minimo locale dell'hamiltoniana, o lo stato fondamentale ⬢, poichè $\widehat{H}(⬢) < \widehat{H}(⬡)$, in un tempo inferiore a $e^{(V^*+\varepsilon)\beta}$, uniformemente nella configurazione di partenza per ogni $\varepsilon > 0$. Per tutti i dettagli tecnici rimandiamo alla Sezione 6.3.

TEMPO DI TRANSIZIONE E DESCRIZIONE DI UN VARCO

Prima di enunciare i risultati che abbiamo ottenuto, forniamo una discussione euristica da un punto di vista statico. Consideriamo il regime metastabile (2.3.57) e il limite di β che tende all'infinito. Facciamo un calcolo approssimativo della probabilità di vedere un esagono regolare di raggio r di siti occupati e centrato nell'origine. Indichiamo con μ^* l'insieme ristretto, cioé la misura di Gibbs grancanonica definita in (2.3.17) limitata ad un adeguato sottoinsieme di configurazioni, dove tutti i cluster sufficientemente grandi vengono soppressi. Sotto l'insieme ristretto abbiamo che

$$\mu^*(\text{esagono regolare di raggio } r) \approx \rho^{6r^2} e^{3U(3r^2-r)\beta},$$

poiché la densità del gas ρ è prossima alla probabilità di trovare una particella in un dato sito e $-U$ è l'energia di legame tra due particelle nei siti primi vicini, con $3(3r^2 - r)$ che rappresenra il numero di legami per un esagono di raggio r. Scrivendo $\rho = e^{-\Delta\beta}$ si ottiene

$$\mu^*(\text{esagono regolare di raggio } r) \approx e^{-\beta[6r^2\Delta + 3(r-3r^2)U]},$$

dove l'esponente ha un punto di sella in

$$\bar{r} = \frac{U}{2(3U - 2\Delta)}.$$

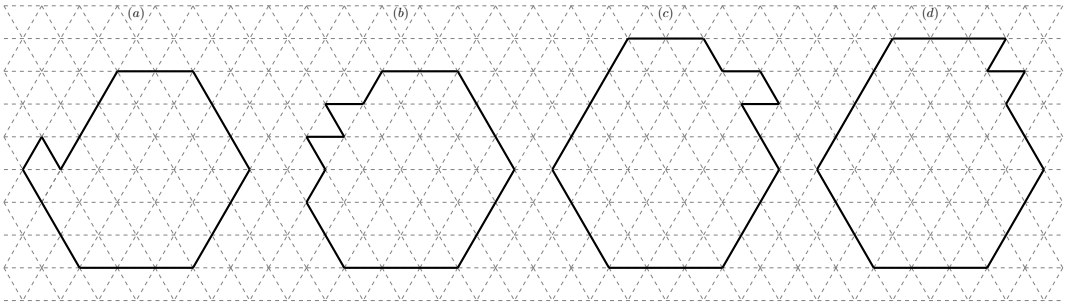

Figura 2.25 – Sulla sinistra forniamo due esempi di configurazioni in $\widetilde{\mathcal{S}}(A_1^* - 1)$, $\widetilde{\mathcal{D}}(A_1^* - 1)$. Sulla destra forniamo due esempi di configurazioni $\widetilde{\mathcal{S}}(A_2^* - 1)$, $\widetilde{\mathcal{D}}(A_2^* - 1)$.

Ciò significa che le gocce con raggio $r < \bar{r}$ appaiono con una probabilità che diminuisce in r e gocce con raggio $r \geqslant \bar{r}$ con una probabilità che aumenta in r. Questo porterebbe alla conclusione che $\bar{r}$ è il raggio della goccia critica. Vedremo nel seguito che la situazione è più delicata (vedi (2.3.63) per la definizione precisa del raggio critico r^*), infatti il meccanismo dinamico per la transizione tra gocce esagonali, che qui non viene considerato, influisce sulla crescita o sul restringimento delle gocce. La scelta $\Delta \in (U, \frac{3}{2}U)$ corrisponde a $r^* \in (1, \infty)$, cioè ad una goccia critica non banale.

Per rendere precisa l'ipotesi precedente su L, introduciamo il cosiddetto *raggio critico* come

$$r^* := \left\lfloor \frac{U}{2(3U - 2\Delta)} - \frac{1}{2} \right\rfloor = \left\lfloor \frac{\Delta - U}{3U - 2\Delta} \right\rfloor. \tag{2.3.63}$$

Abbiamo bisogno di assumere

$$L > 2r^* + 3. \tag{2.3.64}$$

Richiediamo inoltre alcune ipotesi di non degenerazione. In particolare assumiamo che

$$\frac{\Delta - U}{3U - 2\Delta} \notin \mathbb{N}. \tag{2.3.65}$$

Per evitare casi banali patologici, assumiamo inoltre che

$$\Delta \in \left(\frac{7}{5}U, \frac{3}{2}U \right). \tag{2.3.66}$$

Notiamo che la condizione (2.3.66) garantisce che tutte le lunghezze critiche siano maggiori di due. Nel resto di questa sezione assumeremo che tali condizioni (2.3.64)–(2.3.66) siano in vigore. Grazie a (2.3.65), possiamo scrivere

$$r^* = \frac{\Delta - U}{3U - 2\Delta} - \delta,$$

con $\delta \in (0, 1)$ la parte frazionaria di $(\Delta - U)/(3U - 2\Delta)$ fissata. Vedremo che δ ricoprirà un ruolo cruciale in questa analisi. Infatti, a seconda che $\delta \in (0, \frac{1}{2})$ o $\delta \in (\frac{1}{2}, 1)$, il sistema ha un comportamento differente. Il nostro obiettivo è fornire stime per il tempo di transizione da ⬡ e ⬢, e caratterizzare le gocce critiche.

Dimostriamo in seguito che il varco per la transizione $\mathcal{C}^* = \mathcal{C}^*(⬡, ⬢)$ contiene quelle configurazioni costituite da una particella libera e da un unico cluster di forma vicina ad un esagono di raggio r^*. A tal fine ragioniamo come segue. Per prima cosa definiamo l'*area critica* A^* come il numero delle particelle nelle configurazioni in $\mathcal{C}^*$. Formalmente è definita come

$$A^* := \begin{cases} A_1^* & \text{se } \delta \in (0, \frac{1}{2}), \\ A_2^* & \text{se } \delta \in (\frac{1}{2}, 1), \end{cases} \tag{2.3.67}$$

dove A_1^* e A_2^* sono due costanti esplicite che dipendono da r^*. Per caratterizzare le gocce critiche diamo una definizione intuitiva delle configurazioni che indichiamo con $\widetilde{\mathcal{S}}(A^*-1)$ e $\widetilde{\mathcal{D}}(A^*-1)$ e che svolgeranno il ruolo di configurazioni protocritiche. In particolare, le configurazioni in $\widetilde{\mathcal{S}}(A^*-1)$ (risp. $\widetilde{\mathcal{D}}(A^*-1)$) hanno un unico cluster di area A^*-1 e forma come in Fig. 2.25(a)-(c) (risp. Fig. 2.25(b)-(d)). Indicando con $n(\eta)$ il numero di particelle libere della configurazione η, poniamo

$$\begin{aligned}\mathcal{K}(A^*-1) := \{\eta' \in \mathcal{V}_{A^*-1} | \, \exists\, \omega = (\eta, \omega_1, ..., \omega_n, \eta') : \eta \in \widetilde{\mathcal{S}}(A^*-1) \cup \widetilde{\mathcal{D}}(A^*-1), \\ \widehat{H}(\eta) = \widehat{H}(\eta'), n(\omega_j) = 0 \, \forall \, j = 1, ..., n \text{ e } \Phi_{\mathcal{V}_{A^*-1}}(\eta, \eta') \leqslant \widehat{H}(\eta) + U\}\end{aligned} \tag{2.3.68}$$

l'insieme delle configurazioni ottenute a partire da $\widetilde{\mathcal{S}}(A^*-1) \cup \widetilde{\mathcal{D}}(A^*-1)$ con un cammino che non crea particelle libere, l'energia lungo di esso aumenta al massimo di U e le configurazioni iniziali e finali hanno la stessa energia. Notiamo che l'ultima condizione in (2.3.68) equivale a richiedere che $\Phi_{\mathcal{V}_{A^*-1}} < \Gamma_H^*$, dove

$$\Gamma_H^* := \widehat{H}(\mathcal{K}(A^*-1)) + \Delta = \widehat{H}(\widetilde{\mathcal{S}}(A^*-1)) + \Delta = \widehat{H}(\widetilde{\mathcal{D}}(A^*-1)) + \Delta.$$

L'insieme $\mathcal{K}(A^*-1)$ svolge lo stesso ruolo degli insiemi $\widetilde{\mathcal{D}}$ e $\bar{\mathcal{D}}$ introdotti per il modello che evolve sul reticolo quadrato. Infatti, le condizioni richieste in (2.3.68) sono analoghe a quelle in (2.3.31), con l'ulteriore richiesta che il cammino che collega $\eta \in \widetilde{\mathcal{S}}(A^*-1) \cup \widetilde{\mathcal{D}}(A^*-1)$ a $\eta' \in \mathcal{V}_{A^*-1}$ non deve creare alcuna particella libera. Questa condizione garantisce che η' non si ottiene da η spostando una protuberanza, perché sul reticolo esagonale ciò avviene staccando prima la protuberanza stessa. Non abbiamo bisogno di questa condizione sul reticolo quadrato perché una protuberanza può essere spostata lungo un lato di un cluster senza mai staccarsi.

In questa tesi dimostreremo che l'insieme $\mathcal{C}^* = \mathcal{K}(A^*-1)^{fp}$ è un varco per la transizione da $\hexagon$ a $\hexagon$, cosicché il valore energetico Γ_H^* coincide con l'energia delle configurazioni critiche. Sottolineiamo che non abbiamo ottenuto una caratterizzazione geometrica completa di questo insieme. Per ottenere questo, infatti, abbiamo bisogno di identificare geometricamente l'insieme $\mathcal{K}(A^*-1)$. Questo è lasciato come futura direzione di ricerca.

Osservazione 2.3.2. *A differenza di quanto accade sul reticolo quadrato, sul reticolo esagonale molti altri modi di spostare particelle a costo U può verificarsi. Sottolineiamo questa proprietà cruciale del reticolo esagonale perché ha un forte impatto sulla descrizione geometrica del varco. Infatti, ad esempio, considerando una configurazione come in Figura 2.26(a), osserviamo che è possibile spostare una protuberanza appartenente al rombo elementare a sinistra a costo U. Il fatto chiave è che questa non è l'unica possibilità, come avviene sul reticolo quadrato, infatti in questo caso è possibile muovere anche particelle che appartengono alla parte interna di un cluster. Ad esempio, è possibile spostare verso il rombo elementare un'intera fila di particelle dando origine ad una configurazione con la stessa energia (si veda Figura 2.26 per l'intero cammino). Da qui segue che la caratterizzazione geometrica del varco è molto più ricca ed interessante di quella che emerge per il reticolo quadrato. Inoltre, questi ulteriori movimenti regolarizzanti delle particelle porta a diversi meccanismi per entrare nel varco. Segnaliamo al lettore l'Osservazione 2.3.3 per maggiori dettagli.*

Per dimostrare che l'insieme $\mathcal{C}^*$ è varco per la transizione e che il sistema, con probabilità tendente a 1 nel limite per β che tende all'infinito, crea la goccia critica e raggiunge $\hexagon$ in un tempo di ordine $e^{\Gamma_H^* \beta}$ quando parte da $\hexagon$, gli ingredienti fondamentali sono i seguenti:

(i) Dimostrare che $\Phi(\hexagon, \hexagon) \leqslant \Gamma_H^*$.
(ii) Dimostrare che $\Phi(\hexagon, \hexagon) \geqslant \Gamma_H^*$.
(iii) Dimostrare che ogni $\omega \in (\hexagon \to \hexagon)_{opt}$ attraversa l'insieme $\mathcal{C}^*$.

Per (i) è sufficiente costruire un *cammino di riferimento* ω^* che collega $\hexagon$ a $\hexagon$ e che non supera il valore energetico Γ_H^*. In particolare, questo cammino è composto da cluster che crescono il più vicino possibile a forme esagonali quasi–regolari, si veda la Figura 2.27. L'idea per la costruzione di ω^* è la seguente: per prima cosa costruiamo un cammino scheletro $\{\bar{\omega}_r\}_{r=0}^L$ dato da una sequenza di configurazioni che contengono un esagono regolare di raggio r. Ovviamente $\bar{\omega}_r$ non è un cammino poichè la transizione da $\bar{\omega}_r$ a $\bar{\omega}_{r+1}$ non può verificarsi in un singolo passo della dinamica. Così, al fine di ottenere un cammino, interpoliamo ogni elemento del cammino scheletro. Questo avviene in due fasi. Innanzitutto introduciamo tra

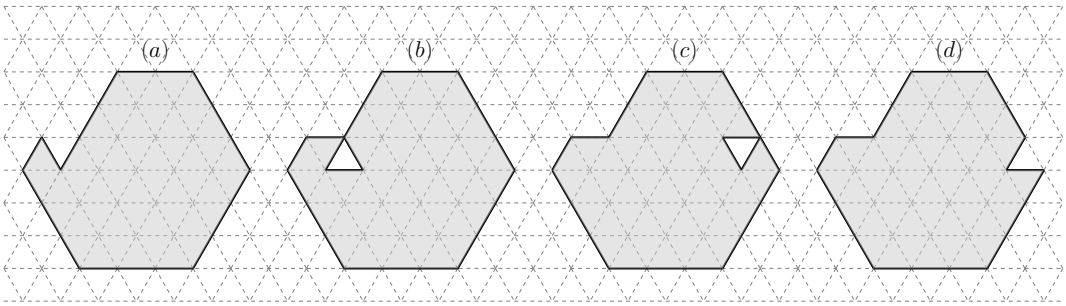

Figura 2.26 – In questa figura forniamo un esempio di movimento di particelle che stanno nella parte interna di un cluster a costo U. Rappresentiamo il cluster in grigio. Partendo dalla configurazione rappresentata in (a), muovendo una particella verso il sito vuoto, l'energia aumenta di U e la configurazione ottenuta è rappresentata in (b). Da ora in poi il sito vuoto si muove a costo 0 fino a quando il cammino raggiunge la configurazione rappresentata in (c). Infine il cammino raggiunge la configurazione in (d) diminuendo l'energia di U, cosicché le configurazioni iniziale e finale hanno la stessa energia.

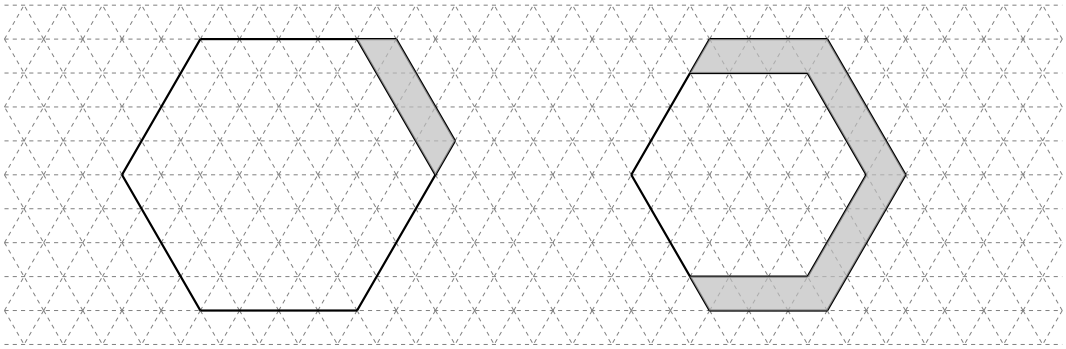

Figura 2.27 – Due esempi di esagoni quasi regolari.

$\bar{\omega}_r$ e $\bar{\omega}_{r+1}$ una sequenza di configurazioni $\tilde{\omega}_r^1, ..., \tilde{\omega}_r^{i_r}$ date da $\bar{\omega}_r$ più una barra, cioè da un esagono quasi regolare. Di nuovo, queste configurazioni sono date da una singola goccia che cresce. Introduciamo infine una seconda interpolazione per ottenere un cammino ω^* dalla sequenza di configurazioni $\tilde{\omega}_r^i$. La sua costruzione è la seguente. Tra ogni coppia di configurazioni consecutive in $\tilde{\omega}$, per cui il cluster è aumentato di una particella, viene inserita una sequenza di configurazioni con una nuova particella. In particolare la nuova particella è inizialmente creata al bordo di Λ e poi portata al sito corretto tramite movimenti consecutivi di questa particella libera.

Per il punto (ii) dobbiamo introdurre l'insieme $\mathcal{E}_{B_i}(r)$, che contiene le configurazioni che hanno un unico cluster con una forma di esagono quasi–regolare, che è un esagono regolare con i barre attaccate in senso orario. Si veda Figura 2.27, dove a sinistra (risp. destra) rappresentiamo una configurazione in $\mathcal{E}_{B_1}(4)$ (risp. $\mathcal{E}_{B_4}(3)$). La dimostrazione procede quindi in tre passi:

1. Se $\delta \in (0, \frac{1}{2})$ (risp. $\delta \in (\frac{1}{2}, 1)$), dimostrare che ogni $\omega \in (\hexagon \to \hexagonblack)_{opt}$ deve passare attraverso una configurazione $\mathcal{E}_{B_5}(r^*)$ (risp. $\mathcal{E}_{B_1}(r^*+1)$).
2. Se $\delta \in (0, \frac{1}{2})$ (risp. $\delta \in (\frac{1}{2}, 1)$), dimostrare che ogni $\omega \in (\hexagon \to \hexagonblack)_{opt}$ deve passare attraverso una configurazione che ha il cluster che appartiene all'insieme $\mathcal{E}_{B_5}(r^*)$ (risp. $\mathcal{E}_{B_1}(r^*+1)$) con l'aggiunta di due particelle.
3. Ogni $\omega \in (\hexagon \to \hexagonblack)_{opt}$ deve raggiungere il livello di energia Γ_H^*.

Per dimostrare questi tre punti consideriamo separatamente i casi $\delta \in (0, \frac{1}{2})$ e $\delta \in (\frac{1}{2}, 1)$. Per dare un'idea delle prove qui ci concentriamo soltanto sul caso $\delta \in (0, \frac{1}{2})$. Per dimostrare il punto 1 l'idea è la seguente. Denotando con $\widetilde{A}$ il numero di particelle delle configurazioni in $\mathcal{E}_{B_5}(r^*)$ e utilizzando un argomento di tipo isoperimetrico realizzato in [4], deduciamo che in

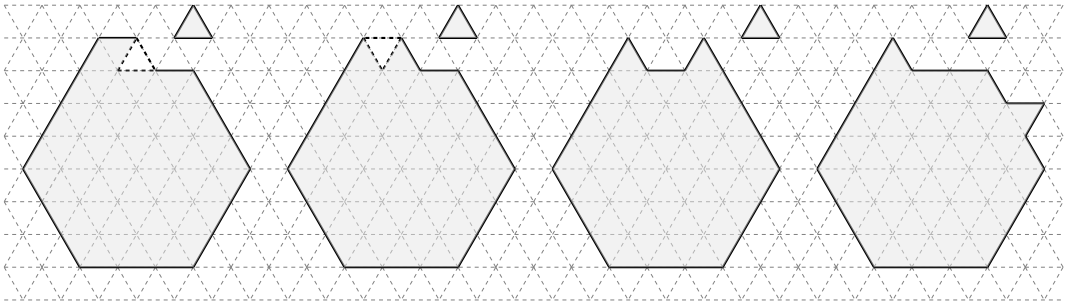

Figura 2.28 – Da sinistra a destra rappresentiamo in grigio chiaro le configurazioni possibili in $\mathcal{X}_{A_1^*-1}$ e attraversate da un cammino ottimale. In grigio scuro trattegiato rappresentiamo la posizione futura della particella libera per riempire l'angolo di $\frac{5}{3}\pi$ nei primi due esempi.

$\mathcal{V}_{\widetilde{A}}$ l'unica (modulo traslazioni e rotazioni) configurazione di perimetro minimo, e quindi di energia minima, è quella in $\mathcal{E}_{B_5}(r^*)$. Da

$$\widehat{H}(\mathcal{E}_{B_5}(r^*)) = \Gamma_H^* - 3\Delta + 2U,$$

qualsiasi altra configurazione in $\mathcal{V}_{\widetilde{A}}$ ha energia almeno $\Gamma_H^* - 3\Delta + 3U$. Per aumentare il numero di particelle partendo da una tale configurazione una particella deve essere creata al costo Δ. La configurazione risultante avrebbe però energia $\Gamma_H^* - 2\Delta + 3U$, che eccede Γ_H^* per la condizione $2\Delta < 3U$. Questo implicherebbe che il cammino supera il valore energetico Γ_H^* e quindi non sarebbe ottimale. Osserviamo che $\widetilde{A} = A_1^* - 3$. Grazie al punto 1, per dimostrare il punto 2 ragioniamo come segue. Poiché il cammino deve attraversare $\mathcal{V}_{A_1^*-1}$, partendo da un esagono quasi regolare con area $A_1^* - 3$ si crea una particella libera dando origine ad una configurazione con energia $\Gamma_H^* - 2\Delta + 2U < \Gamma_H^*$. Prima che venga creata qualsiasi nuova particella libera l'energia deve diminuire di almeno U. L'unico modo per fare questo è spostare la particella verso il cluster e attaccarla all'esagono quasi–regolare, in modo tale che l'energia diminuisce a $\Gamma_H^* - 2\Delta + U$. Ora è possibile creare un'altra particella al costo Δ dando origine ad una configurazione con energia $\Gamma_H^* - \Delta + U < \Gamma_H^*$. Di nuovo, prima di creare una nuova particella libera, l'energia deve diminuire di almeno U. L'unico modo per farlo è spostare la particella fino a quando non è attaccata al cluster, abbassando quindi l'energia a $\Gamma_H^* - \Delta$. Questo ci dà una configurazione η composta da un cluster appartenente a $\mathcal{E}_{B_5}(r^*)$ con l'aggiunta di due particelle, come affermato. Per concludere l'argomentazione con il punto 3, usiamo ancora un argomento di tipo isoperimetrico realizzato in [4], che assicura che l'energia minima in $\mathcal{V}_{A_1^*-1}$ si realizza, anche se non univocamente, in una configurazione come η descritta sopra. Poiché non è possibile ridurre l'energia senza abbassare il numero di particelle e qualsiasi ulteriore mossa per aumentare il numero di particelle comporta la creazione di una nuova particella, l'energia deve raggiungere il valore Γ_H^*.

Infine, grazie ai precedenti punti 2 e 3, per ottenere (iii) dobbiamo dimostrare che qualsiasi cammino ottimale che connette ⬡ a ⬢ attraversa l'insieme $\mathcal{V}_{A^*-1}$ in una configurazione appartenente a $\mathcal{K}(A^* - 1)$ (si ricordi l'equazione (2.3.68)) prima che venga creata una nuova particella, dando origine ad una configurazione in $\mathcal{C}^*$. Questa parte della dimostrazione è tecnica e richiede un'analisi dettagliata. Infatti il punto 2 sopra non dice come le due particelle aggiuntive sono attaccate al cluster esagonale quasi–regolare, si veda ad esempio la Figura 2.28 per quattro esempi ammissibili quando $\delta \in (0, \frac{1}{2})$. Si noti che nei primi due esempi è possibile attaccare la particella libera abbassando l'energia di $2U$, mentre negli altri due casi l'energia diminuisce solo di U. Questo è responsabile di un comportamento diverso della dinamica in questi due casi. Le prime due configurazioni, infatti, appartengono all'insieme $\mathcal{K}(A_1^* - 1)^{fp}$, mentre le altre no. L'idea della dimostrazione è che, quando la dinamica raggiunge una configurazione diversa dalle prime due rappresentate in Figura 2.28, allora non può raggiungere direttamente il ciclo dello stato stabile, ma deve riorganizzare le particelle clusterizzate per ottenere una configurazione in $\mathcal{K}(A_1^* - 1)^{fp}$. Ciò dimostrerà l'affermazione desiderata.

Osservazione 2.3.3. *Sottolineiamo che il risultato riguardante il varco che otteniamo è diverso da [35, Proposizione 2.3.7]. Sul reticolo quadrato, infatti, gli autori sono stati in grado di dimostrare*

che qualsiasi cammino ottimale dallo stato metastabile a quello stabile raggiunge una forma quadrata o quasi–quadrata, quindi viene poi attaccata una protuberanza e infine una particella libera entra nella scatola. Tuttavia, i punti 2 e 3 non sono sufficienti a caratterizzare l'ingresso nel cancello. Sul reticolo esagonale, infatti, appaiono diversi meccanismi per entrare nel varco. Una di queste possibilità è chiaramente aggiungere una particella libera partendo da una configurazione in $\mathcal{K}(A_i^* - 1)$, ma ci sono molti altri modi per entrare in $\mathcal{K}(A_i^* - 1)^{fp}$. Ad esempio, supponiamo che $0 < \delta < \frac{1}{2}$ e che un cammino ottimale $\omega : \hexagon \to \hexagon$ attraversi una configurazione η del tipo del terzo cluster raffigurato in Figura 2.28. Partendo da tale η è possibile che la particella libera sia attaccata al cluster in modo tale da formare un rombo elementare insieme ad una faccia triangolare già attaccata. Pertanto l'energia raggiunge il valore $\Gamma_H^* - U$. Allora è possibile spostare l'altra faccia triangolare a costo U e, quando si stacca, il cammino ω passa da una configurazione in $\mathcal{K}(A_1^* - 1)^{fp}$, ma il cammino non attraversa l'insieme $\mathcal{K}(A_1^* - 1)$. Con questo esempio vogliamo porre l'attenzione sul fatto che diversi meccanismi per entrare nel varco appaiono a causa della particolare forma del reticolo. Infatti sul reticolo quadrato non ha importanza da che parte è attaccata la protuberanza perché è possibile spostarla lungo il lato a costo zero.

L'ultimo risultato che abbiamo dimostrato è un primo passo verso la caratterizzazione del tubo delle traiettorie tipiche, che esula dagli scopi di questa tesi. Caratterizziamo in particolari esagoni quasi–regolari sottocritici e supercritici, cioè gli esagoni quasi–regolari sottocritici si riducono a $\hexagon$, mentre gli esagoni quasi–regolari supercritici crescono fino a $\hexagon$ nel seguente senso. Sia $\mathcal{E}^-_{B_i}(r)$ (risp. $\mathcal{E}^+_{B_i}(r)$) l'insieme delle configurazioni composte da un singolo esagono quasi–regolare contenuto in (risp. contenente) $\mathcal{E}_{B_i}(r)$. Valgono le seguenti affermazioni:

(i) Quando $\delta \in (0, \frac{1}{2})$, abbiamo

$$\begin{aligned} &\text{se } \eta \in \mathcal{E}^-_{B_5}(r^*) \quad &&\Longrightarrow \lim_{\beta\to\infty} \mathbb{P}_\eta(\tau_{\hexagon} < \tau_{\hexagon}) = 1, \\ &\text{se } \eta \in \mathcal{E}^+_{B_0}(r^* + 1) \quad &&\Longrightarrow \lim_{\beta\to\infty} \mathbb{P}_\eta(\tau_{\hexagon} < \tau_{\hexagon}) = 1. \end{aligned} \tag{2.3.69}$$

(ii) Quando $\delta \in (\frac{1}{2}, 1)$, abbiamo

$$\begin{aligned} &\text{se } \eta \in \mathcal{E}^-_{B_1}(r^* + 1) \quad &&\Longrightarrow \lim_{\beta\to\infty} \mathbb{P}_\eta(\tau_{\hexagon} < \tau_{\hexagon}) = 1, \\ &\text{se } \eta \in \mathcal{E}^+_{B_2}(r^* + 1) \quad &&\Longrightarrow \lim_{\beta\to\infty} \mathbb{P}_\eta(\tau_{\hexagon} < \tau_{\hexagon}) = 1. \end{aligned} \tag{2.3.70}$$

La dimostrazione si basa sulla nozione di ciclo (ricordare (2.3.34)). Per dimostrare (i) e (ii) abbiamo bisogno di [92, Teorema 3.2], che afferma che ogni stato in un ciclo è visitato dal processo prima dell'uscita con alta probabilità. Usando questo risultato dobbiamo dimostrare quanto segue:

1. Quando $0 < \delta < \frac{1}{2}$, allora
   (i) se η è un esagono quasi–regolare contenuto in $\mathcal{E}_{B_4}(r^*)$, allora esiste un ciclo $\mathcal{C}^{\hexagon}_{\hexagon}(\Gamma_H^*)$ contenente η e $\hexagon$ e non contenente $\hexagon$;
   (ii) se η è un esagono quasi–regolare contenente $\mathcal{E}_{B_0}(r^* + 1)$, allora esiste un ciclo $\mathcal{C}^{\hexagon}_{\hexagon}(\Gamma_H^* - \widehat{H}(\hexagon))$ contenente η e $\hexagon$ e non contenente $\hexagon$;
2. Quando $\frac{1}{2} < \delta < 1$, allora
   (i) se η è un esagono quasi–regolare contenuto in $\mathcal{E}_{B_0}(r^* + 1)$, allora esiste un ciclo $\mathcal{C}^{\hexagon}_{\hexagon}(\Gamma_H^*)$ contenente η e $\hexagon$ e non contenente $\hexagon$;
   (ii) se η è un esagono quasi–regolare contenente $\mathcal{E}_{B_2}(r^* + 1)$, allora esiste un ciclo $\mathcal{C}^{\hexagon}_{\hexagon}(\Gamma_H^* - \widehat{H}(\hexagon))$ contenente η e $\hexagon$ e non contenente $\hexagon$.

Ciò può essere ottenuto mediante il cammino di riferimento ω^* introdotto sopra. Per tutti i dettagli tecnici rimandiamo alla Sezione 6.3.6.

2.3.4 *Verso il modello originale: il ruolo dell'entropia*

In questa sezione torniamo al modello originale introdotto nella Sezione 2.3.1, cioè le particelle adesso vivono ed evolvono su una scatola quadrata le cui dimensioni crescono in modo esponenziale nella temperatura inversa β. Siamo interessati a come il gas *nuclea* in grandi volumi, cioè a come le particelle formano e dissolvono gocce sottocritiche finché non

riescono a costruire una goccia critica che è abbastanza grande da innescare la nucleazione. L'analisi di questo modello è molto più difficile rispetto a quella del modello locale, perché ora le particelle sono conservate in tutto il dominio ed è necessario un controllo dettagliato dell'interazione tra le gocce ed il gas di "particelle isolate".

In questo contesto il ruolo dell'*entropia* risulta fondamentale. La nozione di entropia, infatti, entra in gioco in ogni tentativo di spiegare la metastabilità e si può sostenere che gli stati metastabili vengono determinati dal principio di *massima entropia* (o minima energia libera) sotto opportuni vincoli. Il passaggio dallo stato metastabile allo stato stabile è un tipico processo termodinamico irreversibile verso il massimo assoluto dell'entropia (o minimo assoluto dell'energia libera). La transizione verso la stabilità è un fenomeno di grandi deviazioni che può essere descritto in termini di opportune funzioni di tasso. L'uscita dalla metastabilità alla stabilità è, in generale, intrinsecamente aleatorio. Per sistemi fisicamente rilevanti il meccanismo di transizione coinvolge quella che può essere chiamata entropia temporale: il passaggio avviene dopo lunghi tempi di attesa aleatori all'interno di opportuni *insiemi di permanenza*, che sono regioni all'interno dello spazio degli stati costruiti come unioni connesse di cicli. Entra in gioco anche l'entropia spaziale: in grandi volumi, anche a basse temperature, l'entropia è in competizione con l'energia perché lo stato metastabile e gli stati che ne derivano sotto la dinamica hanno una struttura spaziale non banale. Se vogliamo capire il comportamento di tali sistemi, allora una descrizione a grana grossa diventa imperativa, poiché a livello microscopico la competizione tra energia ed entropia non consente una corretta comprensione degli stati metastabili e dei loro cammini di transizione.

Il problema della nucleazione per la dinamica di Kawasaki in grandi volumi viene affrontato in una serie di tre lavori. Adottiamo il punto di vista che l'identificazione del "tubo delle traiettorie tipiche" è la chiave per ottenere il pieno controllo sulla transizione metastabile. Già nei primi articoli matematici sulla metastabilità [39, 95, 96, 107], e successivamente negli articoli sulla dinamica di Kawasaki a volume finito [67, 75], la strategia principale era identificare insiemi di configurazioni di *regolarità crescente* che sono *resistenti* alla dinamica su corrispondenti scale temporali crescenti. Questi insiemi di configurazioni costituiscono la spina dorsale nella costruzione del "tubo delle traiettorie tipiche". In particolare l'idea era quella di definire ambienti configurazionali temporali entro cui le traiettorie del processo rimangono confinate con alta probabilità su scale temporali opportune. Questo approccio comporta un'analisi di tutte le possibili evoluzioni del processo e richiede l'esclusione di eventi rari attraverso stime a priori di grandi deviazioni.

Nel primo articolo [65] gli autori hanno dimostrato una *approssimazione di gas ideale*, cioè hanno mostrato che la dinamica è ben approssimata da un processo di *passeggiate aleatorie indipendenti* (IRW). Infatti, se il gas reticolare è sufficientemente rarefatto, ogni particella trascorre la maggior parte del suo tempo muovendosi come una passeggiata aleatoria. Quando due particelle occupano siti primi vicini, l'energia di legame inibisce il loro movimento di camminata casuale, e queste pause sono lunghe quando la temperatura è bassa. Tuttavia, se gli intervalli di tempo in cui una particella sta interagendo con le altre particelle sono brevi rispetto agli intervalli di tempo in cui è libera, l'interazione può essere rappresentata come una piccola perturbazione di un movimento di camminata aleatoria libera. La situazione più difficile è quando la temperatura e la densità del gas tendono a zero contemporaneamente, che è proprio il nostro caso. Il motivo è che ad una bassa temperatura corrisponde una forte interazione, cosicché l'approssimazione di gas ideale è tutt'altro che banale. Questa è anche la situazione più interessante dal punto di vista fisico. Infatti $e^{-2U\beta}$ è la densità del gas saturo nel punto di condensazione, si veda [76]. Per densità inferiori a questa, ovvero per $\Delta > 2U$, abbiamo un gas stabile così rarefatto che si comporta come un gas ideale *fino a tempi molto grandi*. Se scegliamo $\Delta < U$ otteniamo un gas instabile che si comporta come un gas ideale solo *fino a tempi brevi*. Se scegliamo $U < \Delta < 2U$, evitando la presenza di gocce della fase liquida, otteniamo un gas metastabile. In questo regime abbiamo ancora un gas rarefatto e gli autori hanno dimostrato che si comporta come un gas ideale *fino a tempi relativamente grandi*. Il gas ideale è rappresentato da un processo di IRW e l'approssimazione di gas ideale è descritta da un processo di *Quasi–Random Walks* (QRW), che è definito come segue. Consiste in un processo di N particelle etichettate che può essere accoppiato ad un processo di N IRW in modo tale che i due processi seguano gli stessi cammini al di fuori di rari intervalli di tempo, detti *intervalli di pausa*, in cui i percorsi del processo di QRW rimangono confinati in

piccole regioni. Nel regime metastabile tipicamente alcune pause sono molto più brevi di $e^{\Delta\beta}$, mentre altre sono molto più lunghe. Gli autori hanno dimostrato che la dinamica di Kawasaki a bassa densità con particelle etichettate è un processo di QRW. Incoraggiamo il lettore ad ispezionare le principali proprietà dei QRW, che saranno uno strumento chiave per l'analisi di questo modello. Ci riferiamo in particolare a [62, Teoremi 3.2.3, 3.2.4, 3.2.5, 3.3.1] rispettivamente per la proprietà di *non-superdiffusività* e per i limiti superiore ed inferiore relativi alla *proprietà di spalmatura*.

Analizziamo ora le principali difficoltà che emergono nell'analisi di una dinamica pienamente conservativa mostrando le differenze che appaiono rispetto al modello locale e a quello semplificato. Da un lato, nel modello locale (si veda la Sezione 2.3.2) le particelle si muovono secondo la dinamica di Kawasaki solo all'interno di una scatola finita Λ_0 e al bordo le particelle vengono create e distrutte. Pertanto non vi è alcun effetto delle gocce in Λ_0 sul gas fuori da Λ_0. Per quanto riguarda il modello semplificato (si veda la Sezione 2.3.1), il serbatoio di gas è ora costituito da IRW. Il numero totale di particelle è fissato e questo modello è ben approssimato dal modello locale per $\beta \to \infty$ per quanto riguarda il suo comportamento metastabile, si veda [75]. Si noti che il gas all'esterno di Λ_0 influenza il gas di Kawasaki all'interno di Λ_0 e viceversa. Questa influenza reciproca è stata descritta per mezzo di QRW: le particelle del gas eseguono passeggiate aleatorie, intervallate da pause durante le quali interagiscono con le altre particelle, e intervallate da salti corrispondenti alla differenza tra le posizioni della particella alla fine e all'inizio intervallo di pausa. Poichè Λ_0 è finito i salti sono piccoli rispetto allo spostamento delle passeggiate aleatorie su scale temporali esponenzialmente grandi in β. Inoltre, il numero degli intervalli di pausa è controllato dai rari ritorni della passeggiata aleatoria a Λ_0. Questi due ingredienti —pochi intervalli di pausa e piccoli salti— erano sufficienti per controllare la dinamica. Per quanto riguarda il modello pienamente conservativo, purché i cluster siano piccoli, possiamo aspettarci che i salti nei QRW siano piccoli: al massimo dell'ordine della dimensione dei cluster. L'ostacolo cruciale nell'approssimazione delle particelle del gas con QRW è che l'interazione agisce ovunque. Le particelle devono arrivare o ritornare al gas, che funge da serbatoio, e quindi la dinamica non è propriamente locale. Pertanto non è possibile disaccoppiare la dinamica delle particelle all'interno di Λ_0 dalla dinamica del gas fuori da Λ_0. Quindi dobbiamo sostituire il controllo sui rari ritorni di una passeggiata aleatoria verso una scatola finita fissa mediante un controllo sul numero di collissioni particella–particella e particella–cluster. Questo si ottiene con l'aiuto delle stime di non collisione sviluppate in [61].

In questa tesi, che corrisponde al secondo lavoro della serie, usiamo i risultati in [65] per analizzare come le gocce sottocritiche si formano e dissolvono su scale spazio-temporali multiple quando il volume è *moderatamente grande*, ovvero $\Theta < 2\Delta - U$. In grandi volumi le possibili evoluzioni del gas reticolare di Kawasaki sono molto più complicate che in piccoli volumi, e devono essere considerati e controllati più eventi rispetto al caso di volume finito trattato in precedenza. In particolare, è importante controllare la *storia* delle particelle. Per questo motivo introduciamo diversi nuovi strumenti, come l'assegnazione di colori alle particelle che riassume le informazioni su come hanno interagito con il gas circostante in passato. L'attenzione rimane sul "tubo delle traiettorie tipiche", anche se il controllo di tutte le possibili evoluzioni del gas reticolare di Kawasaki richiede l'uso di molteplici grafi che descrivono gli ambienti configurazionali temporali. Questi grafi saranno identificati nella Sezione 7.5, che è il fulcro di questa analisi e contiene le dimostrazioni di tutti i lemmi principali.

Infine, nell'articolo successivo [12], che è l'ultimo di una serie di tre articoli che si occupano della dinamica di Kawasaki in grandi volumi, consideriamo il contesto in cui il volume è *molto grande*, cioè $\Theta < \Gamma^* - (2\Delta - U)$ (ricordiamo che Γ^* è l'energia della goccia critica nel modello locale), e usiamo i risultati dei primi due articoli [11, 62] per identificare il *tempo di nucleazione*. Il risultato complessivo dei tre articoli mostra quanto segue:

(1) Le gocce sottocritiche si comportano come Quasi–Random Walks, si veda [65].
(2) La maggior parte del tempo la configurazione consiste di *quasi–quadrati* e *particelle libere*. Ecco perché usiamo la terminologia *dinamica di gocce*. Il tempo di transizione tra configurazioni di questo tipo è individuato su una scala temporale esponenziale in β (si veda Teorema 7.1.2).
(3) A partire dalle configurazioni costituite da quasi–quadrati e particelle libere, la dina-

mica tipicamente *resiste*, cioè le dimensioni dei quasi–quadrati non cambiano, per una scala temporale esponenziale in β dipendente solo dalle dimensioni del più piccolo quasi–quadrato (si veda Teorema 7.1.3).

(4) A partire dalle configurazioni costituite da quasi–quadrati e particelle libere, la dinamica tipicamente crea un quasi–quadrato più grande o un quasi–quadrato più piccolo, a seconda delle dimensioni del quasi–quadrato di partenza (si veda Teorema 7.1.5). C'è una probabilità non trascurabile che un quasi–quadrato *sottocritico* segua una transizione *atipica*, cioè cresce in un quasi–quadrato più grande, e questo fa sì che la dinamica *sfugga alla metastabilità* (si veda Teorema 7.1.6).

(5) Il passaggio da gas a liquido (= nucleazione) avviene perché un *quasi–quadrato supercritico* viene creato da qualche parte in una scatola moderatamente grande e *successivamente cresce in una goccia grande*. Questo problema verrà affrontato in [12].

(6) Le configurazioni in scatole moderatamente grandi si comportano come se fossero *essenzialmente indipendenti* e come se il gas circostante fosse *ideale*. Nessuna informazione viaggia tra queste scatole sulla scala temporale rilevante che cresce esponenzialmente con β. Il quasi–quadrato supercritico appare più o meno indipendentemente in scatole diverse, un fenomeno chiamato *nucleazione omogenea*. Questo problema verrà affrontato in [12].

(7) Il *tubo delle traiettorie tipiche che porta alla nucleazione* è descritto attraverso una serie di eventi in cui l'evoluzione del gas è costituita da *gocce che vagano su più scale spazio–temporali*. Questo controllo si ottiene tramite quello che chiamiamo *approccio deduttivo* nella Sezione 7.5.

(8) Il comportamento asintotico del tempo di nucleazione è individuato su una scala temporale che è esponenziale in β e dipende dal *fattore entropico* relativo alla dimensione della scatola. Questo problema verrà affrontato in [12].

Vedremo che nel regime metastabile $\Delta \in (U, 2U)$ gocce piccole con "lunghezza laterale" minore di una lunghezza critica avranno la tendenza a restringersi, mentre gocce grosse avranno la tendenza a crescere. Ci riferiremo al primo tipo come *gocce sottocritiche* e a quest'ultimo come *gocce supercritiche*. La configurazione iniziale η_0 viene scelta in base alla misura *ristretta* $\mu_{\mathcal{R}}$, che è la misura di Gibbs grancanonica associata a H e condizionata a $\mathcal{R}$, cioè *condizionata all'avere in* Λ_β *soltanto gocce sottocritiche*. Più precisamente, richiamando la definizione della lunghezza critica per il modello locale ℓ_c data in (2.3.21), definiamo

$$\mathcal{R} := \{\eta \in \mathcal{X}_\beta : \text{tutti i cluster di } \eta \text{ hanno volume minore di } \ell_c(\ell_c - 1) + 2\} \tag{2.3.71}$$

e la misura ristretta $\mu_{\mathcal{R}}$ è definita come

$$\mu_{\mathcal{R}}(\eta) = \frac{e^{-\beta[H(\eta)+\Delta|\eta|]}}{Z_{\mathcal{R}}} \mathbb{1}_{\mathcal{R}}(\eta), \qquad \eta \in \mathcal{X}_\beta, \tag{2.3.72}$$

dove

$$Z_{\mathcal{R}} = \sum_{\eta \in \mathcal{R}} e^{-\beta[H(\eta)+\Delta|\eta|]}. \tag{2.3.73}$$

Per descrivere l'evoluzione del nostro sistema in termini di dinamica di gocce mostreremo che su una scala temporale appropriata la dinamica in genere ritorna all'insieme di configurazioni costituite da gocce quasi quadrate, a condizione che il volume non sia troppo grande. I principali risultati di questa tesi consentono una tale descrizione della dinamica in termini di gocce erranti che crescono e si restringono. Come parte del processo di nucleazione le gocce crescono e si restringono scambiando particelle con il gas che le circonda, come è tipico di una dinamica conservativa. Identificheremo in particolare i principal tassi di crescita e restringimento per queste gocce fino ad un orizzonte temporale che va ben oltre l'uscita da $\mathcal{R}$, cioè fino alla formazione di una prima grande goccia di volume di ordine $\lambda(\beta)$, con λ una funzione lentamente crescente ma illimitata. Nell'articolo successivo [12] questi teoremi verranno utilizzati per identificare il tempo di nucleazione, cioè il tempo di uscita da $\mathcal{R}$. I nostri teoremi riguardano soltanto la *fase iniziale* della nucleazione, cioè fino a quando la goccia critica cresce in una goccia che è all'incirca $\sqrt{\lambda(\beta)}$ volte la dimensione della goccia critica. Non forniscono informazioni su cosa succede *dopo*, cioè quando la goccia cresce

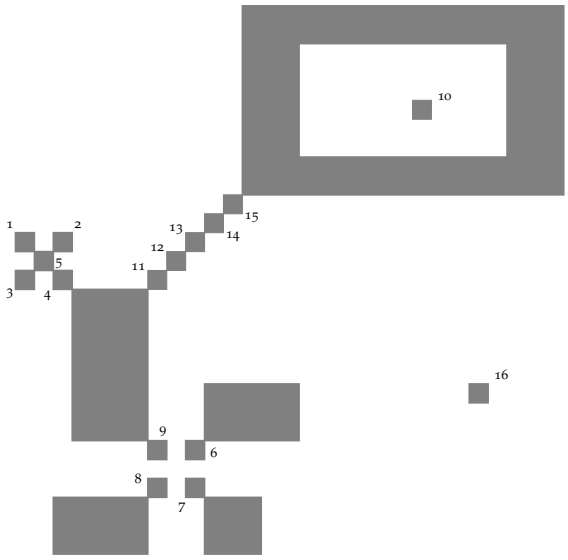

Figura 2.29 – Ciascuna particella è rappresentata da un quadrato unitario. Una particella è clusterizzata quando è parte di un cluster. Una particella è libera quando non tocca nessun'altra particella e può essere spostata all'infinito muovendo soltanto particelle non clusterizzate. Le particelle 1–5 e 16 sono libere, le particelle 6–9, 10, 11–15 non sono libere. Tutte le altre particelle sono clusterizzate.

ancora di più e diventa macroscopicamente grande. In quel regime il gas attorno alla goccia si esaurisce, gocce più piccole si muovono e si fondono in gocce più grandi, ecc. Descrivere cosa succede precisamente in questo regime rimane una grande sfida, che va *oltre* la metastabilità.

Per precisare l'orizzonte temporale a cui siamo interessati abbiamo bisogno delle seguenti definizioni. Poniamo

$$\mathcal{R}' := \left\{ \eta \in \mathcal{X}_\beta : \begin{array}{l} \text{tutti i cluster di } \eta \text{ hanno volume al massimo } \ell_c(\ell_c - 1) + 2 \\ \text{tranne al massimo un cluster con volume inferiore a } \frac{1}{8}\lambda(\beta) \end{array} \right\}, \tag{2.3.74}$$

dove $\lambda(\beta)$ è una funzione illimitata ma lentamente crescente in β che soddisfa

$$\lambda(\beta) \log \lambda(\beta) = o(\log \beta), \qquad \beta \to \infty, \tag{2.3.75}$$

es. $\lambda(\beta) = \sqrt{\log \beta}$. Per $C^\star > 0$ abbastanza grande i nostri teoremi valgono fino al tempo $T^\star$ definito come

$$T^\star = e^{C^\star \beta} \wedge \min\{t \geqslant 0 \colon X(t) \notin \mathcal{R}'\}. \tag{2.3.76}$$

Vedremo in [12] che la nostra dinamica, partendo da $\mu_{\mathcal{R}}$, tipicamente esce da $\mathcal{R}'$ entro un tempo che è esponenzialmente grande in β, e con una probabilità che tende ad 1 lo fa attraverso la formazione di un unico grande cluster $\mathcal{C}$ di volume $\frac{1}{8}\lambda(\beta)$, piuttosto che attraverso la formazione di due gocce supercritiche. Quindi $T^\star$ coincide effettivamente con il tempo di comparsa di $\mathcal{C}$, ammesso che $C^\star$ sia sufficientemente grande.

Come in [62], la nozione di particella attiva e dormiente sarà cruciale durante questa analisi. Poiché la definizione precisa richiede notazioni aggiuntive, diamo qui solo una descrizione intuitiva. Per le definizioni precise facciamo riferimento a Sezione 7.4.3.1.

La divisione delle particelle in attive e dormienti è legata alla nozione di particelle libere, che è leggermente diversa per il modello originale rispetto a quella del modello locale. Intuitivamente una particella è *libera* se non appartiene ad un cluster (= una componente connessa delle particelle più vicine) e può essere spostata all'infinito senza clusterizzazione, cioè spostando solo particelle non clusterizzate (si veda la Figura 2.29). Sia

$$D = U + d,$$

con $d > 0$ sufficientemente piccolo. Per $t > e^{D\beta}$, si dice che una particella è *dormiente* all'istante t se non è libera durante l'intervallo di tempo $[t - e^{D\beta}, t]$. Le particelle non dormienti sono chiamate *attive*. Si noti che essere attivi o dormienti dipende dalla storia della

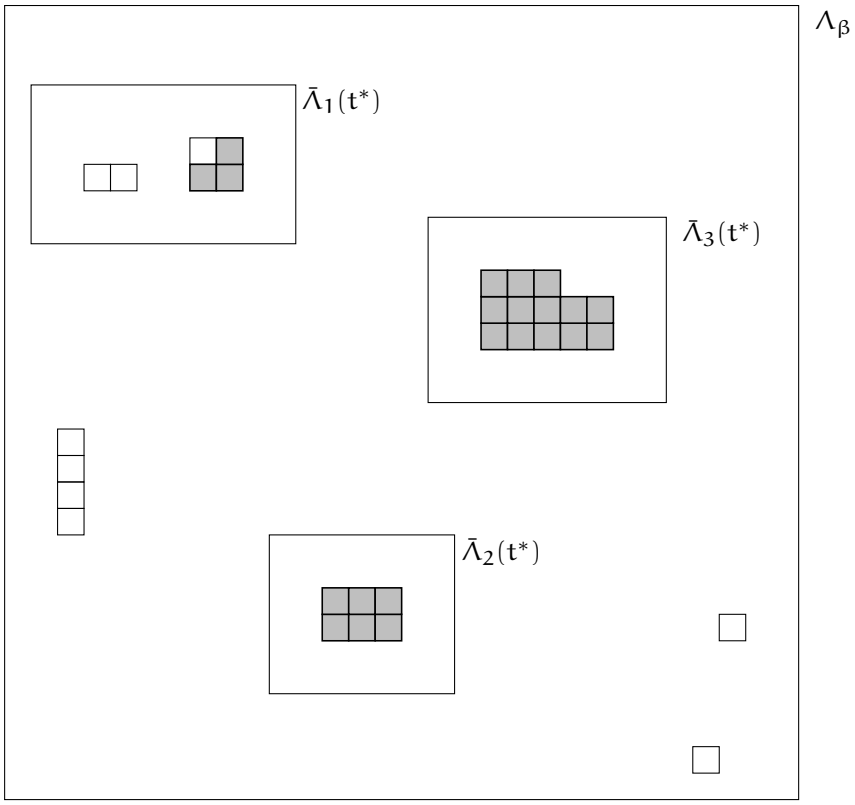

Figura 2.30 – Un esempio di scatole locali $\bar{\Lambda}(t^*) = (\bar{\Lambda}_i(t^*))_{1 \leqslant i \leqslant 3}$ per $t^* > 0$, dove le particelle grigie e bianche sono rispettivamente dormienti e attive.

particella. Per convenzione diciamo che prima del tempo $e^{D\beta}$ le particelle dormienti sono quelle che appartengono a un *quasi-quadrato* abbastanza grande, dove i quasi quadrati sono clusters con dimensioni $\ell_1 \times \ell_2$ nell'insieme

$$QS = \{(\ell_1, \ell_2) \in \mathbb{N}^2 \colon \ell_1 \leqslant \ell_2 \leqslant \ell_1 + 1\}. \tag{2.3.77}$$

Per dichiarare dormienti tutte le particelle del quasi-quadrato prima del tempo $e^{D\beta}$ richiediamo che $\ell_1 \geqslant 2$.

Per definire una scatola finita Λ come unione di un numero finito k di scatole locali disgiunte $\bar{\Lambda}_i$, $1 \leqslant i \leqslant k$, in analogia con il modello locale introdotto in [75], associamo ad ogni configurazione una configurazione locale

$$\bar{\eta} \in \{0,1\}^{\bar{\Lambda}} = \prod_{1 \leqslant i \leqslant k} \{0,1\}^{\bar{\Lambda}_i},$$

che identifichiamo con $\{0,1\}^{\Lambda}$. Queste scatole locali ci permettono di controllare le proprietà globali del gas in termini di proprietà locali, cioè attraverso la dualità tra gas e goccioline, che è rappresentata rispettivamente dalla dualità tra particelle attive e dormienti. Innanzitutto richiediamo che le scatole locali contengano tutte le particelle dormienti. In secondo luogo le scatole locali sono dinamiche, ovvero $\bar{\Lambda}_i = \bar{\Lambda}_i(t)$. Le gocce, infatti, possono muoversi e vogliamo evitare di vedere particelle dormienti fuori dalle scatole locali. In particolare le scatole seguono le gocce, cioè devono essere ridefinite solo quando si verificano i seguenti eventi: due gocce sono troppo vicine l'una all'altra, oppure un cluster è troppo vicino al bordo di una scatola, oppure una particella fuori dalle scatole si addormenta, oppure le particelle in una scatola diventano tutte attive. In qualsiasi momento $t \geqslant 0$ richiediamo che la collezione delle $k(t)$ scatole locali $\bar{\Lambda}(t) = (\bar{\Lambda}_i(t))_{1 \leqslant i \leqslant k(t)}$ soddisfino le precedenti condizioni. Facciamo riferimento alla Definizione 7.1.1 per i dettagli tecnici. Si veda la Figura 2.30 per un esempio di scatole locali.

Poiché ad ogni tempo t tutte le particelle dormienti appartengono a $\bar{\Lambda}(t)$, le scatole inducono una partizione delle particelle dormienti. Diciamo che al tempo t si verifica una

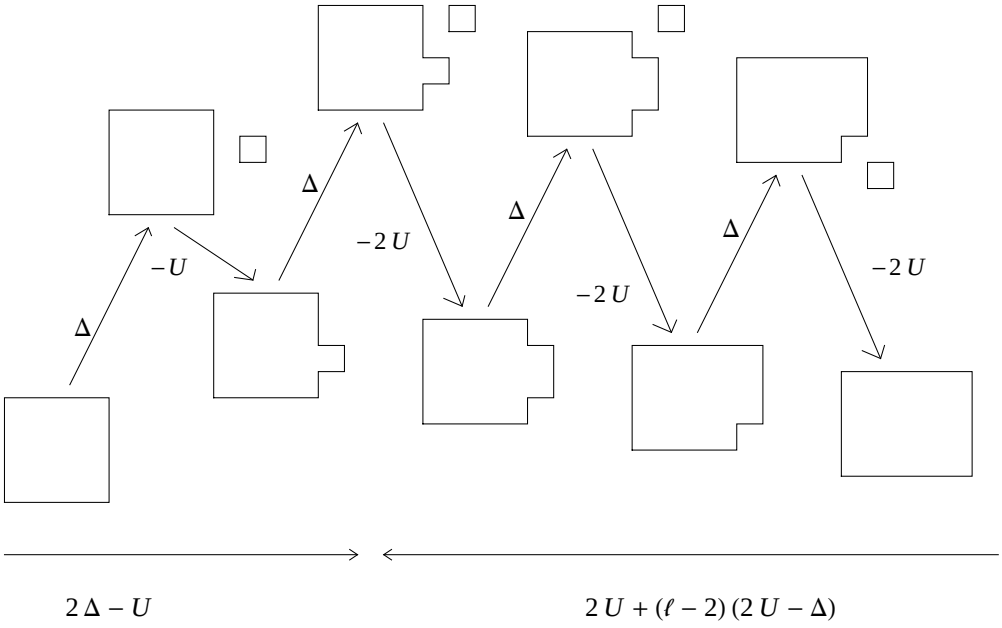

Figura 2.31 – Costo per aggiungere o rimuovere una riga di lunghezza ℓ in volume finito.

coalescenza se esistono due particelle dormienti che si trovano in diverse scatole locali all'istante t^-, ma si trovano nella stessa scatola locale all'istante t, cioè se esistono $1 \leqslant i_1, i_2 \leqslant k(t^-)$, $i_1 \neq i_2$, $1 \leqslant i^* \leqslant k(t)$ e due particelle dormienti s_1, s_2 tali che $s_j \in \bar{\Lambda}_{i_j}(t^-)$ e $s_j \in \bar{\Lambda}_{i^*}(t)$, $j = 1, 2$. Questo fenomeno è legato alla possibilità che due gocce si uniscano per formare un'unica goccia più grande. La coalescenza è difficile da controllare quantitativamente, ragion per cui nel presente lavoro ci limitiamo a cosa succede *in assenza di coalescenza*. Nel lavoro successivo [12] mostriamo che è improbabile che la nucleazione metastabile si verifichi tramite coalescenza.

Sia $\mathcal{X}_{\Delta^+}$ l'insieme delle configurazioni senza gocce o con gocce che sono quasi–quadrati con $\ell_1 \geqslant 2$ (e con ulteriori condizioni di regolarità sul gas che circonda le gocce da specificare nella Definizione 7.2.9). Sia $\mathcal{X}_E$ l'insieme delle configurazioni in $\mathcal{X}_{\Delta^+}$ senza gocce (si veda (7.3.1) e Definizione 7.2.9). Definiamo $(\bar{\tau}_k)_{k\in\mathbb{N}_0}$ come la successione dei tempi di ritorno in $\mathcal{X}_{\Delta^+}$ dopo che una particella attiva è stata vista in Λ, dove $\bar{\tau}_0$ è il tempo di primo arrivo in $\mathcal{X}_{\Delta^+}$. Rimandiamo a (7.1.5) per la definizione precisa. Ricordiamo che $|\Lambda_\beta| = e^{\Theta\beta}$. Supponiamo che $\Delta < \Theta \leqslant \theta$, con θ definito come segue. Sia $\varepsilon = 2U - \Delta$, e sia $r(\ell_1, \ell_2)$ la *resistenza* del quasi–quadrato $\ell_1 \times \ell_2$ con $1 \leqslant \ell_1 \leqslant \ell_2$ dato da (si veda la Figura 2.31)

$$\begin{aligned} r(\ell_1, \ell_2) &= \min\{(\ell_1 - 2)\varepsilon + 2U, 2\Delta - U\} \\ &= \min\{(2U - \Delta)\ell_1 - U + 2\Delta - U, 2\Delta - U\}. \end{aligned} \tag{2.3.78}$$

Sia $\theta = 2\Delta - U - \gamma$ la resistenza del più grande quasi–quadrato sottocritico. Poiché questo quasi–quadrato ha dimensioni $(\ell_c - 1) \times \ell_c$, abbiamo che $2\Delta - U - \gamma = 2U + ((\ell_c - 1) - 2)\varepsilon$, cosicché

$$\gamma = \Delta - U - (\ell_c - 2)\varepsilon. \tag{2.3.79}$$

Vedremo che $\gamma > 0$ è un parametro importante. Le già citate condizioni di regolarità sul gas utilizzano un parametro aggiuntivo $\alpha > 0$ (si veda la Definizione 7.2.9 sotto), che può essere scelto piccolo quanto desiderato. Poiché abbiamo definito $D = U + d$, Δ^+ è definito da $\Delta^+ = \Delta + \alpha$. Chiamiamo una funzione $f(\beta)$ superesponenzialmente piccola, e la indichiamo con $\mathrm{SES}(\beta)$, se

$$\lim_{\beta\to\infty} \frac{1}{\beta} \log f(\beta) = -\infty. \tag{2.3.80}$$

TEOREMI PRINCIPALI: TASSI DI CRESCITA E RIDUZIONE DELLE GOCCE

I principali teoremi che abbiamo derivato controllano le transizioni tra le configurazioni

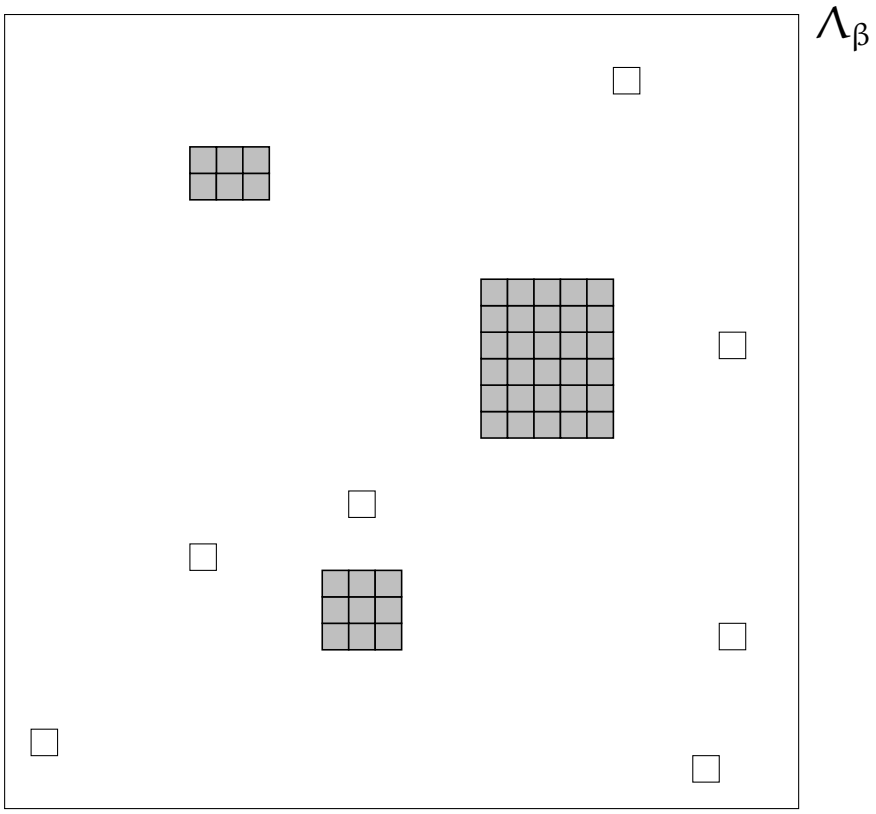

Figura 2.32 – Un esempio di configurazione $\eta \in \mathcal{X}_{\Delta^+}$, dove le particelle grigie e bianche sono rispettivamente dormienti e attive, tale che $\pi(\eta) = \{(2,3),(3,3),(5,6)\}$.

costituite da quasi–quadrati e particelle libere, le scale temporali su cui avvengono queste transizioni, e le traiettorie più probabili che seguono.

Teorema (I) Il nostro primo risultato descrive i tempi di ritorno tipici all'insieme $\mathcal{X}_{\Delta^+}$. In particolare dimostriamo che, partendo da $\mu_{\mathcal{R}}$, con probabilità $1 - \mathrm{SES}(\beta)$ vale che i tempi di ritorno sull'insieme $\mathcal{X}_{\Delta^+}$ sono dell'ordine $e^{(\Delta+\alpha)\beta}$.

Teorema (II) Il nostro secondo teorema descrive i tempi di aggiornamento tipici per una configurazione in $\mathcal{X}_{\Delta^+}$. Indichiamo con π una proiezione da $\mathcal{X}_{\Delta^+}$ ad uno spazio finito

$$\bar{\mathcal{X}}_\Delta = \bigcup_{k \geqslant 0} QS^1 \times \cdots \times QS^k, \tag{2.3.81}$$

dove QS^i sono le dimensioni dei cluster quasi–quadrati contenuti nelle scatole locali $\bar{\Lambda}_i$ e definite in (2.3.77). Si veda la Figura 2.32. Possiamo definire una dinamica sullo spazio $\bar{\mathcal{X}}_\Delta$ delle dimensioni dei quasi–quadrati, disposti ad esempio in ordine lessicografico crescente. Per $i \in \mathbb{N}_0$ indichiamo con $(\ell_{1,i}, \ell_{2,i})$ in QS, con $\ell_{1,i} \geqslant 2$, le dimensioni del quasi–quadrato più piccolo al tempo $\bar{\tau}_i$, se presente, altrimenti impostiamo $\ell_{1,i} = \ell_{2,i} = 0$. Richiamiamo (2.3.78) e definiamo la resistenza di una configurazione in $\mathcal{X}_E$ come

$$r(0,0) = 4\Delta - 2U - \theta. \tag{2.3.82}$$

Dimostriamo che partendo da $\mu_{\mathcal{R}}$ e a meno che non si verifichi una coalescenza, per ogni $i \in \mathbb{N}_0$ la dinamica proiettata tipicamente rimane in $\pi(X(\bar{\tau}_i))$ attraverso visite successive in $\mathcal{X}_{\Delta^+}$ per un tempo di ordine $e^{r(\ell_{1,i},\ell_{2,i})\beta}$. Notiamo che per $\ell_{1,i} \geqslant \ell_c$ tutti i quasi–quadrati hanno la stessa resistenza $2\Delta - U$. Nel caso in cui $X(\bar{\tau}_i)$ non abbia quasi–quadrati, la sua resistenza $r(0,0)$ coinvolge la resistenza della configurazione vuota nel modello locale e l'entropia spaziale che viene dalla posizione in Λ_β dove può apparire la nuova goccia.

Teorema (III) Il nostro terzo risultato descrive la transizione tipica del sistema tra due visite successive a $\mathcal{X}_{\Delta^+}$ a condizione che la dinamica non ritorni nella stessa configurazione al

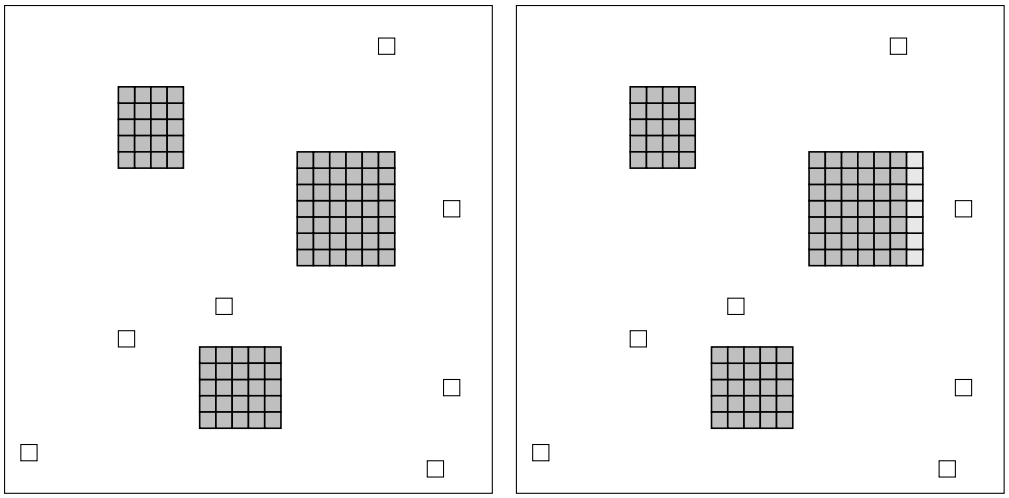

Figura 2.33 – Per $\ell_c = 4$ rappresentiamo sulla sinistra un esempio di configurazione $\eta \in \mathcal{X}_{\Delta^+}$ tale che $\pi(\eta) = \{(4,5),(5,5),(6,7)\}$ e sulla destra una possibile transizione tipica $\pi' = \{(4,5),(5,5),(7,7)\}$, dove le particelle grigie e bianche sono rispettivamente dormienti e attive.

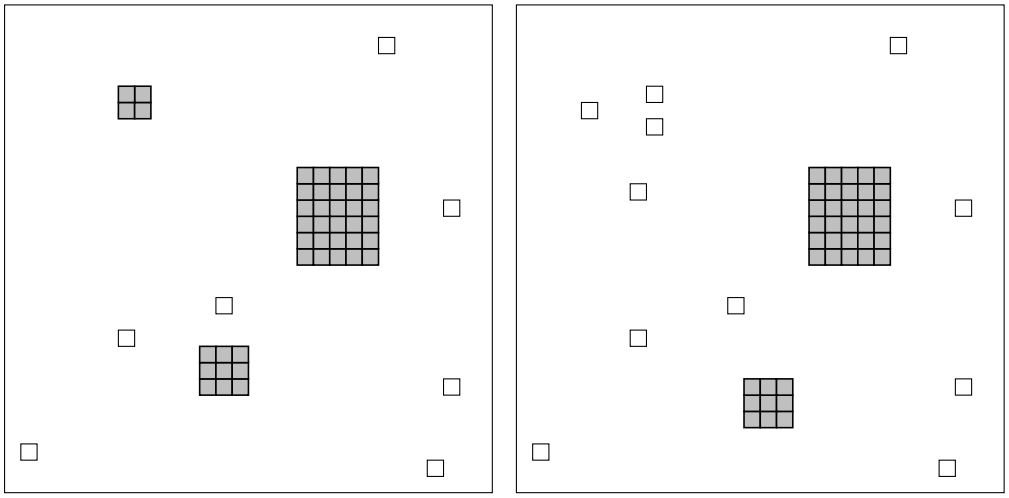

Figura 2.34 – Sulla sinistra rappresentiamo un esempio di configurazione $\eta \in \mathcal{X}_{\Delta^+}$ tale che $\pi(\eta) = \{(2,2),(3,3),(5,6)\}$ e sulla destra la transizione tipica $\pi' = \{(3,3),(5,6)\}$, dove le particelle grigie e bianche sono rispettivamente dormienti e attive.

tempo $\bar{\tau}_{i+1}$. Data una configurazione $X(\bar{\tau}_i) \in \mathcal{X}_{\Delta^+}$ definiamo la transizione tipica π'_i come segue. Per $\ell_{1,i} \geqslant \ell_c$ poniamo

$$\pi'_i = \big\{\pi(\eta') \colon \eta' \text{ è una configurazione ottenuta da } X(\bar{\tau}_i) \text{ aggiungendo una riga a un quasi–quadrato arbitrario}\big\}. \tag{2.3.83}$$

Si veda la Figura 2.33. Per $\ell_{1,i} < \ell_c$ dobbiamo distinguere i casi $\ell_{2,i} \geqslant 3$, $\ell_{2,i} = 2$ e $\ell_{2,i} = 0$. Se $\ell_{1,i} < \ell_c$ e $\ell_{2,i} \geqslant 3$ (risp. $\ell_{2,i} = 2$), allora definiamo π'_i come il singoletto costituito dalla collezione delle dimensioni dei quasi–quadrati ottenuta da $\pi(X(\bar{\tau}_i))$ modificando uno dei quasi–quadrati più piccoli, che diventa $(\ell_{2,i} - 1) \times \ell_{1,i}$ (risp. 0×0). Se $\ell_{1,i} = \ell_{2,i} = 0$ definiamo allora $\pi'_i = \{\pi(\eta')\}$, dove η' è la configurazione ottenuta da $X(\bar{\tau}_i)$ creando una goccia quadrata 2×2, cioè $\pi'_i = \{(2,2)\}$. Si veda la Figura 2.34. Dimostriamo quindi che

$$\lim_{\beta\to\infty} P_{\mu_{\mathcal{R}}}\left(\begin{array}{c}\text{se } \bar{\tau}_{i+1} \leqslant T^\star, \text{ allora } \pi(X(\bar{\tau}_{i+1})) \in \pi'_i \text{ o}\\ \text{si verifica una coalescenza tra } \bar{\tau}_i \text{ e } \bar{\tau}_{i+1}\end{array}\,\middle|\, \pi(X(\bar{\tau}_{i+1})) \neq \pi(X(\bar{\tau}_i))\right) = 1. \tag{2.3.84}$$

Teorema (IV) Il nostro quarto e ultimo teorema caratterizza le transizioni atipiche del sistema, partendo da una configurazione sottocritica costituita da un unico quasi–quadrato, tra due

visite successive a $\mathcal{X}_{\Delta^+}$, senza la creazione di nuove scatole e condizionato ad una dinamica che non torna alla stessa configurazione al tempo $\bar{\tau}_i$. A tal fine, dato $X(\bar{\tau}_i) \in \mathcal{X}_{\Delta^+}$ con $2 \leqslant \ell_{1,i} < \ell_c$, definiamo $\pi_i'' = (\ell_{2,i}, \ell_{1,i} + 1)$. Questo risultato fornisce un limite inferiore per la transizione atipica di "andare controcorrente" nel caso di un quasi–quadrato sottocritico. Come mostreremo nell'articolo successivo [12], la *fuga dalla metastabilità* avviene tramite nucleazione di una goccia supercritica da qualche parte nella scatola Λ_β. Caratterizzeremo, infatti, il tempo che impiega la dinamica per uscire da $\mathcal{R}$, così come le traiettorie tipiche delle configurazioni visitate dal cluster errante fino alla formazione di una goccia grossa I risultati di questa tesi, che sono limitati al caso $\Theta < 2\Delta - U - \gamma$, ci consentiranno di svolgere questa analisi per valori maggiori di Θ, cioè $\Theta < \Gamma^* - (2\Delta - U)$, dove ricordiamo che Γ^* è l'energia della goccia critica nel modello locale.

Osservazione 2.3.4. *Le tecniche sviluppate in questa tesi consentono di dimostrare che, per qualsiasi configurazione quasi–quadrata di dimensioni $\ell_1 \times \ell_2$ in $\mathcal{X}_{\Delta^+}$, il cluster esce da una qualsiasi scatola finita, centrata attorno al cluster e con volume indipendente da β, entro un tempo di ordine $e^{\Gamma(\ell_1,\ell_2)\beta}$. Questo è il motivo per cui si parla di* cluster errante*. Non enunciamo né usiamo questo risultato come teorema formale.*

Il resto di questa sezione è dedicato a fornire l'idea delle prove di questi quattro teoremi principali. Il punto di partenza è formulare determinate proprietà di regolarità per la configurazione iniziale che possiamo imporre perché la loro violazione è estremamente improbabile. In particolare introduciamo un sottoinsieme di configurazioni $\mathcal{X}^* \subset \mathcal{X}_\beta$, che chiamiamo *ambiente tipico*, con la proprietà che se il nostro sistema parte dall'insieme ristretto, poi esce dall'ambito $\mathcal{X}^*$ entro una qualsiasi scala temporale esponenziale in β solo con una probabilità trascurabile, cioè

$$P_{\mu_{\mathcal{R}}}(\tau_{\mathcal{X}_\beta \setminus \mathcal{X}^*} \leqslant T^\star) = \mathrm{SES}(\beta).$$

Questo risultato ci permette di lavorare con configurazioni in $\mathcal{X}^*$. Sostituendo, quindi, la dinamica originale con la dinamica ristretta a $\mathcal{X}^*$, possiamo accoppiare le due dinamiche in modo tale che abbiano le stesse traiettorie fino a qualsiasi tempo esponenziale in β con probabilità $1 - \mathrm{SES}(\beta)$.

L'idea di base per dimostrare il teorema (I) consiste nel raggruppare le configurazioni in una sequenza di sottoinsiemi di configurazioni di regolarità crescente e dimostrare una proprietà di ricorrenza a questi insiemi su una sequenza crescente di scale temporali, cioè la dinamica raggiunge questi insiemi entro il tempo di riferimento con probabilità $1 - \mathrm{SES}(\beta)$. Questo è un argomento standard per sistemi metastabili a bassa temperatura, che è stato eseguito nei minimi dettagli per una versione semplificata del nostro modello [75]. Qui indichiamo le differenze rispetto al lavoro precedente. Sottolineiamo innanzitutto che, rispetto al modello locale, dobbiamo introdurre due insiemi aggiuntivi per controllare la regolarità del gas che circonda le gocce. Inoltre, le scatole locali ora non sono fisse, ma si muovono con le gocce e pertanto è necessario un loro controllo accurato: dobbiamo controllare in particolare la probabilità che una nuova scatola venga creata entro il tempo di riferimento.

Per dimostrare i Teoremi (II)–(IV) dobbiamo fornire stime sulla probabilità di transizione tra configurazioni costituite da quasi–quadrati e particelle libere. In particolare, fornire limiti superiori alla probabilità che si verifichino transizioni tipiche e atipiche rappresenta il principale ostacolo. Dobbiamo controllare, infatti, tutti i possibili meccanismi per crescere e contrarsi. Questi ostacoli sono organizzati in quello che chiamiamo *approccio deduttivo*: il tubo delle traiettorie tipiche che portano alla nucleazione è descritto attraverso una serie di eventi, i cui complementari hanno una probabilità trascurabile, sui quali l'evoluzione del gas consiste in *gocce erranti su scale spazio-temporali multiple* in un modo che può essere descritto da una catena di Markov a grana grossa su uno spazio di gocce.

2.4 METASTABILITÀ PER SISTEMI NON CONSERVATIVI

Consideriamo l'esempio di un sistema ferromagnetico al di sotto della temperatura critica. Facciamo partire il sistema da uno stato di equilibrio quando un campo magnetico esterno positivo si è lentamente spento, e poi lo lasciamo evolvere, dopo aver introdotto un piccolo

campo magnetico negativo. Osserviamo che la situazione iniziale, caratterizzata da una magnetizzazione positiva, persiste per un lungo tempo macroscopico. In altre parole il sistema, invece di subire la giusta transizione di fase, rimane a lungo in una situazione apparentemente stazionaria fino a quando qualche perturbazione esterna o qualche grande fluttuazione spontanea nucleerà la nuova fase, avviando un processo irreversibile che porterà il sistema alla vera fase di equilibrio con magnetizzazione negativa. Il comportamento sopra descritto è tipico di un'evoluzione non conservativa nel senso che la magnetizzazione non si conserva. Per modellizzare matematicamente i fenomeni come quello appena descritto si propone spesso di utilizzare modelli reticolari che evolvono secondo la dinamica di Glauber poiché la dinamica non conserva la magnetizzazione totale del sistema. Sottolineiamo che le dinamiche non conservative hanno le proprie caratteristiche peculiari rispetto a quelle conservative, e nel resto di questa sezione ci proponiamo di evidenziarle.

2.4.1 *Dinamica di Glauber*

Consideriamo un insieme finito di siti V. Ad ogni sito associamo un valore di spin (-1 o $+1$) e definiamo lo spazio delle configurazioni come $\mathcal{X} = \{-1, +1\}^V$. Possiamo associare ad ogni configurazione σ l'energia Hamiltoniana $\widetilde{H}(\sigma)$. Qui non riportiamo la scelta particolare dell'insieme V e dell'energia $\widetilde{H}(\sigma)$, perché cambia a seconda del fenomeno che vogliamo analizzare. Questa scelta verrà mostrata nella Sezione 2.4.2 dove analizzeremo la diffusione di un'opinione all'interno di una comunità. Ponendo β la temperatura inversa, consideriamo la dinamica di Metropolis usuale a cambiamento singolo di spin $(X_t)_{t\in\mathbb{N}}$ su $\mathcal{X}$ indotta da $\widetilde{H}$. Le probabilità di transizione della dinamica di Glauber sono quindi date da

$$P(\sigma,\eta) = q(\sigma,\eta)e^{-\beta[\widetilde{H}(\eta)-\widetilde{H}(\sigma]_+}, \quad \text{per tutti } \sigma \neq \eta, \tag{2.4.1}$$

dove $[\cdot]_+$ denota la parte positiva e $q(\sigma,\eta)$ è una matrice di connettività indipendente da β, definita, per ogni $\sigma \neq \eta$, come

$$q(\sigma,\eta) = \begin{cases} \frac{1}{|V|} & \text{se } \exists\, x \in V \text{ tale che } \sigma^{(x)} = \eta, \\ 0 & \text{altrimenti,} \end{cases} \tag{2.4.2}$$

dove

$$\sigma^{(x)}(z) = \begin{cases} \sigma(z) & \text{se } z \neq x, \\ -\sigma(x) & \text{se } z = x. \end{cases} \tag{2.4.3}$$

Questa dinamica è *reversibile* rispetto alla misura di Gibbs

$$\mu(\sigma) = Z^{-1}\exp(-\beta\widetilde{H}(\sigma)),$$

dove $Z = \sum_{\sigma\in\mathcal{X}} \widetilde{H}(\sigma)$ è la costante di normalizzazione, nel senso che la nostra catena di Markov $(X_t)_{t\in\mathbb{N}}$ soddisfa la condizione di equilibrio dettagliato.

2.4.2 *Un modello per la dinamica di opinioni*

In questa sezione ci concentriamo sul modello di Ising come primo semplice modello canonico per una dinamica di opinione pubblica, c.f. [109, 110], in presenza di una scelta binaria. In questo contesto lo stato di uno spin descrive l'opinione corrente di un individuo, il campo magnetico esterno cattura l'esposizione a informazioni distorte e/o marketing/campagna unilaterale, e gli accoppiamenti tra spin vicini rappresentano l'effetto delle interazioni tra pari sulle opinioni personali. Nei modelli di opinione binaria simili a Ising la temperatura del sistema approssima più o meno eventi aleatori che possono influenzare le opinioni degli individui ma non sono esplicitamente presi in considerazione nel modello, cfr. [110]. In questa tesi studiamo il comportamento metastabile del modello di Ising su una rete con comunità nel limite di temperatura molto bassa, che è utile a descrivere una situazione in cui le interazioni tra pari e fattori esterni hanno una forte influenza sull'opinione di tutti. La bassa temperatura

favorisce motivi di opinioni omogenee in cui ci sono meno individui che non sono d'accordo con i pari con cui interagiscono, che a livello macroscopico significa che le opinioni diventano molto rigide e difficili da cambiare, ad esempio, su una situazione di polarizzazione.

Il modello base di Ising può essere ampliato per avere più di due opinioni e possibilmente interazioni asimmetriche tra loro, come in [111], dove gli autori considerano un modello simile a quello di Ising con tre opinioni ma dove le due opinioni più estreme non interagiscono tra loro. Dal momento che siamo principalmente interessati all'interazione tra dinamiche di opinioni e topologia di rete, in questa tesi ci concentriamo sul caso più semplice di un'opinione binaria. Il modello elettorale è un altro modello simile ad Ising per studiare l'evoluzione delle opinioni binarie che presentano una diversa (e possibilmente irreversibile) regola di aggiornamento della maggioranza, si veda ad esempio [8, 51, 94]. Per una revisione più ampia dei modelli matematici e fisici di dinamica di opinioni rimandiamo il lettore interessato a [114].

È chiaro che assumere che la struttura sottostante sia un reticolo o il grafo completo non è l'ideale quando si analizza una dinamica di opinione pubblica, poiché gli individui hanno reti sociali e motivi di interazione molto eterogenei. In particolare è ragionevole supporre che ogni individuo abbia solo un numero finito di interazioni e che tenderebbe ad allinearsi di più con l'opinione degli individui della comunità a cui appartiene piuttosto che a quella di perfetti sconosciuti. Con l'obiettivo di capire il ruolo della struttura comunitaria nelle dinamiche di opinione, consideriamo qui un famiglia di reti molto eterogenea con comunità molto dense ed interazioni molto deboli tra queste comunità. Vari modelli di dinamiche di opinione sono stati studiati su reti a struttura comunitaria, ad esempio, [83, 108], ma soprattutto mediante simulazioni numeriche, mentre in questa tesi ci concentriamo su risultati matematici rigorosi.

A noi interessa soprattutto capire l'interazione tra le dinamiche di opinione e la struttura comunitaria della rete sottostante. Con l'obiettivo di derivare risultati in forma chiusa, scegliamo una specifica famiglia di reti clusterizzate semplice ma emblematica. Consideriamo in particolare il modello di Ising su un grafo G costituito da k cluster di uguale dimensione, che sono grafi localmente completi, e tale che ogni nodo sia connesso ad un singolo nodo in ciascuno degli altri cluster. Con questa scelta otteniamo una rete con comunità molto fitte che sono solo scarsamente collegate tra loro.

La struttura della rete influenza pesantemente sia le proprietà statiche (cioè l'energia delle configurazioni) che quelle dinamiche (la probabilità delle traiettorie del sistema) del modello di Ising. In questo contesto è interessante studiare i fenomeni di metastabilità o "tunneling" che il modello di dinamica di opinioni può esibire. In presenza di un campo magnetico esterno positivo, ad esempio, lo stato metastabile del sistema descrive la diffusione di una seconda opinione molto rigida che non è allineata con quella principale.

Informalmente, le configurazioni metastabili sono quelle in cui il sistema persiste per molto tempo prima di raggiungere una delle configurazioni stabili, cioè quelle che minimizzano l'energia del sistema. Nel contesto della rete clusterizzata che consideriamo in questa tesi, l'insieme degli stati metastabili dipende fortemente dalla forza relativa delle interazioni tra le comunità della rete e da quella del campo magnetico esterno. In assenza di un campo magnetico esterno le due opinioni sono ugualmente probabili ed i due motivi di opinione omogenei sono entrambi stati stabili. In questo caso è comunque interessante studiare come, iniziando con tutti gli individui che concordano su un'opinione, l'intera rete può passare all'opinione opposta, quanto tempo ci vorrà e quali sono le traiettorie più probabili di questo processo.

Formalmente, per ogni $k \geqslant 2$ e ogni $n \geqslant 2$ consideriamo un grafo non orientato $G = \mathcal{G}(k, n)$ costituito da k cluster, ognuno dei quali è un sottografo completo di dimensione n, in cui colleghiamo ulteriormente ogni nodo, $i = 1, \dots, n$ anche ai suoi $k-1$ "gemelli" negli altri $k-1$ cluster (quelli con lo stesso marchio modulo n), ottenendo così un grafo regolare dove ogni nodo ha grado $n+k-2$. L'insieme dei vertici di $\mathcal{G}(k, n)$ è $V = \bigcup_{i=1}^{k} V^{(i)}$, dove $V^{(i)} := \{n \cdot (i-1)+1, \dots, n \cdot i\}$ sono i nodi nel cluster i-esimo. L'insieme degli archi di $\mathcal{G}(k, n)$ è $E = E_{int} \cup E_{cross}$, dove $E_{int} = \bigcup_{i=1}^{k} E_{int}^{(i)}$ è la collezione dei *lati interni*, cioè dei lati all'interno di un cluster, e E_{cross} quella dei lati tra i cluster, a cui ci riferiamo come *lati incrociati*. Il grafo $\mathcal{G}(k, n)$ ha allora $\frac{1}{2}kn(n+k-2)$ lati, di cui $n\binom{k}{2}$ sono incrociati e $\binom{n}{2}$ sono all'interno di ciascun cluster. Figura 2.35 raffigura un'istanza di $\mathcal{G}(3, 5)$.

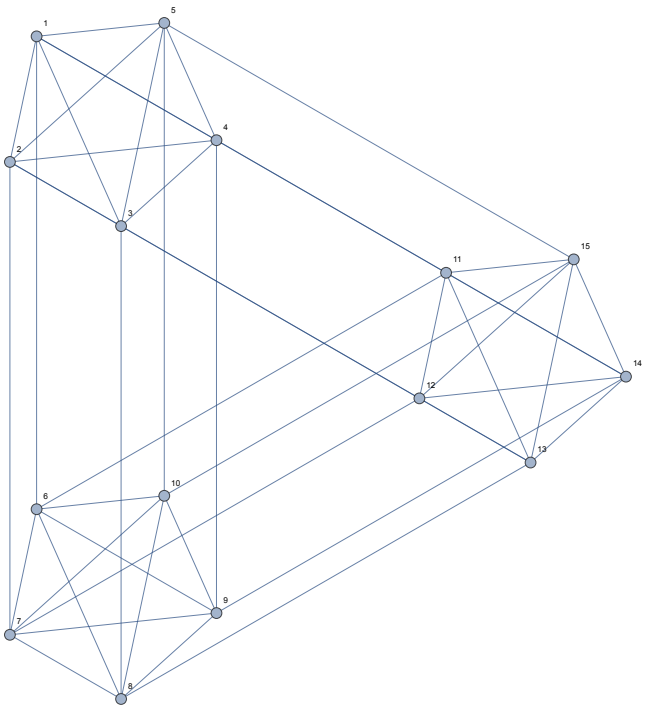

Figura 2.35 – Rappresentazione del grafo $\mathcal{G}(3,5)$.

Ad ogni sito $i \in V$ associamo una variabile di spin $\sigma(i) \in \{-1,+1\}$. Nello spazio delle configurazioni $\mathcal{X} = \{-1,+1\}^V$ definiamo la funzione di energia $\widetilde{H}$ come

$$\widetilde{H}(\sigma) := -\sum_{(i,j)\in E_{int}} \sigma_i\sigma_j - \varepsilon \sum_{(i,j)\in E_{cross}} \sigma_i\sigma_j - h\sum_{i\in V}\sigma_i, \quad \sigma \in \mathcal{X}, \tag{2.4.4}$$

dove assumiamo che la forza dell'interazione tra i cluster sia parametrizzata da uno scalare $\varepsilon \in [-1,1]$, mentre è uguale a 1 lungo tutti gli altri lati interni e $h \geqslant 0$ è il campo magnetico esterno. Considereremo il caso $h \in [0,1]$ dove, come si vedrà, il sistema mostra un comportamento metastabile. È ragionevole supporre che le opinioni degli individui che fanno parte di una comunità diversa hanno meno influenza su ciascuna comunità. Per questo motivo assumiamo che le interazioni tra diversi cluster di rete siano più deboli di quelli all'interno di ciascun cluster, poiché la loro forza è pari a $|\varepsilon| \leqslant 1$. Inoltre, assumendo valori negativi per ε, possiamo considerare situazioni in cui gli individui tendono a non essere d'accordo con individui di altre comunità. La presenza di un campo magnetico esterno diverso da zero di intensità h favorisce le configurazioni in cui gli spin sono allineati nella direzione del campo. Poiché ogni singolo spin sente il campo esterno, il suo contributo energetico deve essere proporzionale al numero di spin con un certo segno.

La dinamica di Glauber è quindi definita come la catena di Markov a tempo discreto con probabilità di transizione definite in (2.4.1) con l'Hamiltoniana definita in (2.4.4). Per questo modello, a seconda dei valori del parametro ε e del campo magnetico esterno h, caratterizzeremo le proprietà asintotiche del tempo di transizione dall'insieme degli stati metastabili (o stabili) all'insieme degli stati stabili, oltre a fornire una caratterizzazione delle configurazioni critiche che sono attraversate dalla dinamica con probabilità tendente a uno nel limite di temperatura molto bassa.

In questa tesi ci interesseremo al caso $k = 2$. La Figura 2.36 raffigura un'istanza di $\mathcal{G}(2,7)$. Il motivo di questa scelta è duplice: in primo luogo il caso $k = 2$ presenta già un comportamento molto vario e ricco, e, in secondo luogo, il caso più generale con $k > 2$ cluster non è concettualmente più difficile da affrontare, ma semplicemente più pesante in termini di notazione e terminologia. Avere una rete con solo $k = 2$ cluster $V^{(1)}$ e $V^{(2)}$ consente una notazione molto compatta per configurazioni di spin equivalenti modulo rietichettatura dei nodi. Per una configurazione $\sigma \in \mathcal{X}$ e $i = 1,2$, sia $V_+^{(i)}(\sigma)$ il sottoinsieme dei nodi nel cluster i

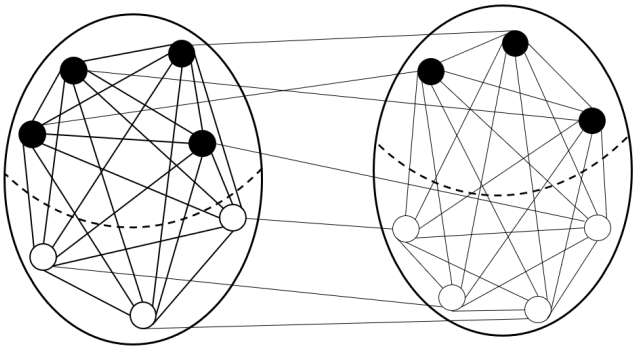

Figura 2.36 – Esempio di una configurazione in $C(4,3,3)$ sulla rete $\mathcal{G}(2,7)$ con gli spin codificati (neri per $+1$ e bianchi per -1). Il primo cluster ha $p_1 = 4$ spin $+1$, ha $p_2 = 3$ spin -1 e ci sono $a = 3$ lati concordi tra spin positivi.

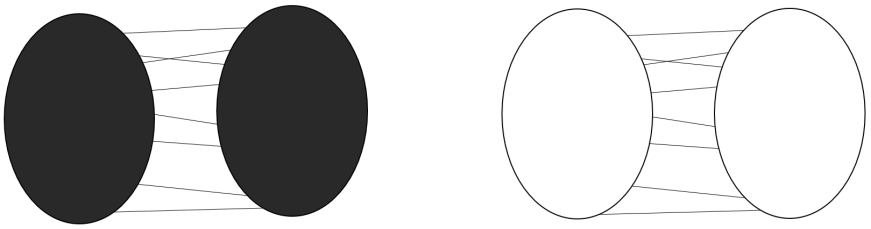

Figura 2.37 – Le due configurazioni uniformi $+\mathbf{1}$ e $-\mathbf{1}$, dove rappresentiamo in bianco (risp. nero) gli spin -1 (risp. $+1$).

il cui spin è uguale a $+1$ in σ e $E_+(\sigma)$ il sottoinsieme dei lati che connettono $V_+^{(1)}(\sigma)$ e $V_+^{(2)}(\sigma)$. Per $0 \leqslant p_1, p_2 \leqslant n$ e $0 \leqslant a \leqslant n$, definiamo il sottoinsieme $C(p_1, p_2, a) \subset \mathcal{X}$ come

$$C(p_1,p_2,a) := \left\{ \sigma \in \mathcal{X} \,:\, |V_+^{(1)}(\sigma)| = p_1,\ |V_+^{(2)}(\sigma)| = p_2,\ \text{e } |E_+(\sigma)| = a \right\}.$$

In parole, $C(p_1, p_2, a)$ è la collezione delle configurazioni σ su $\mathcal{G}(2,n)$ tali che

- σ ha $0 \leqslant p_1 \leqslant n$ spin $+1$ nel primo cluster e $0 \leqslant p_2 \leqslant n$ spin $+1$ nel secondo cluster;
- σ ha a lati incrociati concordi tra gli spin $+1$ nel primo cluster e gli spin $+1$ nel secondo cluster.

Si noti che, dati n, p_1, p_2, il numero a di lati concordi deve soddisfare la seguente disuguaglianza

$$\max\{0, p_1 + p_2 - n\} \leqslant a \leqslant \min\{p_1, p_2\}, \tag{2.4.5}$$

poiché non può esserci una quantità negativa di lati tra una qualsiasi coppia di sottocluster. Si noti che i parametri p_1, p_2 e a identificano in modo univoco l'insieme delle configurazioni in $C(p_1, p_2, a)$, modulo rietichettatura dei nodi. Implicitamente fornisce, infatti, informazioni anche sugli spin -1 nel seguente senso:

- σ ha $0 \leqslant n - p_1 \leqslant n$ spin -1 nel primo cluster e $0 \leqslant n - p_2 \leqslant n$ spin -1 nel secondo cluster;
- σ ha $p_1 - a$ lati incrociati discordi tra gli spin $+1$ nel primo cluster e gli spin -1 nel secondo cluster;
- σ ha $p_2 - a$ lati incrociati discordi tra gli spin -1 nel primo cluster e gli spin $+1$ nel secondo cluster;
- σ ha $n + a - p_1 - p_2$ lati incrociati concordi tra gli spin -1 nel primo cluster e gli spin -1 nel secondo cluster.

La Figura 2.36 mostra un esempio di una configurazione in $C(4,3,3)$ sulla rete $\mathcal{G}(2,7)$.

Indichiamo ulteriormente con $+\mathbf{1}, -\mathbf{1}$ le due configurazioni omogenee su $\mathcal{G}(2,n)$ composte da tutti spin $+1$ e da tutti spin -1, si veda la Figura 2.37. Ci riferiamo alle configurazioni che non sono globalmente omogenee ma localmente uniformi all'interno di ciascun cluster come *configurazioni miste* e le denotiamo con $\pm\mathbf{1}, \mp\mathbf{1}$. Chiaramente ce ne sono solo 2 su $\mathcal{G}(2,n)$, si veda la Figura 2.38.

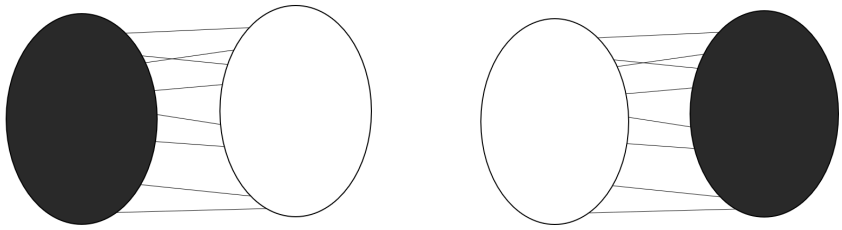

Figura 2.38 – Le due configurazioni miste $\pm\mathbf{1}$ e $\mp\mathbf{1}$, dove rappresentiamo in bianco (risp. nero) gli spin -1 (risp. $+1$).

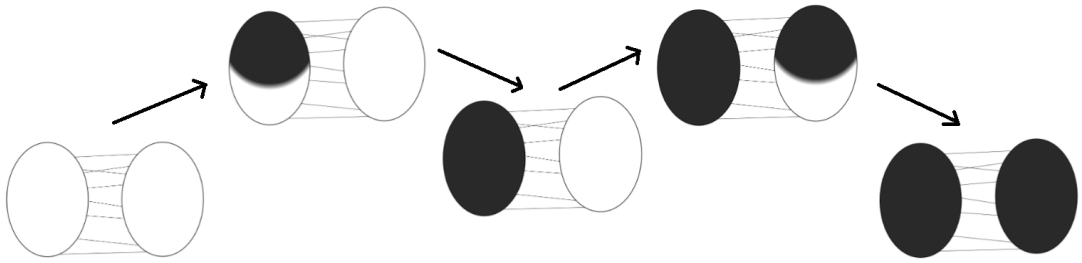

Figura 2.39 – Raffiguriamo il cammino di riferimento $\bar{\omega}$ rappresentando le selle e gli stati metastabili e stabili che attraversa, dove indichiamo in bianco (risp. nero) gli spin -1 (risp. $+1$).

TEOREMI PRINCIPALI: CASO $h = 0$

Qui ci concentriamo sul caso $h = 0$, cioè non c'è campo magnetico esterno. Il primo risultato che forniamo è l'identificazione degli stati metastabili e stabili. In particolare abbiamo che l'insieme degli stati stabili è

$$\mathcal{X}^s = \begin{cases} \{+\mathbf{1}, -\mathbf{1}\} & \text{se } \varepsilon > 0, \\ \{+\mathbf{1}, -\mathbf{1}, \pm\mathbf{1}, \mp\mathbf{1}\} & \text{se } \varepsilon = 0, \\ \{\pm\mathbf{1}, \mp\mathbf{1}\} & \text{se } \varepsilon < 0, \end{cases} \tag{2.4.6}$$

e l'insieme degli stati metastabili è

$$\mathcal{X}^m = \begin{cases} \{\pm\mathbf{1}, \mp\mathbf{1}\} & \text{se } \varepsilon > 0, \\ \{+\mathbf{1}, -\mathbf{1}\} & \text{se } \varepsilon < 0. \end{cases} \tag{2.4.7}$$

Alla luce di ciò è chiaro che il fenomeno interessante da considerare è la *transizione di tunneling*, cioè la transizione tra due stati stabili. A causa della simmetria del sistema si può congetturare che il varco $\mathcal{C}^*$ per questa transizione è composto da due tipi di configurazioni. Il primo corrisponde all'avere $\frac{n}{2}$ spin $+1$ in uno dei due cluster, 0 spin $+1$ nell'altro cluster e 0 spin incrociati concordi tra gli spin $+1$ nei due cluster. Il secondo corrisponde all'avere $\frac{n}{2}$ spin $+1$ in uno dei due cluster, n spin $+1$ nell'altro cluster e $\frac{n}{2}$ lati incrociati concordi tra gli spin $+1$ nei due cluster. Notiamo che se n è dispari, $\frac{n}{2}$ dovrebbe essere sostituito da $\frac{n+1}{2}$ o $\frac{n-1}{2}$ a seconda che $\varepsilon \geqslant 0$ o $\varepsilon < 0$. Deduciamo quindi che il sistema esegue la transizione tra i due stati stabili in un tempo di ordine $e^{\Gamma^*\beta}$ nel limite di $\beta \to \infty$, dove Γ^* è l'energia delle configurazioni critiche e può essere espresso in modo esplicito in termini di n e ε. Indichiamo con s_1 lo stato stabile di partenza e con s_2 lo stato stabile finale. Come abbiamo visto nella Sezione 2.3.3, gli ingredienti fondamentali sono i seguenti:

(i) Dimostrare che $\Phi(s_1, s_2) \leqslant \Gamma^*$.
(ii) Dimostrare che $\Phi(s_1, s_2) \geqslant \Gamma^*$.
(iii) Dimostrare che ogni $\omega \in (s_1 \to s_2)_{opt}$ attraversa l'insieme $\mathcal{C}^*$.

Per il punto (i) è sufficiente costruire un cammino di riferimento che collega s_1 e s_2 e che non supera il valore energetico Γ^*. Se $\varepsilon \geqslant 0$ definiamo un cammino di riferimento $\bar{\omega}$ da $-\mathbf{1}$ a

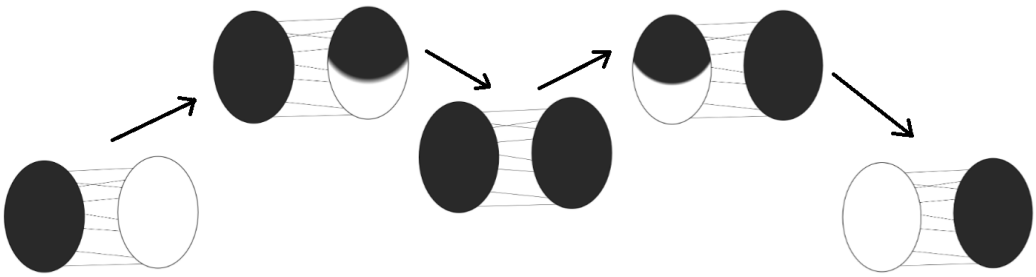

Figura 2.40 – Raffiguriamo il cammino di riferimento $\hat{\omega}$ rappresentando le selle e gli stati metastabili e stabili che attraversa, dove indichiamo in bianco (risp. nero) gli spin -1 (risp. $+1$).

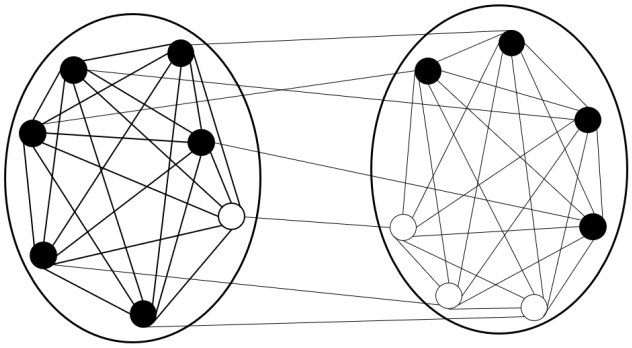

Figura 2.41 – Esempio di una configurazione σ sulla rete $\mathcal{G}(2,7)$ che appartiene alla varietà $\mathcal{C}(10)$, poichè ha $p = 10$ spin $+1$, nello specifico $p_1 = 6$ nel primo cluster e $p_2 = 4$ nel secondo cluster (gli spin $+1/-1$ sono colorati rispettivamente in nero/bianco).

$+\mathbf{1}$, mentre se $\varepsilon < 0$ definiamo un cammino $\hat{\omega}$ da $\pm\mathbf{1}$ a $\mp\mathbf{1}$. A parole, questi percorsi sono costruiti nel modo seguente. Il cammino $\bar{\omega}$, che parte da $-\mathbf{1}$, consiste nel cambiare uno ad uno gli spin -1 in una comunità finché il cammino non raggiunge $\pm\mathbf{1}$ o $\mp\mathbf{1}$ e successivamente gli spin -1 rimanenti vengono cambiati uno ad uno finché il cammino raggiunge $+\mathbf{1}$ (si veda la Figura 2.39). La costruzione del cammino $\hat{\omega}$ è fatto in modo simile (si veda la Figura 2.40).

Ancora una volta, i punti (ii) e (iii) possono essere dimostrati tramite un argomento di tipo disuguaglianza isoperimetrica. L'idea è di partizionare lo spazio degli stati in sottoinsiemi $\mathcal{C}(p)$ di configurazioni aventi precisamente p spin $+1$, si veda la Figura 2.41 per un esempio, e caratterizzare quelle configurazioni che minimizzano l'energia quando p è fissato. Rimandiamo al Capitolo 8 per tutti i dettagli.

TEOREMI PRINCIPALI: CASO $h > 0$

Ci concentriamo qui sul caso $h > 0$, che descrive la situazione in cui c'è un campo magnetico esterno positivo che favorisce gli spin $+1$. Assumiamo inoltre che $0 < h \leqslant 1$ per evitare che il contributo energetico del campo magnetico esterno prevalga sulle energie di legame associate ai lati interni. Come sarà chiaro in seguito, il comportamento dinamico del sistema è diverso nei due casi $0 < h \leqslant |\varepsilon| \leqslant 1$ e $0 \leqslant |\varepsilon| < h \leqslant 1$, specialmente quando $\varepsilon < 0$. Questo corrisponde, infatti, ad una diversa "importanza" data ai lati incrociati e al campo magnetico esterno. Abbiamo che l'insieme degli stati stabili è

$$\mathcal{X}^s = \begin{cases} \{+\mathbf{1}\} & \text{se } 0 \leqslant \varepsilon \leqslant 1 \text{ o } 0 < -\varepsilon < h \leqslant 1, \\ \{+\mathbf{1}, \pm\mathbf{1}, \mp\mathbf{1}\} & \text{se } h = -\varepsilon, \\ \{\pm\mathbf{1}, \mp\mathbf{1}\} & \text{se } 0 < h < -\varepsilon \leqslant 1, \end{cases} \tag{2.4.8}$$

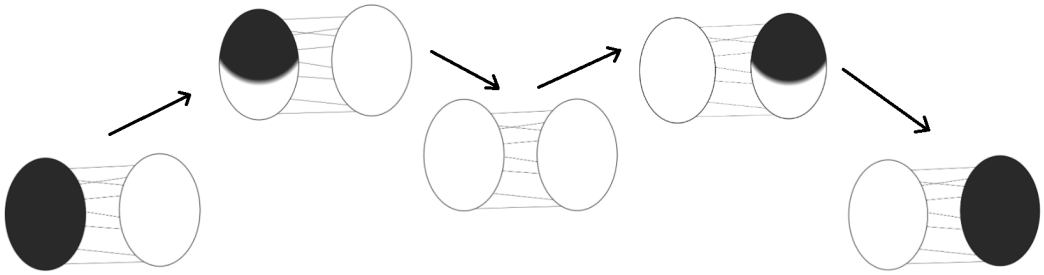

Figura 2.42 – Raffiguriamo il cammino di riferimento $\check{\omega}$ rappresentando le selle e gli stati metastabili e stabili che attraversa, dove indichiamo in bianco (risp. nero) gli spin -1 (risp. $+1$).

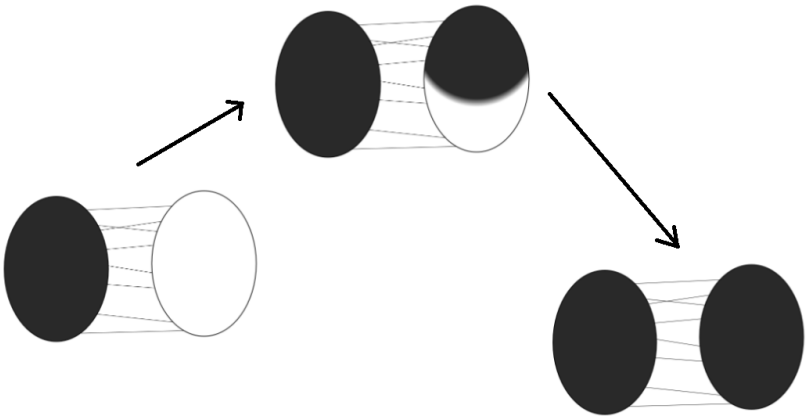

Figura 2.43 – Raffiguriamo il cammino di riferimento $\tilde{\omega}$ rappresentando le selle e gli stati metastabili e stabili che attraversa, dove indichiamo in bianco (risp. nero) gli spin -1 (risp. $+1$).

e l'insieme degli stati metastabili è

$$\mathcal{X}^m = \begin{cases} \{-\mathbf{1}\} & \text{se } 0 \leqslant \varepsilon \leqslant 1 \text{ o } h = -\varepsilon, \\ \{\pm\mathbf{1}, \mp\mathbf{1}\} & \text{se } 0 < -\varepsilon < h \leqslant 1, \\ \{+\mathbf{1}\} & \text{se } 0 < h < -\varepsilon \leqslant 1. \end{cases} \tag{2.4.9}$$

Il nostro interesse è pertanto quello di indagare il comportamento asintotico per $\beta \to \infty$ del tempo di tunneling (risp. tempo di transizione allo stato stabile) del sistema che parte dallo stato stabile s_1 (risp. stato metastabile m) per raggiungere per la prima volta l'altro stato stabile s_2 (risp. lo stato stabile s) se $0 < h < -\varepsilon \leqslant 1$ (risp. se $0 \leqslant \varepsilon \leqslant 1$ o $0 < -\varepsilon < h \leqslant 1$). Come prima, la strategia per caratterizzare il varco e stimare il tempo di transizione è dimostrare la versione corrispondente dei punti precedenti (i)–(iii). Qui discutiamo soltanto il punto (i) esibendo i cammini di riferimento, mentre ci riferiamo al Capitolo 8 per tutti i dettagli relativi ai punti (ii) e (iii). Se $\varepsilon \geqslant 0$, consideriamo il cammino $\bar{\omega}$ rappresentato in Figura 2.39. Se $0 < h < -\varepsilon \leqslant 1$, definiamo $\check{\omega} : \pm\mathbf{1} \to \mp\mathbf{1}$ come il cammino rappresentato in Figura 2.42. Se $0 < -\varepsilon < h \leqslant 1$, definiamo $\tilde{\omega} : \pm\mathbf{1} \to +\mathbf{1}$ come il cammino rappresentato in Figura 2.43.

In questa tesi abbiamo indagato le dinamiche di opinione all'interno di una comunità di individui attraverso l'analisi della metastabilità per il modello di Ising sul grafo $\mathcal{G}(2, n)$. A seconda dei diversi parametri ε e h abbiamo mostrato che gli stati stabili e metastabili del sistema sono diversi. Quindi, a seconda dei diversi scenari, abbiamo utilizzato la struttura dell'approccio traiettoriale [85, 92] per analizzare il tempo di transizione o di tunneling, rispettivamente, e per descrivere le configurazioni critiche. Inoltre, abbiamo dimostrato che la presenza di un campo magnetico esterno positivo, che può essere interpretato come informazioni o influenze esterne, rende la situazione molto più ricca, soprattutto nel caso $\varepsilon < 0$ in cui le comunità tendono ad avere opinioni divergenti. Più specificamente, l'insieme

degli stati stabili è completamente diverso a seconda del ruolo dato alle informazioni esterne per quanto riguarda l'influenza tra le comunità, vale a dire, a seconda che $h < -\varepsilon$ o meno. Questo modello è il nostro primo tentativo di analisi della diffusione di un'opinione all'interno di due comunità. In primo luogo, l'estensione a un numero generale k di comunità nasce naturalmente in questo contesto e sarà al centro del lavoro futuro, unitamente al calcolo del prefattore per il tempo medio di transizione. Questo rappresenta un compito impegnativo nel caso $k > 2$, perché bisogna tener conto di tutti i meccanismi di diffusione della nuova opinione tra le diverse comunità. Inoltre, si possono considerare i modelli con più di due opinioni (modello di Potts) o con diverse forze di interazione tra le comunità. Crediamo che la dinamica di opinione all'interno di una popolazione di individui con una topologia di rete non banale sia un argomento di grande interesse con molte direzioni interessanti da esplorare ulteriormente in futuri lavori di ricerca.

2.5 GRAFI ALEATORI AD ATTACCAMENTO PREFERENZIALE

In questa sezione ci concentriamo sull'analisi del comportamento asintotico dei grafi aleatori ad attaccamento preferenziale. La crescita senza precedenti in termini di dimensioni e complessità delle reti sociali ed economiche negli ultimi due decenni ha suscitato un notevole interesse per la comprensione delle proprietà fondamentali di tali reti. In questo contesto, il modello ad attaccamento preferenziale (PA), introdotto in [19], è un noto modello di rete che cresce nel tempo. Più precisamente, il modello PA è costituito da una sequenza di grafi di dimensione crescenti tale che ogni grafo è ottenuto dal precedente secondo una determinata regola probabilistica. Ad ogni passo un nuovo vertice viene aggiunto e forma connessioni con i vertici nel grafo in modo tale che le connessioni con vertici con gradi maggiori siano più probabili. Qui consideriamo il modello PA senza cappi descritto ad esempio in [59]. In particolare, ogni grafo della sequenza è connesso.

In letteratura compaiono diversi modelli di PA, a seconda dei dettagli concreti del meccanismo di attaccamento. Ad esempio, in [30, 58, 104, 113, 115] gli autori indagano un modello PA *diretto*, mentre in [23, 50, 58, 59, 88, 103] si considera una versione *indiretta*. Tuttavia, le reti PA classiche non sempre si adattano bene ai dati delle reti del mondo reale, o in molte applicazioni è naturale assegnare alcuni tipi di caratteristiche ai vertici o ai lati. Ciò ha portato a prendere in considerazione alcune estensioni del modello PA classico. Ad esempio, in [7] gli autori considerano una famiglia generale di modelli ad attaccamento preferenziale con bordi multitipo, mentre [5, 84, 98] indagano un modello PA che mescola le regole PA con regole di attaccamento uniformi. In questo lavoro consideriamo il modello PA senza cappi descritto in [59]. Facciamo questa scelta per semplificare i calcoli, ma crediamo che il nostro risultato valga anche, ad esempio, per il modello PA con cappi considerato nella referenza [69, Capitolo 8]. Discuteremo di questo più in dettaglio in seguito. Si vedano le Figure 2.44 e 2.45 per esempi di tali grafi aleatori con cappi, dove ogni nuovo nodo ha un numero fisso $m \in \mathbb{N}$ di lati attaccati ad esso e δ è un parametro del modello (si veda (2.5.1) per la definizione precisa). Questo è un caso particolare del modello considerato in [59], dove m è una variabile aleatoria ed è campionato per ogni nuovo nodo.

Il nostro risultato principale è un teorema del limite centrale per la proporzione di nodi con un dato grado. Infatti, dimostriamo questo *congiuntamente* per tutti i conteggi dei gradi. Diamo in particolare un'espressione esplicita per la covarianza asintotica. I primi risultati riguardanti lo studio della normalità asintotica dei conteggi dei gradi nei modelli ad attaccamento preferenziale senza cappi sono dati in [88] usando teoremi del limite centrale per martingale. I nostri risultati generalizzano quelli ottenuti in [103] per l'albero ad attaccamento preferenziale. Più precisamente, in [103] gli autori considerano un modello PA con cappi e tale che $m = 1$. Noi invece consideriamo il modello PA con $m \geqslant 1$ e senza cappi. Tuttavia, questo non influisce il comportamento asintotico dei conteggi dei gradi, poiché quando la dimensione del grafo va all'infinito, la probabilità che un nuovo vertice formi un cappio tende a zero. Per questo ci si aspetterebbe di ritrovare i risultati in [103] quando inseriamo $m = 1$ nel nostro risultato. In effetti questo è il caso se si tiene conto di qualche piccolo errore in [103] di cui parleremo più avanti. Si noti che una grande differenza tra i due modelli è la struttura di connettività risultante. Il nostro modello produce un grafo connesso con probabilità 1 (w.p. 1), mentre il modello in [103] è disconnesso w.p. 1. Questo non ha tuttavia un ruolo nella

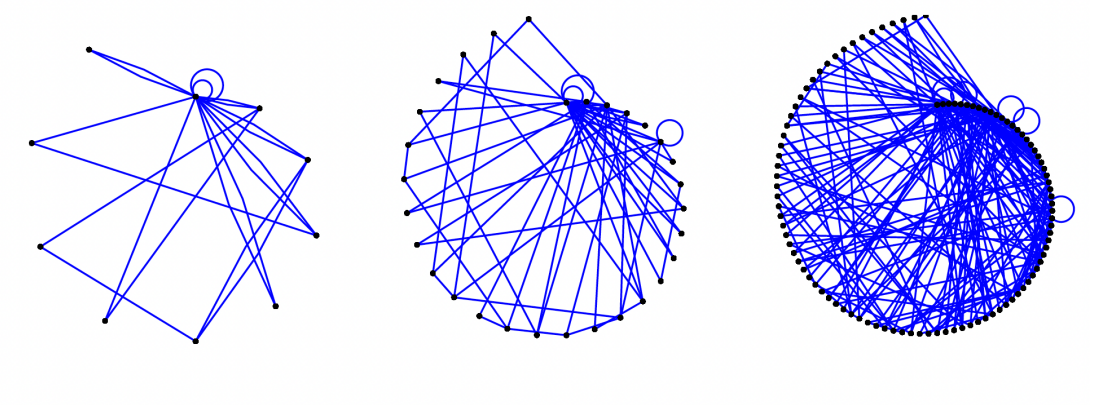

Figura 2.44 – Grafo aleatorio ad attaccamento preferenziale con $m = 2$ e $\delta = 0$ di taglia 10, 30 e 100. Figura presa da [69].

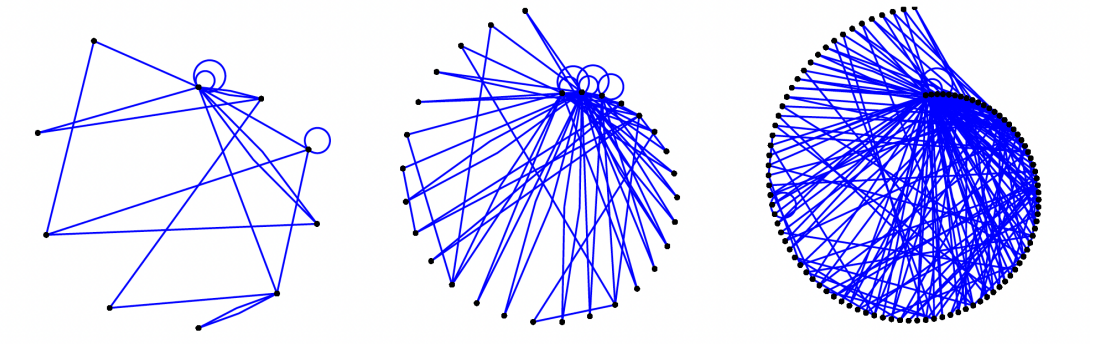

Figura 2.45 – Grafo aleatorio ad attaccamento preferenziale con $m = 2$ e $\delta = -1$ di taglia 10, 30 e 100. Figura presa da [69].

distribuzione dei conteggi dei gradi. In [99] gli autori hanno studiato i conteggi dei gradi congiunti in grafi aleatori ad attaccamento preferenziale lineare. I risultati sono espressi in termini di peso dei vertici, ma possono essere considerati come grado, poiché ogni volta che un vertice riceve un nuovo lato, il suo peso aumenta di uno. La principale differenza tra il nostro ed il loro modello è che noi consideriamo le probabilità di attaccamento proporzionale ad una funzione lineare del grado di un vecchio vertice (si veda (2.5.1)), mentre in [99] sono proporzionali al grado di un vecchio vertice.

In pratica nelle reti del mondo reale non tutti i nodi che entrano nella rete hanno lo stesso grado, e quindi sarebbe interessante estendere il nostro risultato nel caso di una distribuzione aleatoria dei gradi iniziali. Risultati promettenti su questo modello sono stati ottenuti in [54, 59]. In questa tesi assumiamo, inoltre, che i parametri del modello siano noti, ma in molte situazioni pratiche si ha a disposizione una realizzazione del grafo ed il compito sta nella stima dei parametri sconosciuti, si veda [60, 101, 112]. Se consideriamo una classe più generale di grafi ad attaccamento preferenziale, per cui un approccio "senza modello" viene utilizzato e quindi la distribuzione esatta del grafo non è nota (si veda ad esempio [81]), ci aspettiamo che le tecniche presentate in questo lavoro possano essere usate per derivare il teorema del limite centrale per tutti i conteggi dei gradi. Questo è un interessante problema aperto.

Descriviamo ora in dettaglio il modello di grafo aleatorio che consideriamo. Fissiamo una volta per tutte un intero $m \geqslant 1$. Formalmente, il modello ad attaccamento preferenziale è una successione di grafi aleatori $(PA_s)_{s=1}^t$. L'indice s viene interpretato come un parametro temporale. All'istante s il grafo PA_s ha un insieme $V = \{0, 1, ..., s\}$ di $s+1$ vertici. Per $s = 1$, il grafo PA_1 è composto dai vertici 0 e 1, collegati da m archi. Per $s \geqslant 2$, il grafo PA_s è ottenuto da PA_{s-1} aggiungendo un nuovo vertice s di grado m come segue. Definiamo $PA_{s,0} = PA_{s-1}$ e $PA_{s,1}$,...,$PA_{s,m}$ come i grafi intermedi ottenuti aggiungendo un nuovo lato in sequenza a $PA_{s,0}$. Per $i = 1, ..., m$, $PA_{s,i}$ si ottiene da $PA_{s,i-1}$ disegnando un lato da s ad un vertice

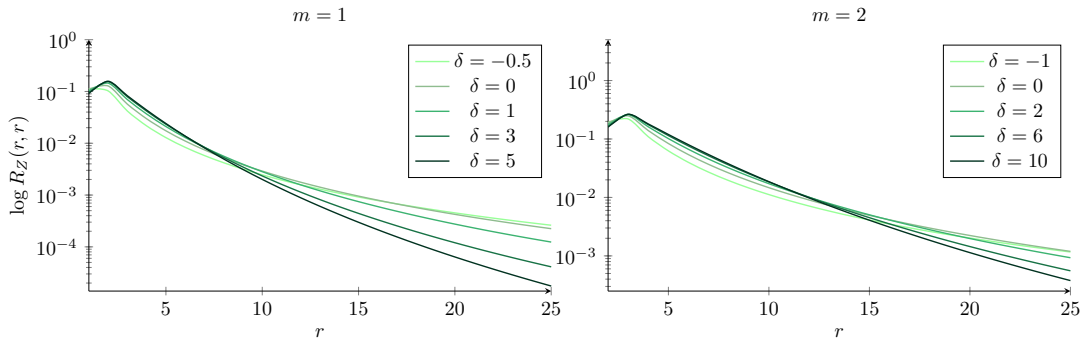

Figura 2.46 – $R_Z(r,r)$ per $m = 1$ e $\delta = -0.5, 0, 1, 3, 5$ sulla sinistra e $R_Z(r,r)$ per $m = 2$ e $\delta = -1, 0, 2, 6, 10$ sulla destra. Per evidenziare il comportamento differente delle diverse funzioni di varianza usiamo la scala logaritmica sull'asse y.

scelto a caso tra $\{0, 1, ..., s-1\}$. La probabilità che un vertice s sia connesso a qualche vertice i è proporzionale al grado di i. In altre parole, vertici con gradi grandi hanno maggiore probabilità di attrarre nuovi lati. Indichiamo con $N_k(s,i)$ per $i = 1, ..., m$ il numero di vertici di grado k dopo che l'i-esimo lato è stato attaccato al tempo s, escluso il vertice s. Poniamo $N_k(s+1,0) := N_k(s,m)$. Inoltre, indichiamo con $D_{s,i}$ il grado del vertice che è stato attaccato al lato i–esimo aggiunto durante la costruzione di PA_s da PA_{s-1}. Consideriamo ora la σ-algebra $\mathcal{F}_{s,i}$ generata dalla costruzione ad attaccamento preferenziale fino all'attaccamento dell'i-esimo lato del nuovo vertice al tempo s. La probabilità condizionata che l'arco i-esimo si colleghi ad un vertice di grado $D_{s,i}$ è

$$\mathbb{P}(D_{s,i} = k | \mathcal{F}_{s,i-1}) = \frac{(k+\delta)N_k(s,i-1)}{\sum_j (j+\delta)N_j(s,i-1)}, \tag{2.5.1}$$

dove $\delta > -m$ è un parametro affine. La costante di normalizzazione in (2.5.1) assume la forma semplice [59]

$$\sum_{j=1}^{\infty} (j+\delta)N_j(s,i-1) = s(2m+\delta) - 2m + i - 1. \tag{2.5.2}$$

Per il modello PA standard considerato in [69, Capitolo 8] si dimostra che esiste una funzione di probabilità di massa $\{p_k,\ k \geqslant m\}$ tale che, uniformemente in $i \in \{0, ..., m\}$,

$$\lim_{s\to\infty} \frac{N_k(s,i)}{s} = p_k \in (0,1), \tag{2.5.3}$$

quasi certamente, dove p_k è dato da

$$p_k = (2 + \delta/m)\frac{\Gamma(k+\delta)\Gamma(m+2+\delta+\delta/m)}{\Gamma(m+\delta)\Gamma(k+3+\delta+\delta/m)}. \tag{2.5.4}$$

Qui $\Gamma(\cdot)$ rappresenta la funzione Gamma. Quando la dimensione del grafo va all'infinito, la probabilità che un nuovo vertice formi un cappio tende a zero e quindi è facile verificare che (2.5.3) e (2.5.4) valgono ancora per il nostro modello senza cappi seguendo la dimostrazione proposta in [69, Sezione 8.6].

Per enunciare il nostro risultato principale abbiamo bisogno di qualche ulteriore notazione. Diciamo che gli eventi $(A_n)_n$ valgono con alta probabilità quando $P(A_n) \to 1$ per $n \to \infty$. Dato un vettore aleatorio $(X_1^{(n)}, X_2^{(n)}, ...)$, scriviamo $(X_1^{(n)}, X_2^{(n)}, ...) \Rightarrow (X_1, X_2, ...)$ per indicare che per ogni $k \in \mathbb{N}$, $(X_1^{(n)}, X_2^{(n)}, ..., X_k^{(n)})$ converge a $(X_1, X_2, ..., X_k)$ in distribuzione come vettori in $\mathbb{R}^n$ per $n \to \infty$. Il nostro risultato principale è il seguente. Per $s \to \infty$, dimostriamo che

$$\left(\sqrt{s}\left(\frac{N_k(s,i)}{s} - p_k\right),\ k = m, m+1, ...\right) \Rightarrow (Z_k, \kappa = m, m+1, ...), \tag{2.5.5}$$

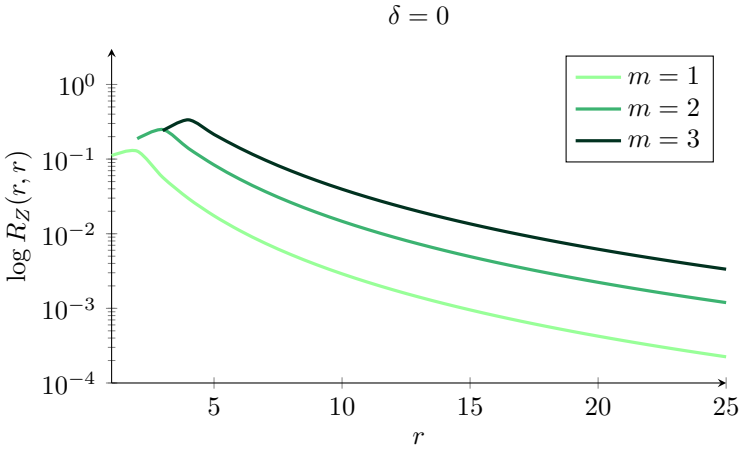

Figura 2.47 – $R_Z(r, r)$ per $\delta = 0$ e $m = 1, 2, 3$. Per evidenziare il comportamento differente delle diverse funzioni di varianza usiamo la scala logaritmica sull'asse y.

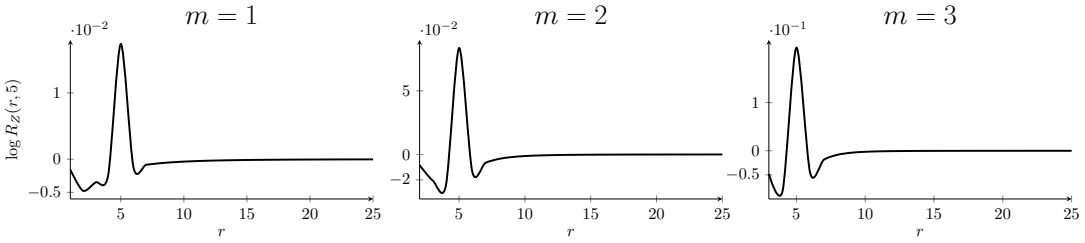

Figura 2.48 – $R_Z(r, 5)$ per $\delta = 0$ e $m = 1, 2, 3$.

dove $(Z_k,\ k = m, m+1, ...)$ è un processo gaussiano con media nulla e funzione di covarianza R_Z data da (9.1.2). La dimostrazione si basa sull'attenta costruzione di un'apposita martingala.

Poiché l'espressione in (9.1.2) è notevolmente complicata, qui non la riportiamo e ci riferiamo al Capitolo 9 per la formula esplicita. Per aiutare la comprensione ne raffiguriamo l'andamento per varie scelte dei parametri. In Figura 2.46 rappresentiamo la funzione $r \mapsto R_Z(r, r)$ per $m = 1$ (risp. $m = 2$) fissato e vari valori di δ. In Figura 2.47 rappresentiamo la funzione $R_Z(r, r)$ per $\delta = 0$ fissato e vari valori di m. In Figura 2.48 tracciamo la funzione $R_Z(r, 5)$ per $\delta = 0$ e $m = 1, 2, 3, 4$. Infine, in Figura 2.49 sul lato sinistro confrontiamo la funzione di covarianza asintotica $R_Z(r, r)$ per $m = 1, \delta = 1$ fissati con la varianza empirica ottenuta dalle simulazioni numeriche del modello PA fino al tempo $t = 100, 1000, 5000$. Inoltre, in Figura 2.49 sul lato destro, confrontiamo la funzione di covarianza asintotica $R_Z(r, 5)$ per $m = 2, \delta = 0$ fissati con la covarianza empirica ottenuta dalle simulazioni numeriche del modello PA fino al tempo $t = 100, 1000, 5000$. Anche se non abbiamo risultati rigorosi sulla velocità di convergenza dei conteggi riscalati dei vertici, Figura 2.49 suggerisce che la convergenza è in effetti abbastanza veloce.

Osservazione 2.5.1. *Come spiegato in [69, Capitolo 8], è possibile definire il modello ad attaccamento preferenziale con $m > 1$ in termini del modello con $m = 1$ collassando i vertici, quindi si potrebbe essere tentati di applicare direttamente questa costruzione ai risultati derivati in [103] per il modello con $m = 1$. Questo è un possibile approccio che presenta le sue difficoltà e ora proviamo a evidenziarle. Il teorema del limite centrale che vogliamo dimostrare coinvolge il numero di vertici con un grado fisso, quindi abbiamo bisogno di trovare una relazione tra quella quantità per il modello $m > 1$ e $m = 1$ per utilizzare il risultato ottenuto in [103]. Questo non è semplice, infatti è richiesto un controllo dettagliato sulla costruzione del grafo ad ogni passo.*

Osservazione 2.5.2. *Qui scegliamo di aggiornare i gradi durante l'attaccamento di un nuovo vertice, ma è possibile considerare anche il caso in cui aggiorniamo i gradi dei vertici solo quando viene aggiunto il lato m-esimo. In questo caso, dopo aver costruito una martingala adatta rispetto alla filtrazione $(\mathcal{F}_s)_{s \geqslant 1}$ generata dalla costruzione del grafo ad attaccamento preferenziale fino al tempo s, è possibile*

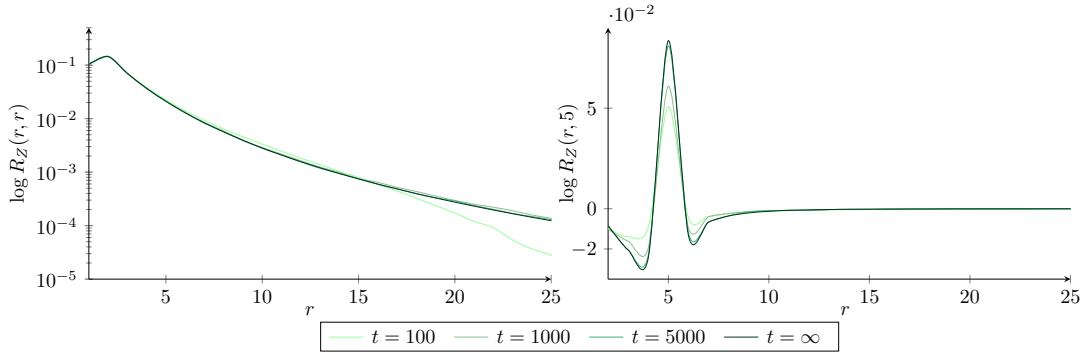

Figura 2.49 – Sulla sinistra rappresentiamo la funzione $R_Z(r,r)$ per $\delta = 1$ e $m = 1$ ($t = \infty$) confrontata con le simulazioni numeriche interrotte al tempo $t = 100, 1000, 5000$. Ciascuna curva empirica è stata ottenuta prendendo una media di $N = 10000$ simulazioni. Sulla destra rappresentiamo la funzione $R_Z(r,5)$ per $\delta = 0$ e $m = 2$ ($t = \infty$) confrontata con le simulazioni numeriche interrotte al tempo $t = 100, 1000, 5000$. Ciascuna curva empirica è stata ottenuta prendendo una media di $N = 10000$ simulazioni. Per evidenziare il comportamento differente delle diverse funzioni di varianza usiamo la scala logaritmica sull'asse y.

riprodurre gli stessi calcoli. Siamo quindi in grado di dimostrare un risultato simile per questo modello utilizzando le tecniche qui presentate.

Seguendo l'argomentazione svolta in [88], siamo in grado di dimostrare un teorema del limite centrale per il vettore composto dal numero riscalato di vertici con grado maggiore di k. In questo caso la matrice di covarianza della legge limite normale diventa semplice ed ora lo calcoliamo. Definiamo il numero di vertici con grado maggiore di k come

$$\psi_k(s,i) := \sum_{j \geqslant k} N_j(s,i) \tag{2.5.6}$$

e

$$\psi(s,i) := (\psi_m(s,i), \psi_{m+1}(s,i), \ldots). \tag{2.5.7}$$

Osserviamo che possiamo scrivere

$$\begin{aligned} &\psi(1,i) = (0,\ldots,0), \\ &\psi(s,i+1) = \psi(s,i) + \delta_{D_{s,i}}, \end{aligned} \tag{2.5.8}$$

dove $\delta_{D_{s,i}}$ è il vettore con tutte le coordinate uguali a 0 tranne il $D_{s,i}$-esimo, che è uguale a 1. Da (2.5.3) segue che le differenze del processo a valori vettoriali $\{\psi(s,i),\ s \geqslant 1,\ i = 1,\ldots,m\}$ diventa sempre più indipendente e identicamente distribuito nel limite di $s \to \infty$. Sia $\pi_k(s,i) := \mathbb{P}(D_{s,i} = k | \mathcal{F}_{s,i-1})$ e

$$\pi_k := \lim_{s\to\infty} \pi_k(s,i) = \frac{k+\delta}{2m+\delta} p_k. \tag{2.5.9}$$

Quindi, quand $s \to \infty$, è vero che

$$\left(\sqrt{s}\Big(\frac{\psi_k(s,i)}{s} - \pi_k \Big),\ k = m, m+1, \ldots \right) \Rightarrow (Z_k,\ k = m, m+1, \ldots), \tag{2.5.10}$$

dove $(Z_k,\ k = m, m+1, \ldots)$ è un processo gaussiano con media nulla e matrice di covarianza $V = (v_{r\ell})_{k\times k}$ data dal limite della dimensione minore in alto a sinistra $i \times i$ della matrice di covarianza condizionale infinita $\mathrm{Var}(\delta_{D_{s,i}} | \mathcal{F}_{s,i-1})$, cioè

$$\begin{aligned} v_{rr} &= \pi_r(1-\pi_r) = \frac{(r+\delta)p_r(2m+\delta-(r+\delta)p_r)}{(2m+\delta)^2}, \\ v_{r\ell} &= -\pi_r\pi_\ell = -\frac{(r+\delta)(\ell+\delta)}{(2m+\delta)^2} p_r p_\ell,\ r \neq \ell. \end{aligned} \tag{2.5.11}$$

2.6 SCHEMA DELLA TESI

Questa tesi è organizzata come segue. I Capitoli 3-7 sono dedicati allo studio della dinamica metastabile conservativa di Kawasaki, mentre il Capitolo 8 allo studio della dinamica metastabile non conservativa di Glauber. Infine, nel Capitolo 9 studiamo le proprietà asintotiche del modello ad attaccamento preferenziale. Più precisamente, il contenuto di ciascun capitolo è il seguente.

Nel Capitolo 3, il nostro obiettivo primario è fornire la descrizione geometrica dell'unione di tutti i varchi minimali $\mathcal{G}(\square, \blacksquare)$ nel caso isotropo. Dimostreremo che ci sono molti varchi minimali distinti, che caratterizzeremo geometricamente insieme alla loro unione. A tal fine diamo prima una *strategia indipendente dal modello* utile ad eliminare alcune selle non essenziali, cioè quelle che non sono essenziali per la caratterizzazione dell'insieme $\mathcal{G}(m, \mathcal{X}^s)$, dove m è l'unico stato metastabile e $\mathcal{X}^s$ è l'insieme degli stati stabili. Applichiamo quindi questa strategia al modello isotropo bidimensionale che evolve sotto la dinamica di Kawasaki, dove $m = \square$ e $\mathcal{X}^s = \{\blacksquare\}$. Per fare questo dobbiamo verificare che gli input dipendenti dal modello richiesti sono validi per il nostro modello. Questo studio, insieme alla caratterizzazione delle selle essenziali, si basa su un'analisi dettagliata del moto delle particelle lungo il bordo delle gocce, che è una caratteristica tipica della dinamica di Kawasaki. Indaghiamo inoltre il gap spettrale ed il tempo di mescolamento del processo. Concludiamo questo capitolo fornendo alcuni risultati indipendenti dal modello relativi alle stime asintotiche forti del tempo medio di transizione, che chiariscono il ruolo delle selle non essenziali nel calcolo del prefattore. Il contenuto di questo capitolo si basa sull'articolo pubblicato [18] e sulla sua versione estesa [15].

Nel Capitolo 4 caratterizziamo geometricamente l'insieme $\mathcal{G}(\square, \blacksquare)$ nel caso debolmente anisotropo. Lo facciamo grazie alla strategia indipendente dal modello introdotta nel capitolo 3 e all'analisi specifica della dinamica del sistema. Indaghiamo inoltre il gap spettrale ed il tempo di miscelazione del processo. Concludiamo questo capitolo fornendo stime asintotiche forti del tempo medio di transizione e della distribuzione uniforme dell'ingresso nel varco. Il contenuto di questo capitolo si basa su l'articolo pubblicato [18] e la sua versione estesa [15].

Il Capitolo 5 è dedicato alla descrizione geometrica dell'insieme $\mathcal{G}(\square, \blacksquare)$ nel regime fortemente anisotropo. Dimostreremo che ci sono molti varchi minimali distinti che caratterizzeremo geometricamente insieme alla loro unione. Applichiamo la strategia introdotta nel Capitolo 3 a questo modello per eliminare alcune selle non essenziali. Dobbiamo quindi verificare che gli input dipendenti dal modello richiesti sono validi nel nostro caso. Questo studio, insieme alla caratterizzazione delle selle essenziali, si basa su un'analisi dettagliata del moto delle particelle lungo il bordo delle gocce. Da un lato questa è una caratteristica tipica della dinamica di Kawasaki, dall'altro questa è una caratteristica peculiare del caso fortemente anisotropo. Forniamo inoltre stime asintotiche forti del tempo medio di transizione ed indaghiamo il gap spettrale ed il tempo di mescolamento. Questo capitolo è basato su [17].

Nel Capitolo 6 studiamo la dinamica locale di Kawasaki sul reticolo esagonale con interazioni isotrope. In particolare, indaghiamo le configurazioni critiche ed il tempo di transizione tra $\hexagon$ (esagono vuoto) e $\hexagonblack$ (esagono pieno) per questo modello. I nostri principali risultati sono i seguenti. Identifichiamo innanzitutto gli stati metastabili e stabili e dimostriamo una convergenza in probabilità, valore atteso e legge per il tempo di transizione, rispondendo alla prima domanda della metastabilità. Dimostriamo, quindi, che il sistema raggiunge con alta probabilità lo stato $\hexagon$ o $\hexagonblack$ in un tempo più breve di $e^{\beta(V^*+\varepsilon)}$, uniformemente nella configurazione di partenza per ogni $\varepsilon > 0$, dove $V^* = \Delta + U$. In altre parole, la dinamica accelerata di un fattore di ordine $e^{\beta V^*}$ raggiunge con alta probabilità $\{\hexagon, \hexagonblack\}$. Forniamo infine una caratterizzazione di un varco per la transizione, rispondendo al secondo problema della metastabilità. Sottolineiamo che questo risultato riflette come il reticolo sottostante sia fondamentale per la dinamica del sistema. Questo capitolo è basato su [13].

Nel Capitolo 7 consideriamo il modello completamente conservativo sul reticolo quadrato bidimensionale. Useremo i risultati di [62] per analizzare come le gocce sottocritiche si formano e si dissolvono su scale spazio-temporali multiple quando il volume è moderatamente grande, cioè quando la scatola ha volume $e^{\Theta\beta}$, con $\Delta < \Theta < 2\Delta - U$. Poiché la dinamica è conservativa, dobbiamo controllare gli effetti non locali nel modo in cui le gocce si formano e si dissolvono. Ciò avviene tramite un *approccio assiomatico*: il tubo delle traiettorie tipiche

che portano alla nucleazione è descritto attraverso una serie di eventi, i cui complementari hanno probabilità trascurabile, su cui l'evoluzione del gas è costituita da gocce erranti su scale spazio-temporali multiple in un modo che può essere descritto da una catena di Markov a grana grossa su uno spazio di gocce. Questo capitolo è basato sulla prestampa [11].

Nel Capitolo 8 analizziamo il modello di Ising su una specifica famiglia di reti clusterizzate, identificando l'insieme degli stati metastabili e stabili e stimando il comportamento asintotico del tempo di transizione tra di loro nel limite di bassa temperatura. Nel contesto della rete clusterizzata che consideriamo in questo capitolo, l'insieme degli stati metastabili dipende fortemente dalla forza relativa delle interazioni tra le comunità della rete e quella del campo magnetico esterno. In assenza di un campo magnetico esterno, le due opinioni sono ugualmente probabili e i due modelli di opinioni omogenee sono entrambi stati stabili. In questo caso è comunque interessante studiare come, iniziando con tutti gli individui che concordano su un'opinione, l'intera rete può passare al parere contrario, quanto tempo ci vorrà e quali sono le traiettorie più probabili di questo processo. Questo capitolo è basato su [10].

Il risultato principale del Capitolo 9 è un teorema del limite centrale per la proporzione di nodi con un dato grado per un modello generale ad attaccamento preferenziale. A tal fine usiamo i teoremi del limite centrale per martingale. Dimostriamo questo *congiuntamente* per tutti i conteggi dei gradi. In particolare, diamo un'espressione esplicita per la covarianza asintotica e usiamo anche simulazioni numeriche per sostenere che la convergenza è abbastanza veloce. La dimostrazione si basa sull'attenta costruzione di un'apposita martingala. Il contenuto di questo capitolo è basato su [9].

Part I

KAWASAKI DYNAMICS: VARIATIONS OF THE LOCALLY CONSERVATIVE MODEL

3

CRITICAL DROPLETS ON THE SQUARE LATTICE: ISOTROPY

This chapter is devoted to the geometrical characterization of the union of all the minimal gates for the local model evolving under Kawasaki dynamics with isotropic interactions, namely, $U_1 = U_2 = U$ in (1.3.11). To this end, we provide a model–independent strategy to identify some unessential saddles, which therefore are not in the minimal gates, and we apply this method to the local isotropic model. We will see how the motion of particles along the border of a cluster plays a crucial role in this analysis and in the isotropic regime this makes a totally explicit geometrical characterization of the minimal gates hard to obtain. Moreover, we investigate the mixing time and spectral gap for this model. Finally, we provide a model–independent discussion about the sharp asymptotics of the mean transition time, in order to clarify the role of the unessential saddles in the computation of the prefactor.

The outline of the chapter is as follows. In Section 3.1 we give some model–independent definitions in order to state our main model-independent results in Propositions 3.1.3 and 3.1.5. In Section 3.2, after giving some geometric definitions valid for Kawasaki dynamics in finite volume (see Section 3.2.1), we state our main results concerning the gates in Section 3.2.2 and concerning the sharp asymptotics in Section 3.2.3. In Section 3.3 we prove the model-independent results that we apply to our model in Section 3.4. In Section 3.5 we give the proof of the main result regarding the identification of the union of all the minimal gates (see Theorem 3.2.7). In Section 3.6 we state and give the proof of the main model–independent theorems about the sharp asymptotics, together with the proof of the asymptotic behaviour of the mixing time and the spectral gap. In Appendix 3.A we give additional explicit proofs and computations.

3.1 MODEL–INDEPENDENT DEFINITIONS AND RESULTS

We will use italic capital letters for subsets of Λ, script capital letters for subsets of $\mathcal{X}$, and boldface capital letters for events under the Kawasaki dynamics. We use this convention in order to keep the various notations apart. We will denote by $\mathbb{P}_{\eta_0}$ the probability law of the Markov process $(\eta_t)_{t\geqslant 0}$ starting at η_0 and by $\mathbb{E}_{\eta_0}$ the corresponding expectation.

3.1.1 *Model–independent definitions*

1. Paths and hitting times.

— A *path* ω is a sequence $\omega = (\omega_1, \dots, \omega_k)$, with $k \in \mathbb{N}$, $\omega_i \in \mathcal{X}$ and $P(\omega_i, \omega_{i+1}) > 0$ for $i = 1, \dots, k-1$. We write $\omega\colon\ \eta \to \eta'$ to denote a path from η to η', namely with $\omega_1 = \eta$, $\omega_k = \eta'$. A set $\mathcal{A} \subset \mathcal{X}$ with $|\mathcal{A}| > 1$ is *connected* if and only if for all $\eta, \eta' \in \mathcal{A}$ there exists a path $\omega : \eta \to \eta'$ such that $\omega_i \in \mathcal{A}$ for all i. We indicate with $\omega_1 \circ \omega_2$ the composition of two paths ω_1 and ω_2, namely if $\omega_1 = (\omega_1^1, ..., \omega_k^1)$ and $\omega_2 = (\omega_1^2, ..., \omega_m^2)$ then $\omega_1 \circ \omega_2 = (\omega_1^1, ..., \omega_k^1, \omega_1^2, ..., \omega_m^2)$.

— Given a non–empty set $\mathcal{A} \subset \mathcal{X}$ and a state $\eta \in \mathcal{X}$, define the *first-hitting time of* $\mathcal{A}$ with initial state η at time $t = 0$ as

$$\tau_{\mathcal{A}}^{\eta} := \min\{t \geqslant 0 : \eta_t \in \mathcal{A} \,|\, \eta_0 = \eta\}. \tag{3.1.1}$$

2. Min-max and communication height

— Given a function $f : \mathcal{X} \to \mathbb{R}$ and a subset $\mathcal{A} \subseteq \mathcal{X}$, we denote by

$$\arg\max_{\mathcal{A}} f := \{\eta \in \mathcal{A} : f(\eta) = \max_{\zeta \in \mathcal{A}} f(\zeta)\} \tag{3.1.2}$$

the set of points where the maximum of f in $\mathcal{A}$ is reached. If $\omega = (\omega_1, ..., \omega_k)$ is a path, in the sequel we will write $\arg\max_{\omega} \widehat{H}$ to indicate $\arg\max_{\mathcal{A}} \widehat{H}$, with $\mathcal{A} = \{\omega_1, ..., \omega_k\}$ and $\widehat{H}$ the Hamiltonian energy.

— The *bottom* $\mathcal{F}(\mathcal{A})$ of a non–empty set $\mathcal{A} \subset \mathcal{X}$ is the set of *global minima* of the Hamiltonian $\widehat{H}$ in $\mathcal{A}$:

$$\mathcal{F}(\mathcal{A}) := \arg\min_{\mathcal{A}} \widehat{H} = \{\eta \in \mathcal{A} : \widehat{H}(\eta) = \min_{\zeta \in \mathcal{A}} \widehat{H}(\zeta)\}. \tag{3.1.3}$$

For a set $\mathcal{A} \subset \mathcal{X}$ such that all the configurations have the same energy, with an abuse of notation we denote this energy by $\widehat{H}(\mathcal{A})$.

— The *communication height* between a pair $\eta, \eta' \in \mathcal{X}$ is

$$\Phi(\eta, \eta') := \min_{\omega : \eta \to \eta'} \max_{\zeta \in \omega} \widehat{H}(\zeta). \tag{3.1.4}$$

Given $\mathcal{A} \subset \mathcal{X}$, we define the *restricted communication height* between $\eta, \eta' \in \mathcal{A}$ as

$$\Phi_{|\mathcal{A}}(\eta, \eta') := \min_{\substack{\omega : \eta \to \eta' \\ \omega \subseteq \mathcal{A}}} \max_{\zeta \in \omega} \widehat{H}(\zeta), \tag{3.1.5}$$

where $(\omega_1, ..., \omega_k) = \omega \subseteq \mathcal{A}$ means $\omega_i \in \mathcal{A}$ for every i.

3. Stability level, stable and metastable states

— We call *stability level* of a state $\zeta \in \mathcal{X}$ the energy barrier

$$V_\zeta := \Phi(\zeta, \mathcal{I}_\zeta) - \widehat{H}(\zeta), \tag{3.1.6}$$

where $\mathcal{I}_\zeta$ is the set of states with energy below $\widehat{H}(\zeta)$:

$$\mathcal{I}_\zeta := \{\eta \in \mathcal{X} : \widehat{H}(\eta) < \widehat{H}(\zeta)\}. \tag{3.1.7}$$

We set $V_\zeta := \infty$ if $\mathcal{I}_\zeta$ is empty.

— We call *V-irreducible states* the set of all states with stability level larger than V:

$$\mathcal{X}_V := \{\eta \in \mathcal{X} : V_\eta > V\}. \tag{3.1.8}$$

— The set of *stable states* is the set of the global minima of the Hamiltonian:

$$\mathcal{X}^s := \mathcal{F}(\mathcal{X}). \tag{3.1.9}$$

— The set of *metastable states* is given by

$$\mathcal{X}^m := \{\eta \in \mathcal{X} : V_\eta = \max_{\zeta \in \mathcal{X} \setminus \mathcal{X}^s} V_\zeta\}. \tag{3.1.10}$$

We denote by Γ_m the stability level of the states in $\mathcal{X}^m$.

4. Optimal paths, saddles and gates

— We denote by $(\eta \to \eta')_{opt}$ the *set of optimal paths* as the set of all paths from η to η' realizing the min-max in $\mathcal{X}$, i.e.,

$$(\eta \to \eta')_{opt} := \{\omega : \eta \to \eta' \text{ such that } \max_{\xi \in \omega} \widehat{H}(\xi) = \Phi(\eta, \eta')\}. \tag{3.1.11}$$

— The set of *minimal saddles* between $\eta, \eta' \in \mathcal{X}$ is defined as

$$\mathcal{S}(\eta, \eta') := \{\zeta \in \mathcal{X} : \ \exists \omega \in (\eta \to \eta')_{opt},\ \omega \ni \zeta \text{ such that } \max_{\xi \in \omega} \widehat{H}(\xi) = \widehat{H}(\zeta)\}. \tag{3.1.12}$$

— A saddle $\xi \in \mathcal{S}(\eta, \eta')$ is called *unessential* if for any $\omega \in (\eta \to \eta')_{opt}$ such that $\omega \cap \xi \neq \emptyset$ we have $\{\arg\max_\omega \widehat{H}\} \setminus \{\xi\} \neq \emptyset$ and there exists $\omega' \in (\eta \to \eta')_{opt}$ such that $\{\arg\max_{\omega'} \widehat{H}\} \subseteq \{\arg\max_\omega \widehat{H}\} \setminus \{\xi\}$.

— A saddle $\xi \in \mathcal{S}(\eta, \eta')$ is called *essential* if it is not unessential, i.e., if either

(i) there exists $\omega \in (\eta \to \eta')_{opt}$ such that $\{\arg\max_\omega \widehat{H}\} = \{\xi\}$ or

(ii) there exists $\omega \in (\eta \to \eta')_{opt}$ such that $\{\arg\max_\omega \widehat{H}\} \supset \{\xi\}$ and $\{\arg\max_{\omega'} \widehat{H}\} \not\subseteq \{\arg\max_\omega \widehat{H}\} \setminus \{\xi\}$ for all $\omega' \in (\eta \to \eta')_{opt}$.

— Given a pair $\eta, \eta' \in \mathcal{X}$, we say that $\mathcal{W} \equiv \mathcal{W}(\eta, \eta')$ is a *gate* for the transition $\eta \to \eta'$ if $\mathcal{W}(\eta, \eta') \subseteq \mathcal{S}(\eta, \eta')$ and $\omega \cap \mathcal{W} \neq \emptyset$ for all $\omega \in (\eta \to \eta')_{\mathtt{opt}}$. In words, a gate is a subset of $\mathcal{S}(\eta, \eta')$ that is visited by all optimal paths.

— We say that $\mathcal{W}(\eta, \eta')$ is a *minimal gate* for the transition $\eta \to \eta'$ if it is a gate and for any $\mathcal{W}' \subsetneq \mathcal{W}(\eta, \eta')$ there exists $\omega' \in (\eta \to \eta')_{\mathtt{opt}}$ such that $\omega' \cap \mathcal{W}' = \emptyset$. In words, a minimal gate is a minimal subset of $\mathcal{S}(\eta, \eta')$ by inclusion that is visited by all optimal paths.

— For a given pair of configurations η, η', we denote by $\mathcal{G}(\eta, \eta')$ the union of all minimal gates:

$$\mathcal{G}(\eta, \eta') := \bigcup_{\mathcal{W}(\eta,\eta') \text{ minimal gate}} \mathcal{W}(\eta, \eta'). \tag{3.1.13}$$

3.1.2 *Model–independent strategy*

In this section we give a general strategy to analyze the geometry of the set $\mathcal{G}(m, \mathcal{X}^s)$, where either $m \in \mathcal{X}^m$ is a metastable state if we analyze metastability or $m \in \mathcal{X}^s$ is a stable state if we analyze tunneling between two stable states. Assume that we are in finite volume and $\mathcal{W}(m, \mathcal{X}^s)$ is a set of configurations that has been proven to be a gate. The following strategy is useful to eliminate some unessential saddles from the set $\mathcal{S}(m, \mathcal{X}^s) \setminus \mathcal{W}(m, \mathcal{X}^s)$ in order to determine the set $\mathcal{G}(m, \mathcal{X}^s)$. Indeed, [85, Theorem 5.1] states the equivalence between being an unessential saddle and not belonging to $\mathcal{G}(m, \mathcal{X}^s)$. This strategy is more effective if the gate proposed is minimal or union of minimal gates.

Since we will apply this strategy to Kawasaki dynamics, we refer to the Hamiltonian energy as $\widehat{H}$, but one could simply replace it with another energy function to get the results for another model. In order to state our results concerning the unessential saddles we need the following definitions.

— A nonempty set $\mathcal{A} \subset \mathcal{X}$ is a cycle if it is either a singleton or it verifies the relation

$$\max_{x,y \in \mathcal{A}} \Phi(x, y) < \Phi(\mathcal{A}, \mathcal{X} \setminus \mathcal{A}). \tag{3.1.14}$$

See [45, equation (3.40)]. In the case of Metropolis dynamics, this definition coincides with [85, equation (2.7)].

— Given $\sigma \in \mathcal{X}$, $\Gamma > 0$ and $\mathcal{A}$ a set of target configurations, we say that the *initial cycle for the transition from* σ *to* $\mathcal{A}$ *with depth* Γ is

$$\mathcal{C}^{\sigma}_{\mathcal{A}}(\Gamma) := \sigma \cup \{\eta \in \mathcal{X} : \ \Phi(\sigma, \eta) - \widehat{H}(\sigma) < \Gamma = \Phi(\sigma, \mathcal{A}) - \widehat{H}(\sigma)\}. \tag{3.1.15}$$

Note that in definition (3.1.15) we emphasize the dependence on σ and $\mathcal{A}$ and that Γ is identified by them. Note that this definition of $\mathcal{C}^{\sigma}_{\mathcal{A}}(\Gamma)$ concides with $\mathcal{C}_{\mathcal{A}}(\sigma)$ defined in [85, equation (2.25)].

In order to apply this strategy to a concrete model, we require the following model-dependent inputs (we encourage the reader to inspect Fig. 3.1):

(i) Identify the sets $\mathcal{X}^m$ and $\mathcal{X}^s = \{\eta^s_1, ..., \eta^s_k\}$, where $\eta^s_1, ..., \eta^s_k$ have to be in $\mathcal{C}^{\mathcal{X}^s}_m(\Gamma_m + \widehat{H}(m) - \widehat{H}(\mathcal{X}^s))$, with $\Gamma_m := \Phi(m, \mathcal{X}^s) - \widehat{H}(m)$ the energy barrier between m and $\mathcal{X}^s$ for a given $m \in \mathcal{X}^m$.

(ii) Find a set $\mathcal{W}(m, \mathcal{X}^s)$ and prove that it is a gate for the transition $m \to \mathcal{X}^s$.

(iii) Find two sets of configurations $\mathcal{L}^G$ and $\mathcal{L}^B$ and prove the following conditions for any $\eta \in \mathcal{W}(m, \mathcal{X}^s)$:

(a) there exist a path $\omega^G_1 : \eta \to \mathcal{L}^G$ such that $\max_{\sigma \in \omega^G_1} \widehat{H}(\sigma) \leqslant \Gamma_m + \widehat{H}(m)$ and a path $\omega^G_2 : \mathcal{L}^G \to \mathcal{X}^s$ such that $\max_{\sigma \in \omega^G_2} \widehat{H}(\sigma) < \Gamma_m + \widehat{H}(m)$;

(b) there exists a path $\omega^B_1 : \eta \to \mathcal{L}^B$ such that $\max_{\sigma \in \omega^B_1} \widehat{H}(\sigma) \leqslant \Gamma_m + \widehat{H}(m)$ and $\nexists\, \omega^B_2 : \mathcal{L}^B \to \mathcal{X}^s$ and $\nexists\, \omega^B_2 : \mathcal{L}^B \to m$ such that $\max_{\sigma \in \omega^B_2} \widehat{H}(\sigma) < \Gamma_m + \widehat{H}(m)$;

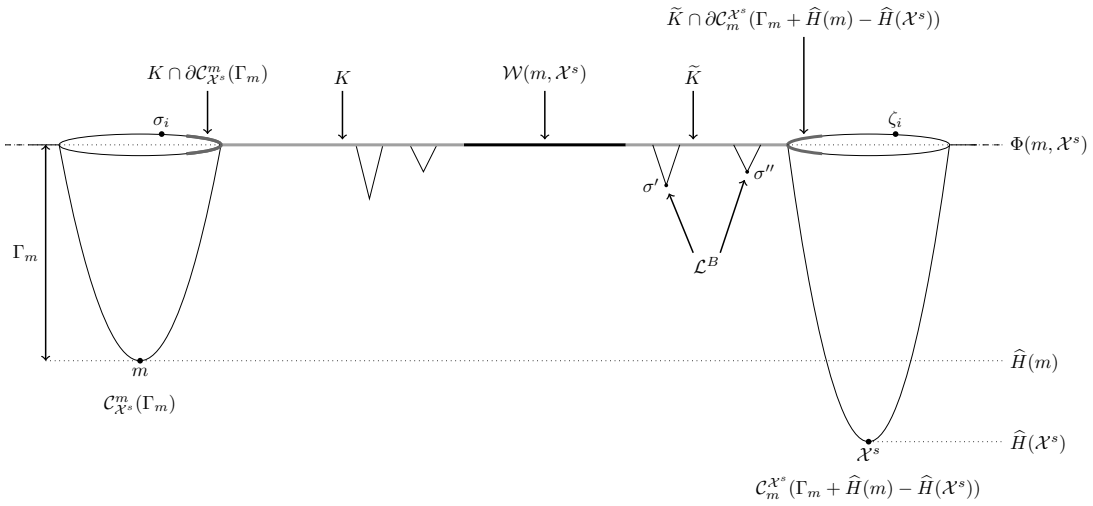

Figure 3.1 – We depict an example of the energy landscape for the transition between the metastable state m and the stable states $\mathcal{X}^s$. We depict on the left the cycle of the metastable state $\mathcal{C}_{\mathcal{X}^s}^m(\Gamma_m)$ and on the right the cycle of the stable states $\mathcal{C}_m^{\mathcal{X}^s}(\Gamma_m + \widehat{H}(m) - \widehat{H}(\mathcal{X}^s))$. We indicate in black $W(m, \mathcal{X}^s)$, in light grey K and $\widetilde{K}$, emphasizing with dark grey the part of K and $\widetilde{K}$ that intersect the boundaries of the two previous cycles. We give an example of two configurations σ' and σ'' that are in $\mathcal{L}^B$.

(iv) Identify the subset K (resp. $\widetilde{K}$) of the saddles that are visited by the optimal paths just before entering (resp. just after visiting) $\mathcal{W}(m, \mathcal{X}^s)$. More precisely,

$$\begin{aligned} K := \{\bar{\eta} \in \mathcal{S}(m, \mathcal{X}^s) \setminus \mathcal{W}(m, \mathcal{X}^s) : \exists\, \eta \in \mathcal{W}(m, \mathcal{X}^s) \text{ and } \omega = \omega_1 \circ \omega_2, \\ \text{with } \omega_1 : \eta \to \bar{\eta} \text{ s.t. } \omega_1 \cap \mathcal{W}(m, \mathcal{X}^s) = \{\eta\},\ \omega_1 \cap \mathcal{C}_{\mathcal{X}^s}^m(\Gamma_m) = \emptyset \\ \text{and } \omega_2 : \bar{\eta} \to m \text{ s.t. } \omega_2 \cap \mathcal{W}(m, \mathcal{X}^s) = \emptyset,\ \max_{\sigma \in \omega} \widehat{H}(\sigma) \leqslant \Gamma_m + \widehat{H}(m)\} \end{aligned} \tag{3.1.16}$$

and

$$\begin{aligned} \widetilde{K} := \{\bar{\eta} \in \mathcal{S}(m, \mathcal{X}^s) \setminus \mathcal{W}(m, \mathcal{X}^s) : \exists\, \eta \in \mathcal{W}(m, \mathcal{X}^s) \text{ and } \omega = \omega_1 \circ \omega_2, \text{ with} \\ \omega_1 : \eta \to \bar{\eta} \text{ s.t. } \omega_1 \cap \mathcal{W}(m, \mathcal{X}^s) = \{\eta\}, \omega_1 \cap \mathcal{C}_m^{\mathcal{X}^s}(\Gamma_m + \widehat{H}(m) - \widehat{H}(\mathcal{X}^s)) = \emptyset \\ \text{and } \omega_2 : \bar{\eta} \to \mathcal{X}^s \text{ s.t. } \omega_2 \cap \mathcal{W}(m, \mathcal{X}^s) = \emptyset,\ \max_{\sigma \in \omega} \widehat{H}(\sigma) \leqslant \Gamma_m + \widehat{H}(m)\}. \end{aligned} \tag{3.1.17}$$

If $\mathcal{X}^s$ is a singleton, then it belongs to $\mathcal{C}_m^{\mathcal{X}^s}(\Gamma_m + \widehat{H}(m) - \widehat{H}(\mathcal{X}^s))$. Conditions (iii)-(a) and (iii)-(b) guarantee that when the dynamics reaches $\mathcal{L}^G$ it has gone "over the hill", while when it reaches $\mathcal{L}^B$ the energy has to increase again to the level $\Gamma_m + \widehat{H}(m)$ to visit m or $\mathcal{X}^s$. In particular, this implies that $\mathcal{L}^G \subset \mathcal{C}_m^{\mathcal{X}^s}(\Gamma_m + \widehat{H}(m) - \widehat{H}(\mathcal{X}^s))$ and $\mathcal{L}^B \not\subseteq \mathcal{C}_m^{\mathcal{X}^s}(\Gamma_m + \widehat{H}(m) - \widehat{H}(\mathcal{X}^s))$. We will show in Section 3.4 how the model-dependent inputs (iii)-(a) and (iii)-(b) apply to the isotropic model evolving under Kawasaki dynamics. For the anisotropic cases, see Sections 4.3 and 5.3. In Section 3.6 we will refer to $\mathcal{C}_{\mathcal{X}^s}^m(\Gamma_m)$ as $\mathcal{X}^{meta}$ and to $\partial \mathcal{C}_m^{\mathcal{X}^s}(\Gamma_m + \widehat{H}(m) - \widehat{H}(\mathcal{X}^s))$ as $\mathcal{X}^{stab}$.

Remark 3.1.1. *Note that it is possible that $K = \emptyset$ and/or $\widetilde{K} = \emptyset$, since the gate $\mathcal{W}(m, \mathcal{X}^s)$ could contain all the configurations with such properties. Indeed, in [26, Lemma 6.4(a)] it is proved that this is the case for the q-state Potts model with negative external magnetic field evolving under Glauber dynamics. In that case $m = \mathbf{1}$, namely, the configuration with all spins 1, and the gate $\mathcal{W}(\mathbf{1}, \mathcal{X}^s)$ is defined as the set of configurations in which all the vertices have spins 1, except those in a rectangle with a protuberance attached to it, which have the same spin different from 1. In particular, assuming $q = 2$, the same result holds for the Ising model.*

See Figure 3.1 for Propositions 3.1.3 and 3.1.5.

Definition 3.1.2. *A saddle σ is of the first type if it is not in $\mathcal{W}(m, \mathcal{X}^s) \cup K$ and belongs to the boundary of the cycle $\mathcal{C}^m_{\mathcal{X}^s}(\Gamma_m)$, i.e., $\sigma \in \partial\mathcal{C}^m_{\mathcal{X}^s}(\Gamma_m) \cap (\mathcal{S}(m, \mathcal{X}^s) \setminus (\mathcal{W}(m, \mathcal{X}^s) \cup K))$, where $\mathcal{C}^m_{\mathcal{X}^s}(\Gamma_m)$ is defined in (3.1.15).*

Note that Definition 3.1.2 for Kawasaki dynamics coincides with Definition 1.3.2.

Proposition 3.1.3. *Any saddle σ of the first type is unessential and therefore it is not in $\mathcal{G}(m, \mathcal{X}^s)$.*

We refer to Section 3.3.1 for the proof of Proposition 3.1.3. As we can see in the proof, it will be clear that this result is guaranteed only by the model-dependent inputs (i), (ii) and (iv).

Definition 3.1.4. *A saddle ζ is of the second type if it is not in $\mathcal{W}(m, \mathcal{X}^s) \cup \widetilde{K}$ and belongs to the boundary of the cycle $\mathcal{C}^{\mathcal{X}^s}_m(\Gamma_m + \widehat{H}(m) - \widehat{H}(\mathcal{X}^s))$, i.e., $\zeta \in \partial\mathcal{C}^{\mathcal{X}^s}_m(\Gamma_m + \widehat{H}(m) - \widehat{H}(\mathcal{X}^s)) \cap (\mathcal{S}(m, \mathcal{X}^s) \setminus (\mathcal{W}(m, \mathcal{X}^s) \cup \widetilde{K}))$, where $\mathcal{C}^{\mathcal{X}^s}_m(\Gamma_m + \widehat{H}(m) - \widehat{H}(\mathcal{X}^s))$ is defined in (3.1.15).*

Note that Definition 3.1.4 for Kawasaki dynamics coincides with Definition 1.3.3.

Proposition 3.1.5. *Any saddle ζ of the second type is unessential and therefore it is not in $\mathcal{G}(m, \mathcal{X}^s)$.*

We refer to Section 3.3.2 for the proof of Proposition 3.1.5. For this result all of the four model-dependent inputs are necessary.

Remark 3.1.6. *This strategy can also be applied in the tunneling scenario, i.e., the transition between two stable states, which corresponds to selecting the starting state $m \in \mathcal{X}^s$. The model-dependent input (i) has to be modified by requiring that the configurations in $\mathcal{X}^s \setminus \{m\}$ are in the same cycle that does not contain m, while the inputs (ii)-(iv) remain the same. Thus, Propositions 3.1.3 and 3.1.5 still hold after replacing the set $\mathcal{X}^s$ by $\mathcal{X}^s \setminus \{m\}$. In this case, since $\widehat{H}(m) = \widehat{H}(\mathcal{X}^s)$, note that the cycles $\mathcal{C}^m_{\mathcal{X}^s \setminus \{m\}}(\Gamma_m)$ and $\mathcal{C}^{\mathcal{X}^s \setminus \{m\}}_m(\Gamma_m + \widehat{H}(m) - \widehat{H}(\mathcal{X}^s))$ have the same depth. The idea of this strategy can be applied also in the tunneling scenario in which the configurations in $\mathcal{X}^s \setminus \{m\}$ are not in the same cycle, but this requires an extension of this strategy. This occurs in the q-state Potts model with q possible spins and zero external magnetic field [25], where the stable states are the configurations with all spins of the same type. In [25, Theorem 3.4] the authors study the gates relevant for the tunneling between one stable state m to the set of the other stable states $\mathcal{X}^s \setminus \{m\}$. For the proof of this theorem they use [25, Theorem 3.2], in which they identify all the unessential saddles for the transition between the selected stable state m to one of the other stable states $s \in \mathcal{X}^s \setminus \{m\}$ when the dynamics is restricted only to the optimal paths that do not visit the rest of the stable states $\mathcal{X}^s \setminus \{m, s\}$. The proof of [25, Theorem 3.2] uses, in the specific model, the ideas presented in this section and the symmetry of the energy landscape for q-state Potts model with zero external magnetic field.*

These model-independent propositions will be applied to the isotropic model evolving under Kawasaki dynamics (in Section 3.4) to identify the set $\mathcal{G}(m, \mathcal{X}^s)$. For the application to the anisotropic models, see Sections 4.3 and 5.3.

3.2 MAIN RESULTS

In this section we state our main results. To this end, in Section 3.2.1 we give some model–dependent definitions, so that in Section 3.2.2 we obtain the geometrical characterization of the union of all minimal gates for the isotropic case. Moreover, we derive the mixing time and spectral gap in Section 3.2.3. For the corresponding results obtained in the weakly and strongly anisotropic cases we refer respectively to Sections 4.1.1 and 5.1.1 for results concerning the gates and union of minimal gates, and to Section 4.1.2 and 5.1.2 for results concerning the asymptotic transition time, mixing time and spectral gap.

3.2.1 *Geometrical definitions for Kawasaki dynamics on the square lattice*

We give some model–dependent definitions and notations in order to state our main theorems.

1. Free particles and clusters

— For $x \in \Lambda_0$, let $nn(x) := \{y \in \Lambda_0 : d(y, x) = 1\}$ be the set of nearest–neighbor sites of x in Λ_0 according to the lattice distance, where d in the entire thesis denotes the lattice distance.

- A *free particle* in $\eta \in \mathcal{X}$ is a site x, with $\eta(x) = 1$, such that either $x \in \partial^- \Lambda$, or $x \in \Lambda_0$ and $\sum_{y \in nn(x) \cap \Lambda_0} \eta(y) = 0$. We denote by η_{fp} the union of free particles in $\partial^- \Lambda$ and free particles in Λ_0. We denote by $n(\eta)$ the number of free particles in η.
  We denote by η_{cl} the clusterized part of the occupied sites of η:

$$\eta_{cl} := \{x \in \Lambda_0 : \ \eta(x) = 1\} \setminus \eta_{fp}. \tag{3.2.1}$$

— We denote by η^{fp} the addition of a free particle anywhere in Λ to the configuration η.
— Given a configuration $\eta \in \mathcal{X}$, consider the subset $C(\eta_{cl})$ of $\mathbb{R}^2$ defined as the union of the 1×1 closed squares centered at the occupied sites of η_{cl} in Λ_0 and call the maximal connected components of this set the clusters of η_{cl}.
— Given a set $A \subset \mathbb{R}^2$, we define the number of 1×1 closed occupied squares in A as

$$|A| := |A \cap C(\eta_{cl})| \tag{3.2.2}$$

and as $\|A\|$ the numbers of 1×1 closed squares in A. Note that $\|\cdot\|$ takes into account the possibility that the squares are occupied or not.

2. Projections, semi-perimeter and vacancies

— For $\eta \in \mathcal{X}$, we denote by $g_1(\eta)$ (resp. $g_2(\eta)$) one half of the horizontal (resp. vertical) length of the Euclidean boundary of $C(\eta_{cl})$. Then, the energy associated with η is given by

$$\widehat{H}(\eta) = -(U_1 + U_2 - \Delta)|C(\eta_{cl})| + U_1 g_2(\eta) + U_2 g_1(\eta) + \Delta n(\eta). \tag{3.2.3}$$

— Let $p_1(\eta)$ and $p_2(\eta)$ be the total lengths of horizontal and vertical projections of $C(\eta_{cl})$, respectively. More precisely, let $r_{j,1} = \{x \in \mathbb{Z}^2 : (x)_1 = j\}$ be the j-th column and $r_{j,2} = \{x \in \mathbb{Z}^2 : (x)_2 = j\}$ be the j-th row, where $(x)_1$ or $(x)_2$ denote the first or second component of x. Let

$$\pi_1(\eta) := \{j \in \mathbb{Z} : \ r_{j,1} \cap C(\eta_{cl}) \neq \emptyset\} \tag{3.2.4}$$

and $p_1(\eta) := |\pi_1(\eta)|$. In a similar way we define the vertical projection $\pi_2(\eta)$ and $p_2(\eta)$.
— We define $g_i'(\eta) := g_i(\eta) - p_i(\eta) \geqslant 0$; we call *monotone* a configuration such that $g_i(\eta) = p_i(\eta)$ for $i = 1, 2$.
— We define the *semi–perimeter* $s(\eta)$ and the *vacancies* $v(\eta)$ as

$$\begin{aligned} s(\eta) &:= p_1(\eta) + p_2(\eta), \\ v(\eta) &:= p_1(\eta)p_2(\eta) - |C(\eta_{cl})|. \end{aligned} \tag{3.2.5}$$

3. n-manifold, rectangles and corners

— The configuration space $\mathcal{X}$ can be partitioned as

$$\mathcal{X} = \bigcup_n \mathcal{V}_n, \tag{3.2.6}$$

where $\mathcal{V}_n := \{\eta \in \mathcal{X} : |C(\eta_{cl})| + n(\eta) = n\}$ is the set of configurations with n particles, called the n-*manifold*.
— We denote by $\mathcal{R}(\ell_1, \ell_2)$ the set of configurations that have no free particle and a single cluster such that $C(\eta_{cl})$ is a rectangle $R(\ell_1, \ell_2)$, with $\ell_1, \ell_2 \in \mathbb{N}$. For any $\eta, \eta' \in \mathcal{R}(\ell_1, \ell_2)$ we have immediately

$$\widehat{H}(\eta) = \widehat{H}(\eta') = \widehat{H}(\mathcal{R}(l_1, l_2)) = U_1 \ell_2 + U_2 \ell_1 - \varepsilon \ell_1 \ell_2, \tag{3.2.7}$$

where

$$\varepsilon := U_1 + U_2 - \Delta. \tag{3.2.8}$$

If $\ell_1 \leqslant \ell_2 \leqslant \ell_1 + 1$, we say that the rectangle $R(\ell_1, \ell_2)$ is a *quasi–square* (recall (1.3.77)).
— A *corner* in $\eta \in \mathcal{X}$ is a closed 1×1 square centered in an occupied site $x \in \Lambda_0$ such that, if we order clockwise its four nearest neighbors x_1, x_2, x_3, x_4, then $\sum_{y \in nn(x)} \eta(y) = 2$, with $\eta(x_i) = \eta(x_{i+1}) = 1$, with $i = 1, ..., 4$ and the convention that $x_5 = x_1$ (see Figure 3.2 on the righ).

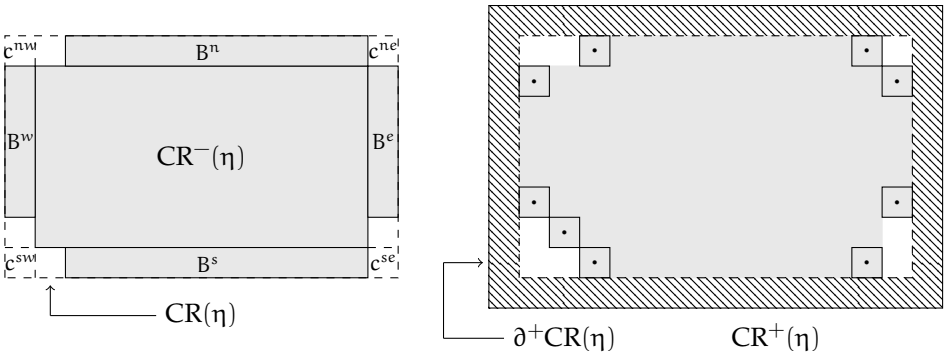

Figure 3.2 – Here we depict the same configuration η on the left and on the right to emphasize different geometrical definitions. The grey area in both pictures represents $C(\eta_{cl})$. In particular, on the left-hand side we stress the frame-angles $c^{\alpha\alpha'}(\eta)$, the bars $B^\alpha(\eta)$, $CR^-(\eta)$ and the circumscribing rectangle $CR(\eta)$ (respresented with a dashed line). While on the right-hand side we stress the sites that are in a corner (represented with a dot), $CR^+(\eta)$ and the external frame $\partial^+CR(\eta)$ (the dashed area).

4. Circumscribed rectangle, frames and bars

— If η is a configuration with a single cluster, then we denote by $CR(\eta)$ the rectangle *circumscribing* $C(\eta_{cl})$, i.e., the smallest rectangle containing η.
We denote $\partial^+CR(\eta)$ the *external frame of* $CR(\eta)$ as the union of squares 1×1 centered at sites that are not contained in $CR(\eta)$ such that those sites have Euclidean distance with sites in $CR(\eta)$ less or equal than $\sqrt{2}$ (see Figure 3.2 on the right-hand side). Note that the external frame of $CR(\eta)$ contains only non occupied sites.
We denote $\partial^-CR(\eta)$ the *internal frame of* $CR(\eta)$ as the union of squares 1×1 centered at sites that are contained in $CR(\eta)$ such that those sites have Euclidean distance with sites not in $CR(\eta)$ less or equal than $\sqrt{2}$. If this distance is equal to $\sqrt{2}$, we say that the unit square is a *frame-angle* $c^{\alpha\alpha'}(\eta)$ in $\partial^-CR(\eta)$, where $\alpha\alpha' \in \{ne, nw, se, sw\}$, with $n =$ north, $s =$ south, etc. Note that the internal frame of $CR(\eta)$ is a geometrical object contained in $\mathbb{R}^2$ that can contain both occupied and non occupied sites (see Figure 3.2 on the left-hand side). We partition the set $\partial^-CR(\eta)$ without frame-angles in *two horizontal and two vertical rows* $r^\alpha(\eta)$, with $\alpha \in \{n, w, e, s\}$.
Moreover, we set

$$\begin{aligned} CR^-(\eta) &= CR(\eta) \setminus \partial^-CR(\eta), \\ CR^+(\eta) &= CR(\eta) \cup \partial^+CR(\eta). \end{aligned} \tag{3.2.9}$$

See Figure 3.2 for an example.
Remark 3.2.1. *Note that, for example, the frame-angles* $c^{ne}(\eta)$ *and* $c^{en}(\eta)$ *are the same, but this distinction will be useful in Definitions 3.2.4 and 3.2.5.*

— A *vertical* (respectively *horizontal*) *bar* $B^\alpha(\eta)$ of a single cluster of η with length k is a $1\times k$ (respectively $k\times 1$) rectangle contained in $C(\eta_{cl})$, with $\alpha \in \{n, w, e, s\}$, $k \geqslant 1$, such that each square 1×1 of the bar is attached only to one square of $C(\eta_{cl}) \setminus B^\alpha(\eta)$ (see Figure 3.2 on the left-hand side). In the cases in which it is not specified if the bar is vertical or horizontal we call it simply *bar*. If $k = 1$ we say that the bar is a *protuberance*.
Remark 3.2.2. *Note that two bars* $B^\alpha(\eta)$ *and* $B^{\alpha'}(\eta)$*, with* $\alpha, \alpha' \in \{n, s, w, e\}$*, can possibly intersect in the frame-angle* $c^{\alpha\alpha'}(\eta)$*. If this is the case, we get* $|B^\alpha(\eta) \cup B^{\alpha'}(\eta)| = |B^\alpha(\eta)| + |B^{\alpha'}(\eta)| - 1$.

5. Motions along the border

Recall definitions of $|\cdot|$ and $\|\cdot\|$ in (3.2.2) and below. In the following, we give the precise notion of translation by 1 of a bar, for example to the left or to the right, while keeping all the squares of the bar attached to the cluster below.

Definition 3.2.3. *Given* η *and a bar* $B^\alpha(\eta)$ *of length* k*, with* $\alpha \in \{n, s, e, w\}$*, we say that it is possible to* translate the bar $B^\alpha(\eta)$ *if*

$$k = |B^\alpha(\eta)| < |\partial^+ B^\alpha(\eta)|. \tag{3.2.10}$$

We define the 1-translation of a bar $B^{\alpha}(\eta)$ *of length* k *as a sequence of configurations* $(\eta_1, ..., \eta_k)$ *such that* $\eta_1 = \eta$ *and* η_i *is obtained from* η_{i-1} *translating by* 1 *a unit square along the rectangle* $\partial^+ B^{\alpha}(\eta) \cap C(\eta_{cl})$ *for any* $2 \leqslant i \leqslant k$.

In Fig. 1.9 (resp. Fig. 1.10) we depict a 1-translation of a horizontal (resp. vertical) bar at cost U_1 (resp. U_2).

In the following, we give the precise notion of sliding a unit square from row $r^{\alpha}(\eta)$ to $r^{\alpha'}(\eta)$ passing through the frame angle $c^{\alpha\alpha'}(\eta)$.

Definition 3.2.4. *Given* η, *let* $\alpha\alpha'$ *such that* $c^{\alpha\alpha'}(\eta)$ *is a frame-angle. We say that it is possible to* slide a unit square around a frame-angle $c^{\alpha\alpha'}(\eta) \subseteq \partial^- CR(\eta)$ *from a row* $r^{\alpha}(\eta) \subseteq \partial^- CR(\eta)$ *to a row* $r^{\alpha'}(\eta) \subseteq \partial^- CR(\eta)$ *via a frame-angle* $c^{\alpha\alpha'}(\eta)$ *if*

$$|c^{\alpha\alpha'}(\eta)| = 0, \quad |r^{\alpha}(\eta)| \geqslant 1, \quad 1 \leqslant |r^{\alpha'}(\eta)| < \|r^{\alpha'}(\eta)\| + 1. \tag{3.2.11}$$

Let $\alpha'' \neq \alpha'$ *such that* $c^{\alpha\alpha''}(\eta)$ *is a frame-angle. See Figure 1.11 for an example. We define a* sliding of a unit square around a frame-angle $c^{\alpha\alpha'}(\eta) \subseteq \partial^- CR(\eta)$ *as the composition of a sequence of* 1*-translations of the bar* $B^{\alpha}(\eta)$ *from* $r^{\alpha}(\eta) \cup c^{\alpha\alpha''}(\eta)$ *to* $r^{\alpha}(\eta) \cup c^{\alpha\alpha'}(\eta)$, *namely* $(\eta^1, ..., \eta^k)$, *and the* 1*-translation of a bar* $B^{\alpha'}(\eta) = C(\eta^k_{cl}) \cap (r^{\alpha'}(\eta) \cup c^{\alpha\alpha'}(\eta))$ *from* $r^{\alpha'}(\eta) \cup c^{\alpha\alpha'}(\eta)$ *to* $r^{\alpha'}(\eta) \cup c^{\alpha'\alpha'''}(\eta)$, *where* $\alpha''' \neq \alpha$ *is such that* $c^{\alpha'\alpha'''}(\eta)$ *is a frame-angle.*

The definition above is used only to define the following sliding of a bar from row $r^{\alpha}(\eta)$ to $r^{\alpha'}(\eta)$ passing through the frame angle $c^{\alpha\alpha'}(\eta)$, that corresponds to iteratively apply the sliding of a unit square around a frame-angle.

Definition 3.2.5. *Given* η, *let* $\alpha\alpha'$ *such that* $c^{\alpha\alpha'}(\eta)$ *is a frame-angle. Before sliding a bar around a frame-angle, we translate the bars* $B^{\alpha}(\eta)$ *and* $B^{\alpha'}(\eta)$ *at distance* 1 *to the frame-angle* $c^{\alpha\alpha'}(\eta)$ *obtaining a configuration* η'. *We say that it is possible to* slide a bar $B^{\alpha}(\eta')$ around a frame-angle $c^{\alpha\alpha'}(\eta') \subseteq \partial^- CR(\eta')$ *if it is possible to move all the unit squares in* $B^{\alpha}(\eta')$ *around a frame-angle* $c^{\alpha\alpha'}(\eta')$ *from a row* $r^{\alpha}(\eta') \cup c^{\alpha\alpha''}(\eta')$ *to a row* $r^{\alpha'}(\eta') \cup c^{\alpha'\alpha'''}(\eta')$, *where* $\alpha'' \neq \alpha'$ *and* $\alpha''' \neq \alpha$ *are such that* $c^{\alpha\alpha''}(\eta')$ *and* $c^{\alpha'\alpha'''}(\eta')$ *are frame-angles. Namely,*

$$|B^{\alpha}(\eta')| + |r^{\alpha'}(\eta')| \leqslant \|r^{\alpha'}(\eta')\| + 1. \tag{3.2.12}$$

Moreover, we define a sliding of a bar $B^{\alpha}(\eta')$ around a frame-angle $c^{\alpha\alpha'}(\eta')$ *as the sequence of* $|B^{\alpha}(\eta')|$ *slidings of unit squares around a frame-angle* $c^{\alpha\alpha'}(\eta')$.

See the path described in Fig. 1.13, that connects the configuration η to the configuration (12) for an example of sliding of the bar $B^e(\eta)$ around the frame-angle $c^{en}(\eta)$, with η as the configuration (3).

3.2.2 *Gate for isotropic interactions*

Recall (3.2.8) for the definition of ε. We will consider $0 < \varepsilon \ll U$, where $\ll$ means sufficiently smaller; for instance $\varepsilon \leqslant \frac{U}{100}$ is enough. In order to state our main result we recall some important definitions that are given in [35]. Recall the definition of the critical length ℓ_c given in (1.3.21) and that we have defined $\bar{\mathcal{Q}}$ as the set of configurations having one cluster consisting of an $(\ell_c - 1) \times \ell_c$ quasi–square anywhere in Λ_0 with a single protuberance attached anywhere to one of the shortest sides. Similarly, the set $\widetilde{\mathcal{Q}}$ contains the configurations having one cluster anywhere in Λ_0 consisting of an $(\ell_c - 1) \times \ell_c$ quasi–square with a single protuberance attached anywhere to one of the longest sides. The critical value of the energy is

$$\Gamma^* = 2U(\ell_c + 1) - (2U - \Delta)(\ell_c(\ell_c - 1) + 2) \tag{3.2.13}$$

and the volume of the clusters in $\mathcal{Q} = \bar{\mathcal{Q}} \cup \widetilde{\mathcal{Q}}$ is

$$n_c = \ell_c(\ell_c - 1) + 1. \tag{3.2.14}$$

Finally, recall (1.3.31) for the definition of the sets $\bar{\mathcal{D}}$ and $\widetilde{\mathcal{D}}$. By [35, Theorem 1.4.1] we obtain the geometric description of the set $\mathcal{D}$ as $\mathcal{D} = \bar{\mathcal{D}} \cup \widetilde{\mathcal{D}}$ that will be useful later on. Roughly

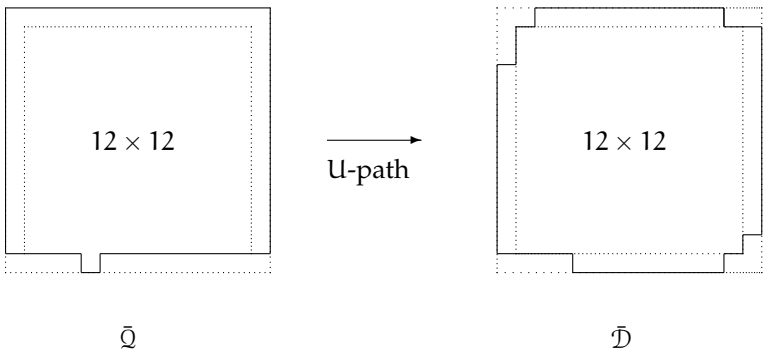

Figure 3.3 – Configurations in $\bar{\mathcal{Q}}$ and $\bar{\mathcal{D}}$ for $\ell_c = 14$. A similar picture applies for $\widetilde{\mathcal{Q}}$ and $\widetilde{\mathcal{D}}$ with a 11×13 rectangle in the center.

speaking, one can think of $\mathcal{D}$ as the set of configurations consisting of a rectangular cluster with four bars attached to its four sides, whose lengths satisfy precise conditions. See Figure 3.3 for an example of a configuration in $\bar{\mathcal{D}}$ that is obtained from a configuration in $\bar{\mathcal{Q}}$ via a U-*path*, i.e., via a path connecting two configurations with the same energy and such that along it no free particle is created and the energy is increased by at most U. Finally, we set

$$\mathcal{C}^* := \mathcal{D}^{fp}. \tag{3.2.15}$$

Note that

$$\begin{aligned} \widehat{H}(\mathcal{C}^*) &= = \widehat{H}(\mathcal{D}^{fp}) = \widehat{H}(\mathcal{D}) + \Delta = \widehat{H}(\mathcal{Q}) + \Delta \\ &= -U((\ell_c - 1)^2 + \ell_c(\ell_c - 2) + 1) + \Delta(\ell_c(\ell_c - 1) + 2) \\ &= 2U(\ell_c + 1) - (2U - \Delta)(\ell_c(\ell_c - 1) + 2) \\ &= \Gamma^*. \end{aligned} \tag{3.2.16}$$

Next we define two types of sets that will be useful in order to characterize the set $\mathcal{G}(\square, \blacksquare)$. For any $i = 0, 1, 2, 3$, we define $\mathcal{P}_i \subseteq \mathcal{S}(\square, \blacksquare)$ to consist of configurations with a single cluster and no free particle, and a fixed number of vacancies that is not monotone with circumscribed rectangle obtained from the one of the configurations in $\mathcal{D}$ via increasing and/or decreasing the horizontal or vertical length. More precisely,

$$\begin{aligned} \mathcal{P}_i := \{\eta \ &: n(\eta) = 0,\, v(\eta) = 2\ell_c - i(i+1) - 2,\, \eta_{cl} \text{ is connected},\, g_1'(\eta) + g_2'(\eta) = 1, \\ &\text{with a } (\ell_c + i + 1) \times (\ell_c - i) \text{ circumscribed rectangle}\},\ i = 0, 1, 2, 3. \end{aligned} \tag{3.2.17}$$

See Figure 1.17(c) for an example of configurations in $\mathcal{P}_1$ and not in $\mathcal{C}^*$.

For any $i = -1, 0, 1, 2$, we define $\mathcal{P}_i^{fp} \subseteq \mathcal{S}(\square, \blacksquare)$ to consist of configurations with a single cluster and one free particle, and a fixed number of vacancies that is monotone with circumscribed rectangle obtained from the one of the configurations in $\mathcal{P}_i$ via decreasing by one the shortest length. More precisely,

$$\begin{aligned} \mathcal{P}_i^{fp} := \ &\{\eta : n(\eta) = 1,\, v(\eta) = \ell_c - i(i+2) - 2,\, \eta_{cl} \text{ is connected},\, g_1'(\eta) + g_2'(\eta) = 0, \\ &\text{with a } (\ell_c + i + 1) \times (\ell_c - i - 1) \text{ circumscribed rectangle}\},\ i = -1, 0, 1, 2. \end{aligned} \tag{3.2.18}$$

See Figure 1.17 for an example of configuration in $\mathcal{P}_{-1}^{fp} \setminus \mathcal{C}^*$ (in (a)) and in $\mathcal{P}_0^{fp}$ and in $\mathcal{C}^*$ (in (b)). Note that other examples of configurations in $\mathcal{C}^*$ can be obtained by those in Figure 3.3 by adding a free particle.

Remark 3.2.6. *Note that $\mathcal{C}^* \subsetneq \mathcal{P}_{-1}^{fp} \cup \mathcal{P}_0^{fp}$. Indeed, there exist configurations that are in $\mathcal{P}_{-1}^{fp} \cup \mathcal{P}_0^{fp}$ and not in $\mathcal{C}^*$: for an example see Fig. 1.17(a).*

The set $\mathcal{G}(\square,\blacksquare)$ contains all the configurations that are in the sets defined in (3.2.17) and (3.2.18) with the following further conditions. First, for any $i=0,1,2,3$ we define the subset $\mathscr{I}_i^{\alpha}$ of the saddles in $\mathcal{P}_i$ with the condition that the configurations have only one occupied unit square in either a row or in one of its two adjacent frame-angles. More precisely,

$$\mathscr{I}_i^{\alpha} := \{\eta \in \mathcal{P}_i : |r^{\alpha}(\eta) \cup c^{\alpha\alpha'}(\eta) \cup c^{\alpha\alpha''}(\eta)| = 1\}, \quad i=0,1,2,3, \tag{3.2.19}$$

with $\alpha,\alpha',\alpha'' \in \{n,s,w,e\}$ such that $c^{\alpha\alpha'}(\eta)$ and $c^{\alpha\alpha''}(\eta)$ are different frame-angles. Next, for any $i=0,1,2$ we define the subset $\mathscr{I}^{\alpha,\alpha'}_{k,k',i}$ of the saddles in $\mathcal{P}_i$ that are obtained from $\eta \in \mathcal{P}_i$ during the sliding of the bar $B^{\alpha'}(\eta)$ around the frame-angle $c^{\alpha'\alpha}(\eta)$. More precisely, for any $i=0,1,2$ we define

$$\begin{aligned}\mathscr{I}^{\alpha,\alpha'}_{k,k',i} \quad &:= \{\eta \in \mathcal{P}_i : |r^{\alpha}(\eta)| = k-1, |r^{\alpha'}(\eta)| = k'-k+1, k' \leqslant 1+\|r^{\alpha}(\eta)\|,\\ &|c^{\alpha'\alpha}(\eta)| = 1, (r^{\alpha}(\eta)\cup c^{\alpha'\alpha}(\eta)) \cap \eta_{cl} = r_{cl}^{\alpha,1} \cup r_{cl}^{\alpha,2} \text{ with } d(r_{cl}^{\alpha,1}, r_{cl}^{\alpha,2}) = 2\},\end{aligned} \tag{3.2.20}$$

where $\alpha,\alpha' \in \{n,s,w,e\}$ is such that $c^{\alpha'\alpha}(\eta)$ is a frame-angle, $r_{cl}^{\alpha,1}$, $r_{cl}^{\alpha,2}$ are two disjoint connected components in $r^{\alpha}(\eta)\cup c^{\alpha'\alpha}(\eta)$ and $k'=2,...,\ell_c$, $k=2,...,k'$ (see for example the configuration in Figure 1.17(c), which is in $\mathscr{I}^{e,s}_{\ell_c-2,\ell_c-1,1}$). The index i in (3.2.20) has to be different from 3 because if the system is in $\mathscr{I}_3^{\alpha}$, then it is not possible to complete the sliding of a bar around the frame-angle. Note that the conditions in (3.2.20) guarantee that these configurations are obtained during a sliding of a bar around a frame-angle, that is identified by the indeces α and α'. Moreover, the index k' denotes the length of the bar that we are sliding. The index k counts the number of particles that are in $r^{\alpha}(\eta)\cup c^{\alpha'\alpha}(\eta)$ during the sliding and can be less or equal than ℓ_c, but for some values of k the set $\mathscr{I}^{\alpha,\alpha'}_{k,k',i}$ can be empty. Our notation does not distinguish whether $\mathscr{I}^{\alpha,\alpha'}_{k,k',i}$ is empty or not in order to avoid the presence of an additional index.

Furthermore, for any $i=-1,0,1,2$ we define the subset $\mathscr{I}_i^{\alpha,\alpha'}$ of the saddles in $\mathcal{P}_i^{fp}$ as the last saddle at the end of a path that describes the sliding of a bar around a frame-angle, i.e., the saddle where the last particle of the bar (protuberance) is detached. (See configuration (12) in the path described in Figure 1.13, imposing $U_1 = U_2 = U$ because we are in the isotropic case). More precisely,

$$\begin{aligned}\mathscr{I}_i^{\alpha,\alpha'} := \{\eta \in \mathcal{P}_i^{fp} \quad &: \exists\, \eta' \in \mathscr{I}^{\alpha,\alpha'}_{2,k',i} \text{ such that } \eta \text{ is obtained from } \eta' \text{ by removing the}\\ &\text{non monotonicity, then removing the protuberance and}\\ &\text{possibly moving the free particle at zero cost}\}, \quad i=-1,0,1,2,\end{aligned} \tag{3.2.21}$$

where $\alpha,\alpha' \in \{n,s,w,e\}$. Again, the indices α and α' identify the frame–angle with respect to which the sliding of the bar takes place. Note that the configuration in Fig. 1.17(a) is in $\mathscr{I}_0^{s,w} \cup \mathscr{I}_0^{e,n}$ and the configuration in Fig. 1.17(b) is in $\mathscr{I}_{-1}^{w,s} \cup \mathscr{I}_{-1}^{w,n} \cup \mathscr{I}_{-1}^{e,n} \cup \mathscr{I}_1^{n,e}$.

In the discussion below [35, Theorem 1.4.3], the authors state that the full identification of the set $\mathcal{G}(\square,\blacksquare)$ is not known. The following result fills this gap.

Theorem 3.2.7. (Union of minimal gates for isotropic interactions). *We obtain the following description for* $\mathcal{G}(\square,\blacksquare)$*:*

$$\mathcal{G}(\square,\blacksquare) = \mathcal{C}^* \cup \bigcup_{i=0}^{3}\bigcup_{\alpha} \mathscr{I}_i^{\alpha} \cup \bigcup_{i=0}^{2}\bigcup_{\alpha,\alpha'}\bigcup_{k,k'} \mathscr{I}^{\alpha,\alpha'}_{k,k',i} \cup \bigcup_{i=-1}^{2}\bigcup_{\alpha,\alpha'} \mathscr{I}_i^{\alpha,\alpha'}. \tag{3.2.22}$$

We refer to Section 3.5 for the proof of the main Theorem 3.2.7.

In [35, Theorem 1.4.3(i)] the authors show that in $\mathcal{S}(\square,\blacksquare)$ there are unessential saddles, also called dead–ends, without fully identifying them, while in Corollary 3.4.4 and Proposition 3.4.5 we identify three types of unessential saddles. Moreover, in Proposition 3.4.2 we prove that $\mathcal{C}^*$ is contained in $\mathcal{G}(\square,\blacksquare)$, which contradicts what is said in the discussion below [35, Theorem 1.4.3].

3.2.3 *Sharp asymptotics*

In this section we investigate the sharp asymptotics concerning the mixing time and spectral gap, and we refer to Section 3.6 for a model–independent argument that provides a correct way to treat the unessential saddles in the computation of the prefactor [32, eq. (1.4.6)].

Recall (1.3.54) and (1.3.55) for the definition of mixing time and spectral gap, respectively.

Theorem 3.2.8. *For any* $\varepsilon \in (0,1)$

$$\lim_{\beta\to\infty} \frac{1}{\beta} \log t_{mix}(\varepsilon) = \Gamma^* = \lim_{\beta\to\infty} -\frac{1}{\beta} \log \rho. \tag{3.2.23}$$

Furthermore, there exist two constants $0 < c_1 \leqslant c_2 < \infty$ *independent of* β *such that for every* $\beta > 0$

$$c_1 e^{-\beta\Gamma^*} \leqslant \rho \leqslant c_2 e^{-\beta\Gamma^*}. \tag{3.2.24}$$

Theorem 3.2.8 holds also for the weakly and strongly anisotropic cases, see Theorems 4.1.7 and 5.1.8, respectively.

3.3 PROOF OF THE MODEL–INDEPENDENT PROPOSITIONS

In this section we give the proof of Propositions 3.1.3 and 3.1.5.

3.3.1 *Proof of Proposition 3.1.3*

We denote by $\sigma_1, ..., \sigma_j$ the saddles in the statement. We want to prove that these saddles are unessential (see Section 3.1.1 point 4 for the definition). Since we can repeat the following argument j times, we may focus on a single configuration σ_i. Consider any $\omega \in (m \to \mathcal{X}^s)_{opt}$ such that $\omega \cap \sigma_i \neq \emptyset$. Since $\mathcal{W}(m, \mathcal{X}^s)$ is a gate for the transition from m to $\mathcal{X}^s$ and $\sigma_i \in \mathcal{S}(m, \mathcal{X}^s) \setminus \mathcal{W}(m, \mathcal{X}^s)$ for any $i = 1, ..., j$, we note that $\{\arg\max_\omega \widehat{H}\} \setminus \{\sigma_i\} \neq \emptyset$. Thus, our strategy consists in finding $\omega' \in (m \to \mathcal{X}^s)_{opt}$ such that $\{\arg\max_{\omega'} \widehat{H}\} \subseteq \{\arg\max_\omega \widehat{H}\} \setminus \{\sigma_i\}$. We analyze separately the two following cases.

Case 1. Suppose that the path ω reaches $\mathcal{S}(m, \mathcal{X}^s)$ for the first time in the configuration $\sigma_i \in \partial\mathcal{C}^m_{\mathcal{X}^s}(\Gamma_m) \cap (\mathcal{S}(m, \mathcal{X}^s) \setminus (\mathcal{W}(m, \mathcal{X}^s) \cup K))$, i.e., there exists the configuration σ_i (as above) such that $\omega = (m, ..., \sigma_i, ..., \eta_1^{(1)}, ..., \mathcal{X}^s)$, where $\eta_1^{(1)} \in \partial\mathcal{C}^m_{\mathcal{X}^s}(\Gamma_m) \cap (\mathcal{W}(m, \mathcal{X}^s) \cup K)$. Any such ω can be written as

$$(m, \omega_1, ..., \omega_{k_1}, \sigma_i, \omega_{k_1+1}, ..., \omega_{k_2}, \gamma_1, \eta_1^{(1)}, ..., \eta_{m_1}^{(1)}, ..., \omega_{k_q}, ..., \omega_{k_{q+1}}, \gamma_q, \eta_1^{(q)}, ..., \eta_{m_q}^{(q)}) \circ \bar{\omega}, \tag{3.3.1}$$

where $\omega_1, ..., \omega_{k_1}, \omega_{k_1+1}, ..., \gamma_1 \in \mathcal{C}^m_{\mathcal{X}^s}(\Gamma_m)$, $\omega_{k_2+1}, ..., \omega_{k_3}, \gamma_2, ..., \omega_{k_q+1}, ..., \omega_{k_{q+1}}$ and γ_q are in $\mathcal{X} \setminus \mathcal{S}(m, \mathcal{X}^s)$, and $\eta_i^{(j)} \in \mathcal{S}(m, \mathcal{X}^s)$ for all $i = 1, ..., m$, $j = 1, ..., q$. At least one among these saddles belongs to $\mathcal{W}(m, \mathcal{X}^s)$ and $\bar{\omega}$ is a path that connects $\eta_{m_q}^{(q)}$ to $\mathcal{X}^s$ such that $\max_{\sigma\in\bar{\omega}} \widehat{H}(\sigma) < \Gamma_m + \widehat{H}(m)$. Note that q and $m_1, ..., m_q$ could be 1. We want to prove that σ_i is unessential, thus we define a new path

$$\omega' = (m, \omega'_1, ..., \omega'_h, \gamma_1, \eta_1^{(1)}, ..., \eta_{m_1}^{(1)}, ..., \omega_{k_q}, ..., \omega_{k_{q+1}}, \gamma_q, \eta_1^{(q)}, ..., \eta_{m_q}^{(q)}) \circ \bar{\omega}, \tag{3.3.2}$$

where $(m, \omega'_1, ..., \omega'_h, \gamma_1)$ is a path that is contained in $\mathcal{C}^m_{\mathcal{X}^s}(\Gamma_m)$ such that its time–reversal exists by [85, Lemma 2.28] with $\eta = \gamma_1$ and $\mathcal{A} = m$. We note that the part of ω' after γ_1 is the same as in equation (3.3.1), thus $\{\arg\max_{\omega'} \widehat{H}\} = \{\eta_1^{(1)}, ..., \eta_{m_1}^{(1)}, ..., \eta_1^{(q)}, ..., \eta_{m_q}^{(q)}\}$ and therefore

$$\{\arg\max_{\omega'} \widehat{H}\} \subseteq \{\arg\max_\omega \widehat{H}\} \setminus \{\sigma_i\}, \quad i = 1, ..., n. \tag{3.3.3}$$

This implies that the saddle σ_i is unessential for any $i = 1, ..., n$ and thus, using [85, Theorem 5.1], $\sigma_i \in \mathcal{S}(m, \mathcal{X}^s) \setminus \mathcal{G}(m, \mathcal{X}^s)$.

Case 2. The path ω reaches $\mathcal{S}(m,\mathcal{X}^s)$ before reaching $\partial\mathcal{C}^m_{\mathcal{X}^s}(\Gamma_m)\cap(\mathcal{S}(m,\mathcal{X}^s)\setminus(\mathcal{W}(m,\mathcal{X}^s)\cup K))$ in σ_i. In this case we can bypass the saddle σ_i by arguing in a similar way as in case 1, indeed we can write the path ω as

$$(m,\omega_1,...,\omega_{k_1},\gamma_1,\eta_1^{(1)},...,\eta_{m_1}^{(1)},...,\sigma_i,...,\gamma_t,\eta_1^{(t)},...,\eta_{m_t}^{(t)},...,\omega_{k_{q+1}},\gamma_q,\eta_1^{(q)},...,\eta_{m_q}^{(q)})\circ\bar{\omega}, \tag{3.3.4}$$

and define

$$\omega'=(m,\omega'_1,...,\omega'_h,\gamma_t,\eta_1^{(t)},...,\eta_{m_t}^{(t)},...,\omega_{k_{q+1}},\gamma_q,\eta_1^{(q)},...,\eta_{m_q}^{(q)})\circ\bar{\omega}, \tag{3.3.5}$$

where $(m,\omega'_1,...,\omega'_h,\gamma_t)$ is a path that is contained in $\mathcal{C}^m_{\mathcal{X}^s}(\Gamma_m)$ such that its time–reversal exists by [85, Lemma 2.28] with $\eta=\gamma_t$ and $\mathcal{A}=m$. Thus,

$$\{\arg\max_{\omega'}\widehat{H}\}=\{\eta_1^{(t)},...,\eta_{m_t}^{(t)},...,\eta_1^{(q)},...,\eta_{m_q}^{(q)}\} \tag{3.3.6}$$

and therefore (3.3.3) holds. □

3.3.2 *Proof of Proposition 3.1.5*

We denote by $\zeta_1,...,\zeta_l$ the saddles in the statement. We want to prove that these saddles are unessential (see Section 3.1.1 point 4 for the definition). Since we can repeat the following argument l times, we may focus on a single configuration ζ_i. Consider any $\omega\in(m\to\mathcal{X}^s)_{opt}$ such that $\omega\cap\zeta_i\neq\emptyset$. Since $\mathcal{W}(m,\mathcal{X}^s)$ is a gate for the transition from m to $\mathcal{X}^s$ and $\zeta_i\in\mathcal{S}(m,\mathcal{X}^s)\setminus\mathcal{W}(m,\mathcal{X}^s)$ for any $i=1,...,j$, we note that $\{\arg\max_\omega\widehat{H}\}\setminus\{\zeta_i\}\neq\emptyset$. Thus, our strategy consists in finding $\omega'\in(m\to\mathcal{X}^s)_{opt}$ such that $\{\arg\max_{\omega'}\widehat{H}\}\subseteq\{\arg\max_\omega\widehat{H}\}\setminus\{\zeta_i\}$. Due to Proposition 3.1.3, we can reduce the proof to consider any $\omega\in(m\to\mathcal{X}^s)_{opt}$ such that the first saddle that is visited is $\eta_1^{(1)}\in\partial\mathcal{C}^m_{\mathcal{X}^s}(\Gamma_m)\cap(\mathcal{W}(m,\mathcal{X}^s)\cup K)$. Note that there exists $\eta_{m_q}^{(q)}\in\partial\mathcal{C}^{\mathcal{X}^s}_m(\Gamma_m+\widehat{H}(m)-\widehat{H}(\mathcal{X}^s))\cap(\mathcal{W}(m,\mathcal{X}^s)\cup\widetilde{K})$, different from ζ_i, that can be connected to the set $\mathcal{L}^G$ via one step of the dynamics. By the model–dependent input (iii) we deduce that ζ_i can be reached either after visiting the set $\mathcal{L}^G$

$$\omega=(m,\omega_1,...,\omega_{k_1},\gamma_1,\eta_1^{(1)},...,\eta_{m_1}^{(1)},...,\omega_{k_q},...,\omega_{k_{q+1}},\gamma_q,\eta_1^{(q)},...,\eta_{m_q}^{(q)},\eta^G,...,\zeta_i)\circ\tilde{\omega}, \tag{3.3.7}$$

or directly from $\eta_{m_q}^{(q)}$

$$\omega=(m,\omega_1,...,\omega_{k_1},\gamma_1,\eta_1^{(1)},...,\eta_{m_1}^{(1)},...,\omega_{k_q},...,\omega_{k_{q+1}},\gamma_q,\eta_1^{(q)},...,\eta_{m_q}^{(q)},\zeta_i,...,\bar{\eta}^G)\circ\bar{\omega}, \tag{3.3.8}$$

where $\omega_1,...,\omega_{k_1},\gamma_1\in\mathcal{C}^m_{\mathcal{X}^s}(\Gamma_m)$ and $\omega_{k_1+1},...,\omega_{k_2},\gamma_2,...,\omega_{k_q+1},...,\omega_{k_{q+1}}\in\mathcal{X}\setminus\mathcal{S}(m,\mathcal{X}^s)$. Additionally, the configurations $\eta_i^{(j)}\in\mathcal{S}(m,\mathcal{X}^s)$ for all $i=1,...,m$, $j=1,...,q$ and at least one among these saddles belongs to $\mathcal{W}(m,\mathcal{X}^s)$. Moreover, η^G (resp. $\bar{\eta}^G$) is in $\mathcal{L}^G$ and $\tilde{\omega}$ (resp. $\bar{\omega}$) is a path that connects ζ_i (resp. $\bar{\eta}^G$) to $\mathcal{X}^s$. Note that q and $m_1,...,m_q$ could be 1. We want to prove that ζ_i is unessential, thus for both ω in (3.3.7) and (3.3.8) we define a new path

$$\omega'=(m,\omega_1,...,\omega_{k_1},\gamma_1,\eta_1^{(1)},...,\eta_{m_1}^{(1)},...,\omega_{k_q},...,\omega_{k_{q+1}},\gamma_q,\eta_1^{(q)},...,\eta_{m_q}^{(q)},\eta^G)\circ\hat{\omega}, \tag{3.3.9}$$

where by the model–dependent input (iii)-(a) there exists a path $\hat{\omega}$ that connects η^G to $\mathcal{X}^s$ such that

$$\max_{\sigma\in\hat{\omega}}\widehat{H}(\sigma)<\Gamma_m+\widehat{H}(m). \tag{3.3.10}$$

Thus, $\{\arg\max_{\omega'}\widehat{H}\}=\{\eta_1^{(1)},...,\eta_{m_1}^{(1)},...,\eta_1^{(q)},...,\eta_{m_q}^{(q)}\}$ and therefore

$$\{\arg\max_{\omega'}\widehat{H}\}\subseteq\{\arg\max_\omega\widehat{H}\}\setminus\{\zeta_i\},\quad i=1,...,n. \tag{3.3.11}$$

This implies that the saddle ζ_i is unessential for any $i=1,...,n$ and thus, using [85, Theorem 5.1], $\zeta_i\in\mathcal{S}(m,\mathcal{X}^s)\setminus\mathcal{G}(m,\mathcal{X}^s)$. □

3.4 MODEL-DEPENDENT STRATEGY

Recall equations (1.3.35)-(1.3.38) and Definition 1.3.4. In this section we give a useful lemma that helps us to characterize the gates and we present our model-dependent strategy to characterize the union of all the minimal gates $\mathcal{G}(\square, \blacksquare)$. Below we state Lemma 3.4.1 for the isotropic case, but it holds also for the anisotropic cases (see Lemmas 4.2.3 and 5.2.3).

Lemma 3.4.1. *Starting from $\mathcal{C}^* \setminus \Omega^{fp}$, if the free particle is attached to a bad site obtaining $\eta^B \in \mathcal{C}^B$, the only transitions that do not exceed the energy Γ^* are either detaching the protuberance, or a sequence of 1-translations of a bar or slidings of a bar around a frame-angle. Moreover, we get:*

(i) if it is possible to slide a bar around a frame-angle, then the saddles that are crossed are essential;

(ii) if it is not possible to slide a bar around a frame-angle, then the path must come back to the starting configuration and the saddles that are crossed are unessential.

Proof. Let $\eta^B \in \mathcal{C}^B$ the configuration obtained by attaching the free particle as a protuberance to a bar, thus $\widehat{H}(\eta^B) = \Gamma^* - U$. Note that it is impossible to move particles in $\partial^- CR(\eta^B)$ before further lowering the energy, since this move costs at least $2U$. Moreover, it is impossible to create a new particle before further lowering the energy, since this move costs Δ. On the other hand there are no moves available to lower the energy. If the protuberance is detached, then the energy reaches the value Γ^*. Analyzing motions of particles along the border of the droplet (both sequence of 1-translations of a bar and sliding around a frame-angle), the energy raises by U at the first step, it is constant in the following steps but the last, when it decreases by U. Thus, these are admissible moves.

First, we prove (i). Let $\xi_1^{(e)}, ..., \xi_m^{(e)} \notin \mathcal{C}^*$ the saddles visited during the sliding of a bar around a frame-angle. We want to prove that these saddles are essential (see Section 3.1.1 point 4 for the definition). Since we can repeat the following argument m times, we may focus on a single configuration $\xi_i^{(e)}$. Since $\mathcal{C}^*$ is a gate for the transition and $\xi_i^{(e)} \in \mathcal{S}(\square, \blacksquare) \setminus \mathcal{C}^*$ for any $i = 1, ..., m$, we note that a path $\omega \in (\square \to \blacksquare)_{opt}$ such that $\{\arg\max_\omega \widehat{H}\} = \{\xi_i^{(e)}\}$ does not exist. Thus, our strategy consists in finding a path $\omega \in (\square \to \blacksquare)_{opt}$ such that for any $\omega' \in (\square \to \blacksquare)_{opt}$

$$\omega \cap \xi_i^{(e)} \neq \emptyset \text{ and } \{\arg\max_{\omega'} \widehat{H}\} \not\subseteq \{\arg\max_\omega \widehat{H}\} \setminus \{\xi_i^{(e)}\}, \quad i = 1, ..., m. \tag{3.4.1}$$

Let η^B be the union of a cluster $\eta \in \mathcal{D}$ and a protuberance attached to one of its bars in a site with coordinates (i, j). Without loss of generality assume that the bar is $B^n(\eta)$ and that $|c^{wn}(\eta)| = 1$, otherwise a sequence of 1-translations of the bars $B^n(\eta)$ and $B^w(\eta)$ can take place before creating the free particle in order to obtain $|c^{wn}(\eta)| = 1$. Note that during these translations the path does not cross any saddle. We define the specific path ω of the strategy above as

$$\omega = (\square, \omega_1, ..., \omega_k, \eta, \eta_1, ..., \eta_{L-j-2}, \eta^B, \xi_1^{(e)}, ..., \xi_m^{(e)}) \circ \bar{\omega}, \tag{3.4.2}$$

where $\omega_1, ..., \omega_k \in \mathcal{C}^{\square}_{\blacksquare}(\Gamma^*)$, $\eta \in \mathcal{D}$, $\eta_1 \in \mathcal{C}^*(L-j-1), ..., \eta_{L-j-2} \in \mathcal{C}^*(2)$, $\eta^B \in \mathcal{C}^B(\hat{\eta}_{L-j-2})$ (see Figure 3.4 for a picture of this situation) and $\bar{\omega}$ is a path that connects $\xi_m^{(e)}$ to $\blacksquare$ such that $\max_{\sigma \in \bar{\omega}} \widehat{H}(\sigma) \leqslant \Gamma^*$. Now we show that for any ω' the condition (3.4.1) is satisfied. If ω' passes through the configuration $\xi_i^{(e)}$, $\{\arg\max_{\omega'} \widehat{H}\} \supseteq \{\xi_i^{(e)}\}$, thus (3.4.1) is satisfied. Therefore we can assume that $\omega' \cap \xi_i^{(e)} = \emptyset$. If ω' crosses the set $\mathcal{S}(\square, \blacksquare)$ through a configuration $\widetilde{\eta}$ such that $\widetilde{\eta} \cap \omega = \emptyset$, then the condition (3.4.1) holds. In the sequel ω' visits the configurations $\eta_1, ..., \eta_{L-j-2} \in \mathcal{C}^*$. Starting from η_{L-j-2}, there are four allowed directions for moving the free particle. If we move it in the direction of the cluster (south in Figure 3.4), we deduce that the path ω' visits the configuration η^B. For the other three choices, the free particle still remains free after the move, indeed by construction of the path ω, starting from η_{L-j-2} it is not possible to reach the set $\mathcal{C}^G$ via one step of the dynamics. Thus, the path ω' can visit either a saddle not already visited by ω (west or east in Figure 3.4) or a saddle that has been already visited by ω (north in Figure 3.4). In the first case, we obtain that (3.4.1) is satisfied. In the latter case, we can iterate this argument and, since ω' goes from $\square$ to $\blacksquare$, we can assume that the path ω' visits the configuration $\eta^B \in \mathcal{C}^B(\hat{\eta}_{L-j-2})$. From now on, starting from η^B, there are two possible scenarios:

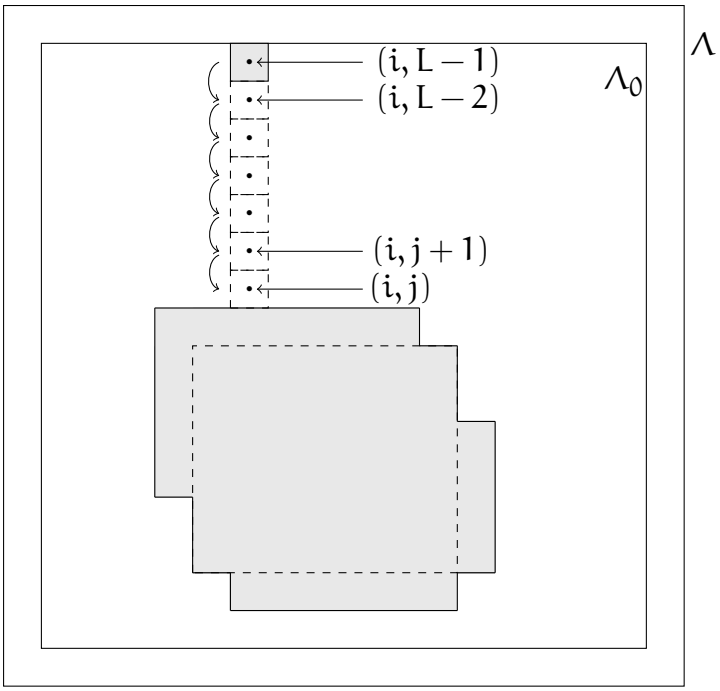

Figure 3.4 – Here we depict the configuration η_1 that consists of a cluster $\eta \in \mathcal{D}$ union a free particle, in grey, that is in position $(i, L-1)$. The dotted unit squares represent the following positions of the free particle that moves as represented by the arrows on the left, until the particle is attached to the cluster in position (i, j). The latter is the configuration η^B.

I. ω' activates the same sliding of a bar around a frame-angle as ω;
II. ω' activates a sliding of a bar around a frame-angle different from ω.

In case I, since $\omega' \cap \xi_i^{(e)} = \emptyset$, the sliding of a bar around a frame-angle has been stopped before hitting $\xi_i^{(e)}$. Thus, we can assume that ω' comes back to η^B, otherwise the energy exceeds Γ^*. Since the path ω' must reach $\blacksquare$, starting from η^B the protuberance is detached and in the sequel is attached in another site. Thus, ω' reaches a saddle that is not visited by ω. This implies that (3.4.1) is satisfied.

In case II, when the path ω' initiates the sliding of a bar around a frame-angle, it reaches at the first step a saddle that it is not visited by ω, thus the condition (3.4.1) is satisfied. Therefore the unique possibility is not to start this sliding and thus the path ω' must come back to η^B, since it has to reach $\blacksquare$. From now on, as before, the path ω' has to detach the protuberance that in the sequel is attached in another site, thus ω' visits a saddle that is not visited by ω. This implies that (3.4.1) is satisfied. Thus, we have proved that the saddle $\xi_i^{(e)}$ is essential for any $i = 1, ..., m$.

Finally, we prove (ii). By assumptions we know that it is not possible to complete a sliding of a bar around a frame–angle and thus this sliding must stop. Let $\xi_1^{(ne)}, ..., \xi_n^{(ne)}$ the saddles that are visited during this motion, we want to prove that these saddles are unessential (see Section 3.1.1 point 4 for the definition). Since we can repeat the following argument n times, we may focus on a single configuration $\xi_i^{(ne)}$. Consider any $\omega \in (\square \to \blacksquare)_{opt}$ such that $\omega \cap \xi_i^{(ne)} \neq \emptyset$. Since $\mathcal{C}^*$ is a gate for the transition from $\square$ to $\blacksquare$ and $\xi_i^{(ne)} \in \mathcal{S}(\square, \blacksquare) \setminus \mathcal{C}^*$ for any $i = 1, ..., n$, we note that $\{\arg\max_\omega \widehat{H}\} \setminus \{\xi_i^{(ne)}\} \neq \emptyset$. Thus, our strategy consists in finding $\omega' \in (\square \to \blacksquare)_{opt}$ such that $\{\arg\max_{\omega'} \widehat{H}\} \subseteq \{\arg\max_\omega \widehat{H}\} \setminus \{\xi_i^{(ne)}\}$. Starting from $\xi_i^{(ne)}$, the unique admissible moves in order to not exceed Γ^* are the time–reversal of the previous moves. This implies that the path must come back to the starting configuration η^B. Thus, we can write

$$\omega = (\square, \omega_1, ..., \omega_k, \gamma_1, ..., \gamma_l, \eta, \eta^B, \xi_1^{(ne)}, ..., \xi_i^{(ne)}, .., \xi_1^{(ne)}, \eta^B) \circ \bar{\omega}, \tag{3.4.3}$$

where $\omega_1, ..., \omega_k \in \mathcal{C}^{\square}_{\blacksquare}(\Gamma^*)$, $\gamma_1, ..., \gamma_l \in \mathcal{X} \setminus \mathcal{C}^{\blacksquare}_{\square}(\Gamma^* - \widehat{H}(\mathcal{X}^s))$ such that $H(\gamma_i) \leqslant \Gamma^*$ for any $i = 1, ..., l$ and $\eta \in \mathcal{C}^*$, $\eta^B \in \mathcal{C}^B(\hat{\eta})$ and $\bar{\omega}$ is a path that connects η^B to $\blacksquare$ such that $\max_{\sigma \in \bar{\omega}} \widehat{H}(\sigma) \leqslant$

Γ^*. For this path we define a new path $\omega' = (\square, \omega_1, ..., \omega_k, \gamma_1, ..., \gamma_l, \eta, \eta^B) \circ \bar{\omega}$. Thus, we deduce that $\{\arg\max_{\omega'} \widehat{H}\} \subseteq \{\arg\max_{\omega} \widehat{H}\} \setminus \{\xi_i^{(ne)}\}$, which implies that the saddle $\xi_i^{(ne)}$ is unessential for any $i = 1, .., n$. □

Our goal is to characterize the union of all the minimal gates. To this end, due to [85, Theorem 5.1], we will characterize all the essential saddles for the transition from the metastable to the stable state. In this section we apply the model–independent strategy explained in Section 3.1.2 in order to identify some unessential saddles. We apply (3.1.15) both for $\sigma = \square$, $\mathcal{A} = \{\blacksquare\}$ and $\Gamma_m = \Gamma^*$ defining $\mathcal{C}^{\square}_{\blacksquare}(\Gamma^*)$, and for $\sigma = \blacksquare$, $\mathcal{A} = \{\square\}$ and $\Gamma_m = \Gamma^* - \widehat{H}(\blacksquare)$ defining $\mathcal{C}^{\blacksquare}_{\square}(\Gamma^* - \widehat{H}(\blacksquare))$. We chose this notation in order to emphasize the dependence on Γ^*. First, we the required model–dependent inputs (iii)-(a) and (iii)-(b) in Section 3.1.2 are satisfied thanks to [35, Proposition 2.3.9]. Second, by [35, Theorem 1.3.3(iii)], we know that $\mathcal{C}^*$ is a gate for the transition from $\square$ to $\blacksquare$. Thus, we apply the model–independent strategy explained in Section 3.1.2 to Kawasaki dynamics by taking $m = \square$, $\mathcal{X}^s = \{\blacksquare\}$, $\mathcal{W}(m, \mathcal{X}^s) = \mathcal{C}^*$, $\mathcal{L}^B = \mathcal{C}^B$ and $\mathcal{L}^G = \mathcal{C}^G$. In Proposition 3.4.2 we prove that $\mathcal{C}^* \subseteq \mathcal{G}(\square, \blacksquare)$, that allows us to study the essentiality only of the saddles that are not in $\mathcal{C}^*$.

In order to apply Propositions 3.1.3 and 3.1.5, we need to characterize the sets K and $\widetilde{K}$ (see (3.1.16) and (3.1.17), respectively, for the definitions) for our models. This is done in Proposition 3.4.3. Due to this result, our strategy consists in partitioning the saddles that are not in $\mathcal{C}^*$ in three types: the saddles that are in the boundary of $\mathcal{C}^{\square}_{\blacksquare}(\Gamma^*)$, i.e., $\sigma \in \partial\mathcal{C}^{\square}_{\blacksquare}(\Gamma^*) \cap (\mathcal{S}(\square, \blacksquare) \setminus \mathcal{C}^*)$, the saddles that are in the boundary of $\mathcal{C}^{\blacksquare}_{\square}(\Gamma^* - \widehat{H}(\blacksquare))$ and not in $\widetilde{K}$, i.e., $\zeta \in \partial\mathcal{C}^{\blacksquare}_{\square}(\Gamma^* - \widehat{H}(\blacksquare)) \cap (\mathcal{S}(\square, \blacksquare) \setminus (\mathcal{C}^* \cup \widetilde{K}))$, and the remaining saddles $\xi \in \mathcal{S}(\square, \blacksquare) \setminus (\partial\mathcal{C}^{\square}_{\blacksquare}(\Gamma^*) \cup (\partial\mathcal{C}^{\blacksquare}_{\square}(\Gamma^* - \widehat{H}(\blacksquare)) \setminus \widetilde{K}) \cup \mathcal{C}^*)$. By Propositions 3.1.3 and 3.1.5, we obtain Corollary 3.4.4 that states that the saddles of the first and second types are respectively unessential. In Proposition 3.4.5 we highlight some of the saddles of type three that are unessential. This analysis is different when we are dealing with isotropic or weakly anisotropic interactions, and with strongly anisotropic interactions due to the different mechanisms to enter $\mathcal{C}^*$ (see [35, Proposition 2.3.7], Lemma 4.3.7 and Lemma 5.3.8, respectively). For the anisotropic cases this strategy is presented in Sections 4.3 and 5.3. Finally, we identify the essential saddles of the third type in Proposition 3.5.1.

3.4.1 *Main Propositions*

In this section we give the main results for our model–dependent strategy. We refer to Section 3.4.3 for the proof of these propositions.

Proposition 3.4.2. $\mathcal{C}^* \subseteq \mathcal{G}(\square, \blacksquare)$.

Proposition 3.4.2 holds also in the weakly and strongly anisotropic regimes, see Propositions 4.3.2 and 5.3.2, respectively.

Proposition 3.4.3. *The following statements hold.*

(i) $K = \emptyset$;

(ii) $\widetilde{K} \cap \partial\mathcal{C}^{\blacksquare}_{\square}(\Gamma^* - \widehat{H}(\blacksquare)) = \{\eta \in \bigcup_i \bigcup_{\alpha,\alpha'} \mathscr{I}_i^{\alpha,\alpha'} \setminus \mathcal{C}^* :$ *it is possible to attach the free particle in* $\partial^- CR(\eta)$ *via one step of the dynamics*$\} =: \bar{\mathscr{I}}$;

For the corresponding result of Proposition 3.4.3 for the anisotropic regimes, see Propositions 4.3.3 and 5.3.3.

Corollary 3.4.4. *The following statements hold.*

(i) The saddles of the first type $\sigma \in \partial\mathcal{C}^{\square}_{\blacksquare}(\Gamma^*) \cap (\mathcal{S}(\square, \blacksquare) \setminus \mathcal{C}^*)$ *are unessential;*

(ii) The saddles of the second type $\zeta \in \partial\mathcal{C}^{\blacksquare}_{\square}(\Gamma^* - \widehat{H}(\blacksquare)) \cap (\mathcal{S}(\square, \blacksquare) \setminus (\mathcal{C}^* \cup \bar{\mathscr{I}}))$ *are unessential;*

Proof. Combining Propositions 3.1.3, 3.1.5 and 3.4.3 we get the claim. □

Proposition 3.4.5. *Any saddle* ξ *that is neither in* $\mathcal{C}^*$, *nor in the boundary of the cycle* $\mathcal{C}^{\square}_{\blacksquare}(\Gamma^*)$, *nor in* $\partial\mathcal{C}^{\blacksquare}_{\square}(\Gamma^* - \widehat{H}(\blacksquare)) \setminus \widetilde{K}$, *i.e.,* $\xi \in \mathcal{S}(\square, \blacksquare) \setminus (\partial\mathcal{C}^{\square}_{\blacksquare}(\Gamma^*) \cup (\partial\mathcal{C}^{\blacksquare}_{\square}(\Gamma^* - \widehat{H}(\blacksquare)) \setminus \widetilde{K}) \cup \mathcal{C}^*)$, *such that* $\tau_\xi < \tau_{\mathcal{C}^B}$ *is unessential. Therefore it is not in* $\mathcal{G}(\square, \blacksquare)$.

For the corresponding result of Proposition 3.4.5 for the anisotropic regimes, see Propositions 4.3.5 and 5.3.5.

3.4.2 *Useful Lemmas for the model-dependent strategy*

In this section we give some useful lemmas about the entrance in the gate and the minimality of the sets $\mathcal{C}^*(i)$ with $i = 3, ..., L^*$. We stress that the behavior for isotropic and weakly anisotropic interactions is very different from that observed for strongly anisotropic interactions, indeed we note that the weakly anisotropic model has some characteristics similar to the isotropic and some similar to the strongly anisotropic model. For the corresponding results obtained in the anisotropic cases we refer to Sections 4.3.2 and 5.3.2.

[35, Proposition 2.3.7] investigates how the entrance in $\mathcal{C}^*$ occurs for the isotropic regime. We encourage the reader to inspect the difference between this proposition and Lemma 4.3.7. and Lemma 5.3.8, where the peculiar entrance in the gate for the strongly anisotropic case is analyzed.

We refer to Section 3.4.4 for the proof of the remaining lemmas. In Lemma 3.4.6 we correct the statement in [35, eq. (3.5.5)] for $\mathcal{C}^*(i)$ with $i = 3, ..., L^*$. Concerning $\mathcal{C}^*(2)$, in Lemma 3.4.8, we replace the minimality of the gate $\mathcal{C}^*(2)$ with the sentence "$\mathcal{C}^*(2)$ is composed by essential saddles". We stress that this correction does not effect the results where the statement was used in [35].

Lemma 3.4.6. *$\mathcal{C}^*(i)$ is a minimal gate for any $i = 3, ..., L^*$.*

Remark 3.4.7. *In the strongly anisotropic case, the statement of Lemma 3.4.6 does not hold. A different result is derived in Lemma 5.3.9.*

Lemma 3.4.8. *The saddles in $\mathcal{C}^*(2)$ are essential.*

3.4.3 *Proof of Propositions*

Proof of Proposition 3.4.2. By Lemma 3.4.8 we know that the saddles in $\mathcal{C}^*(2)$ are essential and thus are in $\mathcal{G}(\square, \blacksquare)$ due to [85, Theorem 5.1]. Moreover, by Lemma 3.4.6 we know that the set $\mathcal{C}^*(i)$ is a minimal gate for any $i = 3, ..., L^*$, thus

$$\mathcal{C}^* = \mathcal{C}^*(2) \cup \bigcup_{i=3}^{L^*} \mathcal{C}^*(i) \subseteq \mathcal{G}(\square, \blacksquare). \tag{3.4.4}$$

□

Proof of Proposition 3.4.3. (i) To prove that $K = \emptyset$ we argue by contradiction. Let $\bar{\eta} \in K$, thus there exist $\eta \in \mathcal{C}^*$ and $\omega = \omega_1 \circ \omega_2$ from η to $\square$ with the properties described in (3.1.16), where $\circ$ denotes the composition of two paths. We know that η is composed by the union of a protocritical droplet in $\mathcal{D}$ and a free particle. Since $\omega_1 \cap \mathcal{C}^* = \{\eta\}$, we note that the free particle must be in Λ^-, otherwise the free particle has to cross at least Λ^- and $\partial\Lambda^-$, the latter in the configuration $\eta' \in \mathcal{C}^*$, with $\eta' \neq \eta$, which contradicts the conditions in (3.1.16). Therefore, starting from η, by the optimality of the path we deduce that the unique admissible move is to remove the free particle. The configuration that is obtained in this way is in $\mathcal{D}$, that belongs to $\mathcal{C}^{\square}_{\blacksquare}(\Gamma^*)$, which is absurd since (3.1.16) requires that $\omega_1 \cap \mathcal{C}^{\square}_{\blacksquare}(\Gamma^*) = \emptyset$. Thus, it is not possible to find such ω_1 and ω_2, therefore $K = \emptyset$.

(ii) Let $\bar{\eta} \in \widetilde{K} \cap \partial\mathcal{C}^{\blacksquare}_{\square}(\Gamma^* - \widehat{H}(\blacksquare))$. By the definition of the set $\widetilde{K}$ we know that there exist $\eta \in \mathcal{C}^*$ and $\omega = \omega_1 \circ \omega_2$ from η to $\blacksquare$ with the properties described in (3.1.17). We know that η is composed by the union of a protocritical droplet $\hat{\eta} \in \mathcal{D}$ and a free particle. Since $\omega_1 \cap \mathcal{C}^* = \{\eta\}$, we note that $\eta \in \mathcal{C}^*(2)$, otherwise the free particle has to cross at least $\bar{B}_2(\hat{\eta})$ and $\bar{B}_3(\hat{\eta})$, the latter in the configuration $\eta' \in \mathcal{C}^*$, with $\eta' \neq \eta$, which contradicts the conditions in (3.1.17). Therefore, starting from η, by the optimality of the path we deduce that the unique admissible move is to attach the free particle to the cluster. If $\bar{\eta}$ is obtained from η by attaching the free particle in a good site giving rise to a configuration in $\mathcal{C}^G(\hat{\eta})$, by [35, Proposition 2.3.9(i)] we know that $\omega_1 \cap \mathcal{C}^{\blacksquare}_{\square}(\Gamma^* - \widehat{H}(\blacksquare)) \neq \emptyset$, that contradicts (3.1.17), thus it is not possible to find such ω_1 and ω_2, therefore $\bar{\eta} \notin \widetilde{K}$, which is in contradiction with the assumption.

Assume now that $\bar{\eta}$ is obtained from η by attaching the free particle in a bad site giving rise to a configuration in $\mathcal{C}^B(\hat{\eta})$. If $\eta \in \Omega^{fp}$, then by [35, Proposition 2.3.8(ii)] the unique

admissible move is the reverse one, thus we may assume that $\eta \in \mathcal{C}^* \setminus \mathcal{Q}^{fp}$ and that the path does not go back to η, otherwise we can iterate this argument for a finite number of steps since the path has to reach $\blacksquare$. Starting from η, by Lemma 3.4.1 we know that $\bar{\eta}$ is obtained either via a sequence of 1-translations of a bar or via a sliding of a bar around a frame-angle. If a sequence of 1-translations takes place, by the optimality of the path we deduce that the unique possibility is either detaching the protuberance or sliding a bar around a frame-angle. In the first case the configuration that is obtained is in $\mathcal{C}^*$ and thus $\bar{\eta} \notin \widetilde{K}$, which contradicts the assumption.

Consider now the case in which a sliding of a bar around a frame–angle takes place. The configurations visited by the path ω during this sliding are $\bar{\eta}_1, ..., \bar{\eta}_m \in \mathscr{I}_{k,k',i}^{\alpha,\alpha'}$ for some $\alpha, \alpha' \in \{n, s, w, e\}$, $k' = 2, ..., \ell_c$ and $k = 2, ..., k'$, while the last configuration is a saddle $\widetilde{\eta} \in \mathscr{I}_i^{\alpha,\alpha'}$ when the last particle of the bar is detached. Thus, $\{\bar{\eta}_1, ..., \bar{\eta}_m\} \cap \partial\mathcal{C}_{\square}^{\blacksquare}(\Gamma^* - \widehat{H}(\blacksquare)) = \emptyset$. Starting from $\widetilde{\eta}$, the free particle can move and be attached in $\partial^+ CR(\widetilde{\eta})$ and another sliding of a bar around a frame–angle can take place. If this is the case, as proved above the saddles visited during this motion are not in $\partial\mathcal{C}_{\square}^{\blacksquare}(\Gamma^* - \widehat{H}(\blacksquare))$ except the last configuration $\widetilde{\widetilde{\eta}}$ visited during the sliding, that is a saddle, if $\mathbb{P}(\widetilde{\widetilde{\eta}}, \mathcal{C}^G) > 0$. Thus, the unique possibility to have $\bar{\eta} \in \widetilde{K} \cap \partial\mathcal{C}_{\square}^{\blacksquare}(\Gamma^* - \widehat{H}(\blacksquare))$ is that $\bar{\eta} \in \mathscr{I}_i^{\alpha,\alpha'} \setminus \mathcal{C}^*$ and it is possible to attach the free particle in $\partial^- CR(\bar{\eta})$ via one step of the dynamics. Taking the union over all $i \in \{-1, 0, 1, 2\}$ and $\alpha, \alpha' \in \{n, s, w, e\}$, we get the claim. □

Proof of Proposition 3.4.5. We denote by $\xi_1, ..., \xi_n$ the saddles in the statement. We want to prove that these saddles are unessential (see Section 3.1.1 point 4 for the definition). Since we can repeat the following argument n times, we may focus on a single configuration ξ_i. Consider any $\omega \in (\square \to \blacksquare)_{opt}$ such that $\omega \cap \xi_i \neq \emptyset$. By hypotheses, we have to analyze only the case in which the path ω reaches the saddle ξ_i before reaching $\mathcal{C}^B$. Since $\mathcal{C}^*$ is a gate for the transition and $\xi_i \in \mathcal{S}(\square, \blacksquare) \setminus \mathcal{C}^*$, we note that $\{\arg\max_\omega \widehat{H}\} \setminus \{\xi_i\} \neq \emptyset$. Thus, our strategy consists in finding $\omega' \in (\square \to \blacksquare)_{opt}$ such that $\{\arg\max_{\omega'} \widehat{H}\} \subseteq \{\arg\max_\omega \widehat{H}\} \setminus \{\xi_i\}$.

First, assume that ω reaches the saddle ξ_i before reaching $\mathcal{C}^G$ and thus ξ_i must be obtained by a configuration $\eta \in \mathcal{C}^*$ without attaching the free particle. In particular, [35, Propositions 2.3.7 and 2.3.8(ii)] imply that the only possibility is that η is composed by the union of a cluster $\hat{\eta} \in \mathcal{Q}$ and a free particle at distance 2 from the cluster. Moreover, ξ_i is the union of a quasi–square $(\ell_c - 1) \times \ell_c$ with a dimer. Thus, starting from ξ_i, by [35, Proposition 2.3.8(ii)] we know that the only transition that does not raise the energy is the reverse move giving rise to the configuration η. Thus by Lemma [35, Proposition 2.3.7] we can write

$$\omega = (\square, \omega_1, ..., \omega_{k_1}, \gamma_1, \eta_1^{(1)}, ..., \eta_{m_1}^{(1)}, ..., \omega_{k_q}, \gamma_q, \eta_1^{(q)}, ..., \eta_{m_q}^{(q)}, \eta, \xi_i, \eta) \circ \bar{\omega}, \tag{3.4.5}$$

where $\omega_1, ..., \omega_{k_1}, ..., \omega_{k_q} \in \mathcal{C}_{\blacksquare}^{\square}(\Gamma^*)$, $\gamma_1, ..., \gamma_q \in \mathcal{D}$, $\eta_1^{(1)}, ..., \eta_{m_1}^{(1)}, ..., \eta_1^{(q)}, ..., \eta_{m_q}^{(q)} \in \mathcal{C}^*$ and $\bar{\omega}$ is a path that connects η to $\blacksquare$ such that $\max_{\sigma \in \bar{\omega}} \widehat{H}(\sigma) \leqslant \Gamma^*$. We define a new path

$$\omega' = (\square, \omega_1, ..., \omega_{k_1}, \gamma_1, \eta_1^{(1)}, ..., \eta_{m_1}^{(1)}, ..., \omega_{k_q}, ..., \omega_{k_{q+1}}, \gamma_q, \eta_1^{(q)}, ..., \eta_{m_q}^{(q)}, \eta) \circ \bar{\omega}. \tag{3.4.6}$$

Thus, $\{\arg\max_{\omega'} \widehat{H}\} = \{\eta_1^{(1)}, ..., \eta_{m_1}^{(1)}, ..., \eta_1^{(q)}, ..., \eta_{m_q}^{(q)}, \eta\} \cup \{\arg\max_{\bar{\omega}} \widehat{H}\}$ and therefore

$$\{\arg\max_{\omega'} \widehat{H}\} \subseteq \{\arg\max_{\omega} \widehat{H}\} \setminus \{\xi_i\}, \quad i = 1, ..., n. \tag{3.4.7}$$

This implies that the saddle ξ_i is unessential for any $i = 1, ..., n$ and thus, using [85, Theorem 5.1], $\xi_i \in \mathcal{S}(\square, \blacksquare) \setminus \mathcal{G}(\square, \blacksquare)$.

Finally, if the path ω reaches the saddle ξ_i after reaching $\mathcal{C}^G$ in the configuration η^G, we can write

$$\omega = (\square, \omega_1, ..., \omega_{k_1}, \gamma_1, \eta_1^{(1)}, ..., \eta_{m_1}^{(1)}, ..., \eta_1^{(q)}, ..., \eta_{m_q}^{(q)}, \eta^G, ..., \xi_i, ..., \blacksquare) \tag{3.4.8}$$

and define

$$\omega' = (\square, \omega_1, ..., \omega_{k_1}, \gamma_1, \eta_1^{(1)}, ..., \eta_{m_1}^{(1)}, ..., \eta_1^{(q)}, ..., \eta_{m_q}^{(q)}, \eta^G) \circ \widetilde{\omega}, \tag{3.4.9}$$

where $\widetilde{\omega}$ is a path such that $\max_{\sigma \in \widetilde{\omega}} \widehat{H}(\sigma) < \Gamma^*$. This path exists by [35, Proposition 2.3.9(i)]. It easy to check that the saddle ξ_i is unessential for any $i = 1, ..., n$ and thus, using [85, Theorem 5.1], $\xi_i \in \mathcal{S}(\square, \blacksquare) \setminus \mathcal{G}(\square, \blacksquare)$. □

3.4.4 *Proof of Lemma 3.4.8*

Let $\xi_1, ..., \xi_n$ the saddles in $\mathcal{C}^*(2)$, we want to prove that these saddles are essential (see Section 3.1.1 point 4 for the definition). Since we can repeat the following argument n times, we may focus on a single configuration ξ_i. We note that a path $\omega \in (\square \to \blacksquare)_{opt}$ such that $\{\arg\max_\omega \widehat{H}\} = \{\xi_i\}$ does not exist, thus our strategy consists in finding a path $\omega \in (\square \to \blacksquare)_{opt}$ such that for any $\omega' \in (\square \to \blacksquare)_{opt}$

$$\omega \cap \xi_i \neq \emptyset \text{ and } \{\arg\max_{\omega'} \widehat{H}\} \not\subseteq \{\arg\max_\omega \widehat{H}\} \setminus \{\xi_i\}, \quad i = 1, ..., n. \tag{3.4.10}$$

Let ξ_i be the union of a cluster $\eta \in \mathcal{D}$ and a free particle in a site with coordinates (i, j) at lattice distance 2 from the cluster. We define the specific path ω of the strategy above as

$$\omega = (\square, \omega_1, ..., \omega_k, \eta, \eta_1, ..., \eta_{L-j-3}, \xi_i, \eta^{(1)}, ..., \eta^{(k)}, \eta^G) \circ \bar{\omega}, \tag{3.4.11}$$

where $\omega_1, ..., \omega_k \in \mathcal{C}^{\square}_{\blacksquare}(\Gamma^*)$, $\eta \in \mathcal{D}$, $\eta_1 \in \mathcal{C}^*(L-j-1), ..., \eta_{L-j-3} \in \mathcal{C}^*(3)$, $\eta^{(1)}, ..., \eta^{(k)} \in \mathcal{C}^*$, $\eta^G \in \mathcal{C}^G(\hat{\eta}^{(k)})$ and $\bar{\omega}$ a path that connects η^G to $\blacksquare$ such that $\max_{\sigma \in \bar{\omega}} \widehat{H}(\sigma) < \Gamma^*$. Note that the part of the path ω from ξ_i to $\eta^{(k)}$ is constructed by moving the free particle at zero cost from (i, j) to a good site depicted in Figure 1.15, so that we obtain a configuration η^G. Moreover, the path $\bar{\omega}$ exists by [35, Proposition 2.3.9(i)]. Now we show that for any ω' condition (3.4.10) is satisfied. If ω' passes through the configuration ξ_i, then $\{\arg\max_{\omega'} \widehat{H}\} \supseteq \{\xi_i\}$, thus (3.4.10) is satisfied. Therefore we can assume that $\omega' \cap \xi_i = \emptyset$. If ω' crosses the set $\mathcal{S}(\square, \blacksquare)$ through a configuration $\widetilde{\eta}$ such that $\omega \cap \widetilde{\eta} = \emptyset$, then condition (3.4.10) holds. Thus, we can reduce our analysis to ω' that visits all the configurations $\eta_1, ..., \eta_{L-j-3} \in \mathcal{C}^*$. Starting from $\eta_{L-j-3} \in \mathcal{C}^*(3)$, there are four allowed directions for moving the free particle. The move cannot be in the direction of the cluster, indeed in that case the path ω' visits $\xi_i \in \mathcal{C}^*(2)$. Concerning the other three choices, we have two cases. In the first case, the path ω' visits a saddle not already present in ω, thus (3.4.10) is satisfied. In the second case, the path ω' visits a saddle that has been already visited by ω, thus we can iterate this argument for a finite number of steps, since the path ω' has to reach $\blacksquare$. Thus, we have proved that the saddle ξ_i is essential for any $i = 1, ..., n$. □

3.5 PROOF OF THE MAIN THEOREM 3.2.7

In this Section we give the proof of the main Theorem 3.2.7 by analyzing the geometry of the set $\mathcal{G}(\square, \blacksquare)$, emphasizing the saddles for the transition from $\square$ to $\blacksquare$ that are essential and the ones that are not. We want to investigate in more detail the saddles $\xi \in \mathcal{S}(\square, \blacksquare) \setminus (\partial\mathcal{C}^{\square}_{\blacksquare}(\Gamma^*) \cup \partial\mathcal{C}^{\blacksquare}_{\square}(\Gamma^* - \widehat{H}(\blacksquare)) \cup \mathcal{C}^*)$ visited after crossing the set $\mathcal{C}^B$.

Proposition 3.5.1. *Any saddle ξ that is neither in $\mathcal{C}^*$, nor in the boundary of the cycle $\mathcal{C}^{\square}_{\blacksquare}(\Gamma^*)$, nor in $\partial\mathcal{C}^{\blacksquare}_{\square}(\Gamma^* - \widehat{H}(\blacksquare)) \setminus \widetilde{K}$, such that $\tau_\xi \geqslant \tau_{\mathcal{C}^B}$ can be essential or not. For those essential, we obtain the following characterization:*

$$\mathcal{G}(\square, \blacksquare) \cap \mathcal{S}(\square, \blacksquare) \setminus (\partial\mathcal{C}^{\square}_{\blacksquare}(\Gamma^*) \cup (\partial\mathcal{C}^{\blacksquare}_{\square}(\Gamma^* - \widehat{H}(\blacksquare)) \setminus \widetilde{K}) \cup \mathcal{C}^*) = \bigcup_{i=0}^{3} \bigcup_{\alpha} \mathscr{I}_i^{\alpha} \cup \bigcup_{i=0}^{2} \bigcup_{\alpha,\alpha'} \bigcup_{k,k'} \mathscr{I}_{k,k',i}^{\alpha,\alpha'} \cup \bigcup_{i=-1}^{2} \bigcup_{\alpha,\alpha'} \mathscr{I}_i^{\alpha,\alpha'}. \tag{3.5.1}$$

We refer to Section 3.5.1 for the proof of the Proposition 3.5.1.

Proof of the main Theorem 3.2.7. By Corollary 3.4.4 we know that the saddles of the first and second type, defined in Definitions 3.1.2 and 3.1.4, respectively, are unessential. By Propositions 3.4.5 and 3.5.1 we have the characterization of the essential saddles of the third type. Use Proposition 3.4.2 to get the claim. □

3.5.1 *Proof of Proposition 3.5.1*

We recall Definitions 3.2.3 and 3.2.5 for the definitions of the 1-translation of a bar and for the sliding of a bar around a frame-angle, respectively, and that $d(\cdot, \cdot)$ denotes the lattice distance. In order to prove Proposition 3.5.1 we need the following lemma.

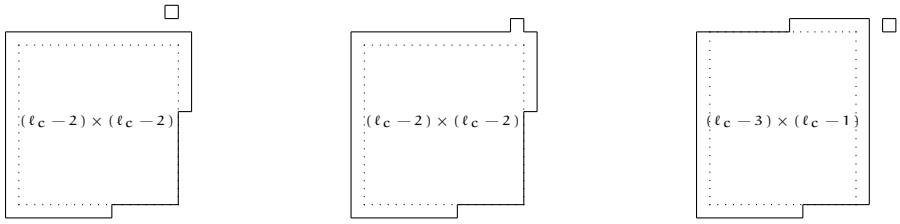

(a) (b) (c)

Figure 3.5 – Here we depict a possible configuration η in (a), its corresponding η' in (b) and the configuration obtained from η' after the sliding of the bar $B^e(\eta)$ around the frame-angle $c^{en}(\eta')$ in (c) for the case 1A.

Lemma 3.5.2. *(i) Starting from $\eta \in \mathscr{I}_0^{\alpha,\alpha'}$ (resp. $\eta \in \mathscr{I}_{-1}^{\alpha,\alpha'}$), if the free particle is attached in $\partial^+ CR(\eta)$ obtaining the configuration η', then the following saddles obtained via a 1-translation of any bar are essential and in $\mathscr{I}_0^\alpha \cup \mathscr{I}_1^\alpha$ (resp. in $\mathscr{I}_0^\alpha$). Moreover, all the saddles in $\mathscr{I}_0^\alpha \cup \mathscr{I}_1^\alpha$ can be obtained from a $\eta \in \mathscr{I}_{-1}^{\alpha,\alpha'} \cup \mathscr{I}_0^{\alpha,\alpha'}$ via a 1-translation of a bar. In particular, starting from $\eta \in \mathcal{C}^*$, if the free particle is attached in a bad site obtaining $\eta^B \in \mathcal{C}^B$, then the following saddles obtained via a 1-translation of any bar are essential. These saddles are in $\mathscr{I}_0^\alpha$ if $\hat{\eta} \in \bar{\mathcal{D}}$ and in $\mathscr{I}_0^\alpha \cup \mathscr{I}_1^\alpha$ if $\hat{\eta} \in \widetilde{\mathcal{D}}$.*

(ii) Starting from $\eta \in \mathscr{I}_1^{\alpha,\alpha'}$, if the free particle is attached in $\partial^+ CR(\eta)$ obtaining the configuration η', then the following saddles obtained via a 1-translation of any bar are essential and in $\mathscr{I}_1^\alpha \cup \mathscr{I}_2^\alpha$. Moreover, all the saddles in $\mathscr{I}_1^\alpha \cup \mathscr{I}_2^\alpha$ can be obtained from a $\eta \in \mathscr{I}_1^{\alpha,\alpha'}$ via a 1-translation of a bar.

(iii) Starting from $\eta \in \mathscr{I}_2^{\alpha,\alpha'}$, if the free particle is attached in $\partial^+ CR(\eta)$ obtaining the configuration η', then the following saddles obtained via a 1-translation of any bar are essential and in $\mathscr{I}_2^\alpha \cup \mathscr{I}_3^\alpha$. Moreover, all the saddles in $\mathscr{I}_2^\alpha \cup \mathscr{I}_3^\alpha$ can be obtained from a $\eta \in \mathscr{I}_2^{\alpha,\alpha'}$ via a 1-translation of a bar.

The proof of the lemma is postponed to Section 3.5.2.

Proof of Proposition 3.5.1. Consider a configuration $\eta \in \mathcal{C}^*(2)$ such that $\eta = (\hat{\eta}, x)$, with $\hat{\eta} \in \mathcal{D}$ and x the site of the free particle such that $d(\hat{\eta}, x) = 2$. By hypotheses we have that the free particle is attached in a bad site obtaining a configuration $\eta' \in \mathcal{C}^B$ (see Figure 3.5(a)-(b) for a possible pair of configuration (η, η')). Due to [85, Theorem 5.1], our strategy consists in characterizing the essential saddles that could be visited after attaching the free particle in a bad site. We consider the following cases:

CASE 1. $\hat{\eta} \in \bar{\mathcal{D}}$;

CASE 2. $\hat{\eta} \in \widetilde{\mathcal{D}}$.

Note that from case 1 one can go to the other cases and viceversa, but since the path has to reach ■ this back and forth must end in a finite number of steps.

Case 1. Let $\hat{\eta} \in \bar{\mathcal{D}}$, thus by [35, Theorem 1.4.1] we know that $\hat{\eta}$ consists in an $(\ell_c - 2) \times (\ell_c - 2)$ square with four bars $B^\alpha(\eta)$, with $\alpha \in \{n, e, w, s\}$, attached to its four sides satisfying

$$1 \leqslant |B^\alpha(\eta)| \leqslant \ell_c, \qquad \sum_\alpha |B^\alpha(\eta)| - \sum_{\alpha\alpha' \in \{nw, ne, sw, se\}} |c^{\alpha\alpha'}(\eta)| = 3\ell_c - 3. \tag{3.5.2}$$

First, note that at most three frame-angles in $\partial^- CR(\hat{\eta})$ can be occupied, otherwise $|\partial^- CR(\hat{\eta})| = 4\ell_c - 4 > 3\ell_c - 3$, which is absurd. Thus, we consider separately the following cases:

A. three frame-angles in $\partial^- CR(\hat{\eta})$ are occupied;
B. two frame-angles in $\partial^- CR(\hat{\eta})$ are occupied;
C. one frame-angle in $\partial^- CR(\hat{\eta})$ is occupied;
D. no frame-angle in $\partial^- CR(\hat{\eta})$ is occupied.

Case 1A. Without loss of generality we consider η as in Figure 3.5(a). If we are considering the case in which a sequence of 1-translations of a bar is possible and takes place, then by Lemma 3.5.2(i) the saddles that are crossed are essential and in $\mathscr{I}_0^\alpha$. If a sequence of

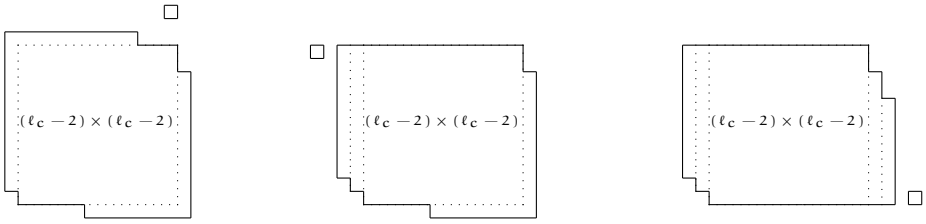

(a) (b) (c)

Figure 3.6 – Case 1B(i): we depict a possible starting configuration $\eta \in \mathcal{C}^*$ in (a), the configuration $\widetilde{\eta}$ obtained from η after the sliding of the bar $B^n(\eta)$ around the frame–angle $c^{nw}(\eta')$ in (b) and the configuration $\bar{\eta}$ obtained from $\widetilde{\eta}$ after the sliding of the bar $B^s(\widetilde{\eta})$ around the frame–angle $c^{se}(\eta'')$ in (c).

1-translations of a bar takes place in such a way that the last configuration has at most two occupied frame–angles, then we can reduce our proof to the cases B, C and D below. Thus, we are left to analyze the case in which there is the activation of a sliding of a bar around a frame–angle. Consider again, for example, η as in Figure 3.5(a). If the free particle is attached to the bar $B^e(\eta)$, then it is not possible to slide the bar $B^n(\eta)$ around the frame–angle $c^{ne}(\eta')$, since the condition (3.2.12) is not satisfied. Thus, by Lemma 3.4.1(ii) we know that the saddles that could be crossed are unessential. If the free particle is attached to the bar $B^s(\eta)$, we conclude as before. If the free particle is attached to the bar $B^n(\eta)$ (see Figure 3.5(b)), then it is not possible to slide the bar $B^w(\eta)$ around the frame–angle $c^{wn}(\eta')$ because condition (3.2.12) is not satisfied and thus we can conclude as before. The unique possibility is to slide the bar $B^e(\eta)$ around the frame–angle $c^{en}(\eta')$ if $|B^e(\eta)| < |B^n(\eta)|$, otherwise (3.2.12) is not satisfied. The saddles that are possibly visited (except the last one) are in $\mathscr{I}^{\alpha,\alpha'}_{k,k',0}$ and by Lemma 3.4.1(i) they are essential. The last configuration visited during this sliding of a bar is depicted in Figure 3.5(c). It belongs to $\mathcal{C}^*$, indeed the cluster is in $\widetilde{\mathcal{D}}$ and therefore the saddles that could be crossed starting from it will be investigated in case 2. If the free particle is attached to the bar $B^w(\eta)$, we conclude in a similar way as before. This concludes case 1A.

Case 1B. We consider separately the following subcases:
(i) the two occupied frame-angles are $c^{\alpha\alpha'}(\eta)$ and $c^{\alpha''\alpha'''}(\eta)$, with all the indeces α, α', α'' and α''' different between each other (see Figure 3.6(a));
(ii) the two occupied frame-angles are $c^{\alpha\alpha'}(\eta)$ and $c^{\alpha'\alpha''}(\eta)$, with $\alpha \neq \alpha''$ (see Figure 3.7(a)).

Case 1B(i). Without loss of generality we consider η as in Figure 3.6(a). If we are considering the case in which a sequence of 1-translations of a bar is possible and takes place, then by Lemma 3.5.2(i) the saddles that are crossed are essential and they are in $\mathscr{I}^{\alpha}_0$. If at least one bar is full, it is possible to activate a sequence of 1-translations of a bar in order to obtain either two occupied frame–angles with a bar in common or three occupied frame–angles. For example, in Figure 3.6(a), if the bar $B^s(\eta)$ is full, one could attach the free particle to $B^e(\eta)$ and translate the bar $B^w(\eta)$ in order to have the frame–angle $c^{sw}(\eta)$ occupied. In both situations the saddles visited up to this point are essential by Lemma 3.5.2(i), while the saddles that follow are analyzed in case 1B(ii) and 1A, respectively. Thus, we can reduce our proof to the case in which there is no translation of a bar and therefore we need to consider only the sliding of a bar around a frame–angle. We may assume without loss of generality that $|B^n(\eta)| < |B^w(\eta)|$ and $|B^s(\eta)| < |B^e(\eta)|$, indeed the other cases can be treated with the same argument. By Lemma 3.4.1 to obtain essential saddles there are one of the following possibilities: attach the free particle to the bar $B^w(\eta)$ (resp. $B^e(\eta)$) and then slide the bar $B^n(\eta)$ (resp. $B^s(\eta)$) around the frame–angle $c^{nw}(\eta')$ (resp. $c^{se}(\eta')$). Assume first that the free particle is attached to $B^w(\eta)$. By Lemma 3.4.1(i) the saddles that are possibly visited are essential and, except the last one, they are in $\mathscr{I}^{\alpha,\alpha'}_{k,k',0}$. The last configuration visited during this sliding of a bar is $\widetilde{\eta} \in \mathscr{I}^{\alpha,\alpha'}_0$ and it is depicted in Figure 3.6(b). Starting from $\widetilde{\eta}$, the unique possibility to visit essential saddles is to attach a free particle in $\partial^+\mathrm{CR}(\widetilde{\eta})$ and then either activate a sequence of 1-translations of bars or slide a bar around a frame–angle. In the first case, by Lemma 3.5.2(i) the saddles that are possibly visited are essential and in $\mathscr{I}^{\alpha}_0 \cup \mathscr{I}^{\alpha}_1$. In the latter case, the unique possibility is to attach the free particle to the bar

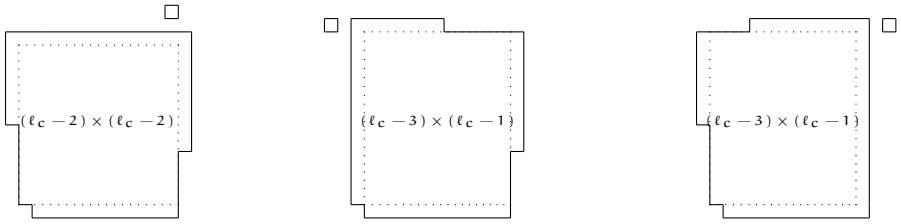

Figure 3.7 – Case 1B(ii): we depict a possible starting configuration $\eta \in \mathcal{C}^*$ in (a), the configuration $\tilde{\eta}$ obtained from η after the sliding of the bar $B^w(\eta)$ around the frame-angle $c^{wn}(\eta')$ in (b) and the configuration $\bar{\eta}$ obtained from η after the sliding of the bar $B^e(\eta)$ around the frame-angle $c^{en}(\eta'')$ in (c).

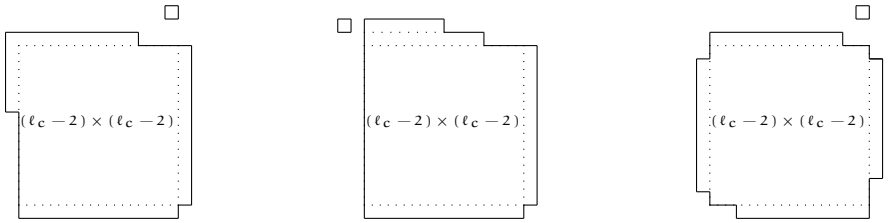

Figure 3.8 – Case 1C: in (a) we depict a possible starting configuration $\eta \in \mathcal{C}^*$ and in (b) the configuration $\tilde{\eta}$ obtained from η after the sliding of the bar $B^w(\eta)$ around the frame-angle $c^{wn}(\eta')$. Case 1D: in (c) we depict a possible starting configuration in $\mathcal{C}^*$.

$B^e(\tilde{\eta})$ obtaining a configuration η'', and then slide $B^s(\tilde{\eta})$ around the frame–angle $c^{se}(\eta'')$. By Lemma 3.4.1(i) the saddles that are possibly visited are essential and, except the last one, they are in $\mathscr{I}^{\alpha,\alpha'}_{k,k',1}$. The last configuration visited during this sliding of a bar is in $\mathscr{I}^{\alpha,\alpha'}_1$ and it is depicted in Figure 3.6(c). Starting from this configuration it is impossible to slide a bar around any frame–angle, thus by Lemma 3.4.1(ii) the saddles that possibly will be crossed if the sliding of a bar is initiated are unessential. If a sequence of 1-translations of bars takes place, by Lemma 3.5.2(ii) the saddles that could be crossed are essential and in $\mathscr{I}^{\alpha}_1 \cup \mathscr{I}^{\alpha}_2$.

Note that if $|B^w(\eta)| < |B^n(\eta)|$ and/or $|B^e(\eta)| < |B^s(\eta)|$ a similar argument can be used. This concludes case 1B(i).

Case 1B(ii). Without loss of generality we consider η as in Figure 3.7(a). If we are considering the case in which a sequence of 1-translations of a bar is possible and takes place, then by Lemma 3.5.2(i) the saddles that are crossed are essential and they are in $\mathscr{I}^{\alpha}_0$. If one bar among $B^w(\eta)$ and $B^e(\eta)$ is full, it is possible to activate a sequence of 1-translations of the bar $B^s(\eta)$ in order to have three occupied frame–angles. This situation has already been analyzed in case 1A. Thus, we can reduce our proof to the case in which there is no translation of a bar and therefore we need to consider only the sliding of a bar around a frame–angle. If the free particle is attached to the bar $B^s(\eta)$, since it is not possible to slide a bar around any frame–angle, by Lemma 3.4.1(ii) we know that the saddles that could be crossed are unessential. If the free particle is attached to one bar among $B^w(\eta)$ and $B^e(\eta)$, then it is not possible to complete the sliding of the bar $B^n(\eta)$ around the frame–angle $c^{nw}(\eta')$ or $c^{ne}(\eta')$. Thus, by Lemma 3.4.1(ii) the saddles that could be crossed are unessential. If the free particle is attached to the bar $B^n(\eta)$, then it is possible to slide the bar $B^w(\eta)$ or $B^e(\eta)$ around the frame–angle $c^{wn}(\eta')$ or $c^{en}(\eta')$, respectively. Thus, by Lemma 3.4.1(i) we know that the saddles that could be crossed are essential and they are in $\mathscr{I}^{\alpha,\alpha'}_{k,k',0}$, except the last one that is in $\mathcal{C}^*$ (see Figure 3.7(b)-(c)). Hence the saddles that could be crossed starting from such configuration will be analyzed in case 2. This concludes case 1B(ii).

Case 1C. Without loss of generality we consider η as in Figure 3.8(a). If we are a considering the case in which a sequence of 1-translations of a bar is possible and takes place, then by Lemma 3.5.2(i) the saddles that are crossed are in $\mathscr{I}^{\alpha}_0$. Starting from this configuration it is possible to obtain two occupied frame–angles: this situation has been already analyzed in case

1B. Thus, we can reduce our proof to the case in which there is no 1-translation of a bar and therefore there is the activation of a sliding of a bar around a frame–angle. If the free particle is attached to the bar $B^e(\eta)$ or $B^s(\eta)$, since it is not possible to complete any sliding of a bar around a frame–angle at cost U, by Lemma 3.4.1(ii) we know that the saddles that could be crossed are unessential. If $|B^w(\eta)| < |B^n(\eta)|$ and the free particle is attached to the bar $B^n(\eta)$, then it is possible to slide the bar $B^w(\eta)$ around the frame–angle $c^{wn}(\eta')$. Thus, by Lemma 3.4.1(i) the saddles that could be crossed are essential and, except the last one, they are in $\mathscr{I}_{k,k',0}^{\alpha,\alpha'}$. Note that the last configuration is in $\mathscr{I}_0^{\alpha,\alpha'}$ (see Figure 3.8(b)). Starting from such a configuration, since it is not possible to complete any sliding of a bar around a frame–angle, by Lemma 3.4.1(ii) we know that the saddles that could be visited are unessential unless a sequence of 1-translations of bars takes place. In this case, by Lemma 3.5.2(ii) the saddles that could be visited are essential and in $\mathscr{I}_0^\alpha \cup \mathscr{I}_1^\alpha$. The case $|B^n(\eta)| < |B^w(\eta)|$ in which the free particle is attached to the bar $B^w(\eta)$ is analogue. This concludes case 1C.

Case 1D. Without loss of generality we consider η as in Figure 3.8(c). If we are considering the case in which a sequence of 1-translations of a bar is possible and takes place, then by Lemma 3.5.2(i) the saddles that are crossed are in $\mathscr{I}_0^\alpha$. Starting from this configuration, it is possible to obtain one or two occupied frame–angles: these situations have been already analyzed in cases 1C and 1B, respectively. Thus, we can reduce our proof to the case in which there is no 1-translation of a bar and therefore there is the activation of a sliding of a bar around a frame–angle. If the free particle is attached to one of the bars, since it is not possible to complete any sliding of bar around a frame–angle, by Lemma 3.4.1(ii) we know that the saddles that could be crossed are unessential. This concludes case 1D.

Case 2. Let $\hat{\eta} \in \widetilde{\mathcal{D}}$, thus by [35, Theorem 1.4.1] we know that $\hat{\eta}$ consists of an $(\ell_c - 3) \times (\ell_c - 1)$ quasi–square with four bars $B^\alpha(\eta)$, with $\alpha \in \{n, w, e, s\}$, attached to its four sides satisfying

$$1 \leqslant |B^\alpha(\eta)|, |B^{\alpha'}(\eta)| \leqslant \ell_c + 1, \qquad 1 \leqslant |B^{\alpha''}(\eta)|, |B^{\alpha'''}(\eta)| \leqslant \ell_c - 1, \tag{3.5.3}$$

where either $\alpha, \alpha' \in \{n, s\}$ and $\alpha'', \alpha''' \in \{w, e\}$, or $\alpha, \alpha' \in \{w, e\}$ and $\alpha'', \alpha''' \in \{n, s\}$, and

$$\sum_\alpha |B^\alpha(\eta)| - \sum_{\alpha\alpha' \in \{nw, ne, sw, se\}} |c^{\alpha\alpha'}(\eta)| = 3\ell_c - 2. \tag{3.5.4}$$

First, note that at most three frame–angles in $\partial^- CR(\hat{\eta})$ can be occupied, otherwise $|\partial^- CR(\hat{\eta})| = 4\ell_c - 4 > 3\ell_c - 2$, which is absurd. By hypotheses we have that the free particle is attached in a bad site obtaining a configuration $\eta' \in \mathcal{C}^B$. We consider separately the following cases:

A. three frame-angles in $\partial^- CR(\eta)$ are occupied;
B. two frame-angles in $\partial^- CR(\eta)$ are occupied;
C. one frame-angle in $\partial^- CR(\eta)$ is occupied;
D. no frame-angle in $\partial^- CR(\eta)$ is occupied.

The argument used in case 2 is analogue to that used above in case 1 and is discussed in details in Appendix 3.A. □

3.5.2 *Proof of Lemma 3.5.2*

(i) Note that $\widehat{H}(\eta') = \Gamma^* - U$, thus it is possible to translate bars at cost U. These saddles are in $\mathscr{I}_0^\alpha$ if $\eta \in \mathscr{I}_{-1}^{\alpha_1\alpha'}$ and in $\mathscr{I}_0^\alpha \cup \mathscr{I}_1^\alpha$ if $\eta \in \mathscr{I}_0^{\alpha,\alpha'}$. To conclude, all the configurations in $\mathscr{I}_0^\alpha \cup \mathscr{I}_1^\alpha$ can be obtained from a configuration $\eta \in \mathscr{I}_{-1}^{\alpha_1\alpha'} \cup \mathscr{I}_0^{\alpha,\alpha'}$ via a 1-translation of a bar. Since $\bar{\mathcal{D}}^{fp} \subseteq \mathscr{I}_{-1}^{\alpha_1\alpha'}$ and $\widetilde{\mathcal{D}}^{fp} \subseteq \mathscr{I}_0^{\alpha,\alpha'}$, we get the particular case in which $\eta' = \eta^B \in \mathcal{C}^B$ as claimed.

It remains to prove that the saddles in $\mathscr{I}_0^\alpha \cup \mathscr{I}_1^\alpha$ are essential. Let $\xi_1, ..., \xi_m \in \mathscr{I}_0^\alpha \cup \mathscr{I}_1^\alpha$ the saddles visited during a 1-translation of a bar. We want to prove that these saddles are essential (see Section 3.1.1 point 4 for the definition). Since we can repeat the following argument m times, we may focus on a single configuration ξ_i. Since $\mathcal{C}^*$ is a gate for the transition and $\xi_i \in \mathcal{S}(\square, \blacksquare) \setminus \mathcal{C}^*$, we note that a path $\omega \in (\square \to \blacksquare)_{opt}$ such that $\{\arg\max_\omega \widehat{H}\} = \{\xi_i\}$ does not exist. Thus, our strategy consists in finding a path $\omega \in (\square \to \blacksquare)_{opt}$ such that for any $\omega' \in (\square \to \blacksquare)_{opt}$

$$\omega \cap \xi_i \neq \emptyset, \ \{\arg\max_{\omega'} \widehat{H}\} \not\subseteq \{\arg\max_\omega \widehat{H}\} \setminus \{\xi_i\}, \qquad i = 1, ..., m. \tag{3.5.5}$$

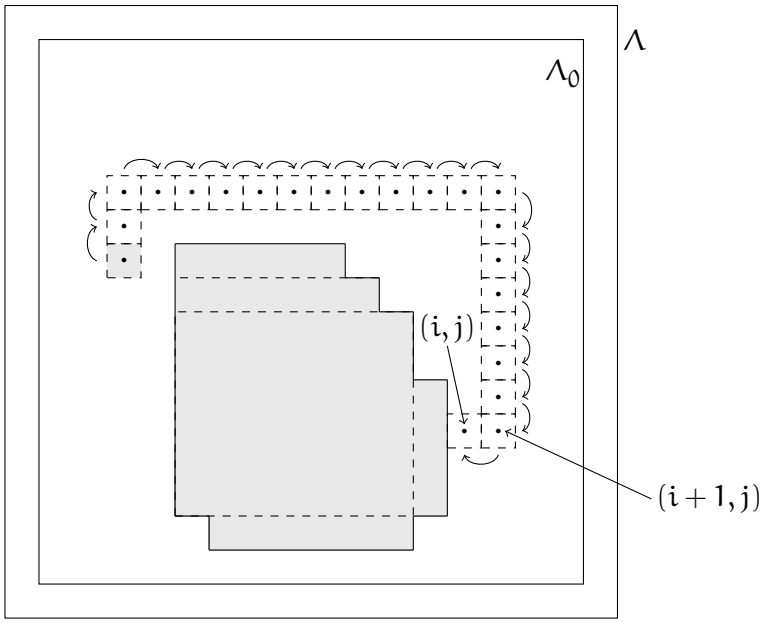

Figure 3.9 – Here we depict in grey the configuration η_1 that consists of the union of a cluster $C(\eta_1)$ and a free particle. The dotted unit squares represent the following positions of the free particle that moves as represented by the arrows on the left, north, east and south, until the particle is attached to the cluster in position (i,j). The latter is the configuration η'. To simplify the exposition we chose to use the path in the external frame of $\partial^+CR(C(\eta_1))$.

Let η' be the configuration with a single cluster obtained as union of a cluster $C(\eta_1)$ and a protuberance attached to one of its bars in a site with coordinates (i,j) such that $\widehat{H}(\eta_1) = \Gamma^*$ and η_1 is the configuration with cluster $C(\eta_1)$ and one free particle. More precisely, by (3.2.21) the configuration η_1 is obtained by the configuration η_0 via a sliding of the bar $B^{\alpha}(\eta_0)$ around the frame–angle $c^{\alpha\alpha'}(\eta_0)$. Without loss of generality we assume that the protuberance of η' is attached to the bar $B^{e}(C(\eta_1))$. We define the specific path ω of the strategy above as

$$\omega = (\square, \omega_1, ..., \omega_k, \gamma_1, ..., \eta_0, ...\gamma_s, \eta_1, ..., \eta_k, \eta', \xi_1, ..., \xi_m) \circ \bar{\omega}, \tag{3.5.6}$$

where $\omega_1, ..., \omega_k \in \mathcal{C}^{\square}_{\blacksquare}(\Gamma^*)$, $\gamma_1, ..., \gamma_s \in \mathcal{X}$ such that $\widehat{H}(\gamma_i) \leqslant \Gamma^*$ for any $i = 1, ..., s$ and $\bar{\omega}$ is a path that connects ξ_m to $\blacksquare$ such that $\max_{\sigma\in\bar{\omega}} \widehat{H}(\sigma) \leqslant \Gamma^*$. Moreover, the saddles $\eta_1, ..., \eta_k$ are composed by the union of the cluster $C(\eta_1)$ and a free particle such that the free particle is at distance $\geqslant 3$ from a site in $\partial^- CR(\eta_1)$ (see Figure 3.9 for a picture of this situation in the case $\alpha = w$ and $\alpha' = n$). In particular, consider that η_1 has the free particle in $\bar{B}_2(\eta_1)$ and η_k in the site with coordinates $(i+1, j) \in \bar{B}_2(\eta_1)$ using the assumption that the protuberance of η' is attached to $B^{e}(\eta_1)$.

Now we show that for any ω' condition (3.5.5) is satisfied. If ω' passes through the configuration ξ_i, $\{\arg\max_{\omega'} \widehat{H}\} \supseteq \{\xi_i\}$, thus (3.5.5) is satisfied. Therefore we can assume that $\omega' \cap \xi_i = \emptyset$. If ω' crosses the set $\mathcal{S}(\square, \blacksquare)$ through a configuration η'' such that $\eta'' \cap \omega = \emptyset$, then condition (3.5.5) holds. Thus, we can reduce our analysis to ω' that visits all the saddles $\eta_1, ..., \eta_k$. Starting from η_k, there are four allowed directions for moving the free particle. If we move it in the direction of the cluster (west in Figure 3.9), we deduce that the path ω' visits the configuration η'. For the other three choices, the free particle still remains free after the move, indeed by construction of the path ω, starting from η_k it is not possible to attach the free particle in $\partial^- CR(\eta_1)$ via one step of the dynamics. Thus, the path ω' can visit either a saddle not already visited by ω (south or east in Figure 3.9) or a saddle that has been already visited by ω (north in Figure 3.9). In the first case, we obtain that (3.5.5) is satisfied. In the latter case, we can iterate this argument and, since ω' goes from $\square$ to $\blacksquare$, we can assume that the path ω' visits the configuration η'. From now on, starting from η', there are two possible scenarios:

I. ω' activates the same 1-translation of a bar as ω;
II. ω' activates a different 1-translation of a bar from ω.

In case I, since $\omega' \cap \xi_i = \emptyset$, we deduce that the 1-translation of a bar has been stopped before hitting ξ_i. Thus, we can assume that ω' comes back to η', otherwise the energy exceeds Γ^*. Since the path ω' has to reach $\blacksquare$, starting from η' the protuberance is detached and in the sequel is attached in another site. Thus, ω' reaches a saddle that is not visited by ω. This implies that (3.5.5) is satisfied.

In case II, when the path ω' initiates a 1-translation of a bar different from ω, it reaches a saddle that it is not visited by ω, thus condition (3.5.5) is satisfied. Therefore we deduce that the path does not start this 1-translation and thus the path ω' must go back to η' (since it has to reach $\blacksquare$). From now on, as before, the path ω' has to detach the protuberance and in the sequel it is attached in another site, thus ω' reaches a saddle that is not visited by ω. This implies that (3.5.5) is satisfied. Thus, we have proved that the saddle ξ_i is essential for any $i = 1, ..., m$.

The proof of (ii) and (iii) is analogue to the one done in (i) by modifying the length of the horizontal and vertical sides of $CR(\eta)$. □

3.6 PROOF OF THE SHARP ASYMPTOTICS

In this section, following the approach initiated in [35] for Kawasaki dynamics and developed in [32, Chapters 16 and 18], we provide a comparison with some model–independent results given in [32, Chapter 16]. For this reason we give our results for a continuous time dynamics, but we encourage the reader to inspect Remark 3.6.8, which translates the aforementioned results to the discrete time Kawasaki dynamics we consider in this thesis.

3.6.1 *Model-independent results for the prefactor*

In order to give the results, we need some definitions. In [32] the authors refer to the protocritical and critical sets as $\mathscr{P}^*(m,s)$ and $\mathscr{C}^*(m,s)$, respectively. Since they differ from our notation, we refer to them as $\mathscr{P}^*_{PTA}(m,s)$ and $\mathscr{C}^*_{PTA}(m,s)$, respectively, where PTA stands for *potential–theoretic approach*. Given $\xi, \xi' \in \mathcal{X}$, we set $\xi \sim \xi'$ if the two configurations can be obtained from each other via an allowed move.

Definition 3.6.1. *[32, Definition 16.3] Recall that*

$$\Gamma_m = \Phi(m,s) - \widehat{H}(m). \tag{3.6.1}$$

Then $(\mathscr{P}^*_{PTA}(m,s), \mathscr{C}^*_{PTA}(m,s))$ *is the maximal subset of* $\mathcal{X} \times \mathcal{X}$ *such that:*

(1) $\forall\ \xi \in \mathscr{P}^*_{PTA}(m,s)\ \exists\ \xi' \in \mathscr{C}^*_{PTA}(m,s) :\ \xi \sim \xi'$ *and* $\forall\ \xi' \in \mathscr{C}^*_{PTA}(m,s)\ \exists\ \xi \in \mathscr{P}^*_{PTA}(m,s) :\ \xi' \sim \xi$;

(2) $\forall\ \xi \in \mathscr{P}^*_{PTA}(m,s),\ \Phi(\xi,m) < \Phi(\xi,s)$;

(3) $\forall\ \xi' \in \mathscr{C}^*_{PTA}(m,s)\ \exists\, \gamma : \xi' \to s$ *such that* $\max_{\zeta\in\gamma} \widehat{H}(\zeta) - \widehat{H}(m) \leqslant \Gamma_m, \gamma \cap \{\zeta \in \mathcal{X} : \Phi(\zeta,m) < \Phi(\zeta,s)\} = \emptyset$.

Now we abbreviate $\mathscr{P}^*_{PTA} = \mathscr{P}^*_{PTA}(m,s)$ and $\mathscr{C}^*_{PTA} = \mathscr{C}^*_{PTA}(m,s)$. In [32] the following results (Theorems 3.6.2 and 3.6.3) are proved subject to the two hypotheses

(H1) $\mathcal{X}^m = \{m\}$ and $\mathcal{X}^s = \{s\}$;

(H2) $\xi' \to |\{\xi \in \mathscr{P}^*_{PTA} :\ \xi \sim \xi'\}|$ is constant on $\mathscr{C}^*_{PTA}$.

Theorem 3.6.2. *[32, Theorem 16.4]*

(a) $\lim_{\beta\to\infty} \mathbb{P}_m(\tau_{\mathscr{C}^*_{PTA}} < \tau_s | \tau_s < \tau_m) = 1$;

(b) $\lim_{\beta\to\infty} \mathbb{P}_m(\xi_{\tau_{\mathscr{C}^*_{PTA}}} = \chi) = \dfrac{1}{|\mathscr{C}^*_{PTA}|}$ *for all* $\chi \in \mathscr{C}^*_{PTA}$.

Theorem 3.6.3. *[32, Theorem 16.5] There exists a constant* $K \in (0,\infty)$ *such that*

$$\lim_{\beta\to\infty} e^{-\beta\Gamma_m} \mathbb{E}_m(\tau_s) = K. \tag{3.6.2}$$

Concerning Theorem 3.6.3, the general strategy developed in [32, Section 16.3.2] is reported in Section 1.3.2 by replacing the Dirichlet form in (1.3.39) with its continuous time version

$$\mathcal{E}_\beta(h) = \frac{1}{2}\sum_{\eta,\eta'\in\mathcal{X}} \mu_\beta(\eta)c_\beta(\eta,\eta')[h(\eta)-h(\eta')]^2, \qquad h\colon \mathcal{X}\to[0,1], \tag{3.6.3}$$

where μ_β is the Gibbs measure defined in [32, eq. (16.1.1)] and c_β is the kernel of transition rates defined in [32, eq. (16.1.2)]. By viewing $\mathcal{X}$ as a graph whose vertices are configurations and whose edges connect communicating configurations, recall the following notation:

- $\mathcal{X}^*$ be the subgraph of $\mathcal{X}$ obtained by removing all vertices η with $H(\eta) > \Gamma^* + H(m)$ and all edges incident to these vertices;
- $\mathcal{X}^{**}$ be the subgraph of $\mathcal{X}^*$ obtained by removing all vertices η with $H(\eta) = \Gamma^* + H(m)$ and all edges incident to these vertices;
- $\mathcal{X}^{meta}$ and $\mathcal{X}^{stab}$ be the connected components of $\mathcal{X}^{**}$ containing m and s respectively.

Moreover, we consider the set

$$\mathcal{X}^{**}\setminus(\mathcal{X}^{meta}\cup\mathcal{X}^{stab}) = \bigcup_{i=1}^{I}\mathcal{X}(i), \tag{3.6.4}$$

where we recall that each $\mathcal{X}(i)$ is a *well* in $\mathcal{S}(m,s)$, i.e., a set of communicating configurations with energy strictly less than $\Gamma_m + \widehat{H}(m)$ but with communication height $\Gamma_m + \widehat{H}(m)$ towards both m and s. Among all the wells $\mathcal{X}(i)$, we can highlight the wells $\mathcal{Z}_j^m$ (resp. $\mathcal{Z}_j^s$) of the unessential saddles of the first (resp. second) type σ_j (resp. ζ_j) (see Definitions 3.1.2 and 3.1.4, and Propositions 3.1.3 and 3.1.5). In particular, these wells can be defined as follows.

Definition 3.6.4. *We define*

1) $\mathcal{Z}_j^m \subset \mathcal{X}^{**}$, $j = 1,\dots,J_m$, *is a connected set such that, for all* $\eta\in\mathcal{Z}_j^m$, $\Phi(m,\eta) = \Phi(s,\eta)$ *and any path* $\omega:\eta\to s$ *must be such that* $\omega\cap\mathcal{X}^{meta}\neq\emptyset$;
2) $\mathcal{Z}_j^s \subset \mathcal{X}^{**}$, $j = 1,\dots,J_s$, *is a connected set such that, for all* $\eta\in\mathcal{Z}_j^m$, $\Phi(s,\eta) = \Phi(m,\eta)$ *and any path* $\omega:\eta\to m$ *must be such that* $\omega\cap\mathcal{X}^{stab}\neq\emptyset$.

Proposition 3.6.5. *If* $\mathcal{Z}_j^m\neq\emptyset$, $\mathcal{X}(i)\equiv\mathcal{Z}_j^m$ *if and only if* $\mathcal{Z}_j^m$ *is a connected component in* $\mathcal{X}^{**}\setminus(\mathcal{X}^{meta}\cup\mathcal{X}^{stab})$ *such that there exists a saddle of the first type* σ_j *that communicates via one step with a configuration in* $\mathcal{Z}_j^m$.

Proof. First, assume that $\mathcal{X}(i)\equiv\mathcal{Z}_j^m$ for some $i\in\{1,\dots,I\}$ and $j\in\{1,\dots,J_m\}$. It is clear that $\mathcal{Z}_j^m$ is a connected component in $\mathcal{X}^{**}\setminus(\mathcal{X}^{meta}\cup\mathcal{X}^{stab})$, indeed any configuration $\eta\in\mathcal{X}^{meta}\cup\mathcal{X}^{stab}$ has $\Phi(\eta,m)\neq\Phi(\eta,s)$. Furthermore, by definition of $\mathcal{Z}_j^m$, we note that $\Phi(s,\eta) = \Gamma_m + \widehat{H}(m)$ and any path $\omega:\eta\to s$ must be such that $\omega\cap\mathcal{X}^{meta}\neq\emptyset$. This implies that there exists $\sigma_j\in\omega\cap\mathcal{S}(s,m)$ that is an unessential saddle of the first type (see Proposition 3.1.3) such that it communicates via one step with a configuration in $\mathcal{Z}_j^m$.

Conversely, assume that any fixed $\mathcal{Z}_j^m$ is a connected component in $\mathcal{X}^{**}\setminus(\mathcal{X}^{meta}\cup\mathcal{X}^{stab})$ such that there exists a saddle of the first type σ_j that communicates via one step with a configuration in $\mathcal{Z}_j^m$. Thus we deduce that $\mathcal{X}(i)\equiv\mathcal{Z}_j^m$ for some $i\in\{1,\dots,I\}$, indeed for all $\eta\in\mathcal{Z}_j^m$ it hold $\Phi(\eta,m) = \Phi(\eta,s) = \Gamma_m + \widehat{H}(m)$ and $\widehat{H}(\eta) < \Gamma_m + \widehat{H}(m)$ since $\mathcal{Z}_j^m\subset\mathcal{X}^{**}$. □

Proposition 3.6.6. *If* $\mathcal{Z}_j^s\neq\emptyset$, $\mathcal{X}(i)\equiv\mathcal{Z}_j^s$ *if and only if* $\mathcal{Z}_j^s$ *is a connected component in* $\mathcal{X}^{**}\setminus(\mathcal{X}^{meta}\cup\mathcal{X}^{stab})$ *such that there exists a saddle of the second type* ζ_j *that communicates via one step with a configuration in* $\mathcal{Z}_j^s$.

Proof. The proof is analogue to the proof of Proposition 3.6.5 by replacing $\mathcal{Z}_j^m$ with $\mathcal{Z}_j^s$ and "$\omega:\eta\to s$ such that $\omega\cap\mathcal{X}^{meta}\neq\emptyset$" with "$\omega:\eta\to m$ such that $\omega\cap\mathcal{X}^{stab}\neq\emptyset$". □

First, note that the unessential saddles of the first and second type are not in the set $\mathscr{C}^*_{PTA}$. Indeed, on the one hand, the saddles $\{\sigma_j\}_{j=1}^{J_m}$ do not verify the condition (3) in Definition 3.6.1, because every optimal path that connects any fixed σ_j to s passes through $\mathcal{X}^{meta}$. On the other hand the saddles $\{\zeta_j\}_{j=1}^{J_s}$ do not verify conditions (1) and (2) in Definition 3.6.1, because they communicate only with configurations that are not in $\mathscr{P}^*_{PTA}$. By [32, eq. (16.3.4)] and

[32, Lemma 16.16], we know that h is constant on each wells, but for the wells $\mathcal{Z}_j^m$ and $\mathcal{Z}_j^s$ we compute this constant in Lemma 3.6.7, indeed [32, Lemma 16.15] can be extended also for these sets together with the unessential saddles of the first and second type.

Lemma 3.6.7. *Recall Definitions 3.1.2 and 3.1.4 for the definition of the saddles σ_j of the first type and ζ_j second type respectively and Definition 3.6.4 for the definition of the wells $\mathcal{Z}_j^m$ and $\mathcal{Z}_j^s$. As $\beta \to \infty$,*

$$Z^{CAP}(m,s) = [1+o(1)]\Theta e^{-\beta \Gamma_m}, \tag{3.6.5}$$

with

$$\Theta = \min_{c_1,\dots,c_{\bar{I}}} \min_{\substack{h:\mathcal{X}^*\to[0,1] \\ h_{|\mathcal{X}_I^{meta}}=1,\ h_{|\mathcal{X}_{II}^{stab}}=0,\ h_{|\mathcal{X}(i)}=c_i, i=1,\dots,\bar{I}}} \frac{1}{2} \sum_{\xi,\xi'\in\mathcal{X}^*} \mathbb{1}_{\{\xi\sim\xi'\}}[h(\xi)-h(\xi')]^2, \tag{3.6.6}$$

where

$$\mathcal{X}_I^{meta} := \mathcal{X}^{meta} \cup \bigcup_{j=1}^{J_m} (\{\sigma_j\} \cup \mathcal{Z}_j^m), \qquad \mathcal{X}_{II}^{stab} := \mathcal{X}^{stab} \cup \bigcup_{j=1}^{J_s} (\{\zeta_j\} \cup \mathcal{Z}_j^s). \tag{3.6.7}$$

and $\mathcal{X}(i)$, $i = 1,\dots,\bar{I}$, are all the wells of the transition except $\bigcup_{j=1}^{J_m} \mathcal{Z}_j^m$ and $\bigcup_{j=1}^{J_s} \mathcal{Z}_j^s$.

Proof. The statement is similar to the one of [32, Lemma 16.17], but the difference is in the variational formula for Θ. More precisely, comparing (3.6.6) with [32, eq. (16.3.11)], the proof is analogue to the one done for [32, Lemma 16.17], but we have to prove that the function h is constant equal to 1 (resp. 0) on $\bigcup_{j=1}^{J_m}(\{\sigma_j\}\cup\mathcal{Z}_j^m)$ (resp. $\bigcup_{j=1}^{J_s}(\{\zeta_j\}\cup\mathcal{Z}_j^s)$).

Fix any saddle of the first type σ_j. By [32, Lemma 16.16] we set $h(\eta) = c_j$ for any $\eta \in \mathcal{Z}_j^m$, $h(\eta) = c_k$ for any $\eta \in \mathcal{Z}_k^m$ with $k \neq j$, and $h(\sigma_j) = \bar{c}_j$. By definition of saddles of the first type, note that σ_j communicates only with configurations either in $\mathcal{X}^{meta}$, or in $\mathcal{Z}_j^m$ or in $\mathcal{Z}_k^m$ with $k \neq j$. Thus the contribution to (3.6.6) of the saddle of the first type σ_j is

$$\sum_{\xi\in\mathcal{X}^{meta}} |\sigma_j\sim\xi|(1-\bar{c}_j)^2 + \sum_{\xi\in\mathcal{Z}_j^m} |\sigma_j\sim\xi|(\bar{c}_j-c_j)^2 + \sum_{\substack{\xi\in\mathcal{Z}_k^m \\ k\neq j}} |\sigma_j\sim\xi|(c_k-\bar{c}_j)^2. \tag{3.6.8}$$

The cases $\mathcal{Z}_j^m = \emptyset$ (resp. $\mathcal{Z}_k^m = \emptyset$) or there is no $\xi \in \mathcal{Z}_j^m$ (resp. $\xi \in \mathcal{Z}_k^m$) such that $\sigma_j \sim \xi$ correspond to the situation in which either there is not the well $\mathcal{Z}_j^m$ (resp. $\mathcal{Z}_k^m$ for any $k \neq j$) or the dynamics does not allow the communication via one step from σ_j and $\mathcal{Z}_j^m$ (resp. $\mathcal{Z}_k^m$). In the first situation we get $\bar{c}_j = 1$ and in the second one we get $\bar{c}_j = c_j = 1$. Otherwise, since the quantity in (3.6.8) is greater or equal than zero, the minimum with respect to c_j, c_k and $\bar{c}_j$ of (3.6.8) is obtained for $c_j = c_k = \bar{c}_j = 1$, thus h is constant equal to 1 on $\bigcup_{j=1}^{J_m}(\{\sigma_j\}\cup\mathcal{Z}_j^m)$. If we consider all the possible transitions of this type and use (3.6.8), we obtain a contribution to (3.6.6) equal to

$$\sum_{j=1}^{J_m} \left(\sum_{\xi\in\mathcal{X}^{meta}} |\sigma_j\sim\xi|(1-\bar{c}_j)^2 + \sum_{\xi\in\mathcal{Z}_j^m} |\sigma_j\sim\xi|(\bar{c}_j-c_j)^2 + \sum_{\substack{\xi\in\mathcal{Z}_k^m \\ k\neq j}} |\sigma_j\sim\xi|(c_k-\bar{c}_j)^2 \right). \tag{3.6.9}$$

Again, the minimum of (3.6.9) with respect to $c_1,\dots,c_{J_m}$ and $\bar{c}_1,\dots,\bar{c}_{J_m}$ is obtained for $c_i = \bar{c}_i = 1$ for any $i = 1,\dots,J_m$.

Similarly, we deduce that h is constant equal to 0 on $\bigcup_{j=1}^{J_s}(\{\zeta_j\}\cup\mathcal{Z}_j^s)$. Indeed, if we fix any saddle of the second type ζ_j, by [32, Lemma 16.16] we set $h(\eta) = c_j$ for any $\eta \in \mathcal{Z}_j^s$, $h(\eta) = c_k$ for any $\eta \in \mathcal{Z}_k^s$ with $k \neq j$, and $h(\zeta_j) = \bar{c}_j$. By definition of saddles of the second type, note that ζ_j communicates only with configurations either in $\mathcal{X}^{stab}$, or in $\mathcal{Z}_j^s$ or in $\mathcal{Z}_k^s$ with $k \neq j$. Thus the contribution to (3.6.6) of the saddle of the second type ζ_j is

$$\sum_{\xi\in\mathcal{X}^{stab}} |\zeta_j\sim\xi|\bar{c}_j^2 + \sum_{\xi\in\mathcal{Z}_j^s} |\zeta_j\sim\xi|(\bar{c}_j-c_j)^2 + \sum_{\substack{\xi\in\mathcal{Z}_k^s \\ k\neq j}} |\zeta_j\sim\xi|(c_k-\bar{c}_j)^2. \tag{3.6.10}$$

The cases $\mathcal{Z}_j^s = \emptyset$ (resp. $\mathcal{Z}_k^s = \emptyset$) or there is no $\xi \in \mathcal{Z}_j^s$ (resp. $\xi \in \mathcal{Z}_k^s$) such that $\zeta_j \sim \xi$ correspond to the situation in which either there is not the well $\mathcal{Z}_j^s$ (resp. $\mathcal{Z}_k^s$ for any $k \neq j$) or the dynamics does not allow the communication via one step from ζ_j and $\mathcal{Z}_j^s$ (resp. $\mathcal{Z}_k^s$). In the first situation we get $\bar{c}_j = 0$ and in the second one we get $\bar{c}_j = c_j = 0$. Otherwise, since the quantity in (3.6.10) is greater or equal than zero, the minimum with respect to c_j, c_k and $\bar{c}_j$ of (3.6.10) is obtained for $c_j = c_k = \bar{c}_j = 0$, thus h is constant equal to 0 on $\bigcup_{j=1}^{J_s}(\{\zeta_j\} \cup \mathcal{Z}_j^s)$. If we consider all the possible transitions of this type, we obtain a contribute to (3.6.6) equal to

$$\sum_{j=1}^{J_s}\left(\sum_{\xi\in\mathcal{X}^{stab}} |\zeta_j \sim \xi|\bar{c}_j^2 + \sum_{\xi\in\mathcal{Z}_j^m} |\zeta_j \sim \xi|(\bar{c}_j - c_j)^2 + \sum_{\substack{\xi\in\mathcal{Z}_k^m \\ k\neq j}} |\zeta_j \sim \xi|(c_k - \bar{c}_j)^2\right). \tag{3.6.11}$$

Again, the minimum of (3.6.11) with respect to $c_1, ..., c_{J_s}$ and $\bar{c}_1, ..., \bar{c}_{J_s}$ is obtained for $c_i = \bar{c}_i = 0$ for any $i = 1, ..., J_s$. Therefore formula (16.3.15) in the proof of [32, Lemma 16.17] should be modified as

$$h = \begin{cases} 1 & \text{on } \mathcal{X}^{meta} \cup \bigcup_{j=1}^{J_m}(\{\sigma_j\} \cup \mathcal{Z}_j^m), \\ 0 & \text{on } \mathcal{X}^{stab} \cup \bigcup_{j=1}^{J_s}(\{\zeta_j\} \cup \mathcal{Z}_j^s), \\ c_i & \text{on } \mathcal{X}(i), i = 1, ..., \bar{I}, \end{cases} \tag{3.6.12}$$

where $\mathcal{X}(i)$, $i = 1, ..., \bar{I}$, are all the wells of the transition except $\bigcup_{j=1}^{J_m} \mathcal{Z}_j^m$ and $\bigcup_{j=1}^{J_s} \mathcal{Z}_j^s$. Thus, we get the claim. □

Remark 3.6.8. *Note that Lemma 3.6.7 can be simply adapted to the discrete time Kawasaki dynamics we consider in this thesis by modifying (3.6.6) as follows. Since the transition rates of the dynamics for the discrete time version are those of the continuous time version rescaled by a factor $1/|\bar{\Lambda}^{*,or ie}|$, equation (3.6.6) should be modified as*

$$\Theta = \min_{c_1,...,c_{\bar{I}}} \min_{\substack{h:\mathcal{X}^*\to[0,1] \\ h_{|\mathcal{X}_I^{meta}}=1,\ h_{|\mathcal{X}_{II}^{stab}}=0,\ h_{|\mathcal{X}(i)}=c_i, i=1,...,\bar{I}}} \frac{1}{2}\sum_{\xi,\xi'\in\mathcal{X}^*} \frac{\mathbb{1}_{\{\xi\sim\xi'\}}}{|\bar{\Lambda}^{*,or ie}|}[h(\xi) - h(\xi')]^2. \tag{3.6.13}$$

Remark 3.6.9. *Lemma 3.6.7 implies that also the unessential saddles σ_j and ζ_j have to be considered in the estimate of the prefactor. However, since $h(\sigma_j) = 1$ and $h(\zeta_j) = 0$ for any j, the transitions that involve these unessential saddles do not contribute numerically to the computation of K. The variational formula for Θ in (3.6.6) is non-trivial because it depends on the geometry of all the wells $\mathcal{X}(i)$, $i = 1, ..., I$, and on the form of the function h on the configurations in $\mathcal{X}^* \setminus \mathcal{X}^{**}$, namely the saddle configurations. These two steps are the model–dependent keys to compute the prefactor $K = 1/\Theta$.*

Remark 3.6.10. *For the hexagonal Ising model that evolves under Glauber dynamics, the estimate of the upper bound of the prefactor, given in [4, Section 6.1], is done setting the equilibrium potential h, for that specific model, according to our discussion (see (3.6.12) and [4, eq. (6.19)])). The authors analyzed the unessential saddles of first and second type that they used for the definition of h together with their valleys. Indeed, they define the sets $\bigcup_{j=1}^{J_A} \mathcal{N}_j^A$ and $\bigcup_{j=1}^{J_B} \mathcal{N}_j^B$ in [4, Section 6.1] that coincide, in their model, with $\bigcup_{j=1}^{J_m} \mathcal{Z}_j^m$ (resp. $\bigcup_{j=1}^{J_s} \mathcal{Z}_j^s$) by Proposition 3.6.5 (resp. Proposition 3.6.6). In [4, Section 6.1] an explicit example of saddle σ_i is given.*

Remark 3.6.11. *In [26, Section 7] the authors study the estimate of the prefactor for the q-state Potts model that evolves under Glauber dynamics using the above discussion and Lemma 3.6.7. In [26, Lemma 7.4(b)] the authors identify geometrically unessential saddles of the first type (see [26, Figure 18(b)]) and describe their wells in the proof. In [26, Lemma 7.4(c)] the authors identify geometrically one unessential saddle of the second type (see [26, Figure 19]). Choosing $q = 2$, this Lemma gives the same results for the standard Ising model. We refer also to [32, Chapter 17], where the authors compute the prefactor in [32, Theorem 17.4] using [32, Lemma 16.17] and some model-dependent properties without identifying the unessential saddles.*

Remark 3.6.12. *For the Ising model with weakly and strongly anisotropic interactions that evolves under Kawasaki dynamics, the estimate of the prefactor is given in Theorems 4.1.4 and 5.1.5, respectively, according to the above discussion and Lemma 3.6.7. For the strongly anisotropic case the authors are able to obtain a sharp estimate for K in (5.1.13). Nevertheless, the asymptotic behavior of the prefactor in the strongly anisotorpic regime as $\Lambda \to \mathbb{Z}^2$ is the same as that of the isotropic and weakly anisotropic regimes, see [35, Theorem 1.4.5] and Theorem 4.1.4), respectively. Moreover, in Figure 5.5 an example of unessential saddle of the second type is given.*

For our model $\mathcal{X}^m = \{\square\}$ and $\mathcal{X}^s = \{\blacksquare\}$, thus (H1) holds and $\Gamma_m = \Phi(\square, \blacksquare) - \widehat{H}(\square) = \Gamma^*$. Moreover, $\mathscr{P}^*_{PTA}(\square, \blacksquare) = \mathcal{D}$ and $\mathscr{C}^*_{PTA}(\square, \blacksquare)$ is the union of all the configurations that are composed by a cluster in $\mathcal{D}$ and a free particle in $\partial^- \Lambda$. Therefore it is clear that $\mathcal{C}^* \neq \mathscr{C}^*_{PTA}(\square, \blacksquare)$. Note that (H2) follows from [35, Proposition 2.3.7]. Here we abbreviate $\mathscr{P}^*_{PTA} = \mathscr{P}^*_{PTA}(\square, \blacksquare)$ and $\mathscr{C}^*_{PTA} = \mathscr{C}^*_{PTA}(\square, \blacksquare)$. Note that $\mathcal{X}^{meta} = \mathcal{C}^{\square}_{\blacksquare}(\Gamma^*)$ and $\mathcal{X}^{stab} = \mathcal{C}^{\blacksquare}_{\square}(\Gamma^* - \widehat{H}(\blacksquare))$. Recall Definition 3.6.4 for the definition of the wells $\mathcal{Z}^{\square}_j$ and $\mathcal{Z}^{\blacksquare}_j$. Concerning Theorem 3.6.3, by [35, Lemma 3.3.2] we know that h is constant on each wells. Thanks to the model–independent discussion given in this section and Lemma 3.6.7, formula (3.6.12) becomes

$$h = \begin{cases} 1 & \text{on } \mathcal{C}^{\square}_{\blacksquare}(\Gamma^*) \cup \bigcup_{j=1}^{J_{\square}} (\{\sigma_j\} \cup \mathcal{Z}^{\square}_j), \\ 0 & \text{on } \mathcal{C}^{\blacksquare}_{\square}(\Gamma^* - \widehat{H}(\blacksquare)) \cup \bigcup_{j=1}^{J_{\blacksquare}} (\{\zeta_j\} \cup \mathcal{Z}^{\blacksquare}_j), \\ c_i & \text{on } \mathcal{X}(i), i = 1, ..., \bar{I}, \end{cases} \tag{3.6.14}$$

where $\mathcal{X}(i)$, $i = 1, ..., \bar{I}$, are all the wells of the transition except $\bigcup_{j=1}^{J_{\square}} \mathcal{Z}^{\square}_j$ and $\bigcup_{j=1}^{J_{\blacksquare}} \mathcal{Z}^{\blacksquare}_j$. Note that formula (3.3.20) in the proof of [35, Proposition 3.3.3] should be modified accordingly to (3.6.14).

3.6.2 *Proof of Theorem 3.2.8*

Thanks to [92, Lemma 3.6], we deduce that for our model the quantity $\widetilde{\Gamma}(B)$, with $B \subsetneq \mathcal{X}$, defined in [92, eq. (21)] is such that $\widetilde{\Gamma}(\mathcal{X} \setminus \{\blacksquare\}) = \Gamma^*$. Thus, Theorem 3.2.8 follows by the following proposition.

Proposition 3.6.13. *[92, Proposition 3.24] For any $\varepsilon \in (0, 1)$ and any $s \in \mathcal{X}^s$*

$$\lim_{\beta \to \infty} \frac{1}{\beta} \log t^{mix}_{\beta}(\varepsilon) = \widetilde{\Gamma}(\mathcal{X} \setminus \{s\}) = \lim_{\beta \to \infty} -\frac{1}{\beta} \log \rho_{\beta}. \tag{3.6.15}$$

Furthermore, there exist two constants $0 < c_1 \leqslant c_2 < \infty$ independent of β such that for every $\beta > 0$

$$c_1 e^{-\beta \widetilde{\Gamma}(\mathcal{X} \setminus \{s\})} \leqslant \rho_{\beta} \leqslant c_2 e^{-\beta \widetilde{\Gamma}(\mathcal{X} \setminus \{s\})}. \tag{3.6.16}$$

APPENDIX

3.A ADDITIONAL MATERIAL FOR SECTION 3.5

We give explicit argument to complete the proof of Proposition 3.5.1, considering the cases that were left in Section 3.5.1, since the proofs are analogue to the ones discussed in that section. Due to [85, Theorem 5.1], our strategy consists in characterizing the essential saddles that could be visited after attaching the free particle in a bad site.

Case 2A. Without loss of generality we consider η as in Figure 3.10(a). If we are considering the case in which a sequence of 1-translations of a bar is possible and takes place, then by Lemma 3.5.2(i) the saddles that are crossed are essential and in $\mathscr{I}^{\alpha}_0 \cup \mathscr{I}^{\alpha}_1$. If a sequence of 1-translations of a bar takes place so that the last configuration has at most two occupied frame-angles and it belongs to the cases 2B, 2C and 2D treated below. Thus we are left to analyze the case in which there is the activation of a sliding of a bar around a frame-angle.

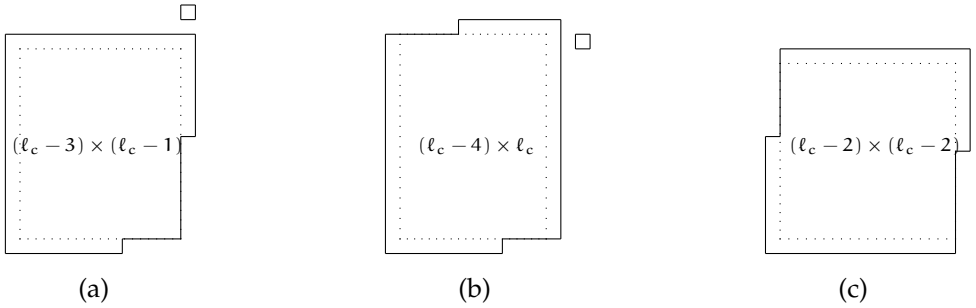

Figure 3.10 – Case 2A: in (a) we depict a possible starting configuration $\eta \in \mathcal{C}^*$, in (b) the configuration $\widetilde{\eta}$ obtained from η after the sliding of the bar $B^e(\eta)$ around the frame-angle $c^{en}(\eta')$ and in (c) the configuration $\widetilde{\eta}$ obtained from η after the sliding of the bar $B^s(\eta)$ around the frame-angle $c^{sw}(\eta')$.

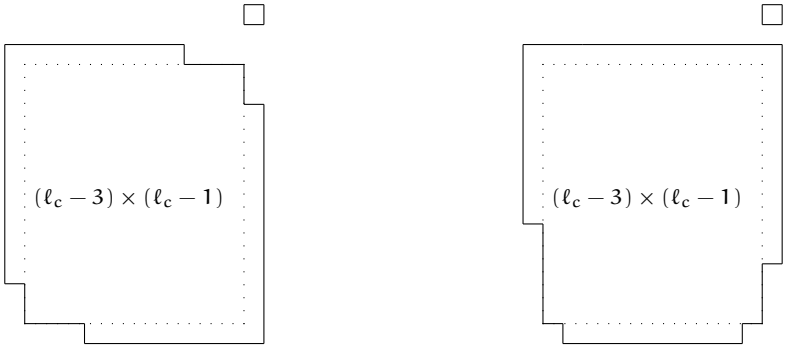

Figure 3.11 – On the left-hand side we depict a possible starting configuration $\eta \in \mathcal{C}^*$ for the case 2B(i) and on the right-hand side a possible starting configuration $\eta \in \mathcal{C}^*$ for the case 2B(ii).

If the free particle is attached to the bar $B^e(\eta)$, then it is not possible to complete the sliding of the bar $B^n(\eta)$ around the frame-angle $c^{ne}(\eta')$, since the condition (3.2.12) is not satisfied. Thus by Lemma 3.4.1(ii) we know that the saddles that could be crossed in this attempt are unessential. If the free particle is attached to the bar $B^s(\eta)$, we conclude as before.

If the free particle is attached to the bar $B^n(\eta)$, then it is not possible to complete the sliding of the bar $B^w(\eta)$ around the frame-angle $c^{wn}(\eta')$ because the condition (3.2.12) is not satisfied and thus we can conclude as before. If $|B^e(\eta)| < |B^n(\eta)|$ the condition (3.2.12) is satisfied, thus it is possible to slide the bar $B^e(\eta)$ around the frame-angle $c^{en}(\eta')$. By Lemma 3.4.1(i) the saddles that are possibly visited are essential and, except the last one, they are in $\mathscr{I}_{k,k',1}^{\alpha,\alpha'}$. The last configuration visited during this sliding of a bar is $\widetilde{\eta} \in \mathscr{I}_1^{\alpha,\alpha'}$, has a free particle and it is depicted in Figure 3.10 (b). Starting from such a configuration, if a sequence of 1-translations of a bar is possible and takes place, then by Lemma 3.5.2(ii) the saddles that could be crossed are essential and in $\mathscr{I}_1^{\alpha} \cup \mathscr{I}_2^{\alpha}$. If this free particle is now attached to $\partial^- CR(\widetilde{\eta})$, then the path reaches $\mathcal{C}_{\blacksquare}^{\square}(\Gamma^*)$ and the saddles are those obtained up to this point. Otherwise, if the free particle is now attached to $B^w(\widetilde{\eta})$ obtaining the configuration η'', and if a sliding of the bar $B^s(\widetilde{\eta})$ around the frame-angle $c^{sw}(\eta'')$ takes place, by Lemma 3.4.1(i) the saddles that could be crossed are essential and, except the last one, are in $\mathscr{I}_{k,k',1}^{\alpha,\alpha'}$. The last configuration is in $\mathcal{C}^*$, because the cluster is in $\widetilde{\mathcal{D}}$. If this sliding of a bar does not take place, the path ω has to go back to a configuration in $\mathscr{I}_1^{\alpha,\alpha'}$ and the saddles that could be crossed are already considered. From now on, we can iterarate this argument for a finite number of steps since the path has to reach $\blacksquare$.

If the free particle is first attached to the bar $B^w(\eta)$, we argue in a similar way as before. Indeed, if $|B^s(\eta)| < |B^w(\eta)|$, it is possible to slide the bar $B^s(\eta)$ around the frame-angle $c^{sw}(\eta')$. By Lemma 3.4.1(i) the saddles that are possibly visited are essential and, except the last one, are in $\mathscr{I}_{k,k',0}^{\alpha,\alpha'}$. The last configuration visited during this sliding of a bar is in $\mathcal{C}^*$ (see Figure 3.10(c)) and it belongs to case 1A. This concludes case 2A.

Case 2B. We consider separately the following subcases:
(i) the two occupied frame-angles are $c^{\alpha\alpha'}(\eta)$ and $c^{\alpha''\alpha'''}(\eta)$, with all the indices $\alpha, \alpha', \alpha''$ and α''' different between each other (see Figure 3.11 on the left-hand side);
(ii) the two occupied frame-angles are $c^{\alpha\alpha'}(\eta)$ and $c^{\alpha'\alpha''}(\eta)$, with $\alpha \neq \alpha''$ (see Figure 3.11 on the right-hand side).

Case 2B(i). Without loss of generality we consider η as in Figure 3.11 on the left-hand side. If we are considering the case in which a sequence of 1-translations of a bar is possible and takes place, then by Lemma 3.5.2(i) the saddles that are crossed are essential and they are in $\mathscr{I}_0^\alpha \cup \mathscr{I}_1^\alpha$. If at least one bar is full and a sequence of 1-translations of a bar takes place, it is possible to obtain a configuration either with two occupied frame-angles with a bar in common or with three occupied frame-angles. The first case will been analyzed in case 2B(ii) and the latter one has been already analyzed in case 2A. Thus we can reduce our proof to the case in which there is no translation of bars and therefore there is the activation of a sliding of a bar around a frame-angle. First, assume that $|B^n(\eta)| < |B^w(\eta)|$ and $|B^s(\eta)| < |B^e(\eta)|$. By Lemma 3.4.1 the only two possibilities to obtain essential saddles is to attach the free particle to the bar $B^w(\eta)$ or $B^e(\eta)$ and then slide the bar $B^n(\eta)$ around the frame-angle $c^{nw}(\eta')$ or $B^s(\eta)$ around $c^{se}(\eta')$ respectively. If the free particle is first attached to $B^w(\eta)$, by Lemma 3.5.2(i) the saddles that are possibly visited are essential and, except the last one, are in $\mathscr{I}^{\alpha,\alpha'}_{k,k',0}$. The last configuration is $\widetilde{\eta} \in \mathscr{I}^{\alpha}_{-1}{}^{\alpha'}$. Starting from $\widetilde{\eta}$, it is possible to attach the free particle to the bar $B^e(\widetilde{\eta})$ obtaining a configuration η'', and then slide the bar $B^s(\widetilde{\eta})$ around the frame-angle $c^{se}(\eta'')$. Thus by Lemma 3.4.1(i) we know that these saddles are essential and, except the last one, are in $\mathscr{I}^{\alpha,\alpha'}_{k,k',0}$. The last configuration is $\bar{\eta} \in \mathscr{I}_0^{\alpha,\alpha'}$. Starting from $\bar{\eta}$, it is not possible to complete any sliding of a bar around a frame-angle and thus by Lemma 3.4.1(ii) we conclude that the saddles that will be possibly crossed are unessential unless a sequence of 1-translations of bars takes place. In this case, by Lemma 3.5.2(i) the saddles that could be crossed are essential and in $\mathscr{I}_0^\alpha \cup \mathscr{I}_1^\alpha$. If the free particle is first attached to $B^e(\eta)$, we conclude similarly.

Assume now that $|B^w(\eta)| < |B^n(\eta)|$ and $|B^e(\eta)| < |B^s(\eta)|$: we argue in the same way as before. If the free particle is first attached to the bar $B^n(\eta)$, the essential saddles that could be crossed are in $\mathscr{I}^{\alpha,\alpha'}_{k,k',1}$ and the last one is $\widetilde{\eta} \in \mathscr{I}_1^{\alpha,\alpha'}$ and has a free particle. Again, starting from $\widetilde{\eta}$, if the free particle is attached to the bar $B^s(\widetilde{\eta})$ obtaining the configuration η'', by Lemma 3.4.1(i) we know that the saddles that will be possibly crossed are essential and, except the last one, are in $\mathscr{I}^{\alpha,\alpha'}_{k,k',2}$. The last configuration is $\bar{\eta} \in \mathscr{I}_2^{\alpha,\alpha'}$. If the free particle is first attached to the bar $B^s(\eta)$, we conclude as above. Starting from $\bar{\eta}$, it is not possible to complete any sliding of a bar around a frame-angle and thus by Lemma 3.4.1(ii) the saddles that could be crossed are unessential unless a sequence of 1-translations of bars takes place. In the latter case, by Lemma 3.5.2(iii) the saddles that could be crossed are essential and in $\mathscr{I}_2^\alpha \cup \mathscr{I}_3^\alpha$.

The cases $|B^w(\eta)| < |B^n(\eta)|$, $|B^s(\eta)| < |B^e(\eta)|$ and $|B^n(\eta)| < |B^w(\eta)|$, $|B^e(\eta)| < |B^s(\eta)|$ can be treated with the same argument as the previous ones and the essential saddles encountered have been already considered. This concludes case 2B(i).

Case 2B(ii). Without loss of generality we consider η as on the right-hand side in Figure 3.11. If we are considering the case in which a sequence of 1-translations of a bar is possible and takes place, then by Lemma 3.5.2(i) the saddles that are crossed are essential and they are in $\mathscr{I}_0^\alpha \cup \mathscr{I}_1^\alpha$. If one bar among $B^w(\eta)$ and $B^e(\eta)$ is full, then it is possible that a sequence of 1-translations of the bar $B^s(\eta)$ takes place in order to have three occupied frame-angles. This situation has already been analyzed in case 2A. Thus we can reduce our proof to the case in which there is no translation of bars and therefore there is the activation of a sliding of a bar around a frame-angle. If the free particle is attached to the bar $B^s(\eta)$, it is not possible to complete any sliding of a bar around a frame-angle at cost U and by Lemma 3.4.1(ii) we know that the saddles that could be crossed are unessential. If the free particle is attached to one bar among $B^w(\eta)$ and $B^e(\eta)$, since (3.2.12) is not satisfied it is not possible to complete the sliding of the bar $B^n(\eta)$ around the frame-angle $c^{nw}(\eta')$ and $c^{ne}(\eta')$ respectively. Thus by Lemma 3.4.1(ii) the saddles that will be possibly crossed are unessential. If the free particle is attached to the bar $B^n(\eta)$, then it is possible to complete the sliding of the bar $B^w(\eta)$ or $B^e(\eta)$ around the frame-angle $c^{wn}(\eta')$ or $c^{en}(\eta')$ respectively. Thus by Lemma 3.4.1(i) we know

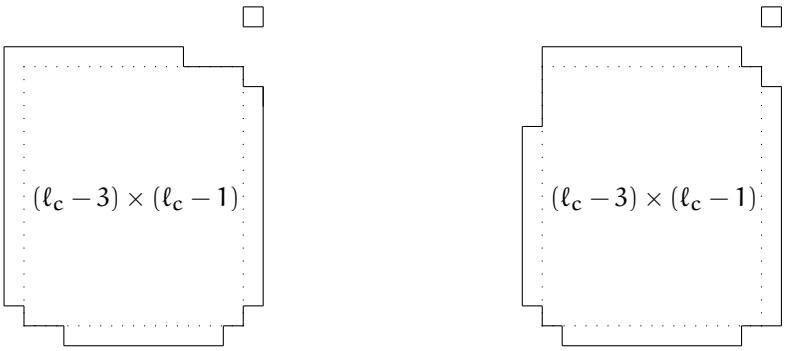

Figure 3.12 – On the left-hand side we depict a possible starting configuration $\eta \in \mathcal{C}^*$ for the case 2C and on the right-hand side a possible starting configuration $\eta \in \mathcal{C}^*$ for the case 2D.

that the saddles that will be crossed are essential and, except the last one, are in $\mathscr{I}_{k,k',1}^{\alpha,\alpha'}$. The last configuration is $\widetilde{\eta} \in \mathscr{I}_1^{\alpha,\alpha'}$ that has a free particle. If this free particle is now attached to $\partial^- CR(\widetilde{\eta})$, then the path reaches $\mathcal{C}_{\blacksquare}^{\square}(\Gamma^*)$ and the saddles are those obtained up to this point. Otherwise, since condition (3.2.12) is not satisfied, it is not possible to complete any sliding of a bar around a frame-angle, thus by Lemma 3.4.1(ii) the saddles that will be possibly crossed during the sliding of a bar are unessential. On the other hand, if a sequence of 1-translations of a bar is possible and takes place, then, starting from $\widetilde{\eta}$, by Lemma 3.5.2(ii) the saddles that could be crossed are essential and in $\mathscr{I}_1^{\alpha} \cup \mathscr{I}_2^{\alpha}$. This concludes case 2B(ii).

Case 2C. Without loss of generality we consider η as in Figure 3.12 on the left-hand side. If we are considering the case in which a sequence of 1-translations of a bar is possible and takes place, then by Lemma 3.5.2(i) the saddles that are crossed are in $\mathscr{I}_0^{\alpha} \cup \mathscr{I}_1^{\alpha}$. Thus we can reduce our proof to the case in which there is no 1-translation of a bar and therefore there is only the activation of a sliding of a bar around a frame-angle. Starting from this configuration it is possible to obtain two occupied frame-angles via a sequence of 1-translations of a bar: this situation has been already analyzed in case 2B. If the free particle is attached to the bar $B^e(\eta)$ or $B^s(\eta)$, since it is not possible to complete any sliding of bar around a frame-angle at cost U, by Lemma 3.4.1(ii) we know that the saddles that could be crossed are unessential. If $|B^w(\eta)| < |B^n(\eta)|$ (resp. $|B^n(\eta)| < |B^w(\eta)|$) and the free particle is attached to the bar $B^n(\eta)$ (resp. $B^w(\eta)$), then it is possible to complete a sliding of the bar $B^w(\eta)$ (resp. $B^n(\eta)$) around the frame-angle $c^{wn}(\eta')$ (resp. $c^{nw}(\eta')$). Thus by Lemma 3.4.1(i) the saddles that could be crossed are essential and in $\mathscr{I}_{k,k',1}^{\alpha,\alpha'}$ (resp. $\mathscr{I}_{k,k',0}^{\alpha,\alpha'}$), except the last one that is $\widetilde{\eta} \in \mathscr{I}_1^{\alpha,\alpha'}$ (resp. $\widetilde{\eta} \in \mathscr{I}_{-1}^{\alpha,\alpha'}$) with a free particle. If this free particle is now attached to $\partial^- CR(\widetilde{\eta})$, then the path reaches $\mathcal{C}_{\blacksquare}^{\square}(\Gamma^*)$ and the saddles are those obtained up to this point. Otherwise, condition (3.2.12) is not satisfied, thus it is not possible to complete any sliding of a bar around a frame-angle. Therefore by Lemma 3.4.1(ii) we know that the saddles that could be visited are unessential unless a sequence of 1-translations of a bar is possible and takes place. In this case, by Lemma 3.5.2(ii) (resp. Lemma 3.5.2(i)) the saddles that could be crossed are essential and in $\mathscr{I}_1^{\alpha} \cup \mathscr{I}_2^{\alpha}$ (resp. $\mathscr{I}_0^{\alpha}$). This concludes case 2C.

Case 2D. Without loss of generality we consider η as in Figure 3.12 on the right-hand side. If we are considering the case in which a sequence of 1-translations of a bar is possible and takes place, then by Lemma 3.5.2(i) the saddles that are crossed are essential and in $\mathscr{I}_0^{\alpha} \cup \mathscr{I}_1^{\alpha}$. Thus, we can reduce our proof to the case in which there is no 1-translation of a bar and therefore there is only the activation of a sliding of a bar around a frame-angle. Starting from this configuration, it is possible to obtain one or two occupied frame-angles via a sequence of 1-translations: these situations have been already analyzed in cases 2C and 2B respectively. If the free particle is attached to one of the bars, since it is not possible to complete any sliding of bar around a frame-angle at cost U, by Lemma 3.4.1(ii) we know that the saddles that could be crossed are unessential. This concludes case 2D.

4

CRITICAL DROPLETS ON THE SQUARE LATTICE: WEAK ANISOTROPY

This chapter is devoted to the geometrical characterization of the union of all the minimal gates for the local model evolving under Kawasaki dynamics with weakly anisotropic interactions, namely, $U_1 < 2U_2$ in (1.3.11). To this end, we apply the model–independent strategy carried out in Chapter 3 to the weakly anisotropic local model. For this regime we are able to fully identify the geometry of the union of all the minimal gates. We observe very different behaviour compared to the strongly anisotropic regime ($U_1 > 2U_2$). Finally, we provide sharp asymptotics concerning the mean transition time, the mixing time and the spectral gap.

This chapter is structured as follows. We state our main results in Section 4.1. In particular, we state the results concerning the gates in Section 4.1.1 and the sharp asymptotics in Section 4.1.2. In Section 4.2 we provide some results that are useful for the model–dependent strategy concerning the minimal gates carried out in Section 4.3. In Section 4.4 we give the proof of the main result regarding the identification of the union of all the minimal gates (see Theorem 3.2.7), while in Section 4.5 we give the proof of the main model–independent theorems about the sharp asymptotics. In Section 4.6 we provide an argument to extend to the simplified weakly anisotropic model the results about the nucleation derived for the local model. Finally, in Appendices 4.A and 4.B we give additional explicit proofs and computations.

4.1 MAIN RESULTS

In this section we state our main results. In Section 4.1.1 we obtain the geometrical characterization of the union of all minimal gates. In order to do this, we need some specific definitions for the weakly anisotropic case (see Section 4.1.1). In Section 4.1.2 we derive sharp estimates for the asymptotic transition time in the weakly anisotropic case. Moreover, we derive the mixing time and spectral gap. For the corresponding results obtained in the isotropic and strongly anisotropic cases we refer to Sections 3.2.2 and 5.1.1 for results concerning the gates and union of minimal gates, respectively. For the corresponding results concerning the asymptotic transition time, mixing time and spectral gap obtained for the isotropic and strongly anisotropic cases we refer to Section 3.2.3 and 5.1.2, respectively.

4.1.1 *Gate for the local model*

In this section we assume $U_1 \neq U_2$ and $U_1 < 2U_2 - 2\varepsilon$ in (1.3.11) (recall (3.2.8) for the definition of ε), i.e., we consider weakly anisotropic interactions between nearest neighboring sites. We will consider $0 < \varepsilon \ll U_2$, where $\ll$ means suffiently smaller; for instance $\varepsilon \leqslant \frac{U_2}{100}$ is enough. In order to state our main results for the gates in the weakly anisotropic regime we need the following definitions. Recall (1.3.30) for the definition of $\bar{\ell}$ and (3.2.5) for the definition of s. For $x \in \mathbb{Z}$, $n \in \mathbb{N}$, we define $[x]_n := x \bmod n$. For any $s > \bar{\ell} + 2$, if s has the same parity as $\bar{\ell}$ i.e., $[s - \bar{\ell}]_2 = [0]_2$, then we define the set of 0-*standard rectangles* as $\mathcal{R}^{0-st}(s) := \mathcal{R}(\ell_1(s), \ell_2(s))$ with side lengths

$$\ell_1(s) := \frac{s + \bar{\ell}}{2}, \qquad \ell_2(s) := \frac{s - \bar{\ell}}{2}, \qquad \text{for } [s - \bar{\ell}]_2 = [0]_2. \tag{4.1.1}$$

If s has the same parity as $\bar{\ell} - 1$ i.e., $[s - \bar{\ell}]_2 = [1]_2$, we define the set of 1-*standard rectangles* to be $\mathcal{R}^{1-st}(s) := \mathcal{R}(\ell_1(s), \ell_2(s))$ with side lengths

$$\ell_1(s) := \frac{s + \bar{\ell} - 1}{2}, \qquad \ell_2(s) := \frac{s - \bar{\ell} + 1}{2}, \qquad \text{for } [s - \bar{\ell}]_2 = [1]_2. \tag{4.1.2}$$

For this value of s we define the set of *quasi-standard* rectangles as $\mathcal{R}^{q-st}(s) := \mathcal{R}(\ell_1(s)+1, \ell_2(s)-1)$. Finally, we set

$$\mathcal{R}^{st}(s) := \begin{cases} \mathcal{R}^{0-st}(s) & \text{if } [s-\bar{\ell}]_2 = [0]_2, \\ \mathcal{R}^{1-st}(s) & \text{if } [s-\bar{\ell}]_2 = [1]_2. \end{cases} \tag{4.1.3}$$

Recall (1.3.22) for the definition of the horizontal and vertical critical lengths ℓ_1^* and ℓ_2^*, respectively. We set the critical value of s as

$$s^* := \ell_1^* + \ell_2^* - 1. \tag{4.1.4}$$

Recall that we have defined $\bar{\mathcal{Q}}$ as the set of configurations having one cluster anywhere in Λ_0 consisting of a $(\ell_1^*-1)\times\ell_2^*$ rectangle with a single protuberance attached to one of the shortest sides. Similarly, the set $\widetilde{\mathcal{Q}}$ contains the configurations having one cluster anywhere in Λ_0 consisting of a $(\ell_1^*-1)\times\ell_2^*$ rectangle with a single protuberance attached to one of the longest sides. The critical value of the energy is

$$\Gamma^* = U_1\ell_2^* + U_2\ell_1^* + U_1 + U_2 + \varepsilon\ell_2^* - \varepsilon\ell_1^*\ell_2^* - 2\varepsilon \tag{4.1.5}$$

and the volume of the clusters in $\bar{\mathcal{Q}}$ is

$$n_c = \ell_2^*(\ell_1^*-1)+1. \tag{4.1.6}$$

Finally, recall (1.3.31) for the definition of the sets $\bar{\mathcal{D}}$ and $\widetilde{\mathcal{D}}$. We encourage the reader to consult Proposition 4.2.1, where we give the geometric description of the sets $\bar{\mathcal{D}}$ and $\widetilde{\mathcal{D}}$. Roughly speaking, one can think of $\bar{\mathcal{D}}$ and $\widetilde{\mathcal{D}}$ as the sets of configurations consisting of a rectangular cluster with four bars attached to its four sides, whose lengths satisfy precise conditions. Finally, we set

$$\mathcal{C}^* = \bar{\mathcal{D}}^{fp}. \tag{4.1.7}$$

The reason why only the set $\bar{\mathcal{D}}$ is relevant for the set $\mathcal{C}^*$ will be clarified in Lemma 5.2.6. Note that

$$\begin{aligned} \widehat{H}(\mathcal{C}^*) &= \widehat{H}(\bar{\mathcal{D}}^{fp}) = \widehat{H}(\bar{\mathcal{D}}) + \Delta = \widehat{H}(\bar{\mathcal{Q}}) + \Delta \\ &= U_1\ell_2^* + U_2(\ell_1^*-1) - \varepsilon\ell_2^*(\ell_1^*-1) + 2\Delta - U_1 \\ &= U_1\ell_2^* + U_2\ell_1^* + U_1 + U_2 + \varepsilon\ell_2^* - \varepsilon\ell_1^*\ell_2^* - 2\varepsilon \\ &= \Gamma^*. \end{aligned} \tag{4.1.8}$$

See Figure 4.1 for examples of configurations in $\mathcal{C}^*$.

Remark 4.1.1. *Note that* $\widehat{H}(\bar{\mathcal{Q}}) < \widehat{H}(\widetilde{\mathcal{Q}})$. *Indeed,*

$$\begin{aligned} \widehat{H}(\bar{\mathcal{Q}}) &= \Gamma^* - \Delta, \\ \widehat{H}(\widetilde{\mathcal{Q}}) &= \Gamma^* - \Delta + U_1 - U_2. \end{aligned} \tag{4.1.9}$$

The first main result of Section 4.1.1 is a refinement of [90, Theorem 2].

Theorem 4.1.2. (Gate for weakly anisotropic interactions). *The set* $\mathcal{C}^*$ *is a gate for the transition from* $\square$ *to* $\blacksquare$.

We refer to Section 4.4.1 for the proof of Theorem 4.1.2.

In order to give the result regarding the geometric characterization of $\mathcal{G}(\square, \blacksquare)$, we need some definitions. For any $i = 0, 1$ we define $\mathcal{P}_i \subseteq \mathcal{S}(\square, \blacksquare)$ to consist of configurations with a single cluster and no free particle, and a fixed number of vacancies that is not monotone with circumscribed rectangles obtained from the one of the configurations in $\bar{\mathcal{D}}$ via increasing by one the horizontal or vertical length. More precisely,

$$\begin{aligned} \mathcal{P}_i := \{\eta : n(\eta) = 0,\, v(\eta) = 2\ell_2^* + i(\ell_1^* - \ell_2^*) - 2,\, g_1'(\eta) = i,\, g_2'(\eta) = 1-i,\, \eta_{cl} \text{ is} \\ \text{connected with circumscribed rectangle in } \mathcal{R}(\ell_1^* - i + 1, \ell_2^* + i)\},\ i = 0, 1. \end{aligned} \tag{4.1.10}$$

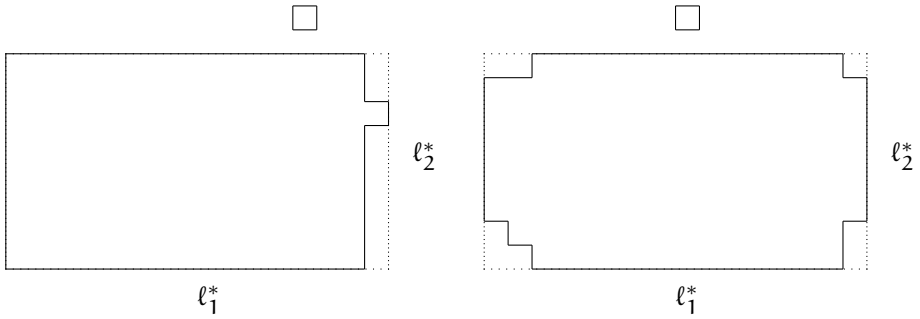

Figure 4.1 – Critical configurations in $\mathcal{C}^*$ in the weakly anisotropic case. Moreover, if we remove the free particle, then we obtain on the left a configuration in $\bar{\mathcal{Q}}$ and on the right a configuration in $\bar{\mathcal{D}} \setminus \bar{\mathcal{Q}}$.

See Figure 1.18 for examples of configurations in $\mathcal{P}_0$ (on the left-hand side) and in $\mathcal{P}_1$ (on the right-hand side).

The set $\mathcal{G}(\square, \blacksquare)$ contains all the configurations that are in the sets defined in (4.1.10) with the following further conditions. First, we define the subset $\mathcal{N}_0^{\alpha'}$ (resp. $\mathcal{N}_1^{\alpha}$) of the saddles in $\mathcal{P}_0$ (resp. $\mathcal{P}_1$) as the set that contains only one occupied unit square in either a vertical (resp. horizontal) row or in one of its two adjacent frame-angles. More precisely,

$$\mathcal{N}_0^{\alpha'} := \{\eta \in \mathcal{P}_0 : |r^{\alpha'}(\eta) \cup c^{\alpha'\bar{\alpha}}(\eta) \cup c^{\alpha'\widetilde{\alpha}}(\eta)| = 1\}, \tag{4.1.11}$$

for any $\alpha' \in \{w, e\}$ and $\bar{\alpha}, \widetilde{\alpha} \in \{n, s\}$ such that $\bar{\alpha} \neq \widetilde{\alpha}$, and

$$\mathcal{N}_1^{\alpha} := \{\eta \in \mathcal{P}_1 : |r^{\alpha}(\eta) \cup c^{\alpha\alpha''}(\eta) \cup c^{\alpha\alpha'''}(\eta)| = 1\}, \tag{4.1.12}$$

for any $\alpha \in \{n, s\}$ and $\alpha'', \alpha''' \in \{w, e\}$ such that $\alpha'' \neq \alpha'''$. Note that in Figure 1.18 the configuration on the left-hand side is in $\mathcal{N}_0^{e}$ and the configuration on the right-hand side is in $\mathcal{N}_1^{n}$.

Next, we define the subset $\mathcal{N}_{k,k'}^{\alpha,\alpha'}$ of the saddles in $\mathcal{P}_0$ as the set of configurations that are obtained from $\eta \in \mathcal{P}_0$ during the sliding of the bar $B^{\alpha'}(\eta)$ around the frame-angle $c^{\alpha'\alpha}(\eta)$. More precisely,

$$\begin{aligned}\mathcal{N}_{k,k'}^{\alpha,\alpha'} := \quad & \{\eta \in \mathcal{P}_0 : |r^{\alpha}(\eta)| = k-1, |r^{\alpha'}(\eta)| = k'-k+1, k' \leqslant 1 + \|r^{\alpha}(\eta)\|, \\ & |c^{\alpha'\alpha}(\eta)| = 1, (r^{\alpha}(\eta) \cup c^{\alpha'\alpha}(\eta)) \cap \eta_{cl} = r_{cl}^{\alpha,1} \dot{\cup} r_{cl}^{\alpha,2} \text{ with } d(r_{cl}^{\alpha,1}, r_{cl}^{\alpha,2}) = 2\},\end{aligned} \tag{4.1.13}$$

where $\alpha \in \{n, s\}$, $\alpha' \in \{w, e\}$, $r_{cl}^{\alpha,1}$, $r_{cl}^{\alpha,2}$ are two disjoint connected components in $r^{\alpha}(\eta) \cup c^{\alpha'\alpha}(\eta)$ and $k' = \ell_1^* - \ell_2^* + 1, ..., \ell_2^*$, $k = 2, ..., k'$. Note that the conditions in (4.1.13) guarantee that these configurations are obtained during a sliding of a bar around a frame-angle, that is identified by the indeces α and α'. Note that the index k' denotes the length of the bar that we are sliding. The index k counts the number of particles that are in $r^{\alpha}(\eta) \cup c^{\alpha'\alpha}(\eta)$ during the sliding and can be less or equal than ℓ_2^*, but it is possible that for some values of k the set $\mathcal{N}_{k,k'}^{\alpha,\alpha'}$ is empty. Our notation does not distinguish whether $\mathcal{N}_{k,k'}^{\alpha,\alpha'}$ is empty or not in order to avoid the presence of an additional index.

Now we are able to give the second main result of Section 4.1.1.

Theorem 4.1.3. (Union of minimal gates for weakly anisotropic interactions). *We obtain the following description for* $\mathcal{G}(\square, \blacksquare)$*:*

$$\mathcal{G}(\square, \blacksquare) = \mathcal{C}^* \cup \bigcup_{\alpha} \bigcup_{\alpha'} \bigcup_{k'=\ell_1^*-\ell_2^*+1}^{\ell_2^*} \bigcup_{k=2}^{k'} \mathcal{N}_{k,k'}^{\alpha,\alpha'} \cup \bigcup_{\alpha'} \mathcal{N}_0^{\alpha'} \cup \bigcup_{\alpha} \mathcal{N}_1^{\alpha}. \tag{4.1.14}$$

We refer to Section 4.4.2 for the proof of Theorem 4.1.3.

4.1.2 *Sharp asymptotics*

Below we state the main results concerning the sharp asymptotics, whose proof and some discussions are deferred to Section 4.5. Equation (4.1.16) below corrects a minor mistake in [18, eq. (4.14)], where the multiplicative factor $|\bar{\Lambda}^{*,\,\mathrm{orie}}|$ in the asymptotic behaviour of the prefactor is missing.

Theorem 4.1.4. *There exists a constant* $K = K(\Lambda, \ell_2^*)$ *such that*

$$\mathbb{E}_{\square}(\tau_{\blacksquare}) = K e^{\Gamma^* \beta}\,[1 + o(1)], \qquad \beta \to \infty. \tag{4.1.15}$$

Moreover, as $\Lambda \to \mathbb{Z}^2$,

$$K(\Lambda, \ell_2^*) \to \frac{|\bar{\Lambda}^{*,\,\mathrm{orie}}|}{4\pi N}\,\frac{\log|\Lambda|}{|\Lambda|}, \tag{4.1.16}$$

where

$$N = \sum_{k=1}^{4} \binom{4}{k}\binom{\ell_2^* + k - 2}{2k-1} \tag{4.1.17}$$

is the cardinality of $\bar{\mathcal{D}} = \bar{\mathcal{D}}(\Lambda, \ell_2^*)$ *modulo shifts.*

Theorem 4.1.4 investigates the prefactor for the weakly anisotropic case. This analysis for the isotropic case is given in [35, Theorem 1.4.4], while for the strongly anisotropic case is given in Theorem 5.1.5.

Theorem 4.1.5. *Let* $\tau_{\mathcal{C}^*-}$ *be the time just prior* $\tau_{\mathcal{C}^*}$. *Then the entrance distribution of* $\mathcal{C}^*$ *is uniform, i.e.,*

$$\lim_{\beta\to\infty} \mathbb{P}_{\square}\Big(\eta_{\tau_{\mathcal{C}^*-}} = \eta | \tau_{\mathcal{C}^*} < \tau_{\square}\Big) = \frac{1}{|\bar{\mathcal{D}}|} \quad \forall\, \eta \in \bar{\mathcal{D}}. \tag{4.1.18}$$

Remark 4.1.6. *Note that Theorem 4.1.5 concerning the uniform entrance distribution in the gate cannot be extended to the strongly anisotropic case due to the two possible entrances in the gate, see Lemma 5.3.8.*

Recall (1.3.54) and (1.3.55) for the definition of mixing time and spectral gap, respectively.

Theorem 4.1.7. *For any* $\varepsilon \in (0,1)$,

$$\lim_{\beta\to\infty} \frac{1}{\beta} \log t_{\mathrm{mix}}(\varepsilon) = \Gamma^* = \lim_{\beta\to\infty} -\frac{1}{\beta} \log \rho. \tag{4.1.19}$$

Furthermore, there exist two constants $0 < c_1 \leqslant c_2 < \infty$ *independent of* β *such that for every* $\beta > 0$,

$$c_1 e^{-\beta\Gamma^*} \leqslant \rho \leqslant c_2 e^{-\beta\Gamma^*}. \tag{4.1.20}$$

Theorem 4.1.7 holds also for the isotropic and strongly anisotropic cases, see Theorems 3.2.8 and 5.1.8, respectively. in the isotropic regime

4.2 USEFUL MODEL–DEPENDENT TOOLS

4.2.1 *Geometric description of the protocritical droplets*

In [35, Theorem 1.4.1] the authors obtain the geometric description of the set $\mathcal{D}$ as $\mathcal{D} = \bar{\mathcal{D}} \cup \widetilde{\mathcal{D}}$. In this section we derive the geometric description of the analogous sets for the weakly anistropic regime following the argument proposed in [35]. The geometric description of these sets for the strongly anisotropic regime is given in Proposition 5.2.1.

Proposition 4.2.1. (Geometric description of $\widetilde{\mathcal{D}}$ and $\bar{\mathcal{D}}$). *For the weakly anisotropic regime we obtain the following geometric description of* $\bar{\mathcal{D}}$ *and* $\widetilde{\mathcal{D}}$*:*

(a) $\bar{\mathcal{D}}$ *is the set of configurations having one cluster* η *anywhere in* Λ_0 *consisting of a* $(\ell_1^* - 2) \times (\ell_2^* - 2)$ *rectangle with four bars* $B^\alpha(\eta)$*, with* $\alpha \in \{n, w, e, s\}$*, attached to its four sides satisfying*

$$1 \leqslant |B^w(\eta)|, |B^e(\eta)| \leqslant \ell_2^*, \qquad \ell_1^* - \ell_2^* + 1 \leqslant |B^n(\eta)|, |B^s(\eta)| \leqslant \ell_1^*, \tag{4.2.1}$$

and

$$\sum_\alpha |B^\alpha(\eta)| - \sum_{\alpha\alpha' \in \{nw, ne, sw, se\}} |c^{\alpha\alpha'}(\eta)| = 2\ell_1^* + \ell_2^* - 3. \tag{4.2.2}$$

(b) $\widetilde{\mathcal{D}}$ *is the set of configurations having one cluster* η *anywhere in* Λ_0 *consisting of a* $(\ell_1^* - 3) \times (\ell_2^* - 1)$ *rectangle with four bars* $B^\alpha(\eta)$*, with* $\alpha \in \{n, w, e, s\}$*, attached to its four sides satisfying*

$$1 \leqslant |B^w(\eta)|, |B^e(\eta)| \leqslant \ell_2^* + 1, \qquad 1 \leqslant |B^n(\eta)|, |B^s(\eta)| \leqslant \ell_1^* - 1, \tag{4.2.3}$$

and

$$\sum_\alpha |B^\alpha(\eta)| - \sum_{\alpha\alpha' \in \{nw, ne, sw, se\}} |c^{\alpha\alpha'}(\eta)| = \ell_1^* + 2\ell_2^* - 2. \tag{4.2.4}$$

Remark 4.2.2. *Let* $\eta \in \bar{\mathcal{D}}$.

(i) Note that (4.2.2) takes into account the number of occupied unit squares in $\partial^- CR(\eta)$ *due to Remark 3.2.2. We deduce that at most three frame-angles of* $CR(\eta)$ *can be occupied, otherwise* $|\partial^- CR(\eta)| = 2\ell_1^* + 2\ell_2^* - 4 > 2\ell_1^* + \ell_2^* - 3$*, which is absurd.*

(ii) Since $|B^s(\eta)| + |B^w(\eta)| \leqslant \ell_1^* + \ell_2^* - 4 + k - |c^{ne}(\eta)|$*, we get*

$$|B^n(\eta)| + |B^e(\eta)| = 2\ell_1^* + \ell_2^* - 3 - (|B^s(\eta)| + |B^w(\eta)|) + k \geqslant \ell_1^* + 1 + |c^{ne}(\eta)|. \tag{4.2.5}$$

By symmetry, we generalize the inequality above for any $\alpha \in \{n, s\}$ *and* $\alpha' \in \{w, e\}$*: we get* $|B^\alpha(\eta)| + |B^{\alpha'}(\eta)| \geqslant \ell_1^* + 1 + |c^{\alpha\alpha'}(\eta)|$.

Proof of Proposition 4.2.1. (a) We denote by $\bar{\mathcal{D}}_{geo}$ the geometric set with the properties specified in point (a) that we introduce to make the argument more clear. The proof will be given in two steps:

(i) $\bar{\mathcal{D}}_{geo} \subseteq \bar{\mathcal{D}}$;

(ii) $\bar{\mathcal{D}}_{geo} \supseteq \bar{\mathcal{D}}$.

Proof of (i). To prove (i) we must show that for all $\eta \in \bar{\mathcal{D}}_{geo}$,

(i1) $\widehat{H}(\eta) = \widehat{H}(\bar{Q})$;

(i2) $\exists\ \omega : \bar{Q} \to \eta$, i.e., $\omega = (\omega_1, ..., \omega_k = \eta)$, such that $\max_i \widehat{H}(\omega_i) \leqslant \widehat{H}(\bar{Q}) + U_1$, with $|\omega_i| = n_c$ for all $i = 1, ..., k$ and $\omega_1 \in \bar{Q}$ (see (4.1.6) for the value of n_c).

Proof of (i1). Any $\eta \in \bar{\mathcal{D}}_{geo}$ satisfies $n(\eta) = 0$, $|C(\eta_{cl})| = (\ell_1^* - 2)(\ell_2^* - 2) + 2\ell_1^* + \ell_2^* - 3 = n_c$, and $g_1(\eta) = \ell_1^*$ and $g_2(\eta) = \ell_2^*$ since the configuration is monotone. Thus by (3.2.3) we deduce that $\widehat{H}$ is constant on $\bar{\mathcal{D}}_{geo}$. Since $\bar{Q} \subseteq \bar{\mathcal{D}}_{geo}$, this completes the proof of (i1).

Proof of (i2). Consider $\zeta \in \bar{Q}$ and $\eta \in \bar{\mathcal{D}}_{geo}$. Here, without loss of generality, we assume that the protuberance is in $r^w(\zeta)$. Then we have

- $|B^w(\zeta)| = 1$;
- $|B^n(\zeta)| = |B^s(\zeta)| = \ell_1^* - 1$;
- $|B^e(\zeta)| = \ell_2^*$;
- $|c^{ne}(\zeta)| = |c^{se}(\zeta)| = 1$.

Using the sliding of a unit square around a frame-angle described in Figure 1.11 (see Definition 3.2.4), we move, one by one, $|B^n(\zeta)| - |B^n(\eta)|$ particles around the frame-angle $c^{nw}(\zeta)$. After that we move $|B^e(\zeta)| - |B^e(\eta)| + |B^s(\zeta)| - |B^s(\eta)|$ particles around the frame-angle $c^{sw}(\zeta)$. Finally, we move $|B^e(\zeta)| - |B^e(\eta)|$ particles around the frame-angle $c^{es}(\zeta)$. The result is the configuration $\eta \in \bar{\mathcal{D}}_{geo}$. This concludes the proof of (i2).

Proof of (ii). By (i2), we know that all configurations in $\bar{\mathcal{D}}_{geo}$ are connected via U_1-path to $\bar{Q}$. Since $\bar{Q} \subseteq \bar{\mathcal{D}} \cap \bar{\mathcal{D}}_{geo}$, in order to prove (ii) it suffices to show that following U_1-paths it is not possible to exit $\bar{\mathcal{D}}_{geo}$. We call a path *clustering* if all the configurations in the path consist of a single cluster and no free particles. Below we will prove that for any $\eta \in \bar{\mathcal{D}}_{geo}$ and any η' connected to η by a clustering U_1-path,

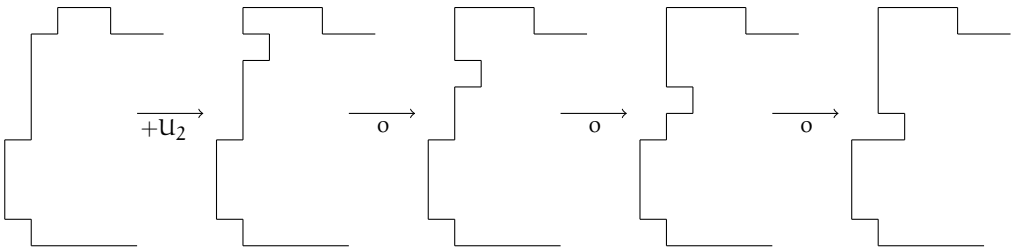

Figure 4.2 – Creation and motion of the recess at cost 0.

(A) $\mathrm{CR}(\eta') = \mathrm{CR}(\eta)$;
(B) $\eta' \supseteq \mathrm{CR}^-(\eta)$.

Proof of (A). Starting from any $\eta \in \mathcal{X}$, it is geometrically impossible to modify $\mathrm{CR}(\eta)$ without detaching a particle, that contradicts the hypotheses of clustering U_1-path.

Proof of (B). Fix $\eta \in \bar{\mathcal{D}}_{geo}$. The proof is done in two steps.

1. First, we consider clustering U_1-paths along which we do not move a particle from $\mathrm{CR}^-(\eta)$. Along such paths we only encounter configurations in $\bar{\mathcal{D}}_{geo}$ or those obtained from $\bar{\mathcal{D}}_{geo}$ by breaking one of the bars in $\partial^-\mathrm{CR}(\eta)$ into two pieces at cost U_1 (resp. U_2) if the bar is horizontal (resp. vertical). This holds because there is no particles outside $\mathrm{CR}(\eta)$ that can lower the cost.

If the broken bar is horizontal, then only moves at zero cost are admissible, so any particle can be detached. This implies that the unique way to regain U_1 and complete the U_1-path is to restore the bar.

If the broken bar is vertical, then the admissible moves are those with cost less or equal than $U_1 - U_2$. Again any particle can be detached, indeed its cost is at least U_1. The moves at cost U_2 are not possible, since $U_1 < 2U_2 - 2\varepsilon$. Thus, the unique way to complete the U_1-path is to restore the broken bar. We have therefore proved that $\eta' \supseteq \mathrm{CR}^-(\eta)$.

2. Consider now clustering U_1-paths along which we move a particle from a corner of $\mathrm{CR}^-(\eta)$. It is not allowed to move at cost $U_1 + U_2$, because it exceeds U_1, thus the overshoot U_2 must be regained by letting the particle slide next to a bar that is attached to a side of $\mathrm{CR}^-(\eta)$ (see Figure 4.2). If the particle moves vertically (resp. horizontally), we regain U_1 (resp. U_2). Since there are never two bars attached to the same side, we can at most regain U_1, thus it is not possible to move a particle from $\mathrm{CR}^-(\eta)$ other than from a corner. From now on, since $U_2 < 2U_1 - 2\varepsilon$, only moves at cost at most zero are admissible. There are no protuberances present anymore, because only the configurations in $\bar{\Omega}$ have a protuberance. Thus, no particle outside $\mathrm{CR}^-(\eta)$ can move, except those just detached from $\mathrm{CR}^-(\eta)$. These particles can move back, in which case we return to the same cofiguration η (see Figure 4.2). In fact, all possible moves at zero cost consist in moving the recess just created in $\mathrm{CR}^-(\eta)$ along the same side of $\mathrm{CR}^-(\eta)$, until it reaches the top of the bar, after which it cannot advance anymore at zero cost (see Figure 4.2). All these moves do not change the energy, except the last one that returns the particle to its original position and regains U_1. This concludes the proof of (B).

From (A), we deduce that $\mathrm{CR}(\eta') = \mathcal{R}(\ell_1^*, \ell_2^*)$. From (A) and (B), we deduce that the number of particles that are in $\partial^-\mathrm{CR}(\eta)$ is equal to the number of particles that are in $\partial^-\mathrm{CR}(\eta')$, thus (4.2.2), $1 \leqslant |B^w(\eta')|, |B^e(\eta')| \leqslant l_2^*$ and $1 \leqslant |B^n(\eta')|, |B^s(\eta')| \leqslant l_1^*$ hold. In order to prove that following clustering U_1-paths it is not possible to exit $\bar{\mathcal{D}}_{geo}$, we have to prove the lower bound in (4.2.1) for the lengths $|B^n(\eta')|$ and $|B^s(\eta')|$. We set

$$k = \sum_{\alpha\alpha' \in \{nw,ne,sw,se\}} |c^{\alpha\alpha'}(\eta')|. \tag{4.2.6}$$

Since $|B^w(\eta')| + |B^e(\eta')| \leqslant 2\ell_2^* - 4 + k$, by (4.2.2) we get

$$|B^n(\eta')| + |B^s(\eta')| = 2\ell_1^* + \ell_2^* - 3 - (|B^w(\eta')| + |B^e(\eta')|) + k \geqslant 2\ell_1^* - \ell_2^* + 1. \tag{4.2.7}$$

Since $|B^s(\eta')| \leqslant \ell_1^*$, (4.2.7) implies

$$|B^n(\eta')| \geqslant 2\ell_1^* - \ell_2^* + 1 - |B^s(\eta')| \geqslant \ell_1^* - \ell_2^* + 1. \tag{4.2.8}$$

By symmetry we can similarly argue for the length $|B^s(\eta')|$. This implies that following U_1-paths it is not possible to exit $\bar{\mathcal{D}}_{geo}$. The argument goes as follows. Detaching a particle costs at least $U_1 + U_2$ unless the particle is a protuberance, in which case the cost is U_1. The only configurations in $\bar{\mathcal{D}}_{geo}$ having a protuberance are those in $\bar{\Omega}$. If we detach the protuberance from a configuration in $\bar{\Omega}$, then we obtain a $(\ell_1^* - 1) \times \ell_2^*$ rectangle with a free particle. Since in the sequel only moves at zero cost are allowed, it is only possible to move the free particle. Since in a U_1-path the particle number is conserved, the only way to regain U_1 and complete the U_1-path is to reattach the free particle to a vertical side of the rectangle, thus return to $\bar{\Omega}$. This implies that for any $\eta \in \bar{\mathcal{D}}_{geo}$ and any η' connected to η by a U_1-path we must have that $\eta' \in \bar{\mathcal{D}}_{geo}$. This concludes the proof.

(b) The proof is analogue to the one in (a). □

4.2.2 *Useful lemmas for the gates*

In this section we give some useful lemmas that help us to characterize the gates.

Below we state Lemma 4.2.3 for the weakly anisotropic model, but it holds also for the isotropic and strongly anisotropic cases, see Lemmas 3.4.1 and 5.2.3, respectively.

Lemma 4.2.3. *Starting from $\mathcal{C}^* \setminus \Omega^{fp}$, if the free particle is attached to a bad site obtaining $\eta^B \in \mathcal{C}^B$, the only transitions that does not exceed the energy Γ^* are either detaching the protuberance, or a sequence of 1-translations of a bar or slidings of a bar around a frame-angle. Moreover, we get:*

(i) if it is possible to slide a bar around a frame-angle, then the saddles that are crossed are essential;

(ii) if it is not possible to slide a bar around a frame-angle, then the path must come back to the starting configuration and the saddles that are crossed are unessential.

Proof. The proof is analogue to the one of Lemma 3.4.1. □

Lemmas 4.2.5 and 4.2.6 are valid also in the strongly anisotropic case (see Lemmas 5.2.5 and 5.2.6 , respectively), while Lemma 4.2.4 has a corresponding version for the strongly anisotropic case, see Lemma 5.2.4. We postone the proof of the following lemmas to Appendix 4.A.

Lemma 4.2.4. *Starting from $\eta^B \in \mathcal{C}^B$, the saddles obtained by a 1-translation of a bar are essential and in $\mathcal{N}_0^{\alpha'} \cup \mathcal{N}_1^{\alpha}$. Moreover, all the saddles in $\mathcal{N}_0^{\alpha'} \cup \mathcal{N}_1^{\alpha}$ can be obtained from this η^B by a 1-translation of a bar.*

Lemma 4.2.5. *Starting from a configuration $\eta \in \mathcal{C}^*$, it is not possible to slide a vertical bar around a frame-angle without exceeding the energy Γ^*.*

With the following Lemma we can justify the definition of $\mathcal{C}^*$ given in (4.1.7).

Lemma 4.2.6. *Starting from $\widetilde{\mathcal{D}}$, the dynamics either passes through $\bar{\mathcal{D}}$ or it is not possible that a free particle is created without exceeding the energy level Γ^*.*

4.3 MODEL-DEPENDENT STRATEGY

Our goal is to characterize the union of all the minimal gates in the weakly anisotropic regime. To this end, we follow the model–dependent strategy carried out in Section 3.4 for the isotropic regime. In order to apply Propositions 3.1.3 and 3.1.5, we need to characterize the sets K and $\widetilde{K}$ (see (3.1.16) and (3.1.17) respectively for the definitions) for our model. This is done in Proposition 4.3.3. By Propositions 3.1.3 and 3.1.5, we obtain Corollary 4.3.4 that states that the saddles of the first and second types are respectively unessential. In Proposition 4.3.5 we highlight some of the saddles of type three that are unessential. This analysis is different when we are dealing with isotropic or weakly anisotropic interactions, and with strongly anisotropic interactions due to the different mechanisms to enter $\mathcal{C}^*$ (see [35, Proposition 2.3.7], Lemma 4.3.7 and Lemma 5.3.8, respectively). For the isotropic and strongly anisotropic cases this strategy is presented in Sections 3.4 and 5.3, respectively. Finally, we identify the essential saddles of the third type in Proposition 4.4.2.

4.3.1 *Main Propositions*

In this section we give the main results for our model-dependent strategy. We refer to Section 4.3.3 for the proof of these propositions.

The next proposition shows that when the dynamics reaches $\mathcal{C}^G$ it has gone "over the hill", while when it reaches $\mathcal{C}^B$ the energy has to increase again to the level Γ^* to visit $\square$ or $\blacksquare$. An analogue version for the isotropic case is proven in [35, Proposition 2.3.9], while here we extend that result to the weakly anisotropic case following a similar argument. Note that this result holds also in the strongly anisotropic case, see Proposition 5.3.1.

Proposition 4.3.1. *The following statements hold.*

(i) If $\eta \in \mathcal{C}^G$*, then there exists a path* $\omega : \eta \to \blacksquare$ *such that* $\max_{\zeta\in\omega} \widehat{H}(\zeta) < \Gamma^*$.

(ii) If $\eta \in \mathcal{C}^B$*, then there are no* $\omega : \eta \to \square$ *or* $\omega : \eta \to \blacksquare$ *such that* $\max_{\zeta\in\omega} \widehat{H}(\zeta) < \Gamma^*$.

Proposition 4.3.2. $\mathcal{C}^* \subseteq \mathcal{G}(\square, \blacksquare)$.

Proposition 4.3.2 holds also in the isotropic and strongly anisotropic cases, see Propositions 3.4.2 and 5.3.2, respectively.

Proposition 4.3.3. *The following statements hold.*

(i) $K = \emptyset$;

(ii) $\widetilde{K} \cap \partial\mathcal{C}^{\blacksquare}_{\square}(\Gamma^* - \widehat{H}(\blacksquare)) = \bigcup_\alpha \bigcup_{\alpha'} \bigcup_{k'} \mathcal{N}^{\alpha,\alpha'}_{2,k'}$.

For the corresponding result of Proposition 4.3.3 for the isotropic and strongly anisotropic regimes, see Propositions 3.4.3 and 5.3.3, respectively.

Corollary 4.3.4. *The following statements hold.*

(i) The saddles of the first type $\sigma \in \partial\mathcal{C}^{\square}_{\blacksquare}(\Gamma^*) \cap (\mathcal{S}(\square, \blacksquare) \setminus \mathcal{C}^*)$ *are unessential;*

(ii) The saddles of the second type $\zeta \in \partial\mathcal{C}^{\blacksquare}_{\square}(\Gamma^* - \widehat{H}(\blacksquare)) \cap (\mathcal{S}(\square, \blacksquare) \setminus (\mathcal{C}^* \cup \bigcup_\alpha \bigcup_{\alpha'} \bigcup_{k'} \mathcal{N}^{\alpha,\alpha'}_{2,k'}))$ *are unessential.*

Proof. Combining Propositions 3.1.3, 3.1.5 and 4.3.3 we get the claim. □

Proposition 4.3.5. *Any saddle* ξ *that is neither in* $\mathcal{C}^*$*, nor in the boundary of the cycle* $\mathcal{C}^{\square}_{\blacksquare}(\Gamma^*)$*, nor in* $\partial\mathcal{C}^{\blacksquare}_{\square}(\Gamma^* - \widehat{H}(\blacksquare)) \setminus \widetilde{K}$*, i.e.,* $\xi \in \mathcal{S}(\square, \blacksquare) \setminus (\partial\mathcal{C}^{\square}_{\blacksquare}(\Gamma^*) \cup (\partial\mathcal{C}^{\blacksquare}_{\square}(\Gamma^* - \widehat{H}(\blacksquare)) \setminus \widetilde{K}) \cup \mathcal{C}^*)$*, such that* $\tau_\xi < \tau_{\mathcal{C}^B}$ *is unessential. Therefore it is not in* $\mathcal{G}(\square, \blacksquare)$.

For the corresponding result of Proposition 4.3.5 for the isotropic and strongly anisotropic regimes, we refer to Propositions 3.4.5 and 5.3.5, respectively.

4.3.2 *Useful Lemmas for the model-dependent strategy*

In this section we give some useful lemmas about the entrance in the gate and the minimality of the sets $\mathcal{C}^*(i)$ with $i = 3, ..., L^*$. We stress that the behavior for the isotropic and weakly anisotropic regimes is very different from that observed in the strongly anisotropic regime, indeed we note that the weakly anisotropic model has some characteristics similar to the isotropic and some similar to the strongly anisotropic model. For the corresponding results obtained in the isotropic and strongly anisotropic cases, we refer to Sections 3.4.2 and 5.3.2, respectively. The next lemma generalizes [32, Proposition 2.3.8], proved for the isotropic case, to the weakly anisotropic case following similar arguments. In the strongly anisotropic case, this result is given in Lemma 5.2.3.

Lemma 4.3.6. *The following statements hold.*

(i) Starting from $\mathcal{C}^* \setminus \mathcal{Q}^{fp}$*, the only transitions that do not raise the energy are motions of the free particle in the region where the free particle is at lattice distance* $\geqslant 3$ *from the protocritical droplet.*

(ii) Starting from $\mathcal{Q}^{fp}$*, the only transitions that do not raise the energy are motions of the free particle in the region where the free particle is at lattice distance* $\geqslant 3$ *from the protocritical droplet and motions of the protuberance along the side of the rectangle where it is attached. When the lattice distance is 2, either the free particle can be attached to the protocritical droplet*

or the protuberance can be detached from the protocritical droplet and attached to the free particle, to form a rectangle plus a dimer. From the latter configuration the only transition that does not raise the energy is the reverse move.

(iii) Starting from $\mathcal{C}^*$, the only configurations that can be reached by a path that lowers the energy and does not decrease the particle number, are those where the free particle is attached to the protocritical droplet.

Proof. The proof is analogue to the one reported in [32] for the isotropic case: the path we consider is the same as in the isotropic case, but the energy of the moves is different. Indeed, the energy decreases by U in the isotropic regime and now by either U_1 or U_2 depending whether it is attached to the vertical or horizontal side respectively. □

The next lemma investigates how the entrance in $\mathcal{C}^*$ occurs in the weakly anisotropic case. This result is proven in [35, Proposition 2.3.7] for the isotropic case. We encourage the reader to inspect the difference between Lemma 4.3.7 and Lemma 5.3.8, where the peculiar entrance in the gate for the strongly anisotropic case is analyzed.

Lemma 4.3.7. *Any $\omega \in (\square \to \blacksquare)_{\mathrm{opt}}$ passes first through $\mathcal{Q}$, then possibly through $\mathcal{D} \setminus \mathcal{Q}$, and finally through $\mathcal{C}^*$.*

We postpone the proof of Lemma 4.3.7 in Appendix 4.A. We refer to Section 4.3.4 for the proof of the remaining lemmas.

Lemma 4.3.8. *$\mathcal{C}^*(i)$ is a minimal gate for any $i = 3, ..., L^*$.*

Remark 4.3.9. *In the strongly anisotropic case, the statement of Lemma 4.3.8 does not hold. A different result is derived in Lemma 5.3.9.*

Lemma 4.3.10. *The saddles in $\mathcal{C}^*(2)$ are essential.*

4.3.3 *Proof of Propositions*

Proof of Proposition 4.3.1. (i) If $\eta \in \mathcal{C}^G$, then its energy is either $\Gamma^* - U_1 - U_2$ or $\Gamma^* - U_1$ (resp. $\Gamma^* - U_2$), depending on whether the attached particle is in a corner or is a protuberance on a vertical (resp. horizontal) side. In the latter case we can move the particle at no cost and gain an extra $-U_2$ (resp. $-U_1$) when it has become a corner. After that it is possible to create a new particle and attach it, which leads to energy $\Gamma^* - U_1 - U_2 - (U_1 + U_2 - \Delta) < \Gamma^*$. We can continue in this way, filling up all the sites in $\partial^- \mathrm{CR}(\eta)$. Now we can proceed along the reference path for the nucleation constructed in [90, Section 3.2] until the path reaches ■. We have exhibited a path ω such that $\max_{\sigma \in \omega} \widehat{H}(\sigma) < \Gamma^*$.

(ii) If $\eta \in \mathcal{C}^B$, then $\widehat{H}(\eta) = \Gamma^* - U_1$ (resp. $\widehat{H}(\eta) = \Gamma^* - U_2$) if the protuberance has been attached to a vertical (resp. horizontal) side. As long as the energy does not exceed Γ^*, it is impossible to create a new particle before further lowering the energy. But there are no moves available to lower the energy. As a consequence the unique admissible moves are those where the last particle that was attached is moving along the side at zero cost or detaching again, or start a sliding of a bar around a frame-angle (see the explanation in the third case). In the first case we obtain a configuration that is analogue to $\eta \in \mathcal{C}^B$ and therefore we can iterate the argument by taking this configuration as η^B for a finite number of steps, since the path has to reach ■. In the second case, we obtain a configuration that is in $\mathcal{C}^*$, thus the path has to reach again the energy value Γ^*. In the third case, we justify separately when the sliding is at cost U_1 or at cost U_2. If $\widehat{H}(\eta) = \Gamma^* - U_1$, the only admissible motions along the border of the droplet that do not exceed Γ^* are those at cost U_1, since the unique possibility is to move the particle in a frame-angle in such a way that it connects to the protuberance, otherwise all the other moves have cost at least $U_1 + U_2$. Similarly, by symmetry we deduce that if $\widehat{H}(\eta) = \Gamma^* - U_2$, then the only admissible move is starting a sliding of a bar around a frame-angle at cost U_2. In both cases the energy returns to Γ^*, which concludes the proof. □

Proof of Proposition 4.3.2. By Lemma 4.3.10 we know that the saddles in $\mathcal{C}^*(2)$ are essential and thus are in $\mathcal{G}(\square,\blacksquare)$ due to [85, Theorem 5.1]. Moreover, by Lemma 4.3.8 we know that the set $\mathcal{C}^*(i)$ is a minimal gate for any $i = 3, ..., L^*$, thus

$$\mathcal{C}^* = \mathcal{C}^*(2) \cup \bigcup_{i=3}^{L^*} \mathcal{C}^*(i) \subseteq \mathcal{G}(\square,\blacksquare). \tag{4.3.1}$$

□

Proof of Proposition 4.3.3. (i) The proof is analogue to the one of Proposition 3.4.3(i).

(ii) The proof is analogue to the one of Proposition 3.4.3(ii), except for the case in which a sliding of a bar around a frame–angle takes place, for which we use the following argument. By (3.2.12), Proposition 4.2.1(a) and Lemma 4.2.5 we deduce that the unique possibility to slide a bar around a frame–angle is that the bar is horizontal and it has length between $\ell_1^* - \ell_2^* + 1$ and $\ell_2^* - 1$. Thus, the configurations visited by the path ω during this sliding are $\bar{\eta}_1, ..., \bar{\eta}_m \in \mathcal{N}_{k,k'}^{\alpha,\alpha'}$ for some $\alpha \in \{n, s\}$, $\alpha' \in \{w, e\}$, $k' = \ell_1^* - \ell_2^* + 1, ..., \ell_2^* - 1$ and $k = 2, ..., k'$, while the last configuration $\widetilde{\eta}$ obtained when the last particle of the bar is detached is not a saddle. Note that $\widetilde{\eta}$ is not in the set $\mathcal{B}$ defined in [90, eq. (3.64)], since $s(\widetilde{\eta}) = s^* + 1$ and $v(\widetilde{\eta}) = 2\ell_2^* - \ell_1^* - 2 < p_{min}(\widetilde{\eta}) - 1 = \ell_2^* - 1$. Thus, by [90, Proposition 11] we know that $\widetilde{\eta} \in \mathcal{C}_{\square}^{\blacksquare}(\Gamma^* - \widehat{H}(\blacksquare))$. This implies that only the configuration $\bar{\eta}_m$, that belongs to $\mathcal{N}_{2,k'}^{\alpha,\alpha'}$, is in $\widetilde{K} \cap \partial\mathcal{C}_{\square}^{\blacksquare}(\Gamma^* - \widehat{H}(\blacksquare))$. Taking the union of $\mathcal{N}_{2,k'}^{\alpha,\alpha'}$ over all $\alpha \in \{n, s\}$ and $\alpha' \in \{w, e\}$, xwe get the claim. □

Proof of Proposition 4.3.5. The proof is analogue to the one of Proposition 3.4.5 after considering that the saddle ξ_i, if crossed by the path before reaching $\mathcal{C}^G$, is the union of a rectangle $(\ell_1^* - 1) \times \ell_2^*$ with an horizontal dimer □

4.3.4 *Proof of Lemmas*

Proof of Lemma 4.3.8. First, we prove that $\mathcal{C}^*(i)$ is a gate. By Lemma 4.3.7 we know that any $\omega \in (\square \to \blacksquare)_{opt}$ enters $\mathcal{C}^*$ through a configuration of the form $(\hat{\eta}, z)$, with $\hat{\eta} \in \bar{\mathcal{D}}$ a protocritical droplet and z the site occupied by the free particle. Note that either $z \in B_i(\hat{\eta})$ if $d(\partial^- \Lambda_4, \hat{\eta}) > i$ or $z \in \bar{B}_i(\hat{\eta})$ if $d(\partial^- \Lambda_4, \hat{\eta}) \leqslant i$, thus $\mathcal{C}^*(i)$ is a gate.

Now we prove that $\mathcal{C}^*(i)$ is a minimal gate. For any $\eta \in \mathcal{C}^*(i)$, our strategy consists in proving that $\mathcal{C}^*(i) \setminus \{\eta\}$ is not a gate by defining a path $\omega \in (\square \to \blacksquare)_{opt}$ such that $\omega \cap (\mathcal{C}^*(i) \setminus \{\eta\}) = \emptyset$. For the following the reader can visualize the path described using Figure 1.16 on the right-hand side. We take an arbitrary path starting from □ and that enters $\mathcal{C}^*(i)$ in $\eta = (\hat{\eta}, z)$. Then the path proceeds by moving the free particle from z to $\hat{\eta}$ such that the distance between the free particle and $\hat{\eta}$ at the first step is strictly decreasing, and at the later steps is not increasing. Finally the free particle is attached in a site $x \in \partial^- CR(\hat{\eta})$ giving rise to a configuration in $\mathcal{C}^G(\hat{\eta})$. From this configuration, the path proceeds towards ■ as the one in Proposition 4.3.1(i). Since the constructed $\omega \in (\square \to \blacksquare)_{opt}$ and $\omega \cap \mathcal{C}^*(i) = \{\eta\}$, the proof is concluded. □

Proof of Lemma 4.3.10. The proof is analogue to the one of Proposition 3.4.8. □

4.4 PROOF OF THE MAIN RESULTS

4.4.1 *Proof of the main Theorem 4.1.2*

In this section we give the proof of the main Theorem 4.1.2. Recall the definitions of standard rectangles given in (4.1.3). Now we recall the definition of the set $\mathcal{P}$ given in [90] as

$$\begin{aligned}\mathcal{P} := \{\eta \ &: n(\eta) = 1,\ v(\eta) = \ell_2(s^*) - 1,\ \eta_{cl} \text{ is connected, monotone,} \\ &\text{with circumscribed rectangle in } \mathcal{R}(\ell_1(s^*) + 1, \ell_2(s^*))\}.\end{aligned} \tag{4.4.1}$$

In particular, in order to state that the set $\mathcal{C}^*$ is a gate for the transition from □ to ■, we need the following

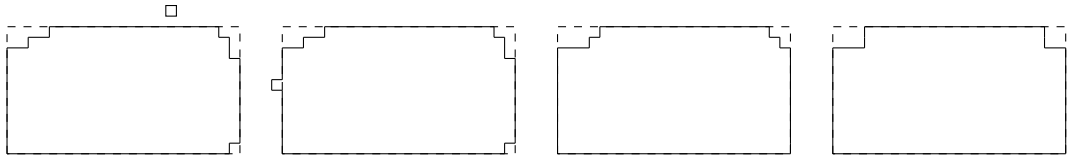

Figure 4.3 – Here we depict in (a) the configuration η; in (b) the configuration obtained by η by attaching the free particle at cost $-U_1$ to $B^w(\eta)$; in (c) the configuration η' obtained from η by attaching the free particle to $c^{se}(\eta)$ and then detaching the particle in $c^{nw}(CR^-(\eta))$ and attach it to $B^e(\eta)$, and in (d) the configuration η'' obtained from η' by detaching the particle in $c^{ne}(CR^-(\eta'))$ attach it to $B^n(\eta')$.

Lemma 4.4.1. *If $\omega \in (\square \to \blacksquare)_{opt}$ passes through the set $\mathcal{P}$, then $\omega \cap \mathcal{C}^* \neq \emptyset$.*

We postpone the proof of Lemma 4.4.1 after the proof of the main Theorem 4.1.2.

Proof of the main Theorem 4.1.2. By [90, Theorem 2], we know that the set $\mathcal{P}$ is a gate for the transition from $\square$ to $\blacksquare$. By Lemma 4.4.1 we know that every path $\omega \in (\square \to \blacksquare)_{opt}$ that crosses $\mathcal{P}$ has to intersect also $\mathcal{C}^*$. This implies that every optimal path ω from $\square$ to $\blacksquare$ is such that $\omega \cap \mathcal{C}^* \neq \emptyset$ and thus $\mathcal{C}^* \cap \mathcal{P} \equiv \mathcal{C}^*$ is a gate. □

Proof of Lemma 4.4.1. Consider $\omega \in (\square \to \blacksquare)_{opt}$. If $\omega \cap \mathcal{C}^* \neq \emptyset$, we get the claim. Thus, we can reduce our analysis to the case in which the path ω reaches the set $\mathcal{P}$ in a configuration $\eta \in \mathcal{P} \setminus \mathcal{C}^*$. We set $\omega = (\square, \omega_1, ..., \omega_k, \eta) \circ \bar{\omega}$, where $\bar{\omega}$ is a path that connects η to $\blacksquare$ such that $\max_{\sigma \in \omega} \widehat{H}(\sigma) \leqslant \Gamma^*$. We are interested in the time–reversal of the path ω. Since $\eta \in \mathcal{P} \setminus \mathcal{C}^*$, we know that it is composed by the union of a cluster $CR^-(\eta) = \mathcal{R}(\ell_1^* - 2, \ell_2^* - 2)$, such that at least one frame-angle of $CR^-(\eta)$ is empty, a free particle and four bars attached to the four sides of $CR^-(\eta)$ in such a way that η contains $n_c + 1$ particles (see (4.1.6) for the precise value of n_c). Suppose that $CR^-(\eta)$ contains x empty frame-angles, with $1 \leqslant x \leqslant 4$, (see Figure 4.3(a) to visualize the configuration η in the case $x = 1$). Since $\widehat{H}(\eta) = \Gamma^*$, the move from η to ω_k must have a non–positive cost and thus the unique admissible moves are:

(i) either moving the free particle at zero cost;
(ii) or removing the free particle;
(iii) or attaching the free particle at cost $-U_1$ (see Figure 4.3(b)) or $-U_2$, or $-U_1 - U_2$.

Case (i). In this case the configuration ω_k is analogue to η and therefore we can iterate this argument by taking this configuration as η.

Case (ii). In this case $\widehat{H}(\omega_k) = \Gamma^* - \Delta$. We may assume that the configuration ω_{k-1} is not obtained by ω_k via adding a free particle, otherwise ω_{k-1} is analogue to η and thus we can iterate the argument by taking this configuration as η. By the optimality of the path, again considering the time-reversal, we deduce that the unique admissible move to obtain ω_{k-1} from ω_k is breaking a horizontal (resp. vertical) bar at cost U_1 (resp. U_2). Thus, it is possible that either a sequence of 1-translations of a bar or a sliding of a bar around a frame-angle takes place. In the first case, we obtain a configuration that is analogue to ω_{k-1} and thus we can iterate the argument for a finite number of steps, since the path has to reach $\square$. In the latter case, by Remark 4.2.2(ii) we deduce that the condition (3.2.12) is not satisfied and therefore it is not possible to complete any sliding of a bar around a frame-angle. This implies that the unique admissible moves are the reverse ones, thus we obtain a configuration that is analogue to ω_{k-1} and therefore we can iterate the argument f or a finite number of steps, since the path has to reach $\square$. In this way we can reduce ourselves to consider case (iii).

Case (iii). (a) We consider the case where from η, again considering the time-reversal, we attach a particle at cost $-U_1$ in $\partial^+ CR(\eta)$ giving rise to the configuration ω_k, i.e., $\widehat{H}(\omega_k) = \Gamma^* - U_1$ (see Figure 4.3(b)). Thus, it is possible that either a sequence of 1-translations of a bar or a sliding of a bar around a frame-angle takes place. In the first case, we obtain a configuration that is analogue to ω_k and thus we can iterate the argument for a finite number of steps, since the path has to reach $\square$. In the latter case, by Remark 4.2.2(ii) we deduce that the condition (3.2.12) is not satisfied and therefore it is not possible to complete any sliding of a bar around a frame-angle. This implies that the unique admissible moves are the reverse

ones, thus we obtain a configuration that is analogue to ω_k and therefore we can iterate the argument for a finite number of steps, since the path has to reach $\square$.

(b) We consider the case where from η, again considering the time-reversal, we attach a particle at cost $-U_2$ in $\partial^+\mathrm{CR}(\eta)$ giving rise to the configuration ω_k, i.e., $\widehat{H}(\omega_k) = \Gamma^* - U_2$. We argue in a similar way as above.

(c) We consider the case where from η, again considering the time-reversal, we attach a particle at cost $-U_1 - U_2$ in $\partial^-\mathrm{CR}(\eta)$ giving rise to the configuration ω_k, i.e., $\widehat{H}(\omega_k) = \Gamma^* - U_1 - U_2$. Thus, it is possible either to have a sequence of 1-translations of a bar, or to have a sliding of a bar around a frame-angle, or to detach a particle at cost $U_1 + U_2$. In the first two possibilities, analogously to what has been discussed previously in (a) and (b), the unique admissible moves are the reverse ones a nd therefore we conclude as above. In the latter possibility, we have that either ω_{k-1} is obtained from ω_k by detaching a particle from a bar at cost $U_1 + U_2$ or from a corner of η that is in $\mathrm{CR}^-(\eta)$. In the first case, the particle can be attached to an empty frame-angle of $\mathrm{CR}^-(\eta)$ and we can repeat these steps at most $x-1$ times (if $x \geqslant 2$), that implies that there exists $\bar{k} < k-1$ such that $\omega_{\bar{k}}$ is composed by the union of a free particle and a rectangle $\mathcal{R}(\ell_1^*-2, \ell_2^*-2)$ with four bars attached to its four sides in such a way $\omega_{\bar{k}}$ contains n_c+1 particles, namely, $\omega_{\bar{k}} \in \mathcal{C}^*$. In the second case, we may assume that the detached particle is attached to a bar in $\partial^-\mathrm{CR}(\eta)$ giving rise to a configuration η' (see Figure 4.3(c)), otherwise we obtain a configuration that is analogue to η. Starting from η', similarly we obtain η'' (see Figure 4.3(d)) if η' has a corner in $\mathrm{CR}^-(\eta')$. If this is the case, we can proceed in a similar way until we obtain a configuration η''' that has no corner in $\mathrm{CR}^-(\eta''')$. Starting from η''', by the optimality of the path we deduce that the unique admissible moves are the reverse ones and therefore the path goes back to η. This concludes the proof. $\square$

4.4.2 *Proof of the main Theorem 4.1.3*

In this section we analyze the geometry of the set $\mathcal{G}(\square, \blacksquare)$ (recall (3.1.13)). In particular, we give the proof of the main Theorem 4.1.3 by giving in Proposition 4.4.2 the geometric characterization of the essential saddles of the third type that are not in $\mathcal{C}^*$ and that are visited after crossing the set $\mathcal{C}^B$.

Proposition 4.4.2. *Any saddle ξ that is neither in $\mathcal{C}^*$, nor in the boundary of the cycle $\mathcal{C}^{\square}_{\blacksquare}(\Gamma^*)$, nor in $\partial\mathcal{C}^{\blacksquare}_{\square}(\Gamma^* - \widehat{H}(\blacksquare)) \setminus \widetilde{K}$, such that $\tau_\xi \geqslant \tau_{\mathcal{C}^B}$ can be essential or not. For those essential, we obtain the following characterization:*

$$\mathcal{G}(\square,\blacksquare) \cap \mathcal{S}(\square,\blacksquare) \setminus (\partial\mathcal{C}^{\square}_{\blacksquare}(\Gamma^*) \cup (\partial\mathcal{C}^{\blacksquare}_{\square}(\Gamma^* - \widehat{H}(\blacksquare)) \setminus \widetilde{K}) \cup \mathcal{C}^*) = \\ = \bigcup_{\alpha}\bigcup_{\alpha'}\bigcup_{k'}\bigcup_{k=2}^{k'} \mathcal{N}_{k,k'}^{\alpha,\alpha'} \cup \bigcup_{\alpha'} \mathcal{N}_0^{\alpha'} \cup \bigcup_{\alpha} \mathcal{N}_1^{\alpha}. \tag{4.4.2}$$

Since the proof of Proposition 4.4.2 is similar to that of Proposition 5.4.3, we postpone it to Appendix 4.B.

Proof of Theorem 4.1.3. By Corollary 4.3.4 we know that the saddles of the first and second type, defined in Definitions 3.1.2 and 3.1.4, respectively, are unessential. By Propositions 4.3.5 and 4.4.2 we have the characterization of the essential saddles of the third type. We use Proposition 4.3.2 to get the claim. $\square$

4.5 PROOF OF THE SHARP ASYMPTOTICS

Thanks to the model-independent discussion given in Section 3.6.1 together with the application to our model, and Lemma 3.6.7, also for the weakly anisotropic case formula (3.6.12) becomes

$$h = \begin{cases} 1 & \text{on } \mathcal{C}^{\square}_{\blacksquare}(\Gamma^*) \cup \bigcup_{j=1}^{J_\square} (\{\sigma_j\} \cup \mathcal{Z}_j^{\square}), \\ 0 & \text{on } \mathcal{C}^{\blacksquare}_{\square}(\Gamma^* - \widehat{H}(\blacksquare)) \cup \bigcup_{j=1}^{J_\blacksquare} (\{\zeta_j\} \cup \mathcal{Z}_j^{\blacksquare}), \\ c_i & \text{on } \mathcal{X}(i), i = 1, ..., \bar{I}, \end{cases} \tag{4.5.1}$$

where $\mathcal{X}(i)$, $i = 1, ..., \bar{I}$, are all the wells of the transition except $\bigcup_{j=1}^{J_\square} \mathcal{Z}_j^{\square}$ and $\bigcup_{j=1}^{J_\blacksquare} \mathcal{Z}_j^{\blacksquare}$.

We give now the proof of Theorem 4.1.4, that represents sharp asymptotics for the weakly anisotropic case. Recall (1.3.42). The guiding idea behind the sharp estimate of $Z^{\,\mathrm{CAP}}(\square, \blacksquare)$ is that $h^*_{\square,\blacksquare}$ is exponentially close to 1 on $\mathcal{C}^{\square}_{\blacksquare}(\Gamma^*)$ and exponentially close to 0 on $\mathcal{C}^{\blacksquare}_{\square}(\Gamma^* - \widehat{H}(\blacksquare))$. By [35, Lemma 3.3.1] we know that $h^*_{\square,\blacksquare}$ is trivial on $\mathcal{C}^{\square}_{\blacksquare}(\Gamma^*) \cup \mathcal{C}^{\blacksquare}_{\square}(\Gamma^* - \widehat{H}(\blacksquare))$, thus it remains to understand what $h^*_{\square,\blacksquare}$ looks like on the set

$$\mathcal{X}^* \setminus (\mathcal{C}^{\square}_{\blacksquare}(\Gamma^*) \cup \mathcal{C}^{\blacksquare}_{\square}(\Gamma^* - \widehat{H}(\blacksquare))) = \{\eta \in \mathcal{X}^* : \ \Phi(\eta, \square) = \Phi(\eta, \blacksquare)\}, \tag{4.5.2}$$

which separates $\mathcal{C}^{\square}_{\blacksquare}(\Gamma^*)$ and $\mathcal{C}^{\blacksquare}_{\square}(\Gamma^* - \widehat{H}(\blacksquare))$ and contains $\mathcal{S}(\square, \blacksquare)$. Before doing so, we first show that $h^*_{\square,\blacksquare}$ is also trivial on $\mathcal{X}^{**} \setminus (\mathcal{C}^{\square}_{\blacksquare}(\Gamma^*) \cup \mathcal{C}^{\blacksquare}_{\square}(\Gamma^* - \widehat{H}(\blacksquare)))$. This set can be partitioned into maximally connected components as in (1.3.43). By [35, Lemma 3.3.2] applied to the weakly anisotropic model we know that $h^*_{\square,\blacksquare}$ is close to a constant on each of these wells. By Proposition 4.3.1(ii) we know that for each $\hat{\eta} \in \bar{\mathcal{D}}$ the four bars of bad sites in $\partial^+ \mathrm{CR}(\hat{\eta})$ form a well. These are not the only wells, but [35, Lemma 3.3.2] applied to the weakly anisotropic model shows that we not need care too much about wells anyway. Thus, *only the transitions in and out of the wells contribute to the Dirichlet form* at the order we are after, not those inside the wells. Since the mechanism to enter the gate $\mathcal{C}^*$ for both isotropic and weakly anisotropic model is analogue, it easy to check that [35, Proposition 3.3.4] and [35, Lemma 3.4.1] can be adapted to the weakly anisotropic model. Thus, using them together with Lemma 3.6.7 and Remark 3.6.8, in order to prove Theorem 4.1.4 it remains to count the cardinality of the set $\bar{\mathcal{D}}$ modulo shifts, which we refer to as N.

Proposition 4.5.1.

$$N = \sum_{k=1}^{4} \binom{4}{k} \binom{\ell_2^* + k - 2}{2k - 1}.$$

Proof. We have to count the number of different shapes of the clusters in $\bar{\mathcal{D}}$. We do this by counting in how many ways $\ell_2^* - 1$ particles can be removed from the four bars of a $\ell_1^* \times \ell_2^*$ rectangle starting from the corners. We split the counting according to the number $k = 1, 2, 3, 4$ of corners from which particles are removed. The number of ways in which we can choose k corners is $\binom{4}{k}$. After we have removed the particles at these corners, we need to remove $\ell_2^* - 1 - k$ more particles from either side of each corner. The number of ways in which this can be done is

$$\begin{aligned} &|\{(m_1, ..., m_{2k}) \in \mathbb{N}_0^{2k} : \ m_1 + ... + m_{2k} = \ell_2^* - 1 - k\}| \\ &\quad = |\{(m_1, ..., m_{2k}) \in \mathbb{N}^{2k} : \ m_1 + ... + m_{2k} = \ell_2^* - 1 + k\}| \\ &\quad = \binom{\ell_2^* + k - 2}{2k - 1}. \end{aligned} \tag{4.5.3}$$

Thus, we get the claim. □

4.5.1 *Proof of Theorem 4.1.5*

In this section we give the proof of Theorem 4.1.5, that represents the uniform entrance distribution. Let $\partial^- \mathcal{C}^*$ be those configurations in $\mathcal{C}^*$ where the free particle is in $\partial^- \Lambda$. Following the same argument used in [35] for the isotropic regime, since $\bar{\mathcal{D}} \subseteq \mathcal{C}^{\square}_{\blacksquare}(\Gamma^*)$ by [35, Theorem 2.3.10(ii)], it follows from [35, Lemma 3.3.1] and $\mathcal{C}^* \subseteq \mathcal{S}(\square, \blacksquare)$ that

$$\min_{\eta' \in \bar{\mathcal{D}}} h^*_{\square, \partial^- \mathcal{C}^*}(\eta') \geqslant 1 - Ce^{-\delta\beta}, \tag{4.5.4}$$

where

$$h^*_{\square, \partial^- \mathcal{C}^*}(\eta') = \begin{cases} 0 & \text{if } \eta' \in \partial^- \mathcal{C}^*, \\ \mathbb{P}_{\eta'}(\tau_{\square} < \tau_{\partial^- \mathcal{C}^*}) & \text{otherwise.} \end{cases} \tag{4.5.5}$$

Moreover, letting $\partial^{--} \mathcal{C}^*$ be the set of configurations obtained from $\partial^- \mathcal{C}^*$ by moving the free particle from $\partial^- \Lambda$ to $\partial^{--} \Lambda = \partial^-(\Lambda^-)$, we deduce that

$$\max_{\eta' \in \partial^{--} \mathcal{C}^*} h^*_{\square, \partial^- \mathcal{C}^*}(\eta') \leqslant Ce^{-\delta\beta}. \tag{4.5.6}$$

From now on, following the argument proposed in [35] we are able to prove the assertion in (4.1.18).

4.5.2 *Proof of Theorem 4.1.7*

Thanks to [92, Lemma 3.6], we deduce that for our model the quantity $\widetilde{\Gamma}(B)$, with $B \subsetneq \mathcal{X}$, defined in [92, eq. (21)] is such that $\widetilde{\Gamma}(\mathcal{X} \setminus \{\blacksquare\}) = \Gamma^*$. Thus, Theorem 4.1.7 follows by [92, Proposition 3.24].

4.6 EXTENSIONS TO THE SIMPLIFIED MODEL

In this section we provide a discussion aiming at extending the results proved for the local model to the simplified version of the model in the weakly anisotropic model. To this end, we follow the strategy proposed in [75] for the isotropic case. In [75, Section 2] the authors give several large deviation estimates concerning exponential clocks, that hold also for the weakly anisotropic case. In [75, Section 3] the authors give several large deviation estimates concerning random walks. All these results are valid for the weakly anisotropic case without changes except for [75, Proposition 3.13], in which we have to replace U with U_1. The recurrence property for the weakly anisotropic simplified model is obtained with similar arguments carried out in [75, Section 6]. To this end, we modify the definition of the set $\bar{\mathcal{X}}_2$ given in [75, eq. (5.8)] by replacing U with U_1. Therefore also the definition of the set $\mathcal{X}_2$ given in [75, eq. (6.1)] should be modified accordingly. Thus, if we define for the weakly anisotropic model $T_1 = e^{0\beta}$, $T_2 = e^{U_1\beta}$ and $T_3 = e^{\Delta\beta}$, [75, Proposition 6.2] holds also for the weakly anisotropic case. Concerning the reduction, we follow the strategy proposed in [75, Section 7]. In particular, we have to study the behavior of the gas and its interaction with the dynamics in the box Λ. There are two classes of gas particles with different behavior: particles that have been in $\Lambda^\beta \setminus \Lambda$ for a long time (say of order T_3), which we call green particles; and particles that exit from Λ and afterwards return to Λ in a short time (say of order 1), which we call red particles. The effect of green (resp. red) particles is studied in [75, Section 7.6] (resp. [75, Section 7.7]) and can be extended to the weakly anisotropic case by modifying the times T_1, T_2 and T_3, and the sets $\mathcal{X}_2$ and $\bar{\mathcal{X}}_2$ as above.

APPENDIX

4.A ADDITIONAL MATERIAL FOR SECTION 4.2

Proof of Lemma 4.2.4. Note that $\widehat{H}(\eta^B) = \Gamma^* - U_2$ (resp. $\widehat{H}(\eta^B) = \Gamma^* - U_1$) if the free particle has been attached to an horizontal (resp. vertical) bar. In the first case, in order to avoid

exceeding the energy value Γ^* it is possible to translate only the vertical bars. These saddles are in $\mathcal{N}_1^\alpha$. In the latter case, it is possible to translate both vertical and horizontal bars. If the translated bar is horizontal, the saddles that are crossed are in $\mathcal{N}_0^{\alpha'}$. If the translated bar is vertical, the configurations obtained do not reach the level Γ^*, thus they are not saddles. To conclude, all the configurations in $\mathcal{N}_0^{\alpha'} \cup \mathcal{N}_1^\alpha$ can be obtained from a configuration η^B via a 1-translation of a bar.

It remains to prove that the saddles in $\mathcal{N}_0^{\alpha'} \cup \mathcal{N}_1^\alpha$ are essential. This part of the proof is analogue to the corresponding one done for the isotropic case in Lemma 3.5.2. □

Proof of Lemma 4.2.5. Since $\widehat{H}(\eta) = \Gamma^*$, it is possible to activate a sliding of a vertical bar around a frame–angle only after lowering the energy. Thus, the only admissible move is to attach the free particle to an horizontal bar, since we want to slide a vertical bar. When this happens, the energy reaches the value $\Gamma^* - U_2$. Now the only possibility to slide the bar is to activate a 1-translation of the vertical bar at cost U_2, thus the subsequent moves must be at zero cost, until the last one that costs $-U_2$. This implies that the last configuration has energy $\Gamma^* - U_2$. If a 1-translation of a horizontal bar is activated, the energy increases by U_1 and thus it reaches the value $\Gamma^* - U_2 + U_1 > \Gamma^*$, which is in contradiction with the optimality of the path. □

Proof of Lemma 4.2.6. By Proposition 4.2.1(a) we know the geometric description of $\widetilde{\mathcal{D}}$. Starting from a configuration $\eta \in \widetilde{\mathcal{D}}$, since $\widehat{H}(\eta) = \Gamma^* - \Delta + U_1 - U_2$, by the optimality of the path, it is possible to create a free particle only after lowering the energy. This is possible only if $\eta \in \widetilde{\mathcal{Q}}$, where it is possible to detach the protuberance and reattach it to a vertical side, thus we obtain a configuration in $\bar{\mathcal{Q}}$. This concludes the proof. □

Proof of Lemma 4.3.7. The proof is analogue to that of Lemma 5.3.8 done for the strongly anisotropic interactions. The difference is only in case (iii), indeed, considering the time-reversal of the path ω from $\eta \in \mathcal{C}^*$ to □, if a sliding of a bar around a frame–angle takes place at cost U_1, the configuration $\omega_{\bar{k}}$ that we obtain does not belong to the set $\mathcal{B}$ defined in [90, eq. (3.64)], because $s(\omega_{\bar{k}}) = s^* + 1$ and $v(\omega_{\bar{k}}) = 2\ell_2^* - \ell_1^* - 2 < p_{min}(\omega_{\bar{k}}) - 1 = \ell_2^* - 1$. Thus, by [90, Proposition 11] we know that the time–reversal of the path ω visits a configuration $\bar{\sigma} \in \mathcal{C}^*$. We can therefore iterate the argument by taking this configuration as η and the iteration involves a finite number of steps since ω has to reach □. This concludes the proof. □

4.B ADDITIONAL MATERIAL FOR SECTION 4.4

Proof of Proposition 4.4.2. Consider a configuration $\eta \in \mathcal{C}^*(2)$ such that $\eta = (\hat{\eta}, x)$, with $\hat{\eta} \in \bar{\mathcal{D}}$ and $d(\hat{\eta}, x) = 2$. By Proposition 4.2.1(a) we deduce that that $\hat{\eta}$ consists of an $(\ell_1^* - 2) \times (\ell_2^* - 2)$ rectangle with four bars B^α, with $\alpha \in \{n, s, w, e\}$, attached to its four sides satisfying

$$1 \leqslant |B^w(\eta)|, |B^e(\eta)| \leqslant \ell_2^*, \quad \ell_1^* - \ell_2^* + 1 \leqslant |B^n(\eta)|, |B^s(\eta)| \leqslant \ell_1^*, \tag{4.B.1}$$

and

$$\sum_\alpha |B^\alpha(\eta)| - \sum_{\alpha\alpha' \in \{nw, ne, sw, se\}} |c^{\alpha\alpha'}(\eta)| = 2\ell_1^* + \ell_2^* - 3. \tag{4.B.2}$$

Assume that the free particle is attached in a bad site obtaining a configuration $\eta' \in \mathcal{C}^B$. Due to [85, Theorem 5.1] and Proposition 4.3.5, our strategy consists in characterizing the essential saddles that could be visited after attaching the free particle in a bad site. By Remark 4.2.2(i) we consider separately the following cases:

A. three frame-angles of $CR(\hat{\eta})$ are occupied;
B. two frame-angles of $CR(\hat{\eta})$ are occupied;
C. one frame-angle of $CR(\hat{\eta})$ is occupied;
D. no frame-angle of $CR(\hat{\eta})$ is occupied.

Note that from case A one can go to the other cases and viceversa, but since the path has to reach ■ this back and forth must end in a finite number of steps.

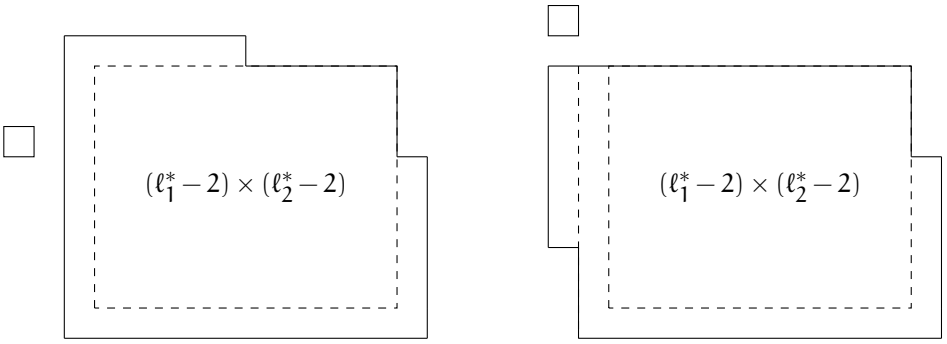

Figure 4.4 – Case A: on the left-hand side we represent a possible starting configuration $\eta \in \mathcal{C}^*$ and on the right-hand side the configuration $\widetilde{\eta}$ obtained from η after the sliding of the bar $B^n(\eta)$ around the frame-angle $c^{nw}(\eta')$.

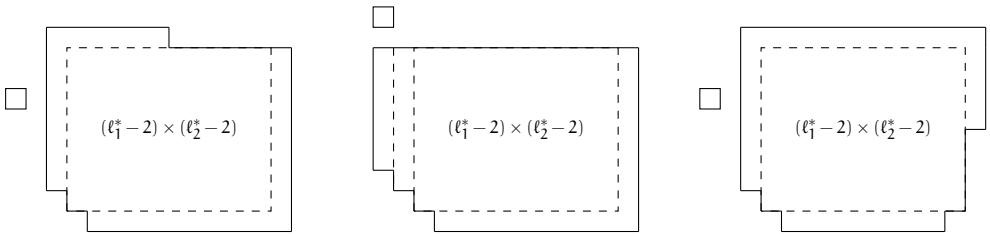

Figure 4.5 – Case B(i): in (a) we depict a possible starting configuration $\eta \in \mathcal{C}^*$ and in (b) the configuration $\widetilde{\eta}$ obtained from η after the sliding of the bar $B^n(\eta)$ around the frame-angle $c^{nw}(\eta')$. Case B(ii): in (c) we depict a possible starting configuration $\eta \in \mathcal{C}^*$.

Case A. Without loss of generality we consider η as in Figure 4.4 on the left-hand side. If we are considering the case in which a 1-translation of a bar is possible and takes place, then by Lemma 4.2.4 the saddles that are crossed are essential and in $\mathcal{N}_0^{\alpha'} \cup \mathcal{N}_1^{\alpha}$. If a sequence of 1-translations of a bar takes place in such a way that the last configuration has at most two occupied frame-angles, then the saddles that could be visited starting from such a configuration will be analyzed in cases B, C and D. Thus, we are left to analyze the case in which there is the activation of a sliding of a bar around a frame-angle. In the following we quickly exclude the cases in which the particle is attached to $B^n(\eta)$, $B^s(\eta)$ or $B^e(\eta)$ and then explain the more interesting case in which it is attached to $B^w(\eta)$ giving rise to Figure 4.4 on the right-hand side. If the free particle is attached to the bar $B^n(\eta)$ (resp. $B^s(\eta)$), by Lemma 4.2.5 we know that it is not possible to complete the sliding of the bar $B^w(\eta)$ (resp. $B^e(\eta)$) around the frame-angle $c^{wn}(\eta')$ (resp. $c^{es}(\eta')$). If the free particle is attached to the bar $B^e(\eta)$ or $B^w(\eta)$, then it is not possible to slide the bar $B^s(\eta)$ around the frame-angle $c^{se}(\eta')$ or $c^{sw}(\eta')$ respectively, since (3.2.12) is not satisfied. In the last two cases by Lemma 4.2.3(ii), we know that the saddles that are visited are unessential. This implies that the unique possibility to activate and complete a sliding of a bar around a frame-angle is attaching the free particle to the bar $B^w(\eta)$, then sliding the bar $B^n(\eta)$ around the frame-angle $c^{nw}(\eta')$ when $|B^n(\eta)| < |B^w(\eta)|$, otherwise (3.2.12) is not satisifed. The saddles that are possibly visited by the sliding path are in $\mathcal{N}_{k,k'}^{\alpha,\alpha'}$ (see Definition (4.1.13)) except the last one, thus by Lemma 4.2.3(i) they are essential. The last configuration visited during this sliding of a bar is depicted in Figure 4.4 on the right-hand side. This configuration has energy $\Gamma^* - U_1 + U_2$ and therefore it is not a saddle and is in $\mathcal{C}_{\square}^{\blacksquare}(\Gamma^* - \widehat{H}(\blacksquare))$. By Propositions 3.1.5 and 4.3.3(ii)-(b), the latter implies that the saddles that could be visited are either unessential or in $\mathcal{N}_{2,k'}^{\alpha,\alpha'}$ and therefore the case A is concluded.

Case B. If we are considering the case in which a 1-translation of a bar is possible and takes place, then by Lemma 4.2.4 the saddles that are crossed are essential and in $\mathcal{N}_0^{\alpha'} \cup \mathcal{N}_1^{\alpha}$. We consider separately the following subcases:

(i) The two occupied frame-angles are $c^{\alpha\alpha'}(\eta)$ and $c^{\alpha''\alpha'''}(\eta)$, with all the indices α, α', α'' and α''' different between each other (see Figure 4.5(a));

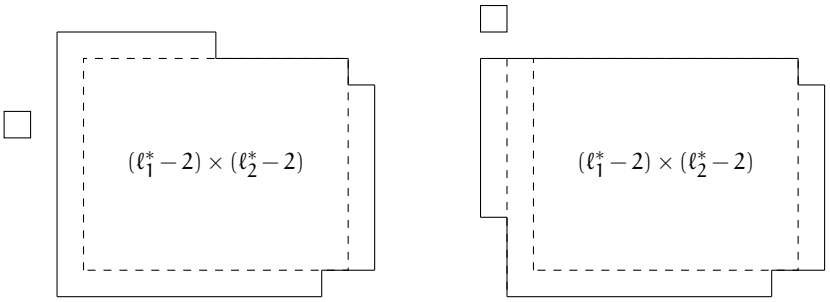

Figure 4.6 – Case B(iii): on the left-hand side we depict a possible starting configuration $\eta \in \mathcal{C}^*$ and on the right-hand side the configuration $\widetilde{\eta}$ obtained from η after the sliding of the bar $B^n(\eta)$ around the frame-angle $c^{nw}(\eta')$.

(ii) The two occupied frame-angles are $c^{\alpha\alpha'}(\eta)$ and $c^{\alpha'\alpha''}(\eta)$, with $\alpha' \in \{n, s\}$ and $\alpha \neq \alpha''$ (see Figure 4.5(c));

(iii) The two occupied frame-angles are $c^{\alpha\alpha'}(\eta)$ and $c^{\alpha'\alpha''}(\eta)$, with $\alpha' \in \{e, w\}$ and $\alpha \neq \alpha''$ (see Figure 4.6 on the left-hand side).

Case B(i). Without loss of generality we consider η as in Figure 4.5(a). We can reduce our proof to the case in which there is no translation of a bar and therefore there is the activation of a sliding of a bar around a frame-angle. If the free particle is attached to the bar $B^n(\eta)$ (resp. $B^s(\eta)$), by Lemma 4.2.5 we know that it is not possible to complete the sliding of the bar $B^w(\eta)$ (resp. $B^e(\eta)$) around the frame-angle $c^{wn}(\eta')$ (resp. $c^{es}(\eta')$). By Lemma 4.2.3(ii), this implies that the saddles that could be crossed are unessential. Note that if the free particle is attached to the bar $B^n(\eta)$ (resp. $B^s(\eta)$), it is not possible to slide the bar $B^e(\eta)$ (resp. $B^w(\eta)$) by definition. If the free particle is attached to the bar $B^w(\eta)$ (resp. $B^e(\eta)$) it is possible to slide the bar $B^n(\eta)$ (resp. $B^s(\eta)$) around the frame-angle $c^{nw}(\eta')$ (resp. $c^{se}(\eta')$) when $|B^n(\eta)| < |B^w(\eta)|$ (resp. $|B^s(\eta)| < |B^e(\eta)|$), otherwise (3.2.12) is not satisifed. The saddles that are possibly visited by the sliding path are in $\mathcal{N}_{k,k'}^{\alpha,\alpha'}$ except the last one, thus by Lemma 3.4.1(i) they are essential. The last configuration visited during this sliding of a bar is depicted in Figure 4.5(b). This configuration has energy $\Gamma^* - U_1 + U_2$ and therefore it is not a saddle and is in $\mathcal{C}_{\square}^{\blacksquare}(\Gamma^* - \widehat{H}(\blacksquare))$. By Propositions 3.1.5 and 4.3.3(ii)-(b), the latter implies that the saddles that could be visited are either unessential or in $\mathcal{N}_{2,k'}^{\alpha,\alpha'}$ and therefore the case B(i) is concluded.

Case B(ii). Without loss of generality we consider η as in Figure 4.5(c). If one bar among $B^w(\eta)$ and $B^e(\eta)$ is full, it is possible to translate $B^s(\eta)$ in order to have three occupied frame-angles. This situation has already been analyzed in case A. Thus, we can reduce our proof to the case in which there is no translation of a bar and therefore there is the activation of a sliding of a bar around a frame-angle. If the free particle is attached to the bar $B^n(\eta)$ or $B^s(\eta)$, by Lemma 4.2.5 we know that it is not possible to complete the sliding of a vertical bar around any frame-angle. If the free particle is attached to the bar $B^w(\eta)$ or $B^e(\eta)$, since the bar $B^n(\eta)$ is full, we deduce that (3.2.12) is not satisfied. This implies that it is not possible to slide the bar $B^n(\eta)$ around the frame-angle $c^{nw}(\eta')$ and $c^{ne}(\eta')$. In the last two cases by Lemma 3.4.1(ii) we know that the saddles that are visited are unessential. This concludes case B(ii).

Case B(iii). Without loss of generality we consider η as in Figure 4.6 on the left-hand side. If the bar $B^n(\eta)$ (resp. $B^s(\eta)$) is full, it is possible to translate $B^e(\eta)$ to occupy the frame-angle $c^{ne}(\eta')$ (resp. $c^{se}(\eta')$). This situation has already been analyzed in case A. Otherwise, it is possible to translate a bar with one occupied frame-angle in order to have two occupied frame-angles in such a way that they have no bar in common. This situation has already been analyzed in case B(i). Thus, we can reduce our proof to the case in which there is no translation of a bar and therefore there is the activation of a sliding of a bar around a frame-angle. If the free particle is attached to the bar $B^n(\eta)$ (resp. $B^s(\eta)$), by Lemma 4.2.5 we know that it is not possible to complete the sliding of the bar $B^w(\eta)$ around the frame-angle $c^{wn}(\eta')$ (resp. $c^{ws}(\eta')$). If the free particle is attached to the bar $B^e(\eta)$, we deduce that (3.2.11) is not satisfied. In the last two cases by Lemma 4.2.3(ii) we know that the saddles

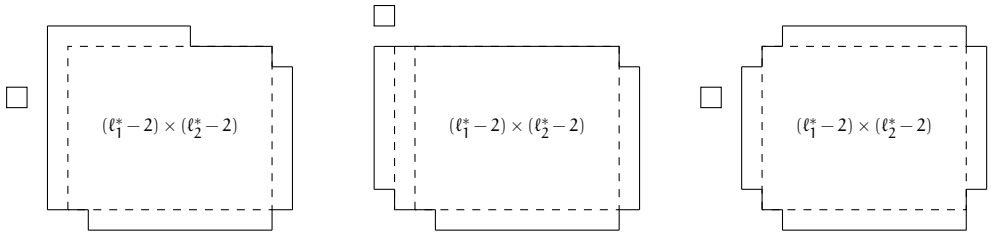

(a) (b) (c)

Figure 4.7 – Case C: in (a) we depict a possible starting configuration $\eta \in \mathcal{C}^*$ and in (b) the configuration $\widetilde{\eta}$ obtained from η after the sliding of the bar $B^n(\eta)$ around the frame-angle $c^{nw}(\eta')$. Case D: in (c) we depict a possible starting configuration $\eta \in \mathcal{C}^*$.

that are visited are unessential. If the free particle is attached to the bar $B^w(\eta)$, it is possible to slide the bar $B^n(\eta)$ (resp. $B^s(\eta)$) around the frame-angle $c^{nw}(\eta')$ (resp. $c^{sw}(\eta')$) when $|B^n(\eta)| < |B^w(\eta)|$ (resp. $|B^s(\eta)| < |B^w(\eta)|$), otherwise (3.2.12) is not satisifed. The saddles that are possibly visited by the sliding path are in $\mathcal{N}_{k,k'}^{\alpha,\alpha'}$ except the last one, thus by Lemma 3.4.1(i) they are essential. The last configuration visited during the sliding of the bar $B^n(\eta)$ around the frame-angle $c^{nw}(\eta')$ is depicted in Figure 4.6 on the right-hand side. This configuration has energy $\Gamma^* - U_1 + U_2$ and therefore it is not a saddle and is in $\mathcal{C}_{\square}^{\blacksquare}(\Gamma^* - \widehat{H}(\blacksquare))$. By Propositions 3.1.5 and and 4.3.3(ii)-(b), the latter implies that the saddles that could be visited are either unessential or in $\mathcal{N}_{2,k'}^{\alpha,\alpha'}$ and therefore the case B(iii) is concluded.

Case C. Without loss of generality we consider η as in Figure 4.7(a). If we are considering the case in which a 1-translation of a bar is possible and takes place, then by Lemma 4.2.4 the saddles that are crossed are essential and in $\mathcal{N}_0^{\alpha'} \cup \mathcal{N}_1^{\alpha}$. Starting from this configuration it is possible to obtain two occupied frame-angles: this situation has been already analyzed in Case B. Thus, we can reduce our proof to the case in which there is no translation of a bar and therefore there is the activation of a sliding of a bar around a frame-angle. If the free particle is attached to the bar $B^n(\eta)$ (resp. $B^s(\eta)$), by Lemma 4.2.5 we know that it is not possible to complete the sliding of the bar $B^w(\eta)$ around the frame-angle $c^{wn}(\eta')$ (resp. $c^{ws}(\eta')$). If the free particle is attached to the bar $B^e(\eta)$, we deduce that (3.2.11) is not satisfied. In the last two cases by Lemma 4.2.3(ii) we know that the saddles that are visited are unessential. If the free particle is attached to the bar $B^w(\eta)$, it is possible to slide the bar $B^n(\eta)$ around the frame-angle $c^{nw}(\eta')$ when $|B^n(\eta)| < |B^w(\eta)|$, otherwise (3.2.12) is not satisifed. The saddles that are possibly visited by the sliding path are in $\mathcal{N}_{k,k'}^{\alpha,\alpha'}$ except the last one, thus by Lemma 4.2.3(i) they are essential. The last configuration visited during this sliding of a bar is depicted in Figure 4.7(b). This configuration has energy $\Gamma^* - U_1 + U_2$ and therefore it is not a saddle and is in $\mathcal{C}_{\square}^{\blacksquare}(\Gamma^* - \widehat{H}(\blacksquare))$. By Propositions 3.1.5 and 4.3.3(ii)-(b), the latter implies that the saddles that could be visited are either unessential or in $\mathcal{N}_{2,k'}^{\alpha,\alpha'}$ and therefore the case C is concluded.

Case D. Without loss of generality we consider η as in Figure 4.7(c). If we are considering the case in which a 1-translation of a bar is possible and takes place, then by Lemma 4.2.4 the saddles that are crossed are essential and in $\mathcal{N}_0^{\alpha'} \cup \mathcal{N}_1^{\alpha}$. Starting from this configuration it is possible to obtain one or two occupied frame-angles: these situations have been already analyzed in Cases C and B, respectively. Thus, we can reduce our proof to the case in which there is no translation of a bar and therefore there is the activation of a sliding of a bar around a frame-angle. If the free particle is attached to the bar $B^n(\eta)$ (resp. $B^s(\eta)$), by Lemma 4.2.5 we know that it is not possible to complete the sliding of the bar $B^w(\eta)$ around the frame-angle $c^{wn}(\eta')$ (resp. $c^{ws}(\eta')$). If the free particle is attached to the bar $B^w(\eta)$ or $B^e(\eta)$, we deduce that (3.2.11) is not satisfied. In the last two cases by Lemma 4.2.3(ii) we know that the saddles that are visited are unessential. This concludes case D. □

5

CRITICAL DROPLETS ON THE SQUARE LATTICE: STRONG ANISOTROPY

This chapter is devoted to the geometrical characterization of the union of all the minimal gates for the local model evolving under Kawasaki dynamics with strongly anisotropic interactions, namely, $U_1 > 2U_2$ in (1.3.11). To this end, we apply the model–independent strategy carried out in Chapter 3 to the strongly anisotropic local model. For this regime we are able to fully identify the geometry of the union of all the minimal gates. We observe very different behaviour compared to the weakly anisotropic regime ($U_1 < 2U_2$). Finally, we provide sharp asymptotics concerning the mean transition time, the mixing time and the spectral gap.

The outline of the chapter is as follows. In Section 5.1 we state our main results. In particular, we state the results concerning the gates in Section 5.1.1 and the sharp asymptotics in Section 5.1.2. In Section 5.2, we give some model-dependent results that are useful for the model–dependent strategy concerning the minimal gates carried out in Section 5.3. In Section 5.4 we give the proof of the main result regarding the identification of the union of all the minimal gates (see Theorem 5.1.3). In Section 5.5 we give the proof of the theorems about the sharp asymptotics.

5.1 MAIN RESULTS: THE GATES FOR OUR MODEL

In this section we state our main results. In particular, in Section 5.1.1 we obtain the geometrical characterization of the union of all minimal gates and in Section 5.1.2 we provide the sharp asymptotics for the mean transition time and for the mixing time and spectral gap. To this end, we need some specific definitions for the strongly anisotropic case provided in Section 5.1.1. For the corresponding results obtained in the isotropic and weakly anisotropic cases, we refer respetively to Sections 3.2.2 and 4.1.1 for the results concerning the gates and union of minimal gates, and to Sections 3.2.3 and 4.1.2 for the results concerning the asymptotic transition time, mixing time and spectral gap.

5.1.1 *Gate for strongly anisotropic interactions*

In this section we assume $U_1 > 2U_2$ in (1.3.11), i.e., we consider strongly anisotropic interactions between nearest neighboring sites. Recall the definition of ε given in (3.2.8). We will consider $0 < \varepsilon \ll U_2$, where $\ll$ means sufficiently smaller; for instance $\varepsilon \leqslant \frac{U_2}{100}$ is enough. In order to state our main results for the gates in the strongly anisotropic regime we need the following definitions. Recall (1.3.22) for the definition of the critical length ℓ_2^* and we set the critical value of s as

$$s^* := 3\ell_2^* - 1. \tag{5.1.1}$$

Recall that we have defined $\bar{\Omega}$ as the set of configurations having one cluster anywhere in Λ_0 consisting of a $(2\ell_2^* - 3) \times \ell_2^*$ rectangle with a single protuberance attached to one of the shortest sides. Similarly, the set $\widetilde{\Omega}$ contains the configurations having one cluster anywhere in Λ_0 consisting of a $(2\ell_2^* - 3) \times \ell_2^*$ rectangle with a single protuberance attached to one of the longest sides. The critical value of the energy is

$$\Gamma^* = U_1\ell_2^* + 2U_2\ell_2^* + U_1 - U_2 - 2\varepsilon(\ell_2^*)^2 + 3\varepsilon\ell_2^* - 2\varepsilon. \tag{5.1.2}$$

and the volume of the clusters in $\bar{\Omega}$ is

$$n_c = \ell_2^*(2\ell_2^* - 3) + 1. \tag{5.1.3}$$

Finally, recall (1.3.31) for the definition of the sets $\bar{\mathcal{D}}$ and $\widetilde{\mathcal{D}}$. We encourage the reader to consult Proposition 5.2.1, where we give the geometrical description of the sets $\bar{\mathcal{D}}$ and $\widetilde{\mathcal{D}}$.

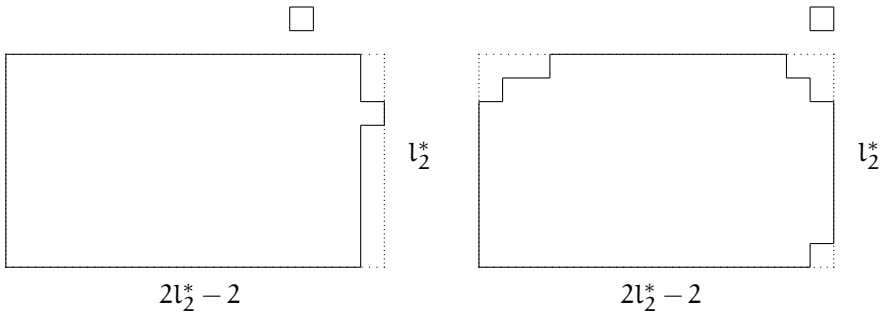

Figure 5.1 – Critical configurations in $\mathcal{C}^*$ in the strongly anisotropic case. Moreover, if we remove the free particle we obtain on the left a configuration in $\bar{\mathcal{Q}}$ and on the right a configuration in $\bar{\mathcal{D}} \setminus \bar{\mathcal{Q}}$.

Roughly speaking, one can think of $\bar{\mathcal{D}}$ as the set of configurations consisting of a rectangular cluster with four bars attached to its four sides, whose lengths satisfy precise conditions. Finally, we set

$$\mathcal{C}^* = \bar{\mathcal{D}}^{fp}. \tag{5.1.4}$$

The reason why only the set $\bar{\mathcal{D}}$ is relevant for the set $\mathcal{C}^*$ will be clarified in Lemma 5.2.6. Note that

$$\begin{aligned} \widehat{H}(\mathcal{C}^*) &= \widehat{H}(\bar{\mathcal{D}}^{fp}) = \widehat{H}(\bar{\mathcal{D}}) + \Delta = \widehat{H}(\mathcal{Q}) + \Delta \\ &= u_1 \ell_2^* + 2u_2 \ell_2^* - u_1 - 3u_2 - \varepsilon \ell_2^* (2\ell_2^* - 3) + 2\Delta \\ &= u_1 \ell_2^* + 2u_2 \ell_2^* + u_1 - u_2 - 2\varepsilon (\ell_2^*)^2 + 3\varepsilon \ell_2^* - 2\varepsilon \\ &= \Gamma^*. \end{aligned} \tag{5.1.5}$$

See Figure 5.1 for an example of configurations in $\mathcal{C}^*$. Note that $\widehat{H}(\bar{\mathcal{Q}}) < H(\widetilde{\mathcal{Q}})$, see Remark 4.1.1.

The first main result of Section 5.1.1 is the following.

Theorem 5.1.1. (Gate for strongly anisotropic interactions). *The set $\mathcal{C}^*$ is a gate for the transition from $\square$ to $\blacksquare$.*

We refer to Section 5.4.1 for the proof of the Theorem 5.1.1.

Remark 5.1.2. *In Theorem 5.1.1 we sharpen the previous result obtained in [16, Theorem 2.4]. Indeed, in [16] the authors proved that $\mathcal{P}_1 \cup \mathcal{P}_2$ is a gate (see (5.1.6) and (5.4.1) for the definitions of $\mathcal{P}_0' = \mathcal{P}_1$ and $\mathcal{P}_2$ respectively), while here we refine that result by proving that $\mathcal{C}^*$ is a gate. In particular, we emphasize that $\mathcal{C}^* \subset \mathcal{P}_1$ and therefore there is an important improvement in the statement since our gate is much smaller than the one found in [16].*

In order to give the result regarding the geometric characterization of $\mathcal{G}(\square, \blacksquare)$, we need some definitions. For any $i = 0, 1$ we define $\mathcal{P}_i' \subseteq \mathcal{S}(\square, \blacksquare)$ that consists of configurations with a single cluster and no free particle, a fixed number of vacancies, that is not monotone with circumscribed rectangles obtained from the one of the configurations in $\bar{\mathcal{D}}$ via increasing by one the horizontal or vertical length. More precisely,

$$\begin{aligned} \mathcal{P}_i' := \quad & \{\eta : n(\eta) = 0,\, v(\eta) = 2\ell_2^* + i\ell_2^* - i(i+1) - 2,\, g_1'(\eta) = i,\, g_2'(\eta) = 1 - i, \eta_{cl} \text{ is} \\ & \text{connected, with circumscribed rectangle in } \mathcal{R}(2\ell_2^* - i - 1, \ell_2^* + i)\},\ i = 0, 1. \end{aligned} \tag{5.1.6}$$

See Figure 1.19 for an example of configurations in $\mathcal{P}_0'$ (on the left-hand side) and in $\mathcal{P}_1'$ (on the right-hand side).

The set $\mathcal{G}(\square, \blacksquare)$ contains all the configurations that are in the sets defined in (5.1.6) with the following further conditions. First, we define the subsets $\mathcal{A}_0^{\alpha'}$ (resp. $\mathcal{A}_1^{\alpha}$) of the saddles in $\mathcal{P}_0'$ (resp. $\mathcal{P}_1'$) that contains only one occupied unit square in either a vertical (resp. horizontal) row or in one of its two adjacent frame-angles. More precisely,

$$\mathcal{A}_0^{\alpha'} := \{\eta \in \mathcal{P}_0' : |r^{\alpha'}(\eta) \cup c^{\alpha' \bar{\alpha}}(\eta) \cup c^{\alpha' \tilde{\alpha}}(\eta)| = 1\}, \tag{5.1.7}$$

for any $\alpha' \in \{w, e\}$ and $\bar{\alpha}, \widetilde{\alpha} \in \{n, s\}$ such that $\bar{\alpha} \neq \widetilde{\alpha}$, and

$$\mathcal{A}_1^{\alpha} := \{\eta \in \mathcal{P}_1' : |r^{\alpha}(\eta) \cup c^{\alpha\alpha''}(\eta) \cup c^{\alpha\alpha'''}(\eta)| = 1\}, \tag{5.1.8}$$

for any $\alpha \in \{n, s\}$ and $\alpha'', \alpha''' \in \{n, s\}$ such that $\alpha' \neq \alpha'''$. Note that in Figure 1.19 the configuration on the right-hand side is in $\mathcal{A}_1^{n}$.

Next, we define the subsets $\mathcal{A}_k^{\alpha,\alpha'}$ of the saddles in $\mathcal{P}_0'$ that are obtained from $\eta \in \mathcal{P}_0'$ during the sliding of the bar $B^{\alpha'}(\eta)$ around the frame-angle $c^{\alpha'\alpha}(\eta)$. More precisely,

$$\begin{aligned}\mathcal{A}_k^{\alpha,\alpha'} := \{\eta \in \mathcal{P}_0' \quad & : |r^{\alpha}(\eta)| = k-1, |r^{\alpha'}(\eta)| = \ell_2^* - k, |c^{\alpha'\alpha}(\eta)| = 1, \\ & (r^{\alpha}(\eta) \cup c^{\alpha'\alpha}(\eta)) \cap \eta_{cl} = r_{cl}^{\alpha,1} \dot{\cup} r_{cl}^{\alpha,2} \text{ with } d(r_{cl}^{\alpha,1}, r_{cl}^{\alpha,2}) = 2\},\end{aligned} \tag{5.1.9}$$

where $\alpha \in \{n, s\}$, $\alpha' \in \{w, e\}$, $r_{cl}^{\alpha,1}$, $r_{cl}^{\alpha,2}$ are two disjoint connected components in $r^{\alpha(\eta)} \cup c^{\alpha'\alpha}(\eta)$ and $k = 2, ..., \ell_2^*$. Note that the conditions in (5.1.9) guarantee that these configurations are obtained during a sliding of a bar around a frame-angle, that is identified by the indeces α and α'. Note that in this case there is not the index k' as in (3.2.20) and (4.1.13) for the isotropic and weakly anisotropic cases, respectively, because in the strongly anisotropic case less sliding on the border of the droplet are allowed. Indeed, in this case $\ell_2^* - 1$ denotes the length of the bar that we are sliding and thus we can consider $k' = \ell_2^* - 1$ fixed. The index k counts the number of particles that are in $r^{\alpha}(\eta) \cup c^{\alpha'\alpha}(\eta)$ during the sliding and can be less or equal than ℓ_2^*. Referring to Figure 1.13, configuration (7) (resp. (11)) is an example of configuration that belongs to $\mathcal{A}_2^{n,e}$ (resp. $\mathcal{A}_{\ell_2^*}^{n,e}$). Note that the set $\mathcal{A}_k^{\alpha,\alpha'}$ contains $k-1$ configurations for any α, α' and k, indeed these configurations are crossed during the sliding of the bar $B^{\alpha'}(\eta)$ around the frame-angle $c^{\alpha'\alpha}(\eta)$, with η the configuration obtained by $\mathcal{R}(2\ell_2^* - 1, \ell_2^* - 1)$ adding a protuberance to one of its longest sides (in Figure 1.13 η corresponds to the configuration (3) and $\alpha = n$, $\alpha' = e$). Thus, we set

$$\mathcal{A}_k^{\alpha,\alpha'} = \{\xi_1^{\alpha,\alpha'}, ..., \xi_{k-1}^{\alpha,\alpha'}\}. \tag{5.1.10}$$

Now we are able to give the second main result of Section 5.1.1.

Theorem 5.1.3. (Union of minimal gates for strongly anisotropic interactions). *We obtain the following description for* $\mathcal{G}(\square, \blacksquare)$*:*

$$\mathcal{G}(\square, \blacksquare) = \mathcal{C}^* \cup \bigcup_{\alpha} \bigcup_{\alpha'} \bigcup_{k=2}^{\ell_2^*} \mathcal{A}_k^{\alpha,\alpha'} \cup \bigcup_{\alpha'} \mathcal{A}_0^{\alpha'} \cup \bigcup_{\alpha} \mathcal{A}_1^{\alpha}. \tag{5.1.11}$$

We refer to Section 5.4.2 for the proof of Theorem 5.1.3.

Remark 5.1.4. *With the strategy carried out in [75] and the argument explained in Section 4.6 the results about the nucleation time and gates derived for the strongly anisotropic local model can be directly extended to the simplified model.*

5.1.2 *Sharp asymptotics for strongly anisotropic interactions*

In this section we investigate the prefactor for the strongly anisotropic case, which is the subject of Theorem 5.1.5. This analysis for the isotropic case is given in [35, Theorem 1.4.4], while for the weakly anisotropic case is given in Theorem 4.1.4. For a model–independent discussion concerning the prefactor we refer to Section 3.6.1. Moreover, in Theorem 5.1.8 we provide sharp asymptotics of mixing time and spectral gap. For the proof of Theorems 5.1.5 and 5.1.8 we refer to Section 5.5. Equation (5.1.14) below corrects a minor mistake in [17, eq. (4.28)], where the multiplicative factor $|\bar{\Lambda}^{*,\,\mathrm{orie}}|$ in the asymptotic behaviour of the prefactor is missing.

Theorem 5.1.5. *There exists a constant* $K = K(\Lambda, \ell_2^*)$ *such that*

$$\mathbb{E}_{\square}(\tau_{\blacksquare}) = K e^{\Gamma^* \beta}\,[1 + o(1)], \qquad \beta \to \infty, \tag{5.1.12}$$

with

$$\frac{1}{\Theta_2} \leqslant K \leqslant \frac{1}{\Theta_1}, \tag{5.1.13}$$

where Θ_1 *and* Θ_2 *are defined in (5.5.17) and (5.5.27), respectively. Moreover, as* $\Lambda \to \mathbb{Z}^2$,

$$K(\Lambda, \ell_2^*) \to \frac{|\bar{\Lambda}^{*,\,\mathrm{orie}}|}{4\pi N} \frac{\log|\Lambda|}{|\Lambda|}, \tag{5.1.14}$$

where

$$N = \sum_{k=1}^{4} \binom{4}{k} \binom{\ell_2^* + k - 2}{2k-1} \tag{5.1.15}$$

is the cardinality of $\bar{\mathcal{D}} = \bar{\mathcal{D}}(\Lambda, \ell_2^*)$ *modulo shifts.*

Remark 5.1.6. *For the strongly anisotropic case we obtain a sharp estimate of* K *in (5.1.13). Nevertheless, the asymptotic behavior of the the prefactor* K *as* $\Lambda \to \mathbb{Z}^2$ *(see (5.1.14)) is the same as the isotropic and weakly anisotropic regimes, see [35, eq. (1.4.9)] and (4.1.16), respectively.*

Remark 5.1.7. *Note that [35, Theorem 1.4.3(iii)] and Theorem 4.1.5 concerning the uniform entrance distribution in the gate does not hold for the strongly anisotropic case due to the two possible entrance mechanisms in* $\mathcal{C}^*$ *(see Lemma 5.3.8).*

Recall (1.3.54) and (1.3.55) for the definition of mixing time and spectral gap, respectively.

Theorem 5.1.8. *For any* $\varepsilon \in (0,1)$

$$\lim_{\beta\to\infty} \frac{1}{\beta} \log t_{\mathrm{mix}}(\varepsilon) = \Gamma^* = \lim_{\beta\to\infty} -\frac{1}{\beta} \log \rho. \tag{5.1.16}$$

Furthermore, there exist two constants $0 < c_1 \leqslant c_2 < \infty$ *independent of* β *such that for every* $\beta > 0$

$$c_1 e^{-\beta\Gamma^*} \leqslant \rho \leqslant c_2 e^{-\beta\Gamma^*}. \tag{5.1.17}$$

Theorem 5.1.8 holds also for the isotropic and weakly anisotropic cases, see Theorems 3.2.8 and 4.1.7, respectively.

5.2 USEFUL MODEL–DEPENDENT TOOLS

5.2.1 *Geometric description of the protocritical droplets*

In this Section we derive the geometric description of the sets $\bar{\mathcal{D}}$ and $\widetilde{\mathcal{D}}$ for the strongly anistropic models following the argument proposed in [35].

Proposition 5.2.1. (Geometric description of $\widetilde{\mathcal{D}}$ and $\bar{\mathcal{D}}$). *For the strongly anisotropic regime we obtain the following geometric description of* $\widetilde{\mathcal{D}}$ *and* $\bar{\mathcal{D}}$*:*

(a) $\widetilde{\mathcal{D}} = \{\eta \in \mathcal{X} : n(\eta) = 0,\ v(\eta) = 2\ell_2^* - 4,\ \eta_{cl}$ *is connected and monotone,* $1 \leqslant |r^\alpha(\eta) \cup c^{\alpha\alpha'}(\eta)| \leqslant 2, |r^\alpha(\eta)| \leqslant 1$, *with* $\alpha \in \{n, s\},\ \alpha' \in \{w, e\}$, *and circumscribed rectangle in* $\mathcal{R}(2\ell_2^* - 3, \ell_2^* + 1)\}$,

(b) $\bar{\mathcal{D}}$ *is the set of configurations having one cluster* η *anywhere in* Λ_0 *consisting of a* $(2\ell_2^* - 4) \times (\ell_2^* - 2)$ *rectangle with four bars* $B^\alpha(\eta)$*, with* $\alpha \in \{n, w, e, s\}$*, attached to its four sides satisfying*

$$1 \leqslant |B^w(\eta)|, |B^e(\eta)| \leqslant \ell_2^*, \qquad \ell_2^* - 1 \leqslant |B^n(\eta)|, |B^s(\eta)| \leqslant 2\ell_2^* - 2, \tag{5.2.1}$$

and

$$\sum_{\alpha} |B^\alpha(\eta)| - \sum_{\alpha\alpha' \in \{nw, ne, sw, se\}} |c^{\alpha\alpha'}(\eta)| = 5\ell_2^* - 7. \tag{5.2.2}$$

Remark 5.2.2. *Let* $\eta \in \bar{\mathcal{D}}$.

(i) Note that (5.2.2) takes into account the number of occupied unit squares in $\partial^- CR(\eta)$ *due to Remark 3.2.2. We deduce that at most three frame-angles of* $CR(\eta)$ *can be occupied, otherwise* $|\partial^- CR(\eta)| = 6\ell_2^* - 8 > 5\ell_2^* - 7$, *which is absurd.*

(ii) Since $|B^s(\eta)| + |B^e(\eta)| \leqslant 3\ell_2^* - 6 + k - |c^{nw}(\eta)|$, *we get*

$$|B^n(\eta)| + |B^w(\eta)| = 5\ell_2^* - 7 - (|B^s(\eta)| + |B^e(\eta)|) + k \geqslant 2\ell_2^* - 1 + |c^{nw}(\eta)|. \quad (5.2.3)$$

By symmetry, we generalize the inequality above for any $\alpha \in \{n, s\}$ *and* $\alpha' \in \{w, e\}$: *we get* $|B^\alpha(\eta)| + |B^{\alpha'}(\eta)| \geqslant 2l_2^* - 1 + |c^{\alpha\alpha'}(\eta)|$.

Proof of Proposition 5.2.1. (a) We introduce only in the proof of this result the following geometrical definition to make the argument more clear

$$\begin{aligned}\widetilde{\mathcal{D}}_{geo} := \{\eta \in \mathcal{X} :\ & n(\eta) = 0,\ v(\eta) = 2\ell_2^* - 4,\ \eta_{cl} \text{ is connected and monotone,} \\ & 1 \leqslant |r^\alpha(\eta) \cup c^{\alpha\alpha'}(\eta)| \leqslant 2, |r^\alpha(\eta)| \leqslant 1, \text{ with } \alpha \in \{n, s\},\ \alpha' \in \{w, e\}, \\ & \text{and circumscribed rectangle in } \mathcal{R}(2\ell_2^* - 3, \ell_2^* + 1)\}.\end{aligned} \quad (5.2.4)$$

The proof will be given in two steps:

(i) $\widetilde{\mathcal{D}}_{geo} \subseteq \widetilde{\mathcal{D}}$;

(ii) $\widetilde{\mathcal{D}}_{geo} \supseteq \widetilde{\mathcal{D}}$.

Proof of (i). To prove (i) we must show that for all $\eta \in \widetilde{\mathcal{D}}_{geo}$,

(i1) $\widehat{H}(\eta) = \widehat{H}(\widetilde{\Omega})$;

(i2) $\exists\ \omega : \widetilde{\Omega} \to \eta$, i.e., $\omega = (\omega_1, ..., \omega_k = \eta)$ such that $\max_i \widehat{H}(\omega_i) \leqslant \widehat{H}(\widetilde{\Omega}) + U_1$, with $|\omega_i| = n_c$ for all $i = 1, ..., k$ (see (5.1.3) for the value of n_c).

Proof of (i1). Any $\eta \in \widetilde{\mathcal{D}}_{geo}$ satisfies $n(\eta) = 0$, $|C(\eta)| = (2\ell_2^* - 3)(\ell_2^* + 1) - v(\eta) = n_c$, and $g_1(\eta) = 2\ell_2^* - 3$ and $g_2(\eta) = \ell_2^* + 1$ since the configuration is monotone. Thus, by (3.2.3) we deduce that $\widehat{H}$ is constant on $\widetilde{\mathcal{D}}_{geo}$. Since $\widetilde{\Omega} \subseteq \widetilde{\mathcal{D}}_{geo}$, this completes the proof of (i1).

Proof of (i2). Consider $\zeta \in \widetilde{\Omega}$ and $\eta \in \widetilde{\mathcal{D}}_{geo}$. If $\eta \in \widetilde{\Omega} \cap \widetilde{\mathcal{D}}_{geo}$, i.e., $|r^\alpha(\eta) \cup c^{\alpha\alpha'}(\eta)| = 1$ for some $\alpha \in \{n, s\}$ and $\alpha' \in \{w, e\}$, then η can be obtained from ζ by moving the protuberance at zero cost along the side which is attached to if the protuberance in ζ is on the same side as the protuberance in η, otherwise η can be obtained detaching the protuberance at cost U_2 and reattaching it to the other side at cost $-U_2$. If $\eta \in \widetilde{\mathcal{D}}_{geo} \setminus \widetilde{\Omega}$, i.e., $|r^\alpha(\eta) \cup c^{\alpha\alpha'}(\eta)| = 2$ with $|r^\alpha(\eta)| = 1$ for some $\alpha \in \{n, s\}$ and $\alpha' \in \{w, e\}$, again we have two cases. If the protuberance in ζ is contained in $r^\alpha(\eta)$ (is in the same side of the rectangle), we deduce that η can be obtained from ζ by moving the protuberance at zero cost until it arrives at distance one from $c^{\alpha\alpha'}(\zeta)$ and then translate the bar $B^{\alpha'}(\zeta)$ towards the frame-angle $c^{\alpha'\alpha}(\zeta)$ at cost U_2. Otherwise, if the protuberance in ζ is contained in $r^{\alpha''}(\eta)$ with $\alpha'' \in \{n, s\} \setminus \{\alpha\}$ (is in the opposite side of the rectangle), the path is constructed as before, provided that first the protuberance is detached at cost U_2 and reattached to the other side at cost $-U_2$. This concludes the proof of (i2).

Proof of (ii). By (i2), we know that all the configurations in $\widetilde{\mathcal{D}}_{geo}$ are connected via U_1-path to $\widetilde{\Omega}$. Since $\widetilde{\Omega} \subseteq \widetilde{\mathcal{D}} \cap \widetilde{\mathcal{D}}_{geo}$, in order to prove (ii) it suffices to show that following U_1-paths it is not possible to exit $\widetilde{\mathcal{D}}_{geo}$. Let $\eta' \in \widetilde{\mathcal{D}}_{geo}$, thus by (i1) and (3.2.3) we get $\widehat{H}(\eta') = \Gamma^* - \Delta + U_1 - U_2$. Note that no particle can arrive because we impose that the number of particles is constant to n_c thus, if $\eta' \in \widetilde{\mathcal{D}}_{geo} \setminus \widetilde{\Omega}$, the unique possibility is to translate the bar $B^{\alpha'}(\eta')$, with $\alpha' \in \{w, e\}$, at cost U_2 giving rise to a configuration that is in $\widetilde{\mathcal{D}}_{geo} \cap \widetilde{\Omega}$. Then it is possible either to move the protuberance at zero cost, or to detach the protuberance at cost U_2 and then necessarily reattach it at cost $-U_2$, giving rise to a configuration that is still in $\widetilde{\mathcal{D}}_{geo} \cap \widetilde{\Omega}$. Note that no other moves are allowed, since it is not possible to complete the sliding of a vertical bar around a frame-angle because the 1-translation of a horizontal bar costs U_1. Indeed, the latter implies that the energy reaches the value $\Gamma^* - \Delta + 2U_1 - U_2 > \Gamma^*$, thus the path described is not a U_1-path. If $\eta' \in \widetilde{\mathcal{D}}_{geo} \cap \widetilde{\Omega}$, with paths similar to the ones described above (possibly in different order), we can conclude case (a).

(b) We denote by $\bar{\mathcal{D}}_{geo}$ the geometric set with the properties specified in point (b) that we introduce to make the argument more clear. The proof will be given in two steps:

(i) $\bar{\mathcal{D}}_{geo} \subseteq \bar{\mathcal{D}}$;
(ii) $\bar{\mathcal{D}}_{geo} \supseteq \bar{\mathcal{D}}$.

Proof of (i). To prove (i) we must show that for all $\eta \in \bar{\mathcal{D}}_{geo}$,
(i1) $\widehat{H}(\eta) = \widehat{H}(\bar{\Omega})$;
(i2) $\exists\ \omega : \bar{\Omega} \to \eta$, i.e., $\omega = (\omega_1, ..., \omega_k = \eta)$ such that $\max_i \widehat{H}(\omega_i) \leqslant \widehat{H}(\bar{\Omega}) + U_1$, with $|\omega_i| = n_c$ for all $i = 1, ..., k$ and $\omega_1 \in \bar{\Omega}$.

Proof of (i1). Any $\eta \in \bar{\mathcal{D}}_{geo}$ satisfies $n(\eta) = 0$, $|C(\eta)| = (2\ell_2^* - 2)(\ell_2^* - 2) + 5\ell_2^* - 7 = n_c$, and $g_1(\eta) = 2\ell_2^* - 2$ and $g_2(\eta) = \ell_2^*$ since the configuration is monotone. Thus, by (3.2.3) we deduce that $\widehat{H}$ is constant on $\bar{\mathcal{D}}_{geo}$. Since $\bar{\Omega} \subseteq \bar{\mathcal{D}}_{geo}$, this completes the proof of (i1).

Proof of (i2). Consider $\zeta \in \bar{\Omega}$ and $\eta \in \bar{\mathcal{D}}_{geo}$. Here, without loss of generality, we assume that the protuberance is in $r^w(\zeta)$. Then we have
- $|B^w(\zeta)| = 1$;
- $|B^n(\zeta)| = |B^s(\zeta)| = 2\ell_2^* - 3$;
- $|B^e(\zeta)| = \ell_2^*$;
- $|c^{ne}(\zeta)| = |c^{se}(\zeta)| = 1$.

Using the sliding of a unit square around a frame-angle described in Figure 1.11 (see Definition 3.2.4), we move, one by one, $|B^n(\zeta)| - |B^n(\eta)|$ particles around the frame-angle $c^{nw}(\zeta)$. After that we move $|B^e(\zeta)| - |B^e(\eta)| + |B^s(\zeta)| - |B^s(\eta)|$ particles around the frame-angle $c^{sw}(\zeta)$. Finally, we move $|B^e(\zeta)| - |B^e(\eta)|$ particles around the frame-angle $c^{es}(\zeta)$. The result is the configuration $\eta \in \bar{\mathcal{D}}_{geo}$. This concludes the proof of (i2).

Proof of (ii). By (i2), we know that all configurations in $\bar{\mathcal{D}}_{geo}$ are connected via U_1-path to $\bar{\Omega}$. Since $\bar{\Omega} \subseteq \bar{\mathcal{D}} \cap \bar{\mathcal{D}}_{geo}$, in order to prove (ii) it suffices to show that following U_1-paths it is not possible to exit $\bar{\mathcal{D}}_{geo}$. We call a path *clustering* if all the configurations in the path consist of a single cluster and no free particles. Below we will prove that for any $\eta \in \bar{\mathcal{D}}_{geo}$ and any η' connected to η by a clustering U_1-path, the following conditions hold:
(A) $CR(\eta') = CR(\eta)$;
(B) $\eta' \supseteq CR^-(\eta)$.

Proof of (A). Starting from any $\eta \in \mathcal{X}$, it is geometrically impossible to modify $CR(\eta)$ without detaching a particle, that contradicts the hypotheses of clustering U_1-path.

Proof of (B). Fix $\eta \in \bar{\mathcal{D}}_{geo}$. The proof is done in two steps.

1. First, we consider clustering U_1-paths along which we do not move a particle from $CR^-(\eta)$. Along such paths we only encounter configurations in $\bar{\mathcal{D}}_{geo}$ or configurations obtained from $\bar{\mathcal{D}}_{geo}$ by breaking one of the bars in $\partial^- CR(\eta)$ into two pieces at cost U_1 (resp. U_2) if the bar is horizontal (resp. vertical). This holds because there is no particle outside $CR(\eta)$ that can lower the cost.

If the broken bar is horizontal, then only moves at zero cost are admissible, so any particle can be detached. This implies that the unique way to regain U_1 and complete the U_1-path is to restore the bar.

If the broken bar is vertical, then the admissible moves in a U_1-path are those with cost less or equal than $U_1 - U_2$. Again any particle can not be detached, indeed its cost is at least U_1. The moves at cost U_2 are possible, thus it is possible to break another vertical bar. From now on, depending on $U_1 - 2U_2 > 0$, it is possible to break other vertical bars. More precisely, let $U_1 = nU_2 + \delta$, with $n \geqslant 2$ and $0 < \delta < U_2$ fixed, thus it is possible to break other $n - 2$ vertical bars in addition to the previous two. When this sequence of moves is completed, the unique way to complete the U_1-path is to restore all the broken bars. Thus, we have proved that $\eta' \supseteq CR^-(\eta)$.

2. Consider now a general clustering U_1-path along which we move a particle from a corner of $CR^-(\eta)$. It is not allowed to move at cost $U_1 + U_2$, because it exceeds U_1, thus the overshoot U_2 must be regained by letting the particle slide next to a bar that is attached to a side of $CR^-(\eta)$ (see Figure 4.2). If the particle moves vertically (resp. horizontally), we regain U_1 (resp. U_2). Since there are never two bars attached to the same side, we can at most regain U_1, thus it is not possible to move a particle from $CR^-(\eta)$ other than from a corner. If the corner particle has been moved vertically (increasing the energy by U_2), the same moves (if possible) are allowed on another corner. Depending on the difference $U_1 - 2U_2 > 0$, it is possible to break some vertical bars. More precisely, let $U_1 = nU_2 + \delta$, with $n \geqslant 2$ and $0 < \delta < U_2$ fixed, it is possible to break $n - 2$ vertical bars. From now on, only moves at cost

at most zero are admissible. There are no protuberances present anymore, because only the configurations in $\bar{\Omega}$ have a protuberance. Thus no particle outside $CR^-(\eta)$ can move, except those just detached from $CR^-(\eta)$. These particles can move back, in which case we return to the same configuration η (see Figure 4.2). In fact, all possible moves at zero cost consist in moving the recess just created in $CR^-(\eta)$ along the same side of $CR^-(\eta)$, until it reaches the top of the bar, after which it cannot advance anymore at zero cost (see Figure 4.2). All these moves do not change the energy, except the last one that returns the particle to its original position and regains U_1. This concludes the proof of (B).

From (A), we deduce that $CR(\eta') = \mathcal{R}(2\ell_2^* - 2, \ell_2^*)$. From (A) and (B), we deduce that the number of particles that are in $\partial^- CR(\eta)$ is equal to the number of particles that are in $\partial^- CR(\eta')$, thus (5.2.2), $1 \leqslant |B^w(\eta')|, |B^e(\eta')| \leqslant \ell_2^*$ and $1 \leqslant |B^n(\eta')|, |B^s(\eta')| \leqslant 2\ell_2^* - 2$ hold. In order to prove that following clustering U_1-paths it is not possible to exit $\bar{\mathcal{D}}_{geo}$, we have to prove the lower bound in (5.2.1) for the lengths $|B^n(\eta')|$ and $|B^s(\eta')|$. We set

$$k = \sum_{\alpha\alpha' \in \{nw, ne, sw, se\}} |c^{\alpha\alpha'}(\eta')|. \tag{5.2.5}$$

Since $|B^w(\eta')| + |B^e(\eta')| \leqslant 2\ell_2^* - 4 + k$, by (5.2.2) we get

$$|B^n(\eta')| + |B^s(\eta')| = 5\ell_2^* - 7 - (|B^w(\eta')| + |B^e(\eta')|) + k \geqslant 3\ell_2^* - 3. \tag{5.2.6}$$

Since $|B^s(\eta')| \leqslant 2\ell_2^* - 2$, (5.2.6) implies

$$|B^n(\eta')| \geqslant 3\ell_2^* - 3 - |B^s(\eta')| \geqslant \ell_2^* - 1. \tag{5.2.7}$$

By symmetry we can similarly argue for the length $|B^s(\eta')|$. This implies that following U_1-paths it is not possible to exit $\bar{\mathcal{D}}_{geo}$. The argument goes as follows. Detaching a particle costs at least $U_1 + U_2$ unless the particle is a protuberance, in which case the cost is U_1. The only configurations in $\bar{\mathcal{D}}_{geo}$ having a protuberance are those in $\bar{\Omega}$. If we detach the protuberance from a configuration in $\bar{\Omega}$, then we obtain a $(2\ell_2^* - 3) \times \ell_2^*$ rectangle with a free particle. Since in the sequel only moves at zero cost are allowed, it is only possible to move the free particle. Since in a U_1-path the particle number is conserved, the only way to regain U_1 and complete the U_1-path is to reattach the free particle to a vertical side of the rectangle, thus return to $\bar{\Omega}$. This implies that for any $\eta \in \bar{\mathcal{D}}_{geo}$ and any η' connected to η by a U_1-path we must have that $\eta' \in \bar{\mathcal{D}}_{geo}$. This concludes the proof. □

5.2.2 *Useful lemmas for the gates*

In this Section we give some useful Lemmas that help us to characterize the gates. below we state Lemma 5.2.3 for the strongly anisotropic case, but it holds also for the isotropic and weakly anisotropic cases, see Lemmas 3.4.1 and 4.2.3. The proof is the same of Lemma 4.2.3 for the weakly anisotropic case.

Lemma 5.2.3. *Starting from $\mathcal{C}^* \setminus \Omega^{fp}$, if the free particle is attached to a bad site obtaining $\eta^B \in \mathcal{C}^B$, the only transitions that does not exceed the energy Γ^* are either detaching the protuberance, or a sequence of 1-translations of a bar or slidings of a bar around a frame-angle. Moreover, we get:*

(i) if it is possible to slide a bar around a frame-angle, then the saddles that are crossed are essential;

(ii) if it is not possible to slide a bar around a frame-angle, then the path must come back to the starting configuration and the saddles that are crossed are unessential.

Lemmas 5.2.5 and 5.2.6 below are valid also in the weakly anisotropic case, see Lemmas 4.2.5 and 4.2.6, respectively, while Lemma 5.2.4 has a corresponding version for the weakly anisotropic case, see Lemma 4.2.4.

Lemma 5.2.4. *Starting from $\eta^B \in \mathcal{C}^B$, the saddles obtained by a 1-translation of a bar are essential and in $\mathcal{A}_0^{\alpha'} \cup \mathcal{A}_1^{\alpha}$. Moreover, all the saddles in $\mathcal{A}_0^{\alpha'} \cup \mathcal{A}_1^{\alpha}$ can be obtained from this η^B by a 1-translation of a bar.*

Proof. Note that $\widehat{H}(\eta^B) = \Gamma^* - U_2$ (resp. $\widehat{H}(\eta^B) = \Gamma^* - U_1$) if the free particle has been attached to an horizontal (resp. vertical) bar. In the first case, in order to avoid exceeding the

energy value Γ^* it is possible to translate only the vertical bars. These saddles are in $\mathcal{A}_1^\alpha$. In the latter case, it is possible to translate both vertical and horizontal bars. If the translated bar is horizontal, the saddles that are crossed are in $\mathcal{A}_0^{\alpha'}$. If the translated bar is vertical, the configurations obtained do not reach the level Γ^*, thus they are not saddles. To conclude, all the configurations in $\mathcal{A}_0^{\alpha'} \cup \mathcal{A}_1^\alpha$ can be obtained from a configuration η^B via a 1-translation of a bar.

It remains to prove that the saddles in $\mathcal{A}_0^{\alpha'} \cup \mathcal{A}_1^\alpha$ are essential. This part of the proof is analogue to the corresponding one done for the isotropic case in Lemma 3.5.2. □

Lemma 5.2.5. *Starting from a configuration $\eta \in \mathcal{C}^*$, it is not possible to slide a vertical bar around a frame-angle without exceeding the energy Γ^*.*

With the following lemma we can justify the definition of $\mathcal{C}^*$ given in (5.1.4).

Lemma 5.2.6. *Starting from $\widetilde{\mathcal{D}}$, the dynamics either passes through $\bar{\mathcal{D}}$ or it is not possible that a free particle is created without exceeding the energy level Γ^*.*

The proof of Lemmas 5.2.5 and 5.2.6 are analogue to those of Lemmas 4.2.5 and 4.2.6, respectively, in the weakly anisotropic case.

5.3 MODEL–DEPENDENT STRATEGY

Our goal is to characterize the union of all the minimal gates in the strongly anisotropic regime. To this end, we follow the model–dependent strategy carried out in Section 3.4 for the isotropic regime. In order to apply Propositions 3.1.3 and 3.1.5, we need to characterize the sets K and $\widetilde{K}$ (see (3.1.16) and (3.1.17) respectively for the definitions) for our model. This is done in Proposition 5.3.3. By Propositions 3.1.3 and 3.1.5, we obtain Corollary 5.3.4 that states that the saddles of the first and second types are respectively unessential. In Proposition 5.3.5 we highlight some of the saddles of type three that are unessential. This analysis is different when we are dealing with isotropic or weakly anisotropic interactions, and with strongly anisotropic interactions due to the different mechanisms to enter $\mathcal{C}^*$ (see [35, Proposition 2.3.7], Lemma 4.3.7 and Lemma 5.3.8, respectively). For the isotropic and weakly anisotropic cases this strategy is presented in Sections 3.4 and 4.3, respectively. Finally, we identify the essential saddles of the third type in Proposition 5.4.3.

5.3.1 *Main Propositions*

In this section, we give the main results for our model–dependent strategy. The next proposition shows that when the dynamics reaches $\mathcal{C}^G$ it has gone "over the hill", while when it reaches $\mathcal{C}^B$ the energy has to increase again to the level Γ^* to visit □ or ■. An analogue version for the isotropic case is proven in [35, Proposition 2.3.9] and for the weakly anisotropic case is proven in Proposition 4.3.1.

Proposition 5.3.1. *The following statements hold.*
(i) If $\eta \in \mathcal{C}^G$, then there exists a path $\omega : \eta \to \blacksquare$ such that $\max_{\zeta\in\omega} \widehat{H}(\zeta) < \Gamma^*$.
(ii) If $\eta \in \mathcal{C}^B$, then there are no $\omega : \eta \to \square$ or $\omega : \eta \to \blacksquare$ such that $\max_{\zeta\in\omega} \widehat{H}(\zeta) < \Gamma^*$.

Proof. The proof is analogue to that of Proposition 4.3.1 for the weakly anisotropic case by using the reference path for the nucleation constructed in [16, Section 3.2]. □

The next Proposition holds also in the isotropic and weakly anisotropic cases, see Propositions 3.4.2 and 4.3.2, respectively. We refer to Section 5.3.3 for the proof of Propositions 5.3.2, 5.3.3 and 5.3.5.

Proposition 5.3.2. $\mathcal{C}^* \subseteq \mathcal{G}(\square, \blacksquare)$.

Proposition 5.3.3. *The following statements hold.*
(i) $K = \emptyset$;
(ii) $\widetilde{K} \cap \partial \mathcal{C}_{\square}^{\blacksquare}(\Gamma^* - \widehat{H}(\blacksquare)) = \emptyset$.

For the corresponding result of Proposition 5.3.3 for isotropic and weakly anisotropic cases, we refer to Propositions 3.4.3 and 4.3.3, respectively.

Corollary 5.3.4. *The following statements hold.*
(i) The saddles of the first type $\sigma \in \partial \mathcal{C}^{\square}_{\blacksquare}(\Gamma^*) \cap (\mathcal{S}(\square,\blacksquare) \setminus \mathcal{C}^*)$ *are unessential;*
(ii) The saddles of the second type $\zeta \in \partial \mathcal{C}^{\blacksquare}_{\square}(\Gamma^* - \widehat{H}(\blacksquare)) \cap (\mathcal{S}(\square,\blacksquare) \setminus \mathcal{C}^*)$ *are unessential.*

Proof. Combining Propositions 3.1.3, 3.1.5 and 5.3.3 we get the claim. □

For the corresponding result of Corollary 5.3.4 for the isotropic and weakly anisotropic cases, we refer to Corollary 3.4.4 and Corollary 4.3.4, respectively.

Proposition 5.3.5. *Any saddle* ξ *that is neither in* $\mathcal{C}^*$, *nor in* $\bigcup_{k,\alpha,\alpha'} \mathcal{A}_k^{\alpha,\alpha'}$, *nor in the boundary of the cycles* $\mathcal{C}^{\square}_{\blacksquare}(\Gamma^*)$ *or* $\mathcal{C}^{\blacksquare}_{\square}(\Gamma^* - \widehat{H}(\blacksquare))$, *i.e.,* $\xi \in \mathcal{S}(\square,\blacksquare) \setminus (\partial \mathcal{C}^{\square}_{\blacksquare}(\Gamma^*) \cup \partial \mathcal{C}^{\blacksquare}_{\square}(\Gamma^* - \widehat{H}(\blacksquare)) \cup \mathcal{C}^* \cup \bigcup_{k,\alpha,\alpha'} \mathcal{A}_k^{\alpha,\alpha'})$, *such that* $\tau_\xi < \tau_{\mathcal{C}^B}$ *is unessential. Therefore it is not in* $\mathcal{G}(\square,\blacksquare)$.

For the corresponding result of Proposition 5.3.5 for the isotropic and weakly anisotropic cases, we refer to Propositions 3.4.5 and 4.3.5, respectively.

5.3.2 *Useful Lemmas for the model-dependent strategy*

In this Section we give some useful lemmas about the entrance in the gate and some properties of the sets $\mathcal{C}^*(i)$ with $i = 3, ..., L^*$. We stress that the behavior for the isotropic and weakly anisotropic cases is very different from that observed for the strongly anisotropic case, indeed we note that the weakly anisotropic model has some characteristics similar to the isotropic and some similar to the strongly anisotropic model. The next lemma generalizes [35, Proposition 2.3.8], proved for the isotropic case, following similar arguments. The proof of Lemma 5.3.6 is analogue to that of Lemma 4.3.6 for the weakly anisotropic case.

Lemma 5.3.6. *(i) Starting from* $\mathcal{C}^* \setminus \mathcal{Q}^{fp}$, *the only transitions that do not raise the energy are motions of the free particle in the region where the free particle is at lattice distance* $\geqslant 3$ *from the protocritical droplet.*
(ii) Starting from $\mathcal{Q}^{fp}$, *the only transitions that do not raise the energy are motions of the free particle in the region where the free particle is at lattice distance* $\geqslant 3$ *from the protocritical droplet and motions of the protuberance along the side of the rectangle where it is attached. When the lattice distance is 2, either the free particle can be attached to the protocritical droplet or the protuberance can be detached from the protocritical droplet and attached to the free particle, to form a rectangle plus a dimer. From the latter configuration the only transition that does not raise the energy is the reverse move.*
(iii) Starting from $\mathcal{C}^*$, *the only configurations that can be reached by a path that lowers the energy and does not decrease the particle number, are those where the free particle is attached to the protocritical droplet.*

Lemma 5.3.7. *The saddles in* $\mathcal{C}^*(2)$ *are essential.*

The proof of Lemma 5.3.7 is analogue to that of Lemmas 3.4.8 and 4.3.10 for the isotropic and weakly anisotropic cases, respectively. The next lemma investigates how the entrance in $\mathcal{C}^*$ occurs. We encourage the reader to inspect the difference between Lemma 5.3.8, [35, Proposition 2.3.7] and Lemma 4.3.7, indeed the entrance in the gate in the strongly anisotropic case is peculiar and different with respect the isotropic and weakly anisotropic ones. Recall (5.1.9) and (5.1.10).

Lemma 5.3.8. *Any* $\omega \in (\square \to \blacksquare)_{opt}$ *enters* $\mathcal{C}^*$ *in one of the following ways:*
(i) ω *passes first through* $\bar{\mathcal{Q}}$, *then possibly through* $\bar{\mathcal{D}} \setminus \bar{\mathcal{Q}}$, *and finally reaches* $\mathcal{C}^*$;
(ii) ω *passes through the configuration* $\mathcal{R}(2\ell_2^* - 1, \ell_2^* - 1)$, *then a free particle is created and moved towards the rectangle until it is attached to an horizontal side* $\alpha \in \{n, s\}$. *Then for some* $\alpha' \in \{w, e\}$ *the path* ω *passes through the sets* $\mathcal{A}_k^{\alpha,\alpha'}$ *for all* $k = 2, ..., \ell_2^*$, *and finally reaches* $\mathcal{C}^*(2)$.

Since in Lemma 5.3.8 we have proved that there are two possible ways to reach $\mathcal{C}^*(2)$, where the possibility (i) is analogue to the isotropic and weakly anisotropic cases, to find the minimal gates in the strongly anisotropic regime for any $i = 3, ..., L^*$ we need to consider $\mathcal{C}^*(i)$ union some particular saddles belonging to the paths described in (ii).

Lemma 5.3.9. *For any $i = 3, ..., L^*$ and $k = 2, ..., \ell_2^*$ the set $\mathcal{C}^*(i) \cup \bigcup_{\alpha,\alpha'} \{\xi_{j(k)}^{\alpha,\alpha'}\}$ is a minimal gate for all $1 \leqslant j(k) \leqslant k-1$, where $\{\xi_{j(k)}^{\alpha,\alpha'}\}$ are the elements in $\mathcal{A}_k^{\alpha,\alpha'}$ defined in (5.1.9) and (5.1.10).*

Remark 5.3.10. *We encourage the reader to inspect the difference between the statement of Lemma 5.3.9 and Lemmas 3.4.6 and 4.3.8: the sets $\mathcal{C}^*(i)$, with $i = 3, ..., L^*$, are minimal gates for the isotropic and weakly anisotropic regimes, while they are not minimal gates for the strongly anisotropic regime.*

Lemma 5.3.11. *For the strongly anisotropic interactions, we have*

$$\mathcal{C}^* \cup \bigcup_{k=2}^{\ell_2^*} \bigcup_{\alpha,\alpha'} \mathcal{A}_k^{\alpha,\alpha'} \subseteq \mathcal{G}(\square, \blacksquare). \tag{5.3.1}$$

5.3.3 *Proof of Propositions*

Proof of Proposition 5.3.2. The statement follows by Lemma 5.3.11. □

Proof of Proposition 5.3.3. (i) The proof is analogue to the one of Proposition 3.4.3(i).

(ii) Let $\bar{\eta} \in \widetilde{K} \cap \partial\mathcal{C}_{\square}^{\blacksquare}(\Gamma^* - \widehat{H}(\blacksquare))$. By the definition of the set $\widetilde{K}$ we know that there exist $\eta \in \mathcal{C}^*$ and $\omega = \omega_1 \circ \omega_2$ from η to $\blacksquare$ with the properties described in (3.1.17). We know that η is composed by the union of a protocritical droplet $\hat{\eta} \in \mathcal{D}$ and a free particle. Since $\omega_1 \cap \mathcal{C}^* = \{\eta\}$, we note that $\eta \in \mathcal{C}^*(2)$, otherwise the free particle has to cross at least $\bar{B}_2(\hat{\eta})$ and $\bar{B}_3(\hat{\eta})$, the latter in the configuration $\eta' \in \mathcal{C}^*$, with $\eta' \neq \eta$, which contradicts the conditions in (3.1.17). Therefore, starting from η, by the optimality of the path we deduce that the unique admissible move is to attach the free particle to the cluster. If $\bar{\eta}$ is obtained from η by attaching the free particle in a good site giving rise to a configuration in $\mathcal{C}^G(\hat{\eta})$, by Proposition 5.3.1(i) we know that $\omega_1 \cap \mathcal{C}_{\square}^{\blacksquare}(\Gamma^* - \widehat{H}(\blacksquare)) \neq \emptyset$, that contradicts (3.1.17), thus it is not possible to find such ω_1 and ω_2, therefore $\bar{\eta} \notin \widetilde{K}$, which is in contradiction with the assumption.

Assume now that $\bar{\eta}$ is obtained from η by attaching the free particle in a bad site giving rise to a configuration in $\mathcal{C}^B(\hat{\eta})$. If $\eta \in \mathcal{Q}^{fp}$, then by Lemma 5.3.6(ii) the unique admissible move is the reverse one, thus we may assume that $\eta \in \mathcal{C}^* \setminus \mathcal{Q}^{fp}$ and that the path does not go back to η, otherwise we can iterate this argument for a finite number of steps since the path has to reach $\blacksquare$. Starting from η, by Lemma 5.2.3 we know that $\bar{\eta}$ is obtained either via a sequence of 1-translations of a bar or via a sliding of a bar around a frame-angle. If a sequence of 1-translations takes place, by the optimality of the path we deduce that the unique possibility is either detaching the protuberance or sliding a bar around a frame-angle. In the first case the configuration that is obtained is in $\mathcal{C}^*$ and thus $\bar{\eta} \notin \widetilde{K}$, which contradicts the assumption. By (3.2.12), Proposition 5.2.1(b) (in particular conditions in (5.2.1)) and Lemma 5.2.5 we deduce that the only possibility to slide a bar around a frame-angle is that the bar is horizontal and it has length exactly $\ell_2^* - 1$. Thus, the configurations visited by the path ω during this sliding are $\bar{\eta}_1, ..., \bar{\eta}_m \in \mathcal{A}_k^{\alpha,\alpha'}$ for some $\alpha \in \{n, s\}$, $\alpha' \in \{w, e\}$ and $k = 2, ..., \ell_2^* - 1$, while the last configuration $\widetilde{\eta}$ obtained when the last particle of the bar is detached is composed by the union of $\mathcal{R}(2\ell_2^* - 1, \ell_2^* - 1)$ and a free particle (see the time–reversal of the path described in Figure 1.13, in particular $\bar{\eta}_m$ is the configuration (7) and $\widetilde{\eta}$ is the configuration (2)). Therefore $\widetilde{\eta}$ belongs to the set $\mathcal{B}$ defined in [16, eq. (3.29)] since $s(\widetilde{\eta}) = s^* - 1$ and $p_2(\widetilde{\eta}) = \ell_2^* - 1$. Thus, by [16, Theorem 3.7] we deduce that $\widetilde{\eta} \notin \mathcal{C}_{\square}^{\blacksquare}(\Gamma^* - \widehat{H}(\blacksquare))$ and therefore $\bar{\eta}_m \notin \partial\mathcal{C}_{\square}^{\blacksquare}(\Gamma^* - \widehat{H}(\blacksquare))$, that implies $\widetilde{K} \cap \partial\mathcal{C}_{\square}^{\blacksquare}(\Gamma^* - \widehat{H}(\blacksquare)) = \emptyset$. □

Proof of Proposition 5.3.5. The proof is analogue to that of Lemmas 3.4.5 and 4.3.5 in the isotropic and weakly anisotropic cases, respectively, but now we use Lemmas 5.3.6(ii) and 5.3.8 and, η as the union of a cluster $\hat{\eta} \in \mathcal{Q}$ and a free particle at distance 2 from the cluster. Moreover, ξ_i is the union of a rectangle $(2\ell_2^* - 3) \times \ell_2^*$ with an horizontal dimer. □

5.3.4 *Proof of Lemmas*

Proof of Lemma 5.3.8. By Theorem 5.1.1 we know that any $\omega \in (\square \to \blacksquare)_{opt}$ passes through $\mathcal{C}^*$. We denote by η this configuration, that is composed by the union of a protocritical droplet $\hat{\eta} \in \bar{\mathcal{D}}$ and a free particle in the site x. Note that there exists $i = 2, ..., L^*$ such that either $x \in B_i(\hat{\eta})$ if $d(\partial^- \Lambda_4, \hat{\eta}) > i$ or $x \in \bar{B}_i(\hat{\eta})$ if $d(\partial^- \Lambda_4, \hat{\eta}) \leqslant i$. We set $\omega = (\square, \omega_1, ..., \omega_k, \eta) \circ \bar{\omega}$, where $\bar{\omega}$ is a path that connects η to $\blacksquare$ such that $\max_{\sigma \in \omega} \widehat{H}(\sigma) \leqslant \Gamma^*$. In order to analyze the entrance in $\mathcal{C}^*$ we consider the time–reversal of the path ω. Since $\widehat{H}(\eta) = \Gamma^*$, the move from η to ω_k must have a non–positive cost and thus the unique admissible moves are:

(i) either moving the free particle at zero cost;
(ii) or removing a free particle at cost $-\Delta$;
(iii) or attaching the free particle at cost $-U_1$ (resp. $-U_2$) or $-U_1 - U_2$.

Case (i). In this case we obtain that the configuration ω_k is still in $\mathcal{C}^*$, thus it is analogue to η and therefore we can iterate the argument by taking this configuration as η.
Case (ii). In this case $\widehat{H}(\omega_k) = \Gamma^* - \Delta$ and $\omega_k \in \bar{\mathcal{D}}$. If $\omega_k \in \bar{\Omega}$ we get the claim, thus in the sequel we assume that $\omega_k \in \bar{\mathcal{D}} \setminus \bar{\Omega}$. Since the path ω starts from $\square$, there exist $k_1 < k_2 < k$ such that $|\omega_{k_1}| = |\omega_k| - 1$ and there is a free particle in ω_{k_2}, i.e., $n(\omega_{k_2}) = 1$. Starting from ω_k and considering the time–reversal of the path ω, in order to obtain a free particle in ω_{k_2} we note that the minimal cost for detaching a particle is $U_1 + U_2$ giving rise to the energy value greater or equal than $\Gamma^* - \Delta + U_1 + U_2 > \Gamma^*$, which is in contradiction with the optimality of the path. Thus, the unique possibility is detaching the protuberance from a configuration in $\bar{\Omega}$ at cost U_1. This implies that ω_k is obtained via a U_1–path starting from a configuration in $\bar{\Omega}$.
Case (iii). First, we consider the case where from η, again considering the time–reversal, we attach a particle at cost $-U_1$ giving rise to the configuration ω_k, i.e., $\widehat{H}(\omega_k) = \Gamma^* - U_1$. Since the path ω starts from $\square$, there exists $k_1 < k$ such that $|\omega_{k_1}| = |\omega_k| - 1$, that implies that there exists a configuration $\omega_{\bar{k}}$ with a free particle during the transition from ω_{k_1} to ω_k (see Figure 1.13 where ω_k is configuration (12) and $\omega_{\bar{k}}$ is configuration (2)). If $\omega_{\bar{k}} \in \mathcal{C}^*$, we can iterate the argument by taking this configuration as η. Otherwise, if $\omega_{\bar{k}} \notin \mathcal{C}^*$, we deduce that $(\omega_{\bar{k}})_{cl} \notin \bar{\mathcal{D}}$. Starting from $\omega_{\bar{k}}$, since the activation of a sequence of 1-translations of bars of configurations in $\bar{\mathcal{D}}$ gives rise to configurations that are in $\bar{\mathcal{D}}$, the unique possibility in order not to exceed Γ^* is that ω_k is obtained from $\omega_{\bar{k}}$ via a sliding of a bar, say $B^{\alpha'}(\omega_k)$, around a frame-angle, say $c^{\alpha' \alpha}(\omega_k)$. In order to do that, by (3.2.12) and Proposition 5.2.1(b), we deduce that the unique possibility to match the two conditions in (5.2.1) is that during the transition the path ω crosses $\mathcal{S}(\square, \blacksquare)$ through the sets $\mathcal{A}_k^{\alpha,\alpha'}$ for any $k = 2, ..., \ell_2^*$, with $\alpha \in \{n, s\}$, $\alpha' \in \{w, e\}$. In Figure 1.13 we represent this transition with $\alpha = n$, $\alpha' = e$ and the configurations (11)–(3) for the sliding. At the end of this sliding we obtain the configuration $\mathcal{R}(2\ell_2^* - 1, \ell_2^* - 1)$ union a free particle. This configuration must be obtained from $\mathcal{R}(2\ell_2^* - 1, \ell_2^* - 1)$ via adding a free particle, otherwise the path ω is not optimal.

Second, we consider the case where from η we attach a particle at cost $-U_2$ giving rise to the configuration ω_k, i.e., $\widehat{H}(\omega_k) = \Gamma^* - U_2$. We argue in a similar way as above, but the difference is that in this case the sliding of a bar around a frame-angle at cost U_2 is not allowed by Lemma 5.2.5.

Third, we consider the case where from η we attach a particle at cost $-U_1 - U_2$ giving rise to the configuration ω_k, i.e., $\widehat{H}(\omega_k) = \Gamma^* - U_1 - U_2$. Since $\eta_{cl} \in \bar{\mathcal{D}}$, the unique possibility is that $\omega_k \in \mathcal{C}^G(\hat{\eta})$, therefore by Lemma 5.3.1(i) we get $\omega_k \in \mathcal{C}^{\blacksquare}_{\square}(\Gamma^* - \widehat{H}(\blacksquare))$. Since by Theorem 5.1.1 we know that $\mathcal{C}^*$ is a gate for the transition, we deduce that there exists $k_1 < k$ such that $\omega_{k_1} \in \mathcal{C}^*$. Thus, we can iterate the argument by taking this configuration as η. □

Proof of Lemma 5.3.9. Let $i \in \{3, ..., L^*\}$, $k \in \{1, ..., n\}$ and $1 \leqslant j(k) \leqslant k - 1$.

First, we prove that $\mathcal{C}^*(i) \cup \bigcup_{\alpha,\alpha'} \{\xi^{\alpha,\alpha'}_{j(k)}\}$ is a gate. By Theorem 5.1.1 we know that any $\omega \in (\square \to \blacksquare)_{opt}$ crosses $\mathcal{C}^*$. If the path ω enters $\mathcal{C}^*$ without crossing the set $\mathcal{P}'_0$, then by Lemma 5.3.8(i) we know that ω has to pass through $\mathcal{C}^*(i)$. If the path ω enters $\mathcal{C}^*$ after crossing the set $\mathcal{P}'_0$, then by Lemma 5.3.8(ii) we know that $\omega \cap \bigcup_{\alpha,\alpha'} \{\xi^{\alpha,\alpha'}_{j(k)}\} \neq \emptyset$.

Now we prove that $\mathcal{C}^*(i) \cup \bigcup_{\alpha,\alpha'} \{\xi^{\alpha,\alpha'}_{j(k)}\}$ is a minimal gate by showing that for any $\eta \in \mathcal{C}^*(i) \cup \bigcup_{\alpha,\alpha'} \{\xi^{\alpha,\alpha'}_{j(k)}\}$ the set $(\mathcal{C}^*(i) \cup \bigcup_{\alpha,\alpha'} \{\xi^{\alpha,\alpha'}_{j(k)}\}) \setminus \{\eta\}$ is not a gate: there exists $\omega \in$

$(\square \to \blacksquare)_{opt}$ such that $\omega \cap ((\mathcal{C}^*(i) \cup \bigcup_{\alpha,\alpha'}\{\xi^{\alpha,\alpha'}_{j(k)}\}) \setminus \{\eta\}) = \emptyset$. We consider separately the cases $\eta \in \bigcup_{\alpha,\alpha'}\{\xi^{\alpha,\alpha'}_{j(k)}\}$ and $\eta \in \mathcal{C}^*(i)$.

Case 1. Let $\eta \in \bigcup_{\alpha,\alpha'}\{\xi^{\alpha,\alpha'}_{j(k)}\}$, thus $\eta = \xi^{\bar\alpha,\bar\alpha'}_{j(k)}$ for some $\bar\alpha \in \{n, s\}$ and $\bar\alpha' \in \{w, e\}$. We can define ω as the reference path defined in [16, Section 3.2] that crosses the configurations $\xi^{\bar\alpha,\bar\alpha'}_1$,...,$\xi^{\bar\alpha,\bar\alpha'}_{k-1}$, then it enters $\mathcal{C}^*(2)$ and finally the free particle is attached in a good site without passing through $\mathcal{C}^*(i)$ with $i = 3, ..., L^*$ (see Figure 1.13). From this configuration, the path proceeds towards $\blacksquare$ as the one in Proposition 5.3.1(i). The constructed ω is optimal and $\omega \cap \bigcup_{\alpha,\alpha'}\{\xi^{\alpha,\alpha'}_{j(k)}\} = \{\xi^{\bar\alpha,\bar\alpha'}_{j(k)}\}$, thus this case is concluded.

Case 2. Let $\eta \in \mathcal{C}^*(i)$. We take an arbitrary path starting from $\square$ and that enters $\mathcal{C}^*(i)$ in $\eta = (\hat\eta, z)$, where $\hat\eta \in \bar{\mathcal{D}}$ is the protocritical droplet and z is the position of the free particle at distance i from the cluster. Then the path proceeds by moving the free particle from z to $\hat\eta$ such that the distance between the free particle and $\hat\eta$ at the first step is strictly decreasing, and at the later steps is not increasing. Finally the free particle is attached in a good site $x \in \partial^- CR(\hat\eta)$ giving rise to a configuration in $\mathcal{C}^G(\hat\eta)$. From this configuration, the path proceeds towards $\blacksquare$ as the one in Proposition 5.3.1(i). Since the constructed $\omega \in (\square \to \blacksquare)_{opt}$ and $\omega \cap \mathcal{C}^*(i) = \{\eta\}$, the proof is completed. □

Proof of Lemma 5.3.11. By Lemma 5.3.7 we know that the saddles in $\mathcal{C}^*(2)$ are essential and thus are in the set $\mathcal{G}(\square, \blacksquare)$ due to [85, Theorem 5.1]. Furthermore, by Lemma 5.3.9 we know that $\mathcal{C}^*(i) \cup \bigcup_{\alpha,\alpha'}\{\xi^{\alpha,\alpha'}_{j(k)}\}$ is a minimal gate for any $i = 3, ..., L^*$ and $j(k) = 1, ..., k-1$, with $k = 2, ..., \ell^*_2$. Therefore we get

$$\mathcal{G}(\square, \blacksquare) \supseteq \mathcal{C}^*(2) \cup \bigcup_{i=3}^{L^*} \bigcup_{k=2}^{\ell^*_2} \bigcup_{j(k),\alpha,\alpha'} (\mathcal{C}^*(i) \cup \{\xi^{\alpha,\alpha'}_{j(k)}\}) = \mathcal{C}^* \cup \bigcup_{k=2}^{\ell^*_2} \bigcup_{\alpha,\alpha'} \mathcal{A}^{\alpha,\alpha'}_k. \tag{5.3.2}$$

□

5.4 PROOF OF THE MAIN RESULTS: STRONGLY ANISOTROPIC CASE

In this Section we give the proof of the main Theorems 5.1.1 and 5.1.3, see Sections 5.4.1 and 5.4.2, respectively.

5.4.1 *Proof of the main Theorem 5.1.1*

In this section we give the proof of the main Theorem 5.1.1. Now we recall the definition of the set $\mathcal{P}_2$ given in [16] as

$$\begin{aligned}\mathcal{P}_2 := \{\eta \quad : n(\eta) = 1,\, \nu(\eta) = \ell^*_2 - 1,\, \eta_{cl} \text{ is connected, monotone,} \\ \text{with circumscribed rectangle in } \mathcal{R}(2\ell^*_2 - 2, \ell^*_2)\}.\end{aligned} \tag{5.4.1}$$

In particular, in order to state that the set $\mathcal{C}^*$ is a gate for the transition from $\square$ to $\blacksquare$, we need the following

Lemma 5.4.1. *If $\omega \in (\square \to \blacksquare)_{opt}$ is such that $\omega \cap \mathcal{P}_2$, then $\omega \cap \mathcal{C}^* \neq \emptyset$.*

We postpone the proof of Lemma 5.4.1 after the proof of the main Theorem 5.1.1.

Proposition 5.4.2. *If $\omega \in (\square \to \blacksquare)_{opt}$ is such that $\omega \cap \mathcal{P}'_0 \neq \emptyset$, then $\omega \cap \mathcal{C}^* \neq \emptyset$.*

We postpone the proof of Proposition 5.4.2 after the proof of Lemma 5.4.1.

Proof of the main Theorem 5.1.1. By [16, Theorem 2.4] taking $\mathcal{P}_1 = \mathcal{P}'_0$, we know that the set $\mathcal{P}'_0 \cup \mathcal{P}_2$ is a gate for the transition from $\square$ to $\blacksquare$. By Lemma 5.4.1 we know that every $\omega \in (\square \to \blacksquare)_{opt}$ that crosses $\mathcal{P}_2$ then crosses $\mathcal{C}^*$, thus we deduce that the set $\mathcal{P}'_0 \cup \mathcal{C}^*$ is a gate. Furthermore, by Proposition 5.4.2 we obtain that every path $\omega \in (\square \to \blacksquare)_{opt}$ that crosses $\mathcal{P}'_0$ then crosses also $\mathcal{C}^*$. This implies that every optimal path ω from $\square$ to $\blacksquare$ is such that $\omega \cap \mathcal{C}^* \neq \emptyset$, thus $\mathcal{C}^*_{sa}$ is a gate. □

Proof of Lemma 5.4.1. Consider $\omega \in (\square \to \blacksquare)_{opt}$. If $\omega \cap \mathcal{C}^* \neq \emptyset$, we get the claim. Thus, we can reduce our analysis to the case in which the path ω reaches the set $\mathcal{P}_2$ in a configuration $\eta \in \mathcal{P}_2 \setminus \mathcal{C}^*$. We set $\omega = (\square, \omega_1, ..., \omega_k, \eta) \circ \bar{\omega}$, where $\bar{\omega}$ is a path that connects η to $\blacksquare$ such that $\max_{\sigma\in\omega} \widehat{H}(\sigma) \leqslant \Gamma^*$. We are interested in the time–reversal of the path. Since $\eta \in \mathcal{P}_2 \setminus \mathcal{C}^*$, we know that it is composed by the union of a cluster $CR^-(\eta) = \mathcal{R}(2\ell_2^* - 4, \ell_2^* - 2)$, such that at least one frame-angle of $CR^-(\eta)$ is empty, a free particle and four bars attached to the four sides of $CR^-(\eta)$ in such a way that η contains $n_c + 1$ particles (see (5.1.3) for the precise value of n_c). For the entire proof we refer to Figure 4.3, where for the strongly anisotropic regime the horizontal and vertical lengths have to be changed to $2\ell_2^* - 2$ and l_2^*, respectively. Suppose that $CR^-(\eta)$ contains x empty frame-angles, with $1 \leqslant x \leqslant 4$. See Figure 4.3(a) to visualize the configuration η in the case $x = 1$. Since $\widehat{H}(\eta) = \Gamma^*$, the move from η to ω_k must have a non-positive cost and thus the unique admissible moves are:

(i) either moving the free particle at zero cost;

(ii) or removing the free particle;

(iii) or attaching the free particle at cost $-U_1$ (see Figure 4.3(b)) or $-U_2$, or $-U_1 - U_2$.

Case (i). In this case the configuration ω_k is analogue to η and therefore we can iterate this argument by taking this configuration as η.

Case (ii). In this case $\widehat{H}(\omega_k) = \Gamma^* - \Delta$. We may assume that the configuration ω_{k-1} is not obtained by ω_k via adding a free particle, otherwise ω_{k-1} is analogue to η and thus we can iterate the argument by taking this configuration as η. By the optimality of the path, again considering the time-reversal, we deduce that the unique admissible move to obtain ω_{k-1} from ω_k is breaking a horizontal (resp. vertical) bar at cost U_1 (resp. U_2). Thus, it is possible that either a sequence of 1-translations of a bar or a sliding of a bar around a frame-angle takes place. In the first case, we obtain a configuration that is analogue to ω_{k-1} and thus we can iterate the argument for a finite number of steps, since the path has to reach $\square$. In the latter case, by Remark 5.2.2(ii) we deduce that the condition (3.2.12) is not satisfied and therefore it is not possible to complete any sliding of a bar around a frame-angle. This implies that the unique admissible moves are the reverse ones, thus we obtain a configuration that is analogue to ω_{k-1} and therefore we can iterate the argument for a finite number of steps, since the path has to reach $\square$. In this way we can reduce ourselves to consider case (iii).

Case (iii). (a) We consider the case where from η, again considering the time-reversal, we attach a particle at cost $-U_1$ in $\partial^+CR(\eta)$ giving rise to the configuration ω_k, i.e., $\widehat{H}(\omega_k) = \Gamma^* - U_1$ (see Figure 4.3(b)). Thus, it is possible that either a sequence of 1-translations of a bar or a sliding of a bar around a frame-angle takes place. In the first case, we obtain a configuration that is analogue to ω_k and thus we can iterate the argument for a finite number of steps, since the path has to reach $\square$. In the latter case, by Remark 5.2.2(ii) we deduce that the condition (3.2.12) is not satisfied and therefore it is not possible to complete any sliding of a bar around a frame-angle. This implies that the unique admissible moves are the reverse ones, thus we obtain a configuration that is analogue to ω_k and therefore we can iterate the argument for a finite number of steps, since the path has to reach $\square$.

(b) We consider the case where from η, again considering the time-reversal, we attach a particle at cost $-U_2$ in $\partial^+CR(\eta)$ giving rise to the configuration ω_k, i.e., $\widehat{H}(\omega_k) = \Gamma^* - U_2$. We argue in a similar way as above.

(c) We consider the case where from η, again considering the time-reversal, we attach a particle at cost $-U_1 - U_2$ in $\partial^-CR(\eta)$ giving rise to the configuration ω_k, i.e., $\widehat{H}(\omega_k) = \Gamma^* - U_1 - U_2$. Thus, it is possible either to have a sequence of 1-translations of a bar, or to have a sliding of a bar around a frame-angle, or to detach a particle at cost $U_1 + U_2$. In the first two possibilities, analogously to what has been discussed previously in (a) and (b), the unique admissible moves are the reverse ones and therefore we conclude as above. In the latter possibility, we have that either ω_{k-1} is obtained from ω_k by detaching a particle from a bar at cost $U_1 + U_2$ or from a corner of η that is in $CR^-(\eta)$. In the first case, the particle can be attached to an empty frame-angle of $CR^-(\eta)$ and we can repeat these steps at most $x - 1$ times (if $x \geqslant 2$), that implies that there exists $\bar{k} < k - 1$ such that $\omega_{\bar{k}}$ is composed by the union of a free particle and a rectangle $\mathcal{R}(2\ell_2^* - 4, \ell_2^* - 2)$ with four bars attached to its four sides in such a way that $\omega_{\bar{k}}$ contains $n_c + 1$ particles, namely, $\omega_{\bar{k}} \in \mathcal{C}^*$. In the second case, we may assume that the detached particle is attached to a bar in $\partial^-CR(\eta)$ giving rise to a configuration η' (see Figure 4.3(c)), otherwise we obtain a configuration that is analogue to

η. Starting from η', similarly we obtain η'' (see Figure 4.3(d)) if η' has a corner in $CR^-(\eta')$. If this is the case, we can proceed in a similar way until we obtain a configuration η''' that has no corner in $CR^-(\eta''')$. Starting from η''', by the optimality of the path we deduce that the unique admissible moves are the reverse ones and therefore the path goes back to η. This concludes the proof. □

Proof of Proposition 5.4.2. Consider any $\omega \in (\square \to \blacksquare)_{opt}$ such that $\omega \cap \mathcal{P}'_0 \neq \emptyset$. We consider separately the following three cases.

Case (i). Assume that the path ω crosses the set $\mathcal{A} := \bigcup_{\alpha,\alpha',k} \mathcal{A}_k^{\alpha,\alpha'}$, with $\alpha \in \{n, s\}$, $\alpha' \in \{w, e\}$ and $k = 2, ..., \ell_2^*$, in the configuration η. Since $\widehat{H}(\eta) = \Gamma^*$, as long as the energy does not exceed Γ^*, it is impossible to create a free particle before further lowering the energy by a quantity greater or equal than $U_1 + U_2$. Since $g_2'(\eta) = 1$, it is possible to connect at cost $-U_1$ the two protuberances or a bar and a protuberance. Moreover, there is no admissible move that costs $-U_2$, since $g_1'(\eta) = 0$ and there is no free particle that could been attached to an horizontal side of the cluster. Thus, the only admissible moves are starting a sliding of a bar around a frame-angle $c^{\alpha\alpha'}(\eta)$ or $c^{\alpha'\alpha}(\eta)$, with $\alpha \in \{n, s\}$, $\alpha' \in \{w, e\}$, at cost less or equal than U_1. We consider separately these two possibilities, that correspond to the two different directions to cross the path described in Figure 1.13 starting from the configuration η. More precisely, one of these possibilities (that we will analyze in (iA)), gives rise to the configuration (12), while the other (that will be treated in (iB)) corresponds to the time-reversal of the path described in Figure 1.13 starting from the configuration η.

(iA). In this situation it is possible to obtain one or more saddles $\xi_1, ..., \xi_{n-1}$ such that $\xi_i \in \mathcal{A}$ for all $i = 1, ..., n-1$ and for the last configuration we have $|r^{\alpha'}(\xi_{n-1}) \cup c^{\alpha\alpha'}(\xi_{n-1})| = 1$, with $\alpha \in \{n, s\}$, $\alpha' \in \{w, e\}$ and $g_2'(\xi_{n-1}) = 1$ (see configuration (12) in Figure 1.13). From this configuration, since $\widehat{H}(\xi_{n-1}) = \Gamma^*$, by the optimality of the path ω it is impossible to detach the protuberance before lowering the energy. Thus, the unique admissible moves are either the reverse move or connect the protuberance and the bar at cost $-U_1$ and then detach the protuberance at cost U_1 (see the move starting from the configuration (12) in Figure 1.13 that is described with a dashed arrow). In the latter situation the path reaches a configuration $\xi_n \in \mathcal{C}^*$. Thus, we have to consider the possibilities that ω visits ξ_n and ω does not visit ξ_n. In the first possibility, since ω passes through $\xi_n \in \mathcal{C}^*$ we get the claim. In the latter possibility, the path ω does not pass through the configuration ξ_n, but assume that the path ω visits the saddles $\xi_i, ..., \xi_j$ for some $1 \leqslant i \leqslant j \leqslant n-1$. We set

$$\omega = (\square, \omega_1, ..., \omega_k, \xi_i, \zeta_i, .., \zeta_h, \xi_{i+1}, \zeta_{h+1}, ..., \zeta_{h+m}, ..., \xi_j) \circ \bar{\omega},$$

where $\zeta_i, ..., \zeta_h$ are not saddles, but are crossed during the sliding of a bar around a frame-angle connecting ξ_i to ξ_{i+1} and so on. Moreover, $\bar{\omega}$ is a path that connects ξ_j to $\blacksquare$ such that $\max_{\sigma\in\omega} \widehat{H}(\sigma) \leqslant \Gamma^*$. Note that the configuration ξ_j coincides with ξ_{i+1} in the case $j = i+1$. If $i = j$, we set

$$\omega = (\square, \omega_1, ..., \omega_k, \xi_i) \circ \bar{\omega},$$

where $\bar{\omega}$ is a path that connects ξ_i to $\blacksquare$ such that $\max_{\sigma\in\omega} \widehat{H}(\sigma) \leqslant \Gamma^*$. To prove our statement we investigate the structure of the path ω before entering $\mathcal{A}$, namely, we consider the time–reversal of the path. Since $\xi_i \in \mathcal{A}$ that implies $\widehat{H}(\xi_i) = \Gamma^*$, we note that the move from ξ_i to ω_k must have a non–positive cost. Thus, the admissible transitions from ξ_i to ω_k are either moving the particle at zero cost or moving a particle at cost $-U_1$. In the first case, we obtain a configuration that is analogue to ξ_i and therefore we can iterate for a finite number of steps this argument until we get the situation described in the latter case. In the latter case $\widehat{H}(\omega_k) = \Gamma^* - U_1$, thus ω_{k-1} can be obtained from ω_k by breaking a bar at cost U_1 or U_2, since it is not possible to detach any particle because its cost is at least $U_1 + U_2$. If the cost is U_1, we deduce that ω_{k-1} is analogue to the initial configuration ξ_i and thus we can iterate this argument for a finite number of steps, because the path has to reach $\square$. If the cost is U_2, we can iterate this argument to deduce that starting from ω_k a sliding of a bar around a frame-angle takes place (see the time–reversal of the path described in Figure 1.13, where ω_{k-1} can be, for example, the configuration (9)). Since the path has to reach $\square$, this implies that there exists $k_1 < k$ such that ω_{k_1} is composed by the union of a

rectangle $\mathcal{R}(2\ell_2^*-1,\ell_2^*-1)$ and a protuberance attached to one of the longest sides. Note that $\widehat{H}(\omega_{k_1})=\Gamma^*-U_1$. Furthermore, since either moving the protuberance along the side or detaching it from the cluster are the only admissible moves with $\max_{\sigma\in\omega}\widehat{H}(\sigma)\leqslant\Gamma^*$, we note that there exists $k_2<k_1$ such that the configuration ω_{k_2} is composed by the union of $\mathcal{R}(2\ell_2^*-1,\ell_2^*-1)$ and a free particle. Note that ω_{k_2} belongs to the set $\mathcal{B}$ defined in [16, Definition 3.5] because $p_2(\omega_{k_2})=\ell_2^*-1$. Thus, by [16, Theorem 3.7] we know that ω reaches a configuration in $\mathcal{P}_2$. We get the claim by using Lemma 5.4.1.

(iB). Note that this situation can be treated as in (iA) for the case in which ω does not visit ξ_n, indeed without loss of generality we may assume that $\eta=\xi_i$ and then we proceed as above.

Case (ii). Assume that ω crosses the set $\mathcal{A}_0^{\alpha'}\cup\mathcal{A}_1^{\alpha}$ in the configuration η, with $\alpha\in\{n,s\}$ and $\alpha'\in\{w,e\}$. By Lemma 5.2.4 we know that η has been obtained from a configuration $\eta^B\in\mathcal{C}^B$, thus there exists a configuration $\bar\eta\in\mathcal{C}^*$ such that ω passes through $\bar\eta$ before crossing η^B.

Case (iii). Assume that ω crosses the set $\mathcal{P}_0'\setminus(\bigcup_{\alpha,\alpha',k}\mathcal{A}_k^{\alpha,\alpha'}\cup\bigcup_{\alpha'}\mathcal{A}_0^{\alpha'}\cup\bigcup_{\alpha}\mathcal{A}_1^{\alpha})$ in the configuration η, thus the path ω crosses either $\eta^B\in\mathcal{C}^B$ or $\eta^G\in\mathcal{C}^G$ before passing through η. In the first case, η is obtained either via a 1-translation of a bar or via a sliding of a bar around a frame-angle that in both cases cannot be completed because η is not in $\bigcup_{\alpha,\alpha',k}\mathcal{A}_k^{\alpha,\alpha'}\cup\bigcup_{\alpha'}\mathcal{A}_0^{\alpha'}\cup\bigcup_{\alpha}\mathcal{A}_1^{\alpha}$. Therefore the path ω, before crossing η^B, passes through a configuration $\bar\eta\in\mathcal{C}^*$. In the latter case, we argue similarly. This concludes the proof. □

5.4.2 *Proof of the main Theorem 5.1.3*

In this section we analyze the geometry of the set $\mathcal{G}(\square,\blacksquare)$ (recall (3.1.13)). In particular, we give the proof of the main Theorem 5.1.3 by giving in Proposition 5.4.3 the geometric characterization of the essential saddles of the third type that are not in $\mathcal{C}^*$ and that are visited after crossing the set $\mathcal{C}^B$.

Proposition 5.4.3. *Any saddle ξ that is neither in $\mathcal{C}^*$, nor in the boundary of the cycles $\mathcal{C}^{\square}_{\blacksquare}(\Gamma^*)$ nor $\mathcal{C}^{\blacksquare}_{\square}(\Gamma^*-\widehat{H}(\blacksquare))$ such that $\tau_\xi\geqslant\tau_{\mathcal{C}^B}$ can be essential or not. For those essential we obtain the following description:*

$$\mathcal{G}(\square,\blacksquare)\cap(\mathcal{S}(\square,\blacksquare)\setminus(\partial\mathcal{C}^{\square}_{\blacksquare}(\Gamma^*)\cup\partial\mathcal{C}^{\blacksquare}_{\square}(\Gamma^*-\widehat{H}(\blacksquare))\cup\mathcal{C}^*))=\bigcup_{\alpha}\bigcup_{\alpha'}\bigcup_{k=2}^{\ell_2^*}\mathcal{A}_k^{\alpha,\alpha'}\cup\bigcup_{\alpha'}\mathcal{A}_0^{\alpha'}\cup\bigcup_{\alpha}\mathcal{A}_1^{\alpha}. \tag{5.4.2}$$

Remark 5.4.4. *In Proposition 5.3.5 we have proved that the saddles ξ of type three that are not in $\bigcup_{k,\alpha,\alpha'}\mathcal{A}_k^{\alpha,\alpha'}$ and such that $\tau_\xi<\tau_{\mathcal{C}^B}$ are unessential. Note that we have not to study separately the essentiality of the saddles $\xi\in\bigcup_{k,\alpha,\alpha'}\mathcal{A}_k^{\alpha,\alpha'}$, since $\bigcup_{k,\alpha,\alpha'}\mathcal{A}_k^{\alpha,\alpha'}$ is included in the essential saddles ξ of type three such that $\tau_\xi\geqslant\tau_{\mathcal{C}^B}$, analyzed in Proposition 5.4.3.*

We postpone the proof of Proposition 5.4.3 after the proof of the main Theorem 5.1.3.

Proof of Theorem 5.1.3. By Corollary 5.3.4 we know that the saddles of the first and second type, defined in Definitions 3.1.2 and 3.1.4, respectively, are unessential. By Propositions 5.3.5 and 5.4.3 we have the characterization of the essential saddles of the third type. We use Proposition 5.3.2 to get the claim. □

Proof of Proposition 5.4.3. Consider a configuration $\eta\in\mathcal{C}^*(2)$ such that $\eta=(\hat\eta,x)$, with $\hat\eta\in\bar{\mathcal{D}}$ and $d(\hat\eta,x)=2$. By Proposition 5.2.1(b), note that $\hat\eta$ consists of an $(2\ell_2^*-4)\times(\ell_2^*-2)$ rectangle with four bars $B^\alpha(\eta)$, with $\alpha\in\{n,s,w,e\}$, attached to its four sides satisfying

$$1\leqslant|B^w(\eta)|,|B^e(\eta)|\leqslant\ell_2^*,\qquad \ell_2^*-1\leqslant|B^n(\eta)|,|B^s(\eta)|\leqslant2\ell_2^*-2, \tag{5.4.3}$$

and

$$\sum_{\alpha}|B^\alpha(\eta)|-k=5\ell_2^*-7, \tag{5.4.4}$$

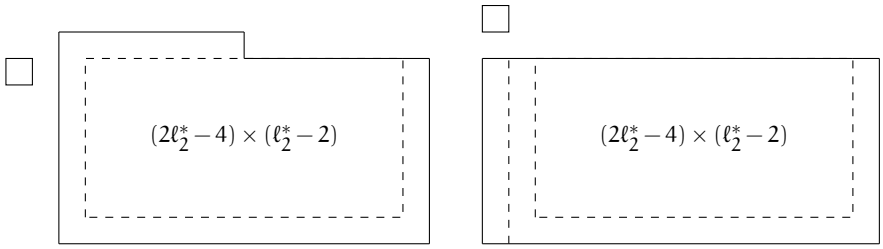

Figure 5.2 – Case A: on the left-hand side we represent a possible starting configuration $\eta \in \mathcal{C}^*$ and on the right-hand side the configuration η' obtained from η after the sliding of the bar $B^n(\eta)$ around the frame-angle $c^{nw}(\eta')$.

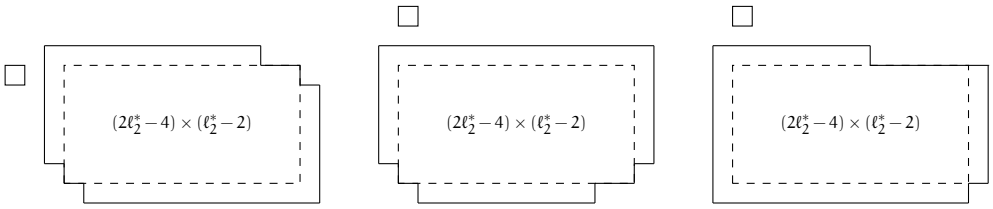

Figure 5.3 – Case B(i): in (a) we depict a possible starting configuration $\eta \in \mathcal{C}^*$. Case B(ii): in (b) we depict a possible starting configuration $\eta \in \mathcal{C}^*$. Case B(iii): in (c) we depict a possible starting configuration $\eta \in \mathcal{C}^*$.

with $k = \sum_{\alpha\alpha' \in \{nw,ne,sw,se\}} |c^{\alpha\alpha'}(\eta)|$. Assume that the free particle is attached in a bad site obtaining a configuration $\eta' \in \mathcal{C}^B$. Due to [85, Theorem 5.1], our strategy consists in characterizing the essential saddles that could be visited after attaching the free particle in a bad site. By Remark 5.2.2(i) we consider separately the following cases:

A. three frame-angles of $CR(\hat{\eta})$ are occupied;
B. two frame-angles of $CR(\hat{\eta})$ are occupied;
C. one frame-angle of $CR(\hat{\eta})$ is occupied;
D. no frame-angle of $CR(\hat{\eta})$ is occupied.

Note that from case A one can go to the other cases and viceversa, but since the path has to reach $\blacksquare$ this back and forth must end in a finite number of steps.

Case A. Without loss of generality we consider η as in Figure 5.2 on the left-hand side. If we are considering the case in which a sequence of 1-translations of a bar is possible and takes place, then by Lemma 5.2.4 the saddles that are crossed are essential and in $\mathcal{A}_0^{\alpha'} \cup \mathcal{A}_1^{\alpha}$. If a sequence of 1-translations of a bar takes place in such a way that the last configuration has at most two occupied frame-angles, then the saddles that are visited starting from it will be analyzed in cases B, C and D. Thus, we are left to analyze the case in which there is the activation of a sliding of a bar around a frame-angle. In the following we quickly exclude the cases in which the particles is attached to $B^n(\eta)$, $B^s(\eta)$ or $B^e(\eta)$ and then explain the more interesting case in which it is attached to $B^w(\eta)$ giving rise to Figure 5.2 on the right-hand side. If the free particle is attached to the bar $B^n(\eta)$ (resp. $B^s(\eta)$), by Lemma 5.2.5 we know that it is not possible to complete the sliding of the bar $B^w(\eta)$ (resp. $B^e(\eta)$) around the frame-angle $c^{wn}(\eta')$ (resp. $c^{es}(\eta')$). If the free particle is attached to the bar $B^e(\eta)$ or $B^w(\eta)$, then it is not possible to slide the bar $B^s(\eta)$ around the frame-angle $c^{se}(\eta')$ or $c^{sw}(\eta')$, respectively, since (3.2.12) is not satisifed. In the last two cases by Lemma 5.2.3(ii) we know that the saddles that are visited are unessential. This implies that the unique possibility to activate and complete a sliding of a bar around a frame-angle is attaching the free particle to the bar $B^w(\eta)$, then sliding the bar $B^n(\eta)$ around the frame-angle $c^{nw}(\eta')$ when $|B^n(\eta)| = \ell_2^* - 1$ and $|B^w(\eta)| = \ell_2^*$, otherwise (3.2.12) is not satisifed. The saddles that are possibly visited by the path we described are in $\mathcal{A}_{k,k'}^{\alpha,\alpha'}$ except the last one, thus by Lemma 5.2.3(i) they are essential. The last configuration visited during this sliding of a bar is depicted in Figure 5.2 on the right-hand side. This configuration has energy $\Gamma^* - U_1 + U_2$ and therefore it is not a saddle. Starting from this configuration, by Lemma 5.3.8 we know that the saddles that could be visited are in $\mathcal{C}^*$ or again in $\mathcal{A}_{k,k'}^{\alpha,\alpha'}$. This concludes case A.

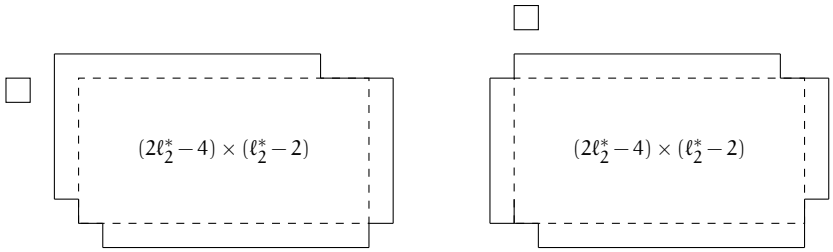

Figure 5.4 – Case C: on the left-hand side we depict a possible starting configuration $\eta \in \mathcal{C}^*$. Case D: on the right-hand side we depict a possible starting configuration $\eta \in \mathcal{C}^*$.

Case B. If we are considering the case in which a sequence of 1-translations of a bar is possible and takes place, then by Lemma 5.2.4 the saddles that are crossed are essential and in $\mathcal{A}_0^{\alpha'} \cup \mathcal{A}_1^{\alpha}$. We consider separately the following subcases:

(i) The two occupied frame-angles are $c^{\alpha\alpha'}(\eta)$ and $c^{\alpha''\alpha'''}(\eta)$, with all the indeces $\alpha, \alpha', \alpha''$ and α''' different between each other (see Figure 5.3(a));

(ii) The two occupied frame-angles are $c^{\alpha\alpha'}(\eta)$ and $c^{\alpha'\alpha''}(\eta)$, with $\alpha' \in \{n, s\}$ and $\alpha \neq \alpha''$ (see Figure 5.3(b));

(iii) The two occupied frame-angles are $c^{\alpha\alpha'}(\eta)$ and $c^{\alpha'\alpha''}(\eta)$, with $\alpha' \in \{e, w\}$ and $\alpha \neq \alpha''$ (see Figure 5.3(c)).

Case B(i). Without loss of generality we consider η as in Figure 5.3(a). We can reduce our proof to the case in which there is no translation of a bar and therefore there is the activation of a sliding of a bar around a frame-angle. If the free particle is attached to the bar $B^n(\eta)$ (resp. $B^s(\eta)$), by Lemma 5.2.5 we know that it is not possible to complete the sliding of the bar $B^w(\eta)$ (resp. $B^e(\eta)$) around the frame-angle $c^{wn}(\eta')$ (resp. $c^{es}(\eta')$). By Lemma 5.2.3(ii), this implies that the saddles that could be crossed are unessential. If the free particle is attached to the bar $B^w(\eta)$ (resp. $B^e(\eta)$), it is possible to slide the bar $B^n(\eta)$ (resp. $B^s(\eta)$) around the frame-angle $c^{nw}(\eta')$ (resp. $c^{se}(\eta')$) when $|B^n(\eta)| < |B^w(\eta)|$ (resp. $|B^s(\eta)| < |B^e(\eta)|$), otherwise (3.2.12) is not satisifed. By (5.4.3) and (5.4.4) we note that $|B^n(\eta)| < |B^w(\eta)|$ (resp. $|B^s(\eta)| < |B^e(\eta)|$) is not possible and the case B(i) is concluded.

Case B(ii). Without loss of generality we consider η as in Figure 5.3(b). If one bar among $B^w(\eta)$ and $B^e(\eta)$ is full, it is possible to translate $B^s(\eta)$ in order to have three occupied frame-angles. This situation has already been analyzed in case A. Thus, we can reduce our proof to the case in which there is no translation of a bar and therefore there is the activation of a sliding of a bar around a frame-angle. If the free particle is attached to the bar $B^n(\eta)$ (or $B^s(\eta)$), by Lemma 5.2.5 we know that it is not possible to complete the sliding of a vertical bar around any frame-angle. If the free particle is attached to the bar $B^w(\eta)$ or $B^e(\eta)$, since the bar $B^n(\eta)$ is full, we deduce that (3.2.12) is not satisfied. This implies that it is not possible to slide the bar $B^n(\eta)$ around the frame-angle $c^{nw}(\eta')$ and $c^{ne}(\eta')$. In the last two cases by Lemma 5.2.3(ii) we know that the saddles that could be visited are unessential. This concludes case B(ii).

Case B(iii). Without loss of generality we consider η as in Figure 5.3(c). If the bar $B^n(\eta)$ (or $B^s(\eta)$) is full, it is possible to translate $B^e(\eta)$ to occupy the frame-angle $c^{ne}(\eta')$ (or $c^{se}(\eta')$). This situation has already been analyzed in case A. Otherwise, it is possible to translate a bar with one occupied frame-angle in order to have two occupied frame-angles in such a way that they have no bar in common. This situation has already been analyzed in case B(i). Thus, we can reduce our proof to the case in which there is no translation of a bar and therefore we can consider only the activation of a sliding of a bar around a frame-angle. If the free particle is attached to the bar $B^n(\eta)$ (resp. $B^s(\eta)$), by Lemma 5.2.5 we know that it is not possible to complete the sliding of the bar $B^w(\eta)$ around the frame-angle $c^{wn}(\eta')$ (resp. $c^{ws}(\eta')$). If the free particle is attached to the bar $B^e(\eta)$, we deduce that (3.2.11) is not satisfied. In the last two cases by Lemma 5.2.3(ii) we know that the saddles that are visited are unessential. If the free particle is attached to the bar $B^w(\eta)$, it is possible to slide the bar $B^n(\eta)$ (resp. $B^s(\eta)$) around the frame-angle $c^{nw}(\eta')$ (resp. $c^{sw}(\eta')$) when $|B^n(\eta)| < |B^w(\eta)|$ (resp. $|B^s(\eta)| < |B^w(\eta)|$), otherwise (3.2.12) is not satisifed. By (5.4.3) and (5.4.4) we note that $|B^n(\eta)| < |B^w(\eta)|$ (resp. $|B^s(\eta)| < |B^w(\eta)|$) is not possible and the case B(iii) is concluded.

Case C. Without loss of generality we consider η as in Figure 5.4 on the left-hand side. If we are considering the case in which a sequence of 1-translations of a bar is possible and takes place, then by Lemma 5.2.4 the saddles that are crossed are essential and in $\mathcal{A}_0^{\alpha'} \cup \mathcal{A}_1^{\alpha}$. Starting from this configuration it is possible to obtain two occupied frame–angles, which has been already analyzed in Case B. Thus, we can reduce our proof to the case in which there is no translation of a bar and therefore there is the activation of a sliding of a bar around a frame-angle. If the free particle is attached to the bar $B^n(\eta)$ (resp. $B^s(\eta)$), by Lemma 5.2.5 we know that it is not possible to complete the sliding of the bar $B^w(\eta)$ around the frame-angle $c^{wn}(\eta')$ (resp. $c^{ws}(\eta')$). If the free particle is attached to the bar $B^e(\eta)$, we deduce that (3.2.12) is not satisfied. In the last two cases by Lemma 5.2.3(ii) we know that the saddles that are visited are unessential. If the free particle is attached to the bar $B^w(\eta)$, it is possible to slide the bar $B^n(\eta)$ around the frame-angle $c^{nw}(\eta')$ when $|B^n(\eta)| < |B^w(\eta)|$, otherwise (3.2.12) is not satisfied. By (5.4.3) and (5.4.4) we note that $|B^n(\eta)| < |B^w(\eta)|$ is not possible and case C is concluded.
Case D. Without loss of generality we consider η as in Figure 5.4 on the right-hand side. If we are considering the case in which a sequence of 1-translations of a bar is possible and takes place, then by Lemma 5.2.4 the saddles that are crossed are essential and in $\mathcal{A}_0^{\alpha'} \cup \mathcal{A}_1^{\alpha}$. Starting from this configuration, it is possible to obtain one or two occupied frame-angles: these situations have been already analyzed in cases C and B, respectively. Thus, we can reduce our proof to the case in which there is no translation of a bar and therefore there is the activation of a sliding of a bar around a frame-angle. If the free particle is attached to the bar $B^n(\eta)$ (resp. $B^s(\eta)$), by Lemma 5.2.5 we know that it is not possible to complete the sliding of the bar $B^w(\eta)$ around the frame-angle $c^{wn}(\eta')$ (resp. $c^{ws}(\eta')$). If the free particle is attached to the bar $B^w(\eta)$ or $B^e(\eta)$, we deduce that (3.2.11) is not satisfied. In the last two cases by Lemma 3.4.1(ii) we know that the saddles that are visited are unessential. This concludes case D. □

5.5 PROOF OF THE SHARP ASYMPTOTICS

For the model-independent discussion we refer to Section 3.6.1. Following the strategy given in [35] for the isotropic case, here we apply this argument for the strongly anisotropic one. For the corresponding strategy in the isotropic and weakly anisotropic cases we refer to Sections 3.6 and 4.5, respectively.

5.5.1 *Application of the potential theory to the strongly anisotropic case*

In [32] the authors let the protocritical and critical sets as $\mathscr{P}^*(m,s)$ and $\mathscr{C}^*(m,s)$, respectively (see [32, Definition 16.3] for the definition of $\mathscr{P}^*(m,s)$ and $\mathscr{C}^*(m,s)$). Since they differ from our notation, we refer to them as $\mathscr{P}^*_{\mathrm{PTA}}(m,s)$ and $\mathscr{C}^*_{\mathrm{PTA}}(m,s)$. In [32] the authors proved [32, Theorem 16.4] and [32, Theorem 16.5] subject to the two hypotheses

(H1) $\mathcal{X}^m = \{m\}$ and $\mathcal{X}^s = \{s\}$;

(H2) $\xi' \to |\{\xi \in \mathscr{P}^*_{\mathrm{PTA}}(m,s) : \xi \sim \xi'\}|$ is constant on $\mathscr{C}^*_{\mathrm{PTA}}(m,s)$.

For our model $\mathcal{X}^m = \{\square\}$ and $\mathcal{X}^s = \{\blacksquare\}$, thus (H1) holds and $\Gamma_m = \Phi(\square,\blacksquare) - \widehat{H}(\square) = \Gamma^*$. Now we abbreviate $\mathscr{P}^*_{\mathrm{PTA}} = \mathscr{P}^*_{\mathrm{PTA}}(\square,\blacksquare)$ and $\mathscr{C}^*_{\mathrm{PTA}} = \mathscr{C}^*_{\mathrm{PTA}}(\square,\blacksquare)$. Moreover, we prove that geometrically $\mathscr{P}^*_{\mathrm{PTA}} = \bar{\mathcal{D}} \cup \bigcup_{\alpha,\alpha'} \bar{\mathcal{A}}_2^{\alpha,\alpha'}$ (see (5.5.5) for the definition of $\bar{\mathcal{A}}_2^{\alpha,\alpha'}$) and $\mathscr{C}^*_{\mathrm{PTA}} = \mathcal{C}^*(L^*) \cup \bigcup_{\alpha,\alpha'} \mathcal{A}_2^{\alpha,\alpha'}$ (recall (5.1.9) for the definition of $\mathcal{A}_2^{\alpha,\alpha'}$) with $\alpha \in \{n,s\}$ and $\alpha' \in \{e,w\}$. Therefore it is clear that $\mathcal{C}^* \neq \mathscr{C}^*_{\mathrm{PTA}}$. Note that (H2) follows from Lemma 5.3.8, indeed each configuration in $\mathscr{C}^*_{\mathrm{PTA}}$ has exactly one configuration in $\mathscr{P}^*_{\mathrm{PTA}}$ from which it can be reached via an allowed move. In particular, the configurations in $\mathcal{C}^*(L^*)$ and $\bar{\mathcal{D}}$ are connected by removing the free particle in $\partial^- \Lambda$, while those in $\mathcal{A}_2^{\alpha,\alpha'}$ and $\bar{\mathcal{A}}_2^{\alpha,\alpha'}$ are connected between each other by attaching the two particles separated by an empty site at cost $-U_1$. Since (H1) and (H2) hold, [32, Theorem 16.4] and [32, Theorem 16.5] should hold, but for the strongly anisotropic case this is not true. More precisely, this model represents a counterexample of [32, Theorem 16.4(b)], indeed on the one hand [32, Theorem 16.4(a)] and [32, Theorem 16.5] are valid, but on the other hand [32, Theorem 16.4(b)] does not hold. This relies on a peculiar feature of this model: the entrance in $\mathscr{C}^*_{\mathrm{PTA}}$ cannot be uniform due to the

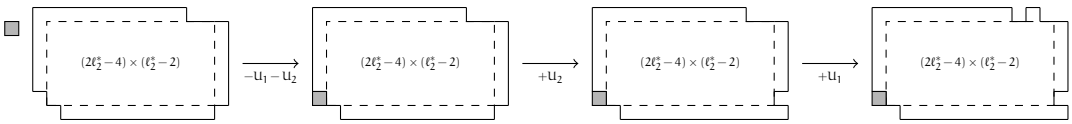

Figure 5.5 – We depict the transition that, starting from a configuration in $\mathcal{C}^*$, passes through $\mathcal{C}^G$ and after two moves reaches an unessential saddle ζ.

two possibile different entrance mechanisms, as claimed in Lemma 5.3.8. This depends on the hypothesis (H2), that takes into account only the map from $\mathscr{C}^*_{PTA}$ to $\mathscr{P}^*_{PTA}$ and not the reverse one. Therefore we propose to replace the hypothesis (H2) with

(H2′) $\xi' \to |\{\xi \in \mathscr{P}^*_{PTA}(m,s) : \xi \sim \xi'\}|$ is constant on $\mathscr{C}^*_{PTA}(m,s)$ and $\xi \to |\{\xi' \in \mathscr{C}^*_{PTA}(m,s) : \xi' \sim \xi\}|$ is constant on $\mathscr{P}^*_{PTA}(m,s)$.

We are convinced that this could be the correct hypotheses, indeed the analysis of the uniform entrance distribution in $\mathscr{C}^*_{PTA}(m,s)$ has to take into account the number of configurations in $\mathscr{P}^*_{PTA}(m,s)$ that communicate with $\mathscr{C}^*_{PTA}(m,s)$ via one step of the dynamics. Now it is clear that this model does not satisfy (H2′), indeed each configuration in $\bar{\mathcal{D}}$ has exactly $4L-4$ configurations in $\mathcal{C}^*$ from which it can be reached via an allowed move, while each configuration in $\bar{\mathcal{A}}_2^{\alpha,\alpha'}$ has only one configuration in $\mathcal{A}_2^{\alpha,\alpha'}$ with this property. Therefore [32, Theorem 16.4(b)] does not hold for this model.

Recall Definition 3.6.4 for the definition of the wells $\mathcal{Z}^{\square}_{sa,j}$ and $\mathcal{Z}^{\blacksquare}_{sa,j}$ and Definitions 3.1.2 and 3.1.4 for the definition of the saddles $\sigma_{sa,j}$ of the first type and $\zeta_{sa,j}$ of the second type, respectively. Concerning [32, Theorem 16.5], by [32, Lemma 16.16] for the case strongly anisotropic case, we know that h is constant on each wells. For the wells $\mathcal{Z}^m_j$ and $\mathcal{Z}^s_j$ this constant is computed in Lemma 3.6.7 indeed [32, Lemma 16.15] can be extended for these sets together with the unessential saddles of the first and second type. Thanks to the model–independent discussion given in Section 3.6.1 and Lemma 3.6.7, equation (3.6.12) becomes

$$h = \begin{cases} 1 & \text{on } \mathcal{C}^{\square}_{\blacksquare}(\Gamma^*) \cup \bigcup_{j=1}^{J_{\square}} (\{\sigma_j\} \cup \mathcal{Z}^{\square}_j), \\ 0 & \text{on } \mathcal{C}^{\blacksquare}_{\square}(\Gamma^* - \widehat{H}(\blacksquare)) \cup \bigcup_{j=1}^{J_{\blacksquare}} (\{\zeta_j\} \cup \mathcal{Z}^{\blacksquare}_j), \\ c_i & \text{on } \mathcal{X}(i), i = 1, ..., \bar{I}, \end{cases} \tag{5.5.1}$$

where $\mathcal{X}(i)$, $i = 1, ..., \bar{I}$, are all the wells of the transition except $\bigcup_{j=1}^{J_{\square}} \mathcal{Z}^{\square}_j$ and $\bigcup_{j=1}^{J_{\blacksquare}} \mathcal{Z}^{\blacksquare}_j$. This implies that the unessential saddles, not characterizing the typical behavior of the process, can not be neglected in the study of the prefactor K. However, since they do not communicate with some $\mathcal{X}(i)$ via one step of the dynamics together with the fact that $h(\sigma_j) = 1$ and $h(\zeta_j) = 0$ for any j, the transitions that involve these unessential saddles do not contribute numerically to the computation of K. The variational formula for $\Theta = 1/K$ in (3.6.6) is non–trivial because it depends on the geometry of all the wells and on the form of the function h on the configurations in $\mathcal{X}^* \setminus \mathcal{X}^{**}$, namely, the saddle configurations.

Remark 5.5.1. *In Figure 5.5 we depict a transition that, starting from a configuration in $\mathcal{C}^*$, gives an unessential saddle ζ of the third type.*

5.5.2 *Proof of Theorem 5.1.5*

Using Lemma 3.6.7 and Remark 3.6.8, in order to prove Theorem 5.1.5 it remains to analyze in detail the number of possible transitions inside the gates and in–between their boundaries. Finally, we need to count the cardinality of $\bar{\mathcal{D}}$ modulo shifts, which we will refer to as N.

LOWER BOUND

We consider the following sets:

$$\begin{aligned} \mathcal{X}^{\square} &:= \mathcal{C}^{\square}_{\blacksquare}(\Gamma^*) \cup \bigcup_{j=1}^{J_{\square}} (\{\sigma_j\} \cup \mathcal{Z}_j^{\square}), \\ \mathcal{X}^{\blacksquare} &:= \mathcal{C}^{\blacksquare}_{\square}(\Gamma^* - \widehat{H}(\blacksquare)) \cup \bigcup_{j=1}^{J_{\blacksquare}} (\{\zeta_j\} \cup \mathcal{Z}_j^{\blacksquare}). \end{aligned} \tag{5.5.2}$$

The lower bound $\Theta \geqslant \Theta_1$ is obtained by removing all the transitions that do not involve either a protocritical droplet and a free particle that moves or the path described in Figure 1.13. The first type of transitions gives a contribute that can be treated in a similar way as in the lower bound in [35, Proposition 3.3.4]. Indeed, by rescaling the transition rates in the case of discrete time dynamics as explained in Remark 3.6.8, we obtain:

$$\begin{aligned} &\sum_{\hat{\eta} \in \bar{\mathcal{D}}} \min_{c_j(\hat{\eta}), j=1,2,3,4} \min_{\substack{g:\Lambda^* \to [0,1] \\ g_{|\partial^G \hat{\eta}} \equiv 0, g_{|\partial_j^B \hat{\eta}} \equiv c_j, j=1,2,3,4, g_{|\partial^+\Lambda} \equiv 1}} \frac{1}{2|\bar{\Lambda}^*, \, \mathrm{orie}|} \sum_{\substack{x,x' \in \Lambda^+ \\ x \sim x'}} [g(x) - g(x')]^2 \\ &\quad \geqslant \sum_{\hat{\eta} \in \bar{\mathcal{D}}} \mathrm{CAP}^{\Lambda^+}(\partial^+\Lambda, \mathrm{CR}(\hat{\eta})), \end{aligned} \tag{5.5.3}$$

where $g(x) := h(\hat{\eta}, x) = h(\eta)$ for $\hat{\eta} \in \bar{\mathcal{D}}$ and $x \in \Lambda \setminus \mathrm{CR}^{++}(\hat{\eta})$, and $\partial^G \hat{\eta}$ denotes the set of good sites in $\partial^- \mathrm{CR}(\hat{\eta})$, $\partial_j^B \hat{\eta}$, $j = 1, 2, 3, 4$, denote the four bars of bad sites in $\partial^+ \mathrm{CR}(\hat{\eta})$ and for any $F \subseteq \Lambda^+$

$$\mathrm{CAP}^{\Lambda^+}(\partial^+\Lambda, F) = \min_{\substack{g:\Lambda^+ \to [0,1] \\ g_{|\partial^+\Lambda} \equiv 1, g_{|F} \equiv 0}} \frac{1}{2|\bar{\Lambda}^*, \, \mathrm{orie}|} \sum_{\substack{x,x' \in \Lambda^+ \\ x \sim x'}} [g(x) - g(x')]^2. \tag{5.5.4}$$

For $\alpha \in \{n, s\}$, $\alpha' \in \{w, e\}$ and $k = 2, ..., \ell_2^*$, we define

$$\begin{aligned} \bar{\mathcal{A}}_k^{\alpha,\alpha'} := \{&\eta : n(\eta) = 0, v(\eta) = 2\ell_2^* - 2, |r^{\alpha}(\eta)| = k - 1, |r^{\alpha}(\eta)| = \ell_2^* - k, |c^{\alpha\alpha'}(\eta)| = 1, \\ &\eta_{cl} \text{ is connected, monotone, with circumscribed rectangle in } \mathcal{R}(2\ell_2^* - 1, \ell_2^*)\} \end{aligned} \tag{5.5.5}$$

and

$$\begin{aligned} \widetilde{\mathcal{A}}_k^{\alpha,\alpha'} := \{&\eta : n(\eta) = 0, v(\eta) = 2\ell_2^* - 2, |r^{\alpha}(\eta)| = k, |r^{\alpha}(\eta)| = \ell_2^* - k, |c^{\alpha\alpha'}(\eta)| = 0, \\ &\eta_{cl} \text{ is connected, monotone, with circumscribed rectangle in } \mathcal{R}(2\ell_2^* - 1, \ell_2^*)\}. \end{aligned} \tag{5.5.6}$$

Referring to Figure 1.13, note that the configuration (6) is in $\bar{\mathcal{A}}_2^{n,e}$ and the configuration (10) is in $\bar{\mathcal{A}}_3^{n,e}$, while the configuration (8) is in $\widetilde{\mathcal{A}}_2^{n,e}$.

Now we analyze the transitions described in Figure 1.13. The configuration (6) is in $\bar{\mathcal{A}}_2^{n,e} \subseteq \mathcal{C}^{\square}_{\blacksquare}(\Gamma^*) \subseteq \mathcal{X}^{\square}$ and therefore $h(\bigcup_{\alpha,\alpha'} \bar{\mathcal{A}}_2^{n,e}) = 1$. Thanks to [35, Lemma 3.3.2], we know that h is constant on the wells and thus we analyze the transitions to and from each wells. In particular, note that during the transition from $\widetilde{\mathcal{A}}_k^{\alpha,\alpha'}$ and $\bar{\mathcal{A}}_{k+1}^{\alpha,\alpha'}$ only configurations with energy strictly smaller than Γ^* are crossed, thus they belong to the same well and therefore we can set h constant on these configurations. We set $h(\bigcup_{\alpha,\alpha'} \mathcal{A}_2^{\alpha,\alpha'}) = c_1$, $h \equiv c_2$ on $\bigcup_{\alpha,\alpha'} \widetilde{\mathcal{A}}_2^{\alpha,\alpha'}$ and on its wells, and so on until the last set $h(\bigcup_{\alpha,\alpha'} \bar{\mathcal{A}}_{\ell_2^*}^{\alpha,\alpha'}) = c_{2\ell_2^*-2}$ and $h(\eta) = c_{2\ell_2^*-1}$ for any $\eta \in \mathcal{C}^*(2)$. Thus, we have to minimize with respect to $c_1, c_2, ..., c_{2\ell_2^*-1}$ the following term:

$$(1 - c_1)^2 + (c_1 - c_2)^2 + ... + (c_{2\ell_2^*-3} - c_{2\ell_2^*-2})^2 + (c_{2\ell_2^*-2} - c_{2\ell_2^*-1})^2 + k c_{2\ell_2^*-1}^2, \tag{5.5.7}$$

where $k = \ell_2^* - 1$ is the number of good sites of the configuration (12) in Figure 1.13. We prove by induction over n that

$$c_n = \frac{1 + K_n c_{n+1}}{K_n + 1}, \qquad 1 \leqslant n \leqslant 2\ell_2^* - 2, \tag{5.5.8}$$

where K_n satisfies the following recurrence relation

$$\begin{cases} K_n = (K_{n-1}+1)^2, \quad 2 \leqslant n \leqslant 2\ell_2^* - 2, \\ K_1 = 1. \end{cases} \tag{5.5.9}$$

$\underline{n=1}$ We have to prove that $c_1 = \frac{1+c_2}{2}$. This can be easily checked by minimizing the function $f(c_1, c_2) = (1-c_1)^2 + (c_1 - c_2)^2$ with respect to c_1. Indeed, we get

$$\frac{\partial f}{\partial c_1} = 4c_1 - 2c_2 - 2 = 0 \quad \Leftrightarrow \quad c_1 = \frac{1+c_2}{2}. \tag{5.5.10}$$

$\underline{2 \leqslant n \leqslant 2\ell_2^* - 2}$ Assume now that (5.5.8) holds for $n-1$ and we prove that it holds also for n. We consider the function $f(c_{n-1}, c_n, c_{n+1}) = (c_{n-1} - c_n)^2 + (c_n - c_{n+1})^2$ and we replace the expression of c_{n-1} in terms of c_n. Thus, we get

$$f(c_n, c_{n+1}) = \left(\frac{1 + K_{n-1} c_n}{K_{n-1}+1} - c_n \right)^2 + (c_n - c_{n+1})^2 \tag{5.5.11}$$

and therefore

$$\frac{\partial f}{\partial c_n} = 2\left(\frac{K_{n-1}}{K_{n-1}+1} - 1 \right)\left(\frac{1 + K_{n-1} c_n}{K_{n-1}+1} - c_n \right) + 2(c_n - c_{n+1}). \tag{5.5.12}$$

The equation $\frac{\partial f}{\partial c_n} = 0$ gives

$$\frac{c_n - 1}{(K_{n-1}+1)^2} = c_{n+1} - c_n, \tag{5.5.13}$$

that implies (5.5.8) by using (5.5.9). Thus, we get the claim.

Now we have to find the value of the constant $c_{2\ell_2^*-1}$ that minimizes (5.5.7). By considering the function $f(c_{2\ell_2^*-2}, c_{2\ell_2^*-1}) = (c_{2\ell_2^*-2} - c_{2\ell_2^*-1})^2 + (\ell_2^* - 1)c_{2\ell_2^*-1}^2$ and proceeding in a similar way as above, we deduce that

$$c_{2\ell_2^*-1} = \frac{1}{(\ell_2^* - 1)(K_{2\ell_2^*-2}+1)^2 + 1}. \tag{5.5.14}$$

By (5.5.8) and (5.5.14) we get

$$1 - c_1 = \frac{1-c_2}{2} \quad \text{and} \quad c_{n-1} - c_n = \frac{1-c_n}{K_{n-1}+1}. \tag{5.5.15}$$

Finally, by (5.5.15) we deduce that the minimizer of the quantity in (5.5.7) is given by

$$\left(\frac{1-c_2}{2}\right)^2 + \sum_{n=2}^{2\ell_2^*-1} \left(\frac{1-c_n}{K_{n-1}+1} \right)^2 + \frac{\ell_2^* - 1}{((\ell_2^* - 1)(K_{2\ell_2^*-2}+1)^2 + 1)^2}, \tag{5.5.16}$$

where the coefficients $c_2, ..., c_{2\ell_2^*-1}$ can be explicitly derived from (5.5.8) e (5.5.14). Combining (5.5.3) and (5.5.16), we get

$$\begin{aligned} \Theta \quad \geqslant \sum_{\hat{\eta} \in \hat{\mathcal{D}}} \mathrm{CAP}^{\Lambda^+}(\partial^+\Lambda, \mathrm{CR}(\hat{\eta})) + 4 \Bigg[\left(\frac{1-c_2}{2}\right)^2 + \sum_{n=2}^{2\ell_2^*-1} \left(\frac{1-c_n}{K_{n-1}+1} \right)^2 \\ + \frac{\ell_2^* - 1}{[(\ell_2^* - 1)(K_{2\ell_2^*-2}+1)^2 + 1]^2} \Bigg] := \Theta_1. \end{aligned} \tag{5.5.17}$$

The first term in the r.h.s. of (5.5.17) can be treated in a similar way as [35, Lemma 3.4.1] for $\Lambda \to \mathbb{Z}^2$. Since the remaining part of the r.h.s. of (5.5.17) does not depend on the size of the box, that implies that we can neglect its contribute as $\Lambda \to \mathbb{Z}^2$, we deduce that

$$\Theta_1 \to \frac{4\pi N}{|\bar{\Lambda}^{*,\,\mathrm{orie}}|} \frac{|\Lambda|}{\log|\Lambda|} \qquad \text{as} \qquad \Lambda \to \mathbb{Z}^2, \tag{5.5.18}$$

where N is computed in Proposition 5.5.2.

UPPER BOUND

We define

$$\mathcal{C}^{++} := \{\eta = (\hat{\eta}, x) : \ \hat{\eta} \in \bar{\mathcal{D}}, \ x \in \Lambda \setminus \mathrm{CR}^{++}(\hat{\eta})\}. \tag{5.5.19}$$

and we consider the following test function

$$h(\eta) := \begin{cases} 1 & \text{if } \eta \in \mathcal{X}^{\square}, \\ c_i & \text{if } \eta \in \mathcal{X}(i), i = 1, ..., \bar{I} \\ g(x) & \text{if } \eta \in \mathcal{C}^{++}, \\ 0 & \text{if } \eta \in \mathcal{X}^{\blacksquare}, \end{cases} \tag{5.5.20}$$

where $g(x) := h(\hat{\eta}, x) = h(\eta)$ for $\hat{\eta} \in \bar{\mathcal{D}}$ and $x \in \Lambda \setminus \mathrm{CR}^{++}(\hat{\eta})$, i.e., $\eta \in \mathcal{C}^{++}$. Thus, by (3.6.13) we get

$$\begin{aligned} \mathrm{CAP}(\square, \blacksquare) \ \leqslant (1 + o(1)) \Bigg(& \sum_{\hat{\eta} \in \bar{\mathcal{D}}} \mathrm{CAP}^{\Lambda^+}(\partial^+\Lambda, \mathrm{CR}^{++}(\hat{\eta})) + \min_{c_1, ..., c_{\bar{I}}} \\ & \min_{\substack{h : \mathcal{X}^* \to [0,1] \\ h_{|\mathcal{X}^{\square}} = 1, h_{|\mathcal{X}^{\blacksquare}} = 0, h_{|\mathcal{X}(i)} = c_i, i = 1, ..., \bar{I}}} \frac{1}{2} \sum_{\eta, \eta' \in \mathcal{X}^*} \mu_\beta(\eta, \eta') P(\eta, \eta') [h(\eta) - h(\eta')]^2, \end{aligned} \tag{5.5.21}$$

where $\mathrm{CAP}^{\Lambda^+}(\partial^+\Lambda, F)$ is defined in (5.5.4). We have to analyze the possible transitions between $\mathcal{X}^{\blacksquare}$ and $\mathcal{X}(i) \cup \bigcup_j \{\xi_j\}$, between $\mathcal{X}(i)$ and $\mathcal{X}(j)$ with $i \neq j$ and between $\mathcal{X}(i) \cup \bigcup_j \{\xi_j\}$ and $\mathcal{X}^{\square}$, where the saddles ξ_j are neither saddles of the first type nor saddles of the second type (recall Definitions 3.1.2 and 3.1.4). We set

$$\mathcal{X}(1) = \bigcup_{\alpha \in \{n,s\}} \bigcup_{\alpha' \in \{w,e\}} \mathcal{A}_2^{\alpha, \alpha'},$$

where an example is given in Figure 1.13 by the configuration (7)). We set $\mathcal{X}(2)$ as the union of $\widetilde{\mathcal{A}}_2^{\alpha,\alpha'}$, $\bar{\mathcal{A}}_3^{\alpha,\alpha'}$ and the configurations connecting these sets in the path described in Figure 1.13 that are in the same well. We iterate this construction until the last set $\mathcal{X}(2\ell_2^* - 1)$ as we did for the lower bound. Furthermore, we set

$$\mathcal{X}(2\ell_2^*) = \mathcal{C}^B, \quad \mathcal{X}(2\ell_2^* + 1) = \bigcup_{\alpha' \in \{e,w\}} \mathcal{A}_0^{\alpha'}, \quad \mathcal{X}(2\ell_2^* + 2) = \bigcup_{\alpha' \in \{e,w\}} \mathcal{A}_1^{\alpha}.$$

Now we analyze all the transitions that give a non–trivial contribute to (5.5.21).

Transitions between $\mathcal{X}^{\square}$ and $\mathcal{X}(i) \cup \bigcup_j \{\xi_j\}$. The transition via one step of the dynamics from $\eta \in \mathcal{X}^{\square}$ and $\eta' \in \mathcal{X}(i) \cup \bigcup_j \{\xi_j\}$ is possible only if either $\eta \in \bar{\mathcal{D}}$ and $\eta' \in \mathcal{C}^*$ or $\eta \in \bar{\mathcal{A}}_2^{\alpha,\alpha'}$ and $\eta' \in \mathcal{A}_2^{\alpha,\alpha'}$ for some $\alpha \in \{n, s\}$ and $\alpha' \in \{w, e\}$. The latter transition contributes 4 times to the quantity in (5.5.21) depending on which frame-angle is involved in the transition.

Transitions between $\mathcal{X}(i)$ and $\mathcal{X}(j)$. We consider the sequence of transitions that forms the path described in Figure 1.13, the transitions between $\mathcal{C}^*(2)$ and $\mathcal{C}^B$, between $\mathcal{C}^B$ and $\mathcal{X}(2\ell_2^* + 1)$ and between $\mathcal{C}^B$ and $\mathcal{X}(2\ell_2^* + 2)$.

Transitions between $\mathcal{X}(i)$ and $\mathcal{X}^{\blacksquare}$. The transition via one step of the dynamics from $\eta \in \mathcal{X}(i)$ and $\eta' \in \mathcal{X}^{\blacksquare}$ is possible only if $\eta \in \mathcal{C}^*(2)$ and $\eta' \in \mathcal{C}^G$.

Collecting all these transitions, by (5.5.20) and (5.5.21) we get

$$\begin{aligned}\mathrm{CAP}(\square,\blacksquare) \;\leqslant\; & \frac{e^{-\beta\Gamma^*}}{Z}(1+o(1))\Bigg(\frac{1}{|\bar{\Lambda}^*,\mathrm{orie}|}\Bigg[\min_{\bar{c},c_1,\dots,c_{2\ell_2^*+2}} 4\Big[(1-c_1)^2+(c_1-c_2)^2\\ & +\dots+(c_{2\ell_2^*-2}-c_{2\ell_2^*-1})^2+(\ell_2^*-1)c_{2\ell_2^*-1}^2\Big]+\sum_{\substack{\eta\in\mathcal{C}^*(2)\\ \eta'\in\mathcal{C}^G}}\bar{c}^2\\ & +\sum_{\substack{\eta\in\mathcal{C}^*(2)\\ \eta'\in\mathcal{X}(2\ell_2^*)}}(\bar{c}^2-c_{2\ell_2^*})^2+2\sum_{\substack{\eta\in\mathcal{X}(2\ell_2^*)\\ \eta'\in\mathcal{X}(2\ell_2^*+1)}}(c_{2\ell_2^*}-c_{2\ell_2^*+1})^2\\ & +2\sum_{\substack{\eta\in\mathcal{X}(2\ell_2^*)\\ \eta'\in\mathcal{X}(2\ell_2^*+2)}}(c_{2\ell_2^*}-c_{2\ell_2^*+2})^2\Bigg]+\sum_{\hat{\eta}\in\bar{\mathcal{D}}}\mathrm{CAP}^{\Lambda^+}(\partial^+\Lambda,\mathrm{CR}^{++}(\hat{\eta}))\Bigg).\end{aligned} \tag{5.5.22}$$

Rearranging the term, we get

$$\begin{aligned}\mathrm{CAP}(\square,\blacksquare) \;\leqslant\; & \frac{e^{-\beta\Gamma^*}}{Z}(1+o(1))\Bigg(\frac{1}{|\bar{\Lambda}^*,\mathrm{orie}|}\Bigg[\min_{c_1,\dots,c_{2\ell_2^*-1}} 4\Big[(1-c_1)^2+(c_1-c_2)^2\\ & +\dots+(c_{2\ell_2^*-2}-c_{2\ell_2^*-1})^2+(\ell_2^*-1)c_{2\ell_2^*-1}^2\Big]+\min_{\bar{c},c_{2\ell_2^*},\dots,c_{2\ell_2^*+2}}\sum_{\substack{\eta\in\mathcal{C}^*(2)\\ \eta'\in\mathcal{C}^G}}\bar{c}^2\\ & +\sum_{\substack{\eta\in\mathcal{C}^*(2)\\ \eta'\in\mathcal{X}(2\ell_2^*)}}(\bar{c}-c_{2\ell_2^*})^2+2\sum_{\substack{\eta\in\mathcal{X}(2\ell_2^*)\\ \eta'\in\mathcal{X}(2\ell_2^*+1)}}(c_{2\ell_2^*}-c_{2\ell_2^*+1})^2\\ & +2\sum_{\substack{\eta\in\mathcal{X}(2\ell_2^*)\\ \eta'\in\mathcal{X}(2\ell_2^*+2)}}(c_{2\ell_2^*}-c_{2\ell_2^*+2})^2\Bigg]+\sum_{\hat{\eta}\in\bar{\mathcal{D}}}\mathrm{CAP}^{\Lambda^+}(\partial^+\Lambda,\mathrm{CR}^{++}(\hat{\eta}))\Bigg).\end{aligned} \tag{5.5.23}$$

Now we analyze separately the two following terms:

$$\bar{\Theta}=\min_{c_1,\dots,c_{2\ell_2^*-1}} 4\Big[(1-c_1)^2+(c_1-c_2)^2+\dots+(c_{2\ell_2^*-2}-c_{2\ell_2^*-1})^2+(\ell_2^*-1)c_{2\ell_2^*-1}^2\Big] \tag{5.5.24}$$

and

$$\begin{aligned}\widetilde{\Theta} \;=\; & \min_{\bar{c},c_{2\ell_2^*},\dots,c_{2\ell_2^*+2}}\sum_{\substack{\eta\in\mathcal{C}^*(2)\\ \eta'\in\mathcal{C}^G}}\bar{c}^2+\sum_{\substack{\eta\in\mathcal{C}^*(2)\\ \eta'\in\mathcal{X}(2\ell_2^*)}}(\bar{c}-c_{2\ell_2^*})^2+2\sum_{\substack{\eta\in\mathcal{X}(2\ell_2^*)\\ \eta'\in\mathcal{X}(2\ell_2^*+1)}}(c_{2\ell_2^*}-c_{2\ell_2^*+1})^2\\ & +2\sum_{\substack{\eta\in\mathcal{X}(2\ell_2^*)\\ \eta'\in\mathcal{X}(2\ell_2^*+2)}}(c_{2\ell_2^*}-c_{2\ell_2^*+2})^2+\sum_{\hat{\eta}\in\bar{\mathcal{D}}}\mathrm{CAP}^{\Lambda^+}(\partial^+\Lambda,\mathrm{CR}^{++}(\hat{\eta})).\end{aligned} \tag{5.5.25}$$

Note that the minimum of (5.5.24) coincides with 4 times the minimum of (5.5.7) and therefore $\bar{\Theta}$ can be computed in the same way as in the lower bound (see (5.5.8), (5.5.14) and (5.5.16)). It is easy to check that the minimum of (5.5.25) with respect to $\bar{c}$ and $c_{2\ell_2^*},\dots,c_{2\ell_2^*+2}$ is obtained for $\bar{c}=c_{2\ell_2^*}=c_{2\ell_2^*+1}=c_{2\ell_2^*+2}=0$. Thus, the term $\widetilde{\Theta}$ becomes

$$\widetilde{\Theta}=\sum_{\hat{\eta}\in\bar{\mathcal{D}}}\mathrm{CAP}^{\Lambda^+}(\partial^+\Lambda,\mathrm{CR}^{++}(\hat{\eta})) \tag{5.5.26}$$

and therefore

$$\begin{aligned}\Theta \;&\leqslant \frac{e^{-\beta\Gamma^*}}{Z}(1+o(1))\Big(\frac{1}{|\bar{\Lambda}^*,\mathrm{orie}|}\bar{\Theta}+\widetilde{\Theta}\Big)\\ &= \frac{e^{-\beta\Gamma^*}}{Z}(1+o(1))\Bigg[\frac{4}{|\bar{\Lambda}^*,\mathrm{orie}|}\Bigg(\Big(\frac{1-c_2}{2}\Big)^2+\sum_{n=2}^{2\ell_2^*-1}\Big(\frac{1-c_n}{K_{n-1}+1}\Big)^2\\ &\quad+\frac{\ell_2^*-1}{[(\ell_2^*-1)(K_{2\ell_2^*-2}+1)^2+1]^2}\Bigg)+\sum_{\hat{\eta}\in\bar{\mathcal{D}}}\mathrm{CAP}^{\Lambda^+}(\partial^+\Lambda,\mathrm{CR}^{++}(\hat{\eta}))\Bigg]:=\Theta_2,\end{aligned} \tag{5.5.27}$$

where the coefficients $c_2, ..., c_{2\ell_2^*-2}, c_{2\ell_2^*-1}$ can be explictly derived from (5.5.8) and (5.5.14), and the sequence K_n is defined in (5.5.9). The first term in the r.h.s. of (5.5.27) does not depend on the size of the box, thus we can neglect its contribution as $\Lambda \to \mathbb{Z}^2$. Since the remaining part of the r.h.s. of (5.5.27) can be treated in a similar way as [35, Lemma 3.4.1] for $\Lambda \to \mathbb{Z}^2$ up to the rescaling factor $1/|\bar{\Lambda}^{*,\,\mathrm{orie}}|$ since we are dealing with a discrete time dynamics, we deduce that

$$\Theta_2 \to \frac{4\pi N}{|\bar{\Lambda}^{*,\,\mathrm{orie}}|} \frac{|\Lambda|}{\log|\Lambda|} \qquad \text{as} \qquad \Lambda \to \mathbb{Z}^2, \tag{5.5.28}$$

where N is computed in Proposition 5.5.2.

Proposition 5.5.2.

$$N = \sum_{k=1}^{4} \binom{4}{k} \binom{\ell_2^* + k - 2}{2k-1}.$$

Proof. We have to count the number of different shapes of the clusters in $\bar{\mathcal{D}}$. We do this by counting in how many ways $\ell_2^* - 1$ particles can be removed from the four bars of a $(2\ell_2^* - 2) \times \ell_2^*$ rectangle starting from the corners. We split the counting according to the number $k = 1, 2, 3, 4$ of corners from which particles are removed. The number of ways in which we can choose k corners is $\binom{4}{k}$. After we have removed the particles at these corners, we need to remove $\ell_2^* - 1 - k$ more particles from either side of each corner. The number of ways in which this can be done is

$$\begin{aligned} &|\{(m_1, ..., m_{2k}) \in \mathbb{N}_0^{2k} : \; m_1 + ... + m_{2k} = \ell_2^* - 1 - k\}| \\ &\quad = |\{(m_1, ..., m_{2k}) \in \mathbb{N}^{2k} : \; m_1 + ... + m_{2k} = \ell_2^* - 1 + k\}| \\ &\quad = \binom{\ell_2^* + k - 2}{2k-1}. \end{aligned} \tag{5.5.29}$$

Thus, we get the claim. □

5.5.3 *Proof of Theorem 5.1.8*

Thanks to [92, Lemma 3.6], we deduce that for our model the quantity $\widetilde{\Gamma}(B)$, with $B \subsetneq \mathcal{X}$, defined in [92, eq. (21)] is such that $\widetilde{\Gamma}(\mathcal{X} \setminus \{\blacksquare\}) = \Gamma^*$. Thus, Theorem 5.1.8 follows by [92, Proposition 3.24].

6 LOCAL DYNAMICS ON THE HEXAGONAL LATTICE

The goal of this chapter is to investigate the metastable transition for Kawasaki dynamics on the hexagonal lattice in order to understand the role of the underlying lattice on the dynamical properties of the system. In particular, we identify stable and metastable states, we provide the limiting behaviour of the transition time and we characterize a gate for the transition. Concerning the last issue, we emphasize the differences with the analogous model on the standard square lattice. We conclude that the shape of the hexagonal lattice has a crucial impact on the critical configurations and on the mechanisms for entering them.

This chapter is structured as follows. In Section 6.1 we state our main results. In Section 6.2, we give the proof of the theorems concerning the asymptotic behavior of the transition time and the characterization of the critical configurations after identifying the maximal stability level. This is done by providing an upper and lower bound via a reference path and by using the isoperimetric inequality respectively. Finally, in Section 6.3 we prove the recurrence property to the set $\{\hexagon, \hexagonblack\}$ which allows use to identify the metastable and stable states of the system.

6.1 MAIN RESULTS

6.1.1 *Geometrical definitions for Kawasaki dynamics on the hexagonal lattice*

We briefly give some geometrical definitions and notations in order to state our main theorems. In particular, we explicitly provide those depending on the underlying lattice and therefore differs from the corresponding for the square lattice, while we refer to Section 3.2.1 for the others. For the extensive geometrical definitions see Section 6.2.1. Recall that $\mathbb{T}^2$ is the dual of $\mathbb{H}^2$, i.e., $\mathbb{T}^2$ is the discrete triangular lattice embedded in $\mathbb{R}^2$.

- We call *triangular unit* or *triangular face* an equilateral triangle of area one, whose center belongs to the discrete hexagonal lattice and whose vertices belong to its dual (see Figure 1.20). Moreover, a set of two triangular units that share an edge is called *elementary rhombus*.
- Given a configuration $\eta \in \mathcal{X}$ we denote by $C(\eta_{cl})$ its Peierls contour, that lives on the dual lattice and is the union of piecewise linear curves separating the empty triangular faces from the triangular faces with particles inside.

6.1.2 *Main results*

In this section we present our main results for this model. Recall (1.3.58) and (1.3.59) for the definition of the empty configuration and of the configuration that is full in Λ_0 and empty in $\Lambda \setminus \Lambda_0$, respectively. By (1.3.56) and (1.3.58) we have that $\widehat{H}(\hexagon) = 0$. Recall the definition of the critical radius r^* given in (1.3.63) We assume that $\frac{U}{2(3U-2\Delta)} - \frac{1}{2}$ is not integer in order to avoid strong degeneracy of the critical configurations. Similar assumptions are common in the literature (see e.g., [37, 44, 47]). We recall the assumption $3U - 2\Delta \ll U$, in particular $3U - 2\Delta \leqslant \frac{U}{100}$ is enough. In the following theorem, we will identify the stable and metastable states and we will show that for our model the energy barrier Γ_m is equal to

$$\Gamma_H^* := \begin{cases} \Gamma_{H,1}^* & \text{if } \delta \in (0, \frac{1}{2}), \\ \Gamma_{H,2}^* & \text{if } \delta \in (\frac{1}{2}, 1). \end{cases} \tag{6.1.1}$$

where

$$\Gamma_{H,1}^* = -3(3(r^*)^2 - r^*)U + 6(r^*)^2\Delta + 5(2r^* + 1)\Delta - (15r^* + 4)U + \Delta$$

and

$$\Gamma_{H,2}^* = -3(3(r^* + 1)^2 - (r^* + 1))U + 6(r^* + 1)^2\Delta + (2r^* + 3)\Delta - 3(r^* + 1)U + \Delta.$$

The value of $\Gamma^{\text{K-Hex}}$ is obtained by computing the energy of the critical configurations. We will see that these configurations consist of a cluster having a shape that is close to a hexagon with radius r^* and, in particular, we will compute the critical area to be

$$\begin{aligned} A_1^* &= 6(r^*)^2 + 10r^* + 6 && \text{if } \delta \in \left(0, \tfrac{1}{2}\right), \\ A_2^* &= 6(r^*+1)^2 + 2(r^*+1) + 2 && \text{if } \delta \in \left(\tfrac{1}{2}, 1\right). \end{aligned} \tag{6.1.2}$$

Theorem 6.1.1. (Identification of the metastable state). *Let* $L > 2r^* + 3$, *then* $\mathcal{X}^m = \{\hexagon\}$ *and* $\mathcal{X}^s = \{\hexagonblack\}$. *Moreover,* $\Gamma_m = \Phi(\hexagon, \hexagonblack) = \Gamma_H^*$.

The idea is to find an upper bound for Γ_m by building a reference path and a lower bound using an isoperimetric inequality. Another goal is to find the asymptotic behavior as $\beta \to \infty$ of the transition time for the system started at the metastable state $\hexagon$.

Theorem 6.1.2. (Asymptotic behavior of $\tau_{\hexagonblack}$). *For any* $\varepsilon > 0$, *we have*

$$\lim_{\beta\to\infty} \mathbb{P}_{\hexagon}\left(e^{\beta(\Gamma_H^* - \varepsilon)} < \tau_{\hexagonblack} < e^{\beta(\Gamma_H^* + \varepsilon)}\right) = 1, \tag{6.1.3}$$

$$\lim_{\beta\to\infty} \frac{1}{\beta} \log \mathbb{E}_{\hexagon}\tau_{\hexagonblack} = \Gamma_H^*. \tag{6.1.4}$$

Moreover, letting $T_\beta := \inf\{n \geqslant 1 : \mathbb{P}_{\hexagon}(\tau_{\hexagonblack} \leqslant n) \geqslant 1 - e^{-1}\}$, *we have*

$$\lim_{\beta\to\infty} \mathbb{P}_{\hexagon}(\tau_{\hexagonblack} > tT_\beta) = e^{-t} \tag{6.1.5}$$

and

$$\lim_{\beta\to\infty} \frac{\mathbb{E}_{\hexagon}\tau_{\hexagonblack}}{T_\beta} = 1. \tag{6.1.6}$$

We refer to Section 6.3.5 for the proof of Theorem 6.1.2. We recall that a function $\beta \mapsto f(\beta)$ is $\text{SES}(\beta)$ if it satisfies (1.3.80). With this notation we can state our first theorem concerning the recurrence of the system to either the state $\hexagon$ or $\hexagonblack$.

Theorem 6.1.3. (Recurrence property). *Let* $V^* = \Delta + U$, *we have* $\mathcal{X}_{V^*} \subseteq \{\hexagon, \hexagonblack\}$ *and for any* $\varepsilon > 0$ *and sufficiently large* β, *we have*

$$\beta \mapsto \sup_{\sigma\in\mathcal{X}} \mathbb{P}_\sigma(\tau_{\mathcal{X}_{V^*}} > e^{\beta(V^*+\varepsilon)}) \text{ is SES.} \tag{6.1.7}$$

Equation (6.1.7) implies that the system reaches with high probability either the state $\hexagon$ (which is a local minimizer of the Hamiltonian) or the ground state in a time shorter than $e^{\beta(V^*+\varepsilon)}$, uniformly in the starting configuration σ for any $\varepsilon > 0$. The proof of Theorem 6.1.3 follows from Proposition 6.3.1 and [85, Theorem 3.1] (see Section 6.3 for more details).

In order to characterize the gate for the transition, we recall Figure 1.25(a)(c) (resp. Figure 1.25(b)(d)) for an example of configurations in $\tilde{\mathcal{S}}(A^* - 1)$ (resp. $\tilde{\mathcal{D}}(A^* - 1)$). We refer the reader to Definitions 6.2.12 and 6.2.13 for a precise definition of these sets. Recall (1.3.68) for the definition of the set $\mathcal{K}(A^* - 1)$. The following theorem characterizes the gate for the transition from $\hexagon$ to $\hexagonblack$.

Theorem 6.1.4. (Gate for the transition). *Given* $\delta \in (0, 1)$ *and* $A^* \in \{A_1^*, A_2^*\}$ *as in* (6.1.2), *the set* $\mathcal{C}(A^*) := \mathcal{K}(A^* - 1)^{fp}$ *is a gate for the transition from* $\hexagon$ *to* $\hexagonblack$.

We refer to Section 6.3.5 for the proof of Theorem 6.1.4.

In order to state the last result of this section, we recall the set $\mathcal{E}_{B_i}(r)$ that contains the configurations which have a unique cluster with a shape of *quasi–regular hexagon*, that is a regular hexagon with i bars attached clockwise. See Figures 1.27 and 6.1 on the left–hand side and in the middle together with definitions 6.2.7, 6.2.8, 6.2.9 for more details.

Theorem 6.1.5. (Subcritical and supercritical quasi–regular hexagons). *Let* $\mathcal{E}^-_{B_i}(r)$ *(resp.* $\mathcal{E}^+_{B_i}(r)$*) be the set of configurations composed by a single quasi-regular hexagon contained in (resp. containing)* $\mathcal{E}_{B_i}(r)$. *For* $L > 2r^* + 3$, *the following statements hold:*

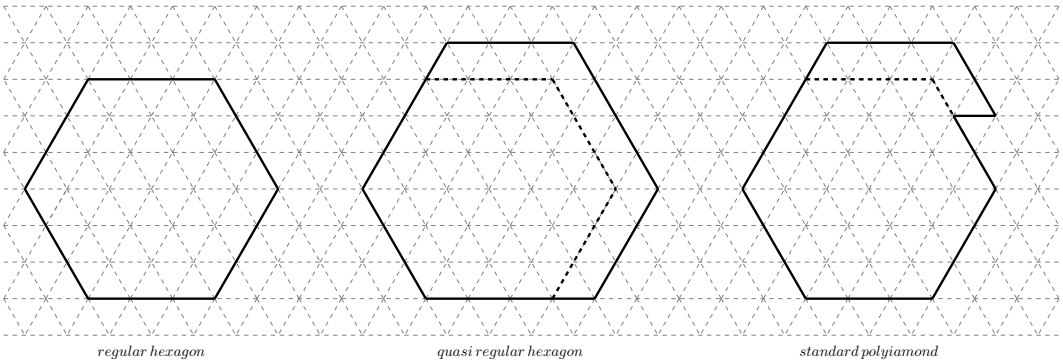

Figure 6.1 – Starting from the left: a regular hexagon with radius length 3, a quasi-regular hexagon with three bars attached clockwise from the top, a standard polyiamond with a complete bar attached on the top and an incomplete bar with cardinality 4 attached close to the top.

(i) If $\delta \in (0, \frac{1}{2})$*, we have*

$$\begin{aligned} &\text{if } \eta \in \mathcal{E}^{-}_{B_5}(r^*) \quad \Longrightarrow \lim_{\beta\to\infty} \mathbb{P}_\eta(\tau_{\hexagon} < \tau_{\hexagon\!\!\!\bullet}) = 1, \\ &\text{if } \eta \in \mathcal{E}^{+}_{B_0}(r^*+1) \quad \Longrightarrow \lim_{\beta\to\infty} \mathbb{P}_\eta(\tau_{\hexagon\!\!\!\bullet} < \tau_{\hexagon}) = 1. \end{aligned} \tag{6.1.8}$$

(ii) If $\delta \in (\frac{1}{2}, 1)$*, we have*

$$\begin{aligned} &\text{if } \eta \in \mathcal{E}^{-}_{B_1}(r^*+1) \quad \Longrightarrow \lim_{\beta\to\infty} \mathbb{P}_\eta(\tau_{\hexagon} < \tau_{\hexagon\!\!\!\bullet}) = 1, \\ &\text{if } \eta \in \mathcal{E}^{+}_{B_2}(r^*+1) \quad \Longrightarrow \lim_{\beta\to\infty} \mathbb{P}_\eta(\tau_{\hexagon\!\!\!\bullet} < \tau_{\hexagon}) = 1. \end{aligned} \tag{6.1.9}$$

In words, we characterize subcritical and supercritical quasi–regular hexagons, i.e., subcritical quasi–regular hexagons shrink to $\hexagon$, while supercritical quasi-regular hexagons grow to $\hexagon\!\!\!\bullet$. We refer to Section 6.3.6 for the proof of Theorem 6.1.5.

6.2 IDENTIFICATION OF MAXIMAL STABILITY LEVEL

6.2.1 *Extensive geometrical definitions*

Now we recall some geometrical definitions and properties about clusters and polyiamonds present in [4].

Definition 6.2.1. *A* polyiamond $P \subset \mathbb{R}^2$ *is a finite maximally connected union of three or more triangular units that share at least a side.*

Note that if two triangular units share only a point these are considered, by definition, two different polyiamonds. We define a new bijection that associates to each cluster a polyiamond with the same shape. This implies that to each cell without a particle, we associate an empty triangular unit.

Definition 6.2.2. *The* boundary *of a polyiamond* P *is the collection of unit edges of the lattice* $\mathbb{T}^2$ *such that each edge separates a triangular unit belonging to* P *from an empty triangular unit. The* edge-perimeter $p(P)$ *of a polyamond* P *is the cardinality of its boundary.*

In other words the perimeter is given by the number of interfaces on the discrete triangular lattice $\mathbb{T}^2$ between the sites inside the polyiamond and those outside. If not specified differently, we will refer to the edge–perimeter simply as perimeter.

Definition 6.2.3. *The* external boundary *of a polyiamond consists of the connected components of the boundary such that for each edge there exists a hexagonal–path in* $\mathbb{H}^2$ *which connects this edge with the boundary of* Λ *without intersecting the polyiamond. The* internal boundary *of a polyiamond consists of the connected components of the boundary that are not external.*

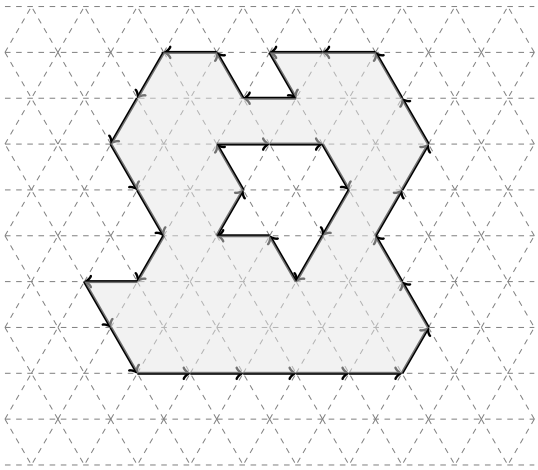

Figure 6.2 – An example of polyiamond with the external boundary oriented counter-clockwise and the internal boundary oriented clockwise.

Definition 6.2.4. *Let us orient counter-clockwise the external boundary and clockwise the internal boundary. For each pair of oriented edges, the angle defined rotating counter-clockwise the second edge on the first edge is called* internal angle *(see Figure 6.2).*

Definition 6.2.5. *A* hole *of a polyiamond* P *is a finite maximally connected component of empty triangular units surrounded by the internal boundary of* P.

We refer to holes consisting of a single empty triangle as *elementary holes*.

Definition 6.2.6. *A polyiamond is* regular *if it has only internal angles of* π *and* $\frac{2}{3}\pi$ *and it has no holes.*

We note that a regular polyiamond has the shape of a hexagon.

Definition 6.2.7. *A polyiamond is a* regular hexagon *if it is a regular polyiamond with all equal sides. We denote by* $E(r)$ *the regular hexagon, where* r *is its radius (see Figure 6.1 on the left-hand side).*

Definition 6.2.8. *A* bar $B(\ell)$ *with larger base* ℓ *is a set of* $\|B(\ell)\| = 2\ell - 1$ *triangular units obtained as a difference between an equilateral triangle with side length* l *and another equilateral triangle with side length* $\ell - 1$ *(see Figure 6.3).*

Definition 6.2.9. *We denote by* $E_{B_1}(r)$ *the polyiamond obtained attaching a bar* B_1 *along its larger base* r *to the regular hexagon (see Figure 6.4). Analogously, we denote by* $E_{B_i}(r)$ *for* $i = 2, ..., 5$ *the polyiamonds obtained attaching a bar* B_i *along its larger base* $r + 1$ *to* $E_{B_{i-1}}(r)$*. Finally, we denote by* $E_{B_6}(r)$ *the polyiamond obtained attaching a bar* B_6 *along its larger base* $r + 2$ *to* $E_{B_5}(r)$*. We call* $E_{B_i}(r)$ *a* quasi-regular hexagon*, where* r *is the radius of the regular hexagon* $E(r)$ *and* $i \in \{1, ..., 6\}$ *is the number of bars attached to it.*

Note that $E_{B_i}(r)$ is always contained in $E(r + 1)$ and it is defined up to a rotation of $z\frac{\pi}{3}$ for $z \in \mathbb{Z}$. Moreover $E(r) \equiv E_{B_0}(r)$ and $E(r + 1) \equiv E_{B_6}(r)$.

Notation 6.2.10. *We denote by* $\mathcal{E}(r)$ *the set of configurations* $\eta \in \mathcal{X}$ *such that* η *has a unique cluster with shape* $E(r)$*. We denote by* $\mathcal{E}_{B_i}(r)$ *the set of configurations* $\eta \in \mathcal{X}$ *such that* η *has a unique cluster with shape* $E_{B_i}(r)$.

Definition 6.2.11. *An* incomplete bar *of cardinality* $k < 2\ell - 1$ *is a subset of a bar with larger base* ℓ *(see Figure 6.5).*

Definition 6.2.12. *A* standard polyiamond *of area* A*, denoted by* $S(A)$*, is a quasi-regular hexagon* $E_{B_i}(r)$ *with possibly an additional incomplete bar of cardinality* k *attached clockwise, such that it is contained in* $E_{B_{i+1}}(r)$*. If* $k = 2$*, we denote it by* $\tilde{S}(A)$.

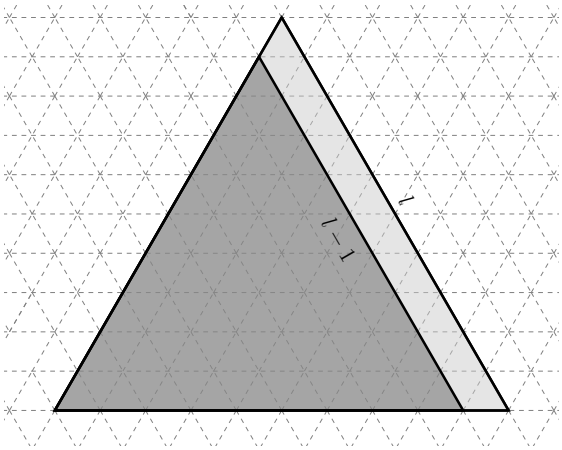

Figure 6.3 – The lightly shaded triangular units form a bar with larger base ℓ and it is obtained as difference between an equilateral triangle with side length l and an equilateral triangle with side length $\ell - 1$.

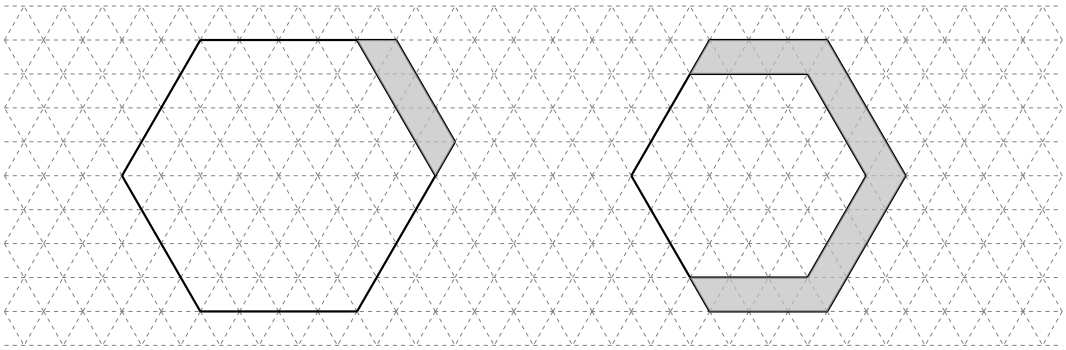

Figure 6.4 – On the left a quasi-regular hexagon $E_{B_1}(4)$. We observe that the cardinality of B_1 of $E_{B_1}(3)$ is $\|B_1\| = 2r - 1 = 5$. On the right a quasi-regular hexagon $E_{B_4}(3)$. We observe that the cardinality of B_1 of $E_{B_1}(3)$ is $\|B_1\| = 2r - 1 = 5$, while the cardinality of B_i of $E_{B_4}(3)$ is $\|B_i\| = 2r + 1 = 7$ with $i = 2, \dots, 4$.

When we refer to a *standard cluster* with area A, our meaning is that the cluster has the shape and the properties of a standard polyiamond $S(A)$. Note that a standard polyiamond $S(A)$ is determined solely by its area A. We characterize $S(A)$ in terms of its radius r, the number i of bars attached to the regular hexagon $E(r)$ to obtain $E_{B_i}(r)$ and the cardinality k of the possible incomplete bar. Starting from the area A, these values can be computed by using [4, algorithm 3.18].

Definition 6.2.13. *A polyiamond consisting of a quasi-regular hexagon with two triangular units attached to one of its longest sides at triangular lattice distance 2 one from the other is called* defective *and it is denoted by $\tilde{D}(A)$, where A is the area.*

Notation 6.2.14. *We denote by $\tilde{\mathcal{S}}(A)$ (resp. $\tilde{\mathcal{D}}(A)$) the set of configurations $\eta \in \mathcal{X}$ such that η has a unique cluster with shape $\tilde{S}(A)$ (resp. $\tilde{D}(A)$). See (a)(c) (resp. (b)(d)) in Figure 1.25 for examples of configurations in $\tilde{\mathcal{S}}(A)$ (resp. $\tilde{\mathcal{D}}(A)$).*

Definition 6.2.15. *We call a* corner *of a standard polyiamond P the pair of triangular faces of P contained in the internal angle of $\frac{2}{3}\pi$.*

6.2.2 *Reference path*

In this section, we construct our *reference path* ω^*, which is a sequence of configurations connecting $\hexagon$ and $\hexagonblack$ such that the maximum of the energy along this path is Γ^*_H. In particular, this path is composed by increasing clusters as close as possible to quasi-regular hexagonal

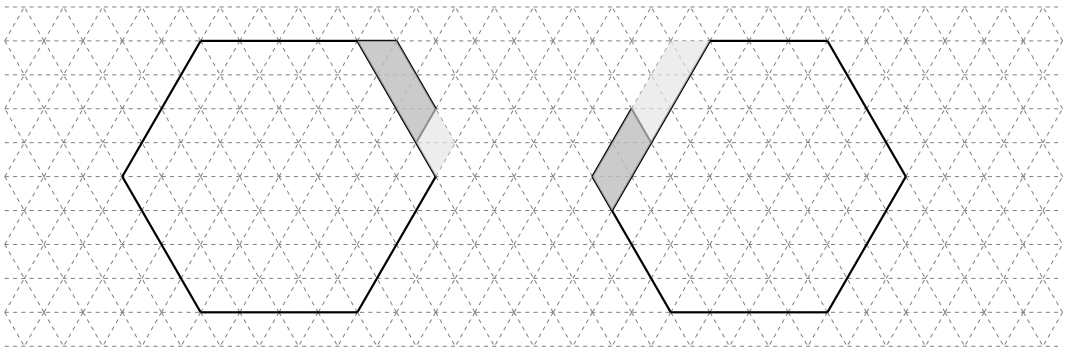

Figure 6.5 – On the left an incomplete bar with trapeze shape and cardinality $k = 5$ attached to the regular hexagon $E(4)$. We observe that the cardinality of the bar containing the incomplete bar is $\|B_1\| = 7 > k$. On the right an incomplete bar with parallelogram shape and cardinality $k = 4$, attached to the quasi-regular hexagon $E_{B_5}(3)$. We observe that the cardinality of the bar containing the incomplete bar is $\|B_6\| = 9 > k$.

shape. The idea of the construction of ω^* is the following: we first construct a skeleton path $\{\bar\omega_r\}_{r=0}^L$ given by a sequence of configurations that contain regular hexagon with radius r. Obviously $\bar\omega_r$ is not a path in the sense that the transition from $\bar\omega_r$ to $\bar\omega_{r+1}$ can not be given in a single step of the dynamics, since $\bar\omega_r$ and $\bar\omega_{r+1}$ contain regular hexagons. Thus in order to obtain a path we have to interpolate each transition of the skeleton path. This is done in two steps. First, we introduce between $\bar\omega_r$ and $\bar\omega_{r+1}$ a sequence of configurations $\tilde\omega_r^1, ..., \tilde\omega_r^{i_r}$ given by $\bar\omega_r$ plus a bar, i.e., a quasi–regular hexagon. Again, these configurations are given by a single increasing droplet. Finally, we introduce a second interpolation to obtain a path ω^* from the sequence of configurations $\tilde\omega_r^i$. Its construction goes as follows. Between every couple of consecutive configurations in $\tilde\omega$, for which the cluster is increased by one particle, a sequence of configurations with a new particle is inserted. In particular, the new particle is initially created at the boundary of Λ and then brought to the correct site via consecutive moves of this free particle.

Skeleton $\bar\omega$: Let us construct a sequence of configurations that contain regular hexagons $\bar\omega = \{\bar\omega_r\}$, with $r = 0, ..., L$, such that $\bar\omega_0 = \hexagon, ..., \bar\omega_L = \hexagon$ and $\bar\omega_r \subset \bar\omega_{r+1}$. Starting from the origin, given $r = 1, ..., L$ let $\bar\omega_r$ the regular hexagon with radius r, i.e., $\bar\omega_r \in \mathcal{E}(r)$.

First interpolation $\tilde\omega$: From $\bar\omega_0$ to $\bar\omega_1$, we define the path $\tilde\omega_0^i$ such that $\tilde\omega_0^0 = \bar\omega_0$ and insert between $\bar\omega_0$ and $\bar\omega_1$ a sequence of configurations $\{\tilde\omega_0^i\}_{i=0}^6$, which correspond to the creation of a hexagon of radius one obtained by adding sequentially particles clockwise. Given a choice for $\bar\omega_r$, with $r < L$, we can construct the path $\tilde\omega_r^i$ such that $\tilde\omega_r^0 = \bar\omega_r$ and insert between $\bar\omega_r$ and $\bar\omega_{r+1}$ a sequence of configurations $\{\tilde\omega_r^i\}_{i=0}^{i_r}$ as follows. Starting from a configuration in $\mathcal{E}(r)$, add consecutive triangular units to the regular hexagon until we obtain a configuration in $\mathcal{E}_{B_1}(r)$. Next we fill the bar on the top right adding consecutive triangular units until we obtain a configuration in $\mathcal{E}_{B_2}(r)$. We go on in the same way adding bars clockwise, until we obtain configurations in $\mathcal{E}_{B_3}(r), ..., \mathcal{E}_{B_6}(r) \equiv \mathcal{E}(r+1)$.

Second interpolation ω^*: For any pair of configurations $(\tilde\omega_r^i, \tilde\omega_r^{i+1})$ such that $\|\tilde\omega_r^i\| < \|\tilde\omega_r^{i+1}\|$, by construction of the path $\tilde\omega_r^i$ the particles are created along the external boundary of the clusters, except for the first particle that is at the origin. So there exist $x_1, ..., x_{j_i}$ a connected chain of nearest-neighbor empty sites of $\tilde\omega_r^i$ such that $x_1 \in \partial^-\Lambda$ and x_{j_i} is the site where is located the additional particle in $\tilde\omega_r^{i+1}$. Define

$$\hat\omega_r^{i,0} = \tilde\omega_r^i, \qquad \hat\omega_r^{i,j_i} = \tilde\omega_r^{i+1}, \quad r = 0, ..., L. \tag{6.2.1}$$

Insert between each pair $(\tilde\omega_r^i, \tilde\omega_r^{i+1})$ a sequence of configurations $\hat\omega_r^{i,j}$, with $j = 1, ..., j_i - 1$, where the free particle is moving from $x_1 \in \partial^-\Lambda$ to the cluster until it reaches the position x_{j_i}. Otherwise, for any pair of configurations $(\tilde\omega_r^i, \tilde\omega_r^{i+1})$ such that $\|\tilde\omega_r^i\| = \|\tilde\omega_r^{i+1}\|$, we define $\hat\omega_r^{i,0} = \tilde\omega_r^i$ and $\hat\omega_r^{i+1,0} = \tilde\omega_s^{i+1}$. This concludes the definition of the reference path.

With an abuse of notation we denote a configuration in $\mathcal{E}_{B_i}(r)$ by $\mathcal{E}_{B_i}(r)$.

Proposition 6.2.16. *The maximum of the energy in ω^* between two consecutive quasi–regular hexagons $\Phi_{\omega^*}(\mathcal{E}_{B_i}(r), \mathcal{E}_{B_{i+1}}(r))$ for every $i = 0, ..., 5$ is achieved in the standard polyiamond obtained adding to $\mathcal{E}_{B_i}(r)$ an elementary rhombus along the longest side and a free particle.*

Proof. Let $A^{(n)}$ be the area obtained after adding n triangular units to the area of the quasi-regular hexagon in $\mathcal{E}_{B_i}(r)$, where $n = 0, ..., \|B_{i+1}\|$. Note that $A^{(n)}$ is the area of the standard polyiamond $\mathcal{S}(A^{(n)})$. We observe that $S(A^{(0)}) = E_{B_i}(r)$ and $S(A^{(\|B_{i+1}\|)}) = E_{B_{i+1}}(r)$. Since the maximum of the energy is obtained after adding a free particle, we obtain

$$\widehat{H}(\mathcal{S}(A^{(n)})^{fp}) - \widehat{H}(\mathcal{S}(A^{(n-1)})^{fp}) = \begin{cases} \Delta - U & \text{if } n = 1, \\ \Delta - U & \text{if } n \text{ is even}, \\ \Delta - 2U & \text{if } n \neq 1 \text{ is odd}. \end{cases} \tag{6.2.2}$$

Therefore we deduce that

$$\widehat{H}(\mathcal{S}(A^{(n)})^{fp}) - \widehat{H}(\mathcal{E}_{B_i}(r)^{fp}) = \begin{cases} U - n\left(\frac{3}{2}U - \Delta\right) & \text{if } n \text{ is even}, \\ \frac{U}{2} - n\left(\frac{3}{2}U - \Delta\right) & \text{if } n \text{ is odd}. \end{cases} \tag{6.2.3}$$

Since the r.h.s. of the last equation decreases with n, due to the fact that $\Delta < \frac{3}{2}U$, in both the odd and even case, it is immediate to check that the maximum is attained for $n = 2$, namely in $\mathcal{S}(A^{(2)})^{fp}$. □

Proposition 6.2.17. *The maximum of the energy in ω^* between two consecutive quasi–regular hexagons $\Phi_{\omega^*}(\mathcal{E}_{B_i}(r), \mathcal{E}_{B_{i-1}}(r))$ for every $i = 1, ..., 6$ is achieved in the standard polyiamond obtained removing counter-clockwise from $\mathcal{E}_{B_i}(r)$ a number of particles equals to $\|B_i\| - 3$ and detaching the $(\|B_i\| - 2)$-th particle from B_i.*

Proof. Let $A^{(n)}$ be the area obtained after adding n triangular units to the area of the quasi-regular hexagon $E_{B_{i-1}}(r)$, where $n = 0, ..., \|B_i\|$. Note that $\mathcal{S}(A^{(n)})$ can be obtained either by removing $\|B_i\| - n$ triangular units from $\mathcal{E}_{B_i}(r)$ or by adding and attaching n triangular units to the quasi-regular hexagon in $\mathcal{E}_{B_{i-1}}(r)$. We recall that *removing* a triangular unit means detaching it from the cluster and moving the free particle outside Λ. Since the maximum of the energy is obtained after adding a free particle, we obtain

$$\widehat{H}(\mathcal{S}(A^{(n-1)})^{fp}) - \widehat{H}(\mathcal{S}(A^{(n)})^{fp}) = \begin{cases} 2U - \Delta & \text{if } n \neq 1 \text{ is odd}, \\ U - \Delta & \text{if } n \text{ is even}, \\ U - \Delta & \text{if } n = 1. \end{cases} \tag{6.2.4}$$

Therefore we deduce that

$$\widehat{H}(\mathcal{S}(A^{(n)})^{fp}) - \widehat{H}(\mathcal{E}_{B_i}(r)^{fp}) = \begin{cases} n\left(\frac{3}{2}U - \Delta\right) - U & \text{if } n \text{ is even}, \\ n\left(\frac{3}{2}U - \Delta\right) - \frac{U}{2} & \text{if } n \text{ is odd}. \end{cases} \tag{6.2.5}$$

Since the r. h. s. of the last equation increases with n, due to the fact that $\Delta < \frac{3}{2}U$, in both the odd and even case, it is immediate to check that the maximum is attained by removing $\|B_i\| - 3$ triangular units from $\mathcal{E}_{B_i}(r)$ and detaching another triangular unit from B_i. Therefore we obtain a configuration in $\mathcal{S}(A^{(2)})^{fp}$. □

Recalling (1.3.63), from now on the strategy is to divide the reference path ω^* into three regions depending on r:

— the region $r \leqslant r^*$ will be considered in Proposition 6.2.18;
— the region $r = r^* + 1$ will be considered in Proposition 6.2.19;
— the region $r \geqslant r^* + 2$ will be considered in Proposition 6.2.20

Proposition 6.2.18. *If $r \leqslant r^*$, then the communication height between two consecutive regular hexagons $\Phi_{\omega^*}(\mathcal{E}(r), \mathcal{E}(r+1))$ along the path ω^* is achieved in a configuration with a free particle and a standard cluster such that the number of its triangular units is $\tilde{A} = 6r^2 + 10r + 5$, that is $\Phi_{\omega^*}(\mathcal{E}(r), \mathcal{E}(r+1)) = \Phi_{\omega^*}(\mathcal{E}_{B_5}(r), \mathcal{E}(r+1)) = \widehat{H}(\mathcal{S}(\tilde{A})) + \Delta$. Moreover, $\Phi_{\omega^*}(\hexagon, \mathcal{E}(r^*+1)) = \Phi_{\omega^*}(\mathcal{E}(r^*), \mathcal{E}(r^*+1)) = \widehat{H}(\mathcal{S}(A_1^* - 1)) + \Delta$ is achieved in a configuration with a free particle and a standard cluster $S(A_1^* - 1)$, where $A_1^* = 6(r^*)^2 + 10r^* + 6$.*

Proof. Let $S(A)$ be a standard polyiamond with an incomplete bar of cardinality two. We obtain:

$$\widehat{H}(\mathcal{S}(A)) = \begin{cases} -3(3r^2 - r)U + 6r^2\Delta + 2(\Delta - U) & \text{if } A = 6r^2 + 2, \\ -3(3r^2 - r)U + 6r^2\Delta + (2r+1)\Delta - 3rU & \text{if } A = 6r^2 + 2r + 1, \\ -3(3r^2 - r)U + 6r^2\Delta + 2(2r+1)\Delta - (6r+1)U & \text{if } A = 6r^2 + 4r + 2, \\ -3(3r^2 - r)U + 6r^2\Delta + 3(2r+1)\Delta - (9r+2)U & \text{if } A = 6r^2 + 6r + 3, \\ -3(3r^2 - r)U + 6r^2\Delta + 4(2r+1)\Delta - (12r+3)U & \text{if } A = 6r^2 + 8r + 4, \\ -3(3r^2 - r)U + 6r^2\Delta + 5(2r+1)\Delta - (15r+4)U & \text{if } A = 6r^2 + 10r + 5. \end{cases} \tag{6.2.6}$$

We compare $\Phi_{\omega^*}(\mathcal{E}(r), \mathcal{E}_{B_1}(r)) = \Phi_{\omega^*}(\mathcal{S}(6r^2), \mathcal{S}(6r^2 + 2r - 1))$ with $\Phi_{\omega^*}(\mathcal{E}_{B_1}(r), \mathcal{E}_{B_2}(r)) = \Phi_{\omega^*}(\mathcal{S}(6r^2 + 2r - 1), \mathcal{S}(6r^2 + 4r))$. By Proposition 6.2.16 we have:

$$\begin{aligned} \Phi_{\omega^*}(\mathcal{E}(r), \mathcal{E}_{B_1}(r)) &= \widehat{H}(\mathcal{S}(6r^2 + 2)) + \Delta, \\ \Phi_{\omega^*}(\mathcal{E}_{B_1}(r), \mathcal{E}_{B_2}(r)) &= \widehat{H}(\mathcal{S}(6r^2 + 2r + 1)) + \Delta. \end{aligned} \tag{6.2.7}$$

By using (6.2.6), we obtain that $\Phi_{\omega^*}(\mathcal{E}(r), \mathcal{E}_{B_1}(r)) \leqslant \Phi_{\omega^*}(\mathcal{E}_{B_1}(r), \mathcal{E}_{B_2}(r))$ if and only if $r \leqslant \frac{2U-\Delta}{3U-2\Delta} = \frac{U}{2(3U-2\Delta)} + \frac{1}{2}$, which is true since we are assuming $r \leqslant r^*$ and $r^* \leqslant \frac{2U-\Delta}{3U-2\Delta}$ due to the condition $2\Delta < 3U$.

We compare the two communication heights $\Phi_{\omega^*}(\mathcal{E}_{B_1}(r), \mathcal{E}_{B_2(r)}) = \Phi_{\omega^*}(\mathcal{S}(6r^2 + 2r - 1), \mathcal{S}(6r^2 + 4r))$ and $\Phi_{\omega^*}(\mathcal{E}_{B_2}(r), \mathcal{E}_{B_3(r)}) = \Phi_{\omega^*}(\mathcal{S}(6r^2 + 4r), \mathcal{S}(6r^2 + 6r + 1))$. By Proposition 6.2.16 we have:

$$\begin{aligned} \Phi_{\omega^*}(\mathcal{E}_{B_1}(r), \mathcal{E}_{B_2}(r)) &= \widehat{H}(\mathcal{S}(6r^2 + 2r + 1)) + \Delta, \\ \Phi_{\omega^*}(\mathcal{E}_{B_2}(r), \mathcal{E}_{B_3}(r)) &= \widehat{H}(\mathcal{S}(6r^2 + 4r + 2)) + \Delta. \end{aligned} \tag{6.2.8}$$

By using (6.2.6), we obtain that $\Phi_{\omega^*}(\mathcal{E}_{B_1}(r), \mathcal{E}_{B_2}(r)) \leqslant \Phi_{\omega^*}(\mathcal{E}_{B_2}(r), \mathcal{E}_{B_3}(r))$ if and only if $r \leqslant \frac{\Delta-U}{3U-2\Delta}$, which is true since we are assuming $r \leqslant r^*$.

We compare the communication heights $\Phi_{\omega^*}(\mathcal{E}_{B_2}(r), \mathcal{E}_{B_3(r)}) = \Phi_{\omega^*}(\mathcal{S}(6r^2 + 4r), \mathcal{S}(6r^2 + 6r + 1))$ and $\Phi_{\omega^*}(\mathcal{E}_{B_3}(r), \mathcal{E}_{B_4(r)}) = \Phi_{\omega^*}(\mathcal{S}(6r^2 + 6r + 1), \mathcal{S}(6r^2 + 8r + 2))$. By Proposition 6.2.16 we have:

$$\begin{aligned} \Phi_{\omega^*}(\mathcal{E}_{B_2}(r), \mathcal{E}_{B_3}(r)) &= \widehat{H}(\mathcal{S}(6r^2 + 4r + 2)) + \Delta, \\ \Phi_{\omega^*}(\mathcal{E}_{B_3}(r), \mathcal{E}_{B_4}(r)) &= \widehat{H}(\mathcal{S}(6r^2 + 6r + 3)) + \Delta. \end{aligned} \tag{6.2.9}$$

By using (6.2.6), we obtain that $\Phi_{\omega^*}(\mathcal{E}_{B_2}(r), \mathcal{E}_{B_3}(r)) \leqslant \Phi_{\omega^*}(\mathcal{E}_{B_3}(r), \mathcal{E}_{B_4}(r))$ if and only if $r \leqslant \frac{\Delta-U}{3U-2\Delta}$, which is true since we are assuming $r \leqslant r^*$.

By performing similar computations, we obtain the following inequalities:

$$\begin{aligned} \Phi_{\omega^*}(\mathcal{E}_{B_3}(r), \mathcal{E}_{B_4}(r)) &\leqslant \Phi_{\omega^*}(\mathcal{E}_{B_4}(r), \mathcal{E}_{B_5}(r)), \\ \Phi_{\omega^*}(\mathcal{E}_{B_4}(r), \mathcal{E}_{B_5}(r)) &\leqslant \Phi_{\omega^*}(\mathcal{E}_{B_5}(r), \mathcal{E}(r+1)). \end{aligned} \tag{6.2.10}$$

Thus, the communication height between two consecutive regular hexagons along the path ω^* is achieved in $\mathcal{S}(6r^2 + 10r + 5)^{fp}$, that is $\Phi_{\omega^*}(\mathcal{E}(r), \mathcal{E}(r+1)) = \Phi_{\omega^*}(\mathcal{E}_{B_5}(r), \mathcal{E}(r+1)) = \widehat{H}(\mathcal{S}(\tilde{A})) + \Delta$, where $\tilde{A} = 6r^2 + 10r + 5$. The maximum of the function $\widehat{H}(\mathcal{S}(\tilde{A})) + \Delta = -3(3r^2 - r)U + 6r^2\Delta + 5(2r+1)\Delta - (15r+4)U + \Delta$ is obtained in $r = \frac{U}{2(3U-2\Delta)} - \frac{5}{6}$. However $r \in \mathbb{N}$ and $r \leqslant r^*$, therefore the maximum is attained in r^* and $\Phi_{\omega^*}(\hexagon, \mathcal{E}(r+1)) = \Phi_{\omega^*}(\mathcal{E}(r^*), \mathcal{E}(r^*+1)) = \widehat{H}(\mathcal{S}(A_1^* - 1)) + \Delta$, where $A_1^* = 6(r^*)^2 + 10r^* + 6$. □

Proposition 6.2.19. *If $r = r^* + 1$, then the communication height $\Phi_{\omega^*}(\mathcal{E}(r^*+1), \mathcal{E}(r^*+2))$ along the path ω^* is achieved in a configuration with a free particle and a standard cluster $S(A_2^* - 1)$, where $A_2^* = 6(r^*+1)^2 + 2(r^*+1) + 2$.*

Proof. Note that in this case $r = \left\lfloor \frac{U}{2(3U-2\Delta)} + \frac{1}{2} \right\rfloor$. We analyze $\Phi_{\omega^*}(\mathcal{E}(r^*+1), \mathcal{E}(r^*+2))$ by using Proposition 6.2.16. We compare the same communication height of Proposition 6.2.18, obtaining the following inequalities since $r = r^* + 1$:

$$\Phi_{\omega^*}(\mathcal{S}(6r^2), \mathcal{S}(6r^2+2r-1)) < \Phi_{\omega^*}(\mathcal{S}(6r^2+2r-1), \mathcal{S}(6r^2+4r)), \tag{6.2.11}$$

and

$$\begin{aligned} \Phi_{\omega^*}(\mathcal{S}(6r^2+2r-1), \mathcal{S}(6r^2+4r)) &> \Phi_{\omega^*}(\mathcal{S}(6r^2+4r), \mathcal{S}(6r^2+6r+1)) \\ &> \Phi_{\omega^*}(\mathcal{S}(6r^2+6r+1), \mathcal{S}(6r^2+8r+2)) \\ &> \Phi_{\omega^*}(\mathcal{S}(6r^2+8r+2), \mathcal{S}(6r^2+10r+3)) \\ &> \Phi_{\omega^*}(\mathcal{S}(6r^2+10r+3), \mathcal{S}(6r^2+12r+6)). \end{aligned} \tag{6.2.12}$$

Then the communication height along the path ω^* between two consecutive regular hexagons with radius r^*+1 is $\Phi_{\omega^*}(\mathcal{E}(r^*+1), \mathcal{E}(r^*+2)) = \Phi_{\omega^*}(\mathcal{S}(6(r^*+1)^2 + 2(r^*+1) - 1), \mathcal{S}(6(r^*+1)^2 + 4(r^*+1)))$ and, by Proposition 6.2.16, it is attained in $\mathcal{S}(A_2^* - 1)^{fp}$, with $A_2^* = 6(r^*+1)^2 + 2(r^*+1) + 2$. □

Proposition 6.2.20. *If $r \geqslant r^* + 2$, then the communication height between two consecutive regular hexagons $\Phi_{\omega^*}(\mathcal{E}(r), \mathcal{E}(r+1))$ along the path ω^* is achieved in a configuration with a free particle and a standard cluster such that the number of its triangular units is $\tilde{A} = 6r^2 + 2$, that is $\Phi_{\omega^*}(\mathcal{E}(r), \mathcal{E}(r+1)) = \Phi_{\omega^*}(\mathcal{E}(r), \mathcal{E}_{B_1}(r)) = \widehat{H}(\mathcal{S}(\tilde{A})) + \Delta$. Moreover, $\Phi_{\omega^*}(\mathcal{E}(r^*+2), \hexagon) = \Phi(\mathcal{E}(r^*+2), \mathcal{E}(r^*+3)) = \widehat{H}(\mathcal{S}(A_3^* - 1)) + \Delta$ is achieved in a configuration with a free particle and a standard cluster $S(A_3^* - 1)$, where $A_3^* = 6(r^*+2)^2 + 3$.*

Proof. We analyze $\Phi_{\omega^*}(\mathcal{E}(r), \mathcal{E}(r+1))$ by using Proposition 6.2.16. We compare the same communication height of Proposition 6.2.18, obtaining the following inequalities since $r \geqslant r^* + 2$:

$$\begin{aligned} \Phi_{\omega^*}(\mathcal{S}(6r^2), \mathcal{S}(6r^2+2r-1)) &\geqslant \Phi_{\omega^*}(\mathcal{S}(6r^2+2r-1), \mathcal{S}(6r^2+4r)) \\ &\geqslant \Phi_{\omega^*}(\mathcal{S}(6r^2+4r), \mathcal{S}(6r^2+6r+1)) \\ &\geqslant \Phi_{\omega^*}(\mathcal{S}(6r^2+6r+1), \mathcal{S}(6r^2+8r+2)) \\ &\geqslant \Phi_{\omega^*}(\mathcal{S}(6r^2+8r+2), \mathcal{S}(6r^2+10r+3)) \\ &\geqslant \Phi_{\omega^*}(\mathcal{S}(6r^2+10r+3), \mathcal{S}(6r^2+12r+6)). \end{aligned} \tag{6.2.13}$$

Thus, the communication height between two consecutive regular hexagons along the path ω^* is attained in $\mathcal{S}(6r^2+2)^{fp}$, that is $\Phi_{\omega^*}(\mathcal{E}(r), \mathcal{E}(r+1)) = \Phi_{\omega^*}(\mathcal{E}(r), \mathcal{E}_{B_1}(r)) = \widehat{H}(\mathcal{S}(\tilde{A})) + \Delta$, where $\tilde{A} = 6r^2 + 2$. The maximum of the function $\widehat{H}(\mathcal{S}(\tilde{A})) + \Delta = -3(3r^2 - r)U + 6r^2\Delta + 2(\Delta - U) + \Delta$ is attained in $r = \frac{U}{2(3U-2\Delta)}$, but $r \in \mathbb{N}$ and $r \geqslant r^* + 2$, so $\Phi_{\omega^*}(\mathcal{E}(r^*+2), \hexagon) = \Phi_{\omega^*}(\mathcal{E}(r^*+2), \mathcal{E}(r^*+3)) = \widehat{H}(\mathcal{S}(A_3^* - 1)) + \Delta$, where $A_3^* = 6(r^*+2)^2 + 3$. □

Proposition 6.2.21. *Let $\delta \in (0,1)$ be such that $\frac{U}{2(3U-2\Delta)} - \frac{1}{2} - \delta$ is an integer number. The maximum $\Phi_{\omega^*}(\hexagon, \hexagon)$ along the path ω^* is attained in a configuration with a free particle and a standard cluster with area $A^* - 1$ (see Figure 6.6), where*

1) *$A^* = A_1^* = 6(r^*)^2 + 10r^* + 6$ if $0 < \delta < \frac{1}{2}$;*
2) *$A^* = A_2^* = 6(r^*+1)^2 + 2(r^*+1) + 2$ if $\frac{1}{2} < \delta < 1$.*

Proof. We compare $\Phi_{\omega^*}(\hexagon, \mathcal{E}(r^*+1))$, $\Phi_{\omega^*}(\mathcal{E}(r^*+1), \mathcal{E}(r^*+2))$ and $\Phi_{\omega^*}(\mathcal{E}(r^*+2), \hexagon)$. By Proposition 6.2.18 we have

$$\begin{aligned} \Phi_{\omega^*}(\hexagon, \mathcal{E}(r^*+1)) &= \widehat{H}(\mathcal{S}(6(r^*)^2 + 10r^* + 5)) + \Delta \\ &= -3(3(r^*)^2 - r^*)U + 6(r^*)^2\Delta + 5(2r^*+1)\Delta - (15r^*+4)U + \Delta. \end{aligned}$$

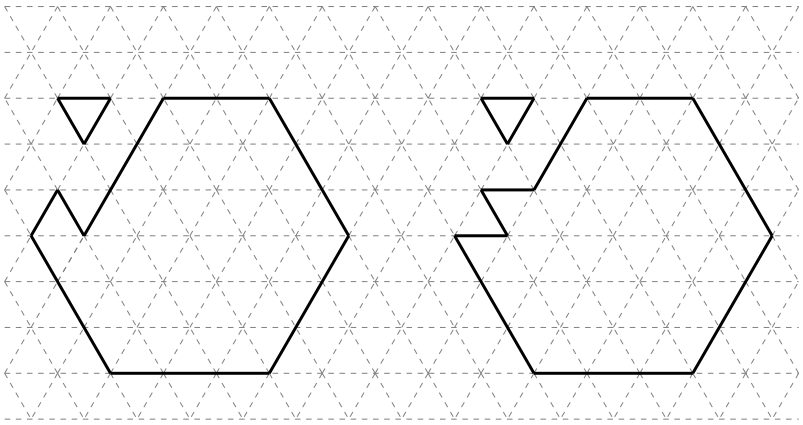

Figure 6.6 – Two standard clusters with critical area $A_1^* - 1$ and a free particle for $0 < \delta < \frac{1}{2}$.

(6.2.14)

By Proposition 6.2.19 we have

$$\begin{aligned}\Phi_{\omega^*}(\mathcal{E}(r^*+1),\mathcal{E}(r^*+2)) &= \widehat{H}(\mathcal{S}(6(r^*+1)^2+2(r^*+1)+1))+\Delta\\ &= -3(3(r^*+1)^2-(r^*+1))U+6(r^*+1)^2\Delta\\ &\quad +(2(r^*+1)+1)\Delta-3(r^*+1)U+\Delta.\end{aligned} \tag{6.2.15}$$

By Proposition 6.2.20 we have

$$\begin{aligned}\Phi_{\omega^*}(\mathcal{E}(r^*+2),\hexagon) &= \widehat{H}(\mathcal{S}(6(r^*+2)^2+2))+\Delta\\ &= -3(3(r^*+2)^2-(r^*+2))U+6(r^*+2)^2\Delta+2(\Delta-U)+\Delta.\end{aligned} \tag{6.2.16}$$

By comparing equations (6.2.14),(6.2.15) and (6.2.16), we obtain

$$\begin{aligned}\Phi_{\omega^*}(\hexagon,\mathcal{E}(r^*+1)) &> \Phi_{\omega^*}(\mathcal{E}(r^*+2),\hexagon),\\ \Phi_{\omega^*}(\mathcal{E}(r^*+1),\mathcal{E}(r^*+2)) &> \Phi_{\omega^*}(\mathcal{E}(r^*+2),\hexagon).\end{aligned} \tag{6.2.17}$$

Thus we deduce that $\Phi_{\omega^*}(\mathcal{E}(r^*+2),\hexagon)$ cannot be the maximum. Moreover, we obtain

$$\begin{aligned}&\Phi_{\omega^*}(\hexagon,\mathcal{E}(r^*+1)) > \Phi_{\omega^*}(\mathcal{E}(r^*+1),\mathcal{E}(r^*+2)) \quad \text{if } 0<\delta<\tfrac{1}{2},\\ &\Phi_{\omega^*}(\hexagon,\mathcal{E}(r^*+1)) < \Phi_{\omega^*}(\mathcal{E}(r^*+1),\mathcal{E}(r^*+2)) \quad \text{if } \tfrac{1}{2}<\delta<1.\end{aligned} \tag{6.2.18}$$

and therefore the maximum $\Phi_{\omega^*}(\hexagon,\hexagon) = \Phi_{\omega^*}(\hexagon,\mathcal{E}(r^*+1))$ is achieved in a configuration $\mathcal{S}(6(r^*)^2+10r^*+5)^{fp}$ if $\delta \in (0,\frac{1}{2})$. Otherwise, if $\delta \in (\frac{1}{2},1)$, then the maximum $\Phi_{\omega^*}(\hexagon,\hexagon) = \Phi_{\omega^*}(\mathcal{E}(r^*+1),\mathcal{E}(r^*+2))$ is achieved in a configuration $\mathcal{S}(6(r^*+1)^2+2(r^*+1)+1)^{fp}$. □

Corollary 6.2.22. *Let Γ_H^* as in (6.1.1). We have*

$$\Phi(\hexagon,\hexagon) \leqslant \Gamma_H^*. \tag{6.2.19}$$

Proof. By definition of communication height and the fact that $\widehat{H}(\hexagon) = 0$, Proposition 6.2.21 implies that

$$\Phi(\hexagon,\hexagon) \leqslant \max_i \widehat{H}(\omega_i^*) = \Gamma_H^* \tag{6.2.20}$$

in the two cases $0 < \delta < \frac{1}{2}$ and $\frac{1}{2} < \delta < 1$. □

6.2.3 *Lower bound of maximal stability level*

In this section we will find a lower bound for Γ_H^*. In particular, we prove that $\Phi(\hexagon,\hexagon) \geqslant \Gamma_H^*$ separately for the case $\delta \in (0,\frac{1}{2})$ and $\delta \in (\frac{1}{2},1)$. The proof comes in three steps, which are the contents of the three following lemmas. The last result of this section combines the upper and lower bound on $\Phi(\hexagon,\hexagon)$ which we have found.

Lemma 6.2.23. *The following statements hold:*

1. *If* $\delta \in \left(0, \frac{1}{2}\right)$, *any* $\omega \in (\hexagon \to \hexagon)_{\mathrm{opt}}$ *must pass through the set* $\mathcal{E}_{B_5}(r^*)$.
2. *If* $\delta \in \left(\frac{1}{2}, 1\right)$, *any* $\omega \in (\hexagon \to \hexagon)_{\mathrm{opt}}$ *must pass through the set* $\mathcal{E}_{B_1}(r^* + 1)$.

Proof. We analyze separately the two cases.

1. Let $\delta \in \left(0, \frac{1}{2}\right)$ and $\tilde{A} = 6(r^*)^2 + 10r^* + 3$. Any path $\omega : \hexagon \to \hexagon$ must cross the set $\mathcal{V}_{\tilde{A}}$. By using [4, Theorem 3.22] and [4, Lemma 3.24] with $m = 5$, in $\mathcal{V}_{\tilde{A}}$ the unique (modulo translations and rotations) configuration of minimal perimeter and hence minimal energy is the standard polyiamond $S(\tilde{A})$, which contains only the quasi-regular hexagon. Thus, the configuration $\mathcal{S}(\tilde{A})$ has energy
$$\begin{aligned} \widehat{H}(\mathcal{S}(\tilde{A})) &= -3(3(r^*)^2 - r^*)U + 6(r^*)^2\Delta + 5(2r^* + 1)\Delta - (15r^* + 1)U \\ &= \Gamma^*_H - 3\Delta + 2U. \end{aligned} \tag{6.2.21}$$
All the other configurations in $\mathcal{V}_{\tilde{A}}$ have energy at least $\Gamma^*_H - 3\Delta + 3U$. To increase the particle number starting from any such a configuration, we must create a particle at cost Δ. But the resulting configuration would have energy $\Gamma^*_H - 2\Delta + 3U$, which exceeds Γ^*_H due to the condition $2\Delta < 3U$. Thus, this would lead to a path exceeding the energy value Γ^*_H and therefore the path would not be optimal.
2. Let $\delta \in \left(\frac{1}{2}, 1\right)$ and $\tilde{A} = 6(r^* + 1)^2 + 2(r^* + 1) - 1$. By observing that [4, Lemma 3.24] holds with $m = 1$, we can argue as before.

□

Lemma 6.2.24. *The following statements hold:*

1. *If* $\delta \in \left(0, \frac{1}{2}\right)$, *any* $\omega \in (\hexagon \to \hexagon)_{\mathrm{opt}}$ *must pass through a configuration composed by a cluster* $E_{B_5}(r^*)$ *with the addition of two triangular faces.*
2. *If* $\delta \in \left(\frac{1}{2}, 1\right)$, *any* $\omega \in (\hexagon \to \hexagon)_{\mathrm{opt}}$ *must pass through a configuration composed by a cluster* $E_{B_1}(r^* + 1)$ *with the addition of two triangular faces.*

Proof. We analyze the two cases separately.

1. Follow the path until it hits $\mathcal{V}_{A^*_1 - 3}$. By Lemma 6.2.23, the configuration in this set must be a quasi-regular hexagon with area $6(r^*)^2 + 10r^* + 3$. Since we need not consider any paths that return to the set $\mathcal{V}_{A^*_1 - 3}$ afterwards and the path has to cross the set $\mathcal{V}_{A^*_1 - 1}$, the path proceeds as follows. Starting from a quasi-regular hexagon with area $A^*_1 - 3$, a free particle is created giving rise to a configuration with energy $\Gamma^*_H - 2\Delta + 2U < \Gamma^*_H$. Before any new particle is created, the energy has to decrease by at least U. The unique way to do this is to move the particle towards the cluster and attach it to the quasi-regular hexagon, which lowers the energy to $\Gamma^*_H - 2\Delta + U$. Now it is possible to create another particle at cost Δ giving rise to a configuration with energy $\Gamma^*_H - \Delta + U < \Gamma^*_H$. Again, before creating a new particle, the energy has to decrease by at least U. The unique way to do this is to move the particle until it is attached to the cluster, which lowers the energy to $\Gamma^*_H - \Delta$. Note that this gives us a configuration composed by a cluster $E_{B_5}(r^*)$ with the addition of two triangular faces, as claimed.
2. We can argue as in the previous case.

□

Lemma 6.2.25. *Any* $\omega \in (\hexagon \to \hexagon)_{\mathrm{opt}}$ *must reach the energy* Γ^*_H.

Proof. By Lemma 6.2.24, we know that any $\omega \in (\hexagon \to \hexagon)_{\mathrm{opt}}$ must cross a configuration composed by two triangular faces attached to a cluster $E_{B_5}(r^*)$ (resp. $E_{B_1}(r^* + 1)$) if $\delta \in \left(0, \frac{1}{2}\right)$ (resp. $\delta \in \left(\frac{1}{2}, 1\right)$). Starting from such a configuration, it is impossible to reduce the energy without lowering the particle number. Indeed, [4, Theorem 3.22] asserts that, for $\delta \in \left(0, \frac{1}{2}\right)$ (resp. $\delta \in \left(\frac{1}{2}, 1\right)$), the minimal energy in $\mathcal{V}_{A^*_1 - 1}$ (resp. $\mathcal{V}_{A^*_2 - 1}$) is realized (although not uniquely) in such a configuration. Since any further move to increase the particles number involves the creation of a new particle, the energy must reach the value Γ^*_H. □

Corollary 6.2.26. *We have*
$$\Phi(\hexagon, \hexagon) = \Gamma^*_H. \tag{6.2.22}$$

Proof. Combining Corollary 6.2.22 and Lemma 6.2.25, we obtain the claim. □

6.2.4 *Structure of the communication level set*

Recalling the two values of the critical area in (6.1.2), we have the following result.

Proposition 6.2.27. *The following statements hold:*

1. *Let* $\delta \in \left(0, \frac{1}{2}\right)$ *and* $A^* = A_1^* = 6(r^*)^2 + 10r^* + 6$. *Any* $\omega \in (\hexagon \to \hexagonblack)_{opt}$ *must pass through the set* $\mathcal{C}(A^*) = \mathcal{K}(A^* - 1)^{fp}$.
2. *Let* $\delta \in \left(\frac{1}{2}, 1\right)$ *and* $A^* = A_2^* = 6(r^* + 1)^2 + 2(r^* + 1) + 2$, *any* $\omega \in (\hexagon \to \hexagonblack)_{opt}$ *must pass through the set* $\mathcal{C}(A^*) = \mathcal{K}(A^* - 1)^{fp}$.

Proof. We analyze the two cases separately.

1. By Lemmas 6.2.23 and 6.2.24, we can obtain a configuration η_0 with a cluster according to the following cases:
   (1) the two triangular faces form an elementary rhombus which is attached to one of the longest sides of the quasi-regular hexagonal cluster, namely the resulting configuration is in $\tilde{\mathcal{S}}(A^* - 1)$ (see Figure 1.28);
   (2) the two triangular faces are attached to one of the longest sides of the quasi-regular hexagonal cluster at triangular lattice distance 2, namely the resulting configuration is in $\tilde{\mathcal{D}}(A^* - 1)$ (see Figure 1.28);
   (3) the two triangular faces are attached to the same side of the quasi-regular hexagonal cluster at triangular lattice distance greater than 2 (see Figure 1.28);
   (4) the two triangular faces are attached to two different sides of the quasi-regular hexagonal cluster (see Figure 1.28);
   (5) the two triangular faces form an elementary rhombus which is attached to one of the sides, other than the longest, of the quasi-regular hexagonal cluster;
   (6) the two triangular faces are attached at triangular lattice distance 2 to the same side, other than the longest, of the quasi-regular hexagonal cluster;
   (7) the two triangular faces form an elementary rhombus which is attached to one of the sides, but the direction of the elementary rhombus is towards the outer direction of the cluster.

   Note that in all these cases the cluster has minimal perimeter, indeed it has the same perimeter as a standard hexagon with the same area. Moreover, in all these cases the configuration η_0 has energy $\Gamma_H^* - \Delta$. We will prove that every $\omega \in (\hexagon \to \hexagonblack)_{opt}$ crosses a configuration in $\mathcal{C}(A^*)$. Since we need not consider any paths that return to the set $\mathcal{V}_{A_1^*-2}$ afterwards and the energy can increase by at most Δ in order to have an optimal path, there are only the following possibilities:
   A. a free particle enters Λ;
   B. a particle is detached from the cluster;
   C. a particle moves at cost U without detaching from the cluster.
   Case A. We may assume that the free particle does not exit from Λ, otherwise we can iterate this argument for a finite number of steps since the path has to reach $\hexagonblack$. Let $\eta_1 = \eta_0^{fp}$. Since $\widehat{H}(\eta_1) = \Gamma_H^*$, in order to have an optimal path the energy cannot increase. Thus the unique admissible moves are the movement of the free particle at zero cost and the attachment of the particle to the cluster. We may assume that the particle attaches to the cluster, otherwise we can iterate this argument.
   In cases (1) and (2), note that η_1 contains an internal angle of $\frac{5}{3}\pi$, thus we consider the configuration η_2 obtained from η_1 by attaching the free particle to cover the internal angle of $\frac{5}{3}\pi$ of the cluster (see Figure 1.28). Thus the energy decreases by $2U$ and therefore it is possible to create a new particle without exceeding the energy value Γ_H^*. Indeed, let η_3 be the configuration obtained from η_2 by creating a new particle, thus we obtain:

$$\begin{aligned} \widehat{H}(\eta_3) &= (\widehat{H}(\eta_3) - \widehat{H}(\eta_2)) + (\widehat{H}(\eta_2) - \widehat{H}(\eta_1)) + \widehat{H}(\eta_1) \\ &= \Gamma_H^* + \Delta - 2U < \Gamma_H^*. \end{aligned} \tag{6.2.23}$$

   From now on the path proceeds as the reference path ω^* without exceeding the energy value Γ_H^*. Note that the path crosses the set $\mathcal{C}(A^*)$ in the configuration η_1.

In cases (5) and (6), since η_1 contains an internal angle of $\frac{5}{3}\pi$, it is possible that the free particle attaches to the cluster at cost $-2U$. If this occurs, we can derive (6.2.23) as before, but we show that now it is not possible to reach ⬣ without exceeding Γ^*_H unless the path reaches a configuration η_0 as in cases (1) or (2). Any side s of $E_{B_5}(r^*)$, other than the longest, has length r^*+1, so the bar B with the larger base r^*+1 has cardinality $\ell = 2r^*-1$. We can write

$$\omega = (⬡, ..., \tilde{\eta}, ..., \eta_0, \eta_1, ..., \eta_{i_\ell}, ..., \eta_{i_{\ell+1}}, ..., \eta_{i_{\ell+2}}, \bar{\eta}, ..., ⬣), \tag{6.2.24}$$

where $\tilde{\eta} = \mathcal{E}_{B_5}(r^*)$, η_0 and η_1 are as above, η_{i_ℓ} is the configuration obtained after filling the new bar B and creating a free particle, $\eta_{i_{\ell+1}}$ is the configuration obtained from η_{i_ℓ} by attaching the free particle and afterwards creating another free particle, and $\eta_{i_{\ell+2}}$ is the configuration obtained from $\eta_{i_{\ell+1}}$ by attaching the free particle to the cluster. Finally, let $\bar{\eta}$ the configuration obtained from $\eta_{i_{\ell+2}}$ by creating a free particle. Thus we obtain the following contradiction:

$$\begin{aligned}\widehat{H}(\bar{\eta}) &= (\widehat{H}(\bar{\eta}) - \widehat{H}(\eta_{i_{\ell+2}})) + (\widehat{H}(\eta_{i_{\ell+2}}) - \widehat{H}(\eta_{i_{\ell+1}})) + (\widehat{H}(\eta_{i_{\ell+1}}) - \widehat{H}(\eta_{i_\ell})) \\ &\quad + (\widehat{H}(\eta_{i_\ell}) - \widehat{H}(\eta_1)) + \widehat{H}(\eta_1) \\ &= \Delta - U + (\Delta - U) + ((2r^*-3)\Delta + (4-3r^*)U) + \Gamma^*_H > \Gamma^*_H.\end{aligned} \tag{6.2.25}$$

Therefore, starting from the configuration η_1, after attaching the protuberance at cost $-2U$ the path cannot sequentially create and attach a particle to the cluster: this follows from (6.2.25). Thus the path has to further lower the energy before reaching the configuration $\eta_{i_{\ell+2}}$. If the path reaches a configuration ξ such that $n(\xi) = 0$, i.e., ξ has no free particle, a free particle has been attached and the energy lowered by $2U$ at most, but this does not suffice due to (6.2.25). But there are no moves that further lower the energy. If the path reaches a configuration ξ such that $n(\xi) = 1$, then the unique way to lower the energy is to attach the free particle at cost $-2U$ or $-U$, but again this does not suffice due to (6.2.25). Since the path ω has to reach ⬣ and therefore the number of particles has to increase, the unique possibility in order to have an optimal path is that the path ω comes back to the configuration η_0. Thus, we are done as claimed before.
If the particle attaches at cost $-U$, motions of particles at cost U can take place. The unique possibility to first move a particle at cost U is to attach it to the elementary rhombus (see Figure 1.23(a)), otherwise it is possible to move the last attached protuberance, but in this case we can iterate the argument. All the configurations that are crossed during these motions have energy either Γ^*_H or $\Gamma^*_H - U$. Since the energy has to further lower in order to create a new particle and reach ⬣, the unique possibility is to detach a protuberance at cost U and attach it to cover the unique internal angle of $\frac{5}{3}\pi$ (see Figure 1.23(b)). Thus, we can argue as before for cases (5) and (6).
In cases (3), (4) and (7) note that the configuration η_1 does not contain an internal angle of $\frac{5}{3}\pi$, thus the free particle can attach only at cost $-U$. Let η_2 be the configuration obtained from η_1 by attaching the free particle to the cluster at cost $-U$, thus $\widehat{H}(\eta_2) = \Gamma^*_H - U$. Note that now the unique admissible moves are those at cost U at most, thus it is not possible to create a new particle before further lowering the energy.
In cases (3) and (7), since the path has to reach ⬣, the unique possibility is to move a protuberance T in such a way it forms an angle of $\frac{5}{3}\pi$ with another protuberance. If the two protuberances in configuration η_0 are not on the longest side, we are left to analyze case A for a configuration η_2 as in cases (5) or (6) and therefore we can argue as before. If the two protuberances in configuration η_0 are on the longest side, we obtain a configuration composed by a cluster as in case (1) or (2) with the addition of a protuberance. As explained before, it is possible that motions at cost U take place. All the configurations that are crossed during these motions have energy either Γ^*_H or $\Gamma^*_H - U$. At the end of these motions, there are only the two following possibilities: there is a unique cluster with an internal angle of $\frac{5}{3}\pi$ and either a free particle (see Figure 1.23(d)) or a single protuberance (see Figure 1.23(c)). In the first case, the configuration that is obtained is in $\mathcal{C}(A^*)$. In the latter case, since the energy has to further lower in order to create a new particle and reach ⬣, the unique possibility is to

detach the single protuberance at cost U and attach to the cluster at cost $-2U$. When the protuberance is detached the path crosses the set $\mathcal{C}(A^*)$.
In case (4), if the third protuberance is attached in such a way all the three protuberances are attached to different sides, then the unique admissible moves are detaching a protuberance. Thus we can iterate this argument for a finite number of steps, since the path has to reach ⬣. We are left to consider the case in which at least two protuberances are attached to the same side. We can argue as above.
Case B. Let η_1 be the configuration obtained from η_0 by detaching a particle from a cluster. Since $\widehat{H}(\eta_0) = \Gamma^*_H - \Delta$ and the path ω has to be optimal, the energy can increase by U at most. Thus, only a protuberance can be detached. After that, only moves with cost 0 at most are admissible. Since the path has to reach ⬣ and therefore the free particle cannot move for infinite time at zero cost, the unique possibility is to attach the free particle to the cluster. Thus we obtain a configuration that is analogue to η_0 and we can iterate this argument for a finite number of steps, until we come back to case A.
Case C. Note that this case is admissible only for configurations η_0 as in cases (1), (2), (5) or (6). Since $\widehat{H}(\eta_0) = \Gamma^*_H - \Delta$ and the path ω has to be optimal, the energy can increase by U at most.
In cases (1) or (2), starting from η_0, all the configurations that can be obtained without exceeding the energy value Γ^*_H are in the set $\mathcal{K}(A^* - 1)$: this directly follows from the definition of that set given in (1.3.68) since no particle is detached from the cluster. From now on, since the energy of the last configuration is $\Gamma^*_H - \Delta$, it is possible either to create a free particle, or to detach a protuberance at cost U, or to move a particle at cost U. In the first case, we can conclude as in case A. Note that the path ω crosses the set $\mathcal{C}(A^*)$ when the free particle is created. In the second case, we can conclude as in case B. In the latter case, we can iterate this argument for a finite number of steps.
In cases (5) or (6), we can argue as for the cases (1) or (2). Indeed, the same kind of motions can take place, but when the free particle is created, we can argue as in the case A for η_1 as in cases (5) or (6). This concludes the proof.

2. The proof of this case is similar to the previous one.

□

6.3 RECURRENCE PROPERTY

The goal of this section is to prove Theorem 6.1.3. Recall (3.1.6) for the definition of stability level. The following theorem states that every configuration of $\mathcal{X}$ different from ⬡ and ⬣ has a stability level $\Delta + U$ at most.

Proposition 6.3.1. *Let $\eta \in \mathcal{X}$ be a configuration such that $\eta \notin \{⬡, ⬣\}$, then $V_\eta \leqslant \Delta + U$.*

An immediate consequence of Proposition 6.3.1 is that the only configurations with a stability level greater than $\Delta + U$ are ⬡ and ⬣, as reported in Theorem 6.1.3. The proof of Proposition 6.3.1 is divided in two steps. First of all, in Section 6.3.1 we prove that the configurations with peculiar geometrical properties has a stability level smaller than or equal to $\Delta + U$ (see Lemmas 6.3.2-6.3.7), and then in Section 6.3.2 we show that all configurations, different from ⬡ and ⬣, has a stability level smaller than or equal to $\Delta + U$, i.e., $\mathcal{X}_{\Delta+U} \setminus \{⬡, ⬣\} = \emptyset$ (see Lemma 6.3.8).

6.3.1 *Configurations with stability level $\Delta + U$ at most*

Recall (3.1.8) for the definition of V-irreducible states. In this Section, we emphasize the different stability level for configurations depending on their particular geometrical properties. For the proof of the lemmas we refer to Section 6.3.3. The following lemma characterizes the configurations in $\mathcal{X}_0$.

Lemma 6.3.2. *Any configuration $\eta \in \mathcal{X}_0$ has no free particles.*

In order to state the following lemmas, we need the following definition. Moreover, recall Definition 6.2.5 for the definition of a hole.

Figure 6.7 – On the left-hand side we depict an example of the cluster in a configuration of Z, while on the right-hand side an example of the cluster in a configuration of R.

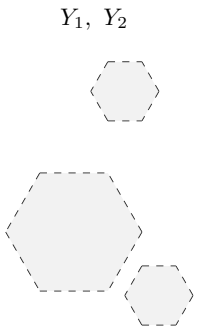

Figure 6.8 – An example of clusters in a configuration of Y.

Definition 6.3.3. *Two clusters are called* interacting *if their lattice distance is two. Otherwise, two clusters are called* non-interacting *if its lattice distance is strictly greater than 2.*

Lemma 6.3.4. *If a configuration σ contains a cluster with an internal angle of $\frac{1}{3}\pi$ and no free particles, no holes and no interacting clusters, then it has a stability level smaller than or equal to U, i.e., $\sigma \notin \mathcal{X}_U$.*

Lemma 6.3.5. *If a configuration σ contains a cluster with an internal angle of $\frac{5}{3}\pi$ and no free particles, no holes and no interacting clusters, then it has a stability level smaller than or equal to Δ, i.e., $\sigma \notin \mathcal{X}_\Delta$.*

Lemma 6.3.6. *If a configuration σ contains a cluster with an internal angle of $\frac{4}{3}\pi$ and no free particles, no holes and no interacting clusters, then it has a stability level smaller than or equal to $2\Delta - U$, i.e., $\sigma \notin \mathcal{X}_{2\Delta-U}$.*

The next lemma investigates the case in which a configuration contains two interacting clusters or a cluster with a hole.

Lemma 6.3.7. *If a configuration σ contains two interacting clusters or a cluster with a hole, then it has a stability level smaller than or equal to $\Delta + U$, i.e., $\sigma \notin \mathcal{X}_{\Delta+U}$.*

6.3.2 *Identification of configurations in $\mathcal{X}_{\Delta+U}$*

In Section 6.3.1, we established that the configurations with particular geometrical properties has a stability level $\Delta + U$ at most. The configurations, that do not satisfy Lemma 6.3.2 and Lemma 6.3.7, has no free particle and no interacting clusters. Moreover, the configurations, that do not satisfy Lemmas 6.3.4-6.3.6, contain clusters with internal angles of π and $\frac{2}{3}\pi$ only. Thus, the clusters contained in these configurations have an hexagonal shape. Now, we partition the set of remaining configurations, different from ⬡ and ⬢, into three subsets Z, R, Y and we prove that also these configurations has a stability level smaller than or equal to $\Delta + U$. Thus, it follows that if there exists a configuration with a stability level strictly greater than $\Delta + U$, then it is ⬡ or ⬢.

Z is the set of configurations consisting of a single quasi–regular hexagonal cluster (see Figure 6.7 on the left-hand side). More precisely, $Z = Z_1 \cup Z_2$, where:

— Z_1 is the collection of configurations such that there exists only one cluster with shape $E_{B_m}(r) \subset \Lambda$ with $r \leqslant r^*$ and $m \in \{0, 1, 2, 3, 4, 5\}$;

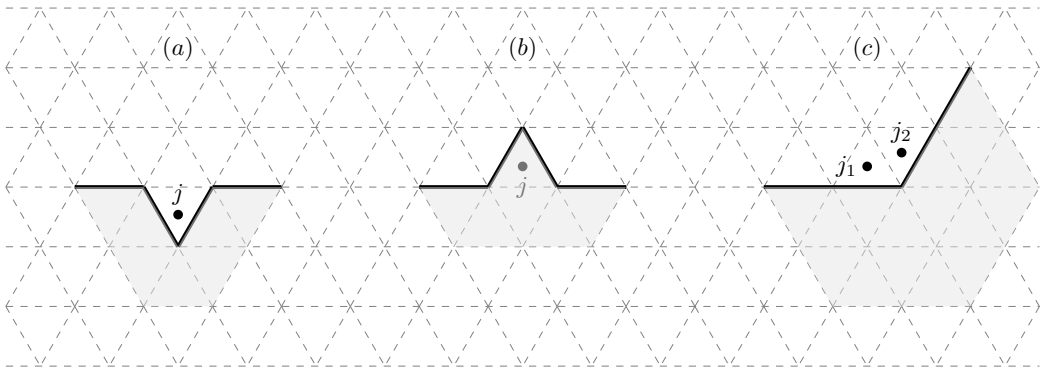

Figure 6.9 – On the left-hand side (resp. center) we depict the site j when σ has an internal angle of $\frac{5}{3}\pi$ (resp. $\frac{1}{3}\pi$). On the right-hand side we depict the two sites j_1, j_2 when σ has an internal angle of $\frac{4}{3}\pi$.

— Z_2 is the collection of configurations such that there exists only one cluster with shape $E_{B_m}(r) \subset \Lambda$ with $r \geqslant r^* + 1$ and $m \in \{0, 1, 2, 3, 4, 5\}$.

We define the set R to be the set of configurations consisting of a single hexagonal cluster (see Figure 6.7 on the right-hand side). Formally, $R = R_1 \cup R_2$, where:

— R_1 is the collection of configurations such that there exists only one cluster with hexagonal shape $E \subset \Lambda$ such that it contains the greatest quasi-regular hexagon with radius $r \leqslant r^*$;

— R_2 is the collection of configurations such that there exists only one cluster with hexagonal shape $E \subset \Lambda$ such that it contains the greatest quasi–regular hexagon with radius $r \geqslant r^* + 1$.

The set Y contains all configurations with more than one hexagonal cluster of the types in Z_1, Z_2, R_1, R_2 (see Figure 6.8). More precisely, we have $Y = Y_1 \cup Y_2$, where:

— Y_1 is the collection of configurations such that there exists a family of non–interacting clusters with hexagonal shape such that it contains the greatest quasi-regular hexagon with radius $r \leqslant r^*$;

— Y_2 is the collection of configurations such that there exists a family of clusters with at least one having hexagonal shape containing the greatest quasi–regular hexagon with radius $r \geqslant r^* + 1$.

In other words, Y_1 contains a collection of clusters of the same type of those in Z_1 or R_1, and Y_2 contains a collection of clusters where at least one is of the same type of those in Z_2 or R_2.

Lemma 6.3.8. *If $\sigma \in Z \cup R \cup Y$, then $V_\sigma \leqslant \Delta + U$.*

We refer to Section 6.3.3 for the proof of this lemma.

6.3.3 *Proof of Lemmas*

Proof of Lemma 6.3.2. If η has a free particle, then η is obviously 0-reducible, i.e., its stability level is 0 and therefore $\eta \notin \mathcal{X}_0$. Indeed, the reducing path is immediately obtained by bringing the free particle outside Λ or attaching it to a cluster. □

Proof of Lemma 6.3.4. Let σ be a configuration as in the statement and let $C(\sigma)$ be a cluster with an internal angle $\alpha = \frac{1}{3}\pi$. Let j be a site such that $\sigma(j) = 1$ and that belongs to the closed triangular face of $C(\sigma)$ intersecting its boundary in two edges (see Figure 6.9(b)). We define η as the configuration obtained from σ by detaching the particle in j and then moving it outside Λ. Note that it is possible to bring the particle outside Λ since σ does not contain clusters with holes or interacting clusters. We construct a path $\omega : \sigma \to \eta$ as

$$\omega = (\sigma, \xi_1, \xi_2, ..., \xi_n, \eta), \tag{6.3.1}$$

where ξ_1 is the configuration obtained from σ by moving the particle at site j in one of the two empty nearest-neighbor sites. The cost of this move is U. Then the particle, after being

detached, can be brought outside Λ passing through the configurations $\xi_2, ..., \xi_n$, possibly interacting with other clusters. We need to bring the particle outside Λ because the energy does not necessarily decreases by $2U$ when the particle interacts with the clusters during the motion. Note that the energy of the configurations $\xi_2, ..., \xi_n$ is $\widehat{H}(\xi_1)$ at most. Thus we obtain

$$\widehat{H}(\eta) - \widehat{H}(\sigma) = U - \Delta < 0, \tag{6.3.2}$$

where the inequality follows from the condition $\Delta > U$. Thus, η belongs to $\mathcal{I}_\sigma$ and $V_\sigma \leqslant U$. □

Proof of Lemma 6.3.5. Let σ be a configuration as in the statement and let $C(\sigma)$ be a cluster with an internal angle $\alpha = \frac{5}{3}\pi$. Let j be the site at distance one to a site in $C(\sigma)$ such that $\sigma(j) = 0$ and that belongs to the closed triangular face intersecting the boundary of $C(\sigma)$ in two or more edges (see Figure 6.9(a)). We define η as the configuration obtained by σ after creating a particle and then attaching it in the site j. Note that it is possible to bring the particle from the boundary of Λ towards the site j since σ does not contain clusters with holes or interacting clusters. We construct a path ω connecting σ and η as

$$\omega = (\sigma, \xi_1, \xi_2, ..., \xi_n, \eta), \tag{6.3.3}$$

where ξ_1 is the configuration obtained from σ by creating a particle in $\partial^-\Lambda$ at cost Δ. Then, this particle moves towards the cluster $C(\sigma)$, passing through the configurations $\xi_2, ..., \xi_n$, until it is attached in the site j at cost $-2U$ giving rise to the configuration η. Note that the energy of the configurations $\xi_2, ..., \xi_n$ is $\widehat{H}(\xi_1)$ at most. Thus we obtain

$$\widehat{H}(\eta) - \widehat{H}(\sigma) = \Delta - 2U < 0, \tag{6.3.4}$$

where the inequality follows from $\Delta < \frac{3}{2}U$. Thus, η belongs to $\mathcal{I}_\sigma$ and $V_\sigma \leqslant \Delta$. □

Proof of Lemma 6.3.6. Let σ be a configuration as in the statement and let $C(\sigma)$ be a cluster with an internal angle $\alpha = \frac{4}{3}\pi$. Let j_1, j_2 be two sites such that $\sigma(j_1) = \sigma(j_2) = 0$, $d(j_1, j_2) = 1$ and let each of them belong to one closed triangular face intersecting the boundary of $C(\sigma)$ in one edge (see Figure 6.9(c)). We define η as the configuration obtained by σ after the following sequence of moves: creation of a particle and movement of it until it is attached in the site j_1; creation of another particle and movement of it until it is attached in the site j_2. Note that it is possible to bring particles from the boundary of Λ towards the sites j_1 and j_2 since σ does not contain clusters with holes. We construct a path ω connecting σ and η as

$$\omega = (\sigma, \xi_{i_1}, \xi_{i_2}, ..., \xi_{i_n}, \xi, \xi_{j_1}, ..., \xi_{j_m}, \eta), \tag{6.3.5}$$

where ξ_{i_1} is the configuration obtained from σ by creating a particle in $\partial^-\Lambda$ at cost Δ. Then, this particle moves towards the cluster $C(\sigma)$, passing through the configurations $\xi_{i_2}, ..., \xi_{i_n}$, until it is attached in the site j_1 at cost $-U$ giving rise to the configuration ξ. Note that the energy of the configurations $\xi_{i_2}, ..., \xi_{i_n}$ is $\widehat{H}(\xi_{i_1})$ at most. The configuration ξ_{j_1} is obtained from ξ by creating a particle in $\partial^-\Lambda$ at cost Δ. Then, this particle moves towards the cluster $C(\sigma)$, passing through the configurations $\xi_{j_2}, ..., \xi_{j_m}$, until it is attached in the site j_2 at cost $-2U$ giving rise to the configuration η. Note that the energy of the configurations $\xi_{j_2}, ..., \xi_{j_m}$ is $\widehat{H}(\xi_{j_1})$ at most. Thus we obtain

$$\widehat{H}(\eta) - \widehat{H}(\sigma) = 2\Delta - 3U < 0, \tag{6.3.6}$$

where the inequality follows from $\Delta < \frac{3}{2}U$. Thus, η belongs to $\mathcal{I}_\sigma$ and $V_\sigma \leqslant 2\Delta - U$. □

Proof of Lemma 6.3.7. We analyze the configuration σ starting from the clusters with minimal distance to the boundary of Λ. If the first clusters $C_1(\sigma)$ and $C_2(\sigma)$, according to this minimal distance, are interacting, we consider the shared vertex $v := C_1(\sigma) \cap C_2(\sigma)$ on the triangular lattice, see the first and the second pictures in Figure 6.10. We let into Λ a particle and we call σ_1 this new configuration. Then this new particle moves until it is attached to v giving rise to the configuration σ_2. In this way, there are two possibilities:

(i) the triangular face of this particle shares an edge with $C_1(\sigma)$, an edge with $C_2(\sigma)$ and contains v, see the second picture in Figure 6.10;

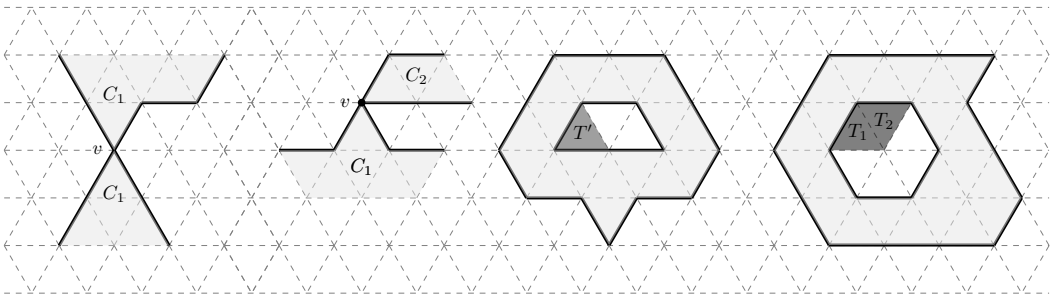

Figure 6.10 – Here we represent clusters in light grey. In the first two pictures we depict two interacting clusters C_1 and C_2, while in the third one (resp. fourth one) we depict an example of configuration belonging to case 2 (resp. case 3) in the proof of Lemma 6.3.7.

(ii) the triangular face of this particle contains v and shares an edge either with $C_1(\sigma)$ or $C_2(\sigma)$, see the first picture in Figure 6.10.

Case (i). We have

$$\begin{aligned} \widehat{H}(\sigma_1) - \widehat{H}(\sigma) &= \Delta, \\ \widehat{H}(\sigma_2) - \widehat{H}(\sigma_1) &= -2U \end{aligned} \tag{6.3.7}$$

and therefore

$$\widehat{H}(\sigma_2) - \widehat{H}(\sigma) = [\widehat{H}(\sigma_2) - \widehat{H}(\sigma_1)] + [\widehat{H}(\sigma_1) - \widehat{H}(\sigma)] = -2U + \Delta < 0. \tag{6.3.8}$$

Thus, the stability level of σ in this case is $V_\sigma = \Delta$.

Case (ii). We may assume without loss of generality that the triangular face T of the new particle shares an edge with $C_1(\sigma)$. We have that

$$\begin{aligned} \widehat{H}(\sigma_1) - \widehat{H}(\sigma) &= \Delta, \\ \widehat{H}(\sigma_2) - \widehat{H}(\sigma_1) &= -U \end{aligned} \tag{6.3.9}$$

and therefore

$$\widehat{H}(\sigma_2) - \widehat{H}(\sigma) = -U + \Delta > 0. \tag{6.3.10}$$

since $\Delta > U$. Thus, the energy has to further lower. We define the configuration σ_3 as the one obtained from σ_2 by creating a new particle. Then this particle moves towards the cluster until it is attached close to the triangular face T in such a way it is attached also to the cluster $C_2(\sigma)$. This configuration is called σ_4. Thus, we have

$$\begin{aligned} \widehat{H}(\sigma_3) - \widehat{H}(\sigma_2) &= \Delta, \\ \widehat{H}(\sigma_4) - \widehat{H}(\sigma_3) &= -2U. \end{aligned} \tag{6.3.11}$$

It follows that

$$\begin{aligned} \widehat{H}(\sigma_4) - \widehat{H}(\sigma) &= [\widehat{H}(\sigma_4) - \widehat{H}(\sigma_3)] + [\widehat{H}(\sigma_3) - \widehat{H}(\sigma_2)] \\ &\quad + [\widehat{H}(\sigma_2) - \widehat{H}(\sigma_1)] + [\widehat{H}(\sigma_1) - \widehat{H}(\sigma)] \\ &= -3U + 2\Delta < 0 \end{aligned} \tag{6.3.12}$$

and the stability level of σ in this case is $V_\sigma = 2\Delta - U$.

Thus, we conclude that the stability level for a configuration with two interacting clusters is $\max\{\Delta, 2\Delta - U\} = 2\Delta - U$.

Next, suppose that the first clusters are not interacting. Let $C(\sigma)$ be the first cluster of σ with a hole. Consider one of the empty triangular faces in the hole that share at least an edge with the cluster. There are three cases:

1. the empty triangular face shares three edges with the cluster;

2. the empty triangular face shares two edges with the cluster, which we represent with the dark grey triangular face T' in the third picture in Figure 6.10;
3. the empty triangular face shares only one edge with the cluster, which we represent with the dark grey triangular face T_1 in the fourth picture in Figure 6.10.

In the first case, we move the empty triangular face until it reaches the internal boundary of the cluster. Since every triangular face in the internal boundary of the cluster shares at least an edge with the empty triangular faces outside the cluster, then

$$\widehat{H}(\eta) - \widehat{H}(\sigma) \leqslant -U, \tag{6.3.13}$$

where η is the configuration obtained from σ by exchanging the empty triangular face of the hole with a triangular face on the internal boundary of the cluster. Thus, $V_\sigma = 0$.

In the second case, as before, we move the empty triangular face T' until it reaches the internal boundary of the cluster giving rise to the configuration σ_1. If σ and σ_1 can be connected via one step of the dynamics, then the energy value remains the same. Otherwise, during the first step, the energy increases by U, indeed the empty triangular face T' can be detached from the other empty triangular face by breaking two bonds and creating only a new bond (see the third picture in Figure 6.10). Thus in both cases it holds that $\widehat{H}(\sigma_1) - \widehat{H}(\sigma) \leqslant U$. Moreover, every triangular face in the internal boundary of the cluster shares one or two edges with the empty triangular face outside the cluster.

— If there exists a triangular face T in the internal boundary of the cluster $C(\sigma)$ with two shared edges with some empty triangular faces, then, denoting by η the configuration obtained from σ_1 by exchanging the empty triangular face of the hole with T, we have

$$\widehat{H}(\eta) - \widehat{H}(\sigma_1) = -2U, \tag{6.3.14}$$

$$\widehat{H}(\eta) - \widehat{H}(\sigma) = [\widehat{H}(\eta) - \widehat{H}(\sigma_1)] + [\widehat{H}(\sigma_1) - \widehat{H}(\sigma)] \leqslant -U. \tag{6.3.15}$$

Thus, $V_\sigma = U$.

— Otherwise, if each triangular face in the internal boundary has only one shared edge with an empty triangular face outside cluster, then we have

$$\widehat{H}(\sigma_2) - \widehat{H}(\sigma_1) = -U, \tag{6.3.16}$$

where σ_2 is the configuration obtained from σ_1 by exchanging the empty triangular face of the hole with a triangular face in the internal boundary of the cluster. Thus, we obtain $\widehat{H}(\sigma_2) = \widehat{H}(\sigma)$, and by construction σ_2 has an internal angle of $\frac{5}{3}\pi$ (see Figure 6.9(a)). We define a configuration σ_3 obtained from σ_2 by getting in Λ a new particle, and we define σ_4 from σ_3 by moving and attaching this particle to cover the internal angle of $\frac{5}{3}\pi$. We have

$$\begin{aligned} \widehat{H}(\sigma_3) - \widehat{H}(\sigma_2) &= \Delta, \\ \widehat{H}(\sigma_4) - \widehat{H}(\sigma_3) &= -2U \end{aligned} \tag{6.3.17}$$

and therefore

$$\begin{aligned} \widehat{H}(\sigma_4) - \widehat{H}(\sigma) &= [\widehat{H}(\sigma_4) - \widehat{H}(\sigma_3)] + [\widehat{H}(\sigma_3) - \widehat{H}(\sigma_2)] + [\widehat{H}(\sigma_2) - \widehat{H}(\sigma)] \\ &\leqslant -2U + \Delta < 0. \end{aligned} \tag{6.3.18}$$

Thus, $V_\sigma = \Delta$.

In the third case, the empty triangular face T_1 has only one shared edge with the cluster, so there exists another empty triangular face T_2 in the hole that is connected with T_1. We move the two empty triangular faces until they reach the internal boundary of the cluster giving rise to the configuration σ_1. If σ and σ_1 can be connected via one step of the dynamics, then the energy value increases by U. Otherwise, during the first step, the energy increases by $2U$, indeed the empty triangular face moves T_1 from the other empty triangular face by breaking two bonds (see the fourth picture in Figure 6.10). Thus in both cases we have that

$$\widehat{H}(\sigma_1) - \widehat{H}(\sigma) \leqslant 2U. \tag{6.3.19}$$

Moreover, every triangular face in the internal boundary of the cluster shares one or two edges with the empty triangular faces outside the cluster, and we proceed as in the previous case.

— If there exist two triangular faces T, T' in the internal boundary of the cluster $C(\sigma)$ such that they both share two edges with some empty triangular faces, then we denote by η the configuration obtained from σ_1 by exchanging the empty triangular face of the hole with T. We have

$$\widehat{H}(\eta) - \widehat{H}(\sigma_1) = -2U, \tag{6.3.20}$$

$$\widehat{H}(\eta) - \widehat{H}(\sigma) = [\widehat{H}(\eta) - \widehat{H}(\sigma_1)] + [\widehat{H}(\sigma_1) - \widehat{H}(\sigma)] \leqslant 0. \tag{6.3.21}$$

Then, in a similar way, we move the empty triangular face T_2 until the internal boundary of the cluster in T'. During the first step, the energy possibly increases by U as in the second case. If we denote by η_1 this configuration, then we have $\widehat{H}(\eta_1) - \widehat{H}(\eta) \leqslant U$. Moreover, T' has two shared edges with some empty triangular face, then, denoting by ξ the configuration obtained from η_1 by exchanging the empty triangular face of the hole with T, we have

$$\widehat{H}(\xi) - \widehat{H}(\eta_1) = -2U, \tag{6.3.22}$$

$$\widehat{H}(\xi) - \widehat{H}(\eta) = [\widehat{H}(\xi) - \widehat{H}(\eta_1)] + [\widehat{H}(\eta_1) - \widehat{H}(\eta)] \leqslant -U. \tag{6.3.23}$$

Thus, we obtain

$$\widehat{H}(\xi) - \widehat{H}(\sigma) = [\widehat{H}(\xi) - \widehat{H}(\eta)] + [\widehat{H}(\eta) - \widehat{H}(\sigma)] = -U \tag{6.3.24}$$

and therefore by (6.3.19) it follows that $V_\sigma = 2U$.

— If there exists only one triangular face T such that it shares two edges with some triangular face outside of the cluster, then we define the configurations σ_1, η, η_1 and ξ as before. Since now $\widehat{H}(\xi) - \widehat{H}(\eta_1) = -U$, we obtain $\widehat{H}(\xi) - \widehat{H}(\sigma) = 0$. By construction ξ has an internal angle of $\frac{5}{3}\pi$, see Figure 6.9(a). We define a configuration ξ_1 obtained from ξ by getting in Λ a new particle, and we define ξ_2 as the configuration obtained from ξ_1 by moving and attaching this particle to cove the internal angle of $\frac{5}{3}\pi$. We have

$$\begin{aligned} \widehat{H}(\xi_1) - \widehat{H}(\xi) &= \Delta, \\ \widehat{H}(\xi_2) - \widehat{H}(\xi_1) &= -2U \end{aligned} \tag{6.3.25}$$

and therefore

$$\widehat{H}(\xi_2) - \widehat{H}(\sigma) = [\widehat{H}(\xi_2) - \widehat{H}(\xi_1)] + [\widehat{H}(\xi_1) - \widehat{H}(\xi)] + [\widehat{H}(\xi) - \widehat{H}(\sigma)] = -2U + \Delta. \tag{6.3.26}$$

Thus, by (6.3.19) $V_\sigma = 2U$.

— If each triangular face in the internal boundary has only one shared edge with an empty triangular face outside cluster, then we have

$$\widehat{H}(\sigma_2) - \widehat{H}(\sigma_1) = -U, \tag{6.3.27}$$

where σ_2 is the configuration obtained from σ_1 by exchanging the empty triangular face of the hole with a triangular face T_1 in the internal boundary of the cluster. Thus, we obtain $\widehat{H}(\sigma_2) - \widehat{H}(\sigma) \leqslant U$, and by construction σ_2 has an internal angle of $\frac{5}{3}\pi$ (see Figure 6.9(a)). We define a configuration σ_3 obtained from σ_2 by getting in Λ a new particle, and we define σ_4 as the configuration obtained from σ_3 by moving and attaching this particle to cover the internal angle of $\frac{5}{3}\pi$. We have

$$\begin{aligned} \widehat{H}(\sigma_3) - \widehat{H}(\sigma_2) &= \Delta, \\ \widehat{H}(\sigma_4) - \widehat{H}(\sigma_3) &= -2U \end{aligned} \tag{6.3.28}$$

and therefore

$$\begin{aligned} \widehat{H}(\sigma_4) - \widehat{H}(\sigma) &= [\widehat{H}(\sigma_4) - \widehat{H}(\sigma_3)] + [\widehat{H}(\sigma_3) - \widehat{H}(\sigma_2)] + [\widehat{H}(\sigma_2) - \widehat{H}(\sigma)] \\ &= -U + \Delta > 0. \end{aligned} \tag{6.3.29}$$

We observe that in σ_4 there is an empty triangular face as in the second case. So, we iterate the same procedure starting from σ_4. Finally we obtain for the energy a total decreasing value $t \leqslant (-U + \Delta) + (-2U + \Delta)$, thus the stability level is $V_\sigma = \Delta + U$, which is obtained in σ_3.

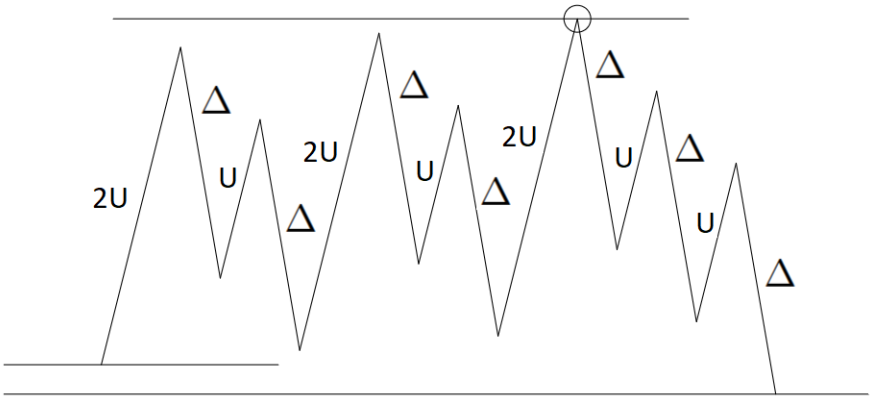

Figure 6.11 – We depict an example of the energy landscape between $\mathcal{E}_{B_m}(r)$ and $\mathcal{E}_{B_{m-1}}(r)$ for the value $r = 4$. We highlight with a circle the maximum of the energy, which is attained in ω_9.

□

Proof of Lemma 6.3.8. We distinguish the three cases $\sigma \in Z$, $\sigma \in R$ and $\sigma \in Y$. Recall Definition 6.2.15 and extend it to clusters. We denote by $\Omega(\eta, \eta')$ the set of all the paths connecting η and η'.

Stability level of Z. We begin by considering the set Z_1. For any configuration $\sigma \in Z_1$ we construct a path $\overline{\omega} \in \Omega(\sigma, \mathcal{I}_\sigma \cap (Z_1 \cup \{\hexagon\}))$ that dismantles the bar on one of the shortest sides of the quasi-regular hexagon starting from one of its corners. Starting from $\sigma \equiv \omega_0 \in Z_1$, we will define ω_1 as follows. Consider a corner in one of the shortest sides of the cluster in $\mathcal{E}_{B_m}(r)$, with $m = 0, ..., 5$ and let j be a site belonging to this corner. Define ω_1 as the configuration obtained starting from ω_0 by moving the particle in j to the empty nearest site. Since ω_1 is obtained by breaking two bonds, we have $\widehat{H}(\omega_1) - \widehat{H}(\omega_0) = 2U$. Then, consider ω_2 as the configuration obtained from ω_1 by moving the same particle outside Λ. We observe that ω_1 and ω_2 are not connected via one step of the dynamics, but there exist some configurations $\xi_1, ..., \xi_n$ such that $(\omega_1, \xi_1, ..., \xi_n, \omega_2)$ is a path with $\widehat{H}(\xi_i) = \widehat{H}(\xi_j)$ for all $i, j \in \{1, ..., n\}$. We have $\widehat{H}(\omega_2) - \widehat{H}(\omega_1) = -\Delta$. Then, we analogously define ω_3 and ω_4 by considering the site j_1, where j_1 is the other site belonging to the same corner. In this case, when a particle is detached from the cluster defining ω_3, only one bond is broken. Thus, we have $\widehat{H}(\omega_3) - \widehat{H}(\omega_2) = U$ and $\widehat{H}(\omega_4) - \widehat{H}(\omega_3) = -\Delta$. By iterating this procedure along the considered side, a bar of the cluster is erased and we obtain the configuration $\eta \equiv \omega_k$ such that $\eta = \mathcal{E}_{B_{m-1}}(r)$ for $m \neq 0$, otherwise $\eta = \mathcal{E}_{B_5}(r-1)$ for $m = 0$. Note that k is twice the cardinality of the bar. See Figure 6.11.

Note that if the initial configuration contains a regular hexagon with radius length one, then the final configuration contains a trapeze composed by three particles.

In order to determine where the maximum is attained, we observe that $\widehat{H}(\omega_{2j}) < \widehat{H}(\omega_{2j+1})$ for every $j = 0, ..., \frac{k-2}{2}$ and $\widehat{H}(\omega_k) < \widehat{H}(\omega_{k-1})$. Thus, we will find the maximum over the configuration with odd index. By (1.3.56), we have

$$\begin{aligned} \widehat{H}(\omega_1) - \widehat{H}(\omega_0) &= 2U, \\ \widehat{H}(\omega_3) - \widehat{H}(\omega_0) &= 3U - \Delta \end{aligned}$$

and for every $s = 2, \cdots, \frac{k-4}{2}$, we have

$$\begin{aligned} \widehat{H}(\omega_{2s+1}) - \widehat{H}(\omega_{2s-3}) &= 3U - 2\Delta, \\ \widehat{H}(\omega_{k-1}) - \widehat{H}(\omega_{k-5}) &= 2U - 2\Delta. \end{aligned}$$

It follows that for $n < k-1$ odd, $n = 2\tilde{s}+1$, we obtain

$$\begin{aligned}\widehat{H}(\omega_n) - \widehat{H}(\omega_0) &= \begin{cases} \sum\limits_{\substack{s=2,..,\tilde{s}\\ s\text{ even}}} [\widehat{H}(\omega_{2s+1}) - \widehat{H}(\omega_{2s-3})] + [\widehat{H}(\omega_1) - \widehat{H}(\omega_0)] & \text{if } \tilde{s} \text{ even} \\ \sum\limits_{\substack{s=3,..,\tilde{s}\\ s\text{ odd}}} [\widehat{H}(\omega_{2s+1}) - \widehat{H}(\omega_{2s-3})] + [\widehat{H}(\omega_3) - \widehat{H}(\omega_0)] & \text{if } \tilde{s} \text{ odd,} \end{cases} \\ &= \begin{cases} \frac{\tilde{s}}{2}(3U-2\Delta)+2U & \text{if } n = 2\tilde{s}+1 \text{ with } \tilde{s} \text{ even,} \\ \frac{\tilde{s}-1}{2}(3U-2\Delta)+3U-\Delta & \text{if } n = 2\tilde{s}+1 \text{ with } \tilde{s} \text{ odd.} \end{cases}\end{aligned} \tag{6.3.30}$$

Thus, for $n = k-1$ we have

$$\begin{aligned}\widehat{H}(\omega_{k-1}) - \widehat{H}(\omega_0) &= [\widehat{H}(\omega_{k-1}) - \widehat{H}(\omega_{k-5})] + [\widehat{H}(\omega_{k-5}) - \widehat{H}(\omega_0)] \\ &= 2U - 2\Delta + \tfrac{k-6}{4}(3U-2\Delta) + 2U \\ &= \tfrac{k-2}{4}(3U-2\Delta) + U,\end{aligned} \tag{6.3.31}$$

where we have used that $\tilde{s}$ is even, indeed $k-1 = 2(2r-j)-1 = 2\tilde{s}-1$ with $j \in \{-1,+1,+3\}$. Since the result is an increasing function of $n = 2\tilde{s}+1$, comparing the three maxima, we see that the absolute maximum is attained in ω_{k-5}. Since k is twice the cardinality of a bar, by Definitions 6.2.8 and 6.2.9, we have

— $k = 2(2r-1)$ if the initial configuration is $\mathcal{E}_{B_1}(r)$;
— $k = 2(2r+1)$ if the initial configuration is $\mathcal{E}_{B_m}(r)$ for $m = 2,3,4,5$;
— $k = 2(2r+3)$ if the initial configuration is $\mathcal{E}(r+1)$.

So, by using (6.3.30) and replacing $k-5 = 2\tilde{s}+1$ with $\tilde{s}$ even, we have

$$\Phi(\overline{\omega}) - \widehat{H}(\omega_0) = \widehat{H}(\omega_{k-5}) - \widehat{H}(\omega_0) = \frac{k-6}{4}(3U-2\Delta) + 2U. \tag{6.3.32}$$

Thus, $\Phi(\overline{\omega})$ depends only on the value k, that is an increasing function of the radius r of the quasi–regular hexagon. The cardinality of the longest bar among those of the quasi–regular hexagon in a configuration in Z_1 is $2r^*+1$ (obtained by removing B_5 from $E_{B_5}(r^*)$), so we choose $k = 2(2r^*+1)$. Note that the maximum is not obtained for $k = 2(2r^*+3)$, since $\mathcal{E}(r^*+1) \notin Z_1$.

Let us check that $\omega_k \in \mathcal{I}_\sigma \cap (Z_1 \cup \{\hexagon\})$. Since $k \leqslant 2(2r^*+1)$, with $r^* = \left\lfloor \frac{U}{2(3U-2\Delta)} - 1/2 \right\rfloor$, and by (6.3.31), we get

$$\begin{aligned}\widehat{H}(\omega_0) - \widehat{H}(\omega_k) &= [\widehat{H}(\omega_0) - \widehat{H}(\omega_{k-1})] + [\widehat{H}(\omega_{k-1}) - \widehat{H}(\omega_k)] \\ &= -\tfrac{k-2}{4}(3U-2\Delta) - U + \Delta \\ &\geqslant -\tfrac{2(2r^*+1)-2}{4}(3U-2\Delta) - U + \Delta = \delta(3U-2\Delta) > 0.\end{aligned} \tag{6.3.33}$$

Finally, by equations (6.3.32) and (6.3.33), we have

$$V_\sigma \leqslant \Phi(\overline{\omega}) - \widehat{H}(\sigma) = \frac{k-6}{4}(3U-2\Delta) + 2U. \tag{6.3.34}$$

Thus, we find $V^*_{Z_1} = \max_{\sigma \in Z_1} V_\sigma$ by choosing $k = 2(2r^*+1)$, i.e.,

$$V^*_{Z_1} \leqslant 3\Delta - 2U. \tag{6.3.35}$$

Next, we analyze the set Z_2. For any configuration $\sigma \in Z_2$ we construct a path $\overline{\omega} \in \Omega(\sigma, \mathcal{I}_\sigma \cap (Z_2 \cup \{\hexagon\}))$. Starting from $\sigma \equiv \omega_0 \in Z_2$, define ω_1 by adding a free particle in Λ. Let us define ω_2 in the following way. Consider a corner in one of the longest sides of the cluster in $\mathcal{E}_{B_m}(r)$ and let j be a site belonging to this corner. Let j_1 be the site at distance one from j such that $\sigma(j_1) = 0$. We define ω_2 by moving the free particle in ω_1 until it reaches the site j_1. We observe that ω_1 and ω_2 are not connected via one step of the dynamics, but there

exist some configurations $\xi_1, ..., \xi_n$ such that $(\omega_1, \xi_1, ..., \xi_n, \omega_2)$ is a path with $\widehat{H}(\xi_i) = \widehat{H}(\xi_j)$ for all $i, j \in \{1, ..., n\}$. Moreover, we have

$$\begin{aligned}\widehat{H}(\omega_1) - \widehat{H}(\omega_0) &= \Delta,\\ \widehat{H}(\omega_2) - \widehat{H}(\omega_1) &= -U.\end{aligned}$$

We consider j_2 the site at distance one from j_1 such that $\sigma(j_2) = 0$ and $d(j_2, j') = 2$ where $j' \neq j$ is another site of the initial cluster. The configuration ω_3 is obtained from ω_2 by adding a free particle, and ω_4 is obtained from ω_3 by moving the free particle until it reaches the site j_2. Again, we have

$$\begin{aligned}\widehat{H}(\omega_3) - \widehat{H}(\omega_2) &= \Delta,\\ \widehat{H}(\omega_4) - \widehat{H}(\omega_3) &= -U.\end{aligned}$$

Let us define ω_5 and ω_6. The configuration ω_5 is obtained from ω_4 by adding a free particle, and ω_6 is obtained from ω_5 by moving the free particle until it reaches the site j_3, where j_3 is the site at distance one from j_2 such that $\sigma(j_3) = 0$ and $d(j_3, j') = 1$ where $j' \neq j$ is another site of the initial cluster. We have

$$\begin{aligned}\widehat{H}(\omega_5) - \widehat{H}(\omega_4) &= \Delta,\\ \widehat{H}(\omega_6) - \widehat{H}(\omega_5) &= -2U.\end{aligned}$$

We note that the energy has decreased by $2U$, since the particle has covered an internal angle of $\frac{5}{3}\pi$. By iterating this procedure along the considered side, a bar is added to the initial cluster. We obtain the configuration $\eta \equiv \omega_k$ such that $\eta = \mathcal{E}_{B_{m+1}}(r)$ for $m \neq 5$, otherwise $\eta = \mathcal{E}(r+1)$ for $m = 5$. Note that the length of the path k is equal to twice the cardinality of the bar.

In order to determine where the maximum is attained, we observe that $\widehat{H}(\omega_{2j}) < \widehat{H}(\omega_{2j+1})$ for every $j = 0, ..., \frac{k-2}{2}$ and $\widehat{H}(\omega_k) < \widehat{H}(\omega_{k-1})$. Thus, we will find the maximum over the configuration with odd index. By (1.3.56), we have

$$\begin{aligned}\widehat{H}(\omega_1) - \widehat{H}(\omega_0) &= \Delta,\\ \widehat{H}(\omega_3) - \widehat{H}(\omega_0) &= 2\Delta - U,\\ \widehat{H}(\omega_5) - \widehat{H}(\omega_0) &= 3\Delta - 2U\end{aligned}$$

and for every $s = 3, ..., \frac{k-2}{2}$ we have

$$\widehat{H}(\omega_{2s+1}) - \widehat{H}(\omega_{2s-3}) = 2\Delta - 3U.$$

It follows that for $n > 5$ odd, $n = 2\tilde{s} + 1$, we obtain

$$\begin{aligned}\widehat{H}(\omega_n) - \widehat{H}(\omega_0) &= \begin{cases} \displaystyle\sum_{\substack{s=3,..,\tilde{s}\\ s\ \text{odd}}} [\widehat{H}(\omega_{2s+1}) - \widehat{H}(\omega_{2s-3})] + [\widehat{H}(\omega_5) - \widehat{H}(\omega_0)] & \text{if } \tilde{s} \text{ odd},\\ \displaystyle\sum_{\substack{s=4,..,\tilde{s}\\ s\ \text{even}}} [\widehat{H}(\omega_{2s+1}) - \widehat{H}(\omega_{2s-3})] + [\widehat{H}(\omega_3) - \widehat{H}(\omega_0)] & \text{if } \tilde{s} \text{ even},\end{cases}\\ &= \begin{cases} \frac{\tilde{s}-2}{2}(2\Delta - 3U) + (3\Delta - 2U) & \text{if } n = 2\tilde{s}+1 \text{ with } \tilde{s} \text{ even},\\ \frac{\tilde{s}-1}{2}(2\Delta - 3U) + (2\Delta - U) & \text{if } n = 2\tilde{s}+1 \text{ with } \tilde{s} \text{ odd}.\end{cases}\end{aligned} \tag{6.3.36}$$

Since $2\Delta - 3U < 0$ and therefore the result is a decreasing function of n, the absolute maximum is attained in ω_5. Thus, we have

$$\Phi(\overline{\omega}) - \widehat{H}(\omega_0) = \widehat{H}(\omega_5) - \widehat{H}(\omega_0) = 3\Delta - 2U. \tag{6.3.37}$$

Finally, let us check that $\omega_k \in \mathcal{I}_\sigma \cap (Z_2 \cup \{\hexagon\})$. If $\sigma \in Z_2 \setminus \mathcal{E}(r^*+1)$, then the cardinality of the smallest bar among those of the quasi–regular hexagon in a configuration in Z_2 is $k_{\min} = 2(r^*+1)+1$. Since $r^* = \left\lfloor \frac{U}{2(3U-2\Delta)} - \frac{1}{2} \right\rfloor$ and by using (6.3.36), we have

$$\begin{aligned}\widehat{H}(\omega_0) - \widehat{H}(\omega_k) &= [\widehat{H}(\omega_0) - \widehat{H}(\omega_{k-2})] + [\widehat{H}(\omega_{k-2}) - \widehat{H}(\omega_k)] = \\ &= \left[\tfrac{k-1}{2}(2\Delta - 3U) + (2\Delta - U)\right] + U - \Delta \\ &= (r^*+1)(2\Delta - 3U) + (2\Delta - U) + U - \Delta = \\ &= -2U + 2\Delta > 0,\end{aligned}$$

since $\Delta > U$. Thus, we deduce that

$$V_\sigma \leqslant \Phi(\overline{\omega}) - \widehat{H}(\sigma) = 3\Delta - 2U. \tag{6.3.38}$$

Now we consider $\mathcal{E}(r^*+1)$ and we note that $\widehat{H}(\mathcal{E}(r^*+1)) < \widehat{H}(\mathcal{E}_{B_1}(r^*+1))$. Thus our path $\overline{\omega}$ is the composition of the path we have previously defined, which connects $\mathcal{E}(r^*+1)$ to $\mathcal{E}_{B_1}(r^*+1)$, and an additional part depending on the value of δ (recall that $\delta \in (0,1)$ is such that $r^* = \frac{U}{2(3U-2\Delta)} - \frac{1}{2} - \delta$). If $0 < \delta < \frac{1}{2}$, then we add the bar B_2 as we have done above for B_1 obtaining that $\overline{\omega}$ connects $\mathcal{E}(r^*+1)$ to $\mathcal{E}_{B_2}(r^*+1)$ passing through $\mathcal{E}_{B_1}(r^*+1)$. If $\frac{1}{2} < \delta < 1$, then in the same manner we add the bars B_2, B_3, B_4, B_5, B_6 obtaining that $\overline{\omega}$ conncets $\mathcal{E}(r^*+1)$ to $\mathcal{E}_{B_6}(r^*+1) \equiv \mathcal{E}(r^*+2)$ passing through $\mathcal{E}_{B_i}(r^*+1)$ for any $i = 2, ..., 5$. In both cases the last configuration of the new paths belongs to $\mathcal{I}_{\mathcal{E}(r^*+1)}$, indeed

$$\begin{aligned}&\widehat{H}(\mathcal{E}(r^*+1)) > \widehat{H}(\mathcal{E}_{B_2}(r^*+1)), && \text{if } \delta \in (0, \tfrac{1}{2}), \\ &\widehat{H}(\mathcal{E}(r^*+1)) > \widehat{H}(\mathcal{E}(r^*+2)), && \text{if } \delta \in (\tfrac{1}{2}, 1).\end{aligned}$$

Thus, using equations (6.3.36), (6.3.37) and (6.3.38), we obtain

$$\begin{aligned}V_\sigma &\leqslant \begin{cases} 3\Delta - 2U + \widehat{H}(\mathcal{E}_{B_1}(r^*+1)) - \widehat{H}(\mathcal{E}(r^*+1)), \text{ for } \delta \in \left(0, \frac{1}{2}\right), \\ 3\Delta - 2U + \widehat{H}(\mathcal{E}_{B_5}(r^*+1)) - \widehat{H}(\mathcal{E}(r^*+1)), \text{ for } \delta \in \left(\frac{1}{2}, 1\right), \end{cases} \\ &= \begin{cases} 3\Delta - 2U + \delta(3U - 2\Delta) < 2\Delta - \frac{U}{2}, \text{ for } \delta \in \left(0, \frac{1}{2}\right), \\ 3\Delta - 2U + (2\delta - 1)(3U - 2\Delta) < \Delta + U, \text{ for } \delta \in \left(\frac{1}{2}, 1\right). \end{cases}\end{aligned}$$

Thus, we find

$$V^*_{Z_2} = \max_{\sigma \in Z_2} V_\sigma \leqslant \Delta + U. \tag{6.3.39}$$

In conclusion, we have that $V^*_Z = \max\{V^*_{Z_1}, V^*_{Z_2}\} \leqslant \Delta + U$.

Stability level of R. Consider the set R_1. For any configuration $\sigma \in R_1$ we construct a path $\overline{\omega} \in \Omega(\sigma, \mathcal{I}_\sigma \cap (R_1 \cup Z_1))$. Starting from $\sigma \equiv \omega_0 \in R_1$, let us define ω_1 as follows. Consider the corner in one of the shortest sides of the cluster and let j be a site belonging to it. Define the configuration ω_1 starting from ω_0 by moving the particle in j to the nearest empty site. Since with this move two bonds are broken, we have $\widehat{H}(\omega_1) - \widehat{H}(\omega_0) = 2U$. Then, consider ω_2 as the configuration obtained from ω_1 by moving the same particle outside Λ. We observe that ω_1 and ω_2 are not connected via one step of the dynamics, but there exist some configurations $\xi_1, ..., \xi_n$ such that $(\omega_1, \xi_1, ..., \xi_n, \omega_2)$ is a path with $\widehat{H}(\xi_i) = \widehat{H}(\xi_j)$ for all $i, j \in \{1, ..., n\}$. We have $\widehat{H}(\omega_2) - \widehat{H}(\omega_1) = -\Delta$. Then, analogously define ω_3 and ω_4 by considering the site j', where j' is the other site belonging to the same corner. In this case, when a particle is detached from the cluster defining ω_3, only one bond is loss. Thus, we have that $\widehat{H}(\omega_3) - \widehat{H}(\omega_2) = U$ and $\widehat{H}(\omega_4) - \widehat{H}(\omega_3) = -\Delta$. By iterating this procedure along the shortest side, a bar of the cluster is erased and we obtain the configuration $\eta \equiv \omega_l$, where l is twice the cardinality of the considered bar. We observe that the greatest value of l is always smaller than k, where k is twice the cardinality of the greatest bar of the quasi-regular hexagon contained in the cluster. Analogously to the case $\omega \in Z_1$, we have that $\omega_l \in \mathcal{I}_\sigma$. Thus, $V_\sigma < 3\Delta - 2U$ and therefore

$$V^*_{R_1} = \max_{\sigma \in R_1} V_\sigma < 3\Delta - 2U. \tag{6.3.40}$$

Next, we consider the set R_2. For any configuration $\sigma \in R_2$ we construct a path $\overline{\omega} \in \Omega(\sigma, \mathcal{I}_\sigma \cap (R_2 \cup Z_2 \cup \{\bullet\}))$. Starting from $\sigma \equiv \omega_0 \in R_2$, let us define ω_1 as follows. Consider a corner in one of the shortest sides of the cluster and let j be a site belonging to it. We distinguish two cases depending on the length of the bar ℓ of the shortest side.

— If the cardinality of the bar ℓ is smaller than $2(r^*+1)-1$, we define ω_1 by detaching the particle in j from the cluster. Then, we define ω_2 by moving the free particle outside Λ. Next, we consider the other site j' belonging to the corner of the cluster and define ω_3 and ω_4 by detaching and moving the particle in j' outside Λ. By iterating this procedure along the shortest side, a bar of the cluster is erased and we obtain the configuration $\eta \equiv \omega_{\tilde{\ell}}$, where $\tilde{\ell} = 2\ell$ is twice the cardinality of the considered bar. Since $\ell < 2(r^*+1)-1$, we observe that the greatest value of $\tilde{\ell}$ is always smaller than k, where k is twice the cardinality of the greatest bar of the quasi–regular hexagon contained in the cluster, that is $\tilde{\ell} < k$. Analogously to the case $\sigma \in Z_1$, we have that $\omega_{\tilde{\ell}} \in \mathcal{I}_\sigma$. Thus, $V_\sigma < 3\Delta - 2U$.

— If the cardinality of the bar ℓ is at least $2(r^*+1)-1$, consider the site j_1 at distance one from j and such that $\sigma(j_1) = 0$. We define the configuration ω_1 starting from ω_0 and by adding a free particle. Then, we define ω_2 by moving the free particle in ω_1 until it reaches the site j_1. Next, we consider j_2 the site at distance one from j_1 such that $\sigma(j_2) = 0$ and $d(j_2, j') = 2$, where $j' \neq j$ is another site of the initial cluster. We define ω_3 and ω_4 in the following way. The configuration ω_3 is obtained from ω_2 by adding a free particle in Λ, and ω_4 is obtained from ω_3 by moving the free particle until it reaches the site j_2. Let j_3 be the site at distance one from j_2 such that $\sigma(j_3) = 0$ and $d(j_3, j') = 1$, where $j' \neq j$ is another site of the initial cluster. We define ω_5 and ω_6 in the same way used before. The configuration ω_5 is obtained from ω_4 by adding a free particle in Λ, and ω_6 is obtained from ω_5 by moving the free particle until it reaches the site j_3. By iterating this procedure along the considered side, a bar is added to the initial cluster. Analogously to the case $\omega \in Z_2$, we have that $\omega_{2\ell} \in \mathcal{I}_\sigma$ since $\ell \geqslant 2(r^*+1)-1$. Thus, $V_\sigma < \Delta + U$ and

$$V^*_{R_2} < \Delta + U. \tag{6.3.41}$$

In conclusion, we have that $V^*_R = \max\{V^*_{R_1}, V^*_{R_2}\} < \Delta + U$.

Stability level of Y. First, consider the set Y_1. For every configuration σ in Y_1, all clusters are non–interacting and are of the same type of those in Z_1 or R_1. If σ contains a cluster that is not a quasi-regular hexagon, then we take our path to be the path that cuts a bar, analogously to what has been done for R_1. We get a configuration in $\mathcal{I}_\sigma \cap Y_1$. Otherwise, if all clusters are quasi-regular hexagons, then we take our path to be the path that cuts a bar of the cluster, analogously to what has been done for Z_1. We get a configuration in $\mathcal{I}_\sigma \cap (Y_1 \cup Z_1)$. So, we have

$$V^*_{Y_1} = \max\{V^*_{R_1}, V^*_{Z_1}\} < 3\Delta - 2U. \tag{6.3.42}$$

Next, consider the set Y_2. For every configuration σ in Y_2, there exists at least a cluster of the same type of those in Z_2 or R_2. If σ contains a cluster of the type of those in R_2, i.e., σ contains a cluster that is not a quasi–regular hexagon, we take our path to be the path that either cuts or adds a bar as it has been done for R_2. We get a configuration in $\mathcal{I}_\sigma \cap Y_2$. Otherwise, if the cluster is like those in Z_2, i.e., the cluster is a quasi-regular hexagon, then we take the path that adds a bar to the quasi-regular hexagon, alike the cases encountered when considering Z_2. We get a configuration in $\mathcal{I}_\sigma \cap (Y_2 \cup \{\bullet\})$. So, we have

$$V^*_{Y_2} = \max\{V^*_{R_2}, V^*_{Z_2}\} < \Delta + U. \tag{6.3.43}$$

We conclude that

$$V^*_Y = \max\{V^*_{Y_1}, V^*_{Y_2}\} = V^*_Z.$$

□

6.3.4 *Proof of Theorem 6.1.1*

In this section, we identify stable and metastable states by proving Theorem 6.1.1.

Proof of Theorem 6.1.1. First, by direct computation we deduce that $\widehat{H}(\hexagon) < \widehat{H}(\hexagon)$ if L is sufficiently large, say $L > 2r^* + 3$. Moreover, we know that $\mathcal{X}^s \subseteq \mathcal{X}_V$ for any $V \geqslant 0$. Thus, using Theorem 6.1.3 and Proposition 6.3.1, we conclude that $\mathcal{X}^s = \{\hexagon\}$. To show that $\mathcal{X}^m = \{\hexagon\}$, we need to prove that $V_{\hexagon} = \Phi(\hexagon, \hexagon) = \Gamma_H^* > V^*$, with $V^* = \Delta + U$. This part of the proof is analogue to that of [90, equation (3.86)]. □

6.3.5 *Proof of Theorems 6.1.2 and 6.1.4*

In this section, we give the proof of the main Theorems 6.1.2 and 6.1.4.

Proof of Theorem 6.1.2. Combining [85, Theorem 4.1], [85, Theorem 4.9], [85, Theorem 4.15], Theorem 6.1.1 and Corollary 6.2.26, we get the claim. □

Proof of Theorem 6.1.4. It follows by Proposition 6.2.27. □

6.3.6 *Proof of Theorem 6.1.5*

We refer to (1.3.34) for the definition of cycle. To prove Theorem 6.1.5 we need [92, Theorem 3.2], which states that every state in a cycle is visited by the process before the exit with high probability. Using this result, to prove Theorem 6.1.5 we need to prove the following:

1. if $0 < \delta < \frac{1}{2}$, then
   (i) if η is a quasi–regular hexagon contained in $\mathcal{E}_{B_4}(r^*)$, then there exists a cycle $\mathcal{C}^{\hexagon}_{\hexagon}(\Gamma_H^*)$ containing η and $\hexagon$ and not containing $\hexagon$;
   (ii) if η is a quasi–regular hexagon containing $\mathcal{E}_{B_0}(r^* + 1)$, then there exists a cycle $\mathcal{C}^{\hexagon}_{\hexagon}(\Gamma_H^* - \widehat{H}(\hexagon))$ containing η and $\hexagon$ and not containing $\hexagon$;
2. if $\frac{1}{2} < \delta < 1$, then
   (i) if η is a quasi-regular hexagon contained in $\mathcal{E}_{B_0}(r^* + 1)$, then there exists a cycle $\mathcal{C}^{\hexagon}_{\hexagon}(\Gamma_H^*)$ containing η and $\hexagon$ and not containing $\hexagon$;
   (ii) if η is a quasi-regular hexagon containing $\mathcal{E}_{B_2}(r^* + 1)$, then there exists a cycle $\mathcal{C}^{\hexagon}_{\hexagon}(\Gamma_H^* - \widehat{H}(\hexagon))$ containing η and $\hexagon$ and not containing $\hexagon$.

Case 1. Let us start with (i). Let $\mathcal{C}^{\hexagon}_{\hexagon}(\Gamma_H^*)$ be the maximal connected set containing $\hexagon$ such that

$$\max_{\eta' \in \mathcal{C}^{\hexagon}_{\hexagon}(\Gamma_H^*)} \widehat{H}(\eta') < \Gamma_H^*.$$

Note that by definition $\mathcal{C}^{\hexagon}_{\hexagon}(\Gamma_H^*)$ is a cycle containing $\hexagon$ and not containing $\hexagon$ since $\Phi(\hexagon, \hexagon) = \Gamma_H^*$. It remains to prove that η belongs to $\mathcal{C}^{\hexagon}_{\hexagon}(\Gamma_H^*)$. The proof goes as follows. We construct a path $\omega^{\eta,\hexagon}$ going from η to $\hexagon$ keeping the energy less than Γ_H^*. This path is obtained by erasing site by site each bar of η, as explain in the first case of the proof of Lemma 6.3.8. Let $\eta \in \mathcal{E}_{B_i}(r)$ with $r \leqslant r^*$ and $0 \leqslant i \leqslant 5$. If $\eta \notin \mathcal{E}_{B_0}(r)$, i.e., if η is not a regular hexagon, consider the sequence of configurations $\{\bar{\omega}_i^{\eta,\hexagon}\}_{i=-\bar{i},\dots,-1}$ connecting η to the regular hexagon $\mathcal{E}_{B_0}(r)$ by erasing site by site each bar. If $\eta \in \mathcal{E}_{B_0}(r)$, we consider this path empty. From now on, let $\{\bar{\omega}_i^{\eta,\hexagon}\}_{i=0,\dots,r}$ be a sequence of configurations that contain regular hexagons, starting from $\mathcal{E}_{B_0}(r)$ and ending in $\hexagon$, with radius $r - i$. To complete the construction we can use the same idea applied in the construction of the reference path. More precisely, between each pair $(\bar{\omega}_i^{\eta,\hexagon}, \bar{\omega}_{i+1}^{\eta,\hexagon})$ we can add a sequence of configurations $\tilde{\omega}_i^{\eta,\hexagon} = \{\tilde{\omega}_{i,j}^{\eta,\hexagon}\}_{j=0,\dots,12r-6}$ such that $\tilde{\omega}_{i,0}^{\eta,\hexagon} = \bar{\omega}_i^{\eta,\hexagon}$ and $\tilde{\omega}_{i,j}^{\eta,\hexagon}$ is obtained from $\bar{\omega}_i^{\eta,\hexagon}$ by erasing j sites for $j > 0$. Again, as in the reference path, the last interpolation consists in inserting between every pair of configurations

in $\tilde{\omega}_i^{\eta,\hexagon}$ a sequence of configurations with a free particle in a suitable sequence of sites connecting the boundary of Λ to the site previously occupied by the erased particle. Either for any $r < r^*$ and $1 \leqslant i \leqslant 6$ or $r = r^*$ and $1 \leqslant i \leqslant 5$, we have that $\widehat{H}(\mathcal{E}_{B_{i-1}}(r)) < \widehat{H}(\mathcal{E}_{B_5}(r^*))$. Thus, by Proposition 6.2.17 for the path $\omega^{\eta,\hexagon}$ we obtain

$$\max_i \widehat{H}(\omega_i^{\eta,\hexagon}) = \max_{r \leqslant r^*} \widehat{H}(\mathcal{E}_{B_{i-1}}(r)) + 3\Delta - 2U < \Gamma_H^*. \tag{6.3.44}$$

The proof of (ii) is similar. Let $\mathcal{C}^{\hexagon}_{\hexagon}(\Gamma_H^* - \widehat{H}(\hexagon))$ be the maximal connected set containing $\hexagon$ such that

$$\max_{\eta' \in \mathcal{C}^{\hexagon}_{\hexagon}(\Gamma_H^* - \widehat{H}(\hexagon))} \widehat{H}(\eta') < \Gamma_H^*.$$

Again $\mathcal{C}^{\hexagon}_{\hexagon}(\Gamma_H^* - \widehat{H}(\hexagon))$ is a cycle containing $\hexagon$ and not containing $\hexagon$ since $\Phi(\hexagon, \hexagon) = \Gamma_H^*$. To prove that $\mathcal{C}^{\hexagon}_{\hexagon}(\Gamma_H^* - \widehat{H}(\hexagon))$ contains η we define a path $\omega^{\eta,\hexagon}$ going from η to $\hexagon$ as follows. It is obtained first by reaching a regular hexagon shape and, from there, following the reference path ω^* defined in Section 6.2.2. Suppose that $\eta \in \mathcal{E}_{B_i}(r)$, with $r \geqslant r^*$ and $0 \leqslant i \leqslant 5$. If η is a regular hexagon, then we define $\omega^{\eta,\hexagon}$ as the part of the reference path going from η to $\hexagon$. Otherwise, we add bars to η with a mechanism similar to the time–reversal of the one used in the construction of $\omega^{\eta,\hexagon}$, until the path reaches a configuration in $\eta \in \mathcal{E}_{B_0}(r+1)$. The remaining part of the path follows the part of the reference path ω^* from $\mathcal{E}_{B_0}(r+1)$ to $\hexagon$. Since for any $r \geqslant r^*$, $0 \leqslant i \leqslant 5$ and $0 < \delta < \frac{1}{2}$, we have that $\widehat{H}(\mathcal{E}_{B_i}(r)) < \widehat{H}(\mathcal{E}_{B_5}(r^*))$, for the path $\omega^{\eta,\hexagon}$ we obtain

$$\max_i \widehat{H}(\omega_i^{\eta,\hexagon}) = \max_{r \geqslant r^*} \widehat{H}(\mathcal{E}_{B_i}(r)) + 3\Delta - 2U < \Gamma_H^*. \tag{6.3.45}$$

Case 2. The proof is analogue to that of case 1 with the following changes. In the proof of (i), since $\frac{1}{2} < \delta < 1$, and either for any $r < r^* + 1$ and $1 \leqslant i \leqslant 6$ or for $r = r^* + 1$ and $i = 1$, we have that $\widehat{H}(\mathcal{E}_{B_{i-1}}(r)) < \widehat{H}(\mathcal{E}_{B_1}(r^* + 1))$. Thus, by Proposition 6.2.17 for the path $\omega^{\eta,\hexagon}$ we obtain

$$\max_i \widehat{H}(\omega_i^{\eta,\hexagon}) = \max_{r \leqslant r^*+1} \widehat{H}(\mathcal{E}_{B_{i-1}}(r)) + 3\Delta - 2U < \Gamma_H^*. \tag{6.3.46}$$

In the proof of (ii), since either for any $r > r^* + 1$ and $0 \leqslant i \leqslant 5$ or for $r = r^* + 1$ and any $2 \leqslant i \leqslant 5$, we have that $\widehat{H}(\mathcal{E}_{B_i}(r)) < \widehat{H}(\mathcal{E}_{B_1}(r^* + 1))$, for the path $\omega^{\eta,\hexagon}$ we obtain

$$\max_i \widehat{H}(\omega_i^{\eta,\hexagon}) = \max_{r \geqslant r^*+1} \widehat{H}(\mathcal{E}_{B_i}(r)) + 3\Delta - 2U < \Gamma_H^*. \tag{6.3.47}$$

This concludes the proof.

Part II

KAWASAKI DYNAMICS: TOWARDS THE FULLY CONSERVATIVE MODEL

7

DROPLET DYNAMICS ON THE 2–D SQUARE LATTICE

The content of this chapter is the second work in a series of three papers in which we study a lattice gas subject to Kawasaki conservative dynamics in a large finite box $\Lambda_\beta \subset \mathbb{Z}^2$ whose volume depends on β. The initial configuration is drawn from the grand–canonical ensemble restricted to the set of configurations where all the droplets are subcritical. Our goal is to describe, in the metastable regime $\Delta \in (U, 2U)$ and in the limit as $\beta \to \infty$, how and when the system nucleates, i.e., grows a supercritical droplet somewhere in Λ_β. In the first paper [62] we showed that subcritical droplets behave as quasi–random walks. Here we use the results in the first paper to analyse how subcritical droplets form and dissolve on multiple space–time scales when the volume is *moderately large*, namely, $|\Lambda_\beta| = e^{\Theta\beta}$ with $\Delta < \Theta < 2\Delta - U$. In the third paper [12] we consider the setting where the volume is *very large*, namely, $|\Lambda_\beta| = e^{\Theta\beta}$ with $\Delta < \Theta < \Gamma^* - (2\Delta - U)$, where Γ^* is the energy of the critical droplet in the local model with fixed volume, and use the results in the first two works to identify the nucleation time. We will see that in a very large volume critical droplets appear more or less independently in boxes of moderate volume, a phenomenon referred to as *homogeneous nucleation*. Since Kawasaki dynamics is *conservative*, we need to control non–local effects in the way droplets are formed and dissolved. This is done via a *deductive approach*: the tube of typical trajectories leading to nucleation is described via a series of events, whose complements have negligible probability, on which the evolution of the gas consists of *droplets wandering around on multiple space-time scales* in a way that can be captured by a coarse-grained Markov chain on a space of droplets.

The outline of the chapter is as follows. In Section 7.1 we state our main theorems. Section 7.2 collects certain key tools that are needed throughout the chapter. In particular, in Section 7.2.1 we introduce key notation, in Section 7.2.2 we formulate certain regularity properties for the initial configuration that we can impose because their failure is extremely unlikely, while in Section 7.2.3 we group the configurations into a sequence of subsets of configurations of increasing regularity and prove a recurrence property to these sets on an increasing sequence of time scales. In Section 7.3.1 we state three key propositions (Propositions 7.3.1–7.3.3) that are needed along the way. The proof of Theorems 7.1.2, 7.1.3, 7.1.5 and 7.1.6 are given in Sections 7.3.2, 7.3.3, 7.3.4 and 7.3.5, respectively, subject to these propositions. The three propositions are proved in Sections 7.4.1–7.4.3. The proof is based on a number of key lemmas (Lemmas 7.4.1, 7.4.3, 7.4.5) whose proof is given in Section 7.5. This section, which uses two more key lemmas (Lemmas 7.5.1–7.5.2), is long and difficult because it contains the main technical hurdles of the work. These hurdles are organised into what we call the *deductive approach*: the tube of typical trajectories leading to nucleation is described via a series of events, whose complements have negligible probability, on which the evolution of the gas consists of *droplets wandering around on multiple space-time scales* in a way that can be captured by a coarse-grained Markov chain on a space of droplets. Finally, Appendices 7.A and 7.B provide additional computations that are needed in the chapter: environment estimates that exclude non-regular configurations, respectively, large deviation estimates for certain events that come up in the deductive approach.

7.1 MAIN RESULTS

7.1.1 *Definitions and notations*

In order to state our main results, we need to introduce some definitions and notations. First, recall (1.3.74) and (1.3.76) for the definition of the set $\mathcal{R}'$ and the time horizon $T^\star$ we are interested in, respectively. To rigorously define the collection of local boxes, we proceed as follows. We denote by $\mathrm{dist}(\cdot,\cdot)$ the distance associated with the ℓ_∞–norm on $\mathbb{R}^2$:

$$\|\cdot\|_\infty \colon (x, y) \in \mathbb{R}^2 \mapsto |x| \vee |y|. \tag{7.1.1}$$

Following [64], we introduce a map g_5 as an iterative map that merges into single rectangles those rectangles that have distance < 5 between them, while we leave the other rectangles unchanged. (We refer to (7.2.6) for the precise definition.) At any time $t \geqslant 0$, we require that the collection of the $k(t)$ local boxes $\bar{\Lambda}(t) = (\bar{\Lambda}_i(t))_{1 \leqslant i \leqslant k(t)}$ satisfy the following conditions associated with $\eta_t = X(t)$:

B1. $\Lambda(t) = \cup_{1 \leqslant i \leqslant k(t)} \bar{\Lambda}_i(t)$ contains all the sleeping particles.

B2. For all $1 \leqslant i \leqslant k(t)$, $\bar{\Lambda}_i(t)$ contains at least one sleeping particle.

B3. For all $1 \leqslant i \leqslant k(t)$, all particles in the restriction $\bar{\eta}_i(t)$ of η_t to $\bar{\Lambda}_i(t)$ are either free or at distance > 1 from the internal border of $\bar{\Lambda}_i(t)$.

B4. For all $1 \leqslant i, j \leqslant k(t)$ with $i \neq j$, $\mathrm{dist}(\bar{\Lambda}_i(t), \bar{\Lambda}_j(t)) \geqslant 5$.

Definition 7.1.1. *The collection of boxes $\bar{\Lambda}(t) = (\bar{\Lambda}_i(t))_{1 \leqslant i \leqslant k(t)}$ is constructed as follows. At time $t = 0$, consider the collection $\bar{S}(0)$ of 5×5 boxes centered at the clusterised particles, and define $\bar{\Lambda}(0) = g_5(\bar{S}(0)) \setminus \bar{\Lambda}^*(0)$, where $\bar{\Lambda}^*(0)$ denotes the collection of boxes belonging to $g_5(\bar{S}(0))$ that contain active particles only. Let $\mathcal{B}$ be the set of special times associated to boxes, refer to as boxes special times, defined by*

$$\mathcal{B} = \big\{ t \geqslant 0 \colon \textit{at time } t \textit{ at least one of the conditions } \textbf{B1–B4} \textit{ above is violated by } \bar{\Lambda}(t^-) \big\}. \tag{7.1.2}$$

For $t > 0$, define $\bar{\Lambda}(t)$ as follows:

- *If $t \in \mathcal{B}$, then define the collection $\bar{S}(t)$ of 5×5 boxes centered at the clusterised particles, and define $\bar{\Lambda}(t) = g_5(\bar{S}(t)) \setminus \bar{\Lambda}^*(t)$, where $\bar{\Lambda}^*(t)$ denotes the collection of boxes belonging to $g_5(\bar{S}(t))$ that contain active particles only.*
- *If $t \notin \mathcal{B}$, then define $\bar{\Lambda}(t) = \bar{\Lambda}(t^-)$.*

We will suppress the dependence on t from the notation whenever it is not relevant. See Fig. 1.30 for an example of local boxes.

7.1.2 *Key theorems: Theorems 7.1.2–7.1.3 and 7.1.5–7.1.6*

• **Sets and hitting times.** Recall that we defined $\mathcal{X}_{\Delta^+}$ as the set of configurations without droplets or with droplets that are quasi–squares with $\ell_1 \geqslant 2$ (and with additional regularity conditions on the gas surrounding droplets to be specified in Definition 7.2.9). Moreover, recall that $\mathcal{X}_E$ is the set of configurations in $\mathcal{X}_{\Delta^+}$ without droplets (see (7.3.1) and Definition 7.2.9). Define $(\bar{\tau}_k)_{k \in \mathbb{N}_0}$ as the sequence of return times in $\mathcal{X}_{\Delta^+}$ after an active particle is seen in Λ. Define the hitting time of the set $A \subset \mathcal{X}_\beta$ for the process X as

$$\tau_A(X) = \inf\{t \geqslant 0 \colon X(t) \in A\}. \tag{7.1.3}$$

Put $\bar{\tau}_0 = \tau_{\mathcal{X}_{\Delta^+}}$ and, for $i \in \mathbb{N}_0$, define

$$\bar{\sigma}_{i+1} = \begin{cases} \inf\big\{t > \bar{\tau}_i \colon \text{there is an active particle in } \Lambda(t) \text{ at time } t\big\}, & \text{if } X(\bar{\tau}_i) \in \mathcal{X}_{\Delta^+} \setminus \mathcal{X}_E, \\ e^{\Delta\beta}, & \text{if } X(\bar{\tau}_i) \in \mathcal{X}_E, \end{cases} \tag{7.1.4}$$

and

$$\bar{\tau}_{i+1} = \inf\{t > \bar{\sigma}_{i+1} \colon X(t) \in \mathcal{X}_{\Delta^+}\}. \tag{7.1.5}$$

Recall (1.3.78) and (1.3.79) for the definition of a quasi–square and of the parameter γ, respectively.

• **Key theorems.** Theorems 7.1.2–7.1.3 and 7.1.5–7.1.6 below control the transitions between configurations consisting of quasi–squares and free particles, the times scales on which these transitions occur, and the most likely trajectories they follow.

(I) Our first theorem describes the typical return times to the set $\mathcal{X}_{\Delta^+}$.

Theorem 7.1.2. [Typical return times] *If $\Delta < \Theta \leqslant \theta$, then for any $\delta > 0$, and any d and α small enough,*

$$P_{\mu_{\mathcal{R}}}\Big(\bar{\tau}_0 \geqslant e^{(\Delta+\alpha+\delta)\beta},\ \bar{\tau}_0 \leqslant T^\star\Big) = \mathrm{SES}(\beta) \tag{7.1.6}$$

and

$$P_{\mu_{\mathcal{R}}}\Big(e^{(\Delta-\alpha-\delta)\beta} \leqslant \bar{\tau}_{i+1} - \bar{\tau}_i \leqslant e^{(\Delta+\alpha+\delta)\beta}\ \forall i \in \mathbb{N}_0 \colon\ \bar{\tau}_{i+1} \leqslant T^\star\Big) = 1 - \mathrm{SES}(\beta). \tag{7.1.7}$$

(II) Our second theorem describes the typical update times for a configuration in $\mathcal{X}_{\Delta^+}$. Recall the definition of the projection π from $\mathcal{X}_{\Delta^+}$ to the finite space defined in (1.3.81). See Fig. 1.32. We can define a dynamics on the space $\bar{\mathcal{X}}_\Delta$ of sizes of quasi–squares, arranged for example in increasing lexicographic order. For $i \in \mathbb{N}_0$, we denote by $(\ell_{1,i}, \ell_{2,i})$ in QS, with $\ell_{1,i} \geqslant 2$, the sizes of the smallest quasi–square at time $\bar{\tau}_i$, if any, and otherwise we set $\ell_{1,i} = \ell_{2,i} = 0$. Define

$$\bar{\tau}_{c,i} = \min\{\bar{\tau}_k \geqslant \bar{\tau}_i \colon\ \pi(X(\bar{\tau}_k)) \neq \pi(X(\bar{\tau}_i))\}, \tag{7.1.8}$$

recall (1.3.78), and recall the resistance of a configuration in $\mathcal{X}_E$ given in (1.3.82).

Theorem 7.1.3. [Typical update times] *If $\Delta < \Theta \leqslant \theta$, then for any $\delta > 0$, any d and α small enough, and any $i \in \mathbb{N}_0$,*

$$P_{\mu_{\mathcal{R}}}\left(\begin{array}{l} \text{if } \bar{\tau}_{c,i} \leqslant T^\star, \text{ then } \bar{\tau}_{c,i} - \bar{\tau}_i \leqslant e^{(r(\ell_{1,i},\ell_{2,i})+\delta)\beta} \\ \text{or a coalescence occurs between } \bar{\tau}_i \text{ and } \bar{\tau}_{c,i} \end{array}\right) = 1 - \mathrm{SES}(\beta) \tag{7.1.9}$$

and

$$\lim_{\beta\to\infty} P_{\mu_{\mathcal{R}}}\left(\begin{array}{l} \text{if } \bar{\tau}_{c,i} \leqslant T^\star, \text{ then } \bar{\tau}_{c,i} - \bar{\tau}_i \geqslant e^{(r(\ell_{1,i},\ell_{2,i})-\delta)\beta} \\ \text{or a coalescence occurs between } \bar{\tau}_i \text{ and } \bar{\tau}_{c,i} \end{array}\right) = 1. \tag{7.1.10}$$

Remark 7.1.4. *Theorem 7.1.3 states that, starting from $\mu_{\mathcal{R}}$ and unless a coalescence occurs, for any $i \in \mathbb{N}_0$ the projected dynamics typically remains in $\pi(X(\bar{\tau}_i))$ through successive visits in $\mathcal{X}_{\Delta^+}$ for a time of order $e^{r(\ell_{1,i},\ell_{2,i})\beta}$. The SES error in (7.1.9) is related to an anomalously large realisation of a geometric random variable, while an anomalously small realisation leads to an error that is only exponentially small in (7.1.10). Note that for $\ell_{1,i} \geqslant \ell_c$ all the quasi-squares have the same resistance $2\Delta - U$. For the case in which $X(\bar{\tau}_i)$ has no quasi-square, its resistance $r(0,0)$ involves the resistance of the empty configuration in the local model and a spatial entropy that comes from the position in Λ_β where the new droplet can appear.*

(III) Our third theorem describes the typical transition of the system between two successive visits to $\mathcal{X}_{\Delta^+}$ conditional on the dynamics not returning to the same configuration at time $\bar{\tau}_{i+1}$. Given a configuration $X(\bar{\tau}_i) \in \mathcal{X}_{\Delta^+}$, recall the definition of the typical transition π'_i given in (1.3.83) and below. define the typical transition π'_i as follows.

Theorem 7.1.5. [Typical transitions] *If $\Delta < \Theta \leqslant \theta$, then for any d and α small enough, and any $i \in \mathbb{N}_0$,*

$$\lim_{\beta\to\infty} P_{\mu_{\mathcal{R}}}\left(\begin{array}{l} \text{if } \bar{\tau}_{i+1} \leqslant T^\star, \text{ then } \pi(X(\bar{\tau}_{i+1})) \in \pi'_i \\ \text{or a coalescence occurs between } \bar{\tau}_i \text{ and } \bar{\tau}_{i+1} \end{array}\ \middle|\ \pi(X(\bar{\tau}_{i+1})) \neq \pi(X(\bar{\tau}_i))\right) = 1. \tag{7.1.11}$$

(IV) Our fourth and last theorem characterises the atypical transitions of the system, starting from a subcritical configuration consisting of a single quasi–square, between two successive visits to $\mathcal{X}_{\Delta^+}$, with no creation of new boxes and conditional on the dynamics not returning to the same configuration at time $\bar{\tau}_i$. To this end, given $X(\bar{\tau}_i) \in \mathcal{X}_{\Delta^+}$ with $2 \leqslant \ell_{1,i} < \ell_c$, we recall that $\pi''_i = (\ell_{2,i}, \ell_{1,i} + 1)$ and that a *box creation occurs at time* t if there exists an active particle at time t^- that does not belong to $\Lambda(t^-)$ and falls asleep at time t.

Theorem 7.1.6. [Atypical transitions] *If $\Delta < \Theta \leqslant \theta$, then for any d and α small enough, and any $i \in \mathbb{N}_0$ such that $X(\bar{\tau}_i) \in \mathcal{X}_{\Delta^+}$ consists of a single quasi-square with $2 \leqslant \ell_{1,i} < \ell_c$,*

$$P_{\mu_{\mathcal{R}}}\left(\begin{array}{l} \text{if } \bar{\tau}_{i+1} \leqslant T^\star, \text{ then } \pi(X(\bar{\tau}_{i+1})) = \pi_i'' \text{ and} \\ \text{no box creation occurs between } \bar{\tau}_i \text{ and } \bar{\tau}_{i+1} \end{array} \middle| \, \pi(X(\bar{\tau}_{i+1})) \neq \pi(X(\bar{\tau}_i)) \right) \geqslant e^{-[(2\Delta - U) - r(\ell_1,\ell_2) + \delta]\beta}. \tag{7.1.12}$$

Remark 7.1.7. *Theorem 7.1.6 provides a lower bound for the atypical transition of 'going against the drift' in the case of a subcritical quasi-square. As we will show in the follow-up paper [12], the escape from metastability occurs via nucleation of a supercritical droplet somewhere in the box Λ_β. Indeed, we will characterise the time the dynamics needs to exit $\mathcal{R}$, as well as the typical paths of configurations visited by the wandering cluster until the formation of a large droplet. The results of the present thesis, which are limited to the case $\Theta < 2\Delta - U - \gamma$, will allow us to accomplish this task for larger values of Θ, namely, $\Theta < \Gamma - (2\Delta - U)$, where Γ is the energy of the critical droplet in the local model.*

Remark 7.1.8. *The techniques developed in the present chapter make it possible to prove that, for any quasi-square configuration of size $\ell_1 \times \ell_2$ in $\mathcal{X}_{\Delta^+}$, the cluster exits any finite box centered around the cluster with a volume that does not depend on β within a time of order $e^{r(\ell_1,\ell_2)\beta}$. This is the reason why we speak of a* wandering cluster. *We will not state this result as a formal theorem. It is similar to the study performed in [22], with the notable difference that the transition time in that paper is of order $e^{2U\beta}$, which is the time needed to detach a corner from a square droplet in the absence of a surrounding gas, while in our case it is of order $e^{\Delta\beta}$, which is the time needed for the arrival of a free particle in our local boxes.*

Remark 7.1.9. *Kawasaki dynamics in large volumes at low temperatures was studied earlier in [36]. There, the average nucleation time was computed for a specific starting distribution called the* last–exit–biased distribution *for the transition from subcritical to supercritical. The techniques employed in that paper rely on potential theory, which is tailored to deal with hitting probabilities and hitting times. It does* not *provide information on* how *the nucleation takes place. Since the last–exit–biased distribution is not a good description of the metastable equilibrium, the resulting average nucleation time is not necessarily physically realistic. However, by controlling the droplet dynamics with the tools of the present chapter, we can show that the last–exit–biased distribution falls into the basin of attraction of the metastable equilibrium, and that therefore the average nucleation time computed in [36] provides an accurate description, including prefactors.*

Remark 7.1.10. *Kawasaki dynamics in large volumes at low temperature was also studied in [68] (with the help of techniques developed in [22]). There, the transitions between the different ground states are analysed in a regime where there is no pure–gas metastable state*[1] *and the process is started from a large square droplet with no surrounding gas. In that setting the interaction between the gas and the droplet, which is at the core of the present work, is largely avoided. Both [22] and [68] are closely related to the aforementioned wandering droplet issue, about which we will say more later on.*

Remark 7.1.11. *It remains a challenge to describe what happens* after *the exit from metastability, i.e., when the system has grown a large supercritical droplet that subsequently grows, moves around, absorbs smaller droplets, thereby depleting the surrounding gas, etc. The fact that Kawasaki lattice-gas dynamics is* conservative *represents a major hurdle. For Glauber spin-flip dynamics, which is* non-conservative, *this phase of the dynamics, which is* beyond metastability, *has been* completely *elucidated at low temperatures in [53] and* partially *elucidated at all subcritical temperatures in [106]. While at low temperatures the escape from metastability and the successive growth of supercritical droplets occurs along increasingly larger Wulff shapes (up to fluctuations), these are used in [106] only as a mathematical tool to control the average transition time via monotonicity, i.e., attractiveness. The description of the typical transition paths for the non-conservative Glauber spin-flip dynamics at all subcritical temperatures is still an open problem: only the Wulff shape of the critical configurations is known, and simulations suggest that subcritical configurations are "rounder" and supercritical configurations are "straighter". Since the techniques used in [66] to control local relaxation times and show the absence of memory of the transition time for Glauber dynamics at all subcritical temperatures*

1. The condition $n^4 L^2 e^{-\beta} \ll 1$ in [68], in the notation introduced in Section 1.3.1, reads $2(\Theta - \Delta) + \Theta - U < 0$, which, together with $\Theta > \Delta$, implies that $\Delta < U$: particles immediately aggregate up to gas depletion.

do not rely on monotonicity, we might hope to be able to extend our understanding of the gas-droplet interaction and thereby extend our control of the transition time for non-monotone Kawasaki dynamics at higher temperatures. However, this will not be sufficient to describe the shape of evaporating subcritical clusters in a depleted gas where critical clusters can still grow. It is also beyond the scope of the present work, in which we analyse the gas-droplet interaction in the much simpler context of low-temperature dynamics and are able to fully characterise the typical escape paths from metastability, while the metastable state of Kawasaki dynamics in large volume does not look like a ground state of a restricted dynamics.

7.2 KEY TOOLS

In this section we provide some tools that are needed to prove the theorems. These tools rely on the notion of QRWs (Quasi-Random Walks). In [62] it was shown that the active particles of a two-dimensional lattice gas under Kawasaki dynamics at low density evolve in a way that is close to an *ideal gas*. The results in [62] are formulated in the general context of QRWs for a large class of initial conditions having no anomalous concentration of particles for time horizons that are much larger than the typical collision time. More precisely, the process of QRWs used to describe the ideal gas approximation consists of N labelled particles that can be coupled to a process of N Independent Random Walks (IRWs) in such a way that the two processes follow the same paths outside rare time intervals, called pause intervals, in which the paths of the QRWs remain confined to small regions.

For the definition of QRWs and their construction, we refer to [62, Sections 2.2-2.4]. We note that for the notion of sleeping and active particles to be well defined, we need to label the *particles* and not work with a dynamics of *configurations* $\eta \in \mathcal{X}_\beta$ only, as defined in (1.3.4). There is flexibility in associating a particle dynamics with a configuration dynamics. In particular, as in [62] we can allow instantaneous permutation of particles inside a given cluster. Later we will use this flexibility by specifying a local permutation rule (see Section 7.4.3.1). For now we only assume that such a rule has been chosen. We encourage the reader to inspect the main properties of QRWs, which will be a key tool in the remaining part of the chapter. In particular, we refer to [62, Theorems 3.2.3, 3.2.4, 3.2.5, 3.3.1] for the *non-superdiffusivity* property and for upper and lower bounds on the *spread-out property*, respectively.

7.2.1 *Definitions and notations*

In this section we introduce some definitions and notations that will be needed throughout the sequel.

Definition 7.2.1.

1. *As in [62], α and d are two positive parameters that can be chosen as small as desired, and $\lambda(\beta)$ is an unbounded but slowly increasing function of β that satisfies (1.3.75). Moreover, $C^\star$ is a positive parameter that can be chosen as large as desired. Once chosen, α, d, λ and $C^\star$ are fixed. We write $O(\delta)$, $O(\alpha)$ and $O(d)$ for quantities with an absolute value that can be bounded by a constant times $|\delta|$, $|\alpha|$ and $|d|$, for small enough values of these parameters. We write $O(\delta, \alpha, d)$ for the sum of three such quantities.*
2. *We use short-hand notation for a few quantities that depend on the old parameters $\Delta \in (\frac{3}{2}U, 2U)$ and $\Theta \in (\Delta, 2\Delta - U)$, and on the new parameters α, d. Recall that*

$$\varepsilon = 2U - \Delta, \qquad \ell_c = \left\lceil \frac{U}{\varepsilon} \right\rceil, \qquad \gamma = \Delta - U - (\ell_c - 2)\varepsilon, \qquad \theta = 2\Delta - U - \gamma,$$

and

$$D = U + d, \qquad \Delta^+ = \Delta + \alpha,$$

and abbreviate

$$S = \frac{4\Delta - \theta}{3} - \alpha. \tag{7.2.1}$$

For $C > 0$, write T_C for the time scale $T_C = e^{C\beta}$.

3. *For convenience we identify a configuration* $\eta \in \mathcal{X}_\beta$ *with its support* $supp(\eta) = \{z \in \Lambda_\beta : \eta(z) = 1\}$ *and write* $z \in \eta$ *to indicate that* η *has a particle at* z*. For* $\eta \in \mathcal{X}_\beta$*, denote by* η^{cl} *the clusterised part of* η*:*

$$\eta^{cl} = \{z \in \eta : \ \| z - z' \| = 1 \text{ for some } z' \in \eta\}. \tag{7.2.2}$$

Call clusters of η *the connected components of the graph drawn on* η^{cl} *obtained by connecting nearest-neighbour sites that are not a singleton.*

4. *Denote by* $B(z, r), z \in \mathbb{R}^2, r > 0$*, the open ball with center* z *and radius* r *in the norm defined in (7.1.1). The closure of* $A \subset \mathbb{R}^2$ *is denoted by* $\overline{A}$*.*
5. *For* $A \subset \mathbb{Z}^2$*, denote by* $\partial^- A$ *the internal boundary of* A*, i.e.,*

$$\partial^- A = \{z \in A : \ \| z - z' \| = 1 \text{ for some } z' \in \mathbb{Z}^2 \setminus A\}. \tag{7.2.3}$$

For $s > 0$*, put*

$$[A, s] = \bigcup_{z \in A} \overline{B(z, e^{\frac{s}{2}\beta})} \cap \mathbb{Z}^2. \tag{7.2.4}$$

Call A *a rectangle on* $\mathbb{Z}^2$ *if there are* $a, b, c, d \in \mathbb{R}$ *such that*

$$A = [a, b] \times [c, d] \cap \mathbb{Z}^2. \tag{7.2.5}$$

Write RC(A), called the circumscribed rectangle of A*, to denote the intersection of all the rectangles on* $\mathbb{Z}^2$ *containing* A*. Moreover, denote by* $\mathcal{R}$ *the set of all finite sets of rectangles on* $\mathbb{Z}^2$*.*

6. *Given* $\sigma \geqslant 0$ *and* $\bar{S} = \{R_1, \dots, R_{|S|}\} \in \mathcal{R}$*, two rectangles* R *and* R' *in* $\bar{S}$ *are said to be in the same equivalence class if there exists a finite sequence* $R_1, \dots, R_k$ *of rectangles in* $\bar{S}$ *such that*

$$R = R_1, \quad R' = R_k, \quad \operatorname{dist}(R_j, R_{j+1}) < \sigma \ \forall\, 1 \leqslant j < k.$$

Let C *indicate the set of equivalent classes, define the map*

$$\bar{g}_\sigma : \bar{S} \in \mathcal{R} \mapsto \left\{ RC\left(\bigcup_{j \in c} R_j \right) \right\}_{c \in C} \in \mathcal{R},$$

and let $(\bar{g}_\sigma^{(k)})_{k \in \mathbb{N}_0} \in \mathcal{R}^{\mathbb{N}}$ *be the sequence of iterates of* $\bar{g}_\sigma$*. Define*

$$g_\sigma(\bar{S}) = \lim_{k \to \infty} \bar{g}_\sigma^{(k)}(\bar{S}). \tag{7.2.6}$$

As discussed in [64], the sequence $(\bar{g}_\sigma^{(k)}(\bar{S}))_{k \in \mathbb{N}_0}$ *ends up being a constant, so the limit is well defined.*

7.2.2 *Environment estimates*

In this section we introduce a subset of configurations $\mathcal{X}^* \subset \mathcal{X}_\beta$, to which we refer as the *typical environment*, with the property that if our system is started from the restricted ensemble, then it can escape from $\mathcal{X}^*$ within any time scale that is exponential in β with a negligible probability only. Boxes are square boxes, and we require that $\Theta > \Delta$. Recall (7.2.1) for the definition of the parameter S.

Remark 7.2.2. *The choice of* S *comes from the fact that we require the probability to have 4 particles anywhere in a box of volume* $e^{S\beta}$ *to tend to zero under the measure* $\mu_{\mathcal{R}}$ *as* $\beta \to \infty$*.*

Definition 7.2.3. *Define*

$$\mathcal{X}^* = \bigcap_{j=1}^{5} \mathcal{X}_j^*, \tag{7.2.7}$$

where, for λ satisfying (1.3.75) and S given by (7.2.1),

$$\mathcal{X}_1^* = \Big\{\eta \in \mathcal{X}_\beta : \textit{in any box of volume } e^{\theta\beta} \textit{ the number of clusters is at most } \lambda(\beta)\Big\},$$

$$\mathcal{X}_2^* = \left\{\eta \in \mathcal{X}_\beta : \begin{array}{l}\textit{in any box of volume } e^{\theta\beta} \textit{ the number of 4-tuples of particles in different}\\ \textit{connected components with diameter smaller than } \sqrt{e^{S\beta}} \textit{ is at most } \lambda(\beta)\end{array}\right\},$$

$$\mathcal{X}_3^* = \left\{\eta \in \mathcal{X}_\beta : \begin{array}{l}\textit{in any box of volume } e^{\theta\beta} \textit{ the number of 4-tuples of particles in}\\ \textit{different connected components with diameter smaller than } \sqrt{e^{A\beta}}\\ \textit{is at most } e^{(3A-4\Delta+\theta+4\alpha)\beta} \textit{ for any } S < A < \Delta^+\end{array}\right\},$$

$$\mathcal{X}_4^* = \left\{\eta \in \mathcal{X}_\beta : \begin{array}{l}\textit{in any box of volume } e^{(\Delta+\alpha)\beta} \textit{ the number of particles is at most } e^{\frac{3}{2}\alpha\beta}\\ \textit{and at least } e^{\frac{1}{2}\alpha\beta}\end{array}\right\},$$

$$\mathcal{X}_5^* = \Big\{\eta \in \mathcal{X}_\beta : \textit{in any box of volume } e^{(\Delta-\frac{\alpha}{4})\beta} \textit{ the number of particles is at most } \tfrac{1}{4}\lambda(\beta)\Big\}.$$

Remark 7.2.4. *The exit time of $\mathcal{X}_5^*$ coincides with the first time $\mathcal{T}_{\alpha,\lambda}$ when an anomalous concentration event occurs ([62]). Since the QRW-estimates of [62] hold up to this time, we can use them as long as the system stays in $\mathcal{X}^* \subset \mathcal{X}_5^*$.*

Remark 7.2.5. *The reason why we define $\mathcal{X}^*$ for any $\Theta > \Delta$ (i.e., without the restriction $\Theta \leqslant \theta$) is that in [12] we will need Proposition 7.2.6, which says that starting from $\mu_{\mathcal{R}}$ the system exits $\mathcal{X}^*$ within any given exponential time with $\mathrm{SES}(\beta)$ probability only. The main theorems of the present thesis, which hold for the dynamics in a box of volume at most $e^{\theta\beta}$, with* periodic *boundary conditions, immediately extend to the case where such a small box is embedded into a larger box of volume $e^{\Theta\beta}$, with* open *boundary conditions, as long as the system remains in the typical environment $\mathcal{X}^*$.*

Recall the definition of the set $\mathcal{R}$ given in (1.3.71), of the set $\mathcal{R}' \supset \mathcal{R}$ given in (1.3.74) and of the time $T^\star$ given in (1.3.76).

Proposition 7.2.6. $P_{\mu_{\mathcal{R}}}(\tau_{\mathcal{X}_\beta \setminus \mathcal{X}^*} \leqslant T^\star) = \mathrm{SES}(\beta)$.

Proof. Denote by A_t the event that the dynamics exits $\mathcal{X}^*$ at time t, and by $A_t^{\mathcal{R}'}$ the event A_t when the dynamics is restricted to $\mathcal{R}'$ (by ignoring jumps that would lead the dynamics out of $\mathcal{R}'$). Given a Poisson process on $\mathbb{R}_+$ with rate $e^{\Theta\beta}$, denote by $M(t)$ the number of times the clock rings up to time $t \geqslant 0$, and write P to denote its law. Let $(\check{X}_k)_{k\in\mathbb{N}}$ be the the embedded discrete-time process such that the original process $(X(t))_{t\geqslant 0}$ can be written as $X(t) = \check{X}_{M(t)}$. Estimate, for $\delta > 0$,

$$\begin{aligned}
P_{\mu_{\mathcal{R}}}(\exists\, t < T^\star, A_t) &= \sum_{\eta\in\mathcal{R}} \frac{\mu(\eta)}{\mu(\mathcal{R})} P_\eta(\exists\, t < T^\star, A_t)\\
&\leqslant \frac{\mu(\mathcal{R}')}{\mu(\mathcal{R})} \sum_{\eta\in\mathcal{R}'} \frac{\mu(\eta)}{\mu(\mathcal{R}')} P_\eta(\exists\, t < T^\star, A_t)\\
&\leqslant \frac{\mu(\mathcal{R}')}{\mu(\mathcal{R})} P_{\mu_{\mathcal{R}'}}\Big(\exists\, t < e^{C^\star\beta}, A_t^{\mathcal{R}'}\Big)\\
&\leqslant \frac{\mu(\mathcal{R}')}{\mu(\mathcal{R})}\Big[P\Big(M(e^{C^\star\beta}) \geqslant e^{(\Theta+C^\star+\delta)\beta}\Big)\\
&\qquad + \sum_{1\leqslant k<e^{(\Theta+C^\star+\delta)\beta}} P_{\mu_{\mathcal{R}'}}(\check{X}_k \in \mathcal{X}_\beta \setminus \mathcal{X}^*)\Big]\\
&\leqslant \frac{\mu(\mathcal{R}')}{\mu(\mathcal{R})}\Big[\mathrm{SES}(\beta) + e^{(\Theta+C^\star+\delta)\beta} \sum_{i=1}^{5} \mu_{\mathcal{R}'}((\mathcal{X}_i^*)^c)\Big],
\end{aligned}$$

where the term $\mathrm{SES}(\beta)$ comes from the Chernoff bound for a Poisson random variable, and $\mu_{\mathcal{R}'}$ stands for the grand-canonical Gibbs measure conditioned to $\mathcal{R}'$. To get the claim, note that, because $\mu(\mathcal{R}')/\mu(\mathcal{R}) \leqslant e^{\bar{C}\beta}$ for some $\bar{C} > 0$, it suffices to prove that $\mu_{\mathcal{R}'}((\mathcal{X}_i^*)^c) = \mathrm{SES}(\beta)$ for any i. This is done in Appendix 7.A. □

Remark 7.2.7. *Proposition 7.2.6 allows us to work with configurations in $\mathcal{X}^*$. Replacing the original dynamics by the dynamics restricted to $\mathcal{X}^*$, we can couple the two dynamics in such a way that they have the same trajectories up to any time that is exponential in β with probability $1 - \mathrm{SES}(\beta)$.*

7.2.3 *Recurrence properties*

In this section we group the configurations in $\mathcal{X}_\beta$ into a sequence of subsets of configurations of *increasing regularity*, and we prove a *recurrence property* of the associated Markov processes restricted to these sets on an *increasing sequence of time scales*. To that end, denote by

$$\bar{H}_i(\bar{\eta}_i) = -U \sum_{\{x,y\}\in\bar{\Lambda}_i(t)^*} \eta(x)\eta(y) + \Delta \sum_{x\in\bar{\Lambda}_i(t)} \eta(x)$$

the *local energy* of $\bar{\eta}_i = \eta_{|\bar{\Lambda}_i}$ at time t inside the box $\bar{\Lambda}_i(t)$, where $\bar{\Lambda}_i(t)^*$ denotes the set of bonds in $\bar{\Lambda}_i(t)$. We emphasise that, alongside the local model, we need to introduce two additional sets, $\mathcal{X}_D$ and $\mathcal{X}_S$, to control the regularity of the gas surrounding the droplets.

Remark 7.2.8. *With each particle i we can associate, at any time $t \geqslant 0$, the time*

$$s_i(t) = \inf\big\{s \in [0,t)\colon \textit{ particle } i \textit{ is not free during the entire time interval } [s,t]\big\}, \tag{7.2.8}$$

so that $s_i^*(t) = e^{D\beta} - (t - s_i(t))$ is the time that particle i needs to remain not free in order to fall asleep. By convention, for a sleeping (respectively, free) particle at time t we put $s_i^*(t) = 0$ (respectively, $s_i^*(t) = \infty$). In this way we are able to characterise active and sleeping particles at any time t. In addition, the process $Y = (X(t), (s_i^*(t))_{i=1}^N, \bar{\Lambda}(t))_{t\geqslant 0}$ is Markovian. In the sequel we will simply refer to this process as the original process $X = (X(t))_{t\geqslant 0}$. In Section 7.4.3.1 we will consider a slight generalisation of the process Y in which more information about particles is included, again referring to it as the original process X.

Definition 7.2.9. *For any time $t \geqslant 0$, given a configuration $\eta_t = X(t) \in \mathcal{X}_\beta$ and the collection $\bar{\Lambda}(t) = (\bar{\Lambda}_i(t))_{1\leqslant i\leqslant k(t)}$ of finite boxes in Λ_β as in Definition 7.1.1, we say that η_t is 0-reducible (respectively, U-reducible) if for some i the local energy of $\bar{\eta}_i$ can be reduced along the dynamics with constant $\bar{\Lambda}(t)$ without exceeding the energy level $\bar{H}_i(\bar{\eta}_i) + 0$ (respectively, $\bar{H}_i(\bar{\eta}_i) + U$). If η_t is not 0-reducible or U-reducible, then we say that η_t is 0-irreducible or U-irreducible, respectively. We define*

$$\begin{aligned}
\mathcal{X}_0 &= \{\eta_t \in \mathcal{X}^*\colon \eta_t \textit{ is 0-irreducible}\},\\
\mathcal{X}_U &= \{\eta_t \in \mathcal{X}_0\colon \eta_t \textit{ is } U\textit{-irreducible}\},\\
\mathcal{X}_D &= \{\eta_t \in \mathcal{X}_U\colon \textit{all the particles in } \Lambda(t) \textit{ are sleeping}\},\\
\mathcal{X}_S &= \{\eta_t \in \mathcal{X}_D\colon \textit{each box of volume } e^{S\beta} \textit{ contains three active particles at most}\},\\
\mathcal{X}_{\Delta^+} &= \left\{\eta_t \in \mathcal{X}_S\colon \begin{array}{l} \bar{\eta}_t \textit{ is a union of at most } \lambda(\beta) \textit{ quasi-squares with}\\ \textit{no particle inside } \bigcup_i [\bar{\Lambda}_i(t), \Delta-\alpha] \textit{ except for those}\\ \textit{in the quasi-squares, one for each local box } \bar{\Lambda}_i(t)\end{array}\right\},
\end{aligned}$$

where $[\bar{\Lambda}_i(t), \Delta - \alpha]$ are the boxes of volume $e^{(\Delta-\alpha)\beta}$ with the same center as $\bar{\Lambda}_i(t)$.

Remark 7.2.10. *Note that if $\eta \in \mathcal{X}_{\Delta^+}$ and $\ell_2 = 2$, then $\ell_1 = 2$. Indeed, a 1×2 dimer does not belong to $\mathcal{X}_U$ and therefore is not in $\mathcal{X}_{\Delta^+}$.*

Recall that $T_A = e^{A\beta}$ for $A \in \{0, U, D, S, \Delta^+\}$. Note that we have used the index Δ^+ to define the set $\mathcal{X}_{\Delta^+}$, despite the fact that it explicitly depends on the quantity $\Delta - \alpha$. This is needed to provide an upper bound for the return times in $\mathcal{X}_{\Delta^+}$, namely, the recurrence property stated in the following proposition, which uses the usual shift operator ϑ_s, $s \geqslant 0$, defined by $\vartheta_s(X) = X(s + \cdot)$, so that $s + \tau_{\mathcal{X}_A} \circ \vartheta_s = \min\{t \geqslant s\colon X(t) \in \mathcal{X}_A\}$.

Proposition 7.2.11. *For all $A \in \{0, U, D, S, \Delta^+\}$, all $\delta > 0$ and any stopping time τ,*

$$P_{\mu_{\mathcal{R}}}\big(\tau_{\mathcal{X}_A} \circ \vartheta_\tau \geqslant T_A e^{\delta\beta},\ \tau + \tau_{\mathcal{X}_A} \circ \vartheta_\tau \leqslant T^\star\big) = \mathrm{SES}(\beta).$$

To prove Proposition 7.2.11, we need the following lemma, whose proof is postponed until after the proof of Proposition 7.2.11.

Lemma 7.2.12. *Let $t \geqslant 0$ be the time at which an active particle p joins a cluster $\mathcal{C}$ with at most two particles, and let $t^* = t + (t_1 \wedge t_2) \circ \vartheta_t$, where t_1 (respectively, t_2) is the first time when the cluster $\mathcal{C}$ contains at least four particles (respectively, does not contain particle p anymore). The probability that particle p falls asleep during the time interval $[t, t^*]$ is* SES(β).

Proof of Proposition 7.2.11. Let $A \in \{0, U, D, S, \Delta^+\}$. Divide the time interval $[0, T_A e^{\delta\beta}]$ into $e^{\frac{3}{4}\delta\beta}$ intervals I_j of length $T_A e^{\frac{\delta}{4}\beta}$. We have

$$\begin{aligned} \sup_{\eta\in\mathcal{X}^*} P_\eta(\tau_{\mathcal{X}_A} \wedge \tau_{\mathcal{X}_\beta\setminus\mathcal{X}^*} > T_A e^{\delta\beta}) &\leqslant \prod_{1\leqslant j<e^{\frac{3}{4}\delta\beta}} \sup_{\eta\in\mathcal{X}^*} P_\eta(\tau_{\mathcal{X}_A}, \tau_{\mathcal{X}_\beta\setminus\mathcal{X}^*} \notin I_j) \\ &= \Big(1 - \inf_{\eta\in\mathcal{X}^*} P_\eta(\tau_{\mathcal{X}_A} \wedge \tau_{\mathcal{X}_\beta\setminus\mathcal{X}^*} \leqslant T_A e^{\frac{\delta}{4}\beta})\Big)^{e^{\frac{3}{4}\delta\beta}}, \end{aligned} \tag{7.2.9}$$

where we use the strong Markov property for the stopping time $\tau_{\mathcal{X}_A}$. By Proposition 7.2.6, it suffices to prove that

$$\inf_{\eta\in\mathcal{X}^*} P_\eta(\tau_{\mathcal{X}_A} \wedge \tau_{\mathcal{X}_\beta\setminus\mathcal{X}^*} \leqslant T_A e^{\frac{\delta}{4}\beta}) \geqslant e^{-\frac{\delta}{4}\beta}. \tag{7.2.10}$$

In other words, for each η in $\mathcal{X}^*$ we have to build a dynamical event on time scale $T_A e^{(\delta/4)\beta}$ and with probability at least $e^{-(\delta/4)\beta}$ such that the final configuration is in $\mathcal{X}_A$, provided our system does not exit $\mathcal{X}^*$. This is a standard estimate for metastable systems at low temperature, which has been carried out in full detail for a simplified version of our model [75]. Here we indicate the differences with respect to the earlier work.

To build $\mathcal{X}_A$, we used $\Lambda(t) = \cup_{1\leqslant i\leqslant k(t)}\bar\Lambda_i(t)$, the connected components of which form our box collection $\bar\Lambda(t)$. For $A \leqslant S$ we use another box collection $\bar\Lambda'(t)$ such that $\Lambda'(t) = \cup_{1\leqslant i\leqslant k'(t)}\bar\Lambda'_i(t)$, for which $\bar\Lambda'_i(t)$, $1 \leqslant i \leqslant k'(t)$, are the connected components of $\Lambda'(t)$, and such that $\Lambda(t) \subset \Lambda'(t)$ for all t. As a consequence, the associated $\mathcal{X}'_A$ is contained in $\mathcal{X}_A$. We need to consider this new collection $\bar\Lambda'(t)$ in order to avoid the creation of new local boxes when some particle outside of $\bar\Lambda(t)$ falls asleep before time $T_A e^{\delta\beta}$. The construction of $\bar\Lambda'(t)$ is analogous to that in Definition 7.1.1, but now without removing the collection $\bar\Lambda^*(t)$, $t \geqslant 0$, i.e., the boxes without sleeping particles, and by redefining the boxes at time t when at least one of the conditions B1′, B3 and B4 is violated by $\bar\Lambda'(t^-)$, with B1′ being defined as B1 but referring to clusterised particles instead of sleeping particles. In this way the new collection satisfies conditions B1′, B3 and B4 for any $t \geqslant 0$.

• Case $A = 0$: Consider $\Lambda'(0)$, which contains all the clusterised particles at time 0 and is such that all particles outside $\Lambda'(0)$ are initially free. Let τ_c be the first time when two of these free particles collide, or one of them enters $\Lambda'(0)$. By [64, Proposition 3.1.1 and Theorem 1], the probability that $\tau_c > e^{\delta\beta}$ when starting from a configuration in $\mathcal{X}^*$ is larger than $e^{-\delta\beta}$ for β large enough. Conditionally on this event, and as long as no clusterised particle in $\Lambda'(0)$ is at distance one from the internal border of $\Lambda'(0)$, the dynamics inside $\Lambda'(0)$ is independent from that outside. By construction, there are at least two particles in each $\bar\Lambda_i(0)$. By grouping them we can perform within time $e^{\delta\beta}$ the 0-reduction in $\bar\Lambda'(0)$ with a non-exponentially small probability, as in [75]: the only difference is that we are not working with a box $\bar\Lambda(0)$ of a bounded size but of a slowly growing size. However, we can deal with this box as in [62, Appendix A].

• Case $A = U$: We can proceed in the same way, except for the fact that to reach a U-irreducible configuration we may have to move some particle outside $\Lambda'(0)$. This happens for example when starting with a protuberance on a quasi-square (see [75]). We set

$$\tilde\Lambda = \{\zeta \in \Lambda_\beta : \exists x \in \Lambda'(0), \|\zeta - x\| \leqslant 2\}$$

and to build the reduction event we ask that each free particle in $\Lambda_\beta \setminus \tilde\Lambda$ remains free, without entering $\tilde\Lambda$, for a time $T_U e^{\delta\beta}$. We also ask that each free particle in $\tilde\Lambda \setminus \Lambda'(0)$ moves to $\Lambda_\beta \setminus \tilde\Lambda$ without visiting $\Lambda'(0)$ or forming a new cluster. Conditionally on this event, the local

configuration in $\Lambda'(0)$ can be U-reduced, with respect to $\Lambda'(0)$, within time $T_U e^{\delta\beta}$ with a non-exponentially small probability. Since no more than $\lambda(\beta)$ particles can leave $\Lambda'(0)$ on the described event, [64, Theorem 1] gives the desired bound.

• Case $A = D$: We can simply use the same event as in the case $A = U$, but built on the slightly longer time scale $T_D e^{\delta\beta}$: all clusterised particles in our U-reduced configuration fall asleep.

• Case $A = S$: We use again the same event, but built on the longer time scale $T_S e^{\delta\beta}$. By the coupling of QRWs and IRWs, the probability that a given quadruple of free particles at time $T_D e^{\delta\beta}$ has a diameter at most $e^{S\beta/2}$ at time $T_S e^{\delta\beta}$ is smaller than $e^{-\delta\beta/2}$, as a consequence of the spread-out property of the simple random walk given by the difference between the position of two of the four particles. By the non-superdiffusivity property, assuming that our process is in $\mathcal{X}_D \subset \mathcal{X}^*$ at time $T_D e^{\delta\beta}$, we only have to consider $\lambda(\beta)$ quadruples to check that by time $T_S e^{\delta\beta}$ we have reached $\mathcal{X}_S$: the probability that a particle exits $\Lambda'(0)$ within time $T_S e^{\delta\beta} \ll e^{2U\beta}$, and before the entrance of a new particle in $\Lambda'(0)$, is exponentially small in β. Consequently,

$$P_\eta(X(T_S e^{\delta\beta}) \in \mathcal{X}_S \text{ or } \tau_{\mathcal{X}^*} < T_S e^{\delta\beta}) \geqslant e^{-\frac{\delta}{4}\beta} - e^{-(2U-S-\delta)\beta} - \lambda(\beta) e^{-\frac{\delta}{2}\beta} \geqslant e^{-\frac{\delta}{3}\beta}$$

for β large enough.

• Case $A = \Delta + \alpha$: We have shown that within time $T_S e^{\delta\beta}$ the dynamics reaches $\mathcal{X}_S$ or exits $\mathcal{X}^*$ with probability $1 - \mathrm{SES}(\beta)$. To build the event, we let particles enter the local boxes in order to form quasi-squares, before emptying the annulus between $[\Lambda(t), \Delta - \alpha]$ and $\Lambda(t)$ for a large enough t, while going to $\mathcal{X}_S$, all without the occurrence of a box creation. To control this event, we provide an upper bound for the probability that a box creation occurs after reaching $\mathcal{X}_S$. A box creation can occur with a non-$\mathrm{SES}(\beta)$ probability only when four particles are in a box of volume $e^{(D+\delta)\beta}$ at the same time $t < T_{\Delta^+} e^{(\delta/4)\beta}$. Indeed, starting from a cluster consisting of two or three particles only, the probability that a particle falls asleep is $\mathrm{SES}(\beta)$ by Lemma 7.2.12. We estimate from above the probability to have four particles in a box of volume $e^{(D+\delta)\beta}$ at the same time $t < T_{\Delta^+} e^{(\delta/4)\beta}$. For $S < A' < \Delta^+$ we can estimate the probability that a given quadruple of particles with diameter $e^{A'\beta/2}$ arrives in a box of volume $e^{(D+\delta)\beta}$ within time $T_{\Delta^+} e^{\delta\beta}$, as follows. Divide the time interval $[e^{A'\beta}, T_{\Delta^+} e^{\delta\beta}]$ into intervals of length $e^{D\beta}$, and divide at each initial time $ie^{D\beta}$ of such a time interval the volume $ie^{(D+\delta)\beta}$ centered at one of the particles into boxes of volume $e^{(D+\delta)\beta}$. Then, by the non-superdiffusivity property and the spread-out property of the QRWs, we get that the required probability is at most

$$e^{\delta\beta} \sum_{e^{A'\beta} \leqslant ie^{D\beta} \leqslant e^{(\Delta+\alpha+\delta)\beta}} \left(\frac{ie^{(D+\delta)\beta}}{e^{(D+\delta)\beta}}\right) \left(\frac{e^{(D+\delta)\beta} e^{\delta\beta}}{ie^{(D+\delta)\beta}}\right)^4 \leqslant e^{2(D-A')\beta + O(\delta)\beta}.$$

When $X(T_S e^{\delta\beta}) \in \mathcal{X}^*$, this implies that the probability to have four particles in a box of volume $e^{(D+\delta)\beta}$ within time $T_{\Delta^+} e^{\delta\beta}$ is at most $e^{(A'+2D-4\Delta+\theta+4\alpha)\beta} e^{O(\delta)\beta}$, which is an increasing function of A'. Since $A' < \Delta^+$, we have that the required probability is less than $e^{\theta\beta} e^{(2D-3\Delta)\beta} e^{(4\alpha+O(\delta))\beta}$, which implies that

$$P\big(\text{a box creation occurs within time } T_{\Delta^+} e^{\delta\beta}\big) \leqslant e^{-(3\Delta-2U-\theta-2d)\beta}. \tag{7.2.11}$$

This is exponentially small, so that we can work with a constant number of boxes.

We can now proceed as in [75] to bring in particles from the gas in order to build quasi-squares. One additional difficulty and one additional simplification occurs. While in [75] the local box was fixed, which makes motion of large droplets inside impossible, here our local boxes move with the droplets, so that there are no lacunary configuration issues. However, we cannot use the simple random walk estimates to give lower bounds on the probability of bringing particles from the gas into the local boxes: these have to be replaced by the strong lower bounds of [62, Theorem 3.3.1]. Once we have obtained quasi-squares only in $\Lambda(\tau)$ for some stopping time $\tau \leqslant T_{\Delta^+} e^{\delta\beta/2}$, we can build the same event that was used to deal with $A = S$ to empty the annulus $[\Lambda(\tau), \Delta - \alpha] \setminus \Lambda(\tau)$ without moving the boxes anymore while going back to $\mathcal{X}_S$. □

Proof of Lemma 7.2.12. Suppose that two active particles join together. Divide the time interval $[0, e^{D\beta}]$ into $e^{\frac{3}{4}d\beta}$ intervals of length $e^{(U+\frac{d}{4})\beta}$. We have

$$P\big(\text{a particle is detached within time } e^{(U+\frac{d}{4})\beta}\big) \geqslant e^{-\frac{d}{4}\beta}$$

and so by the Markov property the probability to have a particle falling asleep is at most $(1-e^{-\frac{d}{4}\beta})^{e^{\frac{3}{4}d\beta}} = \mathrm{SES}(\beta)$. The case in which three active particles join together can be treated similarly. □

7.3 PROOF OF THEOREMS

Section 7.3.1 lists three key propositions that provide bounds on the probability of transitions between configurations consisting of a single quasi-square and free particles. The proofs of these propositions are deferred to Section 7.4. Sections 7.3.2–7.3.5 use the propositions to prove Theorems 7.1.2–7.1.6, respectively.

The pure gas state is defined as

$$\mathcal{X}_E := \{\eta \in \mathcal{X}_{\Delta^+} : \eta \text{ has no quasi-square}\}. \tag{7.3.1}$$

7.3.1 *Key propositions: Propositions 7.3.1–7.3.3*

Recall the definition of $\pi(\eta_0) \in \bar{\mathcal{X}}_\Delta$, $\eta_0 \in \mathcal{X}_{\Delta^+}$, given in Section 7.1. Denote by $(\ell_1, \ell_2) \in QS$ with $\ell_1 \geqslant 2$ the dimensions of the smallest quasi-square, if any, otherwise set $\ell_1 = \ell_2 = 0$. Define the projections $\pi', \pi'' \in \bar{\mathcal{X}}_\Delta$ similarly to the projections π'_i, π''_i defined in Section 7.1.

We start by giving a lower bound for the probability that the dynamics, starting from $\eta_0 \in \mathcal{X}_{\Delta^+}$, has a projection that is distinct from $\pi(\eta_0)$ at time $\bar{\tau}_1$ without exiting the environment $\mathcal{X}^*$.

Proposition 7.3.1. *Assume that $\Delta < \Theta \leqslant \theta$. If $\eta_0 \in \mathcal{X}_{\Delta^+}$, then for any $\delta > 0$,*

$$P_{\eta_0}\left(\begin{array}{l}\pi(X(\bar{\tau}_1)) \neq \pi(\eta_0) \text{ or a coalescence}\\ \text{occurs before } \bar{\tau}_1 \text{ or } \bar{\tau}_1 > \tau_{\mathcal{X}_\beta \setminus \mathcal{X}^*}\end{array}\right) \geqslant e^{-[r(\ell_1,\ell_2)-\Delta+O(\alpha,d,\delta)]\beta}.$$

The proof of Proposition 7.3.1 is given in Section 7.4.1.

We next give a lower bound on the probability that the dynamics, starting from $\eta_0 \in \mathcal{X}_{\Delta^+}$ consisting of a single subcritical quasi-square, at time $\bar{\tau}_1$ reaches a configuration $X(\bar{\tau}_1)$ such that $\pi(X(\bar{\tau}_1)) = \pi''$ without exiting the environment $\mathcal{X}^*$ and no box creation occurs before $\bar{\tau}_1$.

Proposition 7.3.2. *Assume that $\Delta < \Theta \leqslant \theta$. If $\eta_0 \in \mathcal{X}_{\Delta^+}$ consists of a single $\ell_1 \times \ell_2$ quasi-square with $2 \leqslant \ell_1 < \ell_c$, then for any $\delta > 0$,*

$$P_{\eta_0}\left(\begin{array}{l}\pi(X(\bar{\tau}_1)) = \pi'' \text{ and no box creation}\\ \text{occurs before } \bar{\tau}_1, \text{ or } \bar{\tau}_1 > \tau_{\mathcal{X}_\beta \setminus \mathcal{X}^*}\end{array}\right) \geqslant e^{-[\Delta-U+O(\alpha,d,\delta)]\beta}.$$

The proof of Proposition 7.3.2 is given in Section 7.4.2.

We finally provide upper bounds on the probability that typical and atypical transitions occur.

Proposition 7.3.3. *Assume that $\Delta < \Theta \leqslant \theta$.*
(1) If $\eta_0 \in \mathcal{X}_{\Delta^+}$, then

$$\limsup_{\beta\to\infty} \sup_{\pi(\eta_0)} \frac{1}{\beta} \log P_{\eta_0}\left(\begin{array}{l}\pi(X(\bar{\tau}_1)) \neq \pi(\eta_0) \text{ and a}\\ \text{coalescence does not occur}\\ \text{before } \bar{\tau}_1, \text{ or } \bar{\tau}_1 > \tau_{\mathcal{X}_\beta \setminus \mathcal{X}^*}\end{array}\right) \leqslant -[r(\ell_1,\ell_2)-\Delta-O(\alpha,d)]. \tag{7.3.2}$$

(2) If $\eta_0 \in \mathcal{X}_{\Delta^+} \setminus \mathcal{X}_E$, then

$$\limsup_{\beta\to\infty} \sup_{\pi(\eta_0)} \frac{1}{\beta} \log P_{\eta_0}\left(\begin{array}{l}\pi(X(\bar{\tau}_1)) \notin \{\pi(\eta_0)\} \cup \pi' \text{ and}\\ \text{a coalescence does not occur}\\ \text{before } \bar{\tau}_1, \text{ or } \bar{\tau}_1 > \tau_{\mathcal{X}_\beta \setminus \mathcal{X}^*}\end{array}\right) < -[r(\ell_1,\ell_2)-\Delta-O(\alpha,d)]. \tag{7.3.3}$$

The proof of Proposition 7.3.3 is given in Section 7.4.3.

7.3.2 *Proof of Theorem 7.1.2*

Fix $\delta > 0$. From Proposition 7.2.11 we deduce that the event $\{\bar\tau_0 \geqslant e^{(\Delta+\alpha+\delta)\beta}, \bar\tau_0 \leqslant T^\star\}$ has probability SES(β). Consider any $i \in \mathbb{N}_0$ such that $\bar\tau_{i+1} \leqslant T^\star$. The event $\{\bar\tau_{i+1} - \bar\tau_i > e^{(\Delta+\alpha+\delta)\beta}\}$ has probability SES(β). Indeed, this event would imply that either $\bar\sigma_{i+1}$ or $\bar\tau_{i+1}$ exceed $T_{\Delta^+} e^{\delta\beta}$, and both have probability SES(β). Indeed, in the former case, we have to control the probability that none of the particles inside the volume $[\bar\Lambda, \Delta + \alpha]$ enters $\bar\Lambda$ within a time $T_{\Delta^+} e^{\delta\beta}$. These particles are at least $e^{\frac{1}{2}\alpha\beta}$ in number, since the dynamics is in $\mathcal{X}^*$ because of the condition $\bar\tau_{i+1} \leqslant T^\star$. Hence this probability is SES(β) by the strong lower bounds associated with the spread-out property of QRWs (see [62, Theorem 3.3.1]). In the latter case, we conclude by using Proposition 7.2.11. Also the event $\{\bar\tau_{i+1} - \bar\tau_i < e^{(\Delta-\alpha-\delta)\beta}\}$ has probability SES(β). Indeed, this event would imply that $\bar\sigma_{i+1}$ is at most $e^{(\Delta-\alpha-\delta)\beta}$. This event has probability SES(β) by the non-superdiffusivity property if the configuration at time $\bar\tau_i$ is in $\mathcal{X}_{\Delta^+} \setminus \mathcal{X}_E$, otherwise it has probability zero by the condition $\bar\sigma_{i+1} = e^{\Delta\beta}$. □

7.3.3 *Proof of Theorem 7.1.3*

For $i \in \mathbb{N}_0$, define

$$K_i = \min\big\{k \in \mathbb{N}\colon\ \pi(X(\bar\tau_{i+k})) \neq \pi(X(\bar\tau_i))\big\}.$$

Up to coalescence and exit from $\mathcal{X}^*$, Proposition 7.3.1 and the first part of Proposition 7.3.3 show that K_i dominates and is dominated by a geometric random variable with success probability of order $e^{-(r(\ell_1,\ell_2)-\Delta)\beta}$. Together with Theorem 7.1.2, which gives uniform lower and upper bounds on the return times $\bar\tau_{j+1} - \bar\tau_j$, $j \in \mathbb{N}_0$, this proves Theorem 7.1.3: the SES error in (7.1.9) is related to an anomalously large realisation of a geometric random variable, while an anomalously small realisation leads to an error that is only exponentially small in (7.1.10). □

7.3.4 *Proof of Theorem 7.1.5*

Proposition 7.3.1 and the second part of Proposition 7.3.3 prove Theorem 7.1.5 for any $i \in \mathbb{N}_0$ such that $X(\bar\tau_i) \in \mathcal{X}_{\Delta^+} \setminus \mathcal{X}_E$: these propositions provide the necessary lower and upper bounds on the denominator and numerator of the conditional probability. Otherwise, if $X(\bar\tau_i) \in \mathcal{X}_E$, then instead of using Proposition 7.3.3 we conclude by using Remark 7.2.10 and arguing as in (7.2.11) to show that the probability to have more than 4 particles in a box with volume of order $e^{D\beta}$ is exponentially smaller than the bound obtained in Proposition 7.3.1. □

7.3.5 *Proof of Theorem 7.1.6*

Proposition 7.3.2 and the first part of Proposition 7.3.3 prove Theorem 7.1.6: they give the necessary upper and lower bounds on the denominator and numerator of the conditional probability. □

7.4 PROOF OF PROPOSITIONS

In Section 7.4.1–7.4.3 we prove Propositions 7.3.1–7.3.3, respectively. The proof of Proposition 7.3.3 relies on three additional lemmas, whose proof is deferred to Section 7.5.

7.4.1 *Proof of Proposition 7.3.1*

Fix $\delta > 0$. Since

$$P_{\eta_0}(\pi(X(\bar\tau_1)) \neq \pi(\eta_0)) \geqslant P_{\eta_0}(\pi(X(\bar\tau_1)) = \pi'),$$

we need to bound from below the probability that a typical transition of the dynamics on $\mathcal{X}_{\Delta^+}$ occurs.

1. We start by considering the supercritical case $\ell_1 > \ell_c$. Since in this case $r(\ell_1, \ell_2) = 2\Delta - U$, it suffices to exhibit a mechanism to grow within time $T_{\Delta^+} e^{\delta\beta}$ with probability at least $e^{-(\Delta - U + O(\alpha,d,\delta))\beta}$. Within time $T_{\Delta^+} e^{\delta\beta/2}$ bring two particles from the gas inside one of the volumes $[\bar{\Lambda}_i, D - \delta]$. Attach the two particles in time $e^{(D+\delta)\beta}$. Complete the quasi-square with particles from the gas. Let τ be the first time at which there are two active particles inside one of these volumes. On the time scale we are interested in, particles can arrive inside the box Λ, but before time τ only one can be active. Thus, by using the recurrence property to $\mathcal{X}_U$, we know that this active particle can attach itslef to the quasi-square inside Λ, but it does not feel asleep with probability $1 - \text{SES}$. Moreover, via the interaction with this active particle the cluster can move, but in such a way that $\Lambda(t) \subset [\Lambda(0), D - \delta]$ for any t. Indeed, any redefinition of the local box, implied by the movement of the cluster, is related to a free particle that moves in Λ. We show that the probability that the number of these box special times exceeds $e^{O(\alpha,\delta)\beta}$ is SES.

Since the dynamics belongs to the environment $\mathcal{X}^*$, by the non-superdiffusivity property of the QRWs we know that at most $e^{3\alpha\beta/2}$ particles can interact with Λ within time $T_{\Delta^+} e^{\delta\beta}$. Each particle no longer visits Λ after each box special time associated with it with a probability lat least $1/(\log \exp(\Delta + O(\alpha,\delta))\beta)$.Thus,

$$P(\text{there are more than } e^{O(\alpha,\delta)\beta} \text{ visits in } \Lambda) \leqslant \left(1 - \frac{1}{(\Delta + O(\alpha,\delta))\beta}\right)^{e^{O(\alpha,\delta)\beta}} = \text{SES}(\beta).$$

Thus, up to an event of probability SES, we deal with the fixed target volume $[\Lambda(0), D - \delta]$. In addition, we deal with a constant number of local boxes, since we can control the probability that a box creation occurs within time $T_{\Delta^+} e^{\delta\beta}$ via the estimate derived in the proof of Proposition 7.2.11. To check that the resulting order of probability is correct, we proceed as follows. Divide the time interval $[0, T_{\Delta^+} e^{\delta\beta}]$ into intervals $[t_i, t_i + e^{(D+\delta)\beta}]$, with $1 \leqslant i < e^{(\Delta+\alpha-D)\beta}$. By considering $T_i = ie^{(D+\delta)\beta}$, and using the non-superdiffusivity property and the lower bound associated with the spread-out property of the QRWs (see [62, Theorem 3.2.5(ii)]), we get

$$P(\tau < e^{(\Delta+\alpha+\delta)\beta}) \geqslant \sum_{e^{(\Delta+\alpha-\delta)\beta} \leqslant ie^{(D+\delta)\beta} \leqslant e^{(\Delta+\alpha+\delta)\beta}} \left(\frac{e^{(D-\delta)\beta}}{ie^{(D+\delta)\beta} e^{\delta\beta}}\right)^2 \geqslant e^{-[\Delta - U + O(\alpha,d,\delta)]\beta}. \tag{7.4.1}$$

Let these two active particles inside $[\Lambda(0), D - \delta]$ at time τ attach themselves to the quasi-square. By using the non-superdiffusivity property and the stronger, higher resolution, lower bounds associated with the spread-out property of the QRWs, we get that this probability is at least $e^{-O(\delta)\beta}$. Arguing in the same way, we obtain an analogous lower bound for the probability to complete the quasi-square with particles from the gas in time $T_{\Delta^+} e^{\delta\beta/2}$. We conclude by using the strong Markov property at times τ and those corresponding to each attachment of the particles to the cluster in Λ.

2. Next consider the subcritical case $\ell_1 < \ell_c$. We start with $\eta_0 \in \mathcal{X}_E$. Since in this case $r(\ell_1, \ell_2) = 4\Delta - 2U - \theta$, it suffices to exhibit a mechanism to create a 2×2 droplet within time $T_{\Delta^+} e^{\delta\beta}$ with probability at least $e^{-(3\Delta - 2U - \theta + O(\alpha,d,\delta))\beta}$. Within time $T_{\Delta^+} e^{\delta\beta/2}$ bring four particles from the gas inside a box of volume $e^{(D-\delta)\beta}$. Attach two of these particles within time $e^{(D+\delta)\beta}$. Move the other two particles at a finite distance from the dimer within time $e^{(U-\delta/2)\beta}$. Given a fixed site $x \in \Lambda_\beta$, let τ be the first time at which there are four active particles in a box of volume $e^{(D-\delta)\beta}$ centered at x. To check that the resulting order of probability is correct, we proceed as follows. Divide the time interval $[0, T_{\Delta^+} e^{\delta\beta}]$ into intervals $[t_i, t_i + e^{(D+\delta)\beta}]$ with $1 \leqslant i < e^{(\Delta+\alpha-D)\beta}$. By considering $T_i = ie^{(D+\delta)\beta}$, and using the non-superdiffusivity property and the lower bound associated with the spread-out property of the QRWs (see [62, Theorem 3.2.5(ii)]), we get

$$P(\tau < e^{(\Delta+\alpha+\delta)\beta}) \geqslant \sum_{e^{(\Delta+\alpha-\delta)\beta} \leqslant ie^{(D+\delta)\beta} \leqslant e^{(\Delta+\alpha+\delta)\beta}} \left(\frac{e^{(D-\delta)\beta}}{ie^{(D+\delta)\beta} e^{\delta\beta}}\right)^4 \geqslant e^{-3[\Delta - U + O(\alpha,d,\delta)]\beta}.$$

(7.4.2)

Let σ be the first time at which two among these four active particles form a dimer for the first time at a finite distance from the site x. By using the non-superdiffusivity property and the stronger lower bounds associated with the spread-out property of the QRWs, we get

$$P(\sigma < e^{(D+\delta)\beta}) \geqslant \int_{e^{(D-\delta)\beta}}^{e^{(D+\delta)\beta}} \left(\frac{1}{te^{\delta\beta}}\right)^2 dt \geqslant e^{-[U+O(\delta,d)]\beta}. \tag{7.4.3}$$

Now let the other two active particles attach themselves to the dimer formed at time σ within time $e^{(U-\delta/2)\beta}$, so that the dimer is still present with probability $1-$ SES. Arguing as before, we deduce that this probability is at least $e^{-O(\delta)\beta}$. Finally we observe that these creations of a first cluster of sleeping particles around a given site x are disjoint events up to an event with negligible probability, the probability of which is controlled as in (7.2.11). By summing over all the sites $x \in \Lambda_\beta$ and applying the strong Markov property at the times τ, σ and those corresponding to the attachment of the third particle to the dimer, we get the claim.

3. Finally, consider the case $\ell_1 \geqslant 2$. It suffices to exhibit a mechanism to shrink within time $e^{(\Delta-\alpha+\delta)\beta}$ with a probability at least $e^{-(r(\ell_1,\ell_2)-\Delta+O(\alpha,d,\delta))\beta}$. The mechanism to shrink is the following: detach a row of ℓ_1 particles and bring each particle outside the volume $[\Lambda, \Delta-\alpha]$ within time $e^{(\Delta-\alpha/2)\beta}$. Note that at time $t=0$ there are at most $\lambda(\beta)/4$ particles inside the volume $[\Lambda, \Delta-\alpha/4]$ because the dynamics starts in $\mathcal{X}^*$. Thus, by the non-superdiffusivity property it follows that, up to an event of probability SES, these are the only particles that can enter $[\Lambda, \Delta-\alpha]$ within time $e^{(\Delta-\alpha/2)\beta}$. We can therefore argue as in the proof of Proposition 7.2.11 for $A = U$ with the following differences. For the first $\ell_1 - 1$ particles we obtain that the probability for each one of them to be detached is at least $e^{(-(2U-\Delta)-O(\alpha,\delta))\beta}$. Indeed, divide the time interval $[0, e^{(\Delta-\alpha/2)\beta}]$ into intervals S_i of length $e^{D\beta}$, with $1 \leqslant i < e^{(\Delta-D-\alpha/2)\beta}$. Then the probability to detach one of these particles is at least

$$e^{-\delta\beta} \sum_{1\leqslant i<e^{(\Delta-D-\alpha/2)\beta}} P(\text{there is a move of cost } 2U \text{ between } ie^{D\beta} \text{ and } (i+1)e^{D\beta}) \geqslant e^{[-(2U-\Delta)-O(\alpha,\delta)]\beta}.$$

After applying the strong Markov property at each of the detaching times and observing that the probability of detaching the last particle at cost U within time $e^{(\Delta-\alpha/2)\beta}$ is at least $e^{-O(\delta)\beta}$, and also the probability that no particle is inside the annulus $[\Lambda, \Delta-\alpha] \setminus \Lambda$ because of the lower bounds associated with the spread-out property of the QRWs, we get the claim. □

7.4.2 *Proof of Proposition 7.3.2*

Fix $\delta > 0$. Since in this case $\pi'' = (\ell_2 \times (\ell_1 + 1))$, in order to get the claim it suffices to exhibit a mechanism to grow with a probability at least $e^{-[\Delta-U+O(\alpha,d,\delta)]\beta}$. The mechanism is the same as for the supercritical case used in the proof of Proposition 7.3.1. Since now we are interested in not having a box creation before time $\bar{\tau}_1$, we obtain the desired lower bound after using the estimate in (7.2.11). □

7.4.3 *Proof of Proposition 7.3.3*

Since we need to control all the possible mechanisms to grow and shrink, the proof of Proposition 7.3.3 is much more involved than the proofs of Propositions 7.3.1–7.3.2, and is organised into steps. We start by considering the case $\eta_0 \in \mathcal{X}_E$. We assume that there is a single finite box for the starting configuration η_0, namely, $\eta_0 \in \mathcal{X}_{\Delta^+}$ consisting of a single quasi-square of size $\ell_1 \times \ell_2$. Abusing notation, we refer to the current box $\Lambda = \bar{\Lambda}_0$ as $\bar{\Lambda}$ instead of $\bar{\Lambda}_0$. This is needed in order to make the proof clearer. We will see later how to derive the statement for general boxes.

The key steps in the proof are the following:

STEP 1: Introduce coloration and permutation rules (Section 7.4.3.1).

STEP 2: Consider the case $\eta_0 \in \mathcal{X}_E$ (Section 7.4.3.2).

STEP 3: Consider the case $\eta_0 \in \mathcal{X}_{\Delta^+} \setminus \mathcal{X}_E$ and $\ell_2 \geqslant 3$ (Section 7.4.3.3).

STEP 4: Consider the case $\eta_0 \in \mathcal{X}_{\Delta^+} \setminus \mathcal{X}_E$ and $\ell_2 = 2$ (Section 7.4.3.4).

STEP 5: Derive the statement for a general collection of finite boxes $\bar{\Lambda} = (\bar{\Lambda}_i)_{i\in I}$ (Section 7.4.3.5).

In step 1 we introduce the notion of *colours for particles and their permutation rules*, which are needed in steps 2–5. In each of steps 2–4 we state a key lemma and explain how to derive the statement of interest from it. The proofs of the lemmas are deferred to Section 7.5, which is the technical core of the present work.

Recall that we are considering the case in which there is a single finite local box $\bar{\Lambda}$. We call $\mathcal{I}(n)$ the set of configurations η such that $\bar{\eta}$ is of size $|\bar{\eta}| = n$ and is the solution of the associated isoperimetric problem. We use the notation $\mathcal{I}(n)^{fp}$ to indicate the presence of a free particle in $\bar{\Lambda}$. Moreover, we call $\mathcal{I}(0)$ the set of configurations for which there is no local box $\bar{\Lambda}$. We introduce the sequence $(\tau_k)_{k\in\mathbb{N}_0}$ of return times in $\mathcal{X}_D$ after seeing an active particle in $\bar{\Lambda}$ as follows. Put $\tau_0 = 0$ and, for $i \in \mathbb{N}_0$, define

$$\sigma_{i+1} = \inf\left\{t > \tau_i \colon \text{ there is an active particle inside } \bar{\Lambda}(t) \text{ at time } t\right\} \tag{7.4.4}$$

and

$$\tau_{i+1} = \inf\{t > \sigma_{i+1} \colon X(t) \in \mathcal{X}_D\}. \tag{7.4.5}$$

Note the difference between (7.4.4)-(7.4.5) and (7.1.4)-(7.1.5). Let φ^k be the finite-time Markov chain $\varphi^k = (X(\tau_i))_{0\leqslant i\leqslant k}$, and put

$$n = \max\left\{k \geqslant 0 \colon \tau_k < T_{\Delta^+} e^{\delta\beta}\right\}.$$

Finally, set $\iota = \ell_c - U/\varepsilon \in (0, 1)$.

7.4.3.1 *Step 1: Coloration and permutation rules*

Divide the particles into *active* particles and *sleeping* particles: a notion that is related to *free* particle. Define

$$\hat{\mathcal{X}}_N := \{(z_1, \dots, z_N) \colon z_i \neq z_j \,\forall\, i, j \in \{1, ..., N\}, i \neq j\},$$

a set of N labelled particles. We say that a particle $i \in \{1, \dots, N\}$ is free at time $t_0 \geqslant 0$ if there exists a trajectory $\hat{\eta} \colon t \in [t_0, t_0 + T] \mapsto \hat{\eta}(t) \in \hat{\mathcal{X}}_N$ that respects the rules of the dynamics and satisfies (see the construction carried out in [62, Section 2.2] and recall that $T_\alpha = e^{(\Delta-\alpha)\beta}$ with $\alpha > 0$)

(i) $\|\hat{\eta}_i(t_0 + T) - \hat{\eta}_i(t_0)\|_2 > T_\alpha^{1/2}$.

(ii) $\forall\, t \in [t_0, t_0 + T] \colon \mathcal{U}(\hat{\eta}(t))^{cl} = \mathcal{U}(\hat{\eta}(t_0))^{cl}$.

For $t > e^{D\beta}$, a particle is said to be sleeping at time t if it was not free during the entire time interval $[t - e^{D\beta}, t]$. A non-sleeping particle is said to be active. By convention, prior to time $e^{D\beta}$ all particles are active.

• **Coloration rules.** These are for active particles only: sleeping particles have no color.

1. All particles in $[\bar{\Lambda}, \Delta - \delta]^c$ are green and remain green when entering $[\bar{\Lambda}, \Delta - \delta]$. Any particle that leaves $[\bar{\Lambda}, \Delta - \delta]$ is colored green.
2. When a particle wakes up in $\bar{\Lambda}$ at some time t it is colored red if the following rules are satisfied:
   (i) $t = \sigma_i$ for some $i > 0$.
   (ii) The particle is the only one that is active in $\bar{\Lambda}$ at time t.
   (iii) There was a move of cost $2U$ or two "δ-close moves" of cost U, i.e., both in the time interval $[t - e^{\delta\beta}, t]$.
3. Color yellow any particle that wakes up without being colored red.

It follows from these rules that at time $t = 0$ all clusterized particles are without color, all active particles are green, a green particle cannot change color but can only loose color, any particle can loose its color by falling asleep, an awaking particle cannot be colored green at a wake-up time, and a colored particle can change color (from red or yellow to green) only when leaving $[\bar{\Lambda}, \Delta - \delta]$.

• **Permutation rules.** We couple the color rules with labelling rules by building a hierarchy on clusterized particles in the same cluster. The higher particles in this hierarchy are the sleeping ones, followed by yellow, then red, and finally green particles. To compare two sleeping particles or two particles with the same color, we say that the lower one in the hierarchy is the last aggregated particle in their shared cluster, and we break ties by some random rule. At each time t when some particle has to be freed from a cluster, we set particle positions to ensure that this particle is the lowest one in the cluster hierarchy at time t^-. This is compatible with the local permutation rule associated with quasi-random walks.

The reason why we prefer to release green and red particles rather than yellow particles is that we have much less control on the latter. We also want to have to control the smallest possible number of active particles, which is why we place sleeping particles at the highest rank in the hierarchy, and we introduce the time aggregation rule to give more chance to fall asleep to any particle that was about to do so.

7.4.3.2 *Step 2: Starting configuration has no square: Lemma 7.4.1*

Consider the case in which the starting configuration $\eta_0 \in \mathcal{X}_{\Delta^+}$ has no quasi-square, i.e., $\eta_0 \in \mathcal{X}_E$ (recall Definition 7.2.9 and (7.3.1)). Then we need to prove the first part of Proposition 7.3.3 only. The following lemma controls the exit of the dynamics from the pure gas state, which corresponds to the creation of the first droplet and therefore to the creation of a new local box.

Lemma 7.4.1. *Assume that $\Delta < \Theta \leqslant \theta$. For η_0 in $\mathcal{X}_E$,*

$$\limsup_{\beta\to\infty} \frac{1}{\beta} \log P_{\eta_0}(\textit{a box creation occurs within time } \bar{\tau}_1) \leqslant -[3\Delta - 2U - \theta - O(\alpha, d)]. \quad (7.4.6)$$

Remark 7.4.2. *Starting from $\eta_0 \in \mathcal{X}_E$, reaching at time $\bar{\tau}_1$ a configuration such that $\pi(X(\bar{\tau}_1)) \neq \pi(\eta_0)$ implies that a box creation has occurred. Hence the first part of Proposition 7.3.3 follows from Lemma 7.4.1.*

7.4.3.3 *Step 3: Starting configuration has a single large quasi-square: Lemma 7.4.3*

Recall that we are considering a starting configuration $\eta_0 \in \mathcal{X}_{\Delta^+}$ consisting of a single quasi-square of size $\ell_1 \times \ell_2$ with $\ell_1 \leqslant \ell_2$ and $\ell_2 \geqslant 3$. Recall (7.4.4)-(7.4.5) and (1.3.78) for the definition of resistance for a quasi-square of size $\ell_1 \times \ell_2$.

Lemma 7.4.3. *Assume that $\Delta < \Theta \leqslant \theta$. Let $\eta_0 \in \mathcal{X}_{\Delta^+}$ be such that its restriction $\bar{\eta}_0$ to $\bar{\Lambda}$ is a quasi-square of size $\ell_1 \times \ell_2$ with $\ell_1 \leqslant \ell_2$ and $\ell_2 \geqslant 3$. If η_0 is subcritical, i.e., $\ell_1 < \ell_c$, then we set $m = \ell_1 - 2$ and*

$$a = \gamma\Big(\frac{1}{2}\mathbb{1}_{\{\ell_1 < \ell_c - 1\}} + \frac{1}{2}\mathbb{1}_{\{\ell_1 = \ell_c - 1, \iota < \frac{1}{2}\}} + (1-\iota)\mathbb{1}_{\{\ell_1 = \ell_c - 1, \iota \geqslant \frac{1}{2}\}}\Big) > 0.$$

Let $\mathcal{G}_1$ be the graph represented in Fig. 7.1 and $\mathcal{G}_2$ the graph represented in Fig. 7.2. If η_0 is supercritical,i.e., $\ell_1 \geqslant \ell_c$, instead set $m = \ell_c - 2$ and

$$a = (\varepsilon - \gamma)\mathbb{1}_{\{\iota < \frac{1}{2}\}} + \gamma\mathbb{1}_{\{\iota \geqslant \frac{1}{2}\}} > 0.$$

Define the same $\mathcal{G}_1$ (associated with a different m), and let $\mathcal{G}_2$ be the graph represented in Fig. 7.3. Then

$$\limsup_{\beta\to\infty} \frac{1}{\beta} \log P_{\eta_0}(\varphi^n \textit{ escapes from } \mathcal{G}_1) \leqslant -[r(\ell_1, \ell_2) - \Delta - O(\alpha, d)] \quad (7.4.7)$$

and

$$\limsup_{\beta\to\infty} \frac{1}{\beta} \log P_{\eta_0}(\varphi^n \textit{ escapes from } \mathcal{G}_2) \leqslant -[r(\ell_1, \ell_2) - \Delta + a - O(\alpha, d)]. \quad (7.4.8)$$

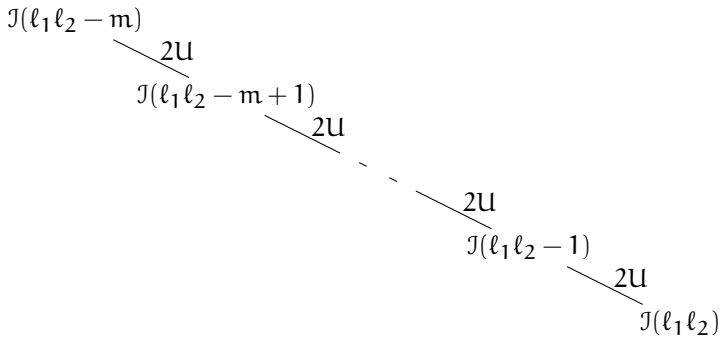

Figure 7.1 – The graph $\mathcal{G}_1$ in both the subcritical and the supercritical case.

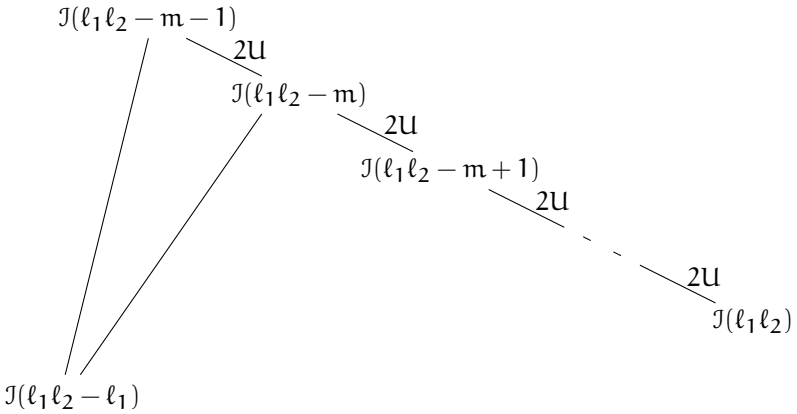

Figure 7.2 – The graph $\mathcal{G}_2$ in the subcritical case.

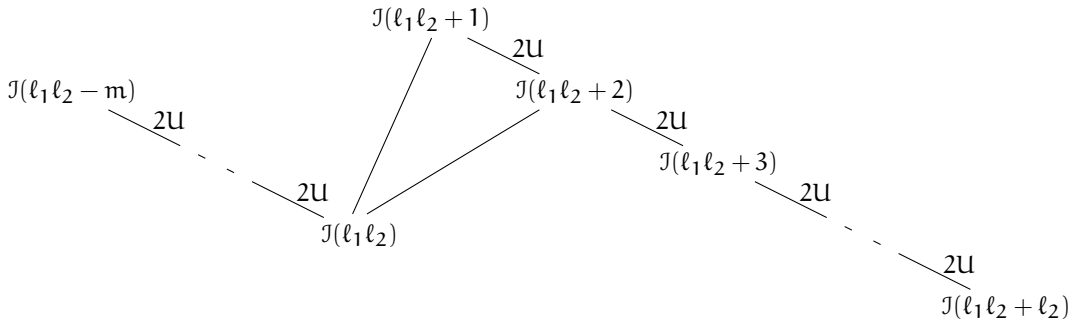

Figure 7.3 – The graph $\mathcal{G}_2$ in the supercritical case.

The proof of Lemma 7.4.3 is given in Section 7.5.

Remark 7.4.4. *Proposition 7.3.3 follows from Lemma 7.4.3 when η_0 consists of a single quasi-square with size $\ell_1 \times \ell_2$ and $\ell_2 \geqslant 3$. First, Lemma 7.4.3 gives us information at the return times to $\mathcal{X}_{\Delta^+}$ after seeing an active particle in $\bar{\Lambda}$. Indeed, note that such a return time can occur only in the time intervals of type $[\tau_k, \sigma_{k+1}]$, because during the time intervals of type $[\sigma_k, \tau_k]$ the configurations that are visited are not in $\mathcal{X}_D$ and therefore not even in $\mathcal{X}_{\Delta^+}$ (recall Definition 7.2.9). It is clear that a return time in $\mathcal{X}_{\Delta^+}$ does not necessarily coincide with a time τ_k, but during the time interval $[\tau_k, \sigma_{k+1}]$ the number of particles of the isoperimetric configuration is conserved, and so the system reaches $\mathcal{X}_{\Delta^+}$ in the same configuration visited at time τ_k. Second, (7.4.7) implies the first part of Proposition 7.3.3. Starting from η_0, if $\pi(X(\bar{\tau}_1)) \neq \pi(\eta_0)$, then φ^n has escaped from $\mathcal{G}_1$. Hence the chain of inequalities holds due to (7.4.7) and we get the claim. Finally, the second part of Proposition 7.3.3 follows in the same*

way. Starting from η_0*, if* $\pi(X(\bar\tau_1)) \notin \{\pi(\eta_0), \pi'\}$*, then* φ^n *has escaped from* $\mathcal{G}_2$*. Hence the chain of inequalities holds due to* (7.4.8).

7.4.3.4 *Step 4: Starting configuration has a single small quasi-square: Lemma 7.4.5*

We recall that we are considering a starting configuration $\eta_0 \in \mathcal{X}_{\Delta^+}$ consisting of a single quasi-square of size $\ell_1 \times \ell_2$ with $\ell_1 \leqslant \ell_2 = 2$. Thus, we need to consider only the case in which η contains a 2×2 square droplet (recall Remark 7.2.10).

Lemma 7.4.5. *Assume that* $\Delta < \Theta \leqslant \theta$*. Let* $\eta_0 \in \mathcal{X}_{\Delta^+}$ *be such that its restriction* $\bar\eta_0$ *to* $\bar\Lambda$ *is a* 2×2 *square. Let* $\mathcal{G}_1$ *be the graph consisting of the vertex* $\mathcal{I}(4)$ *only, and define the graph* $\mathcal{G}_2$ *as*

$$\begin{array}{c} \mathcal{I}(4) \\ / \\ \mathcal{I}(0). \end{array}$$

Then

$$\limsup_{\beta\to\infty} \frac{1}{\beta} \log P_{\eta_0}\left(\varphi^n \text{ escapes from } \mathcal{G}_1\right) \leqslant -[\Gamma(2,2) - \Delta - O(\alpha, d)] \tag{7.4.9}$$

and

$$\limsup_{\beta\to\infty} \frac{1}{\beta} \log P_{\eta_0}\left(\varphi^n \text{ escapes from } \mathcal{G}_2\right) \leqslant -[\Gamma(2,2) - \Delta + \tfrac{1}{2}\gamma - O(\alpha, d)]. \tag{7.4.10}$$

The proof of Lemma 7.4.5 is deferred to Section 7.5.3.

Remark 7.4.6. *In order to deduce Proposition 7.3.3 from Lemma 7.4.5 in case* η_0 *consists of a single* 2×2 *square, we can argue as in Remark 7.4.4.*

7.4.3.5 *Step 5: Result for a general collection of finite boxes*

We close by explaining how to derive Lemmas 7.4.3 and 7.4.5 when the starting configuration is not such that $\bar\Lambda(0) = \bar\Lambda_0(0)$. First, we need to extend the definition of the set $\mathcal{I}(n)$. Given a collection $\bar\Lambda(t) = (\bar\Lambda_i(t))_{1\leqslant i<k(t)}$ of finite boxes in Λ_β, we call $\mathcal{I}(n)$ the set of configurations η such that $\bar\eta$ is of size $\sum_{1\leqslant i<k(t)} |\bar\eta_i| = n$ and is the solution of the isoperimetric problem for a configuration with n particles and $k(t)$ connected components. We use the notation $\mathcal{I}(n)^{fp}$ to indicate the presence of a free particle in one of the boxes. Moreover, in Lemma 7.4.5 we need to replace the set $\mathcal{I}(0)$ by the set $\bar{\mathcal{I}}(n-4)$, defined as the set of configurations for which the collection $\bar\Lambda(t)$ has one local box less than $\bar\Lambda(t^-)$, and there are n particles inside $\bar\Lambda(t^-)$ and $n-4$ particles inside $\bar\Lambda(t)$. This set takes into account the dissolution of a 2×2 square droplet at time t leading to the disappearance of one of the local boxes. Up to any coalescence between local boxes, we can argue as in the proof of Lemmas 7.4.3 and 7.4.5.

7.5 PROOF OF LEMMAS: FROM LARGE DEVIATIONS TO DEDUCTIVE APPROACH

Section 7.5.1 shows that the proof of Lemma 7.4.1 has already been achieved. Section 7.5.2, which is long and constitutes the main technical hurdle of the work, contains the proof of Lemma 7.4.3 and is divided into several parts: Section 7.5.2.1 outlines the structure of the proof, while Sections 7.5.2.2–7.5.2.4 work out the details of this proof for three cases. The latter rely on two further lemmas, whose proof is deferred to Sections 7.5.4–7.5.5.

The structure of the argument used to achieve the proof of Lemma 7.4.3 and Lemma 7.4.5 is common. Indeed, we follow a *deductive approach*, in the sense that we consider a family of large deviation events and use their intricate interrelation to estimate their respective probabilities. In particular, starting from these large deviation events we will prove, by induction in k, a claim $\mathcal{P}(k)$ of the form "if none of these events occurs, then the dynamics does not escape from the graph in the first k steps". This way of going about is inspired by the point of view that the tube of typical paths is the skeleton for the metastable crossover.

Indeed, the role of the different graphs introduced below is that they describe the temporal configurational environment from which the dynamics cannot escape. We will control the evolution of the dynamics in this environment via large deviation a priori estimates, and we will need a detailed case study to be able to proceed.

7.5.1 *Proof of Lemma 7.4.1*

The claim is the same as the one derived in (7.2.11). □

7.5.2 *Proof of Lemma 7.4.3*

7.5.2.1 *Structure of the proof*

By using the coloration and permutation rules introduced in Section 7.4.3.1, we build a list of large deviation events, each having a cost

$$c(\cdot) = -\limsup_{\beta\to\infty} \frac{1}{\beta} \log P(\cdot),$$

to prove by contradiction that if φ^n escapes from $\mathcal{G}_1$, then the union Z_1 of these large deviation events has to occur. We define another event Z_2 by removing from Z_1 some of these large deviation events, resulting in a larger cost, and adding new large deviation events, which also have a larger cost than Z_1. While dealing with Z_1 and $\mathcal{G}_1$, we can consider the subcritical and the supercritical case simultaneously, but we must separate when dealing with Z_2 and $\mathcal{G}_2$. Finally, we prove that if φ^n escapes from $\mathcal{G}_2$, then Z_2 has to occur.

In the sequel we consider three cases for escaping $\mathcal{G}_1$ and $\mathcal{G}_2$:

(I) Escape from $\mathcal{G}_1$.

(II) Escape from $\mathcal{G}_2$ in the subcritical case.

(III) Escape from $\mathcal{G}_2$ in the supercritical case.

7.5.2.2 *Escape case (I)*

• **Large deviation events.** Here is a list of bad events that can lead to φ^n escaping from $\mathcal{G}_1$ or $\mathcal{G}_2$, together with a lower bound on their cost. We call *entrance time* and *exit time* all times t at which a free particle enters or leaves $\bar{\Lambda}(t)$. A *special time* is an entrance time, an exit time, a wake up time, a return time τ_i or a boxes special time (recall (7.1.2)). Note that each σ_i defined in (7.4.4) is a special time, since it is either an entrance time or a wake-up time. As above, we say that two times $t_1 < t_2$ are δ-*close* if $t_2 - t_1 < e^{\delta\beta}$.

A : A recurrence or non-superdiffusivity property is violated within time $T_{\Delta^+} e^{\delta\beta}$. This event has an infinite cost, i.e., its probability is SES.

B : There are more than $e^{(2\alpha+\delta)\beta}$ special times within time $T_{\Delta^+} e^{\delta\beta}$. This event has an infinite cost.

C : Within time $T_{\Delta^+} e^{\delta\beta}$ there is a time interval of length $e^{\delta\beta}$ that contains a special time followed by a move of cost larger than or equal to U. This event costs at least $U - O(\delta)$.

C′ : Within time $T_{\Delta^+} e^{\delta\beta}$ there is a time interval I of length at most $e^{\delta\beta}$ that contains a move of cost larger than or equal to U and ends with the entrance in $\bar{\Lambda}$ of a free particle that was outside $\bar{\Lambda}$ during I. This event costs at least $U - O(\delta)$.

D : Within time $T_{\Delta^+} e^{\delta\beta}$ there is a time interval of length $e^{D\beta}$ that contains a special time followed by a move of cost larger than or equal to $2U$ or two δ-close moves of cost larger than or equal to U. This event costs at least $2U - D - O(\delta)$.

D′ : Within time $T_{\Delta^+} e^{\delta\beta}$ there is a time interval I of length at most $e^{D\beta}$ that contains a move of cost larger than or equal to $2U$ or two δ-close moves of cost larger than or equal to U, and ends with the entrance in $\bar{\Lambda}$ of a free particle that was outside $\bar{\Lambda}$ during I. This event costs at least $2U - D - O(\delta)$.

E : Within time $T_{\Delta^+} e^{\delta\beta}$ there is a time interval $[t_1, t_2]$ such that $|\bar{X}|$ is constant on $[t_1, t_2]$, the local energy difference $\bar{H}(\eta(t_2)) - \bar{H}(\eta(t_1))$ is larger than or equal to $3U$, and t_1 is δ-close to some earlier special time. This event costs at least $3U - \Delta - \alpha - O(\delta)$.

F_{m+1} : There are $m+1$ times $t_1 < \cdots < t_{m+1} < T_{\Delta^+} e^{\delta\beta}$ at which some particle is colored red. This event costs at least $(m+1)(2U-\Delta-\alpha) - O(\delta)$.

G : There are two red particles at a same time $t < T_{\Delta^+} e^{\delta\beta}$ in $[\bar{\Lambda}, D+\delta]$. This event costs at least $U - d + \varepsilon - \alpha - O(\delta)$.

G' : There are a red and a green particles at a same time $t < T_{\Delta^+} e^{\delta\beta}$ in $[\bar{\Lambda}, D+\delta]$. This event costs at least $U - d - \alpha - O(\delta)$.

G'_4 : There are four active particles, red or green, at a same time $t < T_{\Delta^+} e^{\delta\beta}$ in a box of volume $e^{(D+\delta)\beta}$, or a particle that belongs to a cluster consisting of two or three active particles only falls asleep. This event costs at least $3\Delta - 2U - \theta + 3\alpha - 2d - O(\delta)$.

H_2 : There are two green particles at a same time $t < T_{\Delta^+} e^{\delta\beta}$ in $[\bar{\Lambda}, D+\delta]$. This event costs at least $\Delta - D + \alpha - O(\delta)$.

Set

$$Z_1 = A \cup B \cup C \cup C' \cup D \cup D' \cup E \cup F_{m+1} \cup G \cup G' \cup G'_4 \cup H_2, \tag{7.5.1}$$

so that Z_1^c implies A^c,B^c, ..., $G_4'^c$, H_2^c. We will prove by induction that, for all $0 \leqslant k \leqslant n$,

Claim $\mathcal{P}(k)$. *If Z_1 does not occur, then*
(i) φ^k does not escape from $\mathcal{G}_1$.
(ii) A particle is painted red each time φ^k climbs along an $2U$-edge of $\mathcal{G}_1$.
(iii) No particle is painted yellow within τ_k.
(iv) No box creation occurs within τ_k.

Property (iv) avoids the creation of new boxes within time $t \leqslant \tau_k$. Since the cost of Z_1 is given by the smallest cost of its components A, B, ..., we obtain

$$c(Z_1) = \begin{cases} c(F_{m+1}) \geqslant r(\ell_1, \ell_2) - \Delta - O(\alpha) - O(\delta) & \text{if } \ell_1 < \ell_c, \\ c(H_2) \geqslant r(\ell_1, \ell_2) - \Delta - O(\alpha, d) - O(\delta) & \text{if } \ell_1 \geqslant \ell c, \end{cases}$$

and this will prove (7.4.7).

• **Proof of $\mathcal{P}(k)$, $0 \leqslant k \leqslant n$.** $\mathcal{P}(0)$ obviously holds because $\tau_0 = 0$. We prove $\mathcal{P}(k+1)$ by assuming $\mathcal{P}(k)$. Let us assume that Z_1^c occurs. We have to control the process X on the time interval

$$[\tau_k, \tau_{k+1}] = [\tau_k, \sigma_{k+1}] \cup [\sigma_{k+1}, \tau_{k+1}].$$

We analyse these two intervals separately.

▶ *The time interval $[\tau_k, \sigma_{k+1}]$:* Consider the process

$$\Delta\bar{H}\colon\ t \in [\tau_k, \sigma_{k+1}) \mapsto \bar{H}(X(t)) - \bar{H}(X(\tau_k)).$$

It follows from the definition of σ_{k+1} that $|\bar{X}(t)|$ does not change during the time interval $[\tau_k, \sigma_{k+1})$. $\mathcal{P}(k)$ implies, in particular,

$$X(\tau_k) \in \mathcal{I}(\ell_1\ell_2 - i) \tag{7.5.2}$$

for some $1 \leqslant i \leqslant m$, so that $\bar{X}(\tau_k)$ is a solution of the isoperimetric problem, and this implies that $\Delta\bar{H}$ cannot go down below 0. Then E^c implies that $\Delta\bar{H}$ cannot go above $2U$, and it follows that

$$\Delta\bar{H}(t) \in \{0, U, 2U\}, \qquad \tau_k \leqslant t < \sigma_{k+1}.$$

The process $\Delta\bar{H}$ can therefore be seen as a succession of increases and decreases of the local energy to some of these three values. We claim that Z_1^c implies:

(i) Each increase of $\Delta\bar{H}$ to $2U$ is followed by a δ-close decrease to U or 0.
(ii) Each increase of $\Delta\bar{H}$ to U is followed by a δ-close decrease to 0 or a δ-close increase to $2U$.
(iii) After each decrease to U, $\Delta\bar{H}$ has to increase to $2U$ within a time $e^{(U+\delta)\beta}$ or to decrease to 0 within a time $e^{\delta\beta}$.

Indeed, (i) and (ii) follow from the recurrence property to $\mathcal{X}_0$ implied by A^c, while (iii) follows from the recurrence properties to $\mathcal{X}_U$ and $\mathcal{X}_0$ implied by the same event.

Now, σ_{k+1} can be reached either via the entrance of a free particle in $\bar{\Lambda}$ or by freeing some particle in $\bar{\Lambda}$. We will refer to these as the entrance and wake-up case, and we analyse them separately.

ENTRANCE CASE: In this case properties (i)–(iii), C'^c and D'^c imply that $\Delta\bar{H}(\sigma_{k+1}^-) = 0$, hence $X(\sigma_{k+1}^-) \in \mathcal{I}(\ell_1\ell_2 - i)$ with $1 \leqslant i \leqslant m$ defined by (7.5.2). $\bar{X}(\sigma_{k+1})$ is then made up of an isoperimetric configuration of size $\ell_1\ell_2 - i$ and a free particle, for which we use the short-hand notation $X(\sigma_{k+1}) \in \mathcal{I}(\ell_1\ell_2 - i)^{fp}$.

WAKE–UP CASE: Recall (7.5.2) again, and use that E^c and $i \leqslant m < \ell_1 - 1$ imply

$$\bar{H}(X(\sigma_{k+1})) \leqslant \bar{H}(\mathcal{I}(\ell_1\ell_2 - i)) + 2U = \bar{H}(\mathcal{I}(\ell_1\ell_2 - i - 1)) + \Delta.$$

Since a free particle has perimeter 4, we also have the reverse inequality

$$\bar{H}(X(\sigma_{k+1})) \geqslant \bar{H}(\mathcal{I}(\ell_1\ell_2 - i - 1)) + \Delta,$$

and so we conclude that

$$\bar{H}(X(\sigma_{k+1})) = \bar{H}(\mathcal{I}(\ell_1\ell_2 - i - 1)) + \Delta. \tag{7.5.3}$$

Together with properties (i)–(iii) this implies that the waking-up particle is colored red: the requested move of cost $2U$, or two δ-close move of cost U, do not have to be δ-close to σ_{k+1}, and it is not possible that a particle wakes up from a U-reducible configuration that is reached without waking up from a configuration in $\mathcal{X}_D$. Indeed, it is impossible to obtain an isoperimetric configuration with a free particle by detaching a particle from an isoperimetric configuration in $\mathcal{X}_0 \setminus \mathcal{X}_U$: if the free particle is detached from the external boundary of the configuration, then the starting configuration is not isoperimetric, while if the particle is detached from the internal boundary, then it is not in $\mathcal{X}_0$. Equation (7.5.3) also implies that $X(\sigma_{k+1}) \in \mathcal{I}(\ell_1\ell_2 - i - 1)^{fp}$.

The above analysis of the time interval $[\tau_k, \sigma_{k+1}]$ requires a few concluding remarks. First, we proved that no yellow particle can be produced during this time interval. Second, F^c_{m+1} together with $\mathcal{P}(k)$ and $X(0) \in \mathcal{I}(\ell_1\ell_2)$ imply that the wake-up case has to be excluded when $i = m$. Third, we can conclude

$$X(\sigma_{k+1}) \in \begin{cases} \mathcal{I}(\ell_1\ell_2 - j)^{fp} \text{ for some } j \in \{i, i+1\} & \text{if } i < m, \\ \mathcal{I}(\ell_1\ell_2 - j)^{fp} \text{ with } j = i & \text{if } i = m. \end{cases} \tag{7.5.4}$$

► *The time interval* $[\sigma_{k+1}, \tau_{k+1}]$: A^c implies that $\tau_{k+1} - \sigma_{k+1} < e^{(D+\delta/2)\beta}$. From $\mathcal{P}(k)$ and our previous analysis we also know that we have a red or a green particle in $\bar{\Lambda}$ and that no yellow particle was produced during the time interval $[0, \sigma_{k+1}]$. Therefore the non-superdiffusivity property, G^c, G'^c and H_2^c imply that no other (colored) particle can enter $\bar{\Lambda}$ before time τ_{k+1}.

Let us next consider the process

$$\Delta\bar{H}\colon\ t \in [\sigma_{k+1}, \tau_{k+1}] \mapsto \bar{H}(X(t)) - \bar{H}(X(\sigma_{k+1}))$$

and make two preliminary observations:

(i) Since there is a free particle in $\bar{\Lambda}$, the recurrence property to $\mathcal{X}_0$, C^c, C'^c and the fact that no other active particle can enter $\bar{\Lambda}$ before τ_{k+1} imply that $\Delta\bar{H}$ first has to decrease within a time $e^{\delta\beta}$.

(ii) The recurrence property to $\mathcal{X}_U$, D^c and D'^c imply that before time τ_{k+1} there will be neither a move of cost larger than or equal to $2U$, nor a succession of δ-close moves of cost larger than or equal to U.

We now separate two complementary events, to which we will refer as the *good attachment* and the *exit*.

▶ GOOD ATTACHMENT: This occurs when $\Delta\bar{H}$ reaches the level $-2U$ before the free particle leaves $\bar{\Lambda}$. With $1 \leqslant j \leqslant m$ defined in (7.5.4), the local energy is equal to

$$\bar{H}(\mathcal{I}(\ell_1\ell_2 - j)^{fp}) - 2U = \bar{H}(\mathcal{I}(\ell_1\ell_2 - (j-1)))$$

because $j-1 \leqslant m-1 < \ell_1 - 1$ and $j > 0$: good attachment is excluded when $j = 0$ because

$$\bar{H}(\mathcal{I}(\ell_1\ell_2)^{fp}) - 2U < \bar{H}(\mathcal{I}(\ell_1\ell_2 + 1)).$$

The recurrence property to $\mathcal{X}_0$, observation (ii) and the fact that no other free particle can enter $\bar{\Lambda}$ before time τ_{k+1} imply that $\Delta\bar{H}$ can only oscillate between the levels $-2U$ and $-U$. This excludes any possibility for the active particle to leave $\bar{\Lambda}$ before time τ_{k+1}, and X has to reach $\mathcal{X}_D$ by reaching $\mathcal{X}_U$ and making the active particle fall asleep. Since they are reached from level $-2U$, configurations at level $-U$ are U-reducible. It follows that X reaches $\mathcal{X}_D$ at the level $-2U$, i.e., in $\mathcal{I}(\ell_1\ell_2 - (j-1))$.

▶ EXIT: This occurs when $\Delta\bar{H}$ does not reach the level $-2U$ before the free particle leaves $\bar{\Lambda}$. Observation (i) implies that $\Delta\bar{H}$ first decreases to $-\Delta$ or $-U$. In the first case X reaches $\mathcal{X}_D$ in $\mathcal{I}(\ell_1\ell_2 - j)$ with j defined in (7.5.4). In the second case the recurrence property to $\mathcal{X}_0$, observation (ii) and the fact that no other free particle can enter $\bar{\Lambda}$ before τ_{k+1} imply that $\Delta\bar{H}$ can only oscillate between the levels $-U$ and 0 before possibly going down to $-\Delta$. Since configurations at levels $-U$ and 0 are all U-reducible (consider the reverse path to $X(\sigma^-_{k+1})$), $\Delta\bar{H}$ must eventually go down to $-\Delta$: X reaches $\mathcal{X}_D$ in $\mathcal{I}(\ell_1\ell_2 - j)$.

Our permutation rules now imply that no yellow particle can be produced during the time interval $[\sigma_{k+1}, \tau_{k+1}]$, and we conclude that

$$X(\tau_{k+1}) \in \begin{cases} \mathcal{I}(\ell_1\ell_2 - i') \text{ for some } i' \in \{j-1, j\} & \text{if } j > 0, \\ \mathcal{I}(\ell_1\ell_2 - i') \text{ with } i' = j & \text{if } j = 0. \end{cases}$$

Combined with (7.5.4) and the fact that a red particle was produced if $j = i+1$, it remains to prove $\mathcal{P}(k+1)$-iv). But this follows from the event $G_4'^c$ and $\mathcal{P}(k+1)$(iii), and ends our induction.

• **Cost estimates.** To complete the proof of (7.4.7), we only need to check the lower bounds for the cost of each event that makes up Z_1, for which we refer to Appendix 7.B. This concludes Case (I). □

7.5.2.3 *Escape case (II): Lemmas 7.5.1–7.5.2*

• **Special times and large deviation events in the subcritical case.** In the subcritical case, the cost of Z_1 equals the cost of F_{m+1}. We build Z_2 by removing F_{m+1} from Z_1, before adding new large deviation events. With

$$\ell_1' = \ell_2 - 1, \qquad \ell_2' = \ell_1,$$

the proof of (7.4.7) shows that $(Z_1 \setminus F_{m+1})^c$ implies that either φ^n does not escape from $\mathcal{G}_1$, or there is a first return time τ_{k_0} such that $X(\tau_{k_0}) \in \mathcal{I}(\ell_1'\ell_2' + 2)$, and an $(m+1)^{th}$ particle is colored red at time σ_{k_0+1}. The following formula is a definition of k_0:

$$\sigma_{k_0+1} \textit{ is the } (m+1)^{th} \textit{ attribution time of the red color.} \tag{7.5.5}$$

Note that before time τ_{k_0} no particle can be colored yellow and there are at least $\ell_1'\ell_2'$ sleeping particles for any $t \in [0, \tau_{k_0}]$. In proving (7.4.8) we will therefore have to deal with yellow particles. These cannot be controlled by their too low energetic cost, but they are closely related to the notion of U-reducibility. A careful analysis of the possible trajectories between U-reducible clusterized configurations and configurations in $\mathcal{X}_D$ will be the key tool to control the yellow particles. To that end we set $\tilde{\tau}_{k_0} = \tau_{k_0}$ and, for $k \geqslant k_0$,

$$\tilde{\sigma}_{k+1} = \inf\left\{t > \tilde{\tau}_k : \text{ there is a free particle inside } \bar{\Lambda} \text{ at time } t\right\},$$

and

$$\tilde{\tau}_{k+1} = \inf\left\{t > \tilde{\sigma}_{k+1} \colon X(t) \in \mathcal{X}_D \text{ or } X(t) \in \mathcal{I}(\ell_1'\ell_2' + 1) \setminus \mathcal{X}_U\right\}.$$

Note the difference between these definitions and those of the special times σ_{i+1} and τ_{i+1}: they are related to *free* particles and $\mathcal{X}_D \cup (\mathcal{I}(\ell_1'\ell_2' + 1) \setminus \mathcal{X}_U)$, rather than to *active* particles and $\mathcal{X}_D$. However, $(Z_1 \setminus F_{m+1})^c$ implies that $\tilde{\sigma}_{k_0+1} = \sigma_{k_0+1}$. To prove (7.4.8) we must analyze the time intervals $[\tilde{\tau}_k, \tilde{\sigma}_{k+1}]$ and $[\tilde{\sigma}_{k+1}, \tilde{\tau}_{k+1}]$, just like we analyzed the time intervals $[\tau_i, \sigma_{i+1}]$ and $[\sigma_{i+1}, \tau_{i+1}]$ to prove (7.4.7). We needed such an analysis for all $1 \leqslant i < n$, but now it will turn out that it will be enough to consider $1 \leqslant k < \tilde{n}$ with

$$\tilde{n} = \min\{\tilde{n}_1, \tilde{n}_2\} \tag{7.5.6}$$

and

$$\tilde{n}_1 = \max\{k \geqslant k_0 \colon \tilde{\tau}_k \leqslant T_{\Delta^+} e^{\delta\beta}\},$$
$$\tilde{n}_2 = \min\{k > k_0 \colon X(\tilde{\tau}_k) \in \mathcal{I}(\ell_1'\ell_2' + 2)\}.$$

We will add $\tilde{\sigma}_k$ and $\tilde{\tau}_k$, $1 \leqslant k \leqslant \tilde{n}$ to our set of special times.

► *The main obstacle:* With a pair of particles $\{i, j\}$ we associate a family of special times θ_k^{ij}, $k \in \mathbb{N}_0$. Before giving the definition of these stopping times, let us explain what they will be used for. In proving (7.4.7), we could exclude the simultaneous presence of two *free* particles in $\bar{\Lambda}$. This was done by excluding the simultaneous presence of two *active* particles in $[\bar{\Lambda}, D + \delta]$ by the means of large deviation events to control red and green particles and the inductive hypothesis to control yellow particles. In proving (7.4.8), we still need to exclude the simultaneous presence of two *free* particles in $\bar{\Lambda}$, but we have to allow the simultaneous presence of two *active* particles in $\bar{\Lambda}$. We will face this obstacle by using large deviation events and some inductive hypothesis to exclude, on the one hand, the simultaneous presence of *three* active particles in $[\bar{\Lambda}, D + \delta]$, and showing, on the other hand, that the first simultaneous presence of two free particles i and j in $\bar{\Lambda}$ at a time T^{ij} would imply some large deviation event J^{ij} that involves the two particles i and j during a time interval $[\theta_k^{ij}, T^{ij}]$ in which i and j are the only active particles in $[\bar{\Lambda}, D + \delta]$.

Let us now give the precise definitions for θ_k^{ij} and J^{ij}. We call $\theta_0^{ij} < \theta_1^{ij} < \cdots$ the ordered sequence of times t such that one of the following events occurs:

(i) i is clusterized in $\bar{\Lambda}$, j is freed inside $\bar{\Lambda}$, and there was at t^- a single cluster in $\bar{\Lambda}$ that contained i and j.

(ii) i enters $[\bar{\Lambda}, D + \delta]$ and j is in $[\bar{\Lambda}, D + \delta]$, so that i was outside $[\bar{\Lambda}, D + \delta]$ at time t^-.

(iii) i is clusterized in $\bar{\Lambda}$, j is free in $[\bar{\Lambda}, D + \delta]$, a third particle k leaves $[\bar{\Lambda}, D + \delta]$ and there is no other free particle in $[\bar{\Lambda}, D + \delta]$, so that k was inside $[\bar{\Lambda}, D + \delta]$ at time t^-.

We call T^{ij} the first time when particles i and j are both free in $\bar{\Lambda}$. We say that J^{ij} occurs if $T^{ij} \leqslant T_{\Delta^+} e^{\delta\beta}$ and there is some $\theta_k^{ij} < T^{ij}$ such that any active particle in $[\bar{\Lambda}, D + \delta]$ during the time interval $[\theta_k^{ij}, T^{ij}]$ is either i or j. The following lemma expresses one of the main properties of the large deviation event J^{ij}.

Lemma 7.5.1. *If $T^{ij} \leqslant T_{\cdot}\Delta^+ e^{\delta\beta}$, then either J^{ij} occurs or there is a time $t \leqslant T^{ij}$ at which there are at least three active particles inside $[\bar{\Lambda}, D + \delta]$.*

The proof of Lemma 7.5.1 is deferred to Section 7.5.4.

• **Large deviations events.** The event $\tilde{B}$ in the following list contains B because we enlarge our set of *special times* by adding the $\tilde{\sigma}_k$, $\tilde{\tau}_k$ and θ_k^{ij}. In the same way, $\tilde{C}$ and $\tilde{D}$ contain C and D. The event $\tilde{F}_{m+1}$ is instead contained in F_{m+1} and has a larger cost.

$\tilde{B}$: There are more than $e^{(2\alpha+\delta)\beta}$ special times within time $T_{\Delta^+} e^{\delta\beta}$. This event has an infinite cost.

$\tilde{C}$: Within time $T_{\Delta^+} e^{\delta\beta}$ there is a time interval of length $e^{\delta\beta}$ that contains a special time followed by a move of cost larger than or equal to U. This event costs at least $U - O(\delta)$.

$\tilde{D}$: Within time $T_{\Delta^+} e^{\delta\beta}$ there is a time interval of length $e^{D\beta}$ that contains a special time followed by a move of cost larger than or equal to $2U$ or two δ-close moves of cost larger than or equal to U. This event costs at least $2U - D - O(\delta)$.

G_3' : There are three active particles, red or green, together with a particle from a cluster at a same time $t < T_{\Delta^+} e^{\delta\beta}$ in a box of volume $e^{(D+\delta)\beta}$, or a particle that belongs to a cluster consisting of two or three active particles only falls asleep. This event costs at least $3\Delta - 2U - \theta + 3\alpha - 2d - O(\delta)$.

$\tilde F_{m+1}$: Within time $T_{\Delta^+} e^{\delta\beta}$ there are $m+1$ attributions of red color and there are either an extra move of cost larger than or equal to $2U$ or two δ-close moves of cost larger than or equal to U, or else the occurrence of one of the events J^{ij}. Note that $\tilde F_{m+1} = F_{m+1} \cap (F_1 \cup \bigcup_{i,j} J^{ij})$. This event costs at least $(m+\frac{3}{2})(2U - \Delta - \alpha) - O(\delta)$.

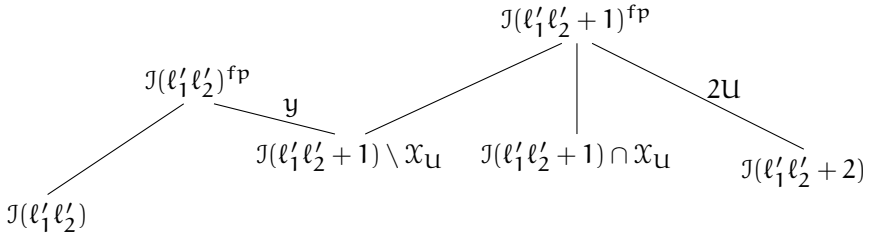

Figure 7.4 – The graph $\tilde{\mathcal{G}}$.

Set

$$Z_2 = A \cup \tilde B \cup \tilde C \cup C' \cup \tilde D \cup D' \cup E \cup \tilde F_{m+1} \cup G \cup G' \cup G_3' \cup G_4' \cup H_2. \tag{7.5.7}$$

Let $\tilde{\mathcal{G}}$ be the graph in Fig. 7.4. Recall (7.5.5) and (7.5.6), and set

$$\tilde\varphi^k = (X(\tilde\tau_{k_0}), X(\tilde\sigma_{k_0+1}), X(\tilde\tau_{k_0+1}), \dots, X(\tilde\sigma_k), X(\tilde\tau_k)), \qquad k_0 \leqslant k \leqslant \tilde n.$$

We will prove by induction that, for all $k_0 \leqslant k \leqslant \tilde n$,

Claim $\tilde{\mathcal{P}}(k)$. *If Z_2 does not occur, then*

(i) $\tilde\varphi^k$ does not escape from $\tilde{\mathcal{G}}$.

(ii) Some particle can be colored yellow during the time interval $[\tilde\tau_{k_0}, \tilde\tau_k]$, but only during the climbing of the y-edge of $\tilde{\mathcal{G}}$.

(iii) There is at most one yellow particle at each time $t \leqslant \tilde\tau_k$.

(iv) Each time $0 \leqslant t \leqslant \tilde\tau_k$ a particle falls asleep there is no yellow particle at the first $\tilde\tau_j$, $1 \leqslant j \leqslant k$, larger than or equal to t.

(v) For all $k_0 < j \leqslant k$, if X visits $\mathcal{X}_U$ during the time interval $[\tilde\sigma_j, \tilde\tau_j)$, then there is no red or green particle in $\bar\Lambda$ at time $\tilde\tau_j$.

(vi) At each time $0 \leqslant t \leqslant \tilde\tau_k$ there are at least $\ell_1'\ell_2'$ sleeping particles.

(vii) No box creation occurs within time $\tilde\tau_k$.

Property (i) is the main one we are interested in. Property (iv) implies that if a particle falls asleep when there is a yellow particle, then it is the yellow particle that falls asleep. Property (vi) is easy to check and simplifies a few steps of the proof. We will use properties (ii)–(iv) to control inductively the yellow particles, in particular, property (iii) will be used to prove property (vii). Property (v) will be used to prove property (iv) with the help of the following lemma, whose proof is deferred to Section 7.5.5.

Lemma 7.5.2. *If Z_2 does not occur, then, for all $k \leqslant \tilde n$, either $X(\tilde\tau_k) \in \mathcal{X}_U$ or $X(t) \notin \mathcal{X}_U$ for all $t \in [\tilde\tau_k, \tilde\sigma_{k+1})$.*

$\trianglerighteq$ Before proving $\tilde{\mathcal{P}}(k)$, $k_0 \leqslant k \leqslant \tilde n$, let us show that $\tilde{\mathcal{P}}(\tilde n)$ implies for both cases $\tilde n = \tilde n_1$ and $\tilde n = \tilde n_2$ that if Z_2^c occurs, then φ^n cannot escape from $\mathcal{G}_2$.

For $\tilde n = \tilde n_1$, since Z_2^c implies that $\tilde\varphi^{\tilde n}$ does not escape from $\tilde{\mathcal{G}}$, it suffices to prove, for all $k_0 \leqslant l \leqslant n$, that $\tau_l = \tilde\tau_k$ for some $k \leqslant \tilde n$. We prove prove by induction on $l \geqslant k_0$. The claim is obvious for $l = k_0$. If this is true for some $l < n$, then $\tilde\sigma_{k+1} = \sigma_{l+1}$ and, since $\tilde n = \tilde n_1$, there is a last time $\tilde\tau_{m^*} > \sigma_{l+1}$ before τ_{l+1}:

$$\tilde\tau_{m^*} = \max\{\tilde\tau_m \leqslant \tau_{l+1} \colon \tilde\tau_m > \sigma_{l+1}\}.$$

If $X(\tilde\tau_{m^*}) \notin \mathcal{X}_U$, then, by Lemma 7.5.2, $\tau_{l+1} \geqslant \tilde\sigma_{m^*+1}$ and $\tilde\tau_{m^*}$ cannot be the *last* time $\tilde\tau_m$ smaller than or equal to τ_{l+1}. It follows that $X(\tilde\tau_{m^*}) \in \mathcal{X}_D$ and, since $\tilde\tau_{m^*} > \sigma_{l+1}$, $\tilde\tau_{m*} \geqslant \tau_{l+1} \geqslant \tilde\tau_{m*}$: the two times coincide.

For $\tilde n = \tilde n_2$, like for $\tilde n = \tilde n_1$, we prove that there is some $k_1 > k_0$ such that $\tau_{k_1} = \tilde\tau_{\tilde n}$ and

$$\{\tau_{k_0}, \tau_{k_0+1}, \dots, \tau_{k_1}\} \subset \{\tilde\tau_{k_0}, \tilde\tau_{k_0+1}, \dots, \tilde\tau_{\tilde n}\}.$$

It follows that Z_2^c implies that φ^{k_1} does not escape from $\mathcal{G}_2$. Since $\tilde n = \tilde n_2$, X reaches $\mathcal{X}_D$ at time $\tilde\tau_{\tilde n}$ and, since $\tilde{\mathcal{P}}(\tilde n)$-i) implies that it does so by making some particle fall asleep, $\tilde{\mathcal{P}}(\tilde n)$(iv) implies that there is no yellow particle at time $\tau_{k_1} = \tilde\tau_{\tilde n}$. Using that $\tilde F_{m+1}^c$ excludes any $(m+2)^{th}$ attribution of the red color, we can show by induction, as in the proof of (7.4.7), that φ^k, for $k \geqslant k_1$, cannot escape anymore from $\mathcal{G}_1$, the subgraph of $\mathcal{G}_2$.

Since the cost of Z_2 is given by the smallest cost of its components, we obtain

$$c(Z_2) = \begin{cases} c(\tilde F_{m+1}) \geqslant r(\ell_1,\ell_2) - \Delta + \frac{\gamma}{2} - O(\alpha, d) - O(\delta) & \text{if } \ell_1 < \ell_c - 1, \\ c(\tilde F_{m+1}) \geqslant r(\ell_1,\ell_2) - \Delta + \frac{\gamma}{2} - O(\alpha, d) - O(\delta) & \text{if } \ell_1 = \ell_c - 1 \text{ and } \iota < 1/2, \\ c(H_2) \geqslant r(\ell_1,\ell_2) - \Delta + (1-\iota)\gamma - O(\alpha, d) - O(\delta) & \text{if } \ell_1 = \ell_c - 1 \text{ and } \iota \geqslant 1/2. \end{cases}$$

To prove (7.4.8) in the subcritical case, it only remains to prove $\tilde{\mathcal{P}}(\tilde n)$ and check the given cost estimates .

• **Proof of $\tilde{\mathcal{P}}(k)$, $k_0 \leqslant k \leqslant \tilde n$.** $\tilde{\mathcal{P}}(k_0)$(iii) and $\tilde{\mathcal{P}}(k_0)$(vi) follow from the argument explained below (7.5.5), while the other items are obvious. For $k \geqslant k_0$, we assume $\tilde{\mathcal{P}}(k)$ to prove $\tilde{\mathcal{P}}(k+1)$. We consider four cases, depending on the configuration at time $\tilde\tau_k$ in one of the sets of $\tilde{\mathcal{G}}$ ordered from right to left.

Case 1: $X(\tilde\tau_k) \in \mathcal{I}(\ell_1'\ell_2' + 2)$. If $k \neq k_0$, then $\tilde n = \tilde n_2 = k$ and there is nothing to prove. We only need to consider the case $k = k_0$, for which $\tilde\sigma_{k+1} = \sigma_{k_0+1}$ and the definition of σ_{k_0+1} gives $X(\sigma_{k_0+1}) \in \mathcal{I}(\ell_1'\ell_2' + 1)^{fp}$. The analysis of the time intervals $[\tau_k, \sigma_{k+1}]$ we gave to prove (7.4.7) also shows that in this case no yellow particle can be produced during the time interval $[\tilde\tau_{k_0}, \tilde\sigma_{k_0+1}]$, and that there are $\ell_1'\ell_2' + 2$ sleeping particles all along $[\tilde\tau_{k_0}, \tilde\sigma_{k_0+1}]$, and $\ell_1'\ell_2' + 1$ sleeping particles at time $\tilde\sigma_{k_0+1}$.

Since the free particle is colored red at time $\tilde\sigma_{k_0+1}$ and no yellow particle was produced during the time interval $[0, \tilde\sigma_{k_0+1}]$, the analysis of the time intervals $[\sigma_{k+1}, \tau_{k+1}]$ we gave to prove (7.4.7) can be reproduced to prove $\tilde{\mathcal{P}}(k_0 + 1)$. There are two differences. One difference is that we have to distinguish between two cases at the end of the "exit case", when reaching an isoperimetric configuration of sleeping particles: if this configuration is U-irreducible, then X reaches $\mathcal{X}_D$ in $\mathcal{I}(\ell_1'\ell_2' + 1) \cap \mathcal{X}_U$, while if not, then X reaches $\mathcal{I}(\ell_1'\ell_2' + 1) \setminus \mathcal{X}_U$. Still, no yellow particle was produced during the time interval $[\tilde\sigma_{k_0+1}, \tilde\tau_{k_0+1}]$, in which we always have $\ell_1'\ell_2' + 1$ sleeping particles at least. The other difference is that we have to check $\mathcal{P}(k_0 + 1)$(v). To do so it suffices to note that the only case for which $X(\tilde\tau_{k_0+1}) \notin \mathcal{X}_D$ is the "exit case" for which X does not visit $\mathcal{X}_U$ during the whole time interval $[\tilde\sigma_{k_0+1}, \tilde\tau_{k_0+1})$. Property $\tilde{\mathcal{P}}(k+1)$(vii) follows from the events $G_4'^c$, $G_3'^c$ and $\tilde{\mathcal{P}}(k+1)$-iii).

Case 2: $X(\tilde\tau_k) \in \mathcal{I}(\ell_1'\ell_2' + 1) \cap \mathcal{X}_U$. In this case the main part of the analysis is that of the time interval $[\tilde\tau_k, \tilde\sigma_{k+1}]$. In particular, we will prove that $X(\tilde\sigma_{k+1})$ belongs to $\mathcal{I}(\ell_1'\ell_2' + 1)^{fp}$, with a cluster made up of sleeping particles only, and there is no yellow particle at time $\tilde\sigma_{k+1}$. After that we can conclude as in Case 1.

We first note that, by the definition of $\tilde\tau_k$, there are only sleeping particles in $\bar\Lambda$ at time $\tilde\tau_k$. Therefore we study once again the process

$$\Delta\bar H\colon\ t \in [\tilde\tau_k, \tilde\sigma_{k+1}) \mapsto \bar H(X(t)) - \bar H(X(\tilde\tau_k)).$$

Similarly to the analysis we gave to prove (7.4.7), the events $\tilde F_{m+1}^c$ and A^c imply that the process can only oscillate between the energy levels 0 and U, and has to go back to 0 within a time $e^{\delta\beta}$ after each increase to U. Since $X(\tilde\tau_k) \in \mathcal{X}_U$, there is no way to free any particle without going above the energy level U. We therefore only have to consider the entrance case. The event C'^c implies that X reaches $\mathcal{I}(\ell_1'\ell_2' + 1)^{fp}$, with a cluster made up of sleeping particles only.

Now, if there were some yellow particle at time $\tilde{\sigma}_{k+1}$, then by $\tilde{\mathcal{P}}(k)$(ii) this should have been produced at some earlier time $\tilde{\sigma}_{k'} < \tilde{\tau}_k$, leaving $\ell_1'\ell_2'$ sleeping particles. Since at time $\tilde{\tau}_k$ there are $\ell_1'\ell_2' + 1$ sleeping particles, we would get a contradiction with $\tilde{\mathcal{P}}(k)$(iv). It therefore remains to prove $\tilde{\mathcal{P}}(k+1)$(vii), for which we can argue as before.

Case 3: $X(\tilde{\tau}_k) \in \mathcal{I}(\ell_1'\ell_2' + 1) \setminus \mathcal{X}_U$. In this case, the same analysis for the time interval $[\tilde{\tau}_k, \tilde{\sigma}_{k+1}]$ can be reproduced with a different conclusion. On the one hand, it is now possible to free some particle with a move of cost U, leading to $\mathcal{I}(\ell_1'\ell_2')^{fp}$ at time $\tilde{\sigma}_{k+1}$, with a cluster of $\ell_1'\ell_2'$ sleeping particles. One yellow particle, *but no more than one*, can subsequently be produced. On the other hand, it is still possible to reach $\mathcal{I}(\ell_1'\ell_2' + 1)^{fp}$ at time $\tilde{\sigma}_{k+1}$, *without producing any new yellow particle*, but in this case too there is a difference with respect to Case 2: it is not true anymore that all the clusterized particles in $\bar{\Lambda}$ are necessarily sleeping at time $\tilde{\sigma}_{k+1}$. Indeed, we cannot exclude anymore the presence of an active particle in $\bar{\Lambda}$ at time $\tilde{\tau}_k$. Also we cannot exclude with the same argument the possibility of having, at time $\tilde{\sigma}_{k+1}$, $l_1'l_2' + 1$ sleeping particles together with a yellow free particle. We will first prove that Z_2^c implies that an eventual red or green particle at time $\tilde{\tau}_k$ cannot fall asleep during the time interval $[\tilde{\tau}_k, \tilde{\sigma}_{k+1}]$. Afterwards we will study the time interval $[\tilde{\sigma}_{k+1}, \tilde{\tau}_{k+1}]$ in the two cases $X(\tilde{\sigma}_{k+1}) \in \mathcal{I}(\ell_1'\ell_2' + 1)^{fp}$ and $X(\tilde{\sigma}_{k+1}) \in \mathcal{I}(\ell_1'\ell_2')^{fp}$, with a cluster of $\ell_1'\ell_2'$ sleeping particles.

A red or a green particle cannot fall asleep in the first time interval. We only have to consider the case when there is some red or green particle i in $\bar{\Lambda}$ at time $\tilde{\tau}_k$. Let us call $\tilde{\tau}_{l^*}$ the last time $\tilde{\tau}_l$ before $\tilde{\tau}_k$ such that $X(\tilde{\tau}_l) \in \mathcal{X}_D$. Lemma 7.5.2 implies that X could not visit $\mathcal{X}_U$ during any time interval $[\tilde{\tau}_j, \tilde{\sigma}_{j+1})$ for $1 \leqslant l^* < j \leqslant k$. Let us call $[\tilde{\sigma}_{j^*}, \tilde{\tau}_{j^*})$ the last time interval $[\tilde{\sigma}_j, \tilde{\tau}_j)$ after $\tilde{\tau}_{l^*}$ and before $\tilde{\tau}_k$ in which X visited $\mathcal{X}_U$. We consider separately the cases in which such an index j^* exists or not. If j^* exists, then by $\tilde{\mathcal{P}}(k)$-v) there was no red or green particle at time $\tilde{\tau}_{j^*}$, in particular, $j^* < k$ and, by construction, X did not visit $\mathcal{X}_U$ during the time interval $[\tilde{\tau}_{j^*}, \tilde{\sigma}_{k+1})$. The recurrence property to $\mathcal{X}_U$, which is described by A^c, then implies

$$\tilde{\sigma}_{k+1} - \tilde{\tau}_{j^*} \leqslant T_U e^{\delta\beta}. \tag{7.5.8}$$

Since at time $\tilde{\tau}_{j^*}$ there was no red or green particle in $\bar{\Lambda}$, if our red or green particle i at time $\tilde{\tau}_k$ was already in $\bar{\Lambda}$ at time $\tilde{\tau}_{j^*}$, then it was sleeping and there must have been some time t_f in $[\tilde{\tau}_{j^*}, \tilde{\tau}_k)$ at which i was free. If i was not in $\bar{\Lambda}$ at time $\tilde{\tau}_k$, then it had to enter $\bar{\Lambda}$ during the time interval $[\tilde{\tau}_{j^*}, \tilde{\tau}_k)$ and, in this case too, it had to be free at some time t_f in $[\tilde{\tau}_{j^*}, \tilde{\tau}_k)$. Inequality (7.5.8) implies that

$$\tilde{\sigma}_{k+1} - t_f \leqslant T_U e^{\delta\beta} < e^{D\beta},$$

so that i cannot fall asleep before time $\tilde{\sigma}_{k+1}$.

If j^* does not exist, then by construction we deduce that $l^* < k$ and

$$\tilde{\sigma}_{k+1} - \tilde{\sigma}_{l^*+1} \leqslant T_U e^{\delta\beta}. \tag{7.5.9}$$

Since all the clusterized particle in $\bar{\Lambda}$ at time $\tilde{\sigma}_{l^*+1}$ were sleeping particles, if i was among them, then there was some time t_f between $\tilde{\sigma}_{l^*+1}$ and $\tilde{\tau}_k$ when i was free. The same conclusion obviously holds if i was the free particle at time $\tilde{\sigma}_{l^*+1}$. Finally, if i was not in $\bar{\Lambda}$ at time $\tilde{\sigma}_{l^*+1}$, then it had to enter $\bar{\Lambda}$ between times $\tilde{\sigma}_{l^*+1}$ and $\tilde{\tau}_k$. But in this case also it had to be free at some time t_f between $\tilde{\sigma}_{l^*+1}$ and $\tilde{\tau}_k$. It follows from (7.5.9) that

$$\tilde{\sigma}_{k+1} - t_f \leqslant T_U e^{\delta\beta} < e^{D\beta},$$

and i cannot fall asleep before time $\tilde{\sigma}_{k+1}$.

► *The case* $X(\tilde{\sigma}_{k+1}) \in \mathcal{I}(\ell_1'\ell_2' + 1)^{fp}$. If all the clusterized particles in $\bar{\Lambda}$ are sleeping at time $\tilde{\sigma}_{k+1}$, then we can conclude as in Case 2: the entrance at $\tilde{\sigma}_{k+1}$ of a yellow particle would imply either the presence of another yellow particle in $\bar{\Lambda}$ at time $\tilde{\tau}_k$, which would contradict $\tilde{\mathcal{P}}(k)$(iii), or the fact that there were only sleeping particles at $\tilde{\tau}_k$, which as before would contradict either $\tilde{\mathcal{P}}(k)$(ii) or $\tilde{\mathcal{P}}(k)$(iv). Let us therefore assume that the isoperimetric cluster at time $\tilde{\sigma}_{k+1}$ contains an active particle. Since there is also a free particle at time $\tilde{\sigma}_{k+1}$ in $\bar{\Lambda}$, we have two active particles in $\bar{\Lambda}$. The events G^c, G'^c and H_2^c imply that at least one of them has to be yellow. Since at time $\tilde{\tau}_k$ there was one yellow particle at most and we did

not produce any new yellow particle during the time interval $[\tilde{\tau}_k, \tilde{\sigma}_{k+1}]$, there is at most one yellow particle. The events G^c, G'^c and H_2^c imply that, among the two active particles in $\bar{\Lambda}$, one is yellow and the other is either red or green, there is no other yellow particle in $\bar{\Lambda}^c$, and no other active particles in $[\bar{\Lambda}, D + \delta] \setminus \bar{\Lambda}$. In particular, as a consequence of A^c, no other particle can enter $\bar{\Lambda}$ before time $\tilde{\tau}_{k+1}$.

Let us consider the process

$$\Delta\bar{H}\colon\ t \in [\tilde{\sigma}_{k+1}, \tilde{\tau}_{k+1}] \mapsto \bar{H}(X(t)) - \bar{H}(X(\tilde{\sigma}_{k+1})).$$

As a consequence of A^c, $\tilde{C}^c$ and the fact that no other particle can enter $\bar{\Lambda}$, this process has to decrease within a time $e^{\delta\beta}$. We then have a flow of alternatives organised as follows. We consider three distinct cases a, b, c: the first two will be conclusive, while the last can either be conclusive in three different ways or bring us to a similar but simpler and binary alternative b'/c'. Once again the first case will be conclusive, while the last case can either be conclusive in three different ways or bring us back to the same binary alternative b'/c'. It will be clear later that Z_2^c will prevent us from running into an infinite loop.

(a) *The free particle at time $\tilde{\sigma}_{k+1}$ leaves $\bar{\Lambda}$ without interacting with any other particle in $\bar{\Lambda}$.* In this case $\Delta\bar{H}$ first decreases to $-\Delta$, which occurs at time $\tilde{\tau}_{k+1}$: X reaches $\mathcal{I}(\ell_1'\ell_2' + 1) \setminus \mathcal{X}_U$ without having time to make the other active particle fall asleep. Indeed, with the same argument as used before, it is possible to prove that the eventual red or green particle cannot fall asleep during the time interval $[\tilde{\tau}_k, \tilde{\sigma}_{k+1} + e^{\delta\beta}]$. If the yellow particle was free at time $\tilde{\sigma}_{k+1}$, then at time $\tilde{\tau}_{k+1}$ it is outside $\bar{\Lambda}$. If the yellow particle was clusterized at time $\tilde{\sigma}_{k+1}$, then at time $\tilde{\tau}_{k+1}$ it is in $\bar{\Lambda}$. In this case the system does not visit $\mathcal{X}_U$ during the time interval $[\tilde{\sigma}_{k+1}, \tilde{\tau}_{k+1}]$.

(b) *$\Delta\bar{H}$ reaches the energy level $-2U$ before a free particle leaves $\bar{\Lambda}$.* In this case we can reproduce the analysis of the good attachment case described to prove (7.4.7). X reaches $\mathcal{X}_D$ in $\mathcal{I}(\ell_1'\ell_2' + 2)$ at time $\tilde{\tau}_{k+1}$ by making fall asleep the two active particles of time $\tilde{\sigma}_{k+1}$.

(c) *The free particle at time $\tilde{\sigma}_{k+1}$ interacts with the clusterized particles and $\Delta\bar{H}$ does not reach the energy level $-2U$ before a free particle leaves $\bar{\Lambda}$.* In this case we can reproduce the analysis of the exit case described to prove (7.4.7), $\Delta\bar{H}$ will reach the energy level $-\Delta$ with the exit of a free particle from $\bar{\Lambda}$ and an isoperimetric configuration in $\bar{\Lambda}$. We note that our permutation rules ensure that at each time t whenever there is a free particle after the first interaction time and before reaching the energy level $-\Delta$, it cannot be yellow. At the time t of the red or green particle exit we distinguish between three cases.

(i) If $X(t) \in \mathcal{I}(\ell_1'\ell_2' + 1) \setminus \mathcal{X}_U$, then $\tilde{\tau}_{k+1} = t$. If some particle fell asleep before time t, then it was the yellow one and there is no yellow particle anymore at time t. If there is still some active particle in $\bar{\Lambda}$ at time t, then it is the yellow one: there is no green or red particle in $\bar{\Lambda}$ at time t.

(ii) If $X(t) \in \mathcal{I}(\ell_1'\ell_2' + 1) \cap \mathcal{X}_U$ and all particles in $\bar{\Lambda}$ are sleeping at time t, then $\tilde{\tau}_{k+1} = t$. There is no yellow particle anymore at time t. There is no green or red particle in $\bar{\Lambda}$ at time t.

(iii) If $X(t) \in \mathcal{I}(\ell_1'\ell_2' + 1) \cap \mathcal{X}_U$ and the yellow particle is still active at time t, then $\tilde{\tau}_{k+1} > t$. As in the good attachment case studied to prove (7.4.7), where $\Delta\bar{H}$ could eventually only oscillate between the two energy levels $-2U$ and $-U$, $\Delta\bar{H}$ can only oscillate between the energy levels $-\Delta$ and $-\Delta + U$ until the first time $t' > t$ when either the yellow particle falls asleep or the red or green particle comes back in $\bar{\Lambda}$. In the former case, to which we will refer as the *conclusive* case, $\tilde{\tau}_{k+1} = t'$, there is no yellow particle anymore at time t', and there is no red or green particle in $\bar{\Lambda}$ at time t'. In the latter case, considering in the same way

$$\Delta\bar{H}\colon\ s \in [t', \tilde{\tau}_{k+1}] \mapsto \bar{H}(X(s)) - \bar{H}(X(t')),$$

we are led to repeat the same kind of analysis, with one more hypothesis with respect to time $\tilde{\sigma}_{k+1}$: we know that the free particle at time t' is either red or green and that the clusterized active particle is the yellow one. We can then define a single alternative (c') to a similar case (b').

(b') *$\Delta\bar{H}$ reaches the energy level $-2U$ before a free particle leaves $\bar{\Lambda}$.* There is no difference in this case with the previous case (b).

(c′) $\Delta\bar{H}$ *does not reach the energy level* $-2U$ *before a free particle leaves* $\bar{\Lambda}$. This case includes a possible absence of interaction between the clusterized particles in $\bar{\Lambda}$ and the green or red free particle before it exits. The same conclusions hold as in the previous case c, with the possibility of going back to the same alternative (b′)/(c′) after a similar time t' when the green or red particle comes back in $\bar{\Lambda}$.

Since each time we go back to the alternative (b′)/(c′) the green or red particle enters again $\bar{\Lambda}$, $\tilde{B}^c$ implies that it can happen a finite number of times only. Ultimately, no yellow particle can be produced during the time interval $[\tilde{\sigma}_{k+1}, \tilde{\tau}_{k+1}]$: if the red or the green particle falls asleep (cases (b) and (b′)), then so does the yellow one, and if the yellow particle falls asleep (cases (b), (b′), (c)(ii), (c′)(ii), conclusive (c)(iii) and (c′)(iii), or (a), (c)(i) and (c′)(i)), then there is no yellow particle anymore at time $\tilde{\tau}_{k+1}$, while if X visited $\mathcal{X}_U$, then a is excluded, which is the only case with a possible green or red particle in $\bar{\Lambda}$ at time $\tilde{\tau}_k$. We also had at least $\ell_1'\ell_2'$ sleeping particles in the whole time interval. For the proof of $\tilde{\mathcal{P}}(k+1)$(vii) we can argue as before.

▶ *The case* $X(\tilde{\sigma}_{k+1}) \in \mathcal{I}(\ell_1'\ell_2')^{fp}$*, with a cluster of* $\ell_1'\ell_2'$ *sleeping particles.* Let us first show by contradiction that there cannot be two yellow particles at time $\tilde{\sigma}_{k+1}$. Indeed, =in this case $\tilde{\mathcal{P}}(k)$(iii) would imply that we just reached $\mathcal{I}(\ell_1'\ell_2')^{fp}$ by producing a yellow particle i during the time interval $[\tilde{\tau}_k, \tilde{\sigma}_{k+1}]$. This is possible only if we had $\ell_1'\ell_2' + 1$ sleeping particles at time $\tilde{\tau}_k$. We note that we could not produce more than one yellow particle in this time interval. Hence there should have been another yellow particle j produced at an earlier time $t < \tilde{\tau}_k$, and we can assume that t was the last emission time of a yellow particle before time $\tilde{\tau}_k$. Since our hypothesis $\tilde{\mathcal{P}}(k)$(ii) implies that there were at most $\ell_1'\ell_2'$ sleeping particles at time t, some particle fell asleep between times t and $\tilde{\tau}_k$ and this would contradict $\tilde{\mathcal{P}}(k)$(iv).

Note that G^c, G'^c and H_2^c imply that there is either 0 or 1 particle in $[\bar{\Lambda}, D+\delta] \setminus \bar{\Lambda}$. We also note that the sleeping particles in $\bar{\Lambda}$ at time $\tilde{\sigma}_{k+1}$ form a quasi-square: this is the only isoperimetrical configuration of size $\ell_1'\ell_2'$.

If there is no particle in $[\bar{\Lambda}, D+\delta] \setminus \bar{\Lambda}$, then, once again, A^c and $\tilde{C}^c$ imply that the local energy first has to decrease within a time $e^{\delta\beta}$.This can be realized in two ways only: waiting either for the attachment of the free particle to the cluster or for the free particle to leave $\bar{\Lambda}$ at some time t. In both cases $\tilde{\tau}_{k+1} = t$. In the former case X goes back to $\mathcal{I}(\ell_1'\ell_2' + 1)$ without making any particle fall asleep and without visiting $\mathcal{X}_U$. In the latter case X reaches $\mathcal{X}_D$ in $\mathcal{I}(\ell_1'\ell_2')$.

If there is another active particle in $[\bar{\Lambda}, D+\delta] \setminus \bar{\Lambda}$, then the events A^c and $\tilde{C}^c$ together with Lemma 7.5.1 and $\tilde{F}^c_{m+1}$ lead to the same conclusion. The free particle at time $\tilde{\sigma}_{k+1}$ indeed has to either leave $\bar{\Lambda}$ or join the cluster before the second active particle can enter $\bar{\Lambda}$. For the proof of $\tilde{\mathcal{P}}(k+1)$(vii) we can argue as before.

Case 4: $X(\tilde{\tau}_k) \in \mathcal{I}(\ell_1'\ell_2')$. In this case we have a quasi-square of sleeping particles at time $\tilde{\tau}_k$, and any move before the entrance of a free particle would cost 2U at least. Such a move is excluded by $\tilde{F}^c_{m+1}$. It follows that X reaches $\mathcal{I}(\ell_1'\ell_2')^{fp}$ with a cluster made up of sleeping particles only at time $\tilde{\sigma}_{k+1}$, and we conclude like in the previous case. This ends our induction.

• **Cost estimates.** To complete the proof of (7.4.7) in the subcritical case, we only need to check the given lower bounds for the cost of each event that compounds Z_2, for which we refer to Appendix 7.B. This concludes Case (II). □

7.5.2.4 *Escape case (III)*

• **Large deviation events in the supercritical case.** In the supercritical case, the cost of Z_1 is that of H_2. We will build Z_2 by removing H_2 from Z_1 before adding new large deviation events. The event $\tilde{H}_2$ in the following list is contained in H_2 and has a larger cost.

H_3 : There are three green particles at a same time $t < T_{\Delta^+}e^{\delta\beta}$ in $[\bar{\Lambda}, D+\delta]$. This event costs at least $2(\Delta - D + \alpha) - O(\delta)$.

H_3' : There are two times $t_1 < t_2 < T_{\Delta^+}e^{\delta\beta}$ at which there is a pair of green particles in $[\bar{\Lambda}, D+\delta]$ at time t_1 and a different pair of green particles in $[\bar{\Lambda}, D+\delta]$ at time t_2. This event costs at least $2(\Delta - D + \alpha) - O(\delta)$.

I : Within time $T_{\Delta^+} e^{\delta\beta}$ there are two green particles at a same time in $[\bar\Lambda, D+\delta]$, and there is one attribution of the red color, or else the occurrence of one of the events J^{ij}. (Note that $I = H_2 \cap (F_1 \cup \bigcup_{i,j} J^{ij})$.) This event costs at least $U - \frac{1}{2}\varepsilon + \frac{1}{2}\alpha - d - O(\delta)$.

$\tilde H_2$: $H_3 \cup H_3' \cup I$. This event costs at least $U - \frac{1}{2}\varepsilon + \frac{1}{2}\alpha - d - O(\delta)$.

• **Z_2 and the escape from $\mathcal{G}_2$ in the supercritical case.** Set

$$Z_2 = A \cup \tilde B \cup \tilde C \cup C' \cup \tilde D \cup D' \cup E \cup F_{m+1} \cup G \cup G' \cup G_4' \cup G_3' \cup \tilde H_2. \tag{7.5.10}$$

Define

$$Z_2'^c = Z_2^c \cap \{\text{no red particles are produced}\}$$

and

$$Z_2''^c = Z_2^c \cap \{\text{red particles can be produced}\},$$

so that $Z_2^c = Z_2'^c \dot\cup Z_2''^c$. If Z_2^c occurs, then either $Z_2'^c$ or $Z_2''^c$ occurs. If $Z_2''^c$ occurs, then, by using the event I^c and arguing in a similar way as in the proof of (7.4.7), we obtain that φ^k does not escape from $\mathcal{G}_1$. If $Z_2'^c$ occurs, then we define $\tilde\tau_0 = \tau_0$ and $\tilde\sigma_k$, τ_k with $k > 0$, as before. If there exists $1 \leqslant k_1 \leqslant \tilde n$ such that at time $\tilde\sigma_{k_1}$ there are two green particles in $\bar\Lambda$, then we define $k_0 = k_1 - 1$, otherwise we put $k_0 = \tilde n$. We will analyze separately the behavior of the process X up to and after time $\tilde\tau_{k_0}$, because before the appearance of two green particles in $\bar\Lambda$ no particle can be painted yellow, otherwise this is possible.

Let $\tilde{\mathcal{G}}'$ be the graph in Fig. 7.5.

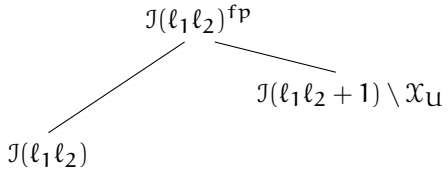

Figure 7.5 – The graph $\tilde{\mathcal{G}}'$.

Recall (7.5.5) and (7.5.6), and set

$$\tilde\varphi'^k = (X(\tilde\tau_0), X(\tilde\sigma_1), X(\tilde\tau_1), \dots, X(\tilde\sigma_k), X(\tilde\tau_k)), \qquad k \leqslant k_0.$$

We will prove by induction that, for all $k \leqslant k_0$,

Claim $\tilde{\mathcal{P}}'(k)$. *If Z_2 does not occur, then*
(i) $\tilde\varphi'^k$ does not escape from $\tilde{\mathcal{G}}'$.
(ii) There is no yellow particle at each time $t \leqslant \tilde\tau_k$.
(iii) For all $0 < j \leqslant k$, if X visited $\mathcal{X}_U$ during the time interval $[\tilde\sigma_j, \tilde\tau_j)$, then there is no green particle in $\bar\Lambda$ at time $\tilde\tau_j$.
(iv) At each time $t \leqslant \tilde\tau_k$ there are $\ell_1\ell_2$ sleeping particles.
(v) No box creation occurs within time $\tilde\tau_k$.

• **Proof of $\tilde{\mathcal{P}}'(k), 0 \leqslant k \leqslant k_0$.** Note that $\tilde{\mathcal{P}}'(0)$ is trivial. For $k \in \mathbb{N}_0$ we assume $\tilde{\mathcal{P}}'(k)$ to prove $\tilde{\mathcal{P}}'(k+1)$. If $k = k_0$, then there is nothing to prove, so assume that $k \neq k_0$. We separate two cases, depending on the configuration at time $\tilde\tau_k$ in one of the bottom sets of $\tilde{\mathcal{G}}'$, ordered from left to right.

Case 1: $X(\tilde\tau_k) \in \mathcal{I}(\ell_1\ell_2)$. In this case we have a quasi-square of sleeping particles at time $\tilde\tau_k$, and any move before the entrance of a free particle would cost $2U$ at least. Such a move is excluded by the fact that no red particles can be produced. It follows that X reaches $\mathcal{I}(\ell_1\ell_2)^{fp}$ with a cluster made up of sleeping particles only at time $\tilde\sigma_{k+1}$. By the fact that no red particles are created and by the event H_3^c, we know that there are at most two active particles in $[\bar\Lambda, D+\delta]$. In particular, the active particles can be green only.

If there is no particle in $[\bar\Lambda, D+\delta]\setminus\bar\Lambda$, then by the events A^c and $\tilde C^c$ we know that the local energy must decrease within a time $e^{\delta\beta}$. This can be realized in two ways only: waiting either for the attachment of the free particle to the cluster or for the free particle to leave $\bar\Lambda$ at some time t. In both cases $\tilde\tau_{k+1}=t$. In the former case X goes back to $\mathcal{I}(\ell_1\ell_2+1)$ without making any particle fall asleep and without visiting $\mathcal{X}_U$. In the latter case X reaches $\mathcal{X}_D$ in $\mathcal{I}(\ell_1\ell_2)$.

If there is one active particle in $[\bar\Lambda, D+\delta]\setminus\bar\Lambda$, then we argue as in the subcritical case by using the events A^c, $\tilde C^c$, I^c and Lemma 7.5.1, and the fact that no red particles can be produced. Indeed, the free particle at time $\tilde\sigma_{k+1}$ has to either leave $\bar\Lambda$ or join the cluster before the second active particle enters $\bar\Lambda$. Property $\tilde{\mathcal{P}}'(k+1)(v)$ follows from the event $G_4'^c$ and $\tilde{\mathcal{P}}'(k+1)(ii)$.

Case 2: $X(\tilde\tau_k)\in\mathcal{I}(\ell_1\ell_2+1)\setminus\mathcal{X}_U$. We can repeat the analysis given in the subcritical case. In particular, with the same arguments we prove that the possible green particle at time $\tilde\tau_k$ cannot feel asleep during the time interval $[\tilde\tau_k,\tilde\sigma_{k+1}]$. Note that $\tilde{\mathcal{P}}'(k)$ implies that at time $\tilde\tau_k$ there is a green particle in $\bar\Lambda$. We have to analyze the time interval $[\tilde\sigma_{k+1},\tilde\tau_{k+1}]$ in the case $X(\tilde\sigma_{k+1})\in\mathcal{I}(\ell_1\ell_2)^{fp}$, with a cluster of $\ell_1\ell_2$ sleeping particles: it is not possible that $X(\tilde\sigma_{k+1})\in\mathcal{I}(\ell_1\ell_2+1)^{fp}$ because $k\leqslant k_0$, and therefore two green particles cannot be in $\bar\Lambda$. We can therefore argue as in the subcritical case. For the proof of $\tilde{\mathcal{P}}'(k+1)(v)$ we can argue as before.

Let $\tilde{\mathcal{G}}$ be the graph in Fig. 7.6.

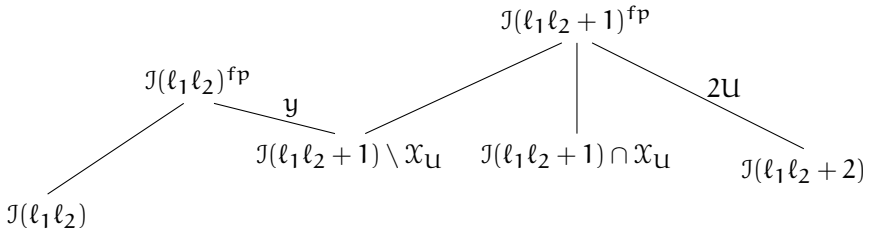

Figure 7.6 – The graph $\tilde{\mathcal{G}}$.

Recall (7.5.5) and (7.5.6), and set

$$\tilde\varphi^k=(X(\tilde\tau_{k_0}),X(\tilde\sigma_{k_0+1}),X(\tilde\tau_{k_0+1}),\dots,X(\tilde\sigma_k),X(\tilde\tau_k)),\qquad k_0<k\leqslant\tilde n.$$

We will prove by induction that, for all $k_0<k\leqslant\tilde n$,

Claim $\tilde{\mathcal{P}}(k)$. *If Z_2 does not occur, then*

(i) $\tilde\varphi^k$ *does not escape from* $\tilde{\mathcal{G}}$.

(ii) Some particle can be colored yellow during the time interval $[\tilde\tau_{k_0},\tilde\tau_k]$*, but only during the climbing of the* y*-edge of* $\tilde{\mathcal{G}}$.

(iii) There is at most one yellow particle at each time $t\leqslant\tilde\tau_k$.

(iv) At each time $1\leqslant t\leqslant\tilde\tau_k$ *when a particle falls asleep there is no yellow particle at the first* $\tilde\tau_j$*,* $1\leqslant j\leqslant k$*, larger than or equal to* t.

(v) For all $0<j\leqslant k$*, if* X *visited* $\mathcal{X}_U$ *during the time interval* $[\tilde\sigma_j,\tilde\tau_j)$*, then there is no red or green particle in* $\bar\Lambda$ *at time* $\tilde\tau_j$.

(vi) At each time $t\leqslant\tilde\tau_k$ *there are at least* $\ell_1\ell_2$ *sleeping particles.*

(vii) Each particle that is yellow at time $t_1\leqslant\tilde\tau_k$ *was green at time* $\tilde\sigma_{k_1}$ *in* $\bar\Lambda$.

(viii) If a green particle falls asleep at time $t\leqslant\tilde\tau_k$*, then it was green at time* $\tilde\sigma_{k_1}$ *in* $\bar\Lambda$.

(ix) No box creation occurs within $\tilde\tau_k$.

Properties (i)-(vi) are the same as considered in the subcritical case, while we will use property (vii) to control inductively the yellow particles. In particular, we cannot exclude anymore the presence of two green particles, but we will exclude the simultaneous presence of two green particles and a yellow particle with the help of property (vii). Property (viii) will be used to prove property (vii). Property (iii) helps us to prove property (ix).

$\trianglerighteq$ Before proving $\tilde{\mathcal{P}}(k)$, $k_0\leqslant k\leqslant\tilde n$, let us show that $\tilde{\mathcal{P}}(\tilde n)$ implies that if Z_2^c occurs, then φ^n cannot escape from $\mathcal{G}_2$. We argue as in the subcritical case, but for $\tilde n=\tilde n_2$ there is one

difference: the attribution of the red color is excluded by the event $Z_2'^c$,and therefore φ^k, $k \geqslant k_1$, cannot escape from $\mathcal{G}_2$.

Since the cost of Z_2 is given by the smallest cost of its constituent components, we obtain

$$c(Z_2) = \begin{cases} c(F_{m+1}) \geqslant r(\ell_1, \ell_2) - \Delta + \varepsilon - \gamma - O(\alpha, d) - O(\delta) & \text{if } \iota < 1/2, \\ c(G_4') \geqslant r(\ell_1, \ell_2) - \Delta + \gamma - O(\alpha, d) - O(\delta) & \text{if } \iota \geqslant 1/2. \end{cases}$$

To prove (7.4.8) in the supercritical case, it remains to prove $\tilde{\mathcal{P}}(\tilde{n})$ and check the given cost estimates .

• **Proof of $\tilde{\mathcal{P}}(k)$, $k_1 \leqslant k \leqslant \tilde{n}$.** We have to prove $\tilde{\mathcal{P}}(k_1)$, and so we consider the time interval $[\tilde{\tau}_{k_0}, \tilde{\tau}_{k_1}]$. By $\tilde{\mathcal{P}}'(k_0)$, either $X(\tilde{\tau}_{k_0}) \in \mathcal{I}(\ell_1\ell_2)$ or $X(\tilde{\tau}_{k_0}) \in \mathcal{I}(\ell_1\ell_2 + 1) \setminus \mathcal{X}_U$. We show by contradiction that $X(\tilde{\tau}_{k_0}) \notin \mathcal{I}(\ell_1\ell_2)$. Indeed, if $X(\tilde{\tau}_{k_0}) \in \mathcal{I}(\ell_1\ell_2)$, then repeating the analysis in the proof of $\tilde{\mathcal{P}}'(k)$ we obtain that $X(\tilde{\sigma}_{k_1}) \in \mathcal{I}(\ell_1\ell_2)^{fp}$, with a cluster made up of sleeping particles only, and the free particle is green. This is in contradiction with the definition of the time $\tilde{\sigma}_{k_1}$. Hence $X(\tilde{\tau}_{k_0}) \in \mathcal{I}(\ell_1\ell_2 + 1) \setminus \mathcal{X}_U$ with $\ell_1\ell_2$ sleeping particles and one active particle, which has to be green. We can repeat the analysis for in the subcritical case to prove that the green particle at time $\tilde{\tau}_{k_0}$ cannot fall asleep during the time interval $[\tilde{\tau}_{k_0}, \tilde{\sigma}_{k_1}]$. By the definition of $\tilde{\sigma}_{k_1}$, we know that $X(\tilde{\sigma}_{k_1}) \in \mathcal{I}(\ell_1\ell_2 + 1)^{fp}$, with $\ell_1\ell_2$ sleeping particles and two green particles. During the time interval $[\tilde{\tau}_{k_0}, \tilde{\sigma}_{k_1}]$ no yellow particle is produced, an so there is no other particle in $[\bar{\Lambda}, D + \delta]$ at time $\tilde{\sigma}_{k_1}$. This implies that no other particle can enter $\bar{\Lambda}$ before time $\tilde{\tau}_{k_1}$. Property $\tilde{\mathcal{P}}'(k+1)$(ix) follows from the event $G_4'^c$, $\tilde{\mathcal{P}}'(k_0)$(ii) and the fact that no yellow particle is produced during the time interval $[\tilde{\tau}_{k_0}, \tilde{\tau}_{k_1}]$. From now on we can argue as in the subcritical case with two differences only: we do not care about yellow particles and have to verify $\tilde{\mathcal{P}}(k_1)$(viii), which is trivial. For $k \geqslant k_1$ we assume $\tilde{\mathcal{P}}(k)$ to prove $\tilde{\mathcal{P}}(k+1)$. We distinguish between four cases, depending on the configuration at time $\tilde{\tau}_k$ in one of the bottom sets of $\tilde{\mathcal{G}}$, ordered from left to right.

Case 1: $X(\tilde{\tau}_k) \in \mathcal{I}(\ell_1\ell_2)$. In this case, as in the proof of $\tilde{\mathcal{P}}'(k)$, we have that $X(\tilde{\sigma}_{k+1}) \in \mathcal{I}(\ell_1\ell_2)^{fp}$, with a cluster made up of sleeping particles only. Note that no yellow particle is produced during the time interval $[\tilde{\tau}_k, \tilde{\sigma}_{k+1}]$. By the fact that no red particle is produced and by the event H_3^c, we know that there are at most three active particles in $[\bar{\Lambda}, D + \delta]$. In particular, the free particle in $\bar{\Lambda}$ at time $\tilde{\sigma}_{k+1}$ is green.

If there is at most one particle in $[\bar{\Lambda}, D + \delta] \setminus \bar{\Lambda}$, then we can argue as in the subcritical case by using the events A^c, $\tilde{C}^c$, I^c and Lemma 7.5.1, and the fact that no red particles can be produced. If there are two particles in $[\bar{\Lambda}, D + \delta] \setminus \bar{\Lambda}$, then there are two green particles and one yellow particle i. Since no yellow particle is produced in $[\tilde{\tau}_k, \tilde{\sigma}_{k+1}]$, we know that particle i was yellow at a time $t \leqslant \tilde{\tau}_k$. Thus, by $\tilde{\mathcal{P}}(k)$(vii) we know that i was green at time $\tilde{\sigma}_{k_1}$ in $\bar{\Lambda}$. This is in contradiction with the event $H_3'^c$, so this case is not admissible.

$\tilde{\mathcal{P}}(k+1)$(i)–(vi) follow by applying the same argument as in the subcritical case. We do not need to check $\tilde{\mathcal{P}}(k+1)$(vii)–(viii), because during the time interval $[\tilde{\tau}_k, \tilde{\tau}_{k+1}]$ no yellow particle is produced and no green particle falls asleep. Property $\tilde{\mathcal{P}}'(k+1)$(ix) follows from the events $G_4'^c$, $G_3'^c$ and $\tilde{\mathcal{P}}'(k+1)$(iii).

Case 2: $X(\tilde{\tau}_k) \in \mathcal{I}(\ell_1\ell_2 + 1) \setminus \mathcal{X}_U$. We can repeat the analysis given for the subcritical case. In particular, with the same argument we are able to prove that the eventual green particle at time $\tilde{\tau}_k$ cannot fall asleep during the time interval $[\tilde{\tau}_k, \tilde{\sigma}_{k+1}]$, and we have to study the time interval $[\tilde{\sigma}_{k+1}, \tilde{\tau}_{k+1}]$ in the two cases $X(\tilde{\sigma}_{k+1}) \in \mathcal{I}(\ell_1\ell_2)^{fp}$, with a cluster of $\ell_1\ell_2$ sleeping particles, and $X(\tilde{\sigma}_{k+1}) \in \mathcal{I}(\ell_1\ell_2 + 1)^{fp}$.

The case $X(\tilde{\sigma}_{k+1}) \in \mathcal{I}(\ell_1\ell_2)^{fp}$, with a cluster of $\ell_1\ell_2$ sleeping particles. As in the subcritical case, we can prove by contradiction that there cannot be two yellow particles at time $\tilde{\sigma}_{k+1}$. By the fact that no red particle can be produced and by the event H_3^c, we know that there are at most three active particles in $[\bar{\Lambda}, D + \delta]$, and so we can conclude as in the previous case. $\tilde{\mathcal{P}}(k+1)$(i)–(vi) follow by applying the same argument carried out in the subcritical case. We do not need to check $\tilde{\mathcal{P}}(k+1)$(viii), because no particle falls asleep during the time interval $[\tilde{\tau}_k, \tilde{\tau}_{k+1}]$. To check $\tilde{\mathcal{P}}(k+1)$(vii), we may suppose that at time $\tilde{\sigma}_{k+1}$ a particle i is colored yellow, because otherwise there is nothing to prove. By the permutation rules, it follows that particle i was sleeping before being colored yellow. Since no particle falls asleep

during the time interval $[\tilde\tau_k, \tilde\sigma_{k+1}]$, particle i was sleeping at $\tilde\tau_k^-$. By $\tilde{\mathcal{P}}(k)$ and the fact that $X(\tilde\sigma_{k+1}) \in \mathcal{I}(\ell_1\ell_2+1)^{fp}$ with two green particles, we know that particle i fell asleep when it was green. Thus, $\tilde{\mathcal{P}}(k+1)$(vii) follows by $\tilde{\mathcal{P}}(k)$(viii). For the proof of $\tilde{\mathcal{P}}'(k+1)$(ix) we can argue as before.

The case $X(\tilde\sigma_{k+1}) \in \mathcal{I}(\ell_1\ell_2+1)^{fp}$. We can argue as in the subcritical case with two differences only: we do not care about red particles and have to check $\tilde{\mathcal{P}}(k+1)$(viii): $\tilde{\mathcal{P}}(k+1)$(vii) is trivial because no particle is colored yellow during the time interval $[\tilde\sigma_{k+1}, \tilde\tau_{k+1}]$. We distinguish between the two following cases: If at time $\tilde\sigma_{k+1}$ the two active particles in $\bar\Lambda$ are green, then $\tilde{\mathcal{P}}(k+1)$(viii) follows by the event $H_3'^c$. If at time $\tilde\sigma_{k+1}$ there is one green and one yellow particles in $\bar\Lambda$, then $\tilde{\mathcal{P}}(k+1)$(viii) follows by $\tilde{\mathcal{P}}(k+1)$(vii) and the event $H_3'^c$. For the proof of $\tilde{\mathcal{P}}'(k+1)$(ix) we can argue as before.

Case 3: $X(\tilde\tau_k) \in \mathcal{I}(\ell_1\ell_2+1) \cap \mathfrak{X}_U$. In this case we can be repeated the analysis in the subcritical case with two differences only: no particle can be colored red and we do not need to check $\tilde{\mathcal{P}}(k+1)$(vii), because no yellow particle is produced during the time interval $[\tilde\tau_k, \tilde\tau_{k+1}]$. $\tilde{\mathcal{P}}(k+1)$(viii) can be checked as in the previous case. For the proof of $\tilde{\mathcal{P}}'(k+1)$(ix) we can argue as before.

Case 4: $X(\tilde\tau_k) \in \mathcal{I}(\ell_1\ell_2+2)$. In this case $k \neq k_0$, so $\tilde n = \tilde n_2 = k$, and there is nothing to prove. This ends our induction.

• **Cost estimates.** To complete the proof of (7.4.8) in the supercritical case, we only need to check the given lower bounds for the cost of each event that compounds Z_2, for which we refer to Appendix 7.B. This concludes case (III). □

7.5.3 *Proof of Lemma 7.4.5*

Recall the definition of the union of events Z_1 and Z_2 in the subcritical case given in (7.5.1) and (7.5.7). We can check that for the escape from $\mathcal{G}_1$ we can argue as in the general case $\ell_2 \geqslant 3$: the cost is given by $c(F_1) \geqslant 2U - \Delta - \alpha - O(\delta)$. For the escape from $\mathcal{G}_2$, again the proof of (7.4.7) shows that $(Z_1 \setminus F_1)^c$ implies that either φ^n does not escape from $\mathcal{G}_1$ or there is a first return time τ_{k_0} such that $X(\tau_{k_0}) \in \mathcal{I}(4)$ and a particle is colored red at time σ_{k_0+1}. Set

$$\bar Z_2 = Z_2 \cup K_1 \cup K_2,$$

where K_1 and K_2 are the following new large deviation events:

K_1 : There are three active particles, which can be green or red, together with one yellow particle in a box of volume $e^{D\beta}$ inside the box $[\bar\Lambda, \Delta+\delta]$ at a same time $t \in [t^*, T_{\Delta^+}e^{\delta\beta}]$ such that $X(t^*) \in \mathcal{I}(0)$ and at time t^* the yellow particle is inside $[\bar\Lambda, D+\delta]$. This event costs at least $\Delta - D + \alpha - O(\delta)$.

K_2 : There are two active particles, which can be green or red, together with two yellow particles in a box of volume $e^{D\beta}$ inside $[\bar\Lambda, \Delta+\delta]$ at a same time $t \in [t^*, T_{\Delta^+}e^{\delta\beta}]$ such that $X(t^*) \in \mathcal{I}(0)$ and at time t^* the two yellow particles are inside $[\bar\Lambda, D+\delta]$. This event costs at least $\Delta - D + \alpha - O(\delta)$.

By defining

$$\bar n = \min\{n, n^*\} \tag{7.5.11}$$

with

$$n^* = \min\{k > k_0 : X(\tau_k) \in \mathcal{I}(4)\} \tag{7.5.12}$$

and

$$\bar\varphi^k = (X(\tau_{k_0}), X(\tau_{k_0+1}), \dots, X(\tau_k)), \qquad k_0 \leqslant k \leqslant \bar n,$$

we will prove by induction that, for all $k_0 \leqslant k \leqslant \bar n$,

Claim $\bar{\mathcal{P}}(k)$. *If $\bar Z_2$ does not occur, then*
(i) $\bar\varphi^k$ does not escape from $\mathcal{G}_2$.
(ii) There are at most three yellow particles at each $t \leqslant \tau_k$.

(iii) If $X(\tau_k) \in \mathcal{I}(4)$*, then at time* τ_k *there is no yellow particle.*
(iv) If $X(\tau_k) \in \mathcal{I}(0)$*, then at time* τ_k *there are three yellow and one red particles in* $[\bar\Lambda, D+\delta]$*, with two yellow particles at distance two from each other.*

Property (i) is the main property we are interested in. We will use properties (ii)–(iv) to control inductively the yellow particles, in particular, property (iii) implies that X reaches $\mathcal{I}(4)$ by putting tosleep all the yellow particles created during the time interval $[\tau_{k_0}, \tau_k]$, while property (iv) implies that $\mathcal{I}(0)$ is reached by breaking a dimer.

$\trianglerighteq$ Before proving $\bar{\mathcal{P}}(k)$, $k_0 \leqslant k \leqslant \bar n$, let us show that $\bar{\mathcal{P}}(\bar n)$ implies in the two cases $\bar n = n$ and $\bar n = n^*$ that if $\bar Z_2^c$ occurs, then φ^n cannot escape from $\mathcal{G}_2$. If $\bar n = n$, then the claim is trivial. If $\bar n = n^*$, then $\bar{\mathcal{P}}(n)$(iii) implies that there is no yellow particle at time τ_{n^*}. Using $\tilde F_1^c$, which excludes any 2^{nd} attribution of the red color, we can show by induction, as in the proof of (7.4.7), that φ^k, for $k \geqslant n^*$, cannot escape anymore from $\mathcal{G}_1$, subgraph of $\mathcal{G}_2$.

• **Proof of $\bar{\mathcal{P}}(k)$, $k_0 \leqslant k \leqslant \bar n$.** $\bar{\mathcal{P}}(k_0)$(i)-(iii) follow from the definition of k_0. Since $X(\tau_{k_0}) \in \mathcal{I}(4)$, we do not need to check $\bar{\mathcal{P}}(k_0)$(iv). For $k \geqslant k_0$ we assume $\bar{\mathcal{P}}(k)$ to prove $\bar{\mathcal{P}}(k+1)$. We distinguish between the two following cases.

Case 1: $X(\tau_k) \in \mathcal{I}(4)$. If $k \neq k_0$, then $\bar n = n^* = k$ and there is nothing to prove. We only have to consider the case $k = k_0$. The definition of σ_{k_0+1} gives $X(\sigma_{k_0+1}) \in \mathcal{I}(3)^{fp}$ with the free particle colored red. Suppose that X does not return to $\mathcal{I}(4)$ within time τ_{k_0+1}. By arguing as in the general case, we deduce that the following moves occur: the red particle exits from $\bar\Lambda$, a particle is detached at cost U and therefore is colored yellow, leading to the configuration $\mathcal{I}(2)^{fp}$. Since we are considering the time interval $[\sigma_{k_0+1}, \tau_{k_0+1}]$ and the times τ_i are return times to $\mathcal{X}_D$, by the recurrence property to $\mathcal{X}_D$ implied by A^c we deduce that no particle can exit from $[\bar\Lambda, D+\delta]$ before time τ_{k_0+1}, in particular, this holds for the red particle. Thus, by the event G'^c, no green particle can enter $[\bar\Lambda, D+\delta]$. Afterwards, the free particle exits from $\bar\Lambda$ and two yellow particles are created after breaking the dimer at time t: X reaches $\mathcal{I}(0)$ at time $t = \tau_{k_0+1}$. By the previous observations it easy to check $\bar{\mathcal{P}}(k_0+1)$(i),(ii),(iv), while we do not need to check $\bar{\mathcal{P}}(k_0+1)$(iii). If X returns in $\mathcal{I}(4)$ at time t, then we have to prove that $t = \tau_{k_0+1}$ because we are analyzing the time interval $[\tau_{k_0}, \tau_{k_0+1}]$. By arguing as in the general case, we deduce that the only possibility, possibly after visiting $\mathcal{I}(2)$ and $\mathcal{I}(3)$ several times, is to reach $\mathcal{X}_D$ in $\mathcal{I}(4)$. Since no particle can enter and exit from $[\bar\Lambda, D+\delta]$ within time τ_{k_0+1}, $\bar{\mathcal{P}}(k_0+1)$(ii),(iii) follow.

Case 2: $X(\tau_k) \in \mathcal{I}(0)$. This part of the proof is directly related to $\bar{\mathcal{P}}(k)$(iv) and the new events K_1 and K_2. Indeed, $\bar{\mathcal{P}}(k)$(iv) gives us control on the distance between the two nearest yellow particles in $[\bar\Lambda, D+\delta]$ and the green particles, which are outside the box $[\bar\Lambda, D+\delta]$ by the event G'^c. By $\bar{\mathcal{P}}(k)$(iv) and the events K_1^c and K_2^c, we deduce that, if a cluster is formed, then it has to be created by attaching the three yellow particles together with one red or green particle, so $X(\tau_{k+1}) \in \mathcal{I}(4)$ and properties (ii) and (iii) follow. The claim follows after checking the given cost estimate for the events K_1 and K_2, for which we refer to Appendix 7.B. □

7.5.4 *Proof of Lemma 7.5.1*

Let us assume that $T^{ij} \leqslant T_{\Delta^+} e^{\delta\beta}$ and there is no such time $t \leqslant T^{ij}$ with three active particles inside $[\bar\Lambda, D+\delta]$. Since at time $t = 0$ either both particles i and j belong to a same unique cluster in $\bar\Lambda$ or at least one is outside $[\bar\Lambda, D+\delta]$, by setting

$$\mathcal{T}_0 = \sup\{t \leqslant T^{ij} : \text{ i or j is outside } [\bar\Lambda, D+\delta] \text{ or both are in a same unique cluster in } \bar\Lambda \text{ at time } t\},$$

we see that $0 \leqslant \mathcal{T}_0 \leqslant T^{ij}$. We distinguish between two cases.

(i) If there are no active particles, but i or j are inside $[\bar\Lambda, D+\delta]$ during the whole time interval $[\mathcal{T}_0, T^{ij}]$, then $\mathcal{T}_0$ is the last θ_k^{ij} before T^{ij}.
(ii) If there is some other active particle inside $[\bar\Lambda, D+\delta]$ at some time t in $[\mathcal{T}_0, T^{ij}]$, then we set

$$\mathcal{T}_1 = \sup\{t \leqslant T^{ij} : \text{ there is an active particle distinct from i and j inside } [\bar\Lambda, D+\delta] \text{ at time } t\}.$$

Since we assumed that there is no time $t \leqslant T^{ij}$ at which three active particles are inside $[\bar{\Lambda}, D+\delta]$, i or j must be sleeping at time $\mathcal{T}_1$ and $\mathcal{T}_1 \leqslant T^{ij}$. $\mathcal{T}_1$ is then the last θ_k^{ij} before T^{ij}.

In both cases there is a last $\theta_k^{ij} \geqslant 0$ before T^{ij} such that any active particle in $[\bar{\Lambda}, D+\delta]$ during the time interval $[\theta_k^{ij}, T^{ij}]$ is either i or j. □

7.5.5 *Proof of Lemma 7.5.2*

We prove the claim by contradiction. Assume that $X(\tilde{\tau}_k) \notin \mathcal{X}_U$ andthat there is a $t \in [\tilde{\tau}_k, \tilde{\sigma}_{k+1})$ such that $X(t) \in \mathcal{X}_U$. Then there is a constant-cluster-size path from $\bar{X}(t)$ to the isoperimetric configuration $\bar{X}(\tilde{\tau}_k)$. By the recurrence property to $\mathcal{X}_U$ implied by A^c, we may also assume that $t - \tilde{\tau}_k \leqslant T_U e^{\delta\beta}$. Then $\tilde{D}^c$ implies that the local energy along this path does not exceed $\bar{H}(X(\tilde{\tau}_k)) + U$. Since $\bar{X}(\tilde{\tau}_k)$ is isoperimetric, we also have $\bar{H}(X(t)) \geqslant \bar{H}(X(\tilde{\tau}_k))$. Since $\bar{X}(\tilde{\tau}_k)$ is U-reducible, we get a contradiction with the fact that $\bar{X}(t)$ is U-irreducible. □

APPENDIX

7.A ENVIRONMENT ESTIMATES

In this appendix we prove that $\mu_{\mathcal{R}'}((\mathcal{X}_i^*)^c) = \mathrm{SES}(\beta)$ for $i = 1, \dots, 5$, where, for $\eta \in \mathcal{X}_\beta$,

$$\mu_{\mathcal{R}'}(\eta) = \frac{e^{-\beta[H(\eta)+\Delta|\eta|]}}{Z_{\mathcal{R}'}} \mathbb{1}_{\mathcal{R}'}(\eta), \qquad Z_{\mathcal{R}'} = \sum_{\eta \in \mathcal{R}'} e^{-\beta[H(\eta)+\Delta|\eta|]}.$$

First, we consider the case $\Delta < \Theta \leqslant \theta$. Given a configuration $\eta \in \mathcal{X}_\beta$, we denote by $\mathcal{C} = \mathcal{C}(\eta)$ its connected component with maximal volume when it is unique. Otherwise, we pick the component containing the highest particle in the lexicographic order. For $C \subset \Lambda_\beta$, we set $\bar{C} = C \cup \partial^+ C$, where $\partial^+ C$ denotes the external boundary of C. We start by showing that there exists a $c > 0$ such that

$$\mu_{\mathcal{R}'}(\mathcal{X}_\beta \setminus \mathcal{X}_i^*) \leqslant e^{c\beta} \mu_{\mathcal{R}}(\mathcal{X}_\beta \setminus \mathcal{X}_i^*).$$

To this end, given a finite set $\Lambda \subset \Lambda_\beta$ and two configurations $\eta_\Lambda \in \{0,1\}^\Lambda$ and $\eta_{\Lambda_\beta \setminus \Lambda} \in \{0,1\}^{\Lambda_\beta \setminus \Lambda}$, we denote by $\eta = \eta_\Lambda \cdot \eta_{\Lambda_\beta \setminus \Lambda} \in \{0,1\}^{\Lambda_\beta}$ the configuration defined by

$$\eta(x) = \begin{cases} \eta_\Lambda(x) & \text{if } x \in \Lambda, \\ \eta_{\Lambda_\beta \setminus \Lambda}(x) & \text{if } x \in \Lambda_\beta \setminus \Lambda. \end{cases}$$

Given a configuration $\sigma \in \{0,1\}^{\Lambda_\beta}$, we introduce the measure $\mu_{\mathcal{R},\Lambda,\sigma}$ on $\{0,1\}^\Lambda$ defined by

$$\mu_{\mathcal{R},\Lambda,\sigma}(\eta_\Lambda) = \frac{1}{Z_{\mathcal{R},\Lambda,\sigma}} e^{-\beta[H(\eta_\Lambda \cdot \sigma_{\Lambda_\beta \setminus \Lambda}) + \Delta(|\eta_\Lambda| + |\sigma_{\Lambda_\beta \setminus \Lambda}|)]} \mathbb{1}_{\mathcal{R}}(\eta_\Lambda \cdot \sigma_{\Lambda_\beta \setminus \Lambda}),$$

where $Z_{\mathcal{R},\Lambda,\sigma}$ is the normalizing constant. For any finite $\Lambda \subset \Lambda_\beta$ and any configuration $\eta \in \{0,1\}^{\Lambda_\beta}$, the DLR equation for the measure $\mu_{\mathcal{R}}$ reads

$$\mu_{\mathcal{R}}(\eta) = \sum_{\sigma \in \Lambda_\beta} \mu_{\mathcal{R}}(\sigma) \mu_{\mathcal{R},\Lambda,\sigma}(\eta_{|\Lambda}).$$

Since a cluster with volume at most $\lambda(\beta)/8$ has perimeter at most $\lambda(\beta)$, and therefore is contained in a box of volume $\lambda^2(\beta)$, it can be arranged inside Λ_β in at most $2^{\lambda^2(\beta)}$ different ways and in at most $e^{\Theta\beta}$ different location. Hence

$$\begin{aligned}\mu_{\mathcal{R}'}(\mathcal{X}_\beta \setminus \mathcal{X}_i^*) &= \frac{\sum_{\eta\in\mathcal{R}'\setminus\mathcal{X}_i^*} e^{-\beta[H(\eta)+\Delta|\eta|]}}{\sum_{\eta\in\mathcal{R}'} e^{-\beta[H(\eta)+\Delta|\eta|]}} \leqslant \sum_{\substack{C\subset\Lambda_\beta\\ |C|\leqslant\lambda^2(\beta)}} \frac{\sum_{\substack{\eta\in\mathcal{R}'\setminus\mathcal{X}_i^*\\ \mathcal{C}=C}} e^{-\beta[H(\eta)+\Delta|\eta|]}}{\sum_{\substack{\eta\in\mathcal{R}'\\ \mathcal{C}=C}} e^{-\beta[H(\eta)+\Delta|\eta|]}}\\ &\leqslant \sum_{\substack{C\subset\Lambda_\beta\\ |C|\leqslant\lambda^2(\beta)}} \frac{e^{-\beta[H(C)+\Delta|C|]}\sum_{\eta\in\mathcal{R}\setminus\mathcal{X}_i^*} e^{-\beta[H(\eta)+\Delta|\eta|]}}{e^{-\beta[H(C)+\Delta|C|]}\sum_{\substack{\eta\in\mathcal{R}\\ |\eta_{|\bar{C}}|=0}} e^{-\beta[H(\eta)+\Delta|\eta|]}}\\ &\leqslant 2^{\lambda^2(\beta)}e^{\Theta\beta}\frac{\mu_{\mathcal{R}}(\mathcal{X}_\beta\setminus\mathcal{X}_i^*)}{\min_{\substack{C\subset\Lambda_\beta\\ |C|\leqslant\lambda^2(\beta)}}\frac{1}{Z_{\mathcal{R}}}\sum_{\substack{\eta\in\mathcal{R}\\ |\eta_{|\bar{C}}|=0}} e^{-\beta[H(\eta)+\Delta|\eta|]}} \leqslant e^{c\beta}\mu_{\mathcal{R}(\mathcal{X}_\beta\setminus\mathcal{X}_i^*)},\end{aligned}$$

where in the last step we use the DLR equation and the fact that, for any configuration $\eta\in\mathcal{R}$, the probability of having $|\eta_{|\bar{C}}|=0$ is at least $1-e^{-(\Delta-\delta)\beta}$ for any $\delta>0$ and β large enough, uniformly in the boundary conditions.

• $\underline{i=1}$. Recall that, for $\eta\in\mathcal{X}_\beta$, η^{cl} is the union of the connected components of size at least two, so that $|\eta\setminus\eta^{cl}|$ denotes the number of connected components that are reduced to single particles. We get

$$\begin{aligned}\mu_{\mathcal{R}}(\mathcal{X}_\beta\setminus\mathcal{X}_1^*) &\leqslant \frac{1}{Z_{\mathcal{R}}}\sum_{k=0}^{e^{\theta\beta}}\sum_{\substack{\eta\in\mathcal{R}\setminus\mathcal{X}_1^*\\ |\eta\setminus\eta^{cl}|=k}} e^{-\beta[H(\eta)+\Delta|\eta|]} \qquad (7.A.1)\\ &\leqslant \frac{1}{Z_{\mathcal{R}}}\left(e^{-(2\Delta-U)\beta}e^{\theta\beta}\right)^{\lambda(\beta)}\sum_{k=0}^{e^{\theta\beta}}\sum_{\substack{\eta\in\mathcal{R}\\ \eta^{cl}=\emptyset,|\eta|=k}} e^{-\beta[H(\eta)+\Delta|\eta|]}\\ &\leqslant \frac{Z_{\mathcal{R}}}{Z_{\mathcal{R}}}e^{-(2\Delta-U-\theta)\beta\lambda(\beta)} = \mathrm{SES}(\beta),\end{aligned}$$

where we use that $\theta<2\Delta-U$.

• $\underline{i=2}$. Note that $\mathcal{X}_\beta\setminus\mathcal{X}_2^*$ implies that the number of disjoint quadruples of particles with diameter smaller than $\sqrt{e^{S\beta}}$ is at least $(\lambda^{1/4}(\beta))/4$. Given $k=\lambda^{1/4}(\beta)/4$ and a collection $x=(x_i^j)_{i<4,j<k}\in\Lambda_\beta^{4\times k}$, we define the set

$$\Lambda_x=\bigcup_{\substack{i<4\\ j<k}} B(x_i^j,\ell_c^2).$$

Using the DLR equation, we obtain

$$\begin{aligned}\mu_{\mathcal{R}}(\mathcal{X}_\beta\setminus\mathcal{X}_2^*) \leqslant \sum_{\substack{x_0^0,\dots,x_3^0\in\Lambda_\beta\\ \mathrm{diam}\{x_i^0,i<4\}<e^{S\beta/2}}}\cdots\sum_{\substack{x_0^{k-1},\dots,x_3^{k-1}\in\Lambda_\beta\\ \mathrm{diam}\{x_i^{k-1},i<4\}<e^{S\beta/2}}}\\ \sum_{\sigma\in\{0,1\}^{\Lambda_\beta}}\mu_{\mathcal{R}}(\sigma)\mu_{\mathcal{R},\Lambda_x,\sigma}\begin{pmatrix}\text{the sites in } x\\ \text{are occupied}\end{pmatrix} \leqslant \left(e^{(3S-4\Delta+\theta)\beta}\right)^{\frac{\lambda^{1/4}(\beta)}{4}} = \mathrm{SES}(\beta),\end{aligned}$$

where $S=\frac{4\Delta-\theta}{3}-\alpha$.

• $\underline{i=3}$. Let $S < A < \Delta$ and divide the box Λ_β into $e^{(3A-4\Delta+\Theta+3\alpha)\beta}$ boxes of volume $e^{(4\Delta-3A-3\alpha)\beta}$. Note that $\mathcal{X}_\beta \setminus \mathcal{X}_3^*$ implies that there exists one box containing at least $(e^{\alpha\beta/4})/4$ disjoint quadruples of particles with diameter smaller than $\sqrt{e^{A\beta}}$. Using the DLR equation and arguing as above, we get

$$\begin{aligned}\mu_{\mathcal{R}}(\mathcal{X}_\beta \setminus \mathcal{X}_3^*) &\leqslant e^{(3A-4\Delta+\Theta+3\alpha)\beta}\Big(e^{-4\Delta\beta}e^{(4\Delta-3A-3\alpha)\beta}\prod_{i=1}^{3}(e^{A\beta}-5i)\Big)^{\frac{e^{\frac{\alpha\beta}{4}}}{4}}\\ &\leqslant e^{(3A-4\Delta+\theta+3\alpha)\beta}e^{-\frac{3}{4}\alpha\beta e^{\frac{\alpha\beta}{4}}} = \mathrm{SES}(\beta).\end{aligned}$$

• $\underline{i=4}$. Note that $\mathcal{X}_\beta \setminus \mathcal{X}_4^*$ implies that there exists a box of volume $e^{(\Delta+\alpha)\beta}$ containing either at least $e^{\frac{3}{2}\alpha\beta}$ or at most $e^{\frac{1}{2}\alpha\beta}$ particles. We consider these cases separately. Concerning the former case, by dividing the box of volume $e^{(\Delta+\alpha)\beta}$ into $e^{\frac{5}{4}\alpha\beta}$ boxes of volume $e^{(\Delta-\frac{\alpha}{4})\beta}$, we have that there exists a box containing at least $e^{\frac{\alpha}{4}\beta}$ particles. Concerning the latter case, by dividing the box of volume $e^{(\Delta+\alpha)\beta}$ into $e^{\frac{\alpha}{2}\beta}$ boxes of volume $e^{(\Delta+\frac{\alpha}{2})\beta}$, we have that there exists a box containing no particle. We proceed to estimate the denominator in this latter case by considering all the configurations with one particle in each box of volume $e^{(\Delta+\frac{\alpha}{4})\beta}$ inside a box of volume $e^{(\Delta+\frac{\alpha}{2})\beta}$, namely, these boxes are $e^{\frac{\alpha}{4}\beta}$. Using the DLR equation and arguing as above, we get

$$\mu_{\mathcal{R}}(\mathcal{X}_\beta \setminus \mathcal{X}_4^*) \leqslant e^{\frac{5}{4}\alpha\beta}\Big(e^{-\Delta\beta}e^{(\Delta-\frac{\alpha}{4}\beta)}\Big)^{e^{\frac{\alpha}{4}\beta}} + e^{\frac{\alpha}{2}\beta}\frac{1}{\Big(e^{-\Delta\beta}e^{(\Delta+\frac{\alpha}{4})\beta}\Big)^{e^{\frac{\alpha}{4}\beta}}} = \mathrm{SES}(\beta).$$

• $\underline{i=5}$. Using the DLR equation and arguing as above, we get

$$\mu_{\mathcal{R}}(\mathcal{X}_\beta \setminus \mathcal{X}_5^*) \leqslant e^{-\Delta\beta\frac{\lambda(\beta)}{4}}\prod_{i<\frac{\lambda(\beta)}{4}}(e^{(\Delta-\frac{\alpha}{4})\beta}-5i) \leqslant e^{-\frac{\alpha}{4}\beta\frac{\lambda(\beta)}{4}} = \mathrm{SES}(\beta).$$

To conclude, consider the case $\Theta > \theta$. Dividing Λ_β into boxes of volume $e^{\theta\beta}$ and arguing as above with the help of the DLR equation, we get the claim.

7.B COST OF LARGE DEVIATION EVENTS

Event A. The cost of event A follows from Proposition 7.2.11 and [62, Theorem 3.2.3].

Event B. Each special time except τ_k is related to a free particle that moves in $\bar{\Lambda}$, but the number of special times τ_k is equal to the one of σ_k by definition. The claim follows after arguing as in the proof of Proposition 7.3.1: at each special time each free particle has a non exponentially small probability to avoid the box after leaving it, so that it visits this box $e^{\delta\beta}$ times with a super-exponentially small probability. Since, by non-superdiffusivity, the special times are associated with no more than $e^{(3\alpha/2+\delta)\beta}$ particles up to a $\mathrm{SES}(\beta)$-event, B occurs with probability $1-\mathrm{SES}(\beta)$.

Event C. Let K denote the number of special times. By the event B, we have $K \leqslant e^{\delta\beta}$ with probability $1-\mathrm{SES}(\beta)$. Let $S_0,\dots,S_{K-1}$ be the special times. Divide the time interval $[0, T_{\Delta^+}e^{\delta\beta}]$ into intervals $[t_i, t_i+e^{\delta\beta}]$ of length $e^{\delta\beta}$, with $1 \leqslant i < e^{(\Delta+\alpha)\beta}$. Introduce the following events: $C_1^i = \{\exists j \in \{0,\dots,K-1\}$ such that $S_j \in [t_i, t_i+e^{\delta\beta}]\}$ and $C_2^i = \{$there is a move of cost $\geqslant U$ in $[S_j, t_i+e^{\delta\beta}]\}$. Using the strong Markov property at the stopping time S_j, we obtain

$$P(C) \leqslant \sum_{i<e^{(\Delta+\alpha)\beta}} P(C_2^i|C_1^i)P(C_1^i) \leqslant e^{-U\beta}e^{\delta\beta}\sum_{i<e^{(\Delta+\alpha)\beta}} P(C_1^i) \leqslant e^{-U\beta}e^{O(\delta)\beta}$$

and therefore $c(C) \geqslant U - O(\delta)$.

Event C′. We control the cost of this event as for the event C by using, instead of the strong Markov property, the independence of the dynamics of particles outside $\bar{\Lambda}$ from the marks used in $\bar{\Lambda}$.

Event D. Divide the time interval $[0, T_{\Delta^+}e^{\delta\beta}]$ into intervals $[t_i, t_i + e^{D\beta}]$ of length $e^{D\beta}$, with $1 \leqslant i < e^{(\Delta+\alpha-D)\beta}e^{\delta\beta}$ and argue as for the event C.

Event D′. Divide the time interval $[0, T_{\Delta^+}e^{\delta\beta}]$ into intervals $[t_i, t_i + e^{D\beta}]$ of length $e^{D\beta}$, with $1 \leqslant i < e^{(\Delta+\alpha-D)\beta}e^{\delta\beta}$ and argue as for the event C.

Event E. Divide the time interval $[0, T_{\Delta^+}e^{\delta\beta}]$ into intervals $[t_i, t_i + e^{\delta\beta}]$ of length $e^{\delta\beta}$, with $1 \leqslant i < e^{(\Delta+\alpha)\beta}$. For t_1, t_2 and $k = |\bar\eta_0|$ fixed, by defining $\bar{\mathcal{X}}_k = \{\bar\eta \in \{0,1\}^{\bar\Lambda} \mid |\bar\eta| = k\}$ and using the reversibility of the measure μ, we obtain

$$\begin{aligned} P_{\eta_0}(\bar H(\bar X(t_2 - t_1)) \geqslant \bar H(\bar X(\bar\eta_0)) + 3U) &\leqslant P_{\bar\eta_0}(\bar H(\bar X(t_2 - t_1)) \geqslant \bar H(\bar X(\bar\eta_0)) + 3U) \\ &\leqslant e^{-3U\beta} \sum_{\substack{\bar\eta \in \bar{\mathcal{X}}_k \\ H(\bar\eta) \geqslant H(\bar\eta_0)+3U}} P_\eta(\bar X^k(t) = \bar\eta_0) \leqslant e^{-3U\beta}e^{\delta\beta}. \end{aligned}$$

Because the temporal entropy is $e^{\delta\beta}$ for t_1 and Δ^+ for t_2, we get follows $c(E) \geqslant 3U - \Delta - \alpha - O(\delta)$.

Event F_{m+1}. Divide the time interval $[0, T_{\Delta^+}e^{\delta\beta}]$ into intervals $[t_i, t_i + e^{D\beta}]$ of length $e^{D\beta}$, with $1 \leqslant i < e^{(\Delta+\alpha-D)\beta}e^{\delta\beta}$. First consider the event F_1, to obtain

$$\begin{aligned} P(F_1) &\leqslant \sum_{1\leqslant i<e^{(\Delta+\alpha-D)\beta}e^{\delta\beta}} \Big[P(\text{move of cost } 2U \text{ in } [s_i, s_i + e^{D\beta}]) + P(\text{move of cost } U \\ &\qquad \text{at time } t \in [s_i, s_i + e^{D\beta}] \text{ and at time } t' \text{ such that } t < t' \text{ are } \delta\text{-close})\Big] \\ &\leqslant e^{(\Delta+\alpha-2U)\beta}e^{O(\delta)\beta}, \end{aligned}$$

which implies $c(F_1) \geqslant 2U - \Delta - \alpha - O(\delta)$. We can easily compute the cost of the event F_{m+1} by applying the strong Markov property at the stopping times related to each attribution of the red color.

Event H_2. Divide the time interval $[0, T_{\Delta^+}e^{\delta\beta}]$ into intervals $[t_i, t_i + e^{D\beta}]$ of length $e^{D\beta}$, with $1 \leqslant i < e^{(\Delta+\alpha-D)\beta}e^{\delta\beta}$. We obtain

$$\begin{aligned} P(H_2) &\leqslant \sum_{1\leqslant i<e^{(\Delta+\alpha-D)\beta}e^{\delta\beta}} P(\text{there are 2 green particles in } [\bar\Lambda, D + 2\delta] \text{ at time } (i+1)e^{D\beta}) \\ &\leqslant \sum_{1\leqslant i<e^{(\Delta+\alpha-D)\beta}e^{\delta\beta}} \left(\frac{e^{(D+2\delta)\beta}e^{\delta\beta}}{e^{(\Delta+\alpha)\beta}}\right)^2 \leqslant e^{(D-\Delta-\alpha)\beta}e^{O(\delta)\beta}, \end{aligned}$$

which implies $c(H_2) \geqslant \Delta - D + \alpha - O(\delta)$. Note that we use the spread-out property on time scale T_{Δ^+} for the green particle because this cannot reach $[\bar\Lambda, D + 2\delta]$ on time scale $e^{D\beta}$.

Event G. For a particle i that is colored red at time S_j, applying the spread-out property and the strong Markov property at time S_j, we get

$$\begin{aligned} P(\xi_i(t) \in [\bar\Lambda, D + \delta]) &\leqslant \mathbb{E}\Big[\frac{e^{(D+\delta)\beta}}{t - S_j} \wedge 1\Big] \leqslant e^{O(\delta)\beta}\int_0^t ds\, e^{-2U\beta}\Big(\frac{e^{D\beta}}{t-s} \wedge 1\Big) \\ &\leqslant e^{-(2U-D-O(\delta))\beta}. \end{aligned}$$

Dividing the time interval $[0, T_{\Delta^+}e^{\delta\beta}]$ into intervals $[t_i, t_i + e^{D\beta}]$ of length $e^{D\beta}$, with $1 \leqslant i < e^{(\Delta+\alpha-D)\beta}e^{\delta\beta}$, we get $c(G) \geqslant U - d + \varepsilon - \alpha - O(\delta)$.

Event G′. Divide the time interval $[0, T_{\Delta^+}e^{\delta\beta}]$ into intervals $[t_i, t_i + e^{D\beta}]$ of length $e^{D\beta}$, with $1 \leqslant i < e^{(\Delta+\alpha-D)\beta}e^{\delta\beta}$. Arguing as for the events H_2 and G, we deduce that $c(G') \geqslant U - d - \alpha - O(\delta)$.

Event G_4'. In case the four particles do not come from a cluster, namely, at time $t = 0$ they are outside the box $[\bar\Lambda, \Delta - \alpha]$, the cost of this event has already been computed in (7.2.11). Consider the case in which the four particles come from a cluster. In particular, we consider the case in which all four particles are green, otherwise the cost of the event is larger. Dividing

Λ_β into boxes of volume $e^{(D+\delta)\beta}$ and the time interval $[0, T_{\Delta^+} e^{\delta\beta}]$ into intervals of length $e^{D\beta}$, we obtain

$$P(G_4') \leqslant \sum_{i<e^{(\theta-D-\delta)\beta}} \sum_{j<e^{(\Delta+\alpha-D+\delta)\beta}} \Big(\frac{e^{(D+\delta)\beta} e^{\delta\beta}}{e^{(\Delta+\alpha)\beta}}\Big)^4 \leqslant e^{-(3\Delta-2U-\theta+3\alpha-2d)\beta} e^{O(\delta)\beta},$$

where we use the spread-out property on time scale $e^{(\Delta+\alpha)\beta}$, because particles cannot be colored green on a shorter time scale. The cases in which there is at least one green particle and one particle not coming from a cluster can be treated in a similar way.

Event $\tilde{B}$. The cost of this event can be computed similarly as the cost of the event B.

Event $\tilde{C}$. The cost of this event can be computed similarly as the cost of the event C.

Event G_3'. We only need to consider the case concerning the presence of one yellow particle from a cluster, otherwise we reduce to a case already taken into account by G_4'. We can argue in a similar way as for the event G_4'.

Event $\tilde{D}$. The cost of this event can be computed similarly as the cost of the event D.

Event $\tilde{F}_{m+1}$. We need to estimate the cost of the occurrence of one of the events J^{ij}. By Proposition 7.2.6 and the event B^c, we have $P(\cup_{i,j} J^{ij}) \leqslant e^{O(\delta)\beta} P(J^{ij})$. In order to estimate the probability that one of the events J^{ij} occurs, we need the following observations:

(i) If the particles i and j are both free in $\bar{\Lambda}$, then the cluster cannot move. Indeed, an $(m+2)^{th}$ attribution of the red color is not allowed.

(ii) In the time intervals in which the particles i and j are both free in $\bar{\Lambda}$, they evolve as independent random walks with simultaneous stops.

Suppose that the cluster does not move via interactions with the free particles. The dynamics of the $\ell_1'\ell_2' + 2$ particles can be seen as the dynamics of two independent simple random walks $\xi = (\xi_t)_{t\geqslant 0}$ and $\xi' = (\xi_t')_{t\geqslant 0}$ with a trap at the origin: the jump rate is $4e^{-U\beta}$ at the origin and 4 at the other sites, towards a nearest-neighbor site chosen uniformly at random. Thus it suffices to prove that, if at least one particle starts either in the origin or at distance $e^{(D+\delta)\beta}$ from the origin, then

$$P(\exists t \leqslant T_{\Delta^+} e^{\delta\beta},\ \xi_t, \xi_t' \in \bar{\Lambda} \setminus \{0\}) \leqslant e^{-\frac{1}{2}(2U-\Delta-\alpha-O(\delta))\beta}. \tag{7.B.1}$$

To this end, note that we can associate to ξ a simple random walk $\tilde{\xi} = (\tilde{\xi}_t)_{t\geqslant 0}$ during every time interval in which $\xi_t \notin 0$. Denoting $s(t) = \max\{s \leqslant t |\ \xi_s = 0\}$ for $t \leqslant T_{\Delta^+} e^{\delta\beta}$, we obtain

$$\begin{aligned} P_0(\xi_t \in \bar{\Lambda} \setminus \{0\}) &= \sum_{x\in\bar{\Lambda}\setminus\{0\}} P_0(\xi_t = x) = \sum_{x\in\bar{\Lambda}\setminus\{0\}} \int_0^t P_0(s(t) \in ds, \xi_t = x) \\ &\leqslant \sum_{x\in\bar{\Lambda}\setminus\{0\}} \int_0^t ds\, 4e^{-U\beta} P_0(\tilde{\xi}_{t-s} = x) \leqslant \sum_{x\in\bar{\Lambda}\setminus\{0\}} \int_0^t ds\, 4e^{-U\beta} \Big(\frac{cst}{1+t-s}\Big) \\ &\leqslant C|\bar{\Lambda}|(\log t + 1)e^{-U\beta} \leqslant C|\bar{\Lambda}|((\Delta+\alpha+\delta)\beta + 1)e^{-U\beta}. \end{aligned} \tag{7.B.2}$$

Hence, by (7.B.2),

$$P_{(0,0)}(\exists t \leqslant T_{\Delta^+} e^{\delta\beta},\ \xi_t, \xi_t' \in \bar{\Lambda} \setminus \{0\}) \leqslant \int_0^{T_{\Delta^+} e^{\delta\beta}} dt\, P_0(\xi_t \in \bar{\Lambda} \setminus \{0\})^2 \leqslant e^{(\Delta+\alpha-2U)\beta} e^{O(\delta)\beta}.$$

Suppose that $x \in [\bar{\Lambda}, D+\delta] \setminus \{0\}$. Letting τ the first time at which a particle detaches from the origin and τ_0' the first time at which ξ' reaches the origin, we get

$$\begin{aligned} P_{(0,x)}(\exists t \leqslant T_\Delta e^{\delta\beta},\ \xi_t, \xi_t' \in \bar{\Lambda} \setminus \{0\}) &\leqslant \int_0^{T_{\Delta^+} e^{\delta\beta}} dt\, P_{(0,0)}(\xi_t, \xi_t' \in \bar{\Lambda} \setminus \{0\}) \\ &\quad + \int_0^{T_{\Delta^+} e^{\delta\beta}} dt\, P_{(0,x)}(\xi_t, \xi_t' \in \bar{\Lambda} \setminus \{0\}, \tau_0' > \tau). \end{aligned}$$

To prove (7.B.1), by the non-superdiffusivity property we can bound the second integral from above as

$$\int_0^{T_{\Delta^+}e^{\delta\beta}} dt \int_0^t ds\, e^{-u\beta} e^{-se^{-u\beta}} P_1(\xi_{t-s} \in \bar{\Lambda}\setminus\{0\}) \sum_{y\in B(x,\sqrt{s}e^{\delta\beta})\setminus\{0\}} \frac{cst}{1+s} P_y(\xi'_{t-s} \in \bar{\Lambda}\setminus\{0\}).$$

Dividing the integral from 0 to t into the integral from 0 to $e^{(u-\frac{1}{2}(\varepsilon-\alpha))\beta}$ and from $e^{(u-\frac{1}{2}(\varepsilon-\alpha))\beta}$ to t, we obtain the desired lower bound. Indeed, the former integral gives $e^{(\Delta+\alpha)\beta}(e^{-u\beta}/e^{(u-\frac{1}{2}(\varepsilon-\alpha))\beta}) = e^{-\frac{1}{2}(\varepsilon-\alpha)\beta}e^{O(\delta)\beta}$ as upper bound, while the second integral gives $e^{-(\varepsilon-\alpha)\beta}e^{O(\delta)\beta}$ as upper bound arguing as in (7.B.2). This concludes the proof of (7.B.1).

It remains to consider the case in which the cluster can move after interacting with the free particles. We observe that if each time the cluster moves we translate it to the origin, then it remains fixed during the whole time interval and there is a resulting perturbation to the remaining free particle. By arguing as before, we get the same result.

Event H_3. We can argue as for the event H_2.

Event H'_3. Divide the time interval $[0, T_{\Delta^+}e^{\delta\beta}]$ into intervals $[t_i, t_i + e^{D\beta}]$ of length $e^{D\beta}$, with $1 \leqslant i < e^{(\Delta+\alpha-D)\beta}e^{\delta\beta}$. If H'_3 occurs, then there are two possible situations: either the two different pairs of green particles are (l,j) and (r,k) with $j \neq k$, which we refer to as $H'_3{}^1$, or (l,j) and (l,k) with l,j,r,k are all different from each other, which we refer to as $H'_3{}^2$. Using an argument similar to the one used for the event H_2, we obtain

$$\begin{aligned} P(H'_3{}^1) &\leqslant e^{2D\beta}e^{-2(\Delta+\alpha)}e^{O(\delta)\beta}, \\ P(H'_3{}^2) &\leqslant e^{2D\beta}e^{-2(\Delta+\alpha)}e^{O(\delta)\beta}, \end{aligned}$$

which imply that $c(H'_3) \geqslant 2(\Delta - D + \alpha) - O(\delta)$.

Event I. We can argue as for the event $\tilde{F}_{m+1}$.

Event $\tilde{H}_2$ We have $c(\tilde{H}_2) = \min\{c(H_3), c(H'_3), c(I)\} \geqslant u - \frac{1}{2}\varepsilon - \frac{3}{2}\alpha - d - O(\delta)$.

Event K_1 Use time scale $e^{(\Delta+\alpha)\beta}$ for the green particles, because of the condition on $\mathcal{X}_{\Delta^+}$ and the fact that the yellow particle is inside the box $[\bar{\Lambda}, D+\delta]$. Using the spread-out property for green/red and yellow particles, we obtain

$$\begin{aligned} P(K_1 \cap G'^c \cap H_2^c) &\leqslant \sum_{t^* \leqslant ie^{D\beta} \leqslant e^{(\Delta+\alpha+\delta)\beta}} \sum_{j<i} \left(\frac{e^{D\beta}e^{\delta\beta}}{e^{(\Delta+\alpha)\beta}}\right)^3 \left(\frac{e^{D\beta}e^{\delta\beta}}{(i+1)e^{D\beta}}\right) \\ &\leqslant e^{(2(D-\Delta)-2\alpha)\beta}e^{O(\delta)\beta}. \end{aligned}$$

This implies that

$$P(K_1) \leqslant P(K_1 \cap G'^c \cap H_2^c) + P(H_2)e^{\delta\beta} \leqslant e^{-(\Delta-D+\alpha-O(\delta))\beta}$$

and therefore $c(K_1) \geqslant \Delta - D + \alpha - O(\delta)$.

Event K_2. We argue as for the event K_1.

Part III

GLAUBER DYNAMICS

8

ISING MODEL ON CLUSTERED NETWORKS

In this chapter we study opinion dynamics on networks with a nontrivial community structure, assuming individuals can update their binary opinion as the result of the interactions with an external influence with strength $h \in [0, 1]$ and with other individuals in the network. To model such dynamics, we consider the Ising model with an external magnetic field on a family of finite networks with a clustered structure. Assuming a unit strength for the interactions inside each community, we assume that the strength of interaction across different communities is described by a scalar $\varepsilon \in [-1, 1]$, which allows a weaker but possibly antagonistic effect between communities. We are interested in the stochastic evolution of this system described by a Glauber-type dynamics parameterized by the inverse temperature β. We focus on the low-temperature regime $\beta \to \infty$, in which homogeneous opinion patterns prevail and, as such, it takes the network a long time to fully change opinion. We investigate the different metastable and stable states of this opinion dynamics model and how they depend on the values of the parameters ε and h. More precisely, using the framework of the pathwise approach [85, 92], we derive rigorous estimates in probability, expectation, and law for the first hitting time between metastable (or stable) states and (other) stable states, together with tight bounds on the mixing time and spectral gap of the Markov chain describing the network dynamics. Lastly, we provide a full characterization of the critical configurations for the dynamics, i.e., those which are visited with high probability along the transitions of interest.

This chapter is structured as follows. In Section 8.1, we outline the main results for the transition time and the critical configurations for the dynamics and we present some preliminary results concerning the energy of the configurations. In Section 8.2, we prove the main results in absence of a external magnetic field, whereas Section 8.3 is devoted to the proofs for the case of a positive external magnetic field.

8.1 MAIN RESULTS AND PRELIMINARIES

For all values of the external magnetic field $h \in [0, 1]$, the considered Ising model exhibits a metastable behavior. In this section, we state our main results, which concern the analysis of the transition either from a metastable to a stable state, or between two stable states, and the description of the corresponding critical configurations (see Section 3.1.1 for the precise definitions of a stable state and a metastable state).

Throughout this chapter we refer to the model–independent definitions and notations of Section 3.1.1, since we can simply adapt them to Glauber dynamics by replacing the Hamiltonian $\widehat{H}$ with $\widetilde{H}$ defined in (1.4.4). The *energy landscape* we consider in this chapter is therefore a 4–tuple $(\mathcal{X}, \Omega, \widetilde{H}, \Delta)$, where $\mathcal{X}$ is the state space, $\Omega \subset \mathcal{X} \times \mathcal{X}$ is the connectivity relation defined in (1.4.2), $\widetilde{H}$ is the energy function defined in (1.4.4), and the *cost function* $\Delta : \Omega \to \mathbb{R}^+$ is defined as $\Delta(x, y) := [\widetilde{H}(y) - \widetilde{H}(x)]_+$.

In Section 8.1.1, we state our main results for the case $h = 0$, while in Section 8.1.2 those for the case $h > 0$. Our results concern the asymptotic behavior of the transition times between metastable and stable configurations in the limit as $\beta \to \infty$, as well as the identification of the *gate* of critical configurations (cf. point 4 in Section 3.1.1 for the precise definition).

8.1.1 *Case* $h = 0$

In this section we focus on the case $h = 0$, namely there is no external magnetic field. The first result we provide is the identification of metastable and stable states, which is the subject of the following theorem.

Theorem 8.1.1 (Stable and metastable states). *Let $(\mathcal{X}, Q, \widetilde{H}, \Delta)$ be the energy landscape corresponding to the Ising model on $\mathcal{G}(2, n)$. Then, the lowest possible energy is equal to*

$$\min_{\sigma\in\mathcal{X}} \widetilde{H}(\sigma) = -n^2 + n - |\varepsilon|n. \tag{8.1.1}$$

The set of stable states is

$$\mathcal{X}^s = \begin{cases} \{+\mathbf{1}, -\mathbf{1}\} & \text{if } \varepsilon > 0, \\ \{+\mathbf{1}, -\mathbf{1}, \pm\mathbf{1}, \mp\mathbf{1}\} & \text{if } \varepsilon = 0, \\ \{\pm\mathbf{1}, \mp\mathbf{1}\} & \text{if } \varepsilon < 0, \end{cases} \tag{8.1.2}$$

and the set of metastable states is

$$\mathcal{X}^m = \begin{cases} \{\pm\mathbf{1}, \mp\mathbf{1}\} & \text{if } \varepsilon > 0, \\ \{+\mathbf{1}, -\mathbf{1}\} & \text{if } \varepsilon < 0. \end{cases} \tag{8.1.3}$$

The next theorem investigates the asymptotic behavior as $\beta \to \infty$ of the tunneling time for the system started at the stable state s_1 to reach for the first time the other stable state s_2, which we denote by $\tau_{s_2}^{s_1}$. Recall (3.1.1) for the precise definition. In order to state the theorem, we need to define

$$\Gamma_s^0 := \begin{cases} \frac{n^2}{2} + |\varepsilon|n & \text{if } n \text{ is even}, \\ \frac{n^2-1}{2} + |\varepsilon|(n+1) & \text{if } n \text{ is odd}, \end{cases} \tag{8.1.4}$$

that represents the maximal value of the energy barrier between two stable states.

Theorem 8.1.2 (Asymptotic behavior of the tunneling time). *For any $\delta > 0$ and for any $s_1, s_2 \in \mathcal{X}^s$, the following statements hold:*

(i) $\lim_{\beta\to\infty} \mathbb{P}(e^{\beta(\Gamma_s^0-\delta)} < \tau_{s_2}^{s_1} < e^{\beta(\Gamma_s^0+\delta)}) = 1$;

(ii) $\lim_{\beta\to\infty} \frac{1}{\beta} \log \mathbb{E}\tau_{s_2}^{s_1} = \Gamma_s^0$;

(iii) $\frac{\tau_{s_2}^{s_1}}{\mathbb{E}\tau_{s_2}^{s_1}} \xrightarrow{d} \mathrm{Exp}(1)$ *as* $\beta \to \infty$;

(iv) there exist two constants $0 < c_1 \leqslant c_2 < \infty$ independent of β such that for every $\beta > 0$

$$c_1 e^{-\beta\Gamma_s^0} \leqslant \rho \leqslant c_2 e^{-\beta\Gamma_s^0}, \tag{8.1.5}$$

where ρ is the spectral gap of the Markov process (recall (1.3.55)).

Remark 8.1.3. *We note that Theorem 8.1.2(iv) implies that*

$$\lim_{\beta\to\infty} \frac{1}{\beta} \log t_{mix}(\varepsilon) = \Gamma_s^0 = \lim_{\beta\to\infty} -\frac{1}{\beta} \log \rho, \tag{8.1.6}$$

where $t_{mix}(\varepsilon)$ is the mixing time of the Markov process, which quantifies how long it takes for the empirical distribution of the process to get close to the stationary distribution (recall (1.3.54)).

The last result of this section concerns the description of a gate for the transition between the stable states s_1 and s_2. To this end, if n is odd, we define

$$C_{odd}^* := \begin{cases} C\left(\frac{n+1}{2}, 0, 0\right) \cup C\left(0, \frac{n+1}{2}, 0\right) \cup C\left(n, \frac{n-1}{2}, \frac{n-1}{2}\right) \cup C\left(\frac{n-1}{2}, n, \frac{n-1}{2}\right) & \text{if } \varepsilon \geqslant 0, \\ C\left(\frac{n-1}{2}, 0, 0\right) \cup C\left(0, \frac{n-1}{2}, 0\right) \cup C\left(n, \frac{n+1}{2}, \frac{n+1}{2}\right) \cup C\left(\frac{n+1}{2}, n, \frac{n+1}{2}\right) & \text{if } \varepsilon < 0, \end{cases} \tag{8.1.7}$$

otherwise if n is even, we define

$$C_{even}^* := C\left(\frac{n}{2}, 0, 0\right) \cup C\left(0, \frac{n}{2}, 0\right) \cup C\left(n, \frac{n}{2}, \frac{n}{2}\right) \cup C\left(\frac{n}{2}, n, \frac{n}{2}\right). \tag{8.1.8}$$

Theorem 8.1.4 (Gate for the tunneling transition). *If n is even (resp. odd), the set C_{even}^* (resp. C_{odd}^*) is a gate for the transition from s_1 to s_2 for any $s_1, s_2 \in \mathcal{X}^s$.*

8.1.2 *Case* $h > 0$

In this section, we focus on the case $h > 0$, which describes the situation in which there is a positive external magnetic field that favors plus spins. Moreover, we assume that $0 < h \leqslant 1$ in order to avoid the energetical contribution of the external magnetic field prevails over the binding energies associated with internal edges. As it will be clear later, the dynamical behavior of the system is different in the two cases $0 < h \leqslant |\varepsilon| \leqslant 1$ and $0 \leqslant |\varepsilon| < h \leqslant 1$, especially when $\varepsilon < 0$. Indeed, this corresponds to a different "importance" given to cross-edges and external magnetic field. The first result we provide is the identification of metastable and stable states, which is the subject of the following theorem.

Theorem 8.1.5 (Stable and metastable states)**.** *Let* $(\mathcal{X}, Q, \widetilde{H}, \Delta)$ *be the energy landscape corresponding to the Ising model on* $\mathcal{G}(2, n)$*. Then, the lowest possible energy is equal to*

$$\min_{\sigma\in\mathcal{X}} \widetilde{H}(\sigma) = \begin{cases} -n^2 + n - \varepsilon n - 2hn & \text{if } 0 \leqslant \varepsilon \leqslant 1 \text{ or } 0 < -\varepsilon < h \leqslant 1, \\ -n^2 + n + \varepsilon n & \text{if } 0 < h \leqslant -\varepsilon \leqslant 1. \end{cases} \tag{8.1.9}$$

The set of stable states is

$$\mathcal{X}^s = \begin{cases} \{+\mathbf{1}\} & \text{if } 0 \leqslant \varepsilon \leqslant 1 \text{ or } 0 < -\varepsilon < h \leqslant 1, \\ \{+\mathbf{1}, \pm\mathbf{1}, \mp\mathbf{1}\} & \text{if } h = -\varepsilon, \\ \{\pm\mathbf{1}, \mp\mathbf{1}\} & \text{if } 0 < h < -\varepsilon \leqslant 1, \end{cases} \tag{8.1.10}$$

and the set of metastable states is

$$\mathcal{X}^m = \begin{cases} \{-\mathbf{1}\} & \text{if } 0 \leqslant \varepsilon \leqslant 1 \text{ or } h = -\varepsilon, \\ \{\pm\mathbf{1}, \mp\mathbf{1}\} & \text{if } 0 < -\varepsilon < h \leqslant 1, \\ \{+\mathbf{1}\} & \text{if } 0 < h < -\varepsilon \leqslant 1. \end{cases} \tag{8.1.11}$$

The next theorems investigate the asymptotic behavior as $\beta \to \infty$ of the tunneling time (resp. transition time to the stable state) for the system started at the stable state s_1 (resp. metastable state m) to reach for the first time the other stable state s_2 (resp. the stable state s) if $0 < h < -\varepsilon \leqslant 1$ (resp. if $0 \leqslant \varepsilon \leqslant 1$ or $0 < -\varepsilon < h \leqslant 1$). Recall (3.1.1) for the precise definition. In order to state the theorems, we need to define:

$$\Gamma^1_m := \begin{cases} \frac{n^2}{2} + n(\varepsilon - h) & \text{if } n \text{ is even,} \\ \frac{n^2-1}{2} + (n+1)(\varepsilon - h) & \text{if } n \text{ is odd and } 0 < h \leqslant \varepsilon \leqslant 1, \\ \frac{n^2-1}{2} + (n-1)(\varepsilon - h) & \text{if } n \text{ is odd and } 0 \leqslant \varepsilon < h \leqslant 1, \end{cases} \tag{8.1.12}$$

$$\Gamma^2_m := \begin{cases} \frac{n^2}{2} - n(\varepsilon + h) & \text{if } n \text{ is even,} \\ \frac{n^2-1}{2} - (n-1)(\varepsilon + h) & \text{if } n \text{ is odd,} \end{cases} \tag{8.1.13}$$

$$\Gamma^h_s := \begin{cases} \frac{n^2}{2} + n(h - \varepsilon) & \text{if } n \text{ is even and } 0 < h - \varepsilon < 1, \\ \frac{n^2-4}{2} + (n+2)(h - \varepsilon) & \text{if } n \text{ is even and } 1 \leqslant h - \varepsilon < 2, \\ \frac{n^2-1}{2} + (n+1)(h - \varepsilon) & \text{if } n \text{ is odd.} \end{cases} \tag{8.1.14}$$

that represent the maximal values of the energy barrier between the set of metastable states to the set of stable states or between two stable states.

Theorem 8.1.6 (Asymptotic behavior of the tunneling time)**.** *If* $0 < h < -\varepsilon \leqslant 1$*, for any* $\delta > 0$ *and for any* $s_1, s_2 \in \mathcal{X}^s$*, the following statements hold*

(i) $\lim_{\beta\to\infty} \mathbb{P}(e^{\beta(\Gamma^h_s - \delta)} < \tau^{s_1}_{s_2} < e^{\beta(\Gamma^h_s + \delta)}) = 1$;

(ii) $\lim_{\beta\to\infty} \frac{1}{\beta} \log \mathbb{E}\tau^{s_1}_{s_2} = \Gamma^h_s$;

(iii) $\dfrac{\tau_{s_2}^{s_1}}{\mathbb{E}\tau_{s_2}^{s_1}} \xrightarrow{d} \mathrm{Exp}(1)$ *as* $\beta \to \infty$;

(iv) there exist two constants $0 < c_1 \leqslant c_2 < \infty$ *independent of* β *such that for every* $\beta > 0$

$$c_1 e^{-\beta \Gamma_s^h} \leqslant \rho \leqslant c_2 e^{-\beta \Gamma_s^h}, \tag{8.1.15}$$

where ρ *is the spectral gap of the Markov process.*

If $0 \leqslant \varepsilon \leqslant 1$ we set $\Gamma_m^* = \Gamma_m^1$, whereas if $0 < -\varepsilon < h \leqslant 1$ we set $\Gamma_m^* = \Gamma_m^2$.

Theorem 8.1.7 (Asymptotic behavior of the transition time). *If* $0 \leqslant \varepsilon \leqslant 1$ *or* $0 < -\varepsilon < h \leqslant 1$, *for any* $\delta > 0$, *for* $m \in \mathcal{X}^m$ *and* $s \in \mathcal{X}^s$, *the following statements hold*

(i) $\lim_{\beta\to\infty} \mathbb{P}(e^{\beta(\Gamma_m^* - \delta)} < \tau_s^m < e^{\beta(\Gamma_m^* + \delta)}) = 1$;

(ii) $\lim_{\beta\to\infty} \dfrac{1}{\beta} \log \mathbb{E}\tau_s^m = \Gamma_m^*$;

(iii) $\dfrac{\tau_s^m}{\mathbb{E}\tau_s^m} \xrightarrow{d} \mathrm{Exp}(1)$ *as* $\beta \to \infty$;

(iv) there exist two constants $0 < c_1 \leqslant c_2 < \infty$ *independent of* β *such that for every* $\beta > 0$

$$c_1 e^{-\beta \Gamma_m^*} \leqslant \rho \leqslant c_2 e^{-\beta \Gamma_m^*}, \tag{8.1.16}$$

where ρ *is the spectral gap of the Markov process.*

Remark 8.1.8. *We note that Theorem 8.1.6(iv) implies that*

$$\lim_{\beta\to\infty} \frac{1}{\beta} \log t_{mix}(\varepsilon) = \Gamma_s^h = \lim_{\beta\to\infty} -\frac{1}{\beta} \log \rho, \tag{8.1.17}$$

where $t_{mix}(\varepsilon)$ *is the mixing time of the Markov process. Analogously, a similar result can be also derived for* Γ_m^* *from Theorem 8.1.7(iv).*

The last main result of this section concerns the description of a gate for the transition between the stable states s_1 and s_2 (resp. between the metastable state m and the stable state s) if $0 < h < -\varepsilon \leqslant 1$ (resp. if $0 \leqslant \varepsilon \leqslant 1$ or $0 < -\varepsilon < h \leqslant 1$). To this end, we need the following definitions.
If $0 \leqslant \varepsilon \leqslant 1$, we define

$$C_1^* := \begin{cases} C\left(\frac{n+1}{2}, 0, 0\right) \cup C\left(0, \frac{n+1}{2}, 0\right) & \text{if } n \text{ is odd and } 0 < h \leqslant \varepsilon \leqslant 1, \\ C\left(\frac{n-1}{2}, 0, 0\right) \cup C\left(0, \frac{n-1}{2}, 0\right) & \text{if } n \text{ is odd and } 0 \leqslant \varepsilon < h \leqslant 1, \\ C\left(\frac{n}{2}, 0, 0\right) \cup C\left(0, \frac{n}{2}, 0\right) & \text{if } n \text{ is even.} \end{cases} \tag{8.1.18}$$

If $0 < -\varepsilon < h \leqslant 1$, we define

$$C_2^* := \begin{cases} C\left(n, \frac{n-1}{2}, \frac{n-1}{2}\right) & \text{if } n \text{ is odd,} \\ C\left(n, \frac{n}{2}, \frac{n}{2}\right) & \text{if } n \text{ is even.} \end{cases} \tag{8.1.19}$$

If $0 < h < -\varepsilon \leqslant 1$, we define

$$C_3^* := \begin{cases} C\left(\frac{n-1}{2}, 0, 0\right) \cup C\left(0, \frac{n-1}{2}, 0\right) & \text{if } n \text{ is odd,} \\ C\left(\frac{n}{2}, 0, 0\right) \cup C\left(0, \frac{n}{2}, 0\right) & \text{if } n \text{ is even and } 0 < h - \varepsilon < 1, \\ C\left(\frac{n-2}{2}, 0, 0\right) \cup C\left(0, \frac{n-2}{2}, 0\right) & \text{if } n \text{ is even and } 1 \leqslant h - \varepsilon < 2. \end{cases} \tag{8.1.20}$$

Theorem 8.1.9 (Gate for the transition). *If* $0 \leqslant \varepsilon \leqslant 1$ *(resp.* $0 < -\varepsilon < h \leqslant 1$*), the set* C_1^* *(resp.* C_2^**) is a gate for the transition from the metastable state* m *to the stable state* s. *If* $0 < h < -\varepsilon \leqslant 1$, *the set* C_3^* *is a gate for the transition from* s_1 *to* s_2 *for any* $s_1, s_2 \in \{\pm\mathbf{1}, \mp\mathbf{1}\}$.

8.1.3 *Energetical properties of the configurations*

In this section, we provide some useful lemmas concerning the energetical properties of the configurations in $C(p_1, p_2, a)$, which will be used in the rest of the chapter. Note that all the configurations in $C(p_1, p_2, a)$ are identical, *modulo permutation of the vertices in each cluster*, since:

- the first cluster gets $n - p_1$ minus spins,
- the second cluster gets $n - p_2$ minus spins,
- $p_1 - a$ is the number of cross edges between plus spins in the first cluster and minus spins in the second cluster,
- $p_2 - a$ is the number of cross edges between minus spins in the first cluster and plus spins in the second cluster,
- $n + a - p_1 - p_2$ is the number of cross edges between minus spins in the first cluster and minus spins in the second cluster.

Lemma 8.1.10 (Energy of the configurations)**.** *For any $\sigma \in C(p_1, p_2, a)$, it holds that*

$$\widetilde{H}(\sigma) = n - \varepsilon n - 2\left(p_1 - \frac{n}{2}\right)^2 - 2\left(p_2 - \frac{n}{2}\right)^2 - 2\varepsilon(2a - p_1 - p_2) - 2h(p_1 + p_2 - n). \quad (8.1.21)$$

Proof. Let $\sigma \in C(p_1, p_2, a)$. Note that in the first cluster there are $\binom{p_1}{2}$ (resp. $\binom{n-p_1}{2}$) internal edges between plus (resp. minus) spins, whereas there are $p_1(n - p_1)$ internal edges between plus and minus spins. By symmetry, analogous relations can be derived for the second cluster. Moreover, there are $n + 2a - p_1 - p_2$ (resp. $p_1 + p_2 - 2a$) cross edges between spins of the same (resp. different) type and $p_1 + p_2$ plus spins in $\mathcal{G}(2, n)$. Thus, by using (1.4.4) we deduce

$$\begin{aligned} H(\sigma) \quad &= -\frac{(n-p_1)(n-p_1-1)}{2} - \frac{p_1(p_1-1)}{2} - \frac{(n-p_2)(n-p_2-1)}{2} - \frac{p_2(p_2-1)}{2} \\ &\quad + p_1(n-p_1) + p_2(n-p_2) - \varepsilon(n + 4a - 2p_1 - 2p_2) - 2h(p_1 + p_2 - n) \\ &= n - \varepsilon n - 2\left(p_1 - \frac{n}{2}\right)^2 - 2\left(p_2 - \frac{n}{2}\right)^2 - 2\varepsilon(2a - p_1 - p_2) - 2h(p_1 + p_2 - n). \end{aligned} \quad (8.1.22)$$

□

From now on, we define up–flip (resp. down–flip) as the move consisting in flipping a minus (resp. plus) spin in a plus (resp. minus) spin.

Lemma 8.1.11 (Energy difference for an up–flip)**.** *Let $\sigma_1 \in C(p_1, p_2, a_1)$ and let $\sigma_2 \in C(p_1 + i, p_2 + j, a_2)$, with $i, j \in \{0, 1\}$ such that $i \neq j$. Then,*

$$\widetilde{H}(\sigma_2) - \widetilde{H}(\sigma_1) = \begin{cases} 2(n - 1 - 2p_1 + \varepsilon - h) & \text{if } i = 1,\ p_1 \leqslant n-1 \text{ and } a_2 = a_1, \\ 2(n - 1 - 2p_1 - \varepsilon - h) & \text{if } i = 1,\ p_1 \leqslant n-1 \text{ and } a_2 = a_1 + 1, \\ 2(n - 1 - 2p_2 + \varepsilon - h) & \text{if } j = 1,\ p_2 \leqslant n-1 \text{ and } a_2 = a_1, \\ 2(n - 1 - 2p_2 - \varepsilon - h) & \text{if } j = 1,\ p_2 \leqslant n-1 \text{ and } a_2 = a_1 + 1. \end{cases} \quad (8.1.23)$$

Proof. In the case $i = 1$ and $p_1 \leqslant n - 1$, by using (8.1.21), we directly get

$$\begin{aligned} \widetilde{H}(\sigma_2) - \widetilde{H}(\sigma_1) \quad &= 2(n - 1 - 2p_1 + 2\varepsilon a_1 - 2\varepsilon a_2 + \varepsilon - h) \\ &= \begin{cases} 2(n - 1 - 2p_1 + \varepsilon - h) & \text{if } a_2 = a_1, \\ 2(n - 1 - 2p_1 - \varepsilon - h) & \text{if } a_2 = a_1 + 1. \end{cases} \end{aligned} \quad (8.1.24)$$

By symmetry, we get the claim also in the case $j = 1$ and $p_2 \leqslant n - 1$. □

Lemma 8.1.12 (Energy difference for a down–flip). *Let* $\sigma_1 \in C(p_1, p_2, a_1)$, $\sigma_2 \in C(p_1 - i, p_2 - j, a_2)$, *with* $i, j \in \{0, 1\}$ *such that* $i \neq j$. *Then,*

$$\widetilde{H}(\sigma_2) - \widetilde{H}(\sigma_1) = \begin{cases} -2(n + 1 - 2p_1 + \varepsilon - h) & \text{if } i = 1,\ p_1 \geqslant 1 \text{ and } a_2 = a_1, \\ -2(n + 1 - 2p_1 - \varepsilon - h) & \text{if } i = 1,\ p_1 \geqslant 1 \text{ and } a_2 = a_1 - 1, \\ -2(n + 1 - 2p_2 + \varepsilon - h) & \text{if } j = 1,\ p_2 \geqslant 1 \text{ and } a_2 = a_1, \\ -2(n + 1 - 2p_2 - \varepsilon - h) & \text{if } j = 1,\ p_2 \geqslant 1 \text{ and } a_2 = a_1 - 1. \end{cases} \tag{8.1.25}$$

Proof. By proceeding as in the proof of Lemma 8.1.11, we get the claim. □

Since the configurations in $C(p_1, p_2, a)$ have all the same energy, see Lemma 8.1.10, with a slight abuse of notation in the rest of the chapter we denote their energy value by $\widetilde{H}(p_1, p_2, a)$.

8.2 PROOF OF THE MAIN RESULTS: CASE $h = 0$

8.2.1 *Reference paths*

If $\varepsilon \geqslant 0$, we define a reference path $\bar{\omega}$ from $-\mathbf{1}$ to $+\mathbf{1}$, while if $\varepsilon < 0$ we define a path $\hat{\omega}$ from $\pm\mathbf{1}$ to $\mp\mathbf{1}$. In words, these paths are constructed in the following way. The path $\bar{\omega}$, which starts from $-\mathbf{1}$, consists in flipping one by one the minus spins in one community until the path reaches either $\pm\mathbf{1}$ or $\mp\mathbf{1}$ and afterward the remaining minuses are flipped one by one until the path reaches $+\mathbf{1}$ (see Figure 1.39). The construction of the path $\hat{\omega}$ is made in a similar way (see Figure 1.40).

Definition 8.2.1 (Reference paths). *If* $\varepsilon \geqslant 0$, *we define* $\bar{\omega} : -\mathbf{1} \to +\mathbf{1}$ *as the path* $(\bar{\omega}_k)_{k=0}^{2n}$ *such that*

$$\bar{\omega}_k \in C(k, 0, 0) \text{ and } \bar{\omega}_{n+k} \in C(n, k, k), \quad \text{for any } k = 0, \dots, n. \tag{8.2.1}$$

If $\varepsilon < 0$, *we define* $\hat{\omega} : \pm\mathbf{1} \to \mp\mathbf{1}$ *as the path* $(\hat{\omega}_k)_{k=0}^{2n}$ *such that*

$$\hat{\omega}_k \in C(n, k, k) \text{ and } \hat{\omega}_{n+k} \in C(n - k, n, n - k), \quad \text{for any } k = 0, \dots, n. \tag{8.2.2}$$

Lemma 8.2.2 (Maximal energy on the reference paths). *Let* $\bar{\omega} : -\mathbf{1} \to +\mathbf{1}$ *and* $\hat{\omega} : \pm\mathbf{1} \to \mp\mathbf{1}$ *be the paths given in Definition 8.2.1. Then,*

$$\Phi_{\bar{\omega}} = \begin{cases} \widetilde{H}(\bar{\omega}_{\frac{n}{2}}) = \widetilde{H}(\bar{\omega}_{n+\frac{n}{2}}) = n - \frac{n^2}{2} & \text{if } n \text{ is even}, \\ \widetilde{H}(\bar{\omega}_{\frac{n+1}{2}}) = \widetilde{H}(\bar{\omega}_{n+\frac{n-1}{2}}) = n - \frac{n^2+1}{2} + \varepsilon & \text{if } n \text{ is odd}, \end{cases} \tag{8.2.3}$$

and

$$\Phi_{\hat{\omega}} = \begin{cases} \widetilde{H}(\hat{\omega}_{\frac{n}{2}}) = \widetilde{H}(\hat{\omega}_{n+\frac{n}{2}}) = n - \frac{n^2}{2} - \varepsilon n & \text{if } n \text{ is even}, \\ \widetilde{H}(\hat{\omega}_{\frac{n+1}{2}}) = \widetilde{H}(\hat{\omega}_{n+\frac{n-1}{2}}) = n - \frac{n^2+1}{2} - \varepsilon & \text{if } n \text{ is odd}. \end{cases} \tag{8.2.4}$$

Proof. Since $\widetilde{H}(C(n-k, n, n-k)) = \widetilde{H}(C(k, 0, 0))$, it suffices to study the maxima of the energy along the path $\bar{\omega}$ connecting $-\mathbf{1}$ and $+\mathbf{1}$. From (8.1.21) and (8.2.1), we have

$$\begin{aligned} \widetilde{H}(\bar{\omega}_k) &= -n^2 + n + 2kn - 2k^2 + 2k\varepsilon - n\varepsilon \\ \widetilde{H}(\bar{\omega}_{n+k}) &= -n^2 + n + 2kn - 2k^2 - 2k\varepsilon + n\varepsilon \end{aligned} \tag{8.2.5}$$

for any $k = 0, \dots, n$. By deriving both equations in (8.2.5) with respect to k, we have that the maxima of the energy along the path $\bar{\omega}$ are $\widetilde{H}(\bar{\omega}_{\frac{n+\varepsilon}{2}})$ and $\widetilde{H}(\bar{\omega}_{n+\frac{n-\varepsilon}{2}})$. This means that on the first part of the path $(\bar{\omega}_k)_{k=0}^{n}$ the maximum is reached at the critical value $k_1^* = \frac{n+\varepsilon}{2}$, while on the second part of the path $(\bar{\omega}_{k+n})_{k=0}^{n}$ the maximum is reached at the critical value $k_2^* = \frac{n-\varepsilon}{2}$.

Let us focus on the value k_1^*. Note that $\widetilde{H}(\bar{\omega}_k)$ is a concave parabola in k, which is symmetric with respect to k_1^*. Since we are interested in finding the integer value of k in which this maximum is achieved, we need to compare the distances $k_1^* - \lfloor k_1^* \rfloor$ and $\lceil k_1^* \rceil - k_1^*$. The minimal distance indicates the value we are interested in. Consider now the case $\varepsilon \geqslant 0$, thus

$$\begin{aligned} \lfloor k_1^* \rfloor &= \begin{cases} \frac{n}{2} & \text{if } n \text{ is even,} \\ \frac{n-1}{2} & \text{if } n \text{ is odd and } 0 \leqslant \varepsilon < 1, \\ \frac{n+1}{2} & \text{if } n \text{ is odd and } \varepsilon = 1, \end{cases} \\ \lceil k_1^* \rceil &= \begin{cases} \frac{n}{2} + 1 & \text{if } n \text{ is even,} \\ \frac{n+1}{2} & \text{if } n \text{ is odd and } 0 \leqslant \varepsilon < 1, \\ \frac{n+3}{2} & \text{if } n \text{ is odd and } \varepsilon = 1, \end{cases} \end{aligned} \tag{8.2.6}$$

and

$$\begin{aligned} \lfloor k_2^* \rfloor &= \begin{cases} \frac{n}{2} - 1 & \text{if } n \text{ is even,} \\ \frac{n-1}{2} & \text{if } n \text{ is odd,} \end{cases} \\ \lceil k_2^* \rceil &= \begin{cases} \frac{n}{2} & \text{if } n \text{ is even,} \\ \frac{n+1}{2} & \text{if } n \text{ is odd.} \end{cases} \end{aligned} \tag{8.2.7}$$

Assume n even. Since $\lfloor \frac{n+\varepsilon}{2} \rfloor = \frac{n}{2}$ and $\lceil \frac{n+\varepsilon}{2} \rceil = \frac{n}{2} + 1$, we have that $k_1^* - \lfloor k_1^* \rfloor = \frac{\varepsilon}{2} \leqslant 1 - \frac{\varepsilon}{2} = \lceil k_1^* \rceil - k_1^*$ and therefore the maximum is achieved in $\widetilde{H}(\bar{\omega}_{\frac{n}{2}})$. By arguing similarly for n odd and k_2^*, we get the claim for $\varepsilon \geqslant 0$. Since $\widetilde{H}(\bar{\omega}_k) = \widetilde{H}(\hat{\omega}_{n+k})$ and $\widetilde{H}(\bar{\omega}_{n+k}) = \widetilde{H}(\hat{\omega}_k)$ for any $k = 0, ..., n$, the case $\varepsilon < 0$ can be studied in a similar way. Note that for $\varepsilon < 0$ the values $\lfloor k_i^* \rfloor$ and $\lceil k_i^* \rceil$, with $i = 1, 2$, are different from the case $\varepsilon > 0$. □

Proposition 8.2.3 (Upper bounds). *Let $(\mathcal{X}, Q, \widetilde{H}, \Delta)$ be the energy landscape corresponding to the Ising model on $\mathcal{G}(2, n)$, then $\Gamma_s \leqslant \Gamma_s^0$, where Γ_s^0 is defined in (8.1.4).*

Proof. By using (8.1.1) and Lemma 8.2.2, we get the claim. □

8.2.2 *Lower bounds*

For every $p \in \{0, \dots, 2n\}$, define the manifold $\mathcal{C}(p) \subset \mathcal{X}$ as the subset of configurations in $\mathcal{X}$ with exactly p plus spins, that is $\mathcal{C}(p) := \{\sigma \in \mathcal{X} : \sum_{i \in V} \mathbf{1}_{\{\sigma_i = +1\}} = p\}$. By fixing the number of plus spins in each of the two clusters, the manifold $\mathcal{C}(p)$ can be decomposed as

$$\mathcal{C}(p) = \bigcup_{\substack{0 \leqslant p_1, p_2 \leqslant n \\ p_1 + p_2 = p}} C(p_1, p_2, a).$$

Assuming the current state $\sigma \in \mathcal{C}(p)$ for some p, since we consider a single-flip dynamics, every nontrivial update will lead to new state σ' that belongs to either $\mathcal{C}(p-1)$ or $\mathcal{C}(p+1)$.

Proposition 8.2.4 (Local minima). *For every $n \geqslant 2$ and $|\varepsilon| \leqslant 1$, regardless of the sign of ε, the minimum value of the energy $\widetilde{H}$ on the manifold $\mathcal{C}(p)$ is given by*

$$\widetilde{H}(p) := \min_{\sigma \in \mathcal{C}(p)} \widetilde{H}(\sigma) = \begin{cases} n - (p-n)^2 - p^2 - \varepsilon(n-2p) & \text{if } 0 \leqslant p \leqslant n, \\ n - (2n-p)^2 - (p-n)^2 - \varepsilon(2p-3n) & \text{if } n \leqslant p \leqslant 2n. \end{cases} \tag{8.2.8}$$

Furthermore, if $0 \leqslant p \leqslant n$, the minimum is achieved on the subsets $C(p, 0, 0)$ and $C(0, p, 0)$, while if $n \leqslant p \leqslant 2n$, the minimum is achieved on the subsets $C(n, p-n, p-n)$ and $C(p-n, n, p-n)$.

Proof. For every fix p, one has consider all the subsets $C(p_1, p_2, a)$ which partition $\mathcal{C}(p)$. In view of (8.1.21), we need to solve the quadratic optimization problem:

$$\min_{\sigma\in\mathcal{C}(p)} \widetilde{H}(\sigma) = n + \varepsilon(2p-n) + \min_{\substack{p_1,p_2,a \\ 0\leqslant p_1,p_2\leqslant n \\ p_1+p_2=p \\ \max\{0,p-n\}\leqslant a\leqslant \min\{p_1,p_2\}}} -2\left(p_1-\frac{n}{2}\right)^2 - 2\left(p_2-\frac{n}{2}\right)^2 - 4\varepsilon a. \tag{8.2.9}$$

If $\varepsilon > 0$, it is clear from (8.2.9) that a should be as large as possible to achieve a possibly lower energy. Without loss of generality, we may assume that $p_1 \leqslant p_2$ and substituting $a = \min\{p_1, p_2\} = p_1$ and then $p_2 = p - p_1$, we have

$$\min_{\sigma\in\mathcal{C}(p)} \widetilde{H}(\sigma) = n - \varepsilon(n-2p) + \min_{\substack{p_1 \\ \max\{0,p-n\}\leqslant p_1\leqslant p/2}} -2\left(p_1-\frac{n}{2}\right)^2 - 2\left(p-p_1-\frac{n}{2}\right)^2 - 4\varepsilon p_1. \tag{8.2.10}$$

Let us define $f(p_1) := -2\left(p_1-\frac{n}{2}\right)^2 - 2\left(p-p_1-\frac{n}{2}\right)^2 - 4\varepsilon p_1$. Recall that p is only a fixed parameter, so $f(p_1)$ single-variable concave function of p_1, which will then achieve its minimum value at the boundary points. The inequality $p_1 \leqslant p/2$ follows from the assumptions $p_1 + p_2 = p$ and $p_1 \leqslant p_2$. Recall that $p \leqslant 2n$ and let us distinguish two cases:

(a) If $0 \leqslant p \leqslant n$, then the boundary points to consider are $p_1 \in \{0, \lfloor p/2 \rfloor\}$, at which the function $f(p_1)$ attains the following values

$$\begin{aligned} f(0) \quad &= -n^2 - 2p^2 + 2np, \\ f(\lfloor \tfrac{p}{2} \rfloor) \quad &= \begin{cases} -n^2 - p^2 + 2np - 2\varepsilon p & \text{if } p \text{ is even,} \\ -n^2 - p^2 + 2np - 2\varepsilon p + 2\varepsilon - 1 & \text{if } p \text{ is odd.} \end{cases} \end{aligned} \tag{8.2.11}$$

By a direct computation, it follows that $f(0) \leqslant f(\lfloor \frac{p}{2} \rfloor)$ either whenever $\varepsilon \leqslant \frac{p}{2}$ if p is even, or whenever $\varepsilon \leqslant \frac{p+1}{2}$ if p is odd. From now on, we consider separately the three following cases.

If $p = 0$, we obtain that $f(\lfloor \frac{p}{2} \rfloor) = f(0)$ and therefore, by using (8.2.10),

$$\min_{\sigma\in\mathcal{C}(0)} \widetilde{H}(\sigma) = n - n^2 - \varepsilon n. \tag{8.2.12}$$

If $p = 1$, we obtain that $f(\lfloor \frac{p}{2} \rfloor) = f(0)$ and therefore, by using (8.2.10),

$$\min_{\sigma\in\mathcal{C}(1)} \widetilde{H}(\sigma) = 3n - n^2 - \varepsilon n + 2\varepsilon - 2. \tag{8.2.13}$$

If $2 \leqslant p \leqslant n$, since $|\varepsilon| \leqslant 1$, we have that $f(0) \leqslant f(\lfloor \frac{p}{2} \rfloor)$. Thus, by using (8.2.10),

$$\min_{\sigma\in\mathcal{C}(p),\ 2\leqslant p\leqslant n} \widetilde{H}(\sigma) = n - (p-n)^2 - p^2 - \varepsilon(n-2p). \tag{8.2.14}$$

(b) If $n \leqslant p \leqslant 2n$, then the boundary points to consider are $p_1 \in \{p-n, \lfloor p/2 \rfloor\}$, at which the function $f(p_1)$ attains the following values

$$\begin{aligned} f(p-n) \quad &= -5n^2 - 2p^2 + 6np - 4\varepsilon p + 4\varepsilon n, \\ f(\lfloor \tfrac{p}{2} \rfloor) \quad &= \begin{cases} -n^2 - p^2 + 2np - 2\varepsilon p & \text{if } p \text{ is even,} \\ -n^2 - p^2 + 2np - 2\varepsilon p + 2\varepsilon - 1 & \text{if } p \text{ is odd.} \end{cases} \end{aligned} \tag{8.2.15}$$

By a direct computation, it follows that $f(p-n) \leqslant f(\lfloor \frac{p}{2} \rfloor)$ either whenever $\varepsilon \leqslant n - \frac{p}{2}$ if p is even, or whenever $\varepsilon \leqslant n - \frac{p-1}{2}$ if p is odd. From now on, we consider separately the three following cases.

If $n \leqslant p \leqslant 2n-2$, since $|\varepsilon| \leqslant 1$, we have that $f(p-n) \leqslant f(\lfloor \frac{p}{2} \rfloor)$. Thus, by using (8.2.10),

$$\min_{\sigma\in\mathcal{C}(p),\ n\leqslant p\leqslant 2n-2} \widetilde{H}(\sigma) = n - (2n-p)^2 - (p-n)^2 - \varepsilon(2p-3n). \tag{8.2.16}$$

If $p = 2n-1$, we obtain that $f(\lfloor \frac{p}{2} \rfloor) = f(n-1)$. Thus, by using (8.2.10),

$$\min_{\sigma \in \mathcal{C}(2n-1)} \widetilde{H}(\sigma) = 3n - n^2 - \varepsilon n + 2\varepsilon - 2. \tag{8.2.17}$$

If $p = 2n$, we obtain that $f(\lfloor \frac{p}{2} \rfloor) = f(n)$. Thus, by using (8.2.10),

$$\min_{\sigma \in \mathcal{C}(2n)} \widetilde{H}(\sigma) = n - n^2 - \varepsilon n. \tag{8.2.18}$$

From the calculations above, it is easy to deduce that if $0 \leqslant p \leqslant n$, the minimum is achieved on the subsets $C(p,0,0)$ and $C(0,p,0)$, while if $n \leqslant p \leqslant 2n$, the minimum is achieved on the subsets $C(n, p-n, p-n)$ and $C(p-n, n, p-n)$.

If $\varepsilon < 0$, it is clear from (8.2.9) that a should be as small as possible to achieve a possibly lower energy. As before, without loss of generality, we assume that $p_1 \leqslant p_2$ and we substitute $p_2 = p - p_1$ in (8.2.9). We need to distinguish two cases depending on the value of p.

(a) If $0 \leqslant p \leqslant n$, then $a = \max\{0, p-n\} = 0$ and (8.2.9) becomes

$$\min_{\sigma \in \mathcal{C}(p)} \widetilde{H}(\sigma) = n - \varepsilon(n-2p) + \min_{\substack{p_1 \\ 0 \leqslant p_1 \leqslant p/2}} -2\left(p_1 - \frac{n}{2}\right)^2 - 2\left(p - p_1 - \frac{n}{2}\right)^2. \tag{8.2.19}$$

The objective function $g(p_1) := -2\left(p_1 - \frac{n}{2}\right)^2 - 2\left(p - p_1 - \frac{n}{2}\right)^2$ is concave in p_1, so again we search the minimum among the boundary points $p_1 \in \{0, \lfloor p/2 \rfloor\}$, at which the function $g(p_1)$ attains the following values

$$\begin{aligned} g(0) \quad &= -n^2 - 2p^2 + 2np, \\ g(\lfloor \tfrac{p}{2} \rfloor) \quad &= \begin{cases} -n^2 - p^2 + 2np & \text{if } p \text{ is even,} \\ -n^2 - p^2 + 2np - 1 & \text{if } p \text{ is odd.} \end{cases} \end{aligned} \tag{8.2.20}$$

By a direct computation, it follows that $g(0) \leqslant g(\lfloor \frac{p}{2} \rfloor)$ in both cases p even and p odd and, thus,

$$\min_{\sigma \in \mathcal{C}(p),\, 0 \leqslant p \leqslant n} \widetilde{H}(\sigma) = n - (p-n)^2 - p^2 - \varepsilon(n-2p). \tag{8.2.21}$$

(b) If $n \leqslant p \leqslant 2n$, then $a = \max\{0, p-n\} = p-n$ and (8.2.9) becomes

$$\min_{\sigma \in \mathcal{C}(p)} \widetilde{H}(\sigma) = n - \varepsilon(2p-3n) + \min_{\substack{p_1 \\ p-n \leqslant p_1 \leqslant p/2}} g(p_1). \tag{8.2.22}$$

The objective function $g(p_1)$ is concave in p_1, so again we search the minimum among the boundary points $p_1 \in \{p-n, \lfloor p/2 \rfloor\}$, at which the function $g(p_1)$ attains the following values

$$\begin{aligned} g(p-n) \quad &= -5n^2 - 2p^2 + 6pn, \\ g(\lfloor \tfrac{p}{2} \rfloor) \quad &= \begin{cases} -n^2 - p^2 + 2pn & \text{if } p \text{ is even,} \\ -n^2 - p^2 + 2pn - 1 & \text{if } p \text{ is odd.} \end{cases} \end{aligned} \tag{8.2.23}$$

By a direct computation, it follows that $g(p-n) \leqslant g(\lfloor \frac{p}{2} \rfloor)$ in both cases p even and p odd and, thus,

$$\min_{\sigma \in \mathcal{C}(p),\, n \leqslant p \leqslant 2n} \widetilde{H}(\sigma) = n - (2n-p)^2 - (p-n)^2 - \varepsilon(2p-3n). \tag{8.2.24}$$

From the calculations above, it is easy to deduce that if $0 \leqslant p \leqslant n$, the minimum is achieved on the subsets $C(p,0,0)$ and $C(0,p,0)$, while if $n \leqslant p \leqslant 2n$, the minimum is achieved on the subsets $C(n, p-n, p-n)$ and $C(p-n, n, p-n)$. □

In order to analyze the manifold $C(p)$ with maximal energy, we need to define

$$p^*_{\text{left}} := \begin{cases} \frac{n}{2} & \text{if } n \text{ is even,} \\ \frac{n+1}{2} & \text{if } n \text{ is odd and } \varepsilon \geqslant 0, \\ \frac{n-1}{2} & \text{if } n \text{ is odd and } \varepsilon < 0, \end{cases} \tag{8.2.25}$$

and

$$p^*_{\text{right}} := \begin{cases} n + \frac{n}{2} & \text{if } n \text{ is even,} \\ n + \frac{n-1}{2} & \text{if } n \text{ is odd and } \varepsilon \geqslant 0, \\ n + \frac{n+1}{2} & \text{if } n \text{ is odd and } \varepsilon < 0. \end{cases} \tag{8.2.26}$$

For any $0 \leqslant p \leqslant 2n$, let $\mathcal{M}_p \in C(p)$ be the set of configurations with minimal energy.

Proposition 8.2.5 (Lower bounds). *Let $(\mathcal{X}, Q, \widetilde{H}, \Delta)$ be the energy landscape corresponding to the Ising model on $\mathcal{G}(2, n)$. The following statements hold:*

— *The maximum of the energy on $\bigcup_{0 \leqslant p \leqslant n} \mathcal{M}_p$ is realized by the configurations in $C(p^*_{\text{left}}, 0, 0) \cup C(0, p^*_{\text{left}}, 0)$;*

— *The maximum of the energy on $\bigcup_{n \leqslant p \leqslant 2n} \mathcal{M}_p$ is realized by the configurations in $C(n, p^*_{\text{right}} - n, p^*_{\text{right}} - n) \cup C(p^*_{\text{right}} - n, n, p^*_{\text{right}} - n)$.*

Moreover, we have that $\Gamma_s \geqslant \Gamma^0_s$, where Γ^0_s is defined in (8.1.4).

Proof. The idea of the proof is to identify, depending on the parity of n and the value of ε, the correct manifold that would give the desired lower bound.

Treating $\widetilde{H}(p)$ as a function of a continuous variable, we see that is concave and, solving for $\frac{d}{dp}\widetilde{H}(p) = 0$, we obtain two stationary points $p_{\text{left}} = \frac{n}{2} + \frac{\varepsilon}{2}$ and $p_{\text{right}} = \frac{3n}{2} - \frac{\varepsilon}{2}$. They both yield the value

$$\max_{0 \leqslant p \leqslant 2n} \widetilde{H}(p) = -\frac{1}{2}\left(n^2 - 2n - \varepsilon^2\right). \tag{8.2.27}$$

Since p_{left} and p_{right} can only take integer values, we deduce that the possible integer optimal values are

$$p^*_1 \in \left\{ \left\lfloor \frac{n}{2} + \frac{\varepsilon}{2} \right\rfloor, \left\lceil \frac{n}{2} + \frac{\varepsilon}{2} \right\rceil \right\}, \quad p^*_2 \in \left\{ \left\lfloor \frac{3n}{2} - \frac{\varepsilon}{2} \right\rfloor, \left\lceil \frac{3n}{2} - \frac{\varepsilon}{2} \right\rceil \right\}. \tag{8.2.28}$$

By performing the same computations as in the proof of Lemma 8.2.2, we obtain that $p^*_1 = p^*_{\text{left}}$ and $p^*_2 = p^*_{\text{right}}$, where p^*_{left} (resp. p^*_{right}) is defined in (8.2.25) (resp. (8.2.25)). Furthermore, by Proposition 8.2.4 we have that the minimum of the energy on the manifold $C(p^*_{\text{left}})$ is realized in $\mathcal{M}_{p^*_{\text{left}}} \equiv C(p^*_{\text{left}}, 0, 0) \cup C(0, p^*_{\text{left}}, 0)$ and on the manifold $C(p^*_{\text{right}})$ in $\mathcal{M}_{p^*_{\text{right}}} \equiv C(n, p^*_{\text{right}} - n, p^*_{\text{right}} - n) \cup C(p^*_{\text{right}} - n, n, p^*_{\text{right}} - n)$.

□

Corollary 8.2.6 (Maximal energy barrier). *We have that*

$$\Gamma_s = \begin{cases} \frac{n^2}{2} + |\varepsilon| n & \text{if } n \text{ is even,} \\ \frac{n^2-1}{2} + |\varepsilon|(n+1) & \text{if } n \text{ is odd.} \end{cases} \tag{8.2.29}$$

Proof. We get the claim by combining Propositions 8.2.3 and 8.2.5. □

8.2.3 *Identification of stable and metastable states*

In this section, we provide the proof of Theorem 8.1.1. To this end, we give two propositions that allow us to accomplish this task. The proof of Propositions 8.2.7 and 8.2.8 are postponed after the proof of Theorem 8.1.1.

Proposition 8.2.7 (Identification of stable states). *Let $(\mathcal{X}, Q, \widetilde{H}, \Delta)$ be the energy landscape corresponding to the Ising model on $\mathcal{G}(2, n)$. Then, the lowest possible value of the energy is equal to*

$$\min_{\sigma \in \mathcal{X}} \widetilde{H}(\sigma) = -n^2 + n - |\varepsilon| n, \tag{8.2.30}$$

and the set of stable states is

$$\mathcal{X}^s = \begin{cases} \{+\mathbf{1}, -\mathbf{1}\} & \text{if } \varepsilon > 0, \\ \{+\mathbf{1}, -\mathbf{1}, \pm\mathbf{1}, \mp\mathbf{1}\} & \text{if } \varepsilon = 0, \\ \{\pm\mathbf{1}, \mp\mathbf{1}\} & \text{if } \varepsilon < 0. \end{cases} \tag{8.2.31}$$

Proposition 8.2.8 (Identification of metastable states). *Let $\sigma \in \mathcal{X} \setminus \{+\mathbf{1}, \pm\mathbf{1}, \mp\mathbf{1}, -\mathbf{1}\}$, then the stability level of σ is zero, i.e., $V_\sigma = 0$. The set of metastable states is*

$$\mathcal{X}^m = \begin{cases} \{\pm\mathbf{1}, \mp\mathbf{1}\} & \text{if } \varepsilon > 0, \\ \{+\mathbf{1}, -\mathbf{1}\} & \text{if } \varepsilon < 0. \end{cases} \tag{8.2.32}$$

Moreover, we have that

$$\Gamma_s = \begin{cases} \frac{n^2}{2} - |\varepsilon| n & \text{if } n \text{ is even}, \\ \frac{n^2-1}{2} - |\varepsilon|(n-1) & \text{if } n \text{ is odd}, \end{cases} \tag{8.2.33}$$

and

$$\Gamma_m = \begin{cases} \frac{n^2}{2} - |\varepsilon| n & \text{if } n \text{ is even}, \\ \frac{n^2-1}{2} - |\varepsilon|(n-1) & \text{if } n \text{ is odd}. \end{cases} \tag{8.2.34}$$

Proof of Theorem 8.1.1. Combining Corollary 8.2.6, Propositions 8.2.7 and 8.2.8 we get the claim. □

Proof of Proposition 8.2.7. Recalling that $\max\{p_1 + p_2 - n, 0\} \leqslant a \leqslant \min\{p_1, p_2\}$, we note that a is a function of p_1 and p_2. In view of the partition

$$\mathcal{X} = \bigcup_{\substack{0 \leqslant p_1, p_2 \leqslant n \\ \max\{0, p_1+p_2-n\} \leqslant a \leqslant \min\{p_1, p_2\}}} C(p_1, p_2, a) \tag{8.2.35}$$

and (8.1.21), we can calculate the minimum energy as

$$\begin{aligned} \min_{p_1, p_2} \widetilde{H}(p_1, p_2, a) &= n - n\varepsilon + 2 \min_{p_1, p_2} \left(-\left(p_1 - \frac{n}{2}\right)^2 - \left(p_2 - \frac{n}{2}\right)^2 + \varepsilon(p_1 + p_2) - 2\varepsilon a \right) \\ &=: n - n\varepsilon + 2 \min_{p_1, p_2} f(p_1, p_2). \end{aligned} \tag{8.2.36}$$

If $\varepsilon \geqslant 0$, we have that

$$\min_{p_1, p_2} f(p_1, p_2) = \min_{p_1, p_2} \left(-\left(p_1 - \frac{n}{2}\right)^2 - \left(p_2 - \frac{n}{2}\right)^2 + \varepsilon(p_1 + p_2) - 2\varepsilon \min\{p_1, p_2\} \right), \tag{8.2.37}$$

so the function $f(p_1, p_2)$ is concave in both variables. Thus, we expect the minimum (p_1^*, p_2^*) to be achieved at the boundary of the feasible region. This immediately implies that $(p_1^*, p_2^*) \in \{(0,0), (0,n), (n,0), (n,n)\}$. By direct computation, we obtain:

$$f(0,0) = f(n,n) = -\frac{n^2}{2}; \quad f(0,n) = f(n,0) = -\frac{n^2}{2} + n\varepsilon. \tag{8.2.38}$$

This implies that the minimum is achieved at $(p_1^*, p_2^*) = (0,0)$ and $(p_1^*, p_2^*) = (n,n)$, which correspond to the configuration $C(0,0,0) \equiv -\mathbf{1}$ and $C(n,n,n) \equiv +\mathbf{1}$, respectively.

If $\varepsilon < 0$, we have that

$$\min_{p_1, p_2} f(p_1, p_2) = \min_{p_1, p_2} \left(-\left(p_1 - \frac{n}{2}\right)^2 - \left(p_2 - \frac{n}{2}\right)^2 + \varepsilon(p_1 + p_2) - 2\varepsilon \max\{p_1 + p_2 - n, 0\} \right),$$

so the function $f(p_1, p_2)$ is concave in both variables as before. Thus, we deduce that the possible configurations in which the minimum is achieved are the same as in (8.2.38). By direct computation, the minimum is attained at $(p_1^*, p_2^*) = (n,0)$ and $(p_1^*, p_2^*) = (0,n)$, which correspond to the configuration $C(n,0,0) \equiv \pm\mathbf{1}$ and $C(0,n,0) \equiv \mp\mathbf{1}$, respectively. □

Proof of Proposition 8.2.8. Consider a configuration $\sigma \in C(p_1, p_2, a)$, with $0 \leqslant p_1, p_2 \leqslant n$ and $\max\{p_1 + p_2 - n, 0\} \leqslant a \leqslant \min\{p_1, p_2\}$. Note that such a configuration σ can communicate via one step of the dynamics with a configuration σ' such that

$$\sigma' \in \begin{cases} C(p_1+1, p_2, a) & \text{if } p_1 \neq n \text{ and } a > \max\{p_1+p_2-n, 0\}, \\ C(p_1, p_2+1, a) & \text{if } p_2 \neq n \text{ and } a > \max\{p_1+p_2-n, 0\}, \\ C(p_1+1, p_2, a+1) & \text{if } p_1 \neq n \text{ and } a = \max\{p_1+p_2-n, 0\}, \\ C(p_1, p_2+1, a+1) & \text{if } p_2 \neq n \text{ and } a = \max\{p_1+p_2-n, 0\}, \\ C(p_1-1, p_2, a) & \text{if } p_1 \neq 0 \text{ and } a < \min\{p_1, p_2\} \text{ or } p_1 > p_2 \text{ and } a = \min\{p_1, p_2\}, \\ C(p_1, p_2-1, a) & \text{if } p_2 \neq 0 \text{ and } a < \min\{p_1, p_2\} \text{ or } p_2 > p_1 \text{ and } a = \min\{p_1, p_2\}, \\ C(p_1-1, p_2, a-1) & \text{if } p_1 \neq 0,\ p_1 \leqslant p_2 \text{ and } a = \min\{p_1, p_2\}, \\ C(p_1, p_2-1, a-1) & \text{if } p_2 \neq 0,\ p_2 \leqslant p_1 \text{ and } a = \min\{p_1, p_2\}. \end{cases} \tag{8.2.39}$$

In other words, σ' is a configuration obtained from σ via either an up–flip or a down–flip in one of the two clusters. First, we will prove that if $\sigma \in C(p_1, p_2, a) \setminus \{-\mathbf{1}, \mp\mathbf{1}, \pm\mathbf{1}, +\mathbf{1}\}$, then $\widetilde{H}(\sigma') - \widetilde{H}(\sigma) < 0$, with σ' one of the configurations described in (8.2.39). To this end, we consider the following cases.

A. $p_1 = n$ and $a \geqslant \max\{p_1 + p_2 - n, 0\}$;
B. $p_1 \neq n$ and $a > \max\{p_1 + p_2 - n, 0\}$;
C. $p_1 \neq n$ and $a = \max\{p_1 + p_2 - n, 0\}$.

Case A. Since it is not possible to have $p_1 = n$ and $a > \max\{p_1 + p_2 - n, 0\}$, we note that now $\sigma \in C(n, p_2, p_2)$. Since $\sigma \notin \{+\mathbf{1}, \pm\mathbf{1}\}$, it follows that $0 < p_2 < n$. By using Lemma 8.1.11, we deduce that

$$\widetilde{H}(C(n, p_2+1, p_2+1)) - \widetilde{H}(C(n, p_2, p_2)) < 0 \iff p_2 \geqslant \left\lceil \frac{n-1}{2} - \frac{\varepsilon}{2} \right\rceil. \tag{8.2.40}$$

Thus, if p_2 satisfies (8.2.40), then we are done. Otherwise, by using Lemma 8.1.12 we deduce that $\widetilde{H}(C(n, p_2-1, p_2-1)) - \widetilde{H}(C(n, p_2, p_2)) < 0$.

Case B. By using Lemma 8.1.11, we deduce that

$$\widetilde{H}(C(p_1+1, p_2, a)) - \widetilde{H}(C(p_1, p_2, a)) < 0 \iff p_1 \geqslant \left\lceil \frac{n-1}{2} + \frac{\varepsilon}{2} \right\rceil. \tag{8.2.41}$$

Thus, if p_1 satisfies (8.2.41), then we are done. Otherwise, we argue as follows. First, we note that the case $p_1 = 0$ implies $a = 0$, but this case is not allowed since $a > \max\{p_1 + p_2 - n, 0\}$.

If $p_1 > p_2$, we get $\widetilde{H}(\sigma') - \widetilde{H}(\sigma) < 0$ with σ' belonging to $C(p_1 - 1, p_2, a)$. Indeed, by using Lemma 8.1.12, we have that

$$\widetilde{H}(C(p_1-1, p_2, a)) - \widetilde{H}(C(p_1, p_2, a)) < 0, \tag{8.2.42}$$

since $p_1 \leqslant \left\lfloor \frac{n-1}{2} + \frac{\varepsilon}{2} \right\rfloor$.

If $p_1 \leqslant p_2$, we get $\widetilde{H}(\sigma') - \widetilde{H}(\sigma) < 0$ with σ' belonging to $C(p_1 - 1, p_2, a - 1)$. Indeed, by using Lemma 8.1.12, we have that

$$\widetilde{H}(C(p_1-1, p_2, a-1)) - \widetilde{H}(C(p_1, p_2, a)) < 0 \tag{8.2.43}$$

since $p_1 \leqslant \left\lfloor \frac{n-1}{2} + \frac{\varepsilon}{2} \right\rfloor$.

Case C. First of all, we note that if $p_2 = n$ then we repeat the argument as in case A. Thus, we assume $p_2 \neq n$. By using Lemma 8.1.11, we deduce that

$$\widetilde{H}(C(p_1+1, p_2, a+1)) - \widetilde{H}(C(p_1, p_2, a)) < 0 \iff p_1 \geqslant \left\lceil \frac{n-1}{2} - \frac{\varepsilon}{2} \right\rceil, \tag{8.2.44}$$

$$\widetilde{H}(C(p_1, p_2+1, a+1)) - \widetilde{H}(C(p_1, p_2, a)) < 0 \iff p_2 \geqslant \left\lceil \frac{n-1}{2} - \frac{\varepsilon}{2} \right\rceil. \tag{8.2.45}$$

Thus, if p_1 satisfies (8.2.44) or p_2 satisfies (8.2.45), then we are done. Otherwise, $a = \max\{p_1 + p_2 - n, 0\} = 0$ and we have $p_1 \neq 0$ or $p_2 \neq 0$ since $\sigma \neq -\mathbf{1}$. Without loss of generality, we suppose $p_1 \neq 0$ and we apply Lemma 8.1.12. We obtain

$$\widetilde{H}(C(p_1 - 1, p_2, a)) - \widetilde{H}(C(p_1, p_2, a)) < 0, \tag{8.2.46}$$

since $p_1 \leqslant \left\lfloor \frac{n-1}{2} - \frac{\varepsilon}{2} \right\rfloor$.

Thus, we proved that the stability level for every configuration different from $-\mathbf{1}$, $\mp\mathbf{1}$, $\pm\mathbf{1}$ and $+\mathbf{1}$ is zero. It remains to show that $\mathcal{X}^m = \{\pm\mathbf{1}, \mp\mathbf{1}\}$ (resp. $\mathcal{X}^m = \{-\mathbf{1}, +\mathbf{1}\}$) if $0 < \varepsilon \leqslant 1$ (resp. $-1 \leqslant \varepsilon < 0$) and to compute the maximal stability level Γ_m. In the case $\varepsilon = 0$, all these states have the same energy and therefore there is no metastable state.

In the case $\varepsilon > 0$, we have $\mathcal{X}^s = \{-\mathbf{1}, +\mathbf{1}\}$. By considering the part of the path $\bar{\omega} : -\mathbf{1} \to +\mathbf{1}$ defined in (8.2.1) connecting $\pm\mathbf{1}$ to $+\mathbf{1}$, and by using (8.2.3), we deduce that

$$\Gamma_m \leqslant \begin{cases} \frac{n^2}{2} - \varepsilon n & \text{if } n \text{ is even,} \\ \frac{n^2-1}{2} - \varepsilon(n-1) & \text{if } n \text{ is odd.} \end{cases}$$

In order to prove also the reverse inequality, we argue as in the proof of [90, eq. (3.86)]. The case $\varepsilon < 0$ can be treated in a similar way. Thus, we get the claim. □

8.2.4 *Asymptotic behavior of the tunneling time*

In this section, we prove Theorem 8.1.2. Recalling (8.2.34), we observe that in all above cases $\Gamma_s - \Gamma_m = 2n|\varepsilon| > 0$ in the case $\varepsilon \neq 0$, which means that the corresponding energy landscape exhibits the absence of deep cycles. In the case $\varepsilon = 0$, we deduce that $\Gamma_s - \Gamma_m = 0$, indeed all the states $\{+\mathbf{1}, \pm\mathbf{1}, \mp\mathbf{1}, -\mathbf{1}\}$ are stable. Thanks to [92, Lemma 3.6], we deduce that for our model the quantity $\tilde{\Gamma}(B)$, with $B \subsetneq \mathcal{X}$, defined in [92, eq. (21)] is such that $\tilde{\Gamma}(\mathcal{X} \setminus \{s_2\}) = \Gamma_s$. Moreover, thanks to the property of absence of deep cycles, [92, Proposition 3.18] implies that $\Theta(s_1, s_2) = \Gamma_s$ for $s_1, s_2 \in \mathcal{X}^s$. Thus, Theorem 8.1.2(i) follows from [92, Corollary 3.16]. Moreover, Theorem 8.1.2(ii) follows from [92, Theorem 3.17] provided that [92, Assumption A] is satisfied: this is implied by the absence of deep cycles and [92, Proposition 3.18]. Finally, Theorem 8.1.2(iii) follows from [92, Theorem 3.19] provided that [92, Assumption B] is satisfied: this is implied by the absence of deep cycles and the argument carried out in [92, Example 4]. theorem 8.1.2(iv) follows from [92, Proposition 3.24] with $\tilde{\Gamma}(\mathcal{X} \setminus \{s_2\}) = \Gamma_s$ for any $s_2 \in \mathcal{X}^s$.

8.2.5 *Gate for the tunneling transition*

In this section, we prove Theorem 8.1.4. If $0 \leqslant \varepsilon \leqslant 1$ (resp. $-1 \leqslant \varepsilon < 0$), consider an optimal path $\omega \in (-\mathbf{1} \to +\mathbf{1})_{opt}$ (resp. $\omega \in (\pm\mathbf{1} \to \mp\mathbf{1})_{opt}$). Since any path from $-\mathbf{1}$ to $+\mathbf{1}$ (resp. from $\pm\mathbf{1}$ to $\mp\mathbf{1}$) has to cross each manifold $C(p)$, with $0 \leqslant p \leqslant 2n$ (resp. either $0 \leqslant p \leqslant n$ or $n \leqslant p \leqslant 2n$), and due to the optimality of the path ω, by Propositions 8.2.4 and 8.2.5 we get the claim.

8.3 PROOF OF THE MAIN RESULTS: CASE $h > 0$

8.3.1 *Reference paths*

If $\varepsilon \geqslant 0$, consider the path $\bar{\omega}$ defined in Definition 8.2.1.

Definition 8.3.1 (Reference paths). *If $0 < h < -\varepsilon \leqslant 1$, we define $\check{\omega} : \pm\mathbf{1} \to \mp\mathbf{1}$ as the path $(\check{\omega}_k)_{k=0}^{2n}$, with*

$$\check{\omega}_k \in C(n-k, 0, 0) \text{ and } \check{\omega}_{n+k} \in C(0, k, 0), \quad \text{for any } k = 0, \dots, n. \tag{8.3.1}$$

If $0 < -\varepsilon < h \leqslant 1$, we define $\tilde{\omega} : \pm\mathbf{1} \to +\mathbf{1}$ as the path $(\tilde{\omega}_k)_{k=0}^{n}$, with

$$\tilde{\omega}_k \in C(n, k, k), \quad \text{for any } k = 0, \dots, n. \tag{8.3.2}$$

See Figure 1.42 (resp. Figure 1.43) to visualize the reference path $\check{\omega}$ (resp. $\bar{\omega}$).

Lemma 8.3.2 (Maximal energy along the reference paths). *If $\varepsilon \geqslant 0$, let $\bar{\omega} : -\mathbf{1} \to +\mathbf{1}$ the path defined in Definition 8.2.1. Then*

$$\Phi_{\bar{\omega}} = \begin{cases} \widetilde{H}(\bar{\omega}_{\frac{n}{2}}) = n - \frac{n^2}{2} + hn & \text{if } n \text{ is even,} \\ \widetilde{H}(\bar{\omega}_{\frac{n+1}{2}}) = n - \frac{n^2+1}{2} + \varepsilon + h(n-1) & \text{if } n \text{ is odd and } 0 < h \leqslant \varepsilon \leqslant 1, \\ \widetilde{H}(\bar{\omega}_{\frac{n-1}{2}}) = n - \frac{n^2+1}{2} - \varepsilon + h(n+1) & \text{if } n \text{ is odd and } 0 \leqslant \varepsilon < h \leqslant 1. \end{cases} \tag{8.3.3}$$

If $0 < h < -\varepsilon \leqslant 1$, let $\check{\omega} : \pm\mathbf{1} \to \mp\mathbf{1}$ be the path given in (8.3.1). Then,

$$\Phi_{\check{\omega}} = \begin{cases} \widetilde{H}(\check{\omega}_{\frac{n}{2}}) = \widetilde{H}(\check{\omega}_{\frac{3n}{2}}) = n - \frac{n^2}{2} + hn & \text{if } n \text{ is even and } 0 < h - \varepsilon < 1, \\ \widetilde{H}(\check{\omega}_{\frac{n+2}{2}}) = \widetilde{H}(\check{\omega}_{\frac{3n-2}{2}}) = n - \frac{n^2+4}{2} - 2\varepsilon + h(n+2) & \text{if } n \text{ is even and } 1 \leqslant h - \varepsilon < 2, \\ \widetilde{H}(\check{\omega}_{\frac{n+1}{2}}) = \widetilde{H}(\check{\omega}_{\frac{3n-1}{2}}) = n - \frac{n^2+1}{2} - \varepsilon + h(n+1) & \text{if } n \text{ is odd.} \end{cases} \tag{8.3.4}$$

If $0 < -\varepsilon < h \leqslant 1$, let $\tilde{\omega} : \pm\mathbf{1} \to +\mathbf{1}$ be the path given in (8.3.2). Then,

$$\Phi_{\tilde{\omega}} = \begin{cases} \widetilde{H}(\tilde{\omega}_{\frac{n}{2}}) = n - \frac{n^2}{2} - hn & \text{if } n \text{ is even,} \\ \widetilde{H}(\tilde{\omega}_{\frac{n-1}{2}}) = n - \frac{n^2+1}{2} + \varepsilon - h(n-1) & \text{if } n \text{ is odd.} \end{cases} \tag{8.3.5}$$

Proof. From (8.1.21) and (8.2.1), we have

$$\begin{aligned} \widetilde{H}(\bar{\omega}_k) &= -n^2 + n + 2kn - 2k^2 + 2k\varepsilon - n\varepsilon - 2h(k-n), \\ \widetilde{H}(\bar{\omega}_{n+k}) &= -n^2 + n + 2kn - 2k^2 - 2k\varepsilon + n\varepsilon - 2hk, \end{aligned} \tag{8.3.6}$$

for any $k = 0, \dots, n$. By deriving both equations in (8.3.6) with respect to k, we have that the maxima of the energy along the path $\bar{\omega}$ are $\widetilde{H}(\bar{\omega}_{\frac{n+\varepsilon-h}{2}})$ and $\widetilde{H}(\bar{\omega}_{n+\frac{n-\varepsilon-h}{2}})$. This means that on the first part of the path $(\bar{\omega}_k)_{k=0}^n$ the maximum is reached at the critical value $k_1^* = \frac{n+\varepsilon-h}{2}$, while on the second part of the path $(\bar{\omega}_{k+n})_{k=0}^n$ the maximum is reached at the critical value $k_2^* = \frac{n-\varepsilon-h}{2}$.

First, consider the case $0 < h \leqslant \varepsilon \leqslant 1$. Let us focus on the value k_1^*. Note that $\widetilde{H}(\bar{\omega}_k)$ is a concave parabola in k, which is symmetric with respect to k_1^*. Since we are interested in finding the integer value of k in which this maximum is achieved, we need to compare the distances $k_1^* - \lfloor k_1^* \rfloor$ and $\lceil k_1^* \rceil - k_1^*$. The minimal distance indicates the value we are interested in. Since $0 \leqslant \varepsilon - h < 1$, we have that

$$\begin{aligned} \lfloor k_1^* \rfloor &= \begin{cases} \frac{n}{2} & \text{if } n \text{ is even,} \\ \frac{n-1}{2} & \text{if } n \text{ is odd,} \end{cases} \\ \lceil k_1^* \rceil &= \begin{cases} \frac{n}{2} + 1 & \text{if } n \text{ is even,} \\ \frac{n+1}{2} & \text{if } n \text{ is odd,} \end{cases} \end{aligned} \tag{8.3.7}$$

and

$$\begin{aligned} \lfloor k_2^* \rfloor &= \begin{cases} \frac{n}{2} - 1 & \text{if } n \text{ is even,} \\ \frac{n-1}{2} & \text{if } n \text{ is odd and } 0 < \varepsilon + h \leqslant 1, \\ \frac{n-3}{2} & \text{if } n \text{ is odd and } 1 < \varepsilon + h \leqslant 2, \end{cases} \\ \lceil k_2^* \rceil &= \begin{cases} \frac{n}{2} & \text{if } n \text{ is even,} \\ \frac{n+1}{2} & \text{if } n \text{ is odd and } 0 < \varepsilon + h \leqslant 1, \\ \frac{n-1}{2} & \text{if } n \text{ is odd and } 1 < \varepsilon + h \leqslant 2. \end{cases} \end{aligned} \tag{8.3.8}$$

Assume n even. Since $\lfloor \frac{n+\varepsilon-h}{2} \rfloor = \frac{n}{2}$ and $\lceil \frac{n+\varepsilon-h}{2} \rceil = \frac{n}{2}+1$, we have that $k_1^* - \lfloor k_1^* \rfloor = \frac{\varepsilon-h}{2} \leqslant 1 - \frac{\varepsilon-h}{2} = \lceil k_1^* \rceil - k_1^*$ and therefore the maximum is achieved in $\widetilde{H}(\bar{\omega}_{\frac{n}{2}})$. By arguing similarly for n odd and for k_2^*, we get the claim.

Consider now the case $0 \leqslant \varepsilon < h \leqslant 1$. By arguing as before, we get the claim.

Consider now the case $0 < h < -\varepsilon \leqslant 1$. From (8.1.21) and (8.3.1), we have

$$\begin{aligned} \widetilde{H}(\check{\omega}_k) &= -n^2 + n + 2kn - 2k^2 - 2k\varepsilon + n\varepsilon + 2hk, \\ \widetilde{H}(\check{\omega}_{n+k}) &= -n^2 + n + 2kn - 2k^2 + 2k\varepsilon - n\varepsilon - 2h(k-n), \end{aligned} \tag{8.3.9}$$

for any $k = 0, \dots, n$. By deriving both equations in (8.3.9) with respect to k, we have that the maxima of the energy along the path $\check{\omega}$ are $\widetilde{H}(\check{\omega}_{\frac{n-\varepsilon+h}{2}})$ and $\widetilde{H}(\check{\omega}_{n+\frac{n+\varepsilon-h}{2}})$. This means that on the first part of the path $(\check{\omega}_k)_{k=0}^n$ the maximum is reached at the critical value $k_1^* = \frac{n-\varepsilon+h}{2}$, while on the second part of the path $(\check{\omega}_{k+n})_{k=0}^n$ the maximum is reached at the critical value $k_2^* = \frac{n+\varepsilon-h}{2}$. We have that

$$\begin{aligned} \lfloor k_1^* \rfloor &= \begin{cases} \frac{n}{2} & \text{if } n \text{ is even,} \\ \frac{n-1}{2} & \text{if } n \text{ is odd and } 0 < h-\varepsilon < 1, \\ \frac{n+1}{2} & \text{if } n \text{ is odd and } 1 \leqslant h-\varepsilon < 2, \end{cases} \\ \lceil k_1^* \rceil &= \begin{cases} \frac{n+2}{2} & \text{if } n \text{ is even,} \\ \frac{n+1}{2} & \text{if } n \text{ is odd and } 0 < h-\varepsilon < 1, \\ \frac{n+3}{2} & \text{if } n \text{ is odd and } 1 \leqslant h-\varepsilon < 2, \end{cases} \end{aligned} \tag{8.3.10}$$

and

$$\begin{aligned} \lfloor k_2^* \rfloor &= \begin{cases} \frac{n-2}{2} & \text{if } n \text{ is even,} \\ \frac{n-1}{2} & \text{if } n \text{ is odd and } 0 < h-\varepsilon \leqslant 1, \\ \frac{n-3}{2} & \text{if } n \text{ is odd and } 1 \leqslant h-\varepsilon < 2, \end{cases} \\ \lceil k_2^* \rceil &= \begin{cases} \frac{n}{2} & \text{if } n \text{ is even,} \\ \frac{n+1}{2} & \text{if } n \text{ is odd and } 0 < h-\varepsilon \leqslant 1, \\ \frac{n-1}{2} & \text{if } n \text{ is odd and } 1 \leqslant h-\varepsilon < 2. \end{cases} \end{aligned} \tag{8.3.11}$$

By arguing as above, we get the claim.

Consider now the case $0 < -\varepsilon < h \leqslant 1$. From (8.1.21) and (8.3.2), we have

$$\widetilde{H}(\tilde{\omega}_k) = -n^2 + n + \varepsilon n - 2k^2 + 2nk - 2\varepsilon k - 2hk. \tag{8.3.12}$$

By deriving the equation in (8.3.12) with respect to k, we have that the maximum of the energy along the path $\tilde{\omega}$ is $\widetilde{H}(\tilde{\omega}_{\frac{n-\varepsilon-h}{2}})$. By arguing as before, we get the claim. □

Proposition 8.3.3 (Upper bounds). *Let $(\mathcal{X}, Q, \widetilde{H}, \Delta)$ be the energy landscape corresponding to the Ising model on $\mathcal{G}(2,n)$. In the case $0 \leqslant \varepsilon \leqslant 1$, we have $\Gamma_m \leqslant \Gamma_m^1$, where Γ_m^1 is defined in (8.1.12). In the case $0 < -\varepsilon < h \leqslant 1$, we have $\Gamma_m \leqslant \Gamma_m^2$, where Γ_m^2 is defined in (8.1.13). In the case $0 < h < -\varepsilon \leqslant 1$, we have $\Gamma_s \leqslant \Gamma_s^h$, where Γ_s^h is defined in (8.1.14).*

Proof. By using (8.1.9) and Lemma 8.3.2, we get the claim. □

8.3.2 *Lower bounds*

Proposition 8.3.4 (Local minima). *For every $n \geqslant 2$ and $|\varepsilon| \leqslant 1$, regardless the sign of ε, the minimum value of the energy $\widetilde{H}$ on the manifold $\mathcal{C}(p)$ is given by*

$$\widetilde{H}(p) := \min_{\sigma \in \mathcal{C}(p)} \widetilde{H}(\sigma) = \begin{cases} n - (p-n)^2 - p^2 - \varepsilon(n-2p) - 2h(p-n) & \text{if } 0 \leqslant p \leqslant n, \\ n - (2n-p)^2 - (p-n)^2 - \varepsilon(2p-3n) - 2h(p-n) & \text{if } n \leqslant p \leqslant 2n. \end{cases}$$

Furthermore, if $0 \leqslant p \leqslant n$, *the minimum is achieved on the subsets* $C(p,0,0)$ *and* $C(0,p,0)$, *while if* $n \leqslant p \leqslant 2n$, *the minimum is achieved on the subsets* $C(n,p-n,p-n)$ *and* $C(p-n,n,p-n)$.

Proof. Note that on the manifold $C(p)$, with $0 \leqslant p \leqslant 2n$, the energy contribution of the external magnetic field is equal to $-2h(p-n)$, which is constant. Thus the claim simply follows by Proposition 8.2.4 by adding this further term to the energy. □

In order to analyze the manifold $C(p)$ with maximal energy, we need to define

$$p_1^* := \begin{cases} \frac{n}{2} & \text{if } n \text{ is even,} \\ \frac{n+1}{2} & \text{if } n \text{ is odd and } 0 < h \leqslant \varepsilon \leqslant 1, \\ \frac{n-1}{2} & \text{if } n \text{ is odd and } 0 \leqslant \varepsilon < h \leqslant 1, \end{cases} \tag{8.3.13}$$

and

$$p_2^* := \begin{cases} \frac{3n}{2} & \text{if } n \text{ is even,} \\ \frac{3n-1}{2} & \text{if } n \text{ is odd,} \end{cases} \tag{8.3.14}$$

and

$$p_3^* := \begin{cases} \frac{n}{2} & \text{if } n \text{ is even and } 0 < h-\varepsilon < 1, \\ \frac{n-2}{2} & \text{if } n \text{ is even and } 1 \leqslant h-\varepsilon < 2, \\ \frac{n-1}{2} & \text{if } n \text{ is odd.} \end{cases} \tag{8.3.15}$$

In the following proposition, depending on the values of the parameters ε and h, we calculate the maximum of the energy over different collections of manifolds $\mathcal{M}_p$, since the relevant starting and target configurations are not always $+\mathbf{1}$ and $-\mathbf{1}$.

Proposition 8.3.5 (Lower bounds). *Let* $(\mathcal{X}, Q, \widetilde{H}, \Delta)$ *be the energy landscape corresponding to the Ising model on* $\mathcal{G}(2,n)$. *The following statements hold:*

- *If* $0 \leqslant \varepsilon \leqslant 1$, *the maximum of the energy on* $\bigcup_{0\leqslant p\leqslant 2n} \mathcal{M}_p$ *is realized by the configurations in* $C(p_1^*,0,0) \cup C(0,p_1^*,0)$. *Moreover, we have that* $\Gamma_m \geqslant \Gamma_m^1$, *where* Γ_m^1 *is defined in* (8.1.12);
- *If* $0 < -\varepsilon < h \leqslant 1$, *the maximum of the energy on* $\bigcup_{n\leqslant p\leqslant 2n} \mathcal{M}_p$ *is realized by the configurations in* $C(n,p_2^*-n,p_2^*-n) \cup C(p_2^*-n,n,p_2^*-n)$. *Moreover, we have that* $\Gamma_m \geqslant \Gamma_m^2$, *where* Γ_m^2 *is defined in* (8.1.13);
- *If* $0 < h < -\varepsilon \leqslant 1$, *the maximum of the energy on* $\bigcup_{0\leqslant p\leqslant 2n} \mathcal{M}_p$ *is realized by the configurations in* $C(p_3^*,0,0) \cup C(0,p_3^*,0)$. *Moreover, we have that* $\Gamma_s \geqslant \Gamma_s^h$, *where* Γ_s^h *is defined in* (8.1.14).

Proof. The idea of the proof is to identify, depending on the parity of n and the values of ε and h, the correct manifold that would give the desired lower bound.

Treating $\widetilde{H}(p)$ as a function of a continuous variable, we see that is concave and, solving for $\frac{d}{dp}\widetilde{H}(p) = 0$, we obtain two stationary points $p_{\text{left}} = \frac{n}{2} + \frac{\varepsilon-h}{2}$ and $p_{\text{right}} = \frac{3n}{2} - \frac{\varepsilon+h}{2}$. Since p_{left} and p_{right} can only take integer values, we deduce that the possible integer optimal values are

$$p_{\text{left}}^* \in \left\{ \left\lfloor \frac{n}{2} + \frac{\varepsilon-h}{2} \right\rfloor, \left\lceil \frac{n}{2} + \frac{\varepsilon-h}{2} \right\rceil \right\}, \quad p_{\text{right}}^* \in \left\{ \left\lfloor \frac{3n}{2} - \frac{\varepsilon+h}{2} \right\rfloor, \left\lceil \frac{3n}{2} - \frac{\varepsilon+h}{2} \right\rceil \right\}.$$

If $0 \leqslant \varepsilon \leqslant 1$ (resp. $0 < h < -\varepsilon \leqslant 1$), since the path from $m \in \mathcal{X}^m$ to $s \in \mathcal{X}^s$ (resp. from $s_1 \in \mathcal{X}^s$ to $s_2 \in \mathcal{X}^s$) has to cross each manifold $C(p)$, with $0 \leqslant p \leqslant 2n$, we need to take into account both p_{left}^* and p_{right}^*. We have that

$$\begin{aligned} \widetilde{H}(C(\tfrac{n}{2} + \tfrac{\varepsilon-h}{2})) &= n - \tfrac{n^2}{2} + nh + \tfrac{1}{2}(\varepsilon-h)^2, \\ \widetilde{H}(C(\tfrac{3n}{2} - \tfrac{\varepsilon+h}{2})) &= n - \tfrac{n^2}{2} - nh + \tfrac{1}{2}(\varepsilon+h)^2. \end{aligned}$$

By direct computation, we deduce that the maximum is reached in $\widetilde{H}(C(\frac{n}{2} + \frac{\varepsilon-h}{2}))$. By performing the same computations in the proof of Lemma 8.3.2, we obtain that $p_{\text{left}}^* = p_1^*$

(resp. $p^*_{\text{left}} = p^*_3$) in the case $0 \leqslant \varepsilon \leqslant 1$ (resp. $0 < h < -\varepsilon \leqslant 1$), where p^*_1 (resp. p^*_3) is defined in (8.3.13) (resp. (8.3.15)). Furthermore, by Proposition 8.3.4 we have that the minimum of the energy on the manifold $C(p^*_1)$ (resp. $C(p^*_3)$) is realized in $\mathcal{M}_{p^*_1} \equiv C(p^*_1, 0, 0) \cup C(0, p^*_1, 0)$ (resp. in $\mathcal{M}_{p^*_3} \equiv C(p^*_3, 0, 0) \cup C(0, p^*_3, 0)$) if $0 \leqslant \varepsilon \leqslant 1$ (resp. $0 < h < -\varepsilon \leqslant 1$).

Consider now the case $0 < -\varepsilon < h \leqslant 1$. In this case, since for any $m \in \{\pm \mathbf{1}, \mp \mathbf{1}\}$ we are interested in the transition from m to $+\mathbf{1}$, we have that every path connecting these two states crosses the foliations $C(p)$ with $n \leqslant p \leqslant 2n$. Thus in this case we have that the critical value of p is

$$p^*_{\text{right}} \in \left\{ \left\lfloor \frac{3n}{2} - \frac{\varepsilon + h}{2} \right\rfloor, \left\lceil \frac{3n}{2} - \frac{\varepsilon + h}{2} \right\rceil \right\}.$$

By performing the same computations in the proof of Lemma 8.3.2, we obtain that $p^*_{\text{right}} = p^*_2$, where p^*_2 is defined in (8.3.14). Furthermore, by Proposition 8.3.4 we have that the minimum of the energy on the manifold $C(p^*_2)$ is realized in $\mathcal{M}_{p^*_2} \equiv C(n, p^*_2 - n, p^*_2 - n) \cup C(p^*_2 - n, n, p^*_2 - n)$. Thus, we get the claim. □

Corollary 8.3.6 (Maximal energy barrier). *Let $(\mathcal{X}, Q, \widetilde{H}, \Delta)$ be the energy landscape corresponding to the Ising model on $\mathcal{G}(2, n)$. If $0 \leqslant \varepsilon \leqslant 1$, we have that*

$$\Gamma_m = \begin{cases} \frac{n^2}{2} + n(\varepsilon - h) & \text{if } n \text{ is even}, \\ \frac{n^2-1}{2} + (n+1)(\varepsilon - h) & \text{if } n \text{ is odd and } 0 < h \leqslant \varepsilon \leqslant 1, \\ \frac{n^2-1}{2} + (n-1)(\varepsilon - h) & \text{if } n \text{ is odd and } 0 \leqslant \varepsilon < h \leqslant 1. \end{cases} \tag{8.3.16}$$

If $0 < -\varepsilon < h \leqslant 1$, we have that

$$\Gamma_m = \begin{cases} \frac{n^2}{2} - n(\varepsilon + h) & \text{if } n \text{ is even}, \\ \frac{n^2-1}{2} - (n-1)(\varepsilon + h) & \text{if } n \text{ is odd}. \end{cases} \tag{8.3.17}$$

If $0 < h < -\varepsilon \leqslant 1$, we have that

$$\Gamma_s = \begin{cases} \frac{n^2}{2} - n(\varepsilon + h) & \text{if } n \text{ is even}, \\ \frac{n^2-1}{2} - (n+1)(\varepsilon + h) & \text{if } n \text{ is odd}. \end{cases} \tag{8.3.18}$$

Proof. We get the claim by combining Propositions 8.3.3 and 8.3.5. □

8.3.3 *Identification of metastable and stable states*

In this section, we provide the proof of Theorem 8.1.5. To this end, we give two propositions that allow us to accomplish this task. The proof of Propositions 8.3.7 and 8.3.8 are postponed after the proof of Theorem 8.1.5.

Proposition 8.3.7 (Identification of stable states). *Let $(\mathcal{X}, Q, \widetilde{H}, \Delta)$ be the energy landscape corresponding to the Ising model on $\mathcal{G}(2, n)$. If $0 \leqslant \varepsilon \leqslant 1$, Then, the lowest possible energy is equal to*

$$\min_{\sigma \in \mathcal{X}} \widetilde{H}(\sigma) = \begin{cases} -n^2 + n - \varepsilon n - 2hn & \text{if } 0 \leqslant \varepsilon \leqslant 1 \text{ or } 0 < -\varepsilon < h \leqslant 1, \\ -n^2 + n + \varepsilon n & \text{if } 0 < h \leqslant -\varepsilon \leqslant 1, \end{cases} \tag{8.3.19}$$

and the set of stable states is

$$\mathcal{X}^s = \begin{cases} \{+\mathbf{1}\} & \text{if } 0 \leqslant \varepsilon \leqslant 1 \text{ or } 0 < -\varepsilon < h \leqslant 1, \\ \{+\mathbf{1}, \pm \mathbf{1}, \mp \mathbf{1}\} & \text{if } h = -\varepsilon, \\ \{\pm \mathbf{1}, \mp \mathbf{1}\} & \text{if } 0 < h < -\varepsilon \leqslant 1. \end{cases}$$

Proposition 8.3.8 (Identification of metastable states). *Let $(\mathcal{X}, Q, \widetilde{H}, \Delta)$ be the energy landscape corresponding to the Ising model on $\mathcal{G}(2, n)$. Let $\sigma \in \mathcal{X} \setminus \{+\mathbf{1}, \pm\mathbf{1}, \mp\mathbf{1}, -\mathbf{1}\}$, then the stability level of σ is zero, i.e., $V_\sigma = 0$. Furthermore, the set of metastable states is*

$$\mathcal{X}^m = \begin{cases} \{-\mathbf{1}\} & \text{if } 0 \leqslant \varepsilon \leqslant 1 \text{ or } h = -\varepsilon, \\ \{\pm\mathbf{1}, \mp\mathbf{1}\} & \text{if } 0 < -\varepsilon < h \leqslant 1, \\ \{+\mathbf{1}\} & \text{if } 0 < h < -\varepsilon \leqslant 1. \end{cases}$$

Moreover, in the case $0 \leqslant \varepsilon \leqslant 1$, we have that

$$\Gamma_m = \begin{cases} \frac{n^2}{2} + n(\varepsilon - h) & \text{if } n \text{ is even}, \\ \frac{n^2-1}{2} + (n+1)(\varepsilon - h) & \text{if } n \text{ is odd and } 0 < h \leqslant \varepsilon \leqslant 1, \\ \frac{n^2-1}{2} + (n-1)(\varepsilon - h) & \text{if } n \text{ is odd and } 0 \leqslant \varepsilon < h \leqslant 1, \end{cases} \tag{8.3.20}$$

whereas in the case $0 < -\varepsilon < h \leqslant 1$, we have that

$$\Gamma_m = \begin{cases} \frac{n^2}{2} - n(\varepsilon + h) & \text{if } n \text{ is even}, \\ \frac{n^2-1}{2} - (n-1)(\varepsilon + h) & \text{if } n \text{ is odd}, \end{cases} \tag{8.3.21}$$

and in the case $0 < h < -\varepsilon \leqslant 1$, we have that

$$\Gamma_s = \begin{cases} \frac{n^2}{2} + n(h - \varepsilon) & \text{if } n \text{ is even and } 0 < h - \varepsilon < 1, \\ \frac{n^2-4}{2} + (n+2)(h - \varepsilon) & \text{if } n \text{ is even and } 1 \leqslant h - \varepsilon < 2, \\ \frac{n^2-1}{2} + (n+1)(h - \varepsilon) & \text{if } n \text{ is odd}, \end{cases} \tag{8.3.22}$$

and

$$\Gamma_m = \begin{cases} \frac{n^2}{2} + n(\varepsilon + h) & \text{if } n \text{ is even}, \\ \frac{n^2-1}{2} + (n-1)(\varepsilon + h) & \text{if } n \text{ is odd}. \end{cases} \tag{8.3.23}$$

Proof of Theorem 8.1.5. Combining Corollary 8.3.6, Propositions 8.3.7 and 8.3.8 we get the claim. □

Proof of Proposition 8.3.7. Recalling that $\max\{p_1 + p_2 - n, 0\} \leqslant a \leqslant \min\{p_1, p_2\}$, we note that a is a function of p_1 and p_2. In view of the partition

$$\mathcal{X} = \bigcup_{\substack{0 \leqslant p_1, p_2 \leqslant n \\ \max\{0, p_1 + p_2 - n\} \leqslant a \leqslant \min\{p_1, p_2\}}} C(p_1, p_2, a)$$

and (8.1.21), we can compute the minimum energy as

$$\begin{aligned} \min_{p_1, p_2} H(p_1, p_2, a) &= n - n(\varepsilon - 2h) \\ &\quad + 2 \min_{p_1, p_2} \left(-\left(p_1 - \frac{n}{2}\right)^2 - \left(p_2 - \frac{n}{2}\right)^2 + (\varepsilon - h)(p_1 + p_2) - 2\varepsilon a \right) \\ &=: n - n(\varepsilon - 2h) + 2 \min_{p_1, p_2} f(p_1, p_2). \end{aligned} \tag{8.3.24}$$

If $\varepsilon \geqslant 0$, we have that

$$\min_{p_1, p_2} f(p_1, p_2) = \min_{p_1, p_2} \left(-\left(p_1 - \frac{n}{2}\right)^2 - \left(p_2 - \frac{n}{2}\right)^2 + (\varepsilon - h)(p_1 + p_2) - 2\varepsilon \min\{p_1, p_2\} \right),$$

so the function $f(p_1, p_2)$ is concave in both variables. Thus, we expect the minimum (p_1^*, p_2^*) to be achieved at the boundary of the feasible region. This immediately implies that $(p_1^*, p_2^*) \in \{(0, 0), (0, n), (n, 0), (n, n)\}$. By direct computation, we obtain:

$$f(0, 0) = -\frac{n^2}{2}; \quad f(0, n) = f(n, 0) = -\frac{n^2}{2} + n(\varepsilon - h); \quad f(n, n) = -\frac{n^2}{2} - 2hn. \tag{8.3.25}$$

This implies that the minimum is achieved at $(p_1^*, p_2^*) = (n, n)$, which corresponds to the configuration $C(n, n, n) \equiv +\mathbf{1}$, as claimed.

If $\varepsilon < 0$, we have that

$$\min_{p_1, p_2} f(p_1, p_2) = \min_{p_1, p_2} -\left(p_1 - \frac{n}{2}\right)^2 - \left(p_2 - \frac{n}{2}\right)^2 + (\varepsilon - h)(p_1 + p_2) - 2\varepsilon \max\{p_1 + p_2 - n, 0\},$$

so the function $f(p_1, p_2)$ is concave in both variables as before. Thus, we deduce that the possible configurations in which the minimum is achieved are the same as in (8.3.25). By direct computation, the minimum is attained either at $(p_1^*, p_2^*) = (n, n)$ whenever $h > -\varepsilon$, which corresponds to the configuration $C(n, n, n) \equiv +\mathbf{1}$, or at $(p_1^*, p_2^*) = (n, 0)$ and $(p_1^*, p_2^*) = (0, n)$ whenever $h < -\varepsilon$, which corresponds to the configurations $C(n, 0, 0) \equiv \pm\mathbf{1}$ and $C(0, n, 0) \mp \mathbf{1}$. In the special case $h = -\varepsilon$, all these configurations realize the minimum of the energy. This concludes the proof. □

Proof of Proposition 8.3.8. Let $0 < \varepsilon \leqslant 1$. Consider a configuration $\sigma \in C(p_1, p_2, a)$, with $0 \leqslant p_1, p_2 \leqslant n$ and $\max\{p_1 + p_2 - n, 0\} \leqslant a \leqslant \min\{p_1, p_2\}$. Note that such a configuration σ can communicate via one step of the dynamics with a configuration σ' as in (8.2.39). In other words, σ' is a configuration obtained from σ via either an up-flip or a down-flip in one of the two clusters. First, we will prove that if $\sigma \in C(p_1, p_2, a) \setminus \{-\mathbf{1}, \mp\mathbf{1}, \pm\mathbf{1}, +\mathbf{1}\}$, then $\widetilde{H}(\sigma') - \widetilde{H}(\sigma) < 0$, with σ' one of the configurations described in (8.2.39). To this end, we consider the following cases.

A. $p_1 = n$ and $a \geqslant \max\{p_1 + p_2 - n, 0\}$;
B. $p_1 \neq n$ and $a > \max\{p_1 + p_2 - n, 0\}$;
C. $p_1 \neq n$ and $a = \max\{p_1 + p_2 - n, 0\}$.

Case A. Since it is not possible to have $p_1 = n$ and $a > \max\{p_1 + p_2 - n, 0\}$, we note that now $\sigma \in C(n, p_2, p_2)$. Since $\sigma \notin \{+\mathbf{1}, \pm\mathbf{1}\}$, it follows that $0 < p_2 < n$. By using Lemma 8.1.11, we deduce that

$$\widetilde{H}(C(n, p_2 + 1, p_2 + 1)) - \widetilde{H}(C(n, p_2, p_2)) < 0 \iff p_2 \geqslant \left\lceil \frac{n-1}{2} - \frac{\varepsilon + h}{2} \right\rceil. \tag{8.3.26}$$

Thus, if p_2 satisfies (8.3.26), then we are done. Otherwise, by using Lemma 8.1.12 we deduce that $\widetilde{H}(C(n, p_2 - 1, p_2 - 1)) - \widetilde{H}(C(n, p_2, p_2)) < 0$.

Case B. By using Lemma 8.1.11, we deduce that

$$\widetilde{H}(C(p_1 + 1, p_2, a)) - \widetilde{H}(C(p_1, p_2, a)) < 0 \iff p_1 \geqslant \left\lceil \frac{n-1}{2} + \frac{\varepsilon - h}{2} \right\rceil. \tag{8.3.27}$$

Thus, if p_1 satisfies (8.3.27), then we are done. Otherwise, we argue as follows. First, we note that the case $p_1 = 0$ implies $a = 0$, but this case is not allowed since $a > \max\{p_1 + p_2 - n, 0\}$.

If $p_1 > p_2$, we get $\widetilde{H}(\sigma') - \widetilde{H}(\sigma) < 0$ with σ' belonging to $C(p_1 - 1, p_2, a)$. Indeed, by using Lemma 8.1.12, we have that

$$\widetilde{H}(C(p_1 - 1, p_2, a)) - \widetilde{H}(C(p_1, p_2, a)) < 0, \tag{8.3.28}$$

since $p_1 \leqslant \lfloor \frac{n-1}{2} + \frac{\varepsilon - h}{2} \rfloor$.

If $p_1 \leqslant p_2$, we get $\widetilde{H}(\sigma') - \widetilde{H}(\sigma) < 0$ with σ' belonging to $C(p_1 - 1, p_2, a - 1)$. Indeed, by using Lemma 8.1.12, we have that

$$\widetilde{H}(C(p_1 - 1, p_2, a - 1)) - \widetilde{H}(C(p_1, p_2, a)) < 0, \tag{8.3.29}$$

since $p_1 \leqslant \lfloor \frac{n-1}{2} + \frac{\varepsilon - h}{2} \rfloor$.

Case C. First of all, we note that if $p_2 = n$, then we repeat the argument as in case A. Thus, we assume $p_2 \neq n$. By using Lemma 8.1.11, we deduce that

$$\widetilde{H}(C(p_1 + 1, p_2, a + 1)) - \widetilde{H}(C(p_1, p_2, a)) < 0 \impliedby p_1 \leqslant \left\lceil \frac{n-1}{2} - \frac{\varepsilon + h}{2} \right\rceil, \tag{8.3.30}$$

$$\widetilde{H}(C(p_1, p_2 + 1, a + 1)) - \widetilde{H}(C(p_1, p_2, a)) < 0 \impliedby p_2 \leqslant \left\lceil \frac{n-1}{2} - \frac{\varepsilon + h}{2} \right\rceil. \tag{8.3.31}$$

Thus, if p_1 satisfies (8.3.30) or p_2 satisfies (8.3.31), then we are done. Otherwise, $a = \max\{p_1 + p_2 - n, 0\} = 0$ and we have $p_1 \neq 0$ or $p_2 \neq 0$, since $\sigma \neq -\mathbf{1}$. Without loss of generality, we suppose $p_1 \neq 0$ and we apply Lemma 8.1.12. We obtain

$$\widetilde{H}(C(p_1 - 1, p_2, a)) - \widetilde{H}(C(p_1, p_2, a)) < 0, \tag{8.3.32}$$

since $p_1 \leqslant \lfloor \frac{n-1}{2} - \frac{\varepsilon+h}{2} \rfloor$.

Thus, we have proven that the stability level for every configuration $\sigma \notin \{-\mathbf{1}, \mp\mathbf{1}, \pm\mathbf{1}, +\mathbf{1}\}$ is zero. It remains to identify the set of metastable states and to compute their stability level Γ_m.

In the case $0 \leqslant \varepsilon \leqslant 1$, we have that $\mathcal{X}^s = \{+\mathbf{1}\}$. By considering the path $\bar{\omega} : -\mathbf{1} \to +\mathbf{1}$ defined in (8.2.1), by using (8.2.3), we deduce that

$$\Phi_{\bar{\omega}}(\pm\mathbf{1}, +\mathbf{1}) - \widetilde{H}(\pm\mathbf{1}) < \Phi_{\bar{\omega}}(-\mathbf{1}, +\mathbf{1}) - \widetilde{H}(-\mathbf{1}) \leqslant \Gamma_m, \tag{8.3.33}$$

where Γ_m is as in (8.3.20). In order to prove also the reverse inequality, we argue as in the proof of [90, eq. (3.86)]. Thus, $\mathcal{X}^m = \{-\mathbf{1}\}$.

In the case $0 < -\varepsilon < h \leqslant 1$, we have that $\mathcal{X}^s = \{+\mathbf{1}\}$. By arguing as above, we deduce that now

$$\Phi_{\bar{\omega}}(-\mathbf{1}, +\mathbf{1}) - \widetilde{H}(-\mathbf{1}) < \Phi_{\bar{\omega}}(\pm\mathbf{1}, +\mathbf{1}) - \widetilde{H}(\pm\mathbf{1}) \leqslant \Gamma_m, \tag{8.3.34}$$

where Γ_m is as in (8.3.21). Thus, $\mathcal{X}^m = \{\pm\mathbf{1}, \mp\mathbf{1}\}$.

In the case $0 < h < -\varepsilon \leqslant 1$, we have that $\mathcal{X}^s = \{\pm\mathbf{1}, \mp\mathbf{1}\}$. By considering the part of the path $\check{\omega}$ defined in (8.3.1) connecting $-\mathbf{1}$ to $\mp\mathbf{1}$, and defining the path $\omega^* = (\omega_1^*, ..., \omega_n^*) : +\mathbf{1} \to \mp\mathbf{1}$ as $\omega_k^* \in C(n-k, n, n-k)$ for $k = 0, ..., n$, we deduce that

$$\Phi_{\check{\omega}}(-\mathbf{1}, \mp\mathbf{1}) - \widetilde{H}(-\mathbf{1}) < \Phi_{\omega^*}(+\mathbf{1}, \mp\mathbf{1}) - \widetilde{H}(+\mathbf{1}) \leqslant \Gamma_m, \tag{8.3.35}$$

where Γ_m is as in (8.3.23). To prove also the reverse inequality, we argue as in the proof of [90, eq. (3.86)]. Thus, $\mathcal{X}^m = \{+\mathbf{1}\}$. □

8.3.4 *Asymptotic behavior of the tunneling time*

In this section, we prove Theorem 8.1.6. We recall (8.3.23). Note that in the case $0 < h < -\varepsilon \leqslant 1$, for which we are interested in studying the tunneling time for the transition from s_1 to s_2, where $s_1, s_2 \in \{\pm\mathbf{1}, \mp\mathbf{1}\}$, we have that

$$\Gamma_s - \Gamma_m = \begin{cases} -2n\varepsilon & \text{if } n \text{ is even and } 0 < h - \varepsilon < 1, \\ -2(1 + n\varepsilon - h + \varepsilon) & \text{if } n \text{ is even and } 1 \leqslant h - \varepsilon < 1, \\ -2(n\varepsilon - h) & \text{if } n \text{ is odd.} \end{cases}$$

In all the above cases we have that $\Gamma_s - \Gamma_m > 0$ since $\varepsilon < 0$, which means that the corresponding energy landscape exhibits the absence of deep cycles.

Here we are interested in the tunneling time from s_1 to s_2 for any $s_1, s_2 \in \mathcal{X}^s$. Thanks to [92, Lemma 3.6], we deduce that for our model the quantity $\tilde{\Gamma}(B)$, with $B \subsetneq \mathcal{X}$, defined in [92, eq. (21)] is such that $\tilde{\Gamma}(\mathcal{X} \setminus \{s_2\}) = \Gamma_s$. Moreover, thanks to the property of absence of deep cycles, [92, Proposition 3.18] implies that $\Theta(s_1, s_2) = \Gamma_s$ for $s_1, s_2 \in \mathcal{X}^s$. Thus, Theorem 8.1.6(i) follows from [92, Corollary 3.16]. Moreover, Theorem 8.1.6(ii) follows from [92, Theorem 3.17] provided that [92, Assumption A] is satisfied: this is implied by the absence of deep cycles and [92, Proposition 3.18]. Finally, Theorem 8.1.6(iii) follows from [92, Theorem 3.19] provided that [92, Assumption B] is satisfied: this is implied by the absence of deep cycles and the argument carried out in [92, Example 4]. Theorem 8.1.6(iv) follows from [92, Proposition 3.24] with $\tilde{\Gamma}(\mathcal{X} \setminus \{s_2\}) = \Gamma_s$ for any $s_2 \in \mathcal{X}^s$.

8.3.5 *Asymptotic behavior of the transition time*

In this section, we prove Theorem 8.1.7. Here we are interested in studying the transition from a metastable to a stable state. Thus, Theorem 8.1.7 follows from [85, Theorems 4.1, 4.9 and 4.15] together with Theorem 8.1.5 and Corollary 8.3.6. Theorem 8.1.7(iv) follows from [92, Proposition 3.24] with $\tilde{\Gamma}(\mathcal{X} \setminus \{s\}) = \Gamma_m$ for any $s \in \mathcal{X}^s$.

8.3.6 *Gate for the transition*

In this section, we prove Theorem 8.1.9. If $0 \leqslant \varepsilon \leqslant 1$, consider $\omega \in (-\mathbf{1} \to +\mathbf{1})_{\mathrm{opt}}$. Since any path from $-\mathbf{1}$ to $+\mathbf{1}$ has to cross each manifold $C(p)$ with $0 \leqslant p \leqslant 2n$, and due to the optimality of the path ω, by Propositions 8.3.4 and 8.3.5 we get the claim.

If $0 < -\varepsilon < h \leqslant 1$, consider either $\omega \in (\pm\mathbf{1} \to +\mathbf{1})_{\mathrm{opt}}$ or $\omega \in (\mp\mathbf{1} \to +\mathbf{1})_{\mathrm{opt}}$. Since any path from either $\pm\mathbf{1}$, or $\mp\mathbf{1}$, to $+\mathbf{1}$ has to cross each manifold $C(p)$ with $n \leqslant p \leqslant 2n$, and due to the optimality of the path ω, by Propositions 8.3.4 and 8.3.5 we get the claim.

If $0 < h < -\varepsilon \leqslant 1$, consider $\omega \in (\pm\mathbf{1} \to \mp\mathbf{1})_{\mathrm{opt}}$. Since any path from $\pm\mathbf{1}$ to $\mp\mathbf{1}$ has to cross each manifold $C(p)$ with $0 \leqslant p \leqslant n$, due to the optimality of the path ω, by Propositions 8.3.4 and 8.3.5 we get the claim.

Part IV

ASYMPTOTIC PROPERTIES OF RANDOM GRAPHS

9 NORMALITY OF DEGREE COUNTS IN A PA MODEL

In this chapter, we consider the preferential attachment model. This is a growing random graph such that at each step a new vertex is added and forms m connections. The neighbors of the new vertex are chosen at random with probability proportional to their degree. It is well known that the proportion of nodes with a given degree at step n converges to a constant as $n \to \infty$. The goal of this chapter is to investigate the asymptotic distribution of the fluctuations around this limiting value. We prove a central limit theorem for the joint distribution of *all* degree counts. In particular, we give an explicit expression for the asymptotic covariance. This expression is rather complex, so we compute it numerically for various parameter choices. We also use numerical simulations to argue that the convergence is quite fast. The proof relies on the careful construction of an appropriate martingale.

The outline of the chapter is as follows. In Section 9.1, we state our main result and in Section 9.2 we prove it.

9.1 MAIN RESULT

Our main result is the following theorem.

Theorem 9.1.1. *As $s \to \infty$,*

$$\left(\sqrt{s}\Big(\frac{N_k(s,i)}{s} - p_k\Big),\ k = m, m+1, \dots\right) \Rightarrow (Z_k,\ k = m, m+1, \dots), \tag{9.1.1}$$

where $(Z_k,\ k = m, m+1, \dots)$ is a mean zero Gaussian process with covariance function R_Z given by

$$\begin{aligned}
R_Z(r,\ell) \quad &= \frac{(-1)^{r+\ell}}{\Gamma(r+\ell+2m+1+3\delta)} \sum_{q=m}^{\infty} (q+\delta)p_q \Big(b_m^{(\ell)} b_m^{(r)} \Gamma(4m+3\delta)(\ell+r-2m)! \\
&\quad + (-1)^{m+q+1}(b_m^{(\ell)} b_q^{(r)} + b_m^{(r)} b_q^{(\ell)})\Gamma(q+3m+3\delta)(\ell+r-q-m)! \\
&\quad + (-1)^{m+q+1}(b_m^{(\ell)} b_{q+1}^{(r)} + b_m^{(r)} b_{q+1}^{(\ell)})\Gamma(q+3m+1+3\delta)(\ell+r-m-q-1)! \\
&\quad + m b_q^{(\ell)} b_q^{(r)} \Gamma(2q+2m+3\delta)(r+\ell-2q)! \\
&\quad + m(b_q^{(\ell)} b_{q+1}^{(r)} + b_q^{(r)} b_{q+1}^{(\ell)})\Gamma(2q+2m+1+3\delta)(\ell+r-2q-1)! \\
&\quad + m b_{q+1}^{(\ell)} b_{q+1}^{(r)} \Gamma(2q+2m+2+3\delta)(\ell+r-2q-2)! \Big) \\
&\quad - \frac{(2m+\delta)\Gamma(\ell+\delta)\Gamma(r+\delta)}{(\Gamma(m+\delta))^2} \sum_{t_1=m}^{\ell} \sum_{t_2=m}^{r} (-1)^{t_1+t_2} \\
&\quad \times \frac{(t_1+t_2+2m+3\delta)^{-1}(t_1+2+\delta-t_1/m)(t_2+2+\delta-t_2/m)}{(t_1-m)!(t_2-m)!(\ell-t_1)!(r-t_2)!(t_1+2+\delta+\delta/m)(t_2+2+\delta+\delta/m)} \\
&\quad - \frac{(2m+\delta)(m-1)\Gamma(\ell+\delta)\Gamma(r+\delta)}{m^2(\Gamma(m+\delta))^2} \sum_{t_1=m}^{\ell} \sum_{t_2=m}^{r} (-1)^{t_1+t_2} \\
&\quad \times \frac{(\delta+t_1)(\delta+t_2)(t_1+t_2+2m+3\delta)^{-1}}{(t_1-m)!(t_2-m)!(\ell-t_1)!(r-t_2)!(t_1+2+\delta+\delta/m)(t_2+2+\delta+\delta/m)},
\end{aligned} \tag{9.1.2}$$

for $r, \ell \geqslant m$. Here $\Gamma(\cdot)$ is the Gamma function and $b_j^{(k)}$ are given by

$$b_j^{(k)} = \prod_{t=j}^{k-1} \frac{t+\delta}{t-k} = (-1)^{k-j} \frac{\Gamma(k+\delta)}{(k-j)!\Gamma(j+\delta)}, \quad 1 \leqslant j \leqslant k. \tag{9.1.3}$$

When $m = 1$, (9.1.2) reduces to [103, (4.28)], but their covariance functions contains a few minor mistakes. More precisely, in the double sum the term $(2+\delta)^2$ should be $(2+\delta)^3$

and the terms $\Gamma(\ell_1 + 2 + 2\delta)$ and $\Gamma(\ell_2 + 2 + 2\delta)$ should be $(\ell_1 + 2 + 2\delta)$ and $(\ell_2 + 2 + 2\delta)$, respectively.

Since the expression in (9.1.2) is remarkably complicated, we plot it for various parameter choices to help the understanding. In particular, we refer to Figures 1.46–1.49.

Following the argument carried out in [88], we are able to prove a central limit theorem for the vector composed by the rescaled number of vertices with degree greater than k. The argument is explained at the end of Section 1.5.

9.2 PROOF OF THE MAIN RESULT

In order to prove Theorem 9.1.1, we apply the following martingale central limit theorem.

Theorem 9.2.1. *[103] Let* $\{X_{n,m}, \mathcal{F}_{m,n}, 1 \leqslant m \leqslant n\}$, $X_{n,m} = (X_{n,m,1}, ..., X_{n,m,d})^T$ *be a* d*–dimensional square–integrable martingale difference array. Consider the* $d \times d$ *non–negative definite random matrices*

$$G_{n,m} = (\mathbb{E}[X_{n,m,i}X_{n,m,j}|\mathcal{F}_{n,m-1}], i, j = 1, .., d), \quad V_n = \sum_{m=1}^{n} G_{n,m}, \tag{9.2.1}$$

and suppose (A_n) *is a sequence of* $\ell \times d$ *matrices with bounded supremum norm. Assume that*

(1) $A_n V_n A_n^T \xrightarrow{P} \Sigma$ *as* $n \to \infty$ *for some non–random (hence non–negative definite) matrix* Σ*;*

(2) $\sum_{m \leqslant n} \mathbb{E}[X^2 \mathbb{1}_{\{|X_{n,m,i}| > \varepsilon\}} | \mathcal{F}_{n,m-1}] \xrightarrow{P} 0$ *as* $n \to \infty$ *for all* $i = 1, ..., d$ *and* $\varepsilon > 0$.

Then,

$$\sum_{m=1}^{n} A_n X_{n,m} \Rightarrow X \quad \text{as } n \to \infty, \tag{9.2.2}$$

in $\mathbb{R}^\ell$*, where* X *is a mean zero* ℓ*-dimensional Gaussian vector with covariance matrix* Σ*.*

We aim at constructing a martingale by appropriate rescaling of the process

$$N_k(1), N_k(2,1), ..., N_k(2, m-1), N_k(2, m), N_k(3, 1), ...,$$

for all $k \geqslant m$. We have the recursion, for $s \geqslant 2$ and $0 \leqslant i \leqslant m-1$,

$$N_k(s, i+1) = N_k(s, i) - \mathbb{1}_{\{D_{s,i+1}=k\}} + \mathbb{1}_{\{k=m\}}\mathbb{1}_{\{i+1=m\}} + \mathbb{1}_{\{k\neq m\}}\mathbb{1}_{\{D_{s,i+1}=k-1\}}. \tag{9.2.3}$$

The second term on the r.h.s. of (9.2.3) accounts for the possibility that the edge being connected at time $i+1$ connects with some vertex of degree k. The third term on the r.h.s. of (9.2.3) takes into account the new vertex joining at time s, after all of its m edges have been connected, while the fourth term accounts for the possibility that the edge being connected at time $i+1$ might connect with some vertex of degree $k-1$.

If we do not update the degrees during the attachment of a new vertex, but simply at the end of the construction of PA_s starting from PA_{s-1}, it is clear that the relation (9.2.3) changes into

$$\begin{cases} N_k(s, i+1) = N_k(s, i), \ i = 0, .., m-2 \\ N_k(s, m) = N_k(s-1, m) + \sum_{i=0}^{m-2} \left[\mathbb{1}_{\{k=m\}}\mathbb{1}_{\{i+1=m\}} + \mathbb{1}_{\{k\neq m\}}\mathbb{1}_{\{D_{s,i+1}=k-1\}} - \mathbb{1}_{\{D_{s,i+1}=k\}}\right]. \end{cases} \tag{9.2.4}$$

For $s \geqslant 2$ and $0 \leqslant i \leqslant m-1$, let us compute

$$\begin{aligned}
\mathbb{E}[N_j(s,i+1)|\mathcal{F}_{s,i}] &= N_j(s,i) - \mathbb{P}(D_{s,i+1} = j|\mathcal{F}_{s,i}) + \mathbb{1}_{\{j=m\}}\mathbb{1}_{\{i+1=m\}} \\
&\quad + \mathbb{1}_{\{j\neq m\}}\mathbb{P}(D_{s,i+1} = j-1|\mathcal{F}_{s,i}) \\
&= N_j(s,i) - \frac{j+\delta}{s(2m+\delta)-2m+i}N_j(s,i) \\
&\quad + \mathbb{1}_{\{j=m\}}\mathbb{1}_{\{i+1=m\}} + \mathbb{1}_{\{j\neq m\}}\frac{j-1+\delta}{s(2m+\delta)-2m+i}N_{j-1}(s,i) \qquad (9.2.5)\\
&= N_j(s,i)\left(1 - \frac{j+\delta}{s(2m+\delta)-2m+i}\right) \\
&\quad + \mathbb{1}_{\{j\neq m\}}\frac{j-1+\delta}{s(2m+\delta)-2m+i}N_{j-1}(s,i) + \mathbb{1}_{\{j=m\}}\mathbb{1}_{\{i+1=m\}}.
\end{aligned}$$

We set

$$M^{(k)}_{s,i} := a^{(k)}_{s,i}\sum_{j=m}^{k} b^{(k)}_j(N_j(s,i) - \mathbb{E}[N_j(s,i)]), \quad s \geqslant 2,\ 0 \leqslant i \leqslant m. \qquad (9.2.6)$$

We will show that, for each $k \geqslant m$, the process $(M^{(k)}_{s,i})$ is a martingale with respect to the same filtration. To this end, we compute

$$\begin{aligned}
\mathbb{E}[M^{(k)}_{s,i+1}|\mathcal{F}_{s,i}] &= \mathbb{E}\left[a^{(k)}_{s,i+1}\sum_{j=m}^{k} b^{(k)}_j(N_j(s,i+1) - \mathbb{E}[N_j(s,i+1)])\middle|\mathcal{F}_{s,i}\right] \\
&= a^{(k)}_{s,i+1}b^{(k)}_m\Bigg(\Big(1 - \frac{m+\delta}{s(2m+\delta)-2m+i}\Big)N_m(s,i) + \mathbb{1}_{\{i+1=m\}} \\
&\quad - \Big(1 - \frac{m+\delta}{s(2m+\delta)-2m+i}\Big)\mathbb{E}[N_m(s,i)] - \mathbb{1}_{\{i+1=m\}}\Bigg) \\
&\quad + a^{(k)}_{s,i+1}\sum_{j=m+1}^{k} b^{(k)}_j\Bigg(N_j(s,i)\Big(1 - \frac{j+\delta}{s(2m+\delta)-2m+i}\Big) \\
&\quad + \frac{j-1+\delta}{s(2m+\delta)-2m+1}N_{j-1}(s,i) + \Big(1 - \frac{j+\delta}{s(2m+\delta)-2m+i}\Big)\mathbb{E}[N_j(s,i)] \\
&\quad - \frac{j-1+\delta}{s(2m+\delta)-2m+i}\mathbb{E}[N_{j-1}(s,i)]\Bigg) \\
&= a^{(k)}_{s,i+1}\sum_{j=m}^{k}\Bigg(b^{(k)}_j\Big(1 - \frac{j+\delta}{s(2m+\delta)-2m+1}\Big) \\
&\quad + b^{(k)}_{j+1}\frac{j+\delta}{s(2m+\delta)-2m+1}\Bigg)(N_j(s,i) - \mathbb{E}[N_j(s,i)]) \\
&\quad + b^{(k)}_k\Big(1 - \frac{k+\delta}{s(2m+\delta)-2m+i}\Big)(N_k(s,i) - \mathbb{E}[N_k(s,i)]).
\end{aligned} \qquad (9.2.7)$$

This is the same as the right–hand side of (9.2.6) if the following holds:

$$\begin{cases}
a^{(k)}_{s,i+1}\left[b^{(k)}_j\Big(1 - \frac{j+\delta}{s(2m+\delta)-2m+1}\Big) + b^{(k)}_{j+1}\frac{j+\delta}{s(2m+\delta)-2m+i}\right] = a^{(k)}_{s,i}b^{(k)}_j,\ j = m, \ldots, k-1, \\
a^{(k)}_{s,i+1}b^{(k)}_k\Big(1 - \frac{k+\delta}{s(2m+\delta)-2m+i}\Big) = a^{(k)}_{s,i}b^{(k)}_k.
\end{cases} \qquad (9.2.8)$$

Let

$$a^{(k)}_{s,i} := \prod_{t=k-m+1}^{s-1}\prod_{r=0}^{m-1}\left(1 - \frac{k+\delta}{t(2m+\delta)-2m+r}\right)^{-1}\prod_{r=0}^{i-1}\left(1 - \frac{k+\delta}{s(2m+\delta)-2m+r}\right)^{-1}. \qquad (9.2.9)$$

Let also

$$b_j^{(k)} := \prod_{t=j}^{k-1} \frac{t+\delta}{t-k} = (-1)^{k-j} \frac{\Gamma(k+\delta)}{(k-j)!\Gamma(j+\delta)}, \quad 1 \leqslant j \leqslant k. \tag{9.2.10}$$

We adopt the usual convention that $b_k^{(k)} = 1$ and $b_j^{(k)} = 0$ for all $j > k$. Direct calculations show that (9.2.9) and (9.2.10) satisfy the conditions in (9.2.8).

Note that

$$a_{s,i+1}^{(k)} = a_{s,i}^{(k)} \left(1 - \frac{k+\delta}{s(2m+\delta) - 2m + i}\right)^{-1}. \tag{9.2.11}$$

Moreover, by the Stirling formula, as $s \to \infty$,

$$\begin{aligned} a_{s,i}^{(k)} &= \prod_{r=0}^{m-1} \frac{\Gamma\left(s + \frac{r-2m}{2m+\delta}\right) \Big/ \Gamma\left(k-m+1+\frac{r-2m}{2m+\delta}\right)}{\Gamma\left(s + \frac{r-k-\delta-2m}{2m+\delta}\right) \Big/ \Gamma\left(k-m+1+\frac{r-k-\delta-2m}{2m+\delta}\right)} \\ &\quad \times \prod_{r=0}^{i-1} \left(1 - \frac{k+\delta}{s(2m+\delta) - 2m + r}\right)^{-1} \\ &\sim s^{\frac{k+\delta}{2m+\delta}} \prod_{r=0}^{m-1} \frac{\Gamma\left(k-m+1+\dfrac{r-k-\delta-2m}{2m+\delta}\right)}{\Gamma\left(k-m+1+\dfrac{r-2m}{2m+\delta}\right)}, \end{aligned} \tag{9.2.12}$$

so that $s \to a_{s,i}^{(k)}$ is regularly varying with index $(k+\delta)/(2m+\delta)$, where $\sim$ means that the ratio of the left–hand and the right–hand side tends to 1 as $s \to \infty$.

Thus, we have proved that the process $(M_{s,i}^{(k)})$ is a martingale with respect to the filtration $(\mathcal{F}_{s,i-1})$.

Remark 9.2.2. *Note that there is not a unique set of coefficients $a_{s,i}^{(k)}$ and $b_j^{(k)}$ that satisfies (9.2.8). For example, if $a_{s,i}^{(k)}, b_j^{(k)}$ is a solution of (9.2.8), then also $\alpha a_{s,i}^{(k)}, b_j^{(k)}$ is a solution for any $\alpha \in \mathbb{R}$. However, if we require that the boundary conditions for $M_{s,i}^{(k)}$ are satisfied, i.e., $M_{s,m}^{(k)} = M_{s+1,0}^{(k)}$ for any $k \geqslant m$, then (9.2.8) admits a unique solution. This implies that the indexing notations for the processes $N_j(s,i)$ and $M_{s,i}^{(k)}$ are consistent.*

There exists a probability mass function $\{p_k,\ k \geqslant m\}$ such that as $s \to \infty$ [69, Chapter 8]

$$\frac{N_k(s,i)}{s} \to p_k, \quad k \geqslant m, \tag{9.2.13}$$

almost surely, uniformly over $i \in \{0, ..., m-1\}$.

For $k = m, m+1, ...$ and $i \in \{0, ..., m-1\}$, define a k-variate triangular array of martingale differences by

$$X_{s,h,j}^{(\ell)} := \frac{M_{h,j}^{(\ell)} - M_{h,j-1}^{(\ell)}}{a_{s,j}^{(\ell)} s^{1/2}}, \quad h = k+1, .., s;\ \ell = m, .., k;\ j = 0, .., i. \tag{9.2.14}$$

In order to use the multivariate martingale central limit theorem, we compute the asymptotic form of the quantities

$$\begin{aligned} G_{s,h,j}(r,\ell) &:= \mathbb{E}[X_{s,h,j}^{(r)} X_{s,h,j}^{(\ell)} | \mathcal{F}_{h,i-1}] \\ &= (a_{s,j}^{(r)} a_{s,j}^{(\ell)} s)^{-1} \mathbb{E}\left[(M_{h,j}^{(r)} - M_{h,j-1}^{(r)})(M_{h,j}^{(\ell)} - M_{h,j-1}^{(\ell)}) \Big| \mathcal{F}_{h,j-1}\right]. \end{aligned} \tag{9.2.15}$$

By the martingale property we get

$$\begin{aligned}
&\mathbb{E}\Big[(M^{(r)}_{h,j}-M^{(r)}_{h,j-1})(M^{(\ell)}_{h,j}-M^{(\ell)}_{h,j-1})\Big|\mathcal{F}_{h,j-1}\Big]\\
&\qquad=\mathbb{E}\Bigg[\sum_{d=m}^{r} b^{(r)}_d(a^{(r)}_{h,j}N_d(h,j))-a^{(r)}_{h,j-1}N_d(h,j-1))\\
&\qquad\quad\times\sum_{t=m}^{\ell} b^{(\ell)}_t(a_{h,j}N_t(h,j)-a_{h,j-1}N_t(h,j-1))\Big|\mathcal{F}_{h,j-1}\Bigg]\\
&\qquad\quad-\sum_{d=m}^{r} b^{(r)}_d(a^{(r)}_{h,j}\mathbb{E}[N_d(h,j)]-a^{(r)}_{h,j-1}\mathbb{E}[N_d(h,j-1)])\\
&\qquad\quad\times\sum_{t=m}^{\ell} b^{(\ell)}_t(a^{(\ell)}_{h,j}\mathbb{E}[N_t(h,j)]-a^{(\ell)}_{h,j-1}\mathbb{E}[N_t(h,j-1)]).
\end{aligned}\tag{9.2.16}$$

We begin by analyzing the behaviour of the deterministic term on the right–hand side of (9.2.16). When $d=m$, by (9.2.11) we obtain

$$\begin{aligned}
&a^{(\ell)}_{s,j}\mathbb{E}[N_m(s,j)]-a^{(\ell)}_{s,j-1}\mathbb{E}[N_m(s,j-1)]\\
&\quad=a^{(\ell)}_{s,j}\Big[\mathbb{1}_{\{j=m\}}+\Big(1-\frac{m+\delta}{s(2m+\delta)-2m+j-1}\Big)\mathbb{E}[N_m(s,j-1)]\Big]-a^{(\ell)}_{s,j-1}\mathbb{E}[N_m(s,j-1)]\\
&\quad=a^{(\ell)}_{s,j}\Big[\mathbb{1}_{\{j=m\}}+\mathbb{E}[N_m(s,j-1)]\frac{\ell-m}{s(2m+\delta)-2m+j-1}\Big]\\
&\quad\sim a^{(\ell)}_{s,j-1}\Big(\mathbb{1}_{\{j=m\}}+p_m\frac{\ell-m}{2m+\delta}\Big),
\end{aligned}\tag{9.2.17}$$

almost surely as $s\to\infty$, since $a^{(\ell)}_{s,j}\sim a^{(\ell)}_{s,j-1}$.

Now consider the case $d\geqslant m+1$:

$$\begin{aligned}
&a^{(\ell)}_{s,j}\mathbb{E}[N_d(s,j)]-a^{(\ell)}_{s,j-1}\mathbb{E}[N_d(s,j-1)]\\
&=a^{(\ell)}_{s,j}\Big(\Big(1-\tfrac{d+\delta}{s(2m+\delta)-2m+j-1}\Big)\mathbb{E}[N_d(s,j-1)]+\tfrac{d-1+\delta}{s(2m+\delta)-2m+j-1}\mathbb{E}[N_{d-1}(s,j-1)]\Big)\\
&\quad-a^{(\ell)}_{s,j-1}\mathbb{E}[N_d(s,j-1)]\\
&=a^{(\ell)}_{s,j}\Big(\tfrac{d-1+\delta}{s(2m+\delta)-2m+j-1}\mathbb{E}[N_{d-1}(s,j-1)]+\tfrac{\ell-d}{s(2m+\delta)-2m+j-1}\mathbb{E}[N_d(s,j-1)]\Big)\\
&\sim\frac{a^{(\ell)}_{s,j-1}}{2m+\delta}\Big((\ell-d)p_d+(d-1+\delta)p_{d-1}\Big),
\end{aligned}\tag{9.2.18}$$

almost surely as $s\to\infty$. Recall that p_d is given by [69, (8.42)].

In conclusion, we get

$$\begin{aligned}
&\lim_{s\to\infty}\frac{1}{a^{(\ell)}_{s,j-1}}\sum_{d=m}^{\ell} b^{(\ell)}_d\Big(a^{(\ell)}_{s,j}\mathbb{E}[N_d(s,j)]-a^{(\ell)}_{s,j-1}\mathbb{E}[N_d(s,j-1)]\Big)\\
&\qquad=b^{(\ell)}_m\mathbb{1}_{\{j=m\}}+\frac{1}{2m+\delta}\sum_{d=m}^{\ell} b^{(\ell)}_d[(\ell-d)p_d+(d-1+\delta)p_{d-1}].
\end{aligned}\tag{9.2.19}$$

Let us focus on the second term of the right-hand side of (9.2.19). Rearranging the terms in the sum, we get

$$\begin{aligned}
\sum_{d=m}^{\ell} b^{(\ell)}_d[(\ell-d)p_d+(d-1+\delta)p_{d-1}] &= \sum_{d=m}^{\ell-1} p_d[(\ell-d)b^{(\ell)}_d+(d+\delta)b^{(\ell)}_{d+1}]\\
&= \sum_{d=m}^{\ell-1} p_d b^{(\ell)}_d\left(\ell-d+(d+\delta)\frac{b^{(\ell)}_{d+1}}{b^{(\ell)}_d}\right)=0,
\end{aligned}\tag{9.2.20}$$

since by (9.2.10) it follows that

$$\frac{b_{d+1}^{(\ell)}}{b_d^{(\ell)}} = \frac{d-\ell}{d+\delta}. \tag{9.2.21}$$

Summarizing, we get

$$\lim_{s\to\infty} \frac{1}{a_{s,j-1}^{(\ell)}} \sum_{d=m}^{\ell} b_d^{(\ell)} \left(a_{s,j}^{(\ell)} \mathbb{E}[N_d(s,j)] - a_{s,j-1}^{(\ell)} \mathbb{E}[N_d(s,j-1)] \right) = b_m^{(\ell)} \mathbb{1}_{\{j=m\}}. \tag{9.2.22}$$

Next, we look at the first term on the right-hand side of (9.2.16). By (9.2.3) we obtain:

$$\begin{aligned} &a_{s,j}^{(r)} N_d(s,j) - a_{s,j-1}^{(r)} N_d(s,j-1) \\ &\quad = a_{s,j}^{(r)} \Big(N_d(s,j-1) + \mathbb{1}_{\{d=m\}}\mathbb{1}_{\{j=m\}} + \mathbb{1}_{\{d\neq m\}}\mathbb{1}_{\{D_{s,j}=d-1\}} - \mathbb{1}_{\{D_{s,j}=d\}} \Big) \\ &\quad\quad - a_{s,j-1}^{(r)} N_d(s,j-1) \\ &\quad = a_{s,j}^{(r)} \Big(N_d(s,j-1) \tfrac{r+\delta}{s(2m+\delta)-2m+j-1} - \mathbb{1}_{\{D_{s,j}=d\}} + \mathbb{1}_{\{d=m\}}\mathbb{1}_{\{j=m\}} \\ &\quad\quad + \mathbb{1}_{\{d\neq m\}}\mathbb{1}_{\{D_{s,j}=d-1\}} \Big) := a_{s,j}^{(r)} \Big(N_d(s,j-1) \tfrac{r+\delta}{s(2m+\delta)-2m+j-1} + B_s^{(j)}(d) \Big), \end{aligned} \tag{9.2.23}$$

where

$$B_s^{(j)}(d) := -\mathbb{1}_{\{D_{s,j}=d\}} + \mathbb{1}_{\{d=m\}}\mathbb{1}_{\{j=m\}} + \mathbb{1}_{\{d\neq m\}}\mathbb{1}_{\{D_{s,j}=d-1\}}. \tag{9.2.24}$$

Thus, we get

$$\begin{aligned} &\mathbb{E}\Bigg[\frac{1}{a_{s,j}^{(r)} a_{s,j}^{(\ell)}} \sum_{d=m}^{r} b_d^{(r)} (a_{s,j}^{(r)} N_d(s,j) - a_{s,j-1}^{(r)} N_d(s,j-1)) \\ &\quad \times \sum_{t=m}^{\ell} b_t^{(\ell)} (a_{s,j}^{(\ell)} N_t(s,j) - a_{s,j-1}^{(\ell)} N_t(s,j-1)) \Big| \mathcal{F}_{s,j-1} \Bigg] \\ &= \mathbb{E}\Bigg[\sum_{d=m}^{r} b_d^{(r)} \left(N_d(s,j-1) \frac{r+\delta}{s(2m+\delta)-2m+j-1} + B_s^{(j)}(d) \right) \\ &\quad \times \sum_{t=m}^{\ell} b_t^{(\ell)} \left(N_t(s,j-1) \frac{\ell+\delta}{s(2m+\delta)-2m+j-1} + B_s^{(j)}(t) \right) \Big| \mathcal{F}_{s,j-1} \Bigg]. \end{aligned} \tag{9.2.25}$$

By direct calculations, the r.h.s of (9.2.25) becomes

$$\begin{aligned} &\sum_{d=m}^{r} b_d^{(r)} (r+\delta) \frac{N_d(s,j-1)}{s(2m+\delta)-2m+j-1} \sum_{t=m}^{\ell} b_t^{(\ell)} (\ell+\delta) \frac{N_t(s,j-1)}{s(2m+\delta)-2m+j-1} \\ &\quad + \sum_{d=m}^{r} b_d^{(r)} (r+\delta) \frac{N_d(s,j-1)}{s(2m+\delta)-2m+j-1} \sum_{t=m}^{\ell} b_t^{(\ell)} \mathbb{E}[B_s^{(j)}(t)|\mathcal{F}_{s,j-1}] \\ &\quad + \sum_{t=m}^{\ell} b_t^{(\ell)} (\ell+\delta) \frac{N_t(s,j-1)}{s(2m+\delta)-2m+j-1} \sum_{d=m}^{r} b_d^{(r)} \mathbb{E}[B_s^{(j)}(d)|\mathcal{F}_{s,j-1}] \\ &\quad + \sum_{d=m}^{r} \sum_{t=m}^{\ell} b_d^{(r)} b_t^{(\ell)} \mathbb{E}[B_s^{(j)}(d) B_s^{(j)}(t)|\mathcal{F}_{s,j-1}] \\ &:= S_{1,s}^{(j)}(r,\ell) + S_{2,s}^{(j)}(r,\ell) + S_{3,s}^{(j)}(r,\ell) + S_{4,s}^{(j)}(r,\ell). \end{aligned} \tag{9.2.26}$$

We are interested in the behaviour of the terms $S_{1,s}^{(j)}(r,\ell)$, $S_{2,s}^{(j)}(r,\ell)$, $S_{3,s}^{(j)}(r,\ell)$ and $S_{4,s}^{(j)}(r,\ell)$ as $s \to \infty$. We first deal with the terms $S_{1,s}^{(j)}(r,\ell)$, $S_{2,s}^{(j)}(r,\ell)$, $S_{3,s}^{(j)}(r,\ell)$. To this end, note that with probability 1 as $s \to \infty$

$$\sum_{d=m}^{r} b_d^{(r)} (r+\delta) \frac{N_d(s,j-1)}{s(2m+\delta)+j-1} \sim \frac{r+\delta}{2m+\delta} \sum_{d=m}^{r} b_d^{(r)} p_d \tag{9.2.27}$$

and that

$$\begin{aligned}\sum_{d=m}^{r} b_d^{(r)}\mathbb{E}[B_s^{(j)}(d)|\mathcal{F}_{s,j-1}] &= b_m^{(r)}\mathbb{E}[\mathbb{1}_{\{j=m\}}-\mathbb{1}_{\{D_{s,j}=m\}}|\mathcal{F}_{s,j-1}]\\ &\quad+\sum_{d=m+1}^{r} b_d^{(r)}\mathbb{E}[\mathbb{1}_{\{D_{s,j}=d-1\}}-\mathbb{1}_{\{D_{s,j}=d\}}|\mathcal{F}_{s,j-1}]\\ &= b_m^{(r)}\mathbb{1}_{\{j=m\}}-b_m^{(r)}\mathbb{P}(D_{s,j}=m|\mathcal{F}_{s,j-1})\\ &\quad+\sum_{d=m+1}^{r} b_d^{(r)}(\mathbb{P}(D_{s,j}=d-1|\mathcal{F}_{s,j-1})-\mathbb{P}(D_{s,j}=d|\mathcal{F}_{s,j-1}))\\ &= b_m^{(r)}\Big(\mathbb{1}_{\{j=m\}}-\frac{m+\delta}{s(2m+\delta)-2m+j-1}N_m(s,j-1)\Big)\\ &\quad+\sum_{d=m+1}^{r} b_d^{(r)}\Big(\frac{d-1+\delta}{s(2m+\delta)-2m+j-1}N_{d-1}(s,j-1)\\ &\quad-\frac{d+\delta}{s(2m+\delta)-2m+j-1}N_d(s,j-1)\Big).\end{aligned} \tag{9.2.28}$$

Thus, we obtain

$$\begin{aligned}&\sum_{d=m}^{r} b_d^{(r)}\mathbb{E}[B_s^{(j)}(d)|\mathcal{F}_{s,j-1}]\\ &\qquad\sim b_m^{(r)}\mathbb{1}_{\{j=m\}}+\frac{1}{2m+\delta}\sum_{d=m}^{r} b_d^{(r)}((d-1+\delta)p_{d-1}-(d+\delta)p_d)\\ &\qquad= b_m^{(r)}\mathbb{1}_{\{j=m\}}-\frac{r+\delta}{2m+\delta}\sum_{d=m}^{r} b_d^{(r)}p_d,\end{aligned} \tag{9.2.29}$$

almost surely as $s\to\infty$, where at the last step we used (9.2.20). Summarizing, with high probability

$$\begin{aligned}S_{1,s}^{(j)}(r,\ell) &\to \frac{(r+\delta)(\ell+\delta)}{(2m+\delta)^2}\sum_{d=m}^{r} b_d^{(r)}p_d\sum_{t=m}^{\ell} b_t^{(\ell)}p_t,\\ S_{2,s}^{(j)}(r,\ell) &\to \frac{r+\delta}{2m+\delta}\sum_{d=m}^{r} b_d^{(r)}p_d\left(b_m^{(\ell)}\mathbb{1}_{\{j=m\}}-\frac{\ell+\delta}{2m+\delta}\sum_{t=m}^{\ell} b_t^{(\ell)}p_t\right),\\ S_{3,s}^{(j)}(r,\ell) &\to \frac{\ell+\delta}{2m+\delta}\sum_{t=m}^{\ell} b_t^{(\ell)}p_t\left(b_m^{(r)}\mathbb{1}_{\{j=m\}}-\frac{r+\delta}{2m+\delta}\sum_{d=m}^{r} b_d^{(r)}p_d\right),\end{aligned} \tag{9.2.30}$$

as $s\to\infty$. Finally, we consider the term $S_{4,s}(r,\ell)$. Note that, by (9.2.24), we have

$$\begin{cases}B_s^{(j)}(m)=\mathbb{1}_{\{j=m\}}-\mathbb{1}_{\{D_{s,j}=m\}},\\ B_s^{(j)}(d)=\mathbb{1}_{\{D_{s,j}=d-1\}}-\mathbb{1}_{\{D_{s,j}=d\}},\quad d\geqslant m+1.\end{cases} \tag{9.2.31}$$

We separate the analysis of these terms according to the following two events:

a) $\{D_{s,j}=m\}$,

b) $\{D_{s,j}=h\}$, $h\geqslant m+1$.

On the event $\{D_{s,j}=m\}$, by (9.2.24), we get

$$\begin{aligned}\mathbb{E}[B_s^{(j)}(d)B_s^{(j)}(t)|\mathcal{F}_{s,j-1}] &= \mathbb{1}_{\{d=t=m\}}\mathbb{1}_{\{j\neq m\}}+\mathbb{1}_{\{d=t=m+1\}}-\mathbb{1}_{\{d=m\}}\\ &\quad\times\mathbb{1}_{\{t=m+1\}}\mathbb{1}_{\{j\neq m\}}-\mathbb{1}_{\{t=m\}}\mathbb{1}_{\{d=m+1\}}\mathbb{1}_{\{j\neq m\}}.\end{aligned} \tag{9.2.32}$$

On $\{D_{s,j}=h\}$, $h\geqslant m+1$, we get

$$\begin{aligned}&\mathbb{E}[B_s^{(j)}(d)B_s^{(j)}(t)|\mathcal{F}_{s,j-1}]\\ &\qquad=\mathbb{1}_{\{d=t=m\}}\mathbb{1}_{\{j=m\}}+\mathbb{1}_{\{d=m\}}\mathbb{1}_{\{j=m\}}\Big(\mathbb{1}_{\{t=h+1\}}-\mathbb{1}_{\{t=h\}}\Big)\\ &\qquad+\mathbb{1}_{\{t=m\}}\mathbb{1}_{\{j=m\}}\Big(\mathbb{1}_{\{d=h+1\}}-\mathbb{1}_{\{d=h\}}\Big)+\mathbb{1}_{\{t=d=h\}}+\mathbb{1}_{\{t=d=h+1\}}\\ &\qquad-\mathbb{1}_{\{d=h\}}\mathbb{1}_{\{t=h+1\}}-\mathbb{1}_{\{d=h+1\}}\mathbb{1}_{\{t=h\}}.\end{aligned} \tag{9.2.33}$$

By (9.2.26), combining (9.2.32) and (9.2.33) we obtain

$$\begin{aligned}
S_{4,s}^{(j)}(r,l) &= \frac{m+\delta}{s(2m+\delta)-2m+j-1} N_m(s,j-1)\Big[\mathbb{1}_{\{j\neq m\}}(b_m^{(r)}b_m^{(\ell)} - b_m^{(r)}b_{m+1}^{(\ell)} \\
&\quad -b_{m+1}^{(r)}b_m^{(\ell)}) + b_{m+1}^{(r)}b_{m+1}^{(\ell)}\Big] + \sum_{h=m+1}^{s} \frac{h+\delta}{s(2m+\delta)-2m+j-1} \\
&\quad \times N_h(s,j-1)\Big[\mathbb{1}_{\{j=m\}}(b_m^{(r)}b_m^{(\ell)} + b_m^{(r)}(b_{h+1}^{(\ell)} - b_h^{(\ell)}) \\
&\quad +b_m^{(\ell)}(b_{h+1}^{(r)} - b_h^{(r)})) + b_h^{(r)}b_h^{(\ell)} + b_{h+1}^{(r)}b_{h+1}^{(\ell)} - b_h^{(r)}b_{h+1}^{(\ell)} - b_{h+1}^{(r)}b_h^{(\ell)}\Big] \\
&\sim \frac{m+\delta}{2m+\delta} p_m\Big[\mathbb{1}_{\{j\neq m\}}(b_m^{(r)}b_m^{(\ell)} - b_m^{(r)}b_{m+1}^{(\ell)} - b_{m+1}^{(r)}b_m^{(\ell)}) + b_{m+1}^{(r)}b_{m+1}^{(\ell)}\Big] \\
&\quad + \sum_{h=m+1}^{\infty} \frac{h+\delta}{2m+\delta} p_h\Big[\mathbb{1}_{\{j=m\}}(b_m^{(r)}b_m^{(\ell)} + b_m^{(r)}(b_{h+1}^{(\ell)} - b_h^{(\ell)}) \\
&\quad +b_m^{(\ell)}(b_{h+1}^{(r)} - b_h^{(r)})) + b_h^{(r)}b_h^{(\ell)} + b_{h+1}^{(r)}b_{h+1}^{(\ell)} - b_h^{(r)}b_{h+1}^{(\ell)} - b_{h+1}^{(r)}b_h^{(\ell)}\Big],
\end{aligned} \tag{9.2.34}$$

almost surely as $s \to \infty$.

Replacing in (9.2.26) the expressions derived in (9.2.30) for the terms $S_{1,s}^{(j)}(r,\ell)$, $S_{2,s}^{(j)}(r,\ell)$ and $S_{3,s}^{(j)}(r,\ell)$ and in (9.2.34) for $S_{4,s}^{(j)}(r,\ell)$, we conclude that, with high probability, as $s \to \infty$,

$$\begin{aligned}
&\mathbb{E}\left[\frac{1}{a_{s,j}^{(r)}a_{s,j}^{(\ell)}}(M_{s,j}^{(r)} - M_{s,j-1}^{(r)})(M_{s,j}^{(\ell)} - M_{s,j-1}^{(\ell)})\Big|\mathcal{F}_{s,j-1}\right] \to a^{(j)}(r,\ell) \\
&\quad := \frac{m+\delta}{2m+\delta} p_m\Big(\mathbb{1}_{\{j\neq m\}}(b_m^{(r)}b_m^{(\ell)} - b_m^{(r)}b_{m+1}^{(\ell)} - b_{m+1}^{(r)}b_m^{(\ell)}) + b_{m+1}^{(r)}b_{m+1}^{(\ell)}\Big) \\
&\qquad + \sum_{h=m+1}^{\infty} \frac{h+\delta}{2m+\delta} p_h\Big(\mathbb{1}_{\{j=m\}}(b_m^{(r)}b_m^{(\ell)} + b_m^{(r)}(b_{h+1}^{(\ell)} - b_h^{(\ell)}) + b_m^{(\ell)}(b_{h+1}^{(r)} \\
&\qquad -b_h^{(r)})) + b_h^{(r)}b_h^{(\ell)} + b_{h+1}^{(r)}b_{h+1}^{(\ell)} - b_h^{(r)}b_{h+1}^{(\ell)} - b_{h+1}^{(r)}b_h^{(\ell)}\Big) - \Big(b_m^{(r)}\mathbb{1}_{\{j=m\}} \\
&\qquad -\frac{r+\delta}{2m+\delta}\sum_{d=m}^{r} b_d^{(r)}p_d\Big)\Big(b_m^{(\ell)}\mathbb{1}_{\{j=m\}} - \frac{\ell+\delta}{2m+\delta}\sum_{t=m}^{\ell} b_t^{(\ell)}p_t\Big).
\end{aligned} \tag{9.2.35}$$

Now we consider the quantity

$$\begin{aligned}
a(r,\ell) &:= \sum_{j=0}^{m-1} a^{(j)}(r,\ell) \\
&= \frac{m+\delta}{2m+\delta} p_m\Big((m-1)(b_m^{(r)}b_m^{(\ell)} - b_m^{(r)}b_{m+1}^{(\ell)} - b_{m+1}^{(r)}b_m^{(\ell)}) + mb_{m+1}^{(r)}b_{m+1}^{(\ell)}\Big) \\
&\quad + \sum_{h=m+1}^{\infty} \frac{h+\delta}{2m+\delta} p_h\Big(b_m^{(r)}b_m^{(\ell)} + b_m^{(r)}(b_{h+1}^{(\ell)} - b_h^{(\ell)}) \\
&\quad +b_m^{(\ell)}(b_{h+1}^{(r)} - b_h^{(r)}) + m(b_h^{(r)}b_h^{(\ell)} + b_{h+1}^{(r)}b_{h+1}^{(\ell)} - b_h^{(r)}b_{h+1}^{(\ell)} - b_{h+1}^{(r)}b_h^{(\ell)})\Big) \\
&\quad -\Big(b_m^{(r)} - \frac{r+\delta}{2m+\delta}\sum_{d=m}^{r} b_d^{(r)}p_d\Big)\Big(b_m^{(\ell)} - \frac{\ell+\delta}{2m+\delta}\sum_{t=m}^{\ell} b_t^{(\ell)}p_t\Big) \\
&\quad -(m-1)\frac{(r+\delta)(\ell+\delta)}{(2m+\delta)^2}\sum_{d=m}^{r} b_d^{(r)}p_d\sum_{t=m}^{\ell} b_t^{(\ell)}p_t \\
&= \sum_{h=m}^{\infty} \frac{h+\delta}{2m+\delta} p_h[(b_m^{(r)} + b_{h+1}^{(r)} - b_h^{(r)})(b_m^{(\ell)} + b_{h+1}^{(\ell)} - b_h^{(\ell)}) \\
&\quad +(m-1)(b_{h+1}^{(\ell)} - b_h^{(\ell)})(b_{h+1}^{(r)} - b_h^{(r)})] \\
&\quad -\Big(b_m^{(r)} - \frac{r+\delta}{2m+\delta}\sum_{d=m}^{r} b_d^{(r)}p_d\Big)\Big(b_m^{(\ell)} - \frac{\ell+\delta}{2m+\delta}\sum_{t=m}^{\ell} b_t^{(\ell)}p_t\Big) \\
&\quad -(m-1)\frac{(r+\delta)(\ell+\delta)}{(2m+\delta)^2}\sum_{d=m}^{r} b_d^{(r)}p_d\sum_{t=m}^{\ell} b_t^{(\ell)}p_t.
\end{aligned} \tag{9.2.36}$$

By [69, Section 8], we can write

$$p_d = \left((2+\delta/m)\frac{\Gamma(m+2+\delta+\delta/m)}{\Gamma(m+\delta)}\right)\frac{\Gamma(d+\delta)}{\Gamma(d+3+\delta+\delta/m)} := c(\delta)\frac{\Gamma(d+\delta)}{\Gamma(d+3+\delta+\delta/m)}. \tag{9.2.37}$$

Then, by (9.2.10) and (9.2.37), we get

$$\begin{aligned}
&\sum_{d=m}^{r-1} p_d b_d^{(r)} = c(\delta)(-1)^r\Gamma(r+\delta)\sum_{d=m}^{r-1}(-1)^d\frac{1}{(r-d)!\Gamma(d+3+\delta+\delta/m)}\\
&= c(\delta)\frac{(-1)^r\Gamma(r+\delta)}{r+2+\delta+\delta/m}\\
&\quad\sum_{d=m}^{r-1}(-1)^d\left[\frac{1}{(r-d)!\Gamma(d+2+\delta+\delta/m)}+\frac{1}{(r-d-1)!\Gamma(d+3+\delta+\delta/m)}\right]\\
&= c(\delta)\frac{(-1)^r\Gamma(r+\delta)}{r+2+\delta+\delta/m}\left[(-1)^m\frac{1}{(r-m)!\Gamma(m+2+\delta+\delta/m)}+(-1)^{r-1}\frac{1}{\Gamma(r+2+\delta+\delta/m)}\right],
\end{aligned} \tag{9.2.38}$$

where at the last step we used the telescoping property of the sum. Thus, by (9.2.38), we get

$$\begin{aligned}
b_m^{(r)} - \frac{r+\delta}{2m+\delta}\sum_{d=m}^{r} b_d^{(r)}p_d &= b_m^{(r)} - \frac{r+\delta}{2m+\delta}p_r - \frac{r+\delta}{2m+\delta}\sum_{d=m}^{r-1} b_d^{(r)}p_d\\
&= (-1)^{r-m}\frac{\Gamma(r+\delta)}{(r-m)!\Gamma(m+\delta)} - (-1)^{r-m}\frac{(r+\delta)(2+\delta/m)\Gamma(r+\delta)}{(2m+\delta)(r-m)!\Gamma(m+\delta)(r+2+\delta+\delta/m)}\\
&= \frac{(-1)^{r-m}\Gamma(r+\delta)}{(r-m)!\Gamma(m+\delta)}\frac{r+2+\delta-r/m}{r+2+\delta+\delta/m}.
\end{aligned} \tag{9.2.39}$$

9.2.1 *First condition of Theorem 9.2.1*

In this section we check that the first condition of Theorem 9.2.1 holds. We know from (9.2.35) that

$$sG_{s,s,j}(r,\ell) \to a^{(j)}(r,\ell), \tag{9.2.40}$$

almost surely as $s\to\infty$. From definition (9.2.15) we have

$$G_{s,h,j}(r,\ell) = \frac{a_{h,j}^{(r)}a_{h,j}^{(\ell)}}{sa_{s,j}^{(r)}a_{s,j}^{(\ell)}}hG_{h,h,j}(r,\ell). \tag{9.2.41}$$

From the regular variation property (9.2.12), the function

$$h \to u(h) := a_{h,j}^{(r)}a_{h,j}^{(\ell)}hG_{h,h,j}(r,\ell) \tag{9.2.42}$$

is regularly varying with index $(r+\ell+2\delta)/(2m+\delta)$. Therefore, from (9.2.41) and Karamata's theorem on integration of regularly varying functions [102, page 25]

$$\begin{aligned}
\sum_{j=0}^{m-1} V_{s,j}(r,\ell) &= \sum_{j=0}^{m-1}\sum_{h=k+1}^{s} G_{s,h,j}(r,\ell) = \sum_{j=0}^{m-1}\sum_{h=k+1}^{s}\frac{a_{h,j}^{(r)}a_{h,j}^{(\ell)}}{sa_{s,j}^{(r)}a_{s,j}^{(\ell)}}hG_{h,h,j}(r,\ell)\\
&= \sum_{j=0}^{m-1}\sum_{h=k+1}^{s}\frac{u(h)}{sa_{s,j}^{(r)}a_{s,j}^{(\ell)}} \sim \sum_{j=0}^{m-1}\frac{u(s)}{\left(\frac{r+\ell+2\delta}{2m+\delta}+1\right)a_{s,j}^{(r)}a_{s,j}^{(\ell)}}\\
&\sim a(r,\ell)\frac{2m+\delta}{r+\ell+2m+3\delta},
\end{aligned} \tag{9.2.43}$$

for $r,\ell = m, m+1, ..., k$.

This verifies the first condition the martingale central limit theorem of Proposition 9.2.1 (with each A_n being a $(k-m+1)\times(k-m+1)$ identity matrix).

9.2.2 *Second condition of Theorem 9.2.1*

Next we show that the second condition of Theorem 9.2.1 holds as well. By (9.2.3), we deduce that

$$|(N_\ell(s,i)-\mathbb{E}[N_\ell(s,i)])-(N_\ell(s,i-1)-\mathbb{E}[N_\ell(s,i-1)])|\leqslant 2 \quad \text{for all } \ell. \tag{9.2.44}$$

Hence the events $\{|X^{(\ell)}_{s,i,j,h}|>\varepsilon\}$ are empty for all ℓ, for all $h\leqslant s$ and for all $j\leqslant i$ as $s\to\infty$, indeed

$$\begin{aligned}\{|X^{(l)}_{s,i,j,h}|>\varepsilon\} &= \{|M^{(\ell)}_{h,j}-M^{(\ell)}_{h,j-1}|>a^{(\ell)}_{s,j}s^{1/2}\varepsilon\}\\ &= \Big\{|a^{(\ell)}_{h,j}\sum_{t=m}^{\ell}b^{(\ell)}_t(N_t(h,j)-\mathbb{E}[N_t(h,j)])-a^{(\ell)}_{h,j-1}\\ &\quad\times\sum_{t=m}^{\ell}b^{(\ell)}_t(N_t(h,j-1)-\mathbb{E}[N_t(h,j-1)])>a^{(\ell)}_{s,j}s^{1/2}\varepsilon\Big\}\\ &\subset\Big\{C_1h^{\frac{\ell+\delta}{2m+\delta}}>\varepsilon s^{\frac{\ell+\delta}{2m+\delta}}s^{1/2}\Big\}\subset\Big\{C_1>\varepsilon s^{1/2}\Big\},\end{aligned} \tag{9.2.45}$$

where $C_1>0$ is a large constant independent of s. Thus, we obtain

$$\mathbb{1}_{\{|X^{(\ell)}_{s,i,j,h}|>\varepsilon\}}\leqslant\mathbb{1}_{\{C_1>\varepsilon s^{1/2}\}}\to 0, \tag{9.2.46}$$

as $s\to\infty$. This implies that the second condition of Proposition 9.2.1 holds.

9.2.3 *The limit process for degree counts*

We conclude that

$$\left(\frac{1}{s^{1/2}}\sum_{j=m}^{k}b^{(k)}_j(N_j(s,i)-\mathbb{E}[N_j(s,i)]),\ k\geqslant m\right)\Rightarrow(Y_k,\ k\geqslant m) \tag{9.2.47}$$

in $\mathbb{R}^{\mathbb{N}}$, where $(Y_k,\ k=m,m+1,...)$ is a mean zero Gaussian process with covariance function R_Y given by

$$R_Y(r,\ell)=\frac{2m+\delta}{r+\ell+2m+3\delta}a(r,\ell),\quad r,\ell\geqslant m. \tag{9.2.48}$$

We use this covariance function to define the $(k-m+1)\times(k-m+1)$ matrix with entries

$$R_{Y,k}=(R_Y(r,\ell),\ m\leqslant r\leqslant k, m\leqslant\ell\leqslant k). \tag{9.2.49}$$

The convergence in (9.2.47) means that for all $k=m,m+1,...$

$$C_k\left(\frac{N_r(s,i)-\mathbb{E}[N_r(s,i)]}{s^{1/2}},\ r=m,...,k\right)^{T}\Rightarrow(Y_r,\ r=m,...,k), \tag{9.2.50}$$

where C_k is a $(k-m+1)\times(k-m+1)$ matrix with entries

$$c_{r,\ell}=\begin{cases}b^{(r)}_\ell & \text{if } \ell\leqslant r,\\ 0 & \text{if } \ell>r.\end{cases} \tag{9.2.51}$$

We are able to conclude that

$$\left(\frac{N_r(s,i)-\mathbb{E}[N_r(s,i)]}{s^{1/2}},\ r=m,...,k\right)\Rightarrow D_k(Y_r,\ r=m,..,k)^{T}, \tag{9.2.52}$$

and the covariance matrix of the limiting Gaussian vector is given by

$$\Sigma_k=D_kR_{Y,k}D_k^{T}. \tag{9.2.53}$$

Using the following identity,

$$\sum_{t=\ell}^{r} x^{t-\ell} b_t^{(r)} b_\ell^{(t)} = b_\ell^{(r)} (1+x)^{r-\ell},\ 1 \leqslant \ell \leqslant r,\ x \in \mathbb{R}, \tag{9.2.54}$$

it can be shown that $D_k = C_k^{-1}$ has entries

$$d_{r,\ell} = \begin{cases} (-1)^{r-\ell} b_\ell^{(r)} & \text{if } \ell \leqslant r, \\ 0 & \text{if } \ell > r. \end{cases} \tag{9.2.55}$$

In order to facilitate the computation of the entries of the matrix Σ_k, by (9.2.36) we can write $R_{Y,k}$ in the form

$$\begin{aligned} R_{Y,k} &= \sum_{q=0}^{\infty} h_q \int_0^{+\infty} (2m+\delta) e^{-(2m+3\delta)x} R_{q,x}^1 dx \\ &\quad + \sum_{q=m}^{\infty} h_q \int_0^{+\infty} (2m+\delta) e^{-(2m+3\delta)x} R_{q,x}^2 dx, \end{aligned} \tag{9.2.56}$$

where

$$h_q = \begin{cases} -1 & \text{if } q = 0, 1, \ldots m-1, \\ \dfrac{q+\delta}{2m+\delta} p_q & \text{if } q \geqslant m, \end{cases} \tag{9.2.57}$$

and the matrix $R_{m,x}$ is the $(k-m+1) \times (k-m+1)$ matrix with entries

$$R_{q,x}^1 = (C_{q,x}^1)^T (C_{q,x}^1), \qquad R_{q,x}^2 = (C_{q,x}^2)^T (C_{q,x}^2). \tag{9.2.58}$$

The vector $C_{q,x}^1$ has the entries

$$C_{q,x}^1(\ell) = \begin{cases} \Big(b_m^{(\ell)} - \dfrac{\ell+\delta}{2m+\delta} \displaystyle\sum_{t=m}^{\ell} b_t^{(\ell)} p_t \Big) e^{-\ell x},\ \ell \geqslant m & \text{if } q = 0, \\ \Big(\dfrac{\ell+\delta}{2m+\delta} \displaystyle\sum_{t=m}^{\ell} b_t^{(\ell)} p_t \Big) e^{-\ell x},\ \ell \geqslant m & \text{if } q = 1, \ldots, m-1, \\ (b_m^{(\ell)} - b_q^{(\ell)} + b_{q+1}^{(\ell)}) e^{-\ell x},\ \ell \geqslant m & \text{if } q \geqslant m. \end{cases} \tag{9.2.59}$$

and

$$C_{q,x}^2(\ell) = \begin{cases} 0 & \text{if } q = 0, 1, \ldots, m-1, \\ \sqrt{m-1} (b_{q+1}^{(\ell)} - b_q^{(\ell)}) e^{-\ell x} & \text{if } q \geqslant m. \end{cases} \tag{9.2.60}$$

Therefore

$$\begin{aligned} \Sigma_k &= \sum_{q=0}^{\infty} h_q \int_0^{+\infty} (2m+\delta) e^{-(2m+3\delta)x} (D_k (C_{q,x}^1)^T) C_{q,x}^1 D_k^T dx \\ &\quad + \sum_{q=m}^{\infty} h_q \int_0^{+\infty} (2m+\delta) e^{-(2m+3\delta)x} (D_k (C_{q,x}^2) T) C_{q,x}^2 D_k^T dx. \end{aligned} \tag{9.2.61}$$

We compute separately the terms in the sum for $q < m$ and $q \geqslant m$. We begin with $C^1_{q,x}$. For $q \geqslant m$ and $\ell = m, m+1, \ldots$, since $b^{(k)}_j = 0$ for all $j > k$, by (9.2.54) and (9.2.55) we have

$$\begin{aligned}
(D_k(C^1_{q,x})^T)(\ell) &= \sum_{t=m}^{\ell} (-1)^{\ell-t} b^{(\ell)}_t (b^{(t)}_m - b^{(t)}_q + b^{(t)}_{q+1}) e^{-tx} \\
&= \sum_{t=m}^{\ell} (-1)^{\ell-t} b^{(\ell)}_t b^{(t)}_m e^{-tx} - \sum_{t=q}^{\ell} (-1)^{\ell-t} b^{(\ell)}_t b^{(t)}_q e^{-tx} \\
&\quad + \sum_{t=q+1}^{\ell} (-1)^{\ell-t} b^{(\ell)}_t b^{(t)}_{q+1} e^{-tx} \\
&= (-1)^{\ell-m} e^{-mx} b^{(\ell)}_m (1-e^{-x})^{\ell-m} \\
&\quad -(-1)^{\ell-q} e^{-qx} b^{(\ell)}_q (1-e^{-x})^{\ell-q} \\
&\quad +(-1)^{\ell-q-1} e^{-(q+1)x} b^{(\ell)}_{q+1} (1-e^{-x})^{\ell-q-1}.
\end{aligned} \tag{9.2.62}$$

Therefore, for $q \geqslant m$ and $r, \ell = m, m+1, \ldots$, we have

$$\begin{aligned}
&(D_k(C^1_{q,x})^T)(\ell)(D_k(C^1_{q,x})^T)(r) \\
&\quad = (-1)^{\ell+r} b^{(\ell)}_m b^{(r)}_m e^{-2mx} (1-e^{-x})^{\ell+r-2m} \\
&\qquad -(-1)^{\ell+r-m-q} (b^{(\ell)}_m b^{(r)}_q + b^{(r)}_m b^{(\ell)}_q) e^{-(m+q)x} (1-e^{-x})^{\ell+r-m-q} \\
&\qquad +(-1)^{\ell+r-q-m-1} (b^{(\ell)}_m b^{(r)}_{q+1} + b^{(r)}_m b^{(\ell)}_{q+1}) e^{-(m+q+1)x} (1-e^{-x})^{\ell+r-m-q-1} \\
&\qquad +(-1)^{\ell+r} b^{(\ell)}_q b^{(r)}_q e^{-2qx} (1-e^{-x})^{r+\ell-2q} \\
&\qquad +(-1)^{\ell+r} (b^{(\ell)}_q b^{(r)}_{q+1} + b^{(r)}_q b^{(\ell)}_{q+1}) e^{-(2q+1)x} (1-e^{-x})^{\ell+r-2q-1} \\
&\qquad +(-1)^{\ell+r} b^{(\ell)}_{q+1} b^{(r)}_{q+1} e^{-2(q+1)x} (1-e^{-x})^{\ell+r-2q-2} \\
&\quad := \sum_{t=1}^{6} \theta^{(t)}_{q,x}(r,\ell).
\end{aligned} \tag{9.2.63}$$

We have

$$\begin{aligned}
&\int_0^{+\infty} (2m+\delta) e^{-(2m+3\delta)x} \theta^{(1)}_{q,x}(r,\ell)\,dx \\
&\qquad = (-1)^{\ell+r} (2m+\delta) b^{(\ell)}_m b^{(r)}_m \int_0^{+\infty} e^{-(4m+3\delta)x} (1-e^{-x})^{\ell+r-2m} dx \\
&\qquad = (-1)^{\ell+r} (2m+\delta) b^{(\ell)}_m b^{(r)}_m B(4m+3\delta, \ell+r-2m+1) \\
&\qquad = (-1)^{\ell+r} (2m+\delta) b^{(\ell)}_m b^{(r)}_m \frac{\Gamma(4m+3\delta)(\ell+r-2m)!}{\Gamma(\ell+r+2m+1+3\delta)},
\end{aligned} \tag{9.2.64}$$

where

$$B(\alpha,\beta) = \frac{\Gamma(\alpha)\Gamma(\beta)}{\Gamma(\alpha+\beta)} \tag{9.2.65}$$

is the Beta function. Similarly,

$$\begin{aligned}
&\int_0^{+\infty} (2m+\delta) e^{-(2m+3\delta)x} \theta^{(2)}_{q,x}(r,\ell)\,dx \\
&\qquad = (-1)^{\ell+r-m-q+1} (2m+\delta) (b^{(\ell)}_m b^{(r)}_q + b^{(r)}_m b^{(\ell)}_q) \frac{\Gamma(3m+q+3\delta)(\ell+r-m-q)!}{\Gamma(\ell+r+2m+1+3\delta)},
\end{aligned} \tag{9.2.66}$$

$$\begin{aligned}
&\int_0^{+\infty} (2m+\delta) e^{-(2m+3\delta)x} \theta^{(3)}_{q,x}(r,\ell)\,dx \\
&\qquad = (-1)^{\ell+r-m-q-1} (2m+\delta) (b^{(\ell)}_m b^{(r)}_{q+1} + b^{(r)}_m b^{(\ell)}_{q+1}) \\
&\qquad\quad \times \frac{\Gamma(3m+q+1+3\delta)(\ell+r-m-q-1)!}{\Gamma(\ell+r+2m+1+3\delta)},
\end{aligned} \tag{9.2.67}$$

$$\int_0^{+\infty}(2m+\delta)e^{-(2m+3\delta)x}\theta^{(4)}_{q,x}(r,\ell)dx$$
$$=(-1)^{r+\ell}(2m+\delta)b^{(\ell)}_q b^{(r)}_q\frac{\Gamma(2q+2m+3\delta)(r+\ell-2q)!}{\Gamma(r+\ell+2m+1+3\delta)}, \tag{9.2.68}$$

$$\int_0^{+\infty}(2m+\delta)e^{-(2m+3\delta)x}\theta^{(5)}_{q,x}(r,\ell)dx$$
$$=(-1)^{\ell+r}(2m+\delta)(b^{(\ell)}_q b^{(r)}_{q+1}+b^{(r)}_q b^{(\ell)}_{q+1})\frac{\Gamma(2q+2m+1+3\delta)(\ell+r-2q-1)!}{\Gamma(\ell+r+2m+1+3\delta)}, \tag{9.2.69}$$

$$\int_0^{+\infty}(2m+\delta)e^{-(2m+3\delta)x}\theta^{(6)}_{q,x}(r,\ell)dx$$
$$=(-1)^{\ell+r}(2m+\delta)b^{(\ell)}_{q+1}b^{(r)}_{q+1}\frac{\Gamma(2q+2m+2+3\delta)(\ell+r-2q-2)!}{\Gamma(\ell+r+2m+1+3\delta)}. \tag{9.2.70}$$

By (9.2.39) and (9.2.55), for $q=0$ and $\ell=m,m+1,\ldots$ we have

$$\begin{aligned}(D_k(C^1_{0,x})^T)(l) &= \sum_{t=m}^{\ell}(-1)^{\ell-t}b^{(\ell)}_t\left(b^{(t)}_m-\frac{t+\delta}{2m+\delta}\sum_{h=m}^{t}b^{(t)}_h p_h\right)e^{-tx}\\ &=\frac{\Gamma(\ell+\delta)}{\Gamma(m+\delta)}\sum_{t=m}^{\ell}(-1)^{t-m}e^{-tx}\frac{t+2+\delta-t/m}{(t-m)!(\ell-t)!(t+2+\delta+\delta/m)}.\end{aligned} \tag{9.2.71}$$

Therefore, by (9.2.71), for $r,\ell\geqslant m$ and $q=0$, we obtain

$$\begin{aligned}&\int_0^{+\infty}(2m+\delta)e^{-(2m+3\delta)x}(D_k(C^1_{0,x})^T)(r)(C^1_{0,x}D^T_k)(\ell)dx\\ &=(2m+\delta)\frac{\Gamma(\ell+\delta)\Gamma(r+\delta)}{(\Gamma(m+\delta))^2}\sum_{t_1=m}^{\ell}\sum_{t_2=m}^{r}(-1)^{t_1+t_2}\\ &\quad\times\frac{(t_1+t_2+2m+3\delta)^{-1}(t_1+2+\delta-t_1/m)(t_2+2+\delta-t_2/m)}{(t_1-m)!(t_2-m)!(\ell-t_1)!(r-t_2)!(t_1+2+\delta+\delta/m)(t_2+2+\delta+\delta/m)}.\end{aligned} \tag{9.2.72}$$

Consider now the case $q=1,\ldots,m-1$ and $\ell=m,m+1,\ldots$. By (9.2.39) and (9.2.55), we have

$$\begin{aligned}(D_k(C^1_{q,x})^T)(l) &= \sum_{t=m}^{\ell}(-1)^{\ell-t}b^{(\ell)}_t\left(\frac{t+\delta}{2m+\delta}\sum_{h=m}^{t}b^{(t)}_h p_h\right)e^{-tx}\\ &=\Gamma(\ell+\delta)\sum_{t=m}^{\ell}\frac{e^{-tx}}{(\ell-t)!\Gamma(t+\delta)}\\ &\quad\times\left(b^{(t)}_m-(-1)^{t-m}\frac{\Gamma(t+\delta)(t+2+\delta-t/m)}{(t-m)!\Gamma(m+\delta)(t+2+\delta+\delta/m)}\right).\end{aligned} \tag{9.2.73}$$

Therefore, by (9.2.73), for $r,\ell\geqslant m$ and $q=1,\ldots,m-1$, we have

$$\begin{aligned}&\int_0^{+\infty}(2m+\delta)e^{-(2m+3\delta)x}(D_k(C^1_{q,x})^T)(r)(C^1_{q,x}D^T_k)(\ell)dx\\ &=(2m+\delta)\Gamma(\ell+\delta)\Gamma(r+\delta)\sum_{t_1=m}^{\ell}\sum_{t_2=m}^{r}\frac{(t_1+t_2+2m+3\delta)^{-1}}{(\ell-t_1)!\Gamma(t_1+\delta)(r-t_2)!\Gamma(t_2+\delta)}\\ &\quad\times\left(b^{(t_1)}_m-(-1)^{t_1-m}\frac{\Gamma(t_1+\delta)(t_1+2+\delta-t_1/m)}{(t_1-m)!\Gamma(m+\delta)(t_1+2+\delta+\delta/m)}\right)\\ &\quad\times\left(b^{(t_2)}_m-(-1)^{t_2-m}\frac{\Gamma(t_2+\delta)(t_2+2+\delta-t_2/m)}{(t_2-m)!\Gamma(m+\delta)(t_2+2+\delta+\delta/m)}\right).\end{aligned} \tag{9.2.74}$$

By using (9.2.10), we deduce that

$$\begin{aligned}\int_0^{+\infty} &(2m+\delta)e^{-(2m+3\delta)x}(D_k(C_{q,x}^1)^T)(r)(C_{q,x}^1 D_k^T)(\ell)dx \\ &= \frac{(2m+\delta)\Gamma(\ell+\delta)\Gamma(r+\delta)}{m^2(\Gamma(m+\delta))^2}\sum_{t_1=m}^{\ell}\sum_{t_2=m}^{r}(-1)^{t_1+t_2} \\ &\quad\times\frac{(\delta+t_1)(\delta+t_2)(t_1+t_2+2m+3\delta)^{-1}}{(t_1-m)!(t_2-m)!(\ell-t_1)!(r-t_2)!(t_1+2+\delta+\delta/m)(t_2+2+\delta+\delta/m)}.\end{aligned} \tag{9.2.75}$$

Now we investigate the behavior of the term $C_{q,x}^2$. For $q \geqslant m$, using (9.2.54), we get

$$\begin{aligned}(D_k(C_{q,x}^2)^T)(\ell) &= \sum_{t=m}^{\ell}\sqrt{m-1}(-1)^{\ell-t}b_t^{(\ell)}(b_{q+1}^{(t)}-b_q^{(t)})e^{-tx} \\ &= \sqrt{m-1}\Big((-1)^{q+1-\ell}e^{-(q+1)x}b_{q+1}^{(\ell)}(1-e^{-x})^{\ell-q-1} \\ &\quad -(-1)^{q-\ell}e^{-qx}b_q^{(\ell)}(1-e^{-x})^{\ell-q}.\end{aligned} \tag{9.2.76}$$

Thus, we obtain

$$\begin{aligned}&(D_k(C_{q,x}^2)^T)(r)(D_k(C_{q,x}^2)^T)(\ell) \\ &\quad= (m-1)\Big((-1)^{r+\ell}e^{-2(q+1)x}b_{q+1}^{(\ell)}b_{q+1}^{(r)}(1-e^{-x})^{\ell+r-2q-2} \\ &\qquad+(-1)^{r+\ell}e^{-2qx}b_q^{(\ell)}b_q^{(r)}(1-e^{-x})^{\ell+r-2q} \\ &\qquad+(-1)^{r+\ell}e^{-(2q+1)x}(b_{q+1}^{(\ell)}b_q^{(r)}+b_q^{(\ell)}b_{q+1}^{(r)})(1-e^{-x})^{\ell+r-2q-1}\Big) \\ &\quad= (m-1)(\theta_{q,x}^{(4)}(r,\ell)+\theta_{q,x}^{(5)}(r,\ell)+\theta_{q,x}^{(6)}(r,\ell)),\end{aligned} \tag{9.2.77}$$

where $\theta_{q,x}^{(t)}(r,\ell)$, $t=4,5,6$, are defined in (9.2.63).

Using (9.2.64)-(9.2.72), (9.2.75) and (9.2.77), we conclude that the covariance function $R_Z(r,\ell)$ of the limiting Gaussian process $(Z_k,\ k=m,m+1,...)$ in (9.1.1) is given by (9.1.2).

[1] L. Alonso and R. Cerf. The three dimensional polyominoes of minimal area. *The Electronic Journal of Combinatorics* 3.1 (1996).

[2] V. Apollonio, R. D'Autilia, B. Scoppola, E. Scoppola, and A. Troiani. Criticality of measures on 2-d Ising configurations: from square to hexagonal graphs. *Journal of Statistical Physics* 177.5 (2019).

[3] V. Apollonio, R. D'Autilia, B. Scoppola, E. Scoppola, and A. Troiani. Shaken dynamics: an easy way to parallel Markov Chain Monte Carlo. *Journal of Statistical Physics* 189.3 (2022).

[4] V. Apollonio, V. Jacquier, F. R. Nardi, and A. Troiani. Metastability for the Ising model on the hexagonal lattice. *Electronic Journal of Probability* 27.38 (2022).

[5] E. Atalay, A. Hortacsu, J. Roberts, and C. Syverson. Network structure of production. *Proceedings of the National Academy of Sciences* 108.13 (2011).

[6] L. Avena, F. Castell, A. Gaudillière, and C. Melot. Approximate and exact solutions of intertwining equations through random spanning forests. *In and Out of Equilibrium 3: Celebrating Vladas Sidoravicius* (2021).

[7] A. Backhausz and B. Rozner. Asymptotic degree distribution in preferential attachment graph models with multiple type edges. *Stochastic Models* 35.4 (2019).

[8] A. S. Balankin, M. A. Martínez-Cruz, F. G. Martínez, B. Mena, A. Tobon, J. Patiño-Ortiz, M. Patiño-Ortiz, and Di. Samayoa. Ising percolation in a three-state majority vote model. *Physics Letters A* 381.5 (2017).

[9] S. Baldassarri and G. Bet. Asymptotic Normality of Degree Counts in a General Preferential Attachment Model. *Markov Processes and Related Fields* 28.4 (2022).

[10] S. Baldassarri, A. Gallo, V. Jacquier, and A. Zocca. Ising model on clustered networks: A model for opinion dynamics. *Physica A: Statistical Mechanics and its Applications* 623 (2023).

[11] S. Baldassarri, A. Gaudillière, F. den Hollander, F. R. Nardi, E. Olivieri, and E. Scoppola. Droplet dynamics in a two-dimensional rarefied gas under Kawasaki dynamics. *arXiv preprint, arXiv:2304.14099* (2023).

[12] S. Baldassarri, A. Gaudillière, F. den Hollander, F. R. Nardi, E. Olivieri, and E. Scoppola. Homogeneous nucleation for two-dimensional Kawasaki dynamics (in preparation).

[13] S. Baldassarri and V. Jacquier. Metastability for Kawasaki dynamics on the hexagonal lattice. *Journal of Statistical Physics* 190.3 (2023).

[14] S. Baldassarri, V. Jacquier, and A. Zocca. Critical configurations of the hard–core model on square grid graphs. *arXiv preprint, arXiv:2308.05041* (2023).

[15] S. Baldassarri and F. R. Nardi. Critical Droplets and sharp asymptotics for Kawasaki dynamics with weakly anisotropic interactions. Extended version. *arXiv preprint, arXiv:2108.02017* (2021).

[16] S. Baldassarri and F. R. Nardi. Metastability in a lattice gas with strong anisotropic interactions under Kawasaki dynamics. *Electronic Journal of Probability* 26.137 (2021).

[17] S. Baldassarri and F. R. Nardi. Critical Droplets and Sharp Asymptotics for Kawasaki Dynamics with Strongly Anisotropic Interactions. *Journal of Statistical Physics* 186.3 (2022).

[18] S. Baldassarri and F. R. Nardi. Critical Droplets and sharp asymptotics for Kawasaki dynamics with weakly anisotropic interactions. *Stochastic Processes and their Applications* 147 (2022).

[19] A.-L. Barabási and R. Albert. Emergence of scaling in random networks. *science* 286.5439 (1999).

[20] J. Beltrán and C. Landim. Tunneling and Metastability of Continuous Time Markov Chains. *Journal of Statistical Physics* 140.6 (2010).

[21] J. Beltrán and C. Landim. A Martingale approach to metastability. *Probability Theory and Related Fields* 161.1-2 (2014).

[22] J. Beltrán and C. Landim. Tunneling of the Kawasaki dynamics at low temperatures in two dimensions. 51.1 (2015).

[23] N. Berger, C. Borgs, J. T. Chayes, and A. Saberi. Asymptotic behavior and distributional limits of preferential attachment graphs. *The Annals of Probability* 42.1 (2014).

[24] G. Bet, A. Gallo, and S. Kim. Metastability of the three-state Potts model with general interactions. *arXiv preprint, arXiv:2208.11869* (2022).

[25] G. Bet, A. Gallo, and F. R. Nardi. Critical Configurations and Tube of Typical Trajectories for the Potts and Ising Models with Zero External Field. *Journal of Statistical Physics* 184.3 (2021).

[26] G. Bet, A. Gallo, and F. R. Nardi. Metastability for the degenerate Potts Model with negative external magnetic field under Glauber dynamics. *Journal of Mathematical Physics* 63.12 (2022).

[27] G. Bet, V. Jacquier, and F. R. Nardi. Effect of Energy Degeneracy on the Transition Time for a Series of Metastable States. *Journal of Statistical Physics* 184.1 (2021).

[28] A. Bianchi and A. Gaudillière. Metastable states, quasi-stationary distributions and soft measures. *Stochastic Processes and their Applications* 126.6 (2016).

[29] A. Bianchi, A. Gaudillière, and P. Milanesi. On Soft Capacities, Quasi-stationary Distributions and the Pathwise Approach to Metastability. *Journal of Statistical Physics* 181.3 (2020).

[30] B. Bollobás, C. Borgs, J. T. Chayes, and O. Riordan. Directed scale-free graphs. In: *SODA*. Vol. 3. 2003.

[31] A. Bovier, M. Eckhoff, V. Gayrard, and M. Klein. Metastability and Low Lying Spectra in Reversible Markov Chains. *Communications in Mathematical Physics* 228.2 (2002).

[32] A. Bovier and F. den Hollander. Metastability. Springer International Publishing, 2015.

[33] A. Bovier, F. den Hollander, and S. Marello. Metastability for Glauber dynamics on the complete graph with coupling disorder. *Communications in Mathematical Physics* 392.1 (2022).

[34] A. Bovier, F. den Hollander, S. Marello, E. Pulvirenti, and M. Slowik. Metastability of Glauber dynamics with inhomogeneous coupling disorder. *arXiv preprint, arXiv:2209.09827* (2022).

[35] A. Bovier, F. den Hollander, and F.R. Nardi. Sharp asymptotics for Kawasaki dynamics on a finite box with open boundary. *Probability Theory and Related Fields* 135.2 (2005).

[36] A. Bovier, F. den Hollander, and C. Spitoni. Homogeneous nucleation for Glauber and Kawasaki dynamics in large volumes at low temperatures. *The Annals of Probability* 38.2 (2010).

[37] A. Bovier and F. Manzo. Metastability in Glauber dynamics in the low temperature limit: beyond exponential asymptotics. *Journal of Statistical Physics* 107.3/4 (2002).

[38] A. Bovier, S. Marello, and E. Pulvirenti. Metastability for the dilute Curie–Weiss model with Glauber dynamics. *Electronic Journal of Probability* 26.47 (2021).

[39] M. Cassandro, A. Galves, E. Olivieri, and M. E. Vares. Metastable behavior of stochastic dynamics: A pathwise approach. *Journal of Statistical Physics* 35.5-6 (1984).

[40] O. Catoni and A. Trouvé. Parallel annealing by multiple trials: a mathematical study. *Simulated annealing* (1992).

[41] R. Cerf and F. Manzo. Nucleation and growth for the Ising model in d dimensions at very low temperatures. *The Annals of Probability* 41.6 (2013).

[42] E. N. M. Cirillo and J. L. Lebowitz. Metastability in the two-dimensional Ising model with free boundary conditions. *Journal of Statistical Physics* 90.1 (1998).

[43] E. N. M. Cirillo and F. R. Nardi. Metastability for a stochastic dynamics with a parallel heath bath updating rule. *Journal of Statistical Physics* 110.1/2 (2003).

[44] E. N. M. Cirillo and F. R. Nardi. Relaxation Height in Energy Landscapes: An Application to Multiple Metastable States. *Journal of Statistical Physics* 150.6 (2013).

[45] E. N. M. Cirillo, F. R. Nardi, and J. Sohier. Metastability for General Dynamics with Rare Transitions: Escape Time and Critical Configurations. *Journal of Statistical Physics* 161.2 (2015).

[46] E. N. M. Cirillo, F. R. Nardi, and C. Spitoni. Competitive nucleation in reversible probabilistic cellular automata. *Physical Review E* 78.4 (2008).

[47] E. N. M. Cirillo, F. R. Nardi, and C. Spitoni. Metastability for Reversible Probabilistic Cellular Automata with Self-Interaction. *Journal of Statistical Physics* 132.3 (2008).

[48] E. N. M. Cirillo, F. R. Nardi, and C. Spitoni. Sum of exit times in a series of two metastable states. *The European Physical Journal Special Topics* 226.10 (2017).

[49] E. N. M. Cirillo and E. Olivieri. Metastability and nucleation for the Blume-Capel model. Different mechanisms of transition. *Journal of Statistical Physics* 83 (1996).

[50] C. Cooper and A. Frieze. A general model of web graphs. *Random Structures & Algorithms* 22.3 (2003).

[51] M. J. De Oliveira, J. F. F. Mendes, and M. A. Santos. Nonequilibrium spin models with Ising universal behaviour. *Journal of Physics A: Mathematical and General* 26.10 (1993).

[52] P. Dehghanpour and R. H. Schonmann. A nucleation-and-growth model. *Probability Theory and Related Fields* 107 (1997).

[53] P. Dehghanpour and R. H. Schonmann. Metropolis dynamics relaxation via nucleation and growth. *Communications in Mathematical Physics* 188.1 (1997).

[54] M. Deijfen, H. van ven Esker, R. van der Hofstad, and G. Hooghiemstra. A preferential attachment model with random initial degrees. *Arkiv för matematik* 47 (2009).

[55] S. Dommers. Metastability of the Ising model on random regular graphs at zero temperature. *Probability Theory and Related Fields* 167 (2017).

[56] S. Dommers, F. den Hollander, O. Jovanovski, and F. R. Nardi. Metastability for Glauber dynamics on random graphs. *The Annals of Applied Probability* 27.4 (2017).

[57] M. I. Freidlin and A. D. Wentzell. Random Perturbations of Dynamical Systems. Springer New York, 1984.

[58] Fengnan G., A. van der Vaart, R. Castro, and R. van der Hofstad. Consistent estimation in general sublinear preferential attachment trees. *Electronic Journal of Statistics* 11.2 (2017).

[59] F. Gao and A. van der Vaart. On the asymptotic normality of estimating the affine preferential attachment network models with random initial degrees. *Stochastic Processes and their Applications* 127.11 (2017).

[60] A. Garavaglia, R. van der Hofstad, and G. Woeginger. The dynamics of power laws: Fitness and aging in preferential attachment trees. *Journal of Statistical Physics* 168 (2017).

[61] A. Gaudillière. Collision probability for random trajectories in two dimensions. *Stochastic Processes and their Applications* 119.3 (2009).

[62] A. Gaudilliere, F. den Hollander, F. R. Nardi, E. Olivieri, and E. Scoppola. Ideal gas approximation for a two-dimensional rarefied gas under Kawasaki dynamics. *Stochastic Processes and their Applications* 119.3 (2009).

[63] A. Gaudillière and F. R. Nardi. An upper bound for front propagation velocities inside moving populations. *Brazilian Journal of Probability and Statistics* 24.2 (2010).

[64] A. Gaudillière. Collision probability for random trajectories in two dimensions. *Stochastic processes and their applications* 119.3 (2009).

[65] A. Gaudillière, F. den Hollander, F. R. Nardi, E. Olivieri, and E. Scoppola. Ideal gas approximation for a two-dimensional rarefied gas under Kawasaki dynamics. *Stochastic Processes and their Applications* 119.3 (2009).

[66] A. Gaudillière, P. Milanesi, and M. E. Vares. Asymptotic exponential law for the transition time to equilibrium of the metastable kinetic Ising model with vanishing magnetic field. *Journal of Statistical Physics* 179.2 (2020).

[67] A. Gaudillière, E. Olivieri, and E. Scoppola. Nucleation pattern at low temperature for local Kawasaki dynamics in two dimensions. *Markov Processes and Related Fields* 11 (2005).

[68] B. Gois and C. Landim. Zero-temperature limit of the Kawasaki dynamics for the Ising lattice gas in a large two-dimensional torus. *The Annals of Probability* 43.4 (2015).

[69] R. van der Hofstad. Random graphs and complex networks. Vol. 43. Cambridge university press, 2016.

[70] F. den Hollander, F. R. Nardi, and S. Taati. Metastability of hard-core dynamics on bipartite graphs. *Electronic Journal of Probability* 23.none (2018).

[71] F. den Hollander, F. R. Nardi, and A. Troiani. Kawasaki Dynamics with Two Types of Particles: Stable/Metastable Configurations and Communication Heights. *Journal of Statistical Physics* 145.6 (2011).

[72] F. den Hollander, F. R. Nardi, and A. Troiani. Kawasaki dynamics with two types of particles: critical droplets. *Journal of Statistical Physics* 149 (2012).

[73] F. den Hollander, F. R. Nardi, and A. Troiani. Metastability for Kawasaki dynamics at low temperature with two types of particles. *Electronic Journal of Probability* 17.2 (2012).

[74] F. den Hollander, F.R. Nardi, E. Olivieri, and E. Scoppola. Droplet growth for three-dimensional Kawasaki dynamics. *Probability Theory and Related Fields* 125.2 (2003).

[75] F. den Hollander, E. Olivieri, and E. Scoppola. Metastability and nucleation for conservative dynamics. *Journal of Mathematical Physics* 41.3 (2000).

[76] F. den Hollander, E. Olivieri, and E. Scoppola. Nucleation in fluids: some rigorous results. *Physica A: Statistical Mechanics and its Applications* 279.1-4 (2000).

[77] M. Kac, G. E. Uhlenbeck, and P. C. Hemmer. On the van der Waals Theory of the Vapor-Liquid Equilibrium. I. Discussion of a One-Dimensional Model. *Journal of Mathematical Physics* 4.2 (1963).

[78] S. Kim and I. Seo. Metastability of Ising and Potts models without external fields in large volumes at low temperatures. *Communications in Mathematical Physics* 396.1 (2022).

[79] R. Kotecký and E. Olivieri. Droplet dynamics for asymmetric Ising model. *Journal of Statistical Physics* 70 (1993).

[80] R. Kotecký and E. Olivieri. Shapes of growing droplets—a model of escape from a metastable phase. *Journal of Statistical Physics* 75 (1994).

[81] A. Krot and L. O. Prokhorenkova. Local clustering coefficient in generalized preferential attachment models. In: *Algorithms and Models for the Web Graph: 12th International Workshop, WAW 2015, Eindhoven, The Netherlands, December 10-11, 2015, Proceedings* 12. 2015.

[82] C. Landim, D. Marcondes, and I. Seo. A resolvent approach to metastability. *arXiv preprint, arXiv:2102.00998* (2021).

[83] A. Lu, C. Sun, and Y. Liu. The impact of community structure on the convergence time of opinion dynamics. *Discrete Dynamics in Nature and Society* 2017 (2017).

[84] H. M. Mahmoud. Local and global degree profiles of randomly grown self-similar hooking networks under uniform and preferential attachment. *Advances in Applied Mathematics* 111 (2019).

[85] F. Manzo, F. R. Nardi, E. Olivieri, and E. Scoppola. On the Essential Features of Metastability: Tunnelling Time and Critical Configurations. *Journal of Statistical Physics* 115.1/2 (2004).

[86] F. Manzo and E. Olivieri. Relaxation patterns for competing metastable states: a nucleation and growth model. *Markov Processes and Related Fields* 4 (1998).

[87] F. Manzo and E. Olivieri. Dynamical Blume–Capel model: competing metastable states at infinite volume. *Journal of Statistical Physics* 104 (2001).

[88] T. Móri. On random trees. *Studia Scientiarum Mathematicarum Hungarica* 39.1-2 (2002).

[89] F. R. Nardi and E. Olivieri. Low temperature stochastic dynamics for an Ising model with alternating field. *Markov Processes and Related Fields* 2 (1996).

[90] F. R. Nardi, E. Olivieri, and E. Scoppola. Anisotropy Effects in Nucleation for Conservative Dynamics. *Journal of Statistical Physics* 119.3-4 (2005).

[91] F. R. Nardi and C. Spitoni. Sharp asymptotics for stochastic dynamics with parallel updating rule. *Journal of Statistical Physics* 146.4 (2012).

[92] F. R. Nardi, A. Zocca, and S. C. Borst. Hitting Time Asymptotics for Hard-Core Interactions on Grids. *Journal of Statistical Physics* 162.2 (2015).

[93] E. J. Neves and R. H. Schonmann. Behavior of droplets for a class of Glauber dynamics at very low temperature. *Probability Theory and Related Fields* 91.3-4 (1992).

[94] M. J. de Oliveira. Isotropic majority-vote model on a square lattice. *Journal of Statistical Physics* 66.1 (1992).

[95] E. Olivieri and E. Scoppola. Markov chains with exponentially small transition probabilities: First exit problem from a general domain. I. The reversible case. *Journal of Statistical Physics* 79.3-4 (1995).

[96] E. Olivieri and E. Scoppola. Markov chains with exponentially small transition probabilities: First exit problem from a general domain. II. The general case. *Journal of Statistical Physics* 84.5-6 (1996).

[97] E. Olivieri and M. E. Vares. Large Deviations and Metastability. Cambridge University Press, 2005.

[98] A. Pachon, L. Sacerdote, and S. Yang. Scale-free behavior of networks with the copresence of preferential and uniform attachment rules. *Physica D: Nonlinear Phenomena* 371 (2018).

[99] E. Peköz, A. Röllin, and N. Ross. Joint degree distributions of preferential attachment random graphs. *Advances in Applied Probability* 49.2 (2017).

[100] O. Penrose and J. L. Lebowitz. Rigorous treatment of metastable states in the van der Waals-Maxwell theory. *Journal of Statistical Physics* 3.2 (1971).

[101] W. Phyllis, W. Tiandong, A. D. Richard, and S. I. Resnick. Fitting the linear preferential attachment model. *Electronic Journal of Statistics* 11.2 (2017).

[102] S. I. Resnick. Heavy-tail phenomena: probabilistic and statistical modeling. Springer Science & Business Media, 2007.

[103] S. I. Resnick and G. Samorodnitsky. Asymptotic normality of degree counts in a preferential attachment model. *Advances in Applied Probability* 48.A (2016).

[104] G. Samorodnitsky, S. I. Resnick, D. Towsley, R. Davis, A. Willis, and P. Wan. Nonstandard regular variation of in-degree and out-degree in the preferential attachment model. *Journal of Applied Probability* 53.1 (2016).

[105] R. H. Schonmann. Slow droplet-driven relaxation of stochastic Ising models in the vicinity of the phase coexistence region. *Communications in Mathematical Physics* 161.1 (1994).

[106] R. H. Schonmann and S. B. Shlosman. Wulff droplets and the metastable relaxation of kinetic Ising models. *Communications in Mathematical Physics* 194 (1998).

[107] E. Scoppola. Renormalization group for Markov chains and application to metastability. *Journal of Statistical Physics* 73 (1993).

[108] X. Si, Y. Liu, and Z. Zhang. Opinion dynamics in populations with implicit community structure. *International Journal of modern physics C* 20.12 (2009).

[109] A. Sîrbu, V. Loreto, V. D. P. Servedio, and F. Tria. Opinion dynamics: models, extensions and external effects. In: *Participatory sensing, opinions and collective awareness*. Springer, 2017, pp. 363–401.

[110] D. Stauffer. Opinion Dynamics and Sociophysics. In: *Encyclopedia of Complexity and Systems Science*. Springer New York, 2009, pp. 6380–6388.

[111] F. Vazquez, P. L. Krapivsky, and S. Redner. Constrained opinion dynamics: Freezing and slow evolution. *Journal of Physics A: Mathematical and General* 36.3 (2003).

[112] P. Wan, T. Wang, R. A. Davis, and S. I. Resnick. Are extreme value estimation methods useful for network data? *Extremes* 23 (2020).

[113] T. Wang and S. I. Resnick. Asymptotic normality of in-and out-degree counts in a preferential attachment model. *Stochastic Models* 33.2 (2017).

[114] Z. Xie, X. Song, and Q. Li. A review of opinion dynamics. *Theory, methodology, tools and applications for modeling and simulation of complex systems* (2016).

[115] P. Zhang and H. M. Mahmoud. On nodes of small degrees and degree profile in preferential dynamic attachment circuits. *Methodology and Computing in Applied Probability* 22 (2020).